

*Advances in*  
**ORGANOMETALLIC  
CHEMISTRY**

VOLUME 35

***Advances in***  
**ORGANOMETALLIC CHEMISTRY**

VOLUME 35

This Page Intentionally Left Blank

# ***Advances in Organometallic Chemistry***

EDITED BY

**F. G. A. STONE**

DEPARTMENT OF CHEMISTRY  
BAYLOR UNIVERSITY  
WACO, TEXAS


**ROBERT WEST**

DEPARTMENT OF CHEMISTRY  
UNIVERSITY OF WISCONSIN  
MADISON, WISCONSIN

VOLUME 35



ACADEMIC PRESS, INC.  
A Division of Harcourt Brace & Company  
San Diego New York Boston  
London Sydney Tokyo Toronto

This book is printed on acid-free paper. 

Copyright © 1993 by ACADEMIC PRESS, INC.

All Rights Reserved.

No part of this publication may be reproduced or transmitted in any form or by any means, electronic or mechanical, including photocopy, recording, or any information storage and retrieval system, without permission in writing from the publisher.

**Academic Press, Inc.**

1250 Sixth Avenue, San Diego, California 92101-4311

*United Kingdom Edition published by*

**Academic Press Limited**

24-28 Oval Road, London NW1 7DX

International Standard Serial Number: 0065-3055

International Standard Book Number: 0-12-031135-6

PRINTED IN THE UNITED STATES OF AMERICA

93 94 95 96 97 98 BB 9 8 7 6 5 4 3 2 1

# Contents

CONTRIBUTORS . . . . .	vii
------------------------	-----

## Chemistry at Diplatinum Centers

GORDON K. ANDERSON

I. Introduction . . . . .	1
II. Complexes with Unsupported Platinum-Platinum Bonds . . . . .	1
III. Halide- and Hydride-Bridged Complexes . . . . .	2
IV. Complexes Containing Organic Bridging Groups . . . . .	5
V. Complexes Containing Orthometalated Phosphine Ligands . . . . .	7
VI. Complexes Bridged by dpdm or Related Ligands . . . . .	11
VII. Complexes Bridged dpdc Ligands . . . . .	32
VIII. Summary . . . . .	35
References. . . . .	35

## Transition Metal Clusters in Homogenous Catalysis

G. SÜSS-FINK and G. MEISTER

I. Introduction . . . . .	41
II. Catalytic Reactions Involving CO . . . . .	44
III. Catalytic Reactions Involving H <sub>2</sub> . . . . .	49
IV. Catalytic Reactions Involving CO and H <sub>2</sub> . . . . .	74
V. Catalytic Reactions Involving CO and H <sub>2</sub> O . . . . .	95
VI. Other Catalytic Reactions . . . . .	107
VII. Conclusions . . . . .	122
References. . . . .	122

## The Interplay of Alkylidyne and Carbaborane Ligands at Metal Centers II: Proton-Mediated Reactions

STEPHEN A. BREW and F. GORDON A. STONE

I. Introduction . . . . .	135
II. Protonations with HBF <sub>4</sub> ·Et <sub>2</sub> O in the Presence of Monodentate Lewis Bases . . . . .	142
III. Protonations with HBF <sub>4</sub> ·Et <sub>2</sub> O in the Presence of Bidentate Phosphines . . . . .	149
IV. Protonations with HX (X = Cl or I). . . . .	152
V. Formation of Dimetal Compounds . . . . .	157
VI. <i>Exo-nido</i> Metallacarboranes. . . . .	172
VII. Spectroscopic and X-Ray Diffraction Analysis . . . . .	176
VIII. Conclusions . . . . .	183
References. . . . .	183

## Di- and Trinuclear Metal Complexes of Diboraheterocycles

WALTER SIEBERT

I.	Introduction . . . . .	187
II.	1,4-Diboracyclohexadiene Metal Complexes . . . . .	191
III.	1,4-Dihydro-1,4-diboranaphthalene Metal Complexes . . . . .	194
IV.	9,10-Dihydro-9,10-diboraanthracene Metal Complexes . . . . .	197
V.	2,3-Dihydro-1,3-diborolyl Metal Complexes . . . . .	202
VI.	1,3-Diborafulvene Metal Complexes. . . . .	205
VII.	Concluding Remarks . . . . .	208
	References. . . . .	209

## Trifluoromethyl-Containing Transition Metal Complexes

JOHN A. MORRISON

I.	Scope of the Review . . . . .	211
II.	Early Studies . . . . .	212
III.	Transition Metal Trifluoromethyl Chemistry of the Past Decade . . . . .	218
IV.	Synopsis of Trifluoromethyl Metal Structural Data. . . . .	234
V.	Prospects . . . . .	235
	References. . . . .	237

## Intramolecular Coordination in Organotin Chemistry

JOHANN T. B. H. JASTRZEBSKI and GERARD VAN KOTEN

I.	Introduction . . . . .	242
II.	Divalent Organotin Compounds Containing a C,Y-Chelating Ligand . . . . .	247
III.	Tetravalent Organotin Compounds Containing a C,Y-Chelating Ligand . . . . .	256
IV.	Concluding Remarks . . . . .	288
	References. . . . .	290

INDEX . . . . .		295
CUMULATIVE LIST OF CONTRIBUTORS . . . . .		303

# Contributors

*Numbers in parentheses indicate the pages on which the authors' contributions begin.*

- GORDON K. ANDERSON (1), Department of Chemistry, University of Missouri, St. Louis, St. Louis, Missouri 63121
- STEPHEN A. BREW (135), Department of Chemistry, Baylor University, Waco, Texas 76798
- JOHANN T. B. H. JASTRZEBSKI (241), Debye Research Institute, Department of Metal-Mediated Synthesis, University of Utrecht, 3584 CH Utrecht, The Netherlands
- G. MEISTER (41), Institut de Chimie, Université de Neuchâtel, CH-2000 Neuchâtel, Switzerland
- JOHN A. MORRISON (211), Department of Chemistry, University of Illinois at Chicago, Chicago, Illinois 60680
- WALTER SIEBERT (187), Anorganisch-Chemisches, Institut der Universität Heidelberg, W-6900 Heidelberg, Germany
- F. GORDON A. STONE (135), Department of Chemistry, Baylor University, Waco, Texas 76798
- G. SÜSS-FINK (41), Institut de Chimie, Université de Neuchâtel, CH-2000 Neuchâtel, Switzerland
- GERARD VAN KOTEN (241), Debye Research Institute, Department of Metal-Mediated Synthesis, University of Utrecht, 3584 CH Utrecht, The Netherlands



This Page Intentionally Left Blank

# Chemistry at Diplatinum Centers

GORDON K. ANDERSON

Department of Chemistry  
University of Missouri—St. Louis  
St. Louis, Missouri 63121

I. Introduction . . . . .	1
II. Complexes with Unsupported Platinum–Platinum Bonds . . . . .	1
III. Halide- and Hydride-Bridged Complexes . . . . .	2
IV. Complexes Containing Organic Bridging Groups . . . . .	5
V. Complexes Containing Orthometalated Phosphine Ligands . . . . .	7
VI. Complexes Bridged by dppm or Related Ligands . . . . .	11
VII. Complexes Bridged by dppc Ligands . . . . .	32
VIII. Summary . . . . .	35
References . . . . .	35

## I

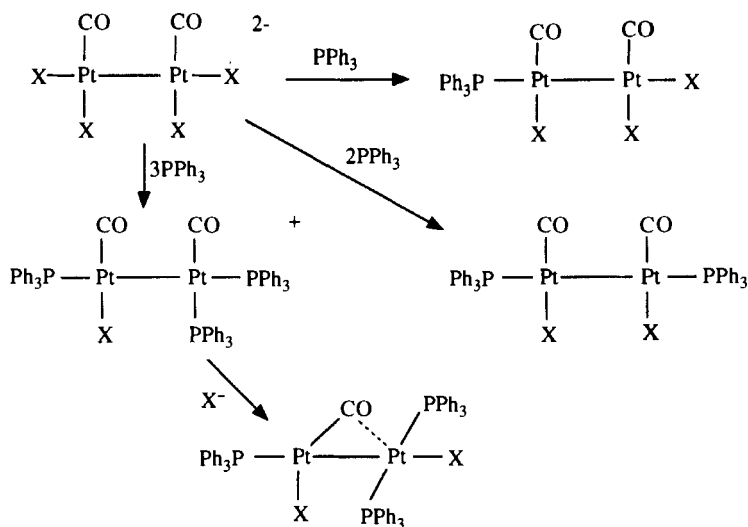
### INTRODUCTION

Dimeric platinum complexes have been well known for many years. In particular, halide-bridged dimers have been valuable precursors to numerous monomeric species, obtained by bridge cleavage reactions. The number and variety of dimeric complexes have increased tremendously, however, with the availability of several bidentate ligands of a bite size suitable to coordinate in a bridging fashion. Most notable among these is bis(diphenylphosphino)methane (dppm), and the remarkable versatility of this ligand has prompted the development of a number of analogs of dppm. We return to complexes of dppm and related ligands, but first, we consider dimeric complexes containing unsupported metal–metal bonds, followed by those bridged by simple ligands, such as halides or hydrides, then a number of compounds with bridging organic fragments.

## II

### COMPLEXES WITH UNSUPPORTED PLATINUM–PLATINUM BONDS

Platinum(I) complexes of the type  $[\text{Pt}_2\text{X}_4(\text{CO})_2]^{2-}$  have been known for some time (1). Treatment of  $[\text{Bu}_4\text{N}]_2[\text{Pt}_2\text{X}_4(\text{CO})_2]$  ( $\text{X} = \text{Cl}, \text{Br}$ ) with  $\text{PPh}_3$  generates  $[\text{Pt}_2\text{X}_3(\text{CO})_2(\text{PPh}_3)]^-$ , in which the  $\text{PPh}_3$  occupies a terminal position. The neutral complex  $[\text{Pt}_2\text{X}_2(\text{CO})_2(\text{PPh}_3)_2]$ , in which both termi-

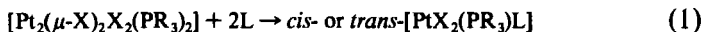
SCHEME 1. Reactions of  $[\text{Pt}_2\text{X}_4(\text{CO})_2]^{2-}$  with  $\text{PPh}_3$ .

nal sites are occupied by  $\text{PPh}_3$ , is obtained with 2 equivalents of  $\text{PPh}_3$  and  $[\text{Pt}_2\text{X}(\text{CO})_2(\text{PPh}_3)_3]^+$  is produced with 3 or more equivalents (Scheme 1). In each of these, the dimer is held together by an unsupported Pt–Pt bond. Addition of  $\text{X}^-$  to  $[\text{Pt}_2\text{X}_2(\text{CO})_2(\text{PPh}_3)_2]$  or  $[\text{Pt}_2\text{X}(\text{CO})_2(\text{PPh}_3)_3]^+$  generates a species containing an asymmetrically bridging carbonyl ligand (2). Treatment of  $[\text{Pt}_3(\text{CO})_3(\text{P}^t\text{Bu}_2\text{Ph})_3]$  with 1.5 equivalents of  $\text{Cl}_2$  yields  $[\text{Pt}_2\text{Cl}_2(\text{CO})_2(\text{P}^t\text{Bu}_2\text{Ph})_2]$ , a species analogous to the neutral one described above (3), whereas the reaction of  $[\text{PtCl}_2(\text{PhCN})_2]$  with  $[\text{Pt}(\text{CO})(\text{PPh}_3)_3]$  yields the bridging carbonyl complex  $[\text{Pt}_2\text{Cl}_2(\mu\text{-CO})(\text{PPh}_3)_3]$  by formal oxidative addition of a Pt–Cl bond to the platinum(0) center (4).

### III

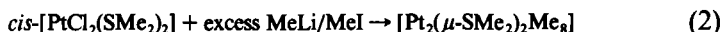
#### HALIDE- AND HYDRIDE-BRIDGED COMPLEXES

Compounds containing simple bridging ligands, such as halides or hydrides, are numerous. Among the most widely used dimers have been Zeise's dimer,  $[\text{Pt}_2(\mu\text{-Cl})_2\text{Cl}_2(\text{C}_2\text{H}_4)_2]$ , and its tertiary phosphine analogs of the type  $[\text{Pt}_2(\mu\text{-X})_2\text{X}_2(\text{PR}_3)_2]$  (5). Cleavage of the latter with a neutral ligand leads to unsymmetrical dihalo complexes of either *cis*- or *trans*-geometry.



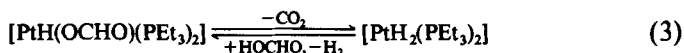
Thus, for example,  $[\text{Pt}_2(\mu\text{-Cl})_2\text{Cl}_2(\text{PR}_3)_2]$  reacts with carbon monoxide to produce *trans*- $[\text{PtCl}_2(\text{CO})(\text{PR}_3)]$ , which, on standing, converts to its *cis*-isomer (6). Other convenient starting materials that have been developed include the arylplatinum dimers prepared by reaction of  $[\text{Pt}_2(\mu\text{-Cl})_2\text{Cl}_2(\text{PR}_3)_2]$  with  $\text{HgAr}_2$  (7) or by treatment of  $[\text{PtCl}_2(\text{C}_2\text{H}_4)(\text{PR}_3)]$  with  $\text{ArSnMe}_3$  (8). These may be cleaved by neutral ligands to generate species of the type  $[\text{PtCl}(\text{Ar})(\text{PR}_3)\text{L}]$ .

Reaction of *cis*- $[\text{PtCl}_2(\text{SMe}_2)_2]$  with methyllithium produces the dimeric complex  $[\text{Pt}_2\text{Me}_4(\mu\text{-SMe}_2)_2]$ , which may also be cleaved, and the dimethylsulfide ligands displaced by a range of neutral species (9). Treatment of the corresponding diethylsulfide-bridged species with silver acetate in the presence of pyridine generates the platinum(III) dimer,  $[\text{Pt}_2\text{Me}_4(\mu\text{-OAc})_2(\text{py})_2]$  (10). Addition of  $[\text{Pt}_2\text{Me}_4(\mu\text{-SMe}_2)_2]$  to a solution of Zeise's dimer generates  $[\text{Pt}_2(\mu\text{-Cl})_2\text{Me}_2(\text{C}_2\text{H}_4)_2]$ , which may be cleaved by alkenes, alkynes, pyridine, or dimethylsulfide (11). Treatment of *cis*- $[\text{PtCl}_2(\text{SMe}_2)_2]$  with  $\text{MeLi}$  and  $\text{MeI}$  yields the platinum(IV) dimers  $[\text{Pt}_2\text{Me}_8(\mu\text{-SMe}_2)_2]$ ,



where the  $\text{SMe}_2$  groups may be displaced by other neutral ligands to give monomeric species of the form  $[\text{PtMe}_4\text{L}_2]$  (12).

Dimeric platinum complexes containing bridging hydrides are also well established. The fluxional cationic trihydride  $[\text{Pt}_2(\mu\text{-H})_2\text{H}(\text{PEt}_3)_4]^+$  may be prepared by irradiation of an acetonitrile solution of the platinum oxalate complex  $[\text{Pt}(\text{C}_2\text{O}_4)(\text{PEt}_3)_2]$  in the presence of  $\text{H}_2$  (13), by reaction of  $[\text{PtH}_2(\text{PEt}_3)_2]$  with  $[\text{PtH}(\text{S})(\text{PEt}_3)_2]^+$  (13,14), or by  $\text{NaBH}_4$  reduction of  $[\text{PtClH}(\text{PEt}_3)_2]$  (14). Reaction of  $[\text{PtD}_2(\text{PEt}_3)_2]$  with  $[\text{PtH}(\text{S})(\text{PEt}_3)_2]^+$  gives  $[\text{Pt}_2(\mu\text{-D})_2\text{H}(\text{PEt}_3)_4]^+$  exclusively, establishing that the dihydride acts as the source of the bridging ligands. The related  $[\text{Pt}_2(\mu\text{-H})_2\text{Ph}(\text{PEt}_3)_4]^+$  cation may be produced by reaction of the dihydride with  $[\text{PtPh}(\text{S})(\text{PEt}_3)_2]^+$  (14). Each of these dimers contains one 4-coordinate and one 5-coordinate platinum. In toluene solution,  $[\text{PtH}_2(\text{PEt}_3)_2]$  inserts  $\text{CO}_2$  to give *trans*- $[\text{Pt-H}(\text{OCHO})(\text{PEt}_3)_2]$ , whereas in acetonitrile or acetone solution,  $[\text{Pt}_2(\mu\text{-H})_2\text{H}(\text{PEt}_3)_4]\text{OCHO}$  is formed which, by dissociation into  $[\text{PtH}_2(\text{PEt}_3)_2]$  and  $[\text{PtH}(\text{OCHO})(\text{PEt}_3)_2]$ , catalyzes the decomposition of formic acid (13):



Related dimeric trihydrides containing various bidentate phosphorus ligands have been prepared by treatment of  $[\text{PtCl}_2\text{L}_2]$  with  $\text{AgBF}_4$ , fol-

lowed by reduction by  $\text{NaBH}_4$  (15). These complexes are fluxional down to  $-95^\circ\text{C}$ . The dppe (1,2-bis(diphenylphosphino)ethane) and dppf (1,1'-bis(diphenylphosphino)ferrocene) complexes have been characterized by X-ray or neutron diffraction methods (15–17). The molecular structure of the  $[\text{Pt}_2(\mu\text{-H})_2\text{H}(\text{dppe})_2]^+$  cation is shown in Fig. 1. The platinum–platinum distances of 2.728(1) and 2.722(1) Å for the dppe and dppf complexes are indicative of the presence of a Pt–Pt bond. Treatment of  $[\text{Pt}_2(\mu\text{-H})_2\text{H}(\text{L}_2)_2]^+$  with carbon monoxide results in the elimination of  $\text{H}_2$  and the formation of the platinum(I) dimer,  $[\text{Pt}_2(\mu\text{-H})(\mu\text{-CO})(\text{L}_2)_2]^+$  ( $\text{L}_2 = \text{dppe}, \text{dppf}$ ), which is also fluxional at ambient temperature (18,19). The loss of  $\text{H}_2$  has been proposed to occur by bridge opening and reductive elimination from a single platinum center (18). A related reaction of  $[\text{Pt}_2(\mu\text{-H})_2\text{H}(\text{dppe})_2]^+$  with styrene yields  $[\text{Pt}_2(\mu\text{-H})(\mu\text{-CHCH}_2\text{Ph})(\text{dppe})_2]^+$ , the first compound containing one alkylidene and one hydride bridging two platinum atoms (20).

The sensitivity of the product nuclearity to the reaction conditions is demonstrated by the following observations. When  $[\text{PtCl}_2(\text{dppe})]$  is treated with  $\text{LiBEt}_3\text{H}$  in THF solution at  $-40^\circ\text{C}$ ,  $[\text{PtH}_2(\text{dppe})]$  is formed, which loses  $\text{H}_2$  on warming to  $25^\circ\text{C}$  to generate a complex proposed to be the platinum (I) dimer,  $[\text{Pt}_2(\mu\text{-H})_2(\text{dppe})_2]$ . Addition of water or methanol converts this to  $[\text{Pt}_2(\mu\text{-H})_2\text{H}(\text{dppe})_2]^+$ , whereas purging the solution with a stream of moist nitrogen generates the  $[\text{Pt}_3(\mu_3\text{-H})\text{H}_2(\text{dppe})_3]^+$  cation (Scheme 2), which has been characterized by X-ray crystallography as its  $\text{BEt}_4^-$  salt (21).

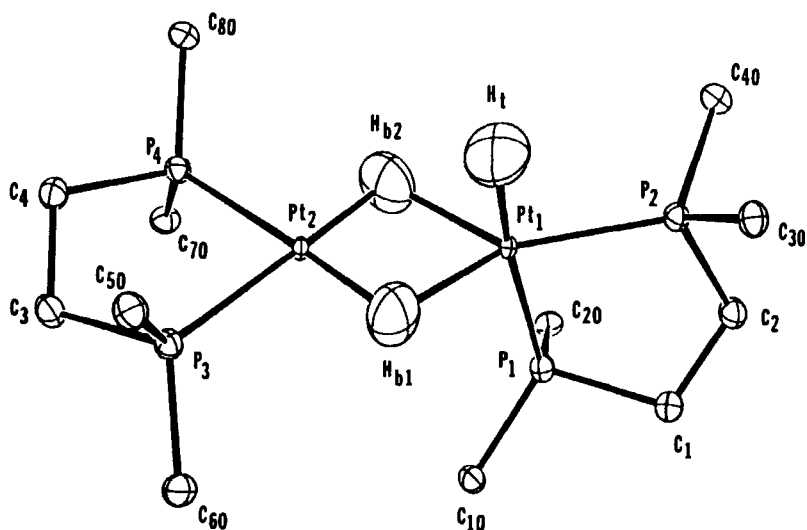
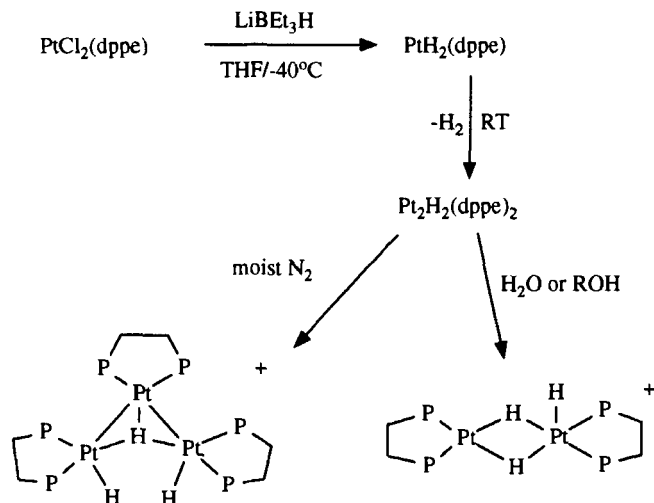


FIG. 1. Molecular structure of the  $[\text{Pt}_2\text{H}_3(\text{dppe})_2]^+$  cation, showing only the central core. [Reproduced with permission from Chiang *et al.* (16).]

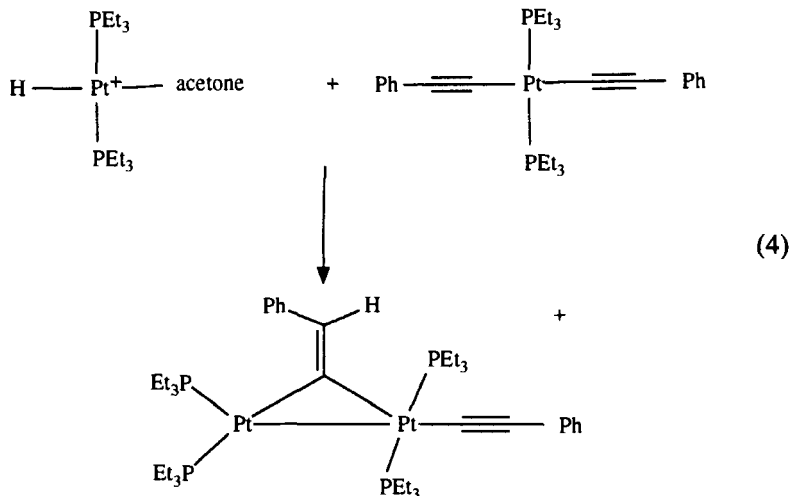


SCHEME 2. Syntheses of platinum hydride complexes containing dppe.

## IV

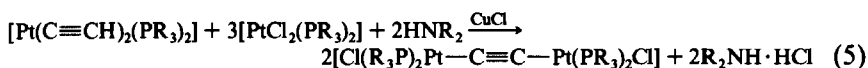
## COMPLEXES CONTAINING ORGANIC BRIDGING GROUPS

There are also compounds containing a variety of bridging organic groups. Reaction of *trans*-[PtH(PEt<sub>3</sub>)<sub>2</sub>(acetone)]BF<sub>4</sub> with *trans*-[Pt(C≡CPh)<sub>2</sub>(PEt<sub>3</sub>)<sub>2</sub>] yields the bridging vinylidene complex [(Et<sub>3</sub>P)<sub>2</sub>Pt(μ-C=CHPh)Pt(C≡CPh)(PEt<sub>3</sub>)<sub>2</sub>]BF<sub>4</sub>. This proceeds by formal addition of the Pt—H bond across the C≡C bond of one of the alkynyl groups.



Isomerization of the C=C double bond occurs in the presence of a free ligand by reversible coordination of the ligand to the CHPh carbon. The synthetic method has been extended to the reaction of  $[\text{PtCH}_3(\text{PEt}_3)_2(\text{acetone})]^+$  with  $[\text{Pt}(\text{C}\equiv\text{CPh})_2(\text{PEt}_3)_2]$ , where formal addition of  $\text{Pt}-\text{CH}_3$  across the alkynyl triple bond takes place (22). The structures of  $[(\text{Et}_3\text{P})\text{XPt}(\mu\text{-C}\equiv\text{CHPh})\text{PtY}(\text{PEt}_3)_2]$  ( $\text{X} = \text{PEt}_3^+$ ,  $\text{Cl}$ ,  $\text{I}$ ;  $\text{Y} = \text{C}\equiv\text{CPh}$  or  $\text{X} = \text{Y} = \text{Br}$ ) have been determined by X-ray diffraction (23,24), and correlations between the Pt-Pt distances and the  $^{31}\text{P}$  and  $^{195}\text{Pt}$  NMR parameters of the complexes have been made (25).

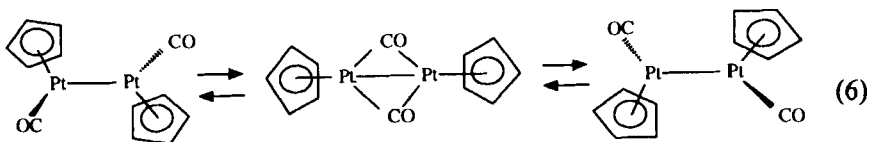
Complexes containing bridging alkynyls may be prepared from  $[\text{Pt}(\text{C}\equiv\text{CH})_2(\text{PR}_3)_2]$  and  $[\text{PtCl}_2(\text{PR}_3)_2]$  in the presence of a secondary amine and a copper(I) chloride catalyst:



Replacement of the terminal chlorides by iodides occurs readily, and the complex  $[\text{Pt}_2(\mu\text{-C}\equiv\text{C})\text{I}_2(\text{PMe}_3)_4]$  has been characterized by X-ray diffraction methods (26).

Complexes containing bridging pentafluorophenyl rings have been generated by reaction of  $[\text{Bu}_4\text{N}]_2[\text{PtCl}(\text{C}_6\text{F}_5)_3]$  with silver perchlorate. The initial product is  $[\text{Bu}_4\text{N}]_2[\text{Pt}_2(\mu\text{-C}_6\text{F}_5)_2(\text{C}_6\text{F}_5)_4]$ , but with additional  $\text{AgClO}_4$  a complex of formulation  $[\text{Bu}_4\text{N}]_2[\text{Pt}_2\text{Ag}(\text{C}_6\text{F}_5)_6(\text{Et}_2\text{O})]$  is obtained. The molecular structure of the latter reveals that the platinum atoms are bridged by two  $\text{C}_6\text{F}_5$  groups, each of which exhibits a short  $\text{Ag}-\text{F}$  contact (27).  $[\text{Bu}_4\text{N}]_2[\text{Pt}_2(\mu\text{-C}_6\text{F}_5)_2(\text{C}_6\text{F}_5)_4]$  may be prepared alternatively by reaction of  $[\text{Bu}_4\text{N}][\text{Pt}(\text{C}_6\text{F}_5)_4]$  with *cis*- $[\text{Pt}(\text{C}_6\text{F}_5)_2(\text{THF})_2]$  (28). Platinum (I) dimers containing perhalophenyl groups have been synthesized from *cis*- $[\text{Pt}(\text{C}_6\text{X}_5)_2\text{L}_2]$  ( $\text{X} = \text{F}$ ,  $\text{Cl}$ ;  $\text{L} = \text{CO}$ ,  $\text{CNR}$ ) and  $[\text{Pt}(\text{C}_2\text{H}_4)(\text{PPh}_3)_2]$ . These contain Pt-Pt bonds but do not contain bridging aryl groups. The Pt-Pt bond distance is 2.599(1) Å in the structurally characterized complex,  $[\text{Pt}_2(\text{C}_6\text{F}_5)_2(\text{CO})_2(\text{PPh}_3)_2]$  (29).

Treatment of Zeise's dimer with  $\text{Mg}(\text{C}_5\text{H}_5)_2$  yields  $[\text{Pt}(\eta^1\text{-C}_5\text{H}_5)(\eta^5\text{-C}_5\text{H}_5)(\text{C}_2\text{H}_4)]$  and a dimeric complex  $[\text{Pt}_2(\eta^5\text{-C}_5\text{H}_5)_2(\mu\text{-C}_{10}\text{H}_{10})]$ , in which two cyclopentadienyl units have combined to form the bridging ligand. The analogous reaction of  $[\text{Bu}_4\text{N}]_2[\text{Pt}_2\text{Cl}_4(\text{CO})_2]$  also produces a monomeric complex,  $[\text{Pt}(\eta^1\text{-C}_5\text{H}_5)(\eta^5\text{-C}_5\text{H}_5)(\text{CO})]$ , but, in addition, the metal-metal bonded species  $[\text{Pt}_2(\eta^5\text{-C}_5\text{H}_5)_2(\text{CO})_2]$  is obtained. This complex contains terminal carbonyl groups, but rapid exchange of CO ligands between the two platinum occurs, presumably by means of a  $[\text{Pt}_2(\eta^5\text{-C}_5\text{H}_5)_2(\mu\text{-CO})_2]$  intermediate (30):



Addition of  $\text{PhC}\equiv\text{CPh}$  causes displacement of one CO and formation of  $[\text{Pt}_2(\eta^5\text{-C}_5\text{H}_5)_2(\mu\text{-CO})(\mu\text{-PhC}\equiv\text{CPh})]$ . The reaction of  $\text{Bu}_4\text{N}[\text{PtCl}_3(\text{CO})]$  with 2 equivalents of  $(\text{C}_5\text{Me}_5)\text{MgCl}\cdot\text{THF}$  generates  $[\text{Pt}_2(\eta^5\text{-C}_5\text{Me}_5)_2(\text{CO})_2]$ , whose molecular structure reveals the presence of terminal CO ligands. Variable temperature  $^{13}\text{C}$  NMR spectroscopy indicates that rapid exchange of CO between platinum occurs in this case also (31).

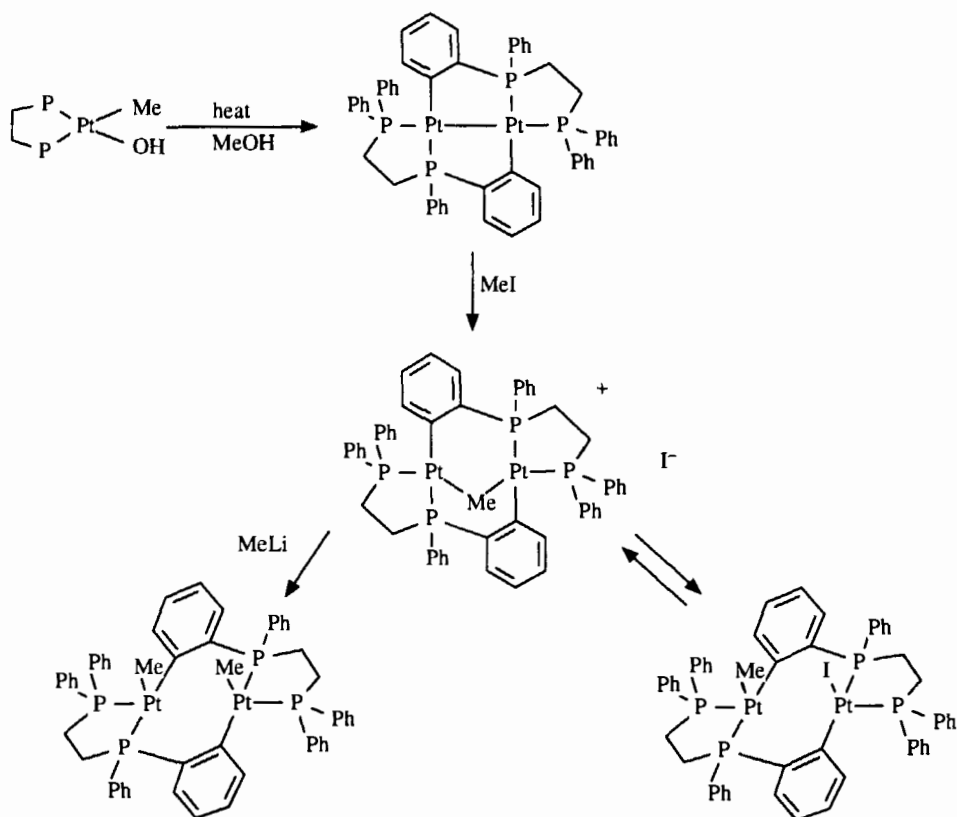
Palladium complexes containing bridging cyclopentadienyl or allyl moieties are well established. The preparation of such species has been extended to platinum. Addition of  $[\text{Pt}(\text{PPR}^i_3)_2]$  to  $[\text{Pt}(\eta^5\text{-C}_5\text{H}_5)(\eta^3\text{-C}_3\text{H}_4\text{Me})]$ , for example, yields the platinum(I) complex  $[\text{Pt}_2(\mu\text{-C}_5\text{H}_5)(\mu\text{-C}_3\text{H}_4\text{Me})(\text{PPR}^i_3)_2]$ . Treatment with  $\text{Me}_3\text{SiBr}$  results in loss of  $\text{C}_5\text{H}_5\text{SiMe}_3$  and formation of the bromide-bridged analog  $[\text{Pt}_2(\mu\text{-Br})(\mu\text{-C}_3\text{H}_4\text{Me})(\text{PPR}^i_3)_2]$ . The availability of the bromide allows further elaboration to heterometallic species by reaction with metal carbonyl anions. Thus, addition of  $\text{Na}[\text{M}(\eta^5\text{-C}_5\text{H}_5)(\text{CO})_3]$  ( $\text{M} = \text{Mo}, \text{W}$ ) produces  $[\text{Pt}_2(\mu\text{-C}_3\text{H}_4\text{Me})(\text{PPR}^i_3)_2(\mu_3\text{-CO})(\mu\text{-CO})_2\text{M}(\eta^5\text{-C}_5\text{H}_5)]$  (32).

## V

### COMPLEXES CONTAINING ORTHOMETALATED PHOSPHINE LIGANDS

It had been reported that heating a methanol solution of  $[\text{Pt}(\text{OH})\text{Me}(\text{dppe})]$  led to an air-stable compound of empirical formula  $[\text{Pt}(\text{dppe})]$  (33). It has since been shown that metalation at an ortho-position in one of the phenyl rings of dppe takes place to yield the metal-metal bonded platinum(I) complex  $[\text{Pt}_2(\mu\text{-C}_6\text{H}_4\text{PPh}(\text{CH}_2)_2\text{PPh}_2)_2]$  (Scheme 3). The Pt-Pt bond distance is 2.628(1) Å (34). Addition of methyl iodide produces a compound of formulation  $[\text{Pt}_2\text{Me}(\mu\text{-C}_6\text{H}_4\text{PPh}(\text{CH}_2)_2\text{PPh}_2)_2]\text{I}$ , in which the methyl group either occupies a bridging position or migrates rapidly between terminal positions on the two metal centers on the NMR time scale. Further treatment with  $\text{CNBu}^t$  and  $\text{NaBF}_4$  yields  $[\text{Pt}_2\text{Me}(\text{CNBu}^t)(\mu\text{-C}_6\text{H}_4\text{PPh}(\text{CH}_2)_2\text{PPh}_2)_2]\text{BF}_4$ , whereas reaction with  $\text{MeLi}$  gives the dimethyl complex  $[\text{Pt}_2\text{Me}_2(\mu\text{-C}_6\text{H}_4\text{PPh}(\text{CH}_2)_2\text{PPh}_2)_2]$ . The latter contains a terminal methyl group on each platinum and no metal-metal bond (35). The formation of  $[\text{Pt}_2(\mu\text{-C}_6\text{H}_4\text{PPh}(\text{CH}_2)_2\text{PPh}_2)_2]$  contrasts with the reaction of  $[\text{Pt}(\text{OSO}_2\text{CF}_3)_2(\text{dppe})]$  with carbon monoxide in which reduc-





SCHEME 3. Complexes containing metalated dppe ligands.

tion to platinum(I) occurs, but this is not accompanied by metalation of dppe. Instead, the product  $[\text{Pt}_2(\text{CO})_2(\text{dppe})_2]^{2+}$  exhibits an unsupported metal-metal bond (36). Reduction of  $[\text{Pd}(\text{OSO}_2\text{CF}_3)_2(\text{dppp})]$  with  $\text{H}_2$  yields a palladium(I) species  $[\text{Pd}_2(\text{dppp})_2]$ , composed of two  $\text{Pd}(\text{dppp})$  units in which there is a weak interaction between one of the phosphorus atoms and the second palladium. Again, metalation of the dppp ligand does not occur (37). In contrast,  $\text{NaBH}_4$  reduction of  $[\text{PtCl}_2(\text{dppp})]$  has been reported to produce  $[\text{Pt}_2(\mu\text{-C}_6\text{H}_4\text{PPh}(\text{CH}_2)_3\text{PPh}_2)_2]$ , albeit in low yield (38), a compound that has also been obtained by heating  $[\text{PtClMe}(\text{dppp})]$  (39).  $[\text{Pt}_2(\mu\text{-C}_6\text{H}_4\text{PPh}(\text{CH}_2)_3\text{PPh}_2)_2]$  reacts with  $[\text{Au}(\text{PPh}_3)\text{BF}_4]$ ,  $\text{Ag}(\text{O}_2\text{CCF}_3)$ ,  $\text{HgCl}_2$ ,  $\text{Hg}(\text{O}_2\text{CCF}_3)_2$ , or  $\text{I}_2$  to generate species of the form  $[\text{Pt}_2(\mu\text{-Z})(\mu\text{-C}_6\text{H}_4\text{PPh}(\text{CH}_2)_3\text{PPh}_2)_2]^{n+}$  ( $n = 0, 1$ ). The species with  $\text{Z} = \text{Au}(\text{PPh}_3)^+$  and  $\text{Hg}(\text{O}_2\text{CCF}_3)_2$  have been characterized by X-ray crystallography (Fig. 2) (38,39), and their Pt-Pt bond distances are

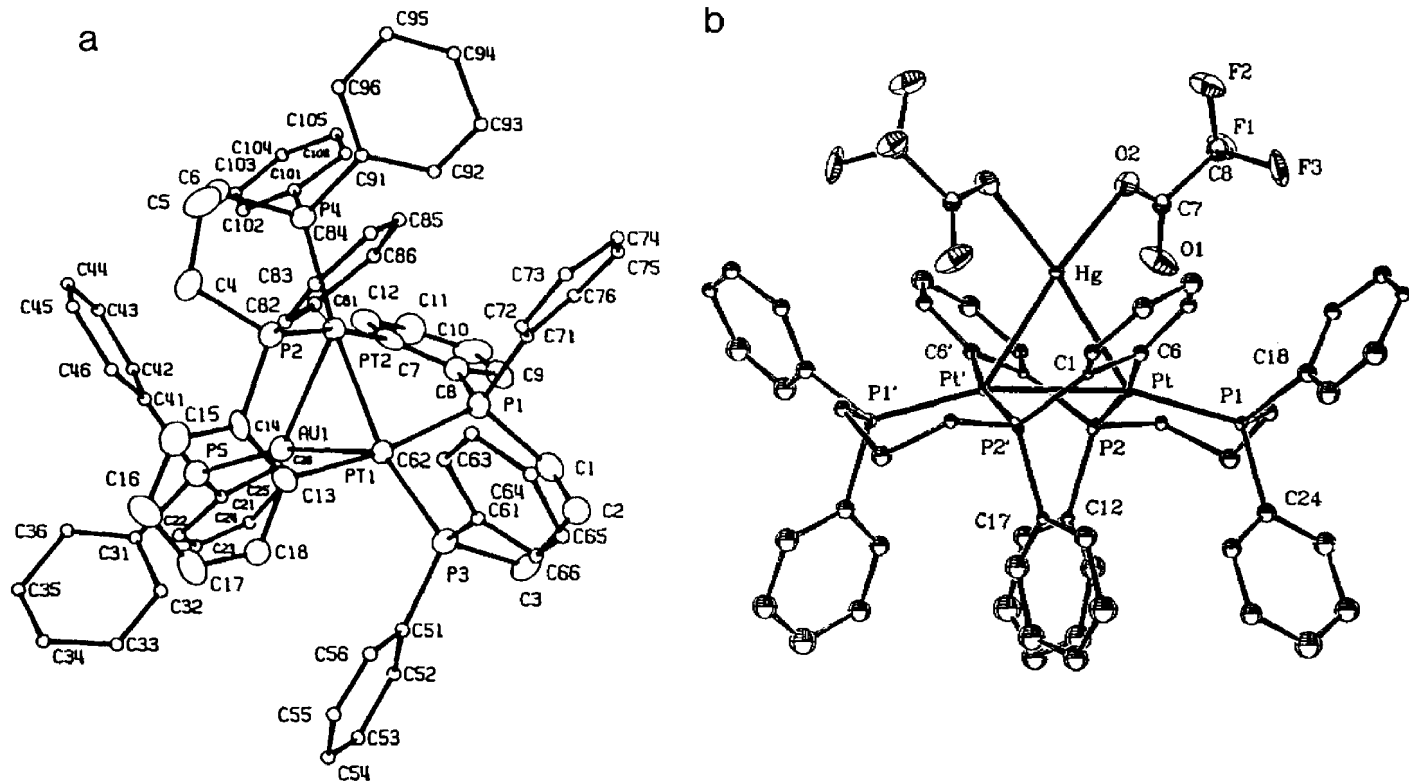
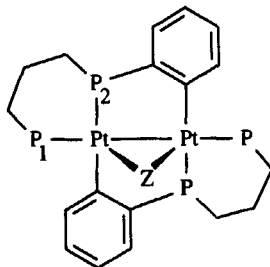


FIG. 2. Molecular structures of  $[\text{Pt}_2(\mu\text{-Z})(\mu\text{-C}_6\text{H}_4\text{PPh}(\text{CH}_2)_3\text{PPh}_2)_2]$ . (a)  $\text{Z} = \text{Au}(\text{PPh}_3)^+$ ; (b)  $\text{Z} = \text{Hg}(\text{O}_2\text{CCF}_3)_2$ . [Reproduced with permission from Bennett *et al.* (38) and Dekker *et al.* (39).]

2.703(1) and 2.7608(7) Å, respectively. These distances indicate that the Pt–Pt bond is not broken on addition of these bridging moieties to  $[\text{Pt}_2(\mu\text{-C}_6\text{H}_4\text{PPh}(\text{CH}_2)_3\text{PPh}_2)_2]$ . The longer Pt–Pt separation in  $[\text{Pt}_2(\mu\text{-Hg}(\text{O}_2\text{CCF}_3)_2)(\mu\text{-C}_6\text{H}_4\text{PPh}(\text{CH}_2)_3\text{PPh}_2)_2]$  is indicative of a weaker bond in this case. There is a good correlation between the Pt–Pt bond strength and the  $^1\text{J}(\text{Pt},\text{P})$  coupling *trans* to the Pt–Pt bond and the  $^2\text{J}(\text{Pt},\text{P})$  couplings (Table I). The two-bond couplings are small and the one-bond coupling is large in the iodide-bridged complex in which there is no formal Pt–Pt bond (39). The relationships between Pt–Pt distances and NMR coupling constants are discussed for dppm-bridged dimers later.

A complex related to those containing metalated diphosphines is obtained from the reaction of  $[\text{Pt}(\text{o-C}_6\text{H}_4\text{PPh}_2)_2]$  with  $[\text{Pt}(\text{PPh}_3)_3]$ . The Pt–Pt bond distance in this platinum(I) dimer,  $[\text{Pt}_2(\mu\text{-C}_6\text{H}_4\text{PPh}_2)_2(\text{PPh}_3)_2]$ , in which the  $\text{PPh}_3$  ligands occupy terminal sites, is 2.630(1) Å. Oxidative addition of iodine generates the “A-frame” complex  $[\text{Pt}_2(\mu\text{-I})(\mu\text{-C}_6\text{H}_4\text{PPh}_2)_2(\text{PPh}_3)_2]\text{I}$ , with a concomitant lengthening of the Pt–Pt distance to 2.931(2) Å (40).

TABLE I  
 $^{195}\text{Pt}$ – $^{31}\text{P}$  COUPLING CONSTANTS<sup>a</sup> IN  
COMPLEXES OF THE TYPE



Z	$^1\text{J}(\text{Pt},\text{P}_1)$	$^2\text{J}(\text{Pt}',\text{P}_1)$	$^2\text{J}(\text{Pt}',\text{P}_2)$
—	1775	996	–143
$\text{Ag}(\text{O}_2\text{CCF}_3)$	2209	767	–139
$\text{Au}(\text{PPh}_3)^+$	2586	538	–126
$\text{HgCl}_2$	3066	312	–174
$\text{Hg}(\text{O}_2\text{CCF}_3)_2$	3353	239	–126
$\text{I}^+$	3719	73	0

<sup>a</sup> Data taken from Ref. (39).

## VI

## COMPLEXES BRIDGED BY dppm OR RELATED LIGANDS

The chemistry of complexes containing dppm or related bifunctional ligands has flourished over the last 15 years. A number of articles reviewing this area have appeared (41–44), and a report describing the development of tripalladium and triplatinum systems bridged by dppm ligands has been published recently (45). We concentrate on diplatinum species here.

Dppm and related ligands have been used to support dimeric complexes containing platinum in the formal oxidation states 0, I, II, III, or IV. The zerovalent complex  $[\text{Pt}_2(\mu\text{-dppm})_3]$ , prepared by reaction of  $[\text{Pt}(\text{PPh}_3)_4]$  with excess dppm or by  $\text{NaBH}_4$  reduction of  $[\text{PtCl}_2(\text{dppm})]$  in the presence of dppm, adopts a “manxane” structure containing no formal Pt–Pt bond (Fig. 3). The Pt–Pt distance is 3.023(1) Å (46). Its primary mode of reaction is by oxidative addition to give platinum(I) or platinum(II) species. The reaction of  $[\text{Pt}(\text{PPh}_3)_3]$  with dmpm (bis(dimethylphosphino)methane) produces  $[\text{Pt}_2(\mu\text{-dmpm})_3]$ ,  $[\text{Pt}_2(\mu\text{-dmpm})_3(\text{PPh}_3)]$ , and  $[\text{Pt}_2(\mu\text{-dmpm})_3(\text{PPh}_3)_2]$ , whereas with depm (bis(diethylphosphino)-

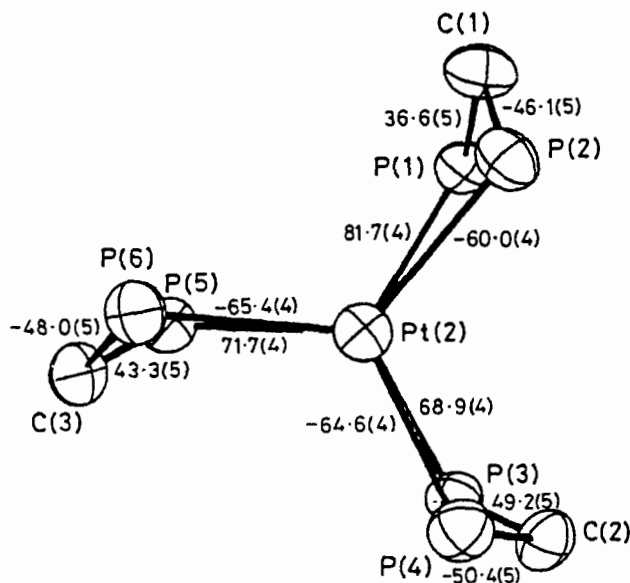
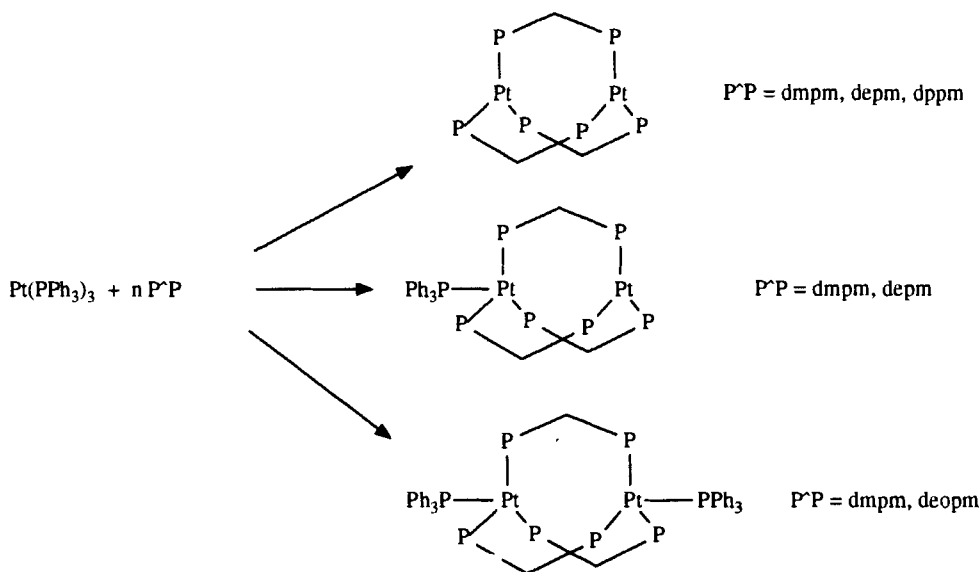


FIG. 3. Molecular structure of  $[\text{Pt}_2(\mu\text{-dppm})_3]$  illustrating the “manxane” structure. [Reproduced with permission from Manojlovic-Muir *et al.* (46).]

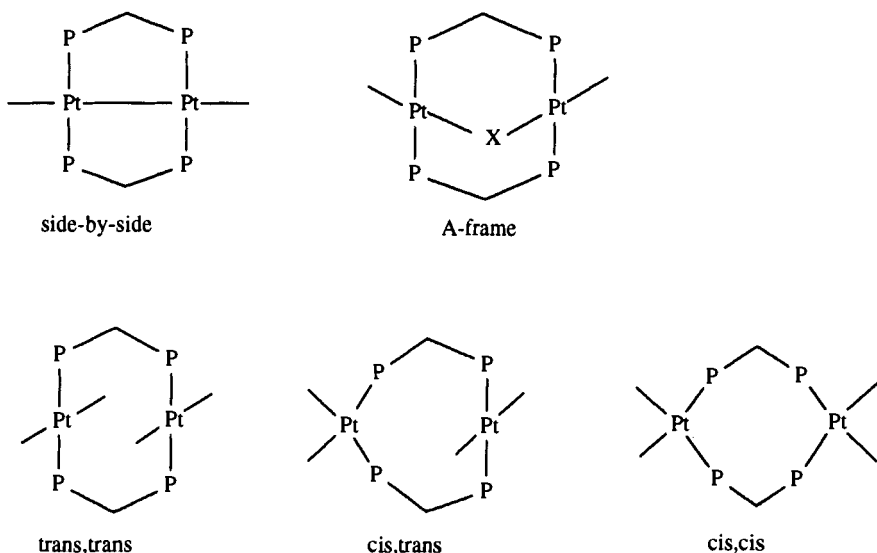
methane,  $[\text{Pt}_2(\mu\text{-depm})_3]$  and  $[\text{Pt}_2(\mu\text{-depm})_3(\text{PPh}_3)]$  are produced. The corresponding reaction of deopm (bis(diethoxyphosphino)methane) generates  $[\text{Pt}_2(\mu\text{-deopm})_3(\text{PPh}_3)_2]$  only (Scheme 4) (47). The smaller steric demands of dmpm, depm, and deopm allow the formation of complexes with four ligands on one or both platinum.

Platinum(I) dimers usually adopt a side-by-side geometry, which is necessary to accommodate the Pt–Pt bond present in such species. For platinum(II), several different geometries are possible. Those containing a bridging moiety, such as H,  $\text{CH}_2$ , or S, adopt an A-frame structure. Such complexes may be formed by addition of the bridging fragment to a side-by-side complex. In platinum(II) complexes containing no bridging ligands other than dppm itself, the complex may adopt a *trans,trans* (or face-to-face), *cis,trans*, or *cis,cis* orientation. The various geometries adopted by platinum(I) or platinum(II) dppm-bridged dimers are depicted in Scheme 5.

The prototypic dppm-bridged platinum(I) dimer is  $[\text{Pt}_2\text{Cl}_2(\mu\text{-dppm})_2]$ . This is prepared by reduction of  $[\text{PtCl}_2(\text{dppm})]$  with  $\text{NaBH}_4$  in methanol, followed by addition of HCl in benzene. Halide exchange may be achieved by treatment with  $\text{Et}_4\text{NBr}$  or NaI. The  $^{31}\text{P}\{^1\text{H}\}$  NMR spectrum of each complex exhibits a single central resonance with complex satellites due to coupling with  $^{195}\text{Pt}$ . For the chloro-complex, these may be analyzed in



SCHEME 4. Platinum(0) complexes containing various diphosphine ligands.



SCHEME 5. Structures of complexes containing bridging dppm or related ligands.

terms of two Pt–P couplings ( $^1J(\text{Pt},\text{P})$  2936 Hz and  $^2J(\text{Pt},\text{P})$  – 136 Hz) and two P–P couplings ( $^2J(\text{P},\text{P})$  63 Hz and  $^3J(\text{P},\text{P})$  26 Hz) (48). The molecular structure of the chloro-complex reveals that it has a side-by-side structure with terminal chlorides and an essentially planar  $\text{Pt}_2\text{Cl}_2\text{P}_4$  unit and a Pt–Pt distance of 2.651(1) Å (49). A mixed palladium–platinum analog has been prepared by treatment of  $[\text{Pd}(\text{PPh}_3)_4]$  with dppm in the presence of  $[\text{PtCl}_2(\text{Bu}^t\text{CN})_2]$  (50). Related metal–metal bonded species include  $[\text{Pt}_2\text{Cl}(\text{C}_6\text{F}_5)(\mu\text{-dppm})_2]$ , prepared by reaction of  $[\text{PtCl}(\text{C}_6\text{F}_5)(\eta^1\text{-dppm})_2]$  with  $[\text{Pt}(\text{cod})_2]$  (51), and  $[\text{Pt}_2(\text{C}\equiv\text{CPh})_2(\mu\text{-dppm})_2]$  which is formed from  $[\text{PtCl}_2(\text{dppm})]$  and  $\text{PhC}\equiv\text{CH}$  in the presence of hydrazine hydrate (52).

$[\text{Pt}_2\text{Cl}_2(\mu\text{-dppm})_2]$  undergoes substitution of the terminal chlorides by a range of neutral ligands in the presence of  $\text{NH}_4\text{PF}_6$  to produce complexes of the type  $[\text{Pt}_2\text{L}_2(\mu\text{-dppm})_2][\text{PF}_6]_2$  ( $\text{L} = \text{PMe}_2\text{Ph}$ ,  $\text{PMePh}_2$ ,  $\text{PPh}_3$ ,  $\text{NH}_3$ ,  $\text{py}$ ). The  $\text{NH}_3$  ligands can be displaced from  $[\text{Pt}_2(\text{NH}_3)_2(\mu\text{-dppm})_2]^{2+}$  by CO, and treatment of  $[\text{Pt}_2(\text{py})_2(\mu\text{-dppm})_2]^{2+}$  with CO produces the unsymmetrical dimer  $[\text{Pt}_2(\text{py})(\text{CO})(\mu\text{-dppm})_2]^{2+}$  (53). Reaction of  $[\text{Pt}_2\text{Cl}_2(\mu\text{-dppm})_2]$  with CO yields  $[\text{Pt}_2\text{Cl}_2(\mu\text{-CO})(\mu\text{-dppm})_2]$ , characterized by an infrared band at  $1638\text{ cm}^{-1}$ . This isomerizes in polar solvents to the  $[\text{Pt}_2\text{Cl}(\text{CO})(\mu\text{-dppm})_2]^+$  cation, which could be isolated as its  $\text{PF}_6^-$  salt (54). The molecular structure of  $[\text{Pt}_2\text{Cl}(\text{CO})(\mu\text{-dppm})_2]\text{PF}_6$  reveals that it contains a terminal carbonyl ligand and it has a Pt–Pt bond distance of 2.620(1) Å (55), shorter than that found in  $[\text{Pt}_2\text{Cl}_2(\mu\text{-dppm})_2]$ .

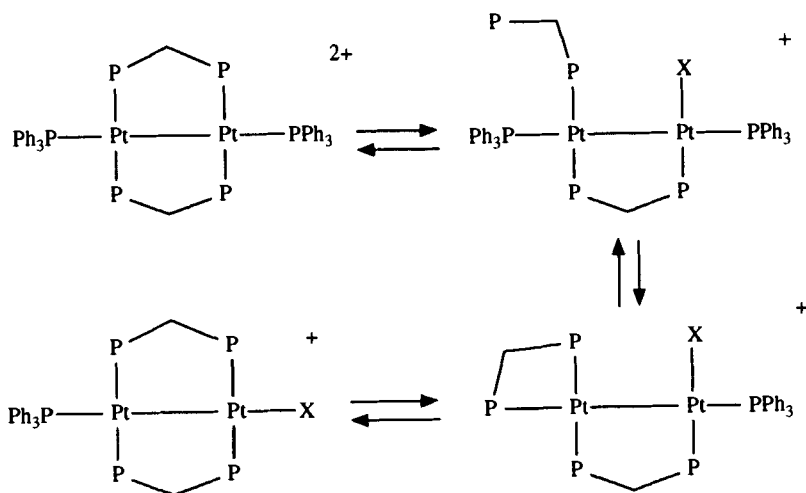
Substitution of one terminal chloride in  $[\text{Pt}_2\text{Cl}_2(\mu\text{-dppm})_2]$  by  $\text{PPh}_3$  produces the unsymmetrical side-by-side complex  $[\text{Pt}_2\text{Cl}(\text{PPh}_3)(\mu\text{-dppm})_2]\text{PF}_6$ . Its molecular structure exhibits some distortion from square-planar geometry at the  $\text{PPh}_3$ -ligated platinum. This distortion alleviates repulsive steric interactions between the  $\text{PPh}_3$  and dppm phenyl substituents, but it also causes a significant increase in the activation energy for the exchange between axial and equatorial hydrogen positions on the  $\text{Pt}_2(\mu\text{-dppm})_2$  ring (56). This structure is less well refined, but the Pt–Pt distance is slightly longer than in the carbonyl analog. The Pt–Pt bond distances found for side-by-side, dppm-bridged platinum(I) complexes are given in Table II.

The reaction of  $[\text{Pt}_2\text{Cl}_2(\mu\text{-dppm})_2]$  with  $\text{PPh}_3$  in  $\text{CH}_2\text{Cl}_2$  solution follows second-order kinetics, with  $k = 15.2 \pm 0.7 \text{ M}^{-1} \text{ s}^{-1}$  at  $25^\circ\text{C}$ . The sole product is  $[\text{Pt}_2\text{Cl}(\text{PPh}_3)(\mu\text{-dppm})_2]\text{Cl}$  in this solvent, but in methanol  $[\text{Pt}_2(\text{PPh}_3)_2(\mu\text{-dppm})_2]\text{Cl}_2$  may be formed also. The reaction of  $[\text{Pt}_2(\text{PPh}_3)_2(\mu\text{-dppm})_2][\text{PF}_6]_2$  with  $\text{Cl}^-$  in  $\text{CH}_2\text{Cl}_2$  solution produces  $[\text{Pt}_2\text{Cl}(\text{PPh}_3)(\mu\text{-dppm})_2]^+$ . In the presence of noncoordinating anions, such as perchlorate, the reaction proceeds by an unusual rate-limiting dissociation of  $\text{PPh}_3$ , which is attributed to the high *trans*-influence of the Pt–Pt bond. In the absence of such anions, the reaction proceeds in three steps, and an intermediate species formulated as  $[(\eta^2\text{-dppm})\text{Pt}(\mu\text{-dppm})\text{-PtCl}(\text{PPh}_3)]^+$ , containing one bridging and one chelated dppm, has been detected at low temperature (Scheme 6) (60).

Reactions of  $[\text{Pt}_2\text{Cl}_2(\mu\text{-dppm})_2]$  or  $[\text{PtCl}_2(\text{dppm})]$  with  $\text{NaBH}_3\text{CN}$  or  $\text{NaBH}_2(\text{CN})_2$  produce a series of complexes of the type  $[\text{Pt}_2\text{X}_2(\mu\text{-dppm})_2]$  ( $\text{X} = \text{NCBH}_3$ ,  $\text{NCBH}_2\text{CN}$ ,  $\text{CNBH}_2\text{CN}$ ,  $\text{CNBH}_3$ ,  $\text{CN}$ ). The two N-bonded species are formed as the kinetic products, but they isomerize over several days to their thermodynamically favored C-bonded analogs. Each of the C-bonded complexes, including the cyano-derivative, has been characterized by X-ray diffraction (Table II) (58).

TABLE II  
PLATINUM–PLATINUM BOND DISTANCES IN  
dppm-BRIDGED PLATINUM(I) DIMERS

Complex	Pt–Pt (Å)	Reference
$[\text{Pt}_2\text{Cl}(\text{CO})(\text{dppm})_2]^+$	2.620(1)	(55)
$[\text{Pt}_2(\text{CO})_2(\text{dppm})_2]^{2+}$	2.642(1)	(57)
$[\text{Pt}_2\text{Cl}_2(\text{dppm})_2]$	2.651(1)	(49)
$[\text{Pt}_2\text{Cl}(\text{PPh}_3)(\text{dppm})_2]^+$	2.665(2)	(56)
$[\text{Pt}_2(\text{CNBH}_2\text{CN})(\text{dppm})_2]$	2.665(1)	(58)
$[\text{Pt}_2(\text{CNBH}_3)_2(\text{dppm})_2]$	2.667(1)	(58)
$[\text{Pt}_2(\text{CN})_2(\text{dppm})_2]$	2.704(1)	(58)
$[\text{Pt}_2\text{H}(\eta^1\text{-dppm})(\text{dppm})_2]^+$	2.770(2)	(59)



SCHEME 6. Proposed mechanism for the substitution of  $\text{PPh}_3$  by chloride in  $[\text{Pt}_2(\text{PPh}_3)_2(\text{dppm})_2]^{2+}$ .

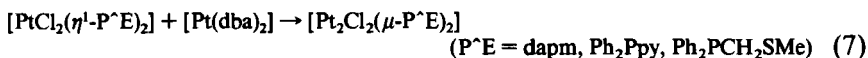
Another type of reaction undergone by  $[\text{Pt}_2\text{Cl}_2(\mu\text{-dppm})_2]$  is insertion into the Pt–Pt bond to give A-frame compounds. As mentioned above, reaction with CO produces  $[\text{Pt}_2\text{Cl}_2(\mu\text{-CO})(\mu\text{-dppm})_2]$ , but this isomerizes to  $[\text{Pt}_2\text{Cl}(\text{CO})(\mu\text{-dppm})_2]\text{Cl}$  (54). The analogous reaction with *p*-tolylisocyanide produces  $[\text{Pt}_2\text{Cl}_2(\mu\text{-CNR})(\mu\text{-dppm})_2]$ ,  $[\text{Pt}_2\text{Cl}(\text{CNR})(\mu\text{-dppm})_2]^+$ ,  $[\text{Pt}_2(\text{CNR})_2(\mu\text{-dppm})_2]^{2+}$ , or  $[\text{Pt}_2(\mu\text{-CNR})(\text{CNR})_2(\mu\text{-dppm})_2]^{2+}$  ( $\text{R} = p\text{-tolyl}$ ), depending on the reaction conditions. The bridging isocyanide complexes may be protonated or alkylated to give bridging aminocarbene species (61). Similarly, insertion of  $\text{CS}_2$  yields  $[\text{Pt}_2\text{Cl}_2(\mu\text{-}\eta^2\text{-C(S)S})(\mu\text{-dppm})_2]$ , which can be methylated with  $\text{MeOSO}_2\text{CF}_3$  to give  $[\text{Pt}_2\text{Cl}_2(\mu\text{-}\eta^2\text{-C(SMe)S})(\mu\text{-dppm})_2]^+$  (62). Treatment of  $[\text{Pt}_2\text{Cl}_2(\mu\text{-dppm})_2]$  with  $\text{NO}^+\text{BF}_4^-$  produces a nonfluxional, symmetrical A-frame complex  $[\text{Pt}_2\text{Cl}_2(\mu\text{-NO})(\mu\text{-dppm})_2]\text{BF}_4$  (63). Transition metal fragments also add to the Pt–Pt bond. Thus, addition of  $\text{Au}(\text{NO}_3)\text{L}$  or  $\text{AuCl}(\text{SMe})$  produces  $[\text{Pt}_2\text{Cl}_2(\mu\text{-AuL})(\mu\text{-dppm})_2]^+$  or  $[\text{Pt}_2\text{Cl}_2(\mu\text{-AuCl})(\mu\text{-dppm})_2]$  (64), whereas addition of  $\text{HgCl}_2$  generates  $[\text{Pt}_2\text{Cl}_2(\mu\text{-HgCl}_2)(\mu\text{-dppm})_2]$  (65).

The reactions of dppm-bridged platinum(I) dimers with  $\text{CH}_2\text{N}_2$ , CO,  $\text{S}_8$ , or  $\text{SO}_2$  have been studied in some detail. When it was reported in 1979, the reaction of  $[\text{Pt}_2\text{Cl}_2(\mu\text{-dppm})_2]$  with  $\text{CH}_2\text{N}_2$  represented the first example of simple methylene insertion into a metal–metal bond (66). The reactions of  $[\text{Pt}_2\text{X}_2(\mu\text{-dppm})_2]$  ( $\text{X} = \text{Cl}, \text{Br}, \text{I}$ ) or  $[\text{Pt}_2\text{L}_2(\mu\text{-dppm})_2]^{2+}$  ( $\text{L} = \text{CO}, \text{py}, \text{NH}_3$ ) with  $\text{CH}_2\text{N}_2$  exhibit second-order rate laws, the reactions being faster for the neutral complexes. The py and  $\text{NH}_3$  complexes



react particularly slowly. The rate constants are characterized by  $\Delta S^\ddagger$  values close to zero, and the rate-determining step is proposed to be transfer of an electron pair from the Pt–Pt bond to the  $\text{CH}_2$  group of diazomethane (67). Treatment of  $[\text{Pt}_2\text{Cl}_2(\mu\text{-dppm})_2]$  with sulfur produces  $[\text{Pt}_2\text{Cl}_2(\mu\text{-S})(\mu\text{-dppm})_2]$  by a second-order process; with a deficiency of  $\text{S}_8$  nearly all eight sulfur atoms are incorporated into the product. Replacement of the terminal chlorides by py,  $\text{NH}_3$ , or CO again greatly reduces the reaction rates, and all the reactions are accelerated by trace amounts of salts such as  $\text{R}_4\text{N}^+\text{X}^-$ . The reaction of  $[\text{Pt}_2\text{Cl}_2(\mu\text{-dppm})_2]$  with  $\text{SO}_2$  has been shown to proceed by preassociation of the reactants to form a loose charge transfer complex. The reactions with  $\text{S}_8$  and  $\text{SO}_2$  are both believed to involve substantial Pt–Pt bond breaking in the activated complex (68). The reactions of the charged complex  $[\text{Pt}_2(\text{PPh}_3)_2(\mu\text{-dppm})_2]^{2+}$  with  $\text{CH}_2\text{N}_2$ , CO,  $\text{S}_8$ , or  $\text{SO}_2$  are believed to occur via a common intermediate. This is most likely to be a species with a dangling dppm ligand, formed by Pt–P bond scission, which is attacked by the substrate leading to A-frame formation (69).

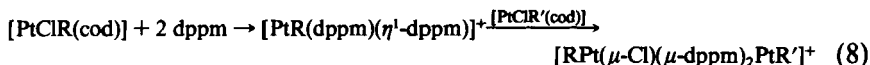
Platinum(I) dimers bridged by dpam [bis(diphenylarsino)methane] and a number of unsymmetrical ligands have been prepared also. Treatment of  $[\text{PtCl}_2(\text{dpam})]$  with dpam yields *trans*- $[\text{PtCl}_2(\eta^1\text{-dpam})_2]$ , and subsequent addition of  $[\text{Pt}_2(\mu\text{-OMe})_2(\text{C}_8\text{H}_{12}\text{OMe})_2]$  gives  $[\text{Pt}_2\text{Cl}_2(\mu\text{-dpam})_2]$ . This undergoes insertion of CO to produce  $[\text{Pt}_2\text{Cl}_2(\mu\text{-CO})(\mu\text{-dpam})_2]$  (70). The unsymmetrical ligands dapm ( $\text{Ph}_2\text{AsCH}_2\text{PPh}_2$ ) (71),  $\text{Ph}_2\text{Ppy}$  [2-(diphenylphosphino)pyridine] (72), or  $\text{Ph}_2\text{PCH}_2\text{SMe}$  (73) each form head-to-tail platinum(I) complexes according to



$[\text{Pt}_2\text{Cl}_2(\mu\text{-dapm})_2]$  reacts with CO to generate  $[\text{Pt}_2\text{Cl}_2(\mu\text{-CO})(\mu\text{-dapm})_2]$ , whereas addition of carbon monoxide to  $[\text{Pt}_2\text{Cl}_2(\text{Ph}_2\text{PCH}_2\text{SMe})_2]$  causes cleavage of the dimeric unit and formation of *cis*- $[\text{PtCl}_2(\eta^1\text{-Ph}_2\text{PCH}_2\text{SMe})_2]$  and *cis*- $[\text{PtCl}_2(\text{CO})(\eta^1\text{-Ph}_2\text{PCH}_2\text{SMe})]$ .

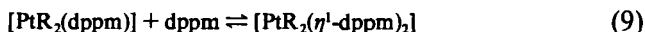
Alternative routes to dppm-bridged A-frame complexes are available. When  $[\text{PtMe}_2(\text{dppm})]$  was treated with 1 equivalent of HCl, it was found that  $[\text{Pt}_2\text{Me}_2(\mu\text{-Cl})(\mu\text{-dppm})_2]\text{Cl}$  and an oligomeric (probably dimeric) form of  $[\text{PtClMe}(\text{dppm})]$  were formed in addition to the expected monomeric  $[\text{PtClMe}(\text{dppm})]$ . The monomer can be prepared cleanly by addition of 1 equivalent of acetyl chloride in  $\text{CH}_2\text{Cl}_2/\text{MeOH}$ , but treatment of  $[\text{PtMe}_2(\text{dppm})]$  with hydrogen chloride in benzene results in precipitation of  $[\text{Pt}_2\text{Me}_2(\mu\text{-Cl})(\mu\text{-dppm})_2]\text{Cl}$  (74). The reactions of  $[\text{PtClR}(\text{cod})]$  with dppm likewise produce mixtures of  $[\text{PtClR}(\text{dppm})]$  and  $[\text{Pt}_2\text{R}_2(\mu\text{-Cl})(\mu\text{-dppm})_2]\text{Cl}$  ( $\text{R} = \text{Me}, \text{Ph}$ ), whereas when  $\text{R} = \text{COPh}$ , only the dimer is

formed (75). Unsymmetrical A-frame complexes can be formed by reaction of  $[\text{PtClR}(\text{cod})]$  with 2 equivalents of dppm, followed by  $[\text{PtClR}'(\text{cod})]$  (76):

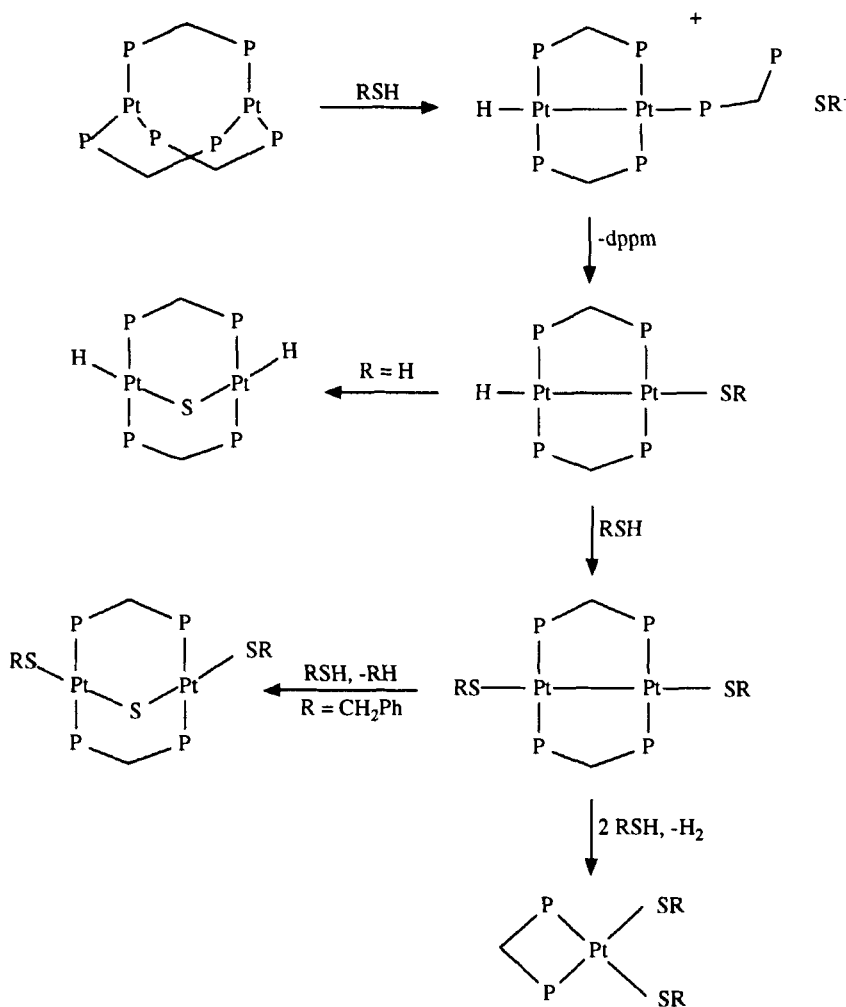


Reaction of  $[\text{Pt}_2(\text{dppm})_3]$  with  $\text{H}_2\text{S}$  leads to  $[\text{Pt}_2\text{H}_2(\mu\text{-S})(\mu\text{-dppm})_2]$ , in addition to  $[\text{Pt}_3\text{H}(\mu_3\text{-S})(\mu\text{-dppm})_3]^+$ , whereas with excess  $\text{RSH}$ , intermediate species of the form  $[\text{Pt}_2\text{H}(\text{SR})(\mu\text{-dppm})_2]$  or  $[\text{Pt}_2(\text{SR})_2(\mu\text{-dppm})_2]$  could be detected prior to their conversion to monomeric compounds  $[\text{Pt}(\text{SR})_2(\text{dppm})]$  (Scheme 7). The reaction with  $\text{PhCH}_2\text{SH}$  results in  $[\text{Pt}_2(\text{SCH}_2\text{Ph})_2(\mu\text{-S})(\mu\text{-dppm})_2]$  as the major product, whose structure has been established by X-ray diffraction (77). The reaction of  $[\text{PtCl}_2(\text{dppm})]$  with  $\text{LiC}\equiv\text{CBu}^t$  in THF solution produces  $[\text{Pt}_2(\text{C}\equiv\text{CBu}^t)_2(\mu\text{-}\eta^1, \eta^2\text{-C}\equiv\text{CBu}^t)(\mu\text{-dppm})_2]\text{Cl}$ . The solid-state structure of the complex, as its tetraphenylborate salt, reveals the presence of an unsymmetrically bridging ( $\eta^1, \eta^2$ -bonded) alkynyl ligand. The cation is fluxional in solution, and this behavior is attributed to rapid switching of the alkynyl group from one platinum to the other (78).

A versatile approach to dppm-bridged platinum(II) species is via  $\eta^1$ -dppm intermediates. A series of equilibrium constants has been established for the process



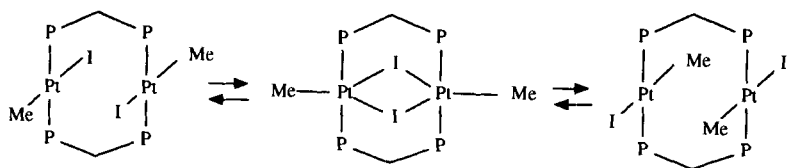
The equilibrium is established rapidly where  $\text{R} = \text{Me}$ , but the reactions take several days to reach equilibrium when  $\text{R} = o\text{-tolyl}$ ,  $o\text{-MeOC}_6\text{H}_4$ , mesityl, or 1-naphthyl. The value of  $K$  is greatest for the methyl case and, as expected, the values of  $K$  increase as the temperature is lowered (79). Reaction of  $[\text{Pt}(o\text{-tolyl})_2(\eta^1\text{-dppm})_2]$  with  $[\text{PtMe}_2(\text{cod})]$ , for example, yields *cis,cis*- $[(o\text{-tolyl})_2\text{Pt}(\mu\text{-dppm})_2\text{PtMe}_2]$ . The presence of the ortho-methyl groups results in formation of syn- and anti-isomers, which equilibrate over a few hours in  $\text{CDCl}_3$  solution. The minor (syn) isomer crystallizes preferentially, and its structure has been established by X-ray diffraction (80). Refluxing *trans*- $[\text{Pt}(\text{C}\equiv\text{CR})_2(\eta^1\text{-dppm})_2]$ , or treating  $[\text{PtCl}_2(\text{dppm})]$  with 2 equivalents of  $\text{LiC}\equiv\text{CR}$ , generates *trans,trans*- $[\text{Pt}_2(\text{C}\equiv\text{CR})_4(\mu\text{-dppm})_2]$  ( $\text{R} = \text{Ph}$ , *p*-tolyl) (81), although *cis,cis*; *cis,trans*; and *trans,trans* isomers of  $[\text{Pt}_2(\text{C}\equiv\text{CR})_4(\mu\text{-dppm})_2]$  ( $\text{R} = \text{Me}$ ,  $\text{Ph}$ ) have been observed (82–84). Reaction of *trans*- $[\text{Pt}(\text{C}\equiv\text{CR})_2(\eta^1\text{-dppm})_2]$  with *trans*- $[\text{PtClH}(\text{PPh}_3)_2]$  produces the A-frame complex  $[\text{Pt}_2(\text{C}\equiv\text{CR})_2(\mu\text{-H})(\mu\text{-dppm})_2]^+$ , which is fluxional at ambient temperature. Deprotonation with  $\text{NaOPr}^i$  leads to the platinum(I) species  $[\text{Pt}_2(\text{C}\equiv\text{CR})_2(\mu\text{-dppm})_2]$ , which

SCHEME 7. Reactions of  $[\text{Pt}_2(\text{dppm})_3]$  with  $\text{RSH}$ .

react with  $\text{CS}_2$  or  $\text{MeOCOC}\equiv\text{CCOOMe}$  to generate A-frame complexes (85).

Whether the *cis,cis* or *trans,trans* isomer, or the corresponding monomeric species, is favored thermodynamically has been shown to depend on the steric requirements of the ligands involved. Increasing steric bulk favors monomeric species and is primarily responsible for determining the ground state conformations of the dimeric complexes. Thus, *dppm*, *dep*m, and *dippm* (bis(diisopropylphosphino)methane) form monomeric dichlorides. On the other hand, *dmpm*, *dtbpm* ( $\text{Bu}^t\text{HPCH}_2\text{PHBu}^t$ ),

and  $(\text{RO})_2\text{PCH}_2\text{P}(\text{OR})_2$  ( $\text{R} = \text{Me}, \text{Et}, \text{Ph}, p\text{-tolyl}$ ) give species of the type  $\text{cis}, \text{cis}-[\text{Pt}_2\text{Cl}_4(\mu\text{-P}^*\text{P})_2]$ , whereas the low steric demand of  $\text{Pr}^i\text{HPCCH}_2\text{P}(\text{HPr}^i)$  allows isolation of the complex  $[\text{Pt}_2\text{Cl}_2(\mu\text{-Pr}^i\text{HPCCH}_2\text{P}(\text{HPr}^i))_3]^{2+}$ . Similarly, monomeric dimethylplatinum species are obtained with dppm and dippm, whereas  $\text{cis}, \text{cis}-[\text{Pt}_2\text{Me}_4(\mu\text{-P}^*\text{P})_2]$  complexes are found for  $\text{P}^*\text{P} = \text{dmpm}, \text{depm}, \text{dppm}, \text{or } (\text{RO})_2\text{PCH}_2\text{P}(\text{OR})_2$ . The dimeric complexes are fluxional, and increasing the steric bulk of the bridging ligands raises the activation energies of these processes. Increasing size also decreases the reactivities of the complexes toward oxidative addition (86–89). We have pointed out above that treatment of  $[\text{PtMe}_2(\text{dppm})]$  with  $\text{HCl}$  yields both  $[\text{PtClMe}(\text{dppm})]$  and the A-frame complex  $[\text{Pt}_2\text{Me}_2(\mu\text{-Cl})(\mu\text{-dppm})_2]\text{Cl}$ . Addition of  $\text{HCl}$  to  $\text{cis}, \text{cis}-[\text{Pt}_2\text{Me}_4(\mu\text{-dppm})_2]$  also generates  $[\text{Pt}_2\text{Me}_2(\mu\text{-Cl})(\mu\text{-dppm})_2]\text{Cl}$ , but similar treatment of the dmpm analog yields  $\text{cis}, \text{cis}-[\text{MeClPt}(\mu\text{-dmpm})_2\text{PtClMe}]$ . Addition of dmpm to  $\text{trans}-[\text{PtIme}(\text{SMe}_2)_2]$  generates  $\text{trans}, \text{trans}-[\text{MeIPt}(\mu\text{-dmpm})_2\text{PtIme}]$ , however, and the A-frame complex can only be formed by iodide removal using  $\text{AgNO}_3$ . The  $\text{trans}, \text{trans}$  complex undergoes fluxional motion that inverts the face-to-face structure. Based on the difficulty in forming the A-frame complex and the fact that the coalescence temperature is the same in  $\text{CDCl}_3$  or  $d_6$ -acetone solution and is unchanged in the presence of  $\text{NaI}$ , the inversion is thought to proceed through a  $[\text{Pt}_2\text{Me}_2(\mu\text{-I})_2(\mu\text{-dmpm})_2]$  intermediate:



(10)

Isolation of the neutral, face-to-face dimers with dmpm, but the ionic, A-frame species with dppm, may be rationalized in terms of steric congestion. Ionization of the halide diminishes the crowding in the molecule, and this becomes more important for the larger dppm ligand (90).

A cation of formulation,  $[\text{Pt}_2\text{Me}_3(\mu\text{-dppm})_2]^+$  has been prepared by a number of routes, including heating  $[\text{PtMe}_2(\text{dppm})]/[\text{PtCl}_2(\text{dppm})]$  or  $[\text{PtMe}_2(\text{dppm})]/[\text{PtClMe}(\text{dppm})]$  mixtures in methanol, treating  $[\text{PtMe}_2(\text{dppm})]$  or  $\text{cis}, \text{cis}-[\text{Pt}_2\text{Me}_4(\mu\text{-dppm})_2]$  with  $\text{HPF}_6$  or  $\text{HClO}_4$ , and adding  $[\text{PtClMe}(\text{cod})]$  to  $[\text{PtMe}_2(\eta^1\text{-dppm})_2]$  (80,90,91). The molecular structure of  $[\text{Pt}_2\text{Me}_3(\mu\text{-dppm})_2]\text{PF}_6$  (Fig. 4) reveals that it contains one  $\text{cis}-\text{PtMe}_2\text{P}_2$  unit and a  $\text{PtMeP}_2$  unit with a  $\text{trans}$ -arrangement of the P atoms. The  $\text{Pt}-\text{Pt}$  distance of  $2.769(1) \text{ \AA}$  is indicative of the presence of a

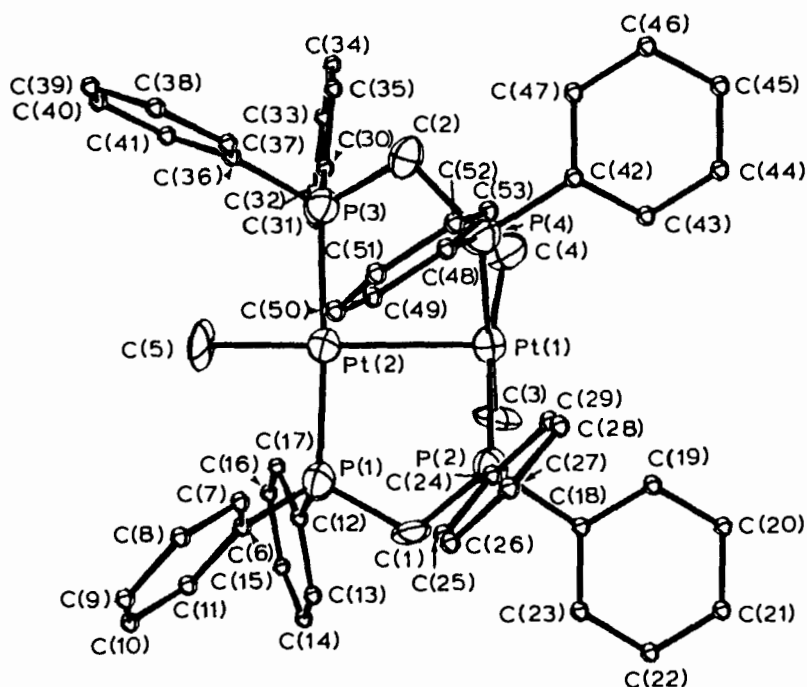


FIG. 4. Molecular structure of the  $[\text{Pt}_2\text{Me}_3(\mu\text{-dppm})_2]^+$  cation. [Reproduced with permission from Brown *et al.* (91).]

metal-metal bond, and this completes the coordination around the second platinum. Since both metal centers are platinum(II), the bond is formulated as a  $\text{Pt(II)} \rightarrow \text{Pt(II)}$  dative bond from the filled  $d_{z^2}$  orbital of the square-planar  $\text{Pt}_2\text{Me}_2$  unit into a vacant acceptor orbital of the 14-electron  $\text{Pt}_2\text{Me}$  fragment. The  $\text{Pt} \rightarrow \text{Pt}$  dative bonds exerts a lower *trans*-influence than  $\text{Pt}-\text{Pt}$  bonds in platinum(I) derivatives, and the  $^1\text{J}(\text{Pt}, \text{Pt})$  coupling is a relatively small 332 Hz (91). Unsymmetrical species containing dppm (92) or dmpm (93) have been prepared by reaction of  $[\text{PtR}_2(\eta^1\text{-P}^+\text{P})_2]$  with  $[\text{PtClR}'(\text{cod})]$  or  $[\text{PtClR}'(\text{SMe}_2)_2]$ . Treatment of  $[\text{PtPh}_2(\eta^1\text{-dmpm})_2]$  with  $[\text{PtClMe}(\text{SMe}_2)_2]$  generates *cis,trans*- $[\text{Ph}_2\text{Pt}(\mu\text{-dmpm})_2\text{PtClMe}]$ , which, on addition of methanol, ionizes to  $[\text{Ph}_2\text{Pt}(\mu\text{-dmpm})_2\text{PtMe}]\text{Cl}$ . After standing for several hours in solution, exchange of organic groups takes place to produce  $[\text{PhMePt}(\mu\text{-dmpm})_2\text{PtPh}]\text{Cl}$ , which may occur via a transient bridging phenyl species (93).

There is some variation in the  $\text{Pt}-\text{Pt}$  bond distances found for side-by-side platinum(I) dimers (2.62–2.77 Å), but the range of values for A-frame and platinum(II) complexes is substantial and has led to considerable

discussion of the nature of the Pt–Pt interactions, as well as attempts to correlate metal–metal distances with NMR coupling constants. Platinum–platinum distances in such compounds bridged by dppm ligands are presented in Table III. For A-frame complexes, these range from 2.71 Å in  $[\text{Pt}_2\text{Cl}_2(\mu\text{-HgCl}_2)(\mu\text{-dppm})_2]$ , where addition of the bridging  $\text{HgCl}_2$  fragment has little effect on the Pt–Pt distance compared with  $[\text{Pt}_2\text{Cl}_2(\mu\text{-dppm})_2]$ , to 3.17 Å in  $[\text{Pt}_2(\text{SCH}_2\text{Ph})_2(\mu\text{-S})(\mu\text{-dppm})_2]$ . In *trans,trans*-dimers, the Pt–Pt distances lie between 3.09 and 3.30 Å (albeit for only three examples), too long to suggest any significant bonding interaction between the two metal centers, and for *cis,cis*-dimers the distances are in excess of 4.0 Å.

The main question surrounds the nature of the bonding in A-frame complexes. As mentioned above, the addition of  $\text{HgCl}_2$  to  $[\text{Pt}_2\text{Cl}_2(\mu\text{-dppm})_2]$  causes only a very slight increase in the Pt–Pt distance [2.712(1) and 2.736(1) Å in the two independent molecules], and the complex clearly still contains a metal–metal bond. The angle between the  $\text{Pt}_2\text{Hg}$  and  $\text{HgCl}_2$  planes is approximately 60°, less than the 90° expected for tetrahedral geometry at mercury, but considerably greater than the 0° required for planar geometry. This is explained in terms of the  $\text{HgCl}_2$  bonding to the  $\text{Pt}_2$  moiety being primarily of  $a_1$  symmetry, with little  $b_2$  component (65). It had been predicted that A-frame complex formation

TABLE III  
PLATINUM–PLATINUM DISTANCES IN A-FRAME AND  
FACE-TO-FACE dppm-BRIDGED PLATINUM DIMERS

Complex	Pt ... Pt (Å)	Reference
$[\text{Pt}_2(\mu\text{-HgCl}_2)\text{Cl}_2(\text{dppm})_2]$	2.712(1) 2.736(1)	(65)
$[\text{Pt}_2\text{Me}_3(\text{dppm})_2]^+$	2.769(1)	(91)
$[\text{Pt}_2(\mu\text{-AuI})(\text{C}\equiv\text{CBu}^t)_2(\text{dppm})_2]$	2.837(1)	(64,94)
$[\text{Pt}_2(\mu\text{-H})\text{Me}_2(\text{dppm})_2]^+$	2.932(1)	(95)
$[\text{Pt}_2(\mu\text{-C}\equiv\text{CMe})\text{Me}_2(\text{dppm})_2]^+$	3.025(2)	(96)
<i>trans, trans</i> - $[\text{Pt}_2\text{Me}_2(\text{NCMe})_2(\text{dppm})_2]^{2+}$	3.093(1)	(97)
$[\text{Pt}_2(\mu\text{-CS}_2)\text{Cl}_2(\text{dppm})_2]$	3.094	(62)
$[\text{Pt}_2(\mu\text{-C}\equiv\text{CBu}^t)(\text{C}\equiv\text{CBu}^t)_2(\text{dppm})_2]^+$	3.117(1)	(78)
$[\text{Pt}_2(\mu\text{-CH}_2)\text{Cl}(\text{CH}_2\text{PPh}_3)(\text{dppm})_2]^+$	3.120(2)	(98)
$[\text{Pt}_2(\mu\text{-CH}_2)\text{Cl}_2(\text{dppm})_2]$	3.151(1)	(98)
$[\text{Pt}_2(\mu\text{-S})(\text{SCH}_2\text{Ph})_2(\text{dppm})_2]$	3.168(1)	(77)
<i>trans, trans</i> - $[\text{Pt}_2\text{Me}_2(\text{CO})_2(\text{dppm})_2]^{2+}$	3.204(1)	(97)
$[\text{Pt}_2(\mu\text{-NO})\text{Cl}_2(\mu\text{-dppm})_2]^+$	3.246(3)	(63)
<i>trans, trans</i> - $[\text{Pt}_2(\text{CN})_4(\text{dppm})_2]$	3.301(1)	(99)
<i>cis, cis</i> - $[\text{Pt}_2\text{Me}_4(\text{dppm})_2]$	4.361(2)	(86)
<i>cis, cis</i> - $[(o\text{-tolyl})_2\text{Pt}(\text{dppm})_2\text{PtMe}_2]$	4.91	(80)

incorporating a  $d^{10}$   $ML_2$  fragment isoelectronic with  $CH_2$  would involve bonding of  $b_2$  symmetry and a planar geometry about M (100). With bonding of  $a_1$  symmetry, the orientation of the  $HgCl_2$  would be determined by steric factors, and this may account for the observed orientation. It is concluded that, as a post-transition metal, the low energies of the  $d$  orbitals of mercury limit their participation in cluster bonding such that the  $b_2$  bonding component is negligible (65).

The bonding in  $[Pt_2(\mu-AuI)(C\equiv C Bu^t)_2(dppm)_2]$  is also described in terms of overlap between the  $a_1$  orbital of the  $[Pt_2(C\equiv C Bu^t)_2(\mu-dppm)_2]$  dimeric unit and the  $a_1$  orbital of the  $AuI$  fragment. It is thus characterized as three-center 2-electron bonding, such that each platinum atom formally attains a 16-electron configuration and the gold attains a 14-electron configuration (94). The longer Pt–Pt distance [2.837(1) Å] compared with  $[Pt_2Cl_2(\mu-HgCl_2)(\mu-dppm)_2]$ , although still a bonding interaction, is primarily a consequence of the higher *trans*-influence of the terminal alkynyl ligands. The lengthening of the Pt–Pt distance that occurs on coordination of the  $AuI$  fragment is unknown, however, since the molecular structure of the  $[Pt_2(C\equiv C Bu^t)_2(\mu-dppm)_2]$  dimer itself is unavailable. In the  $[Pt_2Me_2(\mu-H)(\mu-dppm)_2]^+$  cation (95), the bridging hydrogen is capable of  $a_1$  orbital overlap only, and this again may be described as 3-center 2-electron bonding. The longer Pt–Pt distance of 2.932(1) Å may be explained in terms of the high *trans*-influence of the methyl groups.

In contrast, the Pt–Pt distances in  $[Pt_2Cl_2(\mu-CH_3)(\mu-dppm)_2]$  and  $[Pt_2Cl(CH_2PPh_3)(\mu-CH_3)(\mu-dppm)_2]$  are 3.151(1) and 3.120(2) Å (98), respectively, outside the range of 2.53–2.89 Å characteristic of Pt–Pt single bonds (58). Here there is little, if any, bonding interaction between the two platinum atoms, which can be considered as 16-electron platinum(II) centers in the absence of a Pt–Pt bond.

It has been pointed out that within the linear X–Pt–Pt–Y framework of  $dppm$ - or  $dmpm$ -bridged platinum(I) dimers, the *trans*-influence of X is felt primarily at the Pt–Pt bond, although very high *trans*-influence ligands, such as H or Me, may exert a weaker long-range effect on the Pt–Y bond (101). In complexes of the type  $[XPt(\mu-dppm)_2Pt(PR_3)]^{n+}$  ( $n = 1$  or 2), the  $^1J(Pt,P)$  value for the terminal phosphine is insensitive to the nature of X (102), an observation that is paralleled by the similar Pt–P bond lengths in  $[ClPt(\mu-dppm)_2Pt(PPh_3)]^+$  [2.333(8) Å] and  $[HPt(\mu-dppm)_2Pt(\eta^1-dppm)]^+$  [2.347(4) Å]. On the contrary, the Pt–Pt distances in these two complexes differ considerably [2.665(2) and 2.770(2) Å], and it might be anticipated that the  $^2J(Pt,P)$  value for coupling to the terminal phosphorus might be more sensitive to the *trans*-influence of X. Indeed this is the case, the values of  $^2J(Pt,P)$  in  $[XPt(\mu-dppm)_2Pt(PPh_3)]^{n+}$  de-

creasing in the order  $X = I$  (1290 Hz),  $Cl$  (1232)  $>$   $PPh_3$  (1008)  $>$   $H$  (596)  $>$   $Me$  (490) (102).

The  $^1J(Pt,P)$  values for the dppm phosphorus atoms are also relatively insensitive to changes in the nature of the dimeric system. The  $^nJ(Pt,P)$  ( $n = 2$  or  $3$ ) coupling constant, on the other hand, has been shown to be a valuable indicator of the extent of metal-metal bonding in dppm-bridged complexes (103). In a side-by-side platinum(I) complex, there exist both two-bond  $P-Pt-Pt$  and three-bond  $P-C-P-Pt$  coupling paths, whereas the former is lacking when no metal-metal bond is present. It is found that where a  $Pt-Pt$  bond is present, the coupling in question is negative, whereas it is positive when there is no metal-metal bond. This may be rationalized if the  $P-C-P-Pt$  coupling is positive and the  $P-Pt-Pt$  coupling is negative; when  $Pt-Pt$  bonding is strong, the latter coupling path dominates, whereas in the absence of significant  $Pt-Pt$  bonding, the positive coupling is more important. Data for complexes in which the  $Pt-Pt$  distance and the sign of  $^nJ(Pt,P)$  are both known are presented in Table IV. There is a fairly good correlation between these two parameters. The value of such a relationship lies in its ability to predict the  $Pt-Pt$  distance in compounds for which the molecular structure has not been determined, distinctly negative values indicating the presence of a  $Pt-Pt$  bond, positive values denoting its absence, and values close to zero being indicative of a weak, but significant, metal-metal interaction. Its usefulness, of course,

TABLE IV  
PLATINUM-PLATINUM DISTANCES AND  $^nJ(Pt,P)$  COUPLINGS  
FOR dppm-BRIDGED PLATINUM DIMERS<sup>a</sup>

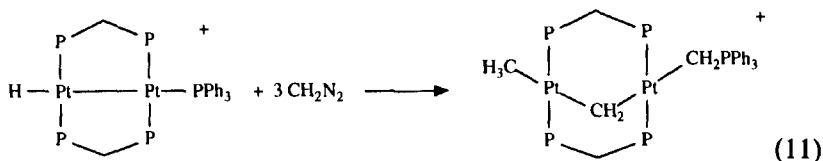
Complex	Pt-Pt (Å)	$^nJ(Pt,P)$ (Hz)
$[Pt_2Cl(CO)(dppm)_2]^+$	2.620(1)	-45, -58
$[Pt_2(CO)_2(dppm)_2]^{2+}$	2.642(1)	-96
$[Pt_2Cl_2(dppm)_2]$	2.651(1)	-136
$[Pt_2(\mu-HgCl_2)Cl_2(dppm)_2]$	2.712(1)	-64
	2.736(1)	
$[Pt_2Me_3(dppm)_2]^+$	2.769(1)	-15, -15
$[Pt_2H(\eta^1-dppm)(dppm)_2]^+$	2.770(2)	-85, -12
$[Pt_2(\mu-AuI)(C\equiv C Bu^t)_2(dppm)_2]$	2.837(1)	-23
$[Pt_2(\mu-H)Me_2(dppm)_2]^+$	2.932(1)	+24
$[Pt_2(\mu-C\equiv C Me)Me_2(dppm)_2]^+$	3.025(2)	+29
$[Pt_2(\mu-C\equiv C Bu^t)(C\equiv C Bu^t)_2(dppm)_2]^+$	3.117(1)	+30
$[Pt_2(\mu-CH_2)Cl_2(dppm)_2]$	3.151(1)	+73
$[Pt_2(\mu-NO)Cl_2(dppm)_2]^+$	3.246(3)	+159

<sup>a</sup> Data for complexes where both parameters have been reported.



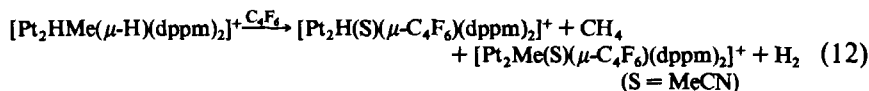
depends on being able to determine the sign of the long-range coupling constant, and this is not always possible from the one-dimensional  $^{31}\text{P}$  NMR spectrum. A convenient method for determining both the magnitude and sign of  $^2J(\text{Pt},\text{P})$  in dimeric platinum complexes by  $^{31}\text{P}$  COSY NMR spectroscopy has been reported recently (104).

We have already indicated that dppm-bridged platinum(I) complexes react with diazomethane to produce methylene-bridged A-frame species (67,69). In certain cases, multiple  $\text{CH}_2$  insertions may take place. Thus,  $[\text{Pt}_2\text{HL}(\mu\text{-dppm})_2]^+$  ( $\text{L} = \text{CO}$ ,  $\text{PMe}_2\text{Ph}$ ) reacts with  $\text{CH}_2\text{N}_2$  to yield  $[\text{Pt}_2(\text{CH}_3)\text{L}(\mu\text{-CH}_2)(\mu\text{-dppm})_2]^+$ . Sodium borohydride reduction of the carbonyl derivative generates  $[\text{Pt}_2\text{Me}_2(\mu\text{-H})(\mu\text{-dppm})_2]^+$ , indicating that the organic fragment can migrate between bridging and terminal positions.  $[\text{Pt}_2\text{H}(\text{PPh}_3)(\mu\text{-dppm})_2]^+$  reacts with 3 equivalents of  $\text{CH}_2\text{N}_2$  to give  $[\text{Pt}_2(\text{CH}_3)(\text{CH}_2\text{PPh}_3)(\mu\text{-CH}_2)(\mu\text{-dppm})_2]^+$ :



which is converted to  $[\text{Pt}_2\text{Cl}(\text{CH}_2\text{PPh}_3)(\mu\text{-CH}_2)(\mu\text{-dppm})_2]^+$  on standing in  $\text{CH}_2\text{Cl}_2$  solution (98).

The neutral methylene-bridged complex  $[\text{Pt}_2\text{Cl}_2(\mu\text{-CH}_2)(\mu\text{-dppm})_2]$  may be protonated with  $\text{HSbF}_6$  to produce  $[\text{Pt}_2\text{ClMe}(\mu\text{-Cl})(\mu\text{-dppm})_2]^+$ , again illustrating the ability of the one-carbon fragment to migrate from a bridging to a terminal position. Borohydride reduction of  $[\text{Pt}_2\text{ClMe}(\mu\text{-Cl})(\mu\text{-dppm})_2]^+$  generates  $[\text{Pt}_2\text{HMe}(\mu\text{-H})(\mu\text{-dppm})_2]^+$ , which undergoes A-frame inversion via an intermediate containing a linear  $\text{HPtHPtMe}$  unit. Addition of hexafluorobut-2-yne in acetonitrile solution yields a 9:1 mixture of two alkyne-bridged species,  $[\text{Pt}_2\text{H}(\text{MeCN})(\mu\text{-C}_4\text{F}_6)(\mu\text{-dppm})_2]^+$  and  $[\text{Pt}_2\text{Me}(\text{MeCN})(\mu\text{-C}_4\text{F}_6)(\mu\text{-dppm})_2]^+$ , the reactions being accompanied by elimination of  $\text{CH}_4$  and  $\text{H}_2$ , respectively:

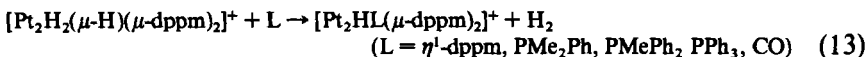


The production of methane or dihydrogen can be accounted for by the elimination of the bridging hydride and one of the terminal groups. Coupling with the methyl group is preferred. The analogous reaction of  $[\text{Pt}_2\text{Me}_2(\mu\text{-H})(\mu\text{-dppm})_2]^+$  with hexafluorobut-2-yne produces  $[\text{Pt}_2\text{Me}(\text{MeCN})(\mu\text{-C}_4\text{F}_6)(\mu\text{-dppm})_2]^+$  and methane only (105).

Reduction of  $[\text{PtCl}_2(\text{dppm})]$  with sodium borohydride yields  $[\text{Pt}_2\text{H}_2(\mu\text{-H})(\mu\text{-dppm})_2]^+$ , obtained as its chloride or hexafluorophosphate salt. The complex is characterized by two hydride resonances in its  $^1\text{H}$  NMR spectrum, one at  $-6.8$  ppm with a  $^1\text{J}(\text{Pt},\text{H})$  coupling of 1162 Hz (due to the terminal hydrides) and one at  $-5.9$  ppm with a  $^1\text{J}(\text{Pt},\text{H})$  coupling of 540 Hz (due to the bridging hydride). Reaction with  $\text{CCl}_4$  or  $\text{HCl}$  gives first  $[\text{Pt}_2\text{H}_2(\mu\text{-Cl})(\mu\text{-dppm})_2]^+$ , followed by  $[\text{Pt}_2\text{Cl}_2(\mu\text{-H})(\mu\text{-dppm})_2]^+$ . Addition of  $\text{HCl}$  to  $[\text{Pt}_2\text{Cl}_2(\mu\text{-dppm})_2]$  in  $\text{CH}_2\text{Cl}_2$  solution produces  $[\text{Pt}_2\text{Cl}_2(\mu\text{-H})(\mu\text{-dppm})_2]\text{Cl}$ , but this reverts to the platinum(I) precursor on standing (106).

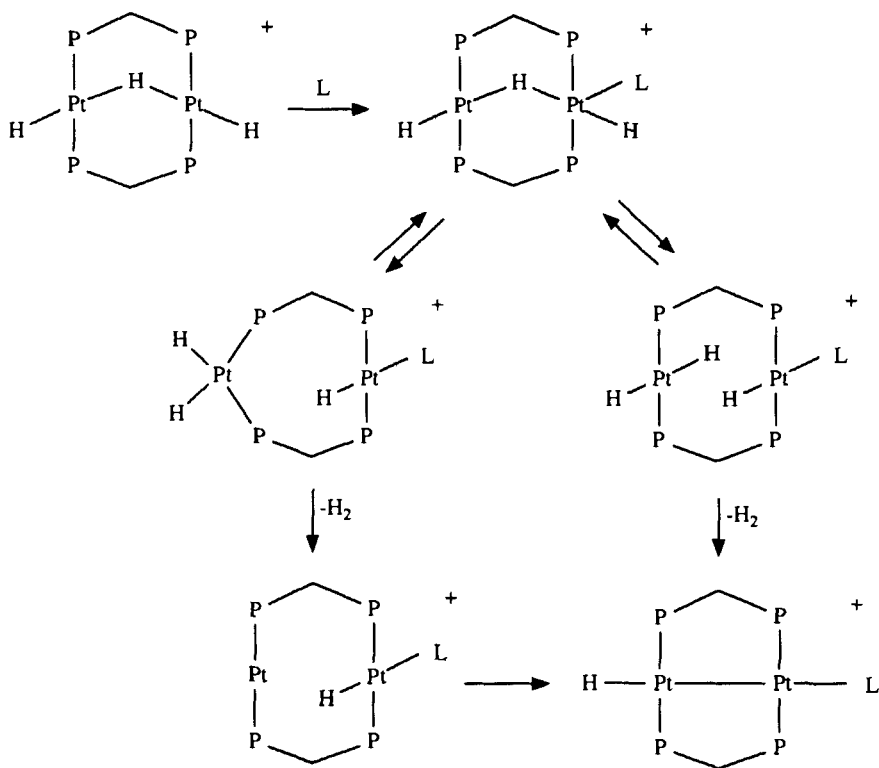
Treatment of an acetonitrile solution of  $[\text{Pt}_2\text{H}_2(\mu\text{-H})(\mu\text{-dppm})_2]\text{PF}_6$  with hexafluorobut-2-yne or dimethylacetylene dicarboxylate results in elimination of dihydrogen and formation of  $[\text{Pt}_2\text{H}(\text{MeCN})(\mu\text{-RC}\equiv\text{CR})(\mu\text{-dppm})_2]^+$  ( $\text{R} = \text{CF}_3, \text{CO}_2\text{Me}$ ), which may be trapped by the addition of sodium chloride as  $[\text{Pt}_2\text{ClH}(\mu\text{-RC}\equiv\text{CR})(\mu\text{-dppm})_2]$ . With trifluoropropyne, the alkyne-bridged alkynyl complex  $[\text{Pt}_2(\text{C}\equiv\text{CCF}_3)_2(\mu\text{-CF}_3\text{C}\equiv\text{CH})(\mu\text{-dppm})_2]$  is produced (107). This contrasts with the reaction of  $[\text{Pt}_2\text{Me}_2(\mu\text{-dppm})_2]^{2+}$  with propyne, where  $[\text{Pt}_2\text{Me}_2(\mu\text{-MeC}\equiv\text{CH})(\mu\text{-dppm})_2]^{2+}$  is formed initially, but it undergoes deprotonation to yield  $[\text{Pt}_2\text{Me}_2(\mu\text{-C}\equiv\text{CMe})(\mu\text{-dppm})_2]^+$  (96).

The reactions of  $[\text{Pt}_2\text{H}_2(\mu\text{-H})(\mu\text{-dppm})_2]\text{PF}_6$  with alkynes serve to introduce a number of studies of the elimination of dihydrogen from this cationic complex. Addition of one of a range of neutral ligands causes  $\text{H}_2$  elimination and formation of a platinum(I) complex of the form  $[\text{Pt}_2\text{HL}(\mu\text{-dppm})_2]^+$  (108,109):



For the reactions with tertiary phosphines, intermediates of the form  $[\text{HPt}(\mu\text{-H})(\mu\text{-dppm})_2\text{PtH}(\text{PR}_3)]^+$  have been detected, and equilibrium constants for their formation at low temperature have been determined (110). Exchange of  $\text{PR}_3$  takes place between the two platinum centers. The elimination of  $\text{H}_2$  has been shown to be intramolecular, and the rate-determining step is the elimination itself. Rearrangement to a second intermediate without a bridging hydride is believed to occur prior to reductive elimination, but it is not possible to determine with certainty whether the elimination occurs at one platinum center or by means of a concerted dinuclear process. Mechanisms involving each type of elimination process have been proposed (Scheme 8) (110).

Similarly, in the reaction of  $[\text{Pt}_2\text{H}_2(\mu\text{-H})(\mu\text{-dppm})_2]^+$  with  $\text{dppm}$  at  $-90^\circ\text{C}$ , an intermediate of the form  $[\text{HPt}(\mu\text{-H})(\mu\text{-dppm})_2\text{PtH}(\eta^1\text{-dppm})]^+$  could be detected. Elimination of  $\text{H}_2$  occurs on raising the tem-

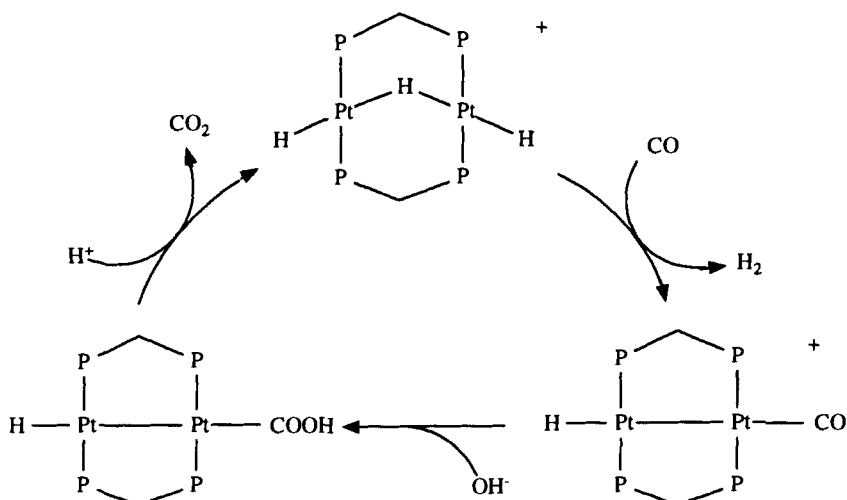


SCHEME 8. Mechanisms for the elimination of  $\text{H}_2$  from  $[\text{Pt}_2\text{H}_3(\text{dppm})_2]^+$ .

perature to  $-10^\circ\text{C}$  (111). Interestingly, the reaction of the depm analog,  $[\text{Pt}_2\text{H}_2(\mu\text{-H})(\mu\text{-depm})_2]^+$ , with depm at  $-90^\circ\text{C}$ , yields  $[\text{Pt}_2\text{H}_2(\mu\text{-H})(\mu\text{-depm})_3]^+$ , which contains a linear  $\text{HPtHPtH}$  unit. Dihydrogen elimination takes place at  $-70^\circ\text{C}$  in this case to generate a platinum(0)–platinum(II) species  $[\text{Pt}(\mu\text{-depm})_3\text{PtH}]^+$ , which may be protonated by  $\text{NH}_4^+$  to give  $[\text{Pt}_2\text{H}_2(\mu\text{-depm})_3]^{2+}$  (111).

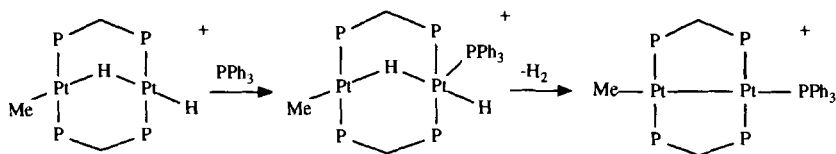
The complex  $[\text{Pt}_2\text{H}_2(\mu\text{-H})(\mu\text{-dppm})_2]\text{PF}_6$  acts as a catalyst precursor for the water–gas shift reaction at  $100^\circ\text{C}$  in methanol. It is most effective at low pressures of carbon monoxide. A possible catalytic cycle is shown in Scheme 9. The catalytic solutions contain various cluster species, however, and a tetra-platinum species  $[\text{Pt}_4(\mu\text{-CO})_2(\mu\text{-dppm})_3(\eta^1\text{-Ph}_2\text{PCH}_2\text{P}(\text{O})\text{Ph}_2)]$  has been isolated and characterized by X-ray crystallography (109,112).

Reductive elimination of dihydrogen from  $[\text{Pt}_2\text{H}_2(\mu\text{-H})(\mu\text{-dppm})_2]^+$  may also be induced photochemically in acetonitrile or pyridine solution.

SCHEME 9. Catalysis of the water-gas shift reaction by  $[\text{Pt}_2\text{H}_2(\mu\text{-H})(\mu\text{-dppm})_2]^+$ .

The reaction is intramolecular, a mixture of  $[\text{Pt}_2\text{H}_2(\mu\text{-H})(\mu\text{-dppm})_2]^+$  and  $[\text{Pt}_2\text{D}_2(\mu\text{-D})(\mu\text{-dppm})_2]^+$  producing  $\text{H}_2$  and  $\text{D}_2$  only, and it is believed to be initiated from a singlet excited state (113). Irradiation of the chloride-bridged dimer  $[\text{Pt}_2\text{H}_2(\mu\text{-Cl})(\mu\text{-dppm})_2]^+$  in THF solution also results in dihydrogen elimination, the product being trapped by addition of carbon monoxide to give  $[\text{Pt}_2\text{Cl}(\text{CO})(\mu\text{-dppm})_2]^+$ . The elimination is proposed to occur through species of the type  $[\text{ClPt}(\mu\text{-H})(\mu\text{-dppm})_2\text{PtH}]^+$  or  $[\text{ClPt}(\mu\text{-dppm})_2\text{PtH}_2]^+$ , formed by exchange of groups between bridging and terminal positions (114).

Treatment of the related  $[\text{Pt}_2\text{HMe}(\mu\text{-H})(\mu\text{-dppm})_2]^+$  cation with  $\text{dppm}$ ,  $\text{PMe}_2\text{Ph}$ , or  $\text{PPh}_3$  causes elimination of dihydrogen (but not methane) and formation of  $[\text{Pt}_2\text{MeL}(\mu\text{-dppm})_2]^+$ . The complex where  $\text{L} = \eta^1\text{-dppm}$  has also been prepared by addition of methyl iodide to  $[\text{Pt}_2(\text{dppm})_3]$ . The elimination follows second-order kinetics, and in the reaction with  $\text{PPh}_3$  the intermediate  $[\text{H}(\text{PPh}_3)\text{Pt}(\mu\text{-H})(\mu\text{-dppm})_2\text{PtMe}]^+$  could be observed by NMR spectroscopy at low temperature (115):



(14)

It is interesting to note that the  $\text{PPh}_3$  coordinates to the platinum atom bearing the terminal hydride ligand. It might be supposed that this would promote migration of the bridging hydride to the other platinum, and hence elimination of methane from the second platinum, but this is clearly not the case. Instead, the  $\text{PPh}_3$  appears to promote reductive elimination of the terminal and bridging hydrides from the first platinum center. Reductive elimination from  $[\text{Pt}_2\text{HMe}(\mu\text{-H})(\mu\text{-dppm})_2]^+$  may be induced photochemically also, but again only  $\text{H}_2$  is generated (116).

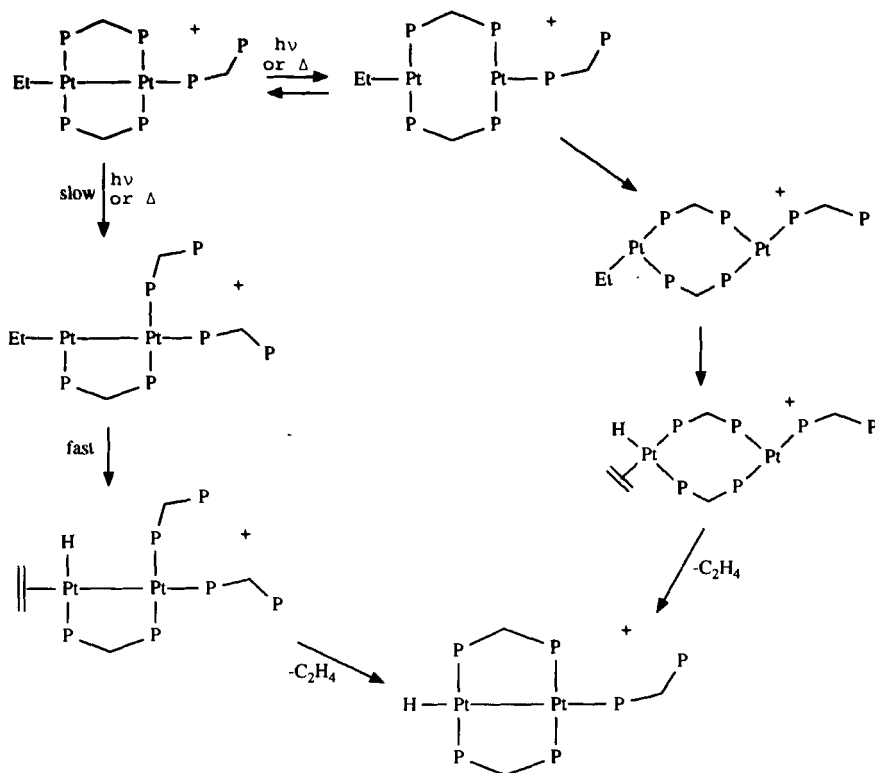
In the case of the dimethyl analog,  $[\text{Pt}_2\text{Me}_2(\mu\text{-H})(\mu\text{-dppm})_2]^+$ , elimination of methane is slow when induced by  $\text{PMe}_2\text{Ph}$ , even at  $50^\circ\text{C}$ . Irradiation of the complex produces methane (and traces of ethene) rapidly, however, and the methane has been shown to be formed by a primarily intramolecular process (95,116,117).

Irradiation of  $[\text{Pt}_2\text{Me}_3(\mu\text{-dppm})_2]^+$  in acetonitrile or acetone solution yields ethane and the solvent-coordinated platinum(I) complex  $[\text{Pt}_2\text{Me}(\text{S})(\mu\text{-dppm})_2]^+$ . As in the previous case, the elimination of ethane is predominantly intramolecular. Photolysis in pyridine solution, however, results in cleavage of the dimer and formation of  $[\text{PtMe}_2(\text{dppm})]$  and  $[\text{PtMe}(\text{py})(\text{dppm})]^+$  (116).

The corresponding ethyl complex,  $[\text{Pt}_2\text{Et}_3(\mu\text{-dppm})_2]\text{SbF}_6$ , undergoes  $\beta$ -elimination of ethene to produce  $[\text{Pt}_2\text{Et}_2(\mu\text{-H})(\mu\text{-dppm})_2]\text{SbF}_6$ . This represents a rare example of  $\beta$ -elimination from a dimeric complex. The reaction is intramolecular, and the  $\beta$ -elimination step is not rate determining. Reductive elimination of ethane does not occur from  $[\text{Pt}_2\text{Et}_2(\mu\text{-H})(\mu\text{-dppm})_2]^+$  under the reaction conditions (118).

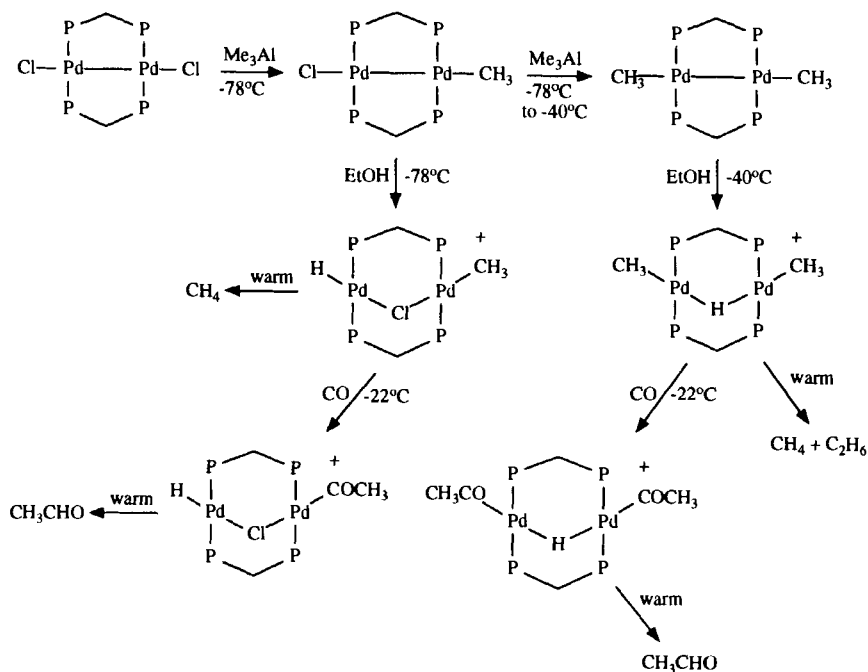
$\beta$ -Elimination also takes place from the platinum(I) species  $[\text{Pt}_2\text{R}(\eta^1\text{-dppm})(\mu\text{-dppm})_2]\text{PF}_6$  ( $\text{R} = \text{Et}, \text{CD}_2\text{CH}_3, \text{Pr}^n, \text{Bu}^n$ ). The reaction proceeds either thermally or photochemically, and the  $\beta$ -elimination step occurs subsequent to the rate-determining step. Two possible mechanisms (Scheme 10), involving initial Pt-Pt or Pt-P bond cleavage, have been proposed. (119).

An interesting and related study involving elimination reactions of dppm-bridged palladium(II) complexes has been reported. Treatment of  $[\text{Pd}_2\text{Cl}_2(\mu\text{-dppm})_2]$  with one or two equivalents of trimethylaluminum, followed by ethanol, yields  $[\text{Pd}_2\text{H}(\text{CH}_3)(\mu\text{-Cl})(\mu\text{-dppm})_2]^+$  or  $[\text{Pd}_2(\text{CH}_3)_2(\mu\text{-H})(\mu\text{-dppm})_2]^+$ , respectively. Reductive elimination from  $[\text{PdH}(\text{CH}_3)(\mu\text{-Cl})(\mu\text{-dppm})_2]^+$  produces methane and  $[\text{Pd}_2\text{Cl}_2(\mu\text{-dppm})_2]$ . Warming a solution of  $[\text{Pd}_2(\text{CH}_3)_2(\mu\text{-H})(\mu\text{-dppm})_2]^+$  results in elimination of both methane and ethane, the latter probably being formed via a transient methyl-bridged species. Treatment of either cation with carbon monoxide results in elimination of acetaldehyde via  $[\text{Pd}_2\text{H}(\text{COCH}_3)(\mu\text{-Cl})(\mu\text{-dppm})_2]^+$ .

SCHEME 10. Elimination of  $\text{C}_2\text{H}_4$  from  $[\text{Pt}_2\text{Et}(\text{dppm})_3]^+\text{PF}_6^-$ .

$\text{dppm})_2]^+$  or  $[\text{Pd}_2(\text{COCH}_3)_2(\mu\text{-H})(\mu\text{-dppm})_2]^+$ , respectively (Scheme 11) (120).

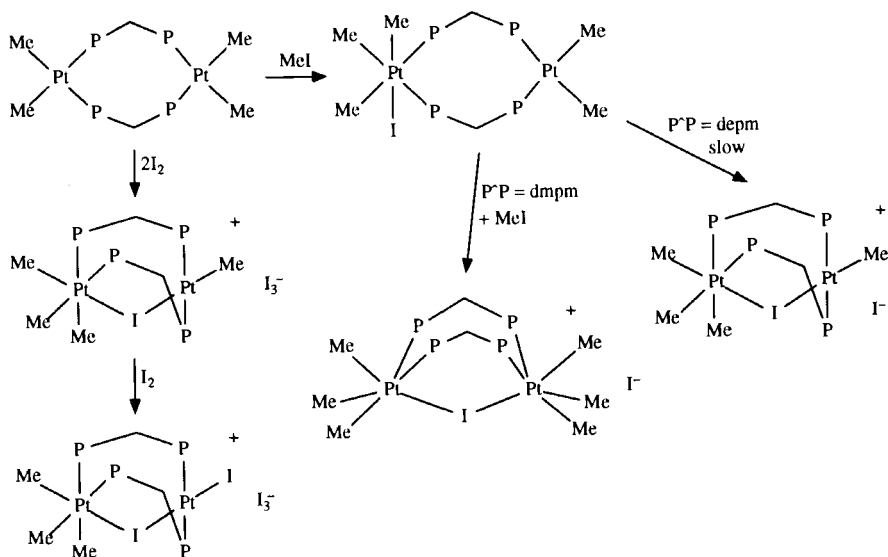
Oxidative addition has been shown to occur for platinum(II) dimers, but only for those containing the smaller and more electron-releasing *dmpm* and *depm*, and only for *cis,cis*-isomers. Addition of  $\text{X}_2$  ( $\text{X} = \text{Cl}, \text{Br}, \text{I}$ ) to *cis,cis*- $[\text{Me}_2\text{Pt}(\mu\text{-dmpm})_2\text{PtMe}_2]$  produces the platinum(IV)-platinum(II) complex *fac,trans*- $[\text{Me}_3\text{Pt}(\mu\text{-X})(\mu\text{-dmpm})_2\text{PtMe}]\text{X}$ , in which migration of a methyl group between platinum atoms takes place. Where  $\text{X} = \text{I}$ , further addition of  $\text{I}_2$  gives *fac,trans*- $[\text{Me}_3\text{Pt}(\mu\text{-I})(\mu\text{-dmpm})_2\text{PtMe}]\text{I}_3$ , and finally *fac,trans*- $[\text{Me}_3\text{Pt}(\mu\text{-I})(\mu\text{-dmpm})_2\text{PtI}]\text{I}_3$ . Treatment of *cis,cis*- $[\text{Me}_2\text{Pt}(\mu\text{-dmpm})_2\text{PtMe}_2]$  with methyl iodide generates the neutral species, *fac,cis*- $[\text{Me}_3\text{IPt}(\mu\text{-dmpm})_2\text{PtMe}_2]$ , since a product analogous to that formed with  $\text{X}_2$  would require a bridging methyl group. Further addition of methyl iodide yields *fac,fac*- $[\text{Me}_3\text{Pt}(\mu\text{-I})(\mu\text{-dmpm})_2\text{PtMe}_3]\text{I}$ .



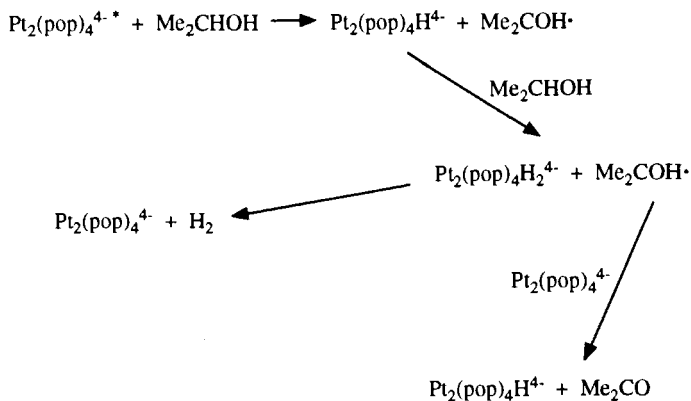
SCHEME 11. Elimination reactions of dppm-bridged palladium complexes.

The reaction of *cis,cis*-[Me<sub>2</sub>Pt(μ-depm)<sub>2</sub>PtMe<sub>2</sub>] with methyl iodide reversibly forms *fac,cis*-[Me<sub>3</sub>IPt(μ-depm)<sub>2</sub>PtMe<sub>2</sub>], which, in the presence of excess methyl iodide, slowly converts to *fac,trans*-[Me<sub>3</sub>Pt(μ-I)(μ-depm)<sub>2</sub>PtMeI]. In contrast, *cis,cis*-[Me<sub>2</sub>Pt(μ-dppm)<sub>2</sub>PtMe<sub>2</sub>] forms no new product with methyl iodide, but it does undergo exchange of methyl groups with CD<sub>3</sub>I (121,122). These reactions are summarized in Scheme 12.

The dianions formed from O{PH(O)OH}<sub>2</sub> (pop) or CH<sub>2</sub>{PH(O)OH}<sub>2</sub> (pcp) have also been employed as bridging ligands in diplatinum complexes. The dianions are formed by deprotonation of the phosphorus atoms, and the presence of a P-O-P or P-C-P backbone means that these ligands closely resemble dppm in their ability to bridge two metal centers. Treatment of K<sub>2</sub>PtCl<sub>4</sub> with CH<sub>2</sub>{PH(O)OH}<sub>2</sub> yields the platinum(II) complex K<sub>4</sub>[Pt<sub>2</sub>(μ-pcp)<sub>4</sub>], whose molecular structure reveals a Pt-Pt distance of 2.9801(2) Å. Addition of chlorine results in the platinum(III) species [ClPt(μ-pcp)<sub>4</sub>PtCl]<sup>4-</sup>, in which the Pt-Pt distance is reduced to 2.7500(3) Å, indicating the presence of a metal-metal bond as expected. In the molecular structure, there is hydrogen bonding between the OH and P=O groups on adjacent phosphorus atoms. The electronic

SCHEME 12. Oxidative addition reactions of  $cis,cis$ -[Pt<sub>2</sub>Me<sub>4</sub>(dppm)<sub>2</sub>].

spectrum exhibits intense absorptions identified as Cl → Pt(III) charge transfer bands. The [Pt<sub>2</sub>(μ-pcp)<sub>4</sub>]<sup>4-</sup> anion is less acidic ( $pK_a$ , 8.0) than its [Pt<sub>2</sub>(μ-pop)<sub>4</sub>]<sup>4-</sup> counterpart ( $pK_a$ , 3.0), due to the less electronegative carbon backbone (123,124). The [Pt<sub>2</sub>(μ-pop)<sub>4</sub>]<sup>4-</sup> anion undergoes photochemically induced oxidative addition of aryl bromides and iodides (but not chlorides) to yield [ArPt(μ-pop)<sub>4</sub>PtX]<sup>4-</sup> (X = Br, I). Exchange of halides, including chloride, takes place under photochemical conditions. [Pt<sub>2</sub>(μ-pop)<sub>4</sub>]<sup>4-</sup> catalyzes the photochemical decomposition of *iso*-pro-

SCHEME 13. Photochemical decomposition of isopropanol catalyzed by [Pt<sub>2</sub>(pop)<sub>4</sub>]<sup>4-</sup>.



panol to acetone and dihydrogen. A proposed catalytic cycle is shown in Scheme 13 (125).

## VII

### COMPLEXES BRIDGED BY dppc LIGANDS

We have used the diphenylphosphinocyclopentadienyl (dppc) ligand to construct diplatinum complexes. Reactions of  $[\text{PtClR}(\text{cod})]$  with  $\text{TiCl}_3\text{H}_4\text{PPh}_2$  produce complexes of the type  $[\text{Pt}_2\text{R}_2(\mu\text{-C}_5\text{H}_4\text{PPh}_2)_2]$  ( $\text{R} = \text{Me, Et, Np, Ph}$ ) (126). These exist as two isomers, which are fluxional in solution at ambient temperature. They have been characterized by NMR spectroscopy at low temperatures, and the major isomer (the only one observed when  $\text{R} = \text{Me}$  or  $\text{Et}$ ) is of an unsymmetrical nature. Examples of each isomer have been characterized by X-ray crystallography and they are shown in Fig. 5. The minor isomer of the phenyl dimer crystallizes from ether solution and it has the expected  $\eta^5$ -coordination of the cyclopentadienyl moiety to both platinum, thus producing two 18-electron metal centers. Similar structures are found for  $[\text{Pd}_2\text{Me}_2(\mu\text{-}\eta^5\text{-C}_5\text{H}_4\text{PPh}_2)_2]$  (127) and  $[\text{Rh}_2(\text{CO})_2(\mu\text{-}\eta^5\text{-C}_5\text{H}_4\text{PPh}_2)_2]$  (128). In the case of the methyl analog, it is the major isomer that is obtained by crystallization from benzene solution. It exhibits one  $\eta^5$ -cyclopentadienyl group, whereas the second ring is coordinated in the  $\eta^1$ -mode and is 1,1-substituted by platinum and phosphorus. The Pt–Pt distance of 2.723(1) Å indicates the presence of a metal–metal bond. This is formulated as a dative bond, with the  $\eta^5$ - and  $\eta^1$ -cyclopentadienyl platinum centers being 18- and 16-electron centers, respectively. This Pt–Pt distance is slightly shorter than the 2.761(1) Å found for the Pt → Pt dative bond in  $[\text{Pt}_2\text{Me}_3(\mu\text{-dppm})_2]^+$ . The  $^1\text{J}(\text{Pt}, \text{Pt})$  coupling of 1134 Hz is also larger than that found for  $[\text{Pt}_2\text{Me}_3(\mu\text{-dppm})_2]^+$  (332 Hz) (91). The complexes  $[\text{Pt}_2\text{R}_2(\mu\text{-C}_5\text{H}_4\text{PPh}_2)_2]$  ( $\text{R} = \text{Me, Et, Np, Ph}$ ) each exhibit two  $^1\text{J}(\text{Pt}, \text{P})$  and two  $^2\text{J}(\text{Pt}, \text{P})$  values. Both two-bond couplings are of negative sign (–305 and –126 Hz for the methyl complex), the larger being due to the phosphorus atom attached to the  $\eta^5$ -cyclopentadienyl–platinum center. The negative coupling constants are consistent with the presence of the Pt–Pt bond (103).

The dppc ligand proves to be a versatile bridging ligand since it may adopt a number of different bonding modes. In addition to the two described above, reactions with CO or  $\text{CNBu}^t$  generate face-to-face platinum(II) dimers of the form  $[\text{Pt}_2\text{R}_2\text{L}_2(\mu\text{-}\eta^1\text{-C}_5\text{H}_4\text{PPh}_2)_2]$ , in which the cyclopentadienyl groups are 1,2-substituted by platinum and phosphorus:

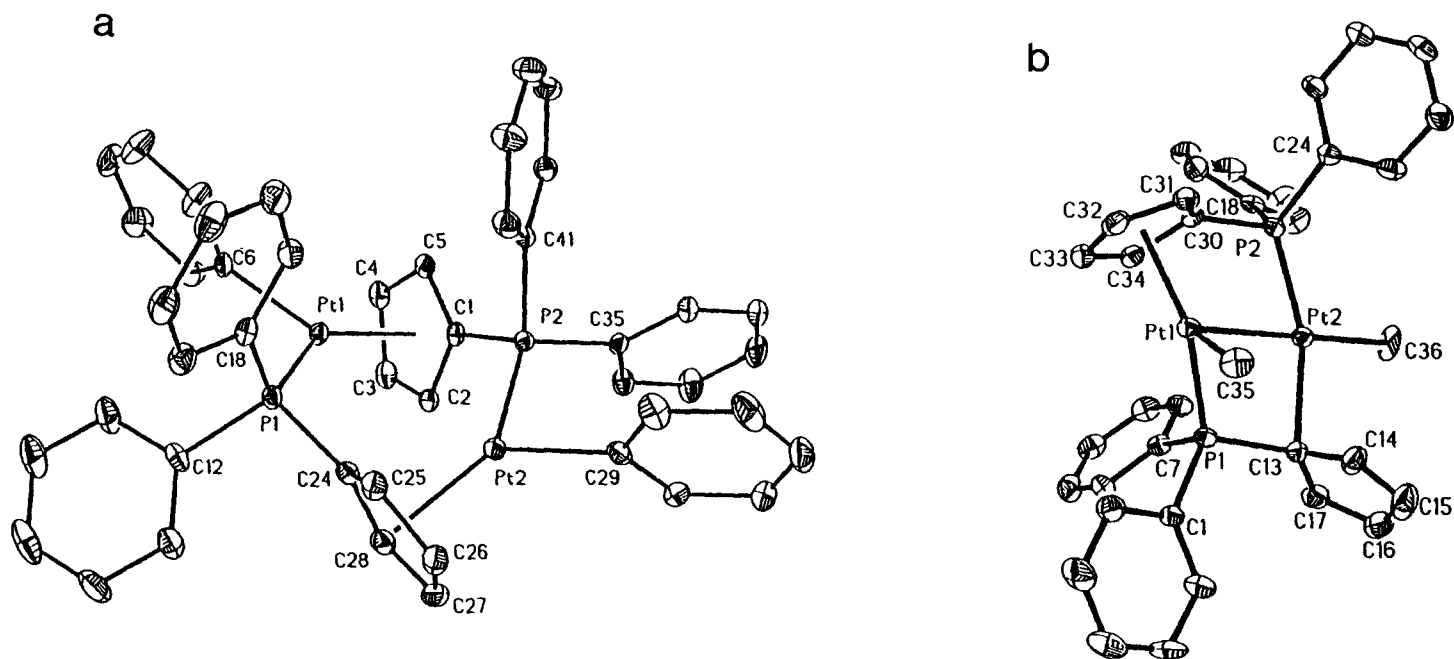
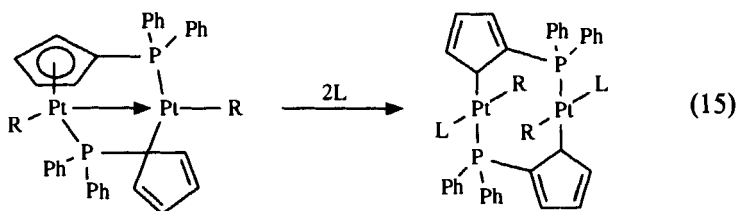
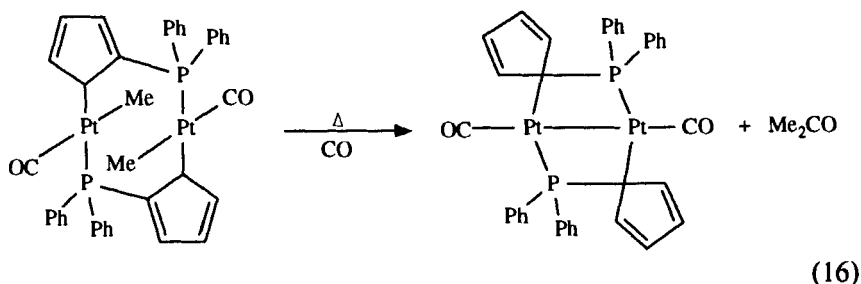


FIG. 5. Molecular structures of  $[\text{Pt}_2\text{R}_2(\mu\text{-dppc})_2]$ , (a)  $\text{R} = \text{Ph}$ ; (b)  $\text{R} = \text{Me}$ , illustrating the two isomeric forms. [Reproduced with permission from Lin *et al.* (126).]



The molecular structure of  $[\text{Pt}_2\text{Me}_2(\text{CO})_2(\mu\text{-}\eta^1\text{-C}_5\text{H}_4\text{PPh}_2)_2]$  reveals a Pt–Pt distance of 3.157(1) Å, outside the range of 2.53–2.89 Å typical of Pt–Pt bonds (58). Heating a solution of  $[\text{Pt}_2\text{Me}_2(\text{CO})_2(\mu\text{-}\eta^1\text{-C}_5\text{H}_4\text{PPh}_2)_2]$  results in reductive elimination of acetone and formation of the platinum(I) dimer  $[\text{Pt}_2(\text{CO})_2(\mu\text{-}\eta^1\text{-C}_5\text{H}_4\text{PPh}_2)_2]$ , in which both cyclopentadienyl rings are 1,1-substituted (129):



The Pt–Pt bond distance is 2.593(1) Å, shorter than those found in dppm-bridged platinum(I) complexes. This is no doubt a consequence of the presence of the four-membered  $\text{Pt}_2\text{PC}$  ring, compared with the five-membered rings found in dppm-bridged species. The stability of the four-membered  $\text{Pt}_2\text{PC}$  ring is illustrated by the fact that the terminal carbonyl ligands may be displaced cleanly to give complexes of the type  $[\text{Pt}_2\text{L}_2(\mu\text{-}\eta^1\text{-C}_5\text{H}_4\text{PPh}_2)_2]$  ( $\text{L} = \text{CNBu}^t, \text{PEt}_3, \text{PMe}_2\text{Ph}, \text{PPh}_3, \text{P}(\text{CH}_2\text{CH}_2\text{CN})_3$ ). Complexes containing four-membered  $\text{Pt}_2\text{PO}$  rings have been prepared by heating  $[\text{Pt}_2(\mu\text{-OH})_2(\text{P}(\text{O})\text{Ph}_2)_2\text{L}_2]$  ( $\text{L} = \text{PMePh}_2, \text{PPh}_3$ ) in ethanol solution. The molecular structure of  $[\text{Pt}_2(\mu\text{-OPPh}_2)_2(\text{PMePh}_2)_2]$  also reveals a short Pt–Pt bond distance of 2.554(1) Å (130).

The elimination of acetone from  $[\text{Pt}_2\text{Me}_2(\text{CO})_2(\mu\text{-}\eta^1\text{-C}_5\text{H}_4\text{PPh}_2)_2]$  to form  $[\text{Pt}_2(\text{CO})_2(\mu\text{-}\eta^1\text{-C}_5\text{H}_4\text{PPh}_2)_2]$  represents an example of the versatility of the dppc ligand, in that there is facile rearrangement between 1,1- and 1,2-substitution of the cyclopentadienyl ring. The former apparently better accommodates the metal–metal bond, whereas the latter bonding mode permits the two metal centers to remain further apart in the face-to-face platinum(II) dimers. Since  $\eta^1$ -cyclopentadienyl complexes of platinum are fluxional even at low temperatures (131), it might be anticipated that,

although migration of the metal around the ring is inhibited by the presence of the  $\text{PPh}_2$  substituent, migration between adjacent ring positions should be a low-energy process.

The reaction of  $[\text{Pt}_2\text{Me}_2(\mu\text{-C}_5\text{H}_4\text{PPh}_2)_2]$  with  $\text{P}(\text{CH}_2\text{CH}_2\text{CN})_3$  produces  $[\text{Pt}_2\{\text{P}(\text{CH}_2\text{CH}_2\text{CN})_3\}_2(\mu\text{-}\eta^1\text{-C}_5\text{H}_4\text{PPh}_2)_2]$  by elimination of ethane. Labeling studies show that this is a strictly intramolecular process at ambient temperature. In contrast, the elimination of acetone from  $[\text{Pt}_2(\text{CH}_3)_2(\text{CO})_2(\mu\text{-}\eta^1\text{-C}_5\text{H}_4\text{PPh}_2)_2]$  and its  $\text{CD}_3$  analog at  $50^\circ\text{C}$  produces a statistical mixture of  $d_0$ -,  $d_3$ -, and  $d_6$ -acetone, suggesting that cleavage of the dimer takes place at some point during the reaction (129). In fact, cleavage of the dimers by tertiary phosphines or  $\text{CNBu}^t$  does occur, producing complexes of the type  $[\text{PtMeL}_2(\text{Ph}_2\text{PC}_5\text{H}_4)]$ , in which the cyclopentadienyl group is uncoordinated (132).

## VIII

### SUMMARY

There is an extensive array of dimeric platinum complexes bridged by ligands as simple as halides or hydrides, or by bidentate ligands with a bite size appropriate to holding two metals together. Among the latter group,  $\text{dppm}$  and related ligands and  $\text{dppc}$  have been found to exhibit wide-ranging chemistry. These ligands confer substantial stability on the diplatinum system, such that substitution, oxidative addition, and reductive elimination reactions within a dimeric framework can be investigated. These are of intrinsic interest, since they provide the opportunity to study the mechanisms of reactions involving two metal centers, and dimeric systems may also be considered as the simplest models for platinum surfaces.

### REFERENCES

1. P. L. Goggin and R. J. Goodfellow, *J. Chem. Soc. Dalton Trans.*, 2355 (1973).
2. R. J. Goodfellow, I. R. Herbert, and A. G. Orpen, *J. Chem. Soc. Chem. Commun.*, 1386 (1983).
3. C. Couture, D. H. Farrar, D. S. Fisher, and R. R. Gukathasan, *Organometallics* 6, 532 (1987).
4. R. Bender, P. Braunstein, A. Tiripicchio, and M. Tiripicchio-Camellini, *J. Chem. Soc. Chem. Commun.*, 42 (1984).
5. F. R. Hartley, "The Chemistry of Platinum and Palladium." Applied Science, London, 1973.
6. G. K. Anderson and R. J. Cross, *J. Chem. Soc. Dalton Trans.*, 1988 (1980).
7. G. K. Anderson and R. J. Cross, *J. Chem. Soc. Dalton Trans.*, 1246 (1979).
8. C. Eaborn, K. J. Odell, and A. Pidcock, *J. Chem. Soc. Dalton Trans.*, 1288 (1978).

9. R. J. Puddephatt, M. A. Thomson, L. Manojlovic-Muir, K. W. Muir, A. A. Frew, and M. P. Brown, *J. Chem. Soc. Chem. Commun.*, 805 (1981).
10. D. P. Bancroft, F. A. Cotton, L. R. Falvello, and W. Schwotzer, *Inorg. Chem.* **25**, 763 (1986).
11. J. D. Scott and R. J. Puddephatt, *J. Chem. Soc. Chem. Commun.*, 193 (1984).
12. M. Lashanizadehgan, M. Rashidi, J. E. Hux, R. J. Puddephatt, and S. S. M. Ling, *J. Organomet. Chem.* **269**, 317 (1984).
13. R. S. Paonessa and W. C. Trogler, *Inorg. Chem.* **22**, 1038 (1983).
14. F. Bachechi, G. Bracher, D. M. Grove, B. Kellenberger, P. S. Pregosin, L. M. Venanzi, and L. Zambonelli, *Inorg. Chem.* **22**, 1031 (1983).
15. C. B. Knobler, H. D. Kaesz, G. Minghetti, A. L. Bandini, G. Banditelli, and F. Bonati, *Inorg. Chem.* **22**, 2324 (1983).
16. M. Y. Chiang, R. Bau, G. Minghetti, A. L. Bandini, G. Banditelli, and T. F. Koetzle, *Inorg. Chem.* **23**, 122 (1984).
17. B. S. Haggerty, C. E. Housecroft, A. L. Rheingold, and B. A. M. Shaykh, *J. Chem. Soc. Dalton Trans.*, 2175 (1991).
18. G. Minghetti, A. L. Bandini, G. Banditelli, F. Bonati, R. Szostak, C. E. Strouse, C. B. Knobler, and H. D. Kaesz, *Inorg. Chem.* **22**, 2332 (1983).
19. A. L. Bandini, G. Banditelli, M. A. Cinellu, G. Sanna, G. Minghetti, F. Desmartin, and M. Manassero, *Inorg. Chem.* **28**, 404 (1989).
20. G. Minghetti, A. Albinati, A. L. Bandini, and G. Banditelli, *Angew. Chem. Int. Ed. Engl.* **24**, 120 (1985).
21. D. Carmichael, P. B. Hitchcock, J. F. Nixon, and A. Pidcock, *J. Chem. Soc. Chem. Commun.*, 1554 (1988).
22. D. Afzal and C. M. Lukehart, *Organometallics* **6**, 546 (1987).
23. D. Afzal, P. G. Lenhert, and C. M. Lukehart, *J. Am. Chem. Soc.* **106**, 3050 (1984).
24. E. Baralt, E. A. Boudreaux, J. N. Demas, P. G. Lenhert, C. M. Lukehart, A. T. McPhail, D. R. McPhail, J. B. Meyers, Jr., L. A. Sacksteder, and W. R. True, *Organometallics* **8**, 2417 (1989).
25. E. Baralt and C. M. Lukehart, *Inorg. Chem.* **29**, 2870 (1990).
26. H. Ogawa, K. Onitsuka, T. Joh, S. Takahashi, Y. Yamamoto, and H. Yamazaki, *Organometallics* **7**, 2257 (1988).
27. R. Uson, J. Fornies, M. Tomas, J. M. Casas, F. A. Cotton, L. R. Falvello, and R. Llusar, *Organometallics* **7**, 2279 (1988).
28. R. Uson, J. Fornies, M. Tomas, J. M. Casas, and R. Navarro, *J. Chem. Soc. Dalton Trans.*, 169 (1989).
29. R. Uson, J. Fornies, P. Espinet, C. Fortuno, M. Tomas, and A. J. Welch, *J. Chem. Soc. Dalton Trans.*, 1583 (1989).
30. N. M. Boag, R. J. Goodfellow, M. Green, B. Hessner, J. A. K. Howard, and F. G. A. Stone, *J. Chem. Soc. Dalton Trans.*, 2585 (1983).
31. N. M. Boag, *Organometallics* **7**, 1446 (1988).
32. P. Thometzek and H. Werner, *Organometallics* **6**, 1169 (1987).
33. T. G. Appleton and M. A. Bennett, *J. Organomet. Chem.* **55**, C88 (1973).
34. D. P. Arnold, M. A. Bennett, M. S. Bilton, and G. B. Robertson, *J. Chem. Soc. Chem. Commun.*, 115 (1982).
35. D. P. Arnold, M. A. Bennett, G. M. McLaughlin, G. B. Robertson, and M. J. Whittaker, *J. Chem. Soc. Chem. Commun.*, 32 (1983).
36. S. Fallis and G. K. Anderson, *J. Organomet. Chem.*, submitted.
37. P. H. M. Budzelaar, P. W. N. M. van Leeuwen, C. F. Roobeek, and A. G. Orpen, *Organometallics* **11**, 23 (1992).

38. M. A. Bennett, D. E. Berry, and K. A. Beveridge, *Inorg. Chem.* **29**, 4148 (1990).
39. G. P. C. M. Dekker, C. J. Elsevier, S. N. Poelsma, K. Vrieze, P. W. N. M. van Leeuwen, W. J. J. Smeets, and A. L. Spek, *Inorg. Chim. Acta* **195**, 203 (1992).
40. M. A. Bennett, D. E. Berry, S. K. Bhargava, E. J. Ditzel, G. B. Robertson, and A. C. Willis, *J. Chem. Soc. Chem. Commun.*, 1613 (1987).
41. R. J. Puddephatt, *Chem. Soc. Rev.* **12**, 99 (1983).
42. A. L. Balch, in "Homogeneous Catalysis with Metal Phosphine Complexes" (L. H. Pignolet, ed.), pp. 167–213. Plenum, New York, 1983.
43. A. L. Balch, *Comments Inorg. Chem.* **3**, 51 (1984).
44. B. Chaudret, B. Delavaux, and R. Poilblanc, *Coord. Chem. Rev.* **86**, 191 (1988).
45. R. J. Puddephatt, L. Manojlovic-Muir, and K. W. Muir, *Polyhedron* **9**, 2767 (1990).
46. L. Manojlovic-Muir, K. W. Muir, M. C. Grossel, M. P. Brown, C. D. Nelson, A. Yavari, E. Kallas, R. P. Moulding, and K. R. Seddon, *J. Chem. Soc. Dalton Trans.*, 1955 (1986).
47. S. S. M. Ling, I. R. Jobe, A. J. McLennan, L. Manojlovic-Muir, K. W. Muir, and R. J. Puddephatt, *J. Chem. Soc. Chem. Commun.*, 566 (1985).
48. M. P. Brown, R. J. Puddephatt, M. Rashidi, and K. R. Seddon, *J. Chem. Soc. Dalton Trans.*, 951 (1977).
49. L. Manojlovic-Muir, K. W. Muir, and T. Solomun, *Acta Crystallogr. Sect. B: Struct. Crystallogr. Cryst. Chem.* **35**, 1237 (1979).
50. P. G. Pringle and B. L. Shaw, *J. Chem. Soc. Chem. Commun.*, 81 (1982).
51. R. Uson, J. Fornies, P. Espinet, and C. Fortuno, *J. Chem. Soc. Dalton Trans.*, 1849 (1986).
52. P. J. M. Ssebuwufu, *Inorg. Chim. Acta* **134**, 185 (1987).
53. M. P. Brown, S. J. Franklin, R. J. Puddephatt, M. A. Thomson, and K. R. Seddon, *J. Organomet. Chem.* **178**, 281 (1979).
54. M. P. Brown, R. J. Puddephatt, M. Rashidi, and K. R. Seddon, *J. Chem. Soc. Dalton Trans.*, 1540 (1978).
55. L. Manojlovic-Muir and T. Solomun, *J. Organomet. Chem.* **179**, 479 (1979).
56. R. J. Blau, J. H. Espenson, S. Kim, and R. A. Jacobson, *Inorg. Chem.* **25**, 757 (1986).
57. J. R. Fisher, A. J. Mills, S. Sumner, M. P. Brown, M. A. Thomson, R. J. Puddephatt, A. A. Frew, L. Manojlovic-Muir, and K. W. Muir, *Organometallics* **1**, 1421 (1982).
58. M. N. I. Khan, C. King, J.-C. Wang, S. Wang, and J. P. Fackler, Jr., *Inorg. Chem.* **28**, 4656 (1989).
59. L. Manojlovic-Muir and K. W. Muir, *J. Organomet. Chem.* **219**, 129 (1981).
60. R. J. Blau and J. H. Espenson, *J. Am. Chem. Soc.* **108**, 1962 (1986).
61. K. R. Grundy and K. N. Robertson, *Organometallics* **2**, 1736 (1983).
62. T. S. Cameron, P. A. Gardner, and K. R. Grundy, *J. Organomet. Chem.* **212**, C19 (1981).
63. F. Neve, M. Ghedini, A. Tiripicchio, and F. Ugozzoli, *Organometallics* **11**, 795 (1992).
64. G. J. Arsenault, L. Manojlovic-Muir, K. W. Muir, R. J. Puddephatt, and I. Treurnicht, *Angew. Chem. Int. Ed. Engl.* **26**, 86 (1987).
65. P. R. Sharp, *Inorg. Chem.* **25**, 4185 (1986).
66. M. P. Brown, J. R. Fisher, R. J. Puddephatt, and K. R. Seddon, *Inorg. Chem.* **18**, 2808 (1979).
67. S. Muralidharan and J. H. Espenson, *Inorg. Chem.* **22**, 2786 (1983).
68. S. Muralidharan, J. H. Espenson, and S. A. Ross, *Inorg. Chem.* **25**, 2557 (1986).
69. S. Muralidharan and J. H. Espenson, *J. Am. Chem. Soc.* **106**, 8104 (1984).
70. G. B. Jacobsen and B. L. Shaw, *J. Chem. Soc. Dalton Trans.*, 151 (1987).
71. A. L. Balch, R. R. Guimerans, J. Linehan, and F. E. Wood, *Inorg. Chem.* **24**, 2021 (1985).

72. J. P. Farr, F. E. Wood, and A. L. Balch, *Inorg. Chem.* **22**, 3387 (1983).
73. G. K. Anderson and R. Kumar, *J. Organomet. Chem.* **342**, 263 (1988).
74. S. J. Cooper, M. P. Brown, and R. J. Puddephatt, *Inorg. Chem.* **20**, 1374 (1981).
75. G. K. Anderson, H. C. Clark, and J. A. Davies, *J. Organomet. Chem.* **210**, 135 (1981).
76. K. A. Fallis, C. Xu, and G. K. Anderson, *Organometallics*, in press.
77. N. Hadj-Bagheri, R. J. Puddephatt, L. Manojlovic-Muir, and A. Stefanovic, *J. Chem. Soc. Dalton Trans.*, 535 (1990).
78. N. W. Alcock, T. J. Kemp, P. G. Pringle, P. Bergamini, and O. Traverso, *J. Chem. Soc. Dalton Trans.*, 1659 (1987).
79. F. S. M. Hassan, D. M. McEwan, P. G. Pringle, and B. L. Shaw, *J. Chem. Soc. Dalton Trans.*, 1501 (1985).
80. A. T. Hutton, P. G. Pringle, and B. L. Shaw, *J. Chem. Soc. Dalton Trans.*, 1677 (1985).
81. P. G. Pringle and B. L. Shaw, *J. Chem. Soc. Chem. Commun.*, 581 (1982).
82. R. J. Puddephatt and M. A. Thomson, *J. Organomet. Chem.* **238**, 231 (1982).
83. A. J. McLennan and R. J. Puddephatt, *Organometallics* **4**, 485 (1985).
84. G. K. Anderson and G. J. Lumetta, *J. Organomet. Chem.* **295**, 257 (1985).
85. C. R. Langrick, P. G. Pringle, and B. L. Shaw, *J. Chem. Soc. Dalton Trans.*, 1015 (1985).
86. L. Manojlovic-Muir, K. W. Muir, A. A. Frew, S. S. M. Ling, M. A. Thomson, and R. J. Puddephatt, *Organometallics* **3**, 1637 (1984).
87. K. A. Azam, G. Ferguson, S. S. M. Ling, M. Parvez, R. J. Puddephatt, and D. Srokowski, *Inorg. Chem.* **24**, 2799 (1985).
88. L. Manojlovic-Muir, I. R. Jobe, B. J. Maya, and R. J. Puddephatt, *J. Chem. Soc. Dalton Trans.*, 2117 (1987).
89. W. Radecka-Paryzek, A. J. McLennan, and R. J. Puddephatt, *Inorg. Chem.* **25**, 3097 (1986).
90. L. Manojlovic-Muir, S. S. M. Ling, and R. J. Puddephatt, *J. Chem. Soc. Dalton Trans.*, 151 (1986).
91. M. P. Brown, S. J. Cooper, A. A. Frew, L. Manojlovic-Muir, K. W. Muir, R. J. Puddephatt, K. R. Seddon, and M. A. Thomson, *Inorg. Chem.* **20**, 1500 (1981).
92. P. G. Pringle and B. L. Shaw, *J. Chem. Soc. Dalton Trans.*, 849 (1984).
93. N. Hadj-Bagheri and R. J. Puddephatt, *Polyhedron* **7**, 2695 (1988).
94. L. Manojlovic-Muir, K. W. Muir, I. Treurnicht, and R. J. Puddephatt, *Inorg. Chem.* **26**, 2418 (1987).
95. M. P. Brown, S. J. Cooper, A. A. Frew, L. Manojlovic-Muir, K. W. Muir, R. J. Puddephatt, and M. A. Thomson, *J. Chem. Soc. Dalton Trans.*, 299 (1982).
96. A. T. Hutton, B. Shabanzadeh, and B. L. Shaw, *J. Chem. Soc. Chem. Commun.*, 549 (1984).
97. A. T. Hutton, B. Shabanzadeh, and B. L. Shaw, *J. Chem. Soc. Chem. Commun.*, 1053 (1983).
98. K. A. Azam, A. A. Frew, B. R. Lloyd, L. Manojlovic-Muir, K. W. Muir, and R. J. Puddephatt, *Organometallics* **4**, 1400 (1985).
99. C.-M. Che, V. W.-W. Yam, W.-T. Wong, and T.-F. Lai, *Inorg. Chem.* **28**, 2908 (1989).
100. D. M. Hoffman and R. Hoffmann, *Inorg. Chem.* **20**, 3543 (1981).
101. S. S. M. Ling and R. J. Puddephatt, *Polyhedron* **5**, 1423 (1986).
102. R. J. Blau and J. H. Espenson, *Inorg. Chem.* **25**, 878 (1986).
103. M. P. Brown, J. R. Fisher, S. J. Franklin, R. J. Puddephatt, and K. R. Seddon, *J. Organomet. Chem.* **161**, C46 (1978).
104. J. V. Zeile Krevor, U. Simonis, A. Karson, C. Castro, and M. Aliakbar, *Inorg. Chem.* **31**, 312 (1992).

105. K. A. Azam and R. J. Puddephatt, *Organometallics* **2**, 1396 (1983).
106. M. P. Brown, R. J. Puddephatt, M. Rashidi, and K. R. Seddon, *J. Chem. Soc. Dalton Trans.*, 516 (1978).
107. R. J. Puddephatt and M. A. Thomson, *Inorg. Chem.* **21**, 725 (1982).
108. M. P. Brown, J. R. Fisher, R. H. Hill, R. J. Puddephatt, and K. R. Seddon, *Inorg. Chem.* **20**, 3516 (1981).
109. J. R. Fisher, A. J. Mills, S. Sumner, M. P. Brown, M. A. Thomson, R. J. Puddephatt, A. A. Frew, L. Manojlovic-Muir, and K. W. Muir, *Organometallics* **1**, 1421 (1982).
110. R. H. Hill and R. J. Puddephatt, *J. Am. Chem. Soc.* **105**, 5797 (1983).
111. A. J. McLennan and R. J. Puddephatt, *J. Chem. Soc. Chem. Commun.*, 422 (1986).
112. A. A. Frew, R. H. Hill, L. Manojlovic-Muir, K. W. Muir, and R. J. Puddephatt, *J. Chem. Soc. Chem. Commun.*, 198 (1982).
113. R. H. Hill, P. de Mayo, and R. J. Puddephatt, *Inorg. Chem.* **21**, 3642 (1982).
114. H. C. Foley, R. H. Morris, T. S. Targos, and G. L. Geoffroy, *J. Am. Chem. Soc.* **103**, 7337 (1981).
115. K. A. Azam, M. P. Brown, R. H. Hill, R. J. Puddephatt, and A. Yavari, *Organometallics* **3**, 697 (1984).
116. K. A. Azam, R. H. Hill, and R. J. Puddephatt, *Can. J. Chem.* **62**, 2029 (1984).
117. M. P. Brown, S. J. Cooper, A. A. Frew, L. Manojlovic-Muir, K. W. Muir, R. J. Puddephatt, and M. A. Thomson, *J. Organomet. Chem.* **198**, C33 (1980).
118. K. A. Azam, M. P. Brown, S. J. Cooper, and R. J. Puddephatt, *Organometallics* **1**, 1183 (1982).
119. M. P. Brown, A. Yavari, R. H. Hill, and R. J. Puddephatt, *J. Chem. Soc. Dalton Trans.*, 2421 (1985).
120. S. J. Young, B. Kellenberger, J. H. Reibenspies, S. E. Himmel, M. Manning, O. P. Anderson, and J. K. Stille, *J. Am. Chem. Soc.* **110**, 5744 (1988).
121. S. S. M. Ling, N. C. Payne, and R. J. Puddephatt, *Organometallics* **4**, 1546 (1985).
122. S. S. M. Ling, I. R. Jobe, L. Manojlovic-Muir, K. W. Muir, and R. J. Puddephatt, *Organometallics* **4**, 1198 (1985).
123. C. King, R. A. Auerbach, F. R. Fronczek, and D. M. Roundhill, *J. Am. Chem. Soc.* **108**, 5626 (1986).
124. C. King, D. M. Roundhill, M. K. Dickson, and F. R. Fronczek, *J. Chem. Soc. Dalton Trans.*, 2769 (1987).
125. D. M. Roundhill, *J. Am. Chem. Soc.* **107**, 4354 (1985).
126. M. Lin, K. A. Fallis, G. K. Anderson, N. P. Rath, and M. Y. Chiang, *J. Am. Chem. Soc.*, **114**, 4687 (1992).
127. F. T. Ladipo and G. K. Anderson, unpublished results.
128. X. He, A. Maisonnat, F. Dahan, and R. Poilblanc, *Organometallics* **8**, 2618 (1989).
129. G. K. Anderson, M. Lin, and N. P. Rath, *Organometallics* **9**, 2880 (1990).
130. N. W. Alcock, P. Bergamini, T. M. Gomes-Carniero, R. D. Jackson, J. Nicholls, A. G. Orpen, P. G. Pringle, S. Sostero, and O. Traverso, *J. Chem. Soc. Chem. Commun.*, 980 (1990).
131. G. K. Anderson, D. M. Black, R. J. Cross, F. J. Robertson, D. S. Rycroft, and R. K. M. Wat, *Organometallics* **9**, 2568 (1990).
132. G. K. Anderson, M. Lin, and M. Y. Chiang, *Organometallics* **9**, 288 (1990).



This Page Intentionally Left Blank

# Transition Metal Clusters in Homogeneous Catalysis

G. SÜSS-FINK and G. MEISTER

*Institut de Chimie  
Université de Neuchâtel  
CH-2000 Neuchâtel, Switzerland*

I. Introduction . . . . .	41
II. Catalytic Reactions Involving CO . . . . .	44
A. Carbonylation of Alcohols, Amines, and Heterocycles . . . . .	44
B. Carbon Monoxide-Mediated Deoxygenation of Oximes and Nitro Compounds . . . . .	46
III. Catalytic Reactions Involving H <sub>2</sub> . . . . .	49
A. Hydrogenation of Olefins . . . . .	49
B. Hydrogenation of Acetylenes . . . . .	60
C. Hydrogenation of Carbonyl Compounds . . . . .	64
D. Hydrogenation of Nitrogen-Containing Functions . . . . .	67
E. Hydrogen Transfer Reactions . . . . .	67
F. Related Reactions . . . . .	72
IV. Catalytic Reactions Involving CO and H <sub>2</sub> . . . . .	74
A. Syngas Reactions . . . . .	74
B. Hydroformylation Reactions . . . . .	80
C. Homologation Reactions . . . . .	90
D. Miscellaneous and Related Reactions . . . . .	93
V. Catalytic Reactions Involving CO and H <sub>2</sub> O . . . . .	95
A. Water-Gas Shift Reaction . . . . .	95
B. Hydroformylation Reactions Using Water as the Hydrogen Source . . . . .	99
C. Hydrogenation Reactions Using Water as the Hydrogen Source . . . . .	102
D. Miscellaneous and Related Reactions . . . . .	104
VI. Other Catalytic Reactions . . . . .	107
A. Isomerization and Rearrangement Reactions . . . . .	107
B. Carbon-Carbon Coupling Reactions . . . . .	112
C. Carbon-Nitrogen Coupling Reactions . . . . .	118
D. Miscellaneous Reactions . . . . .	121
VII. Conclusions . . . . .	122
References . . . . .	122

## I

## INTRODUCTION

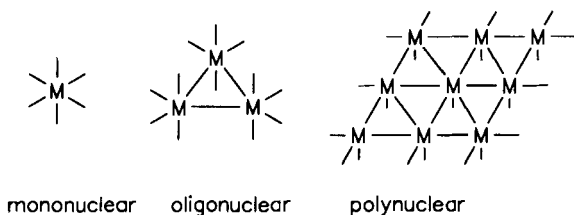
The past two and a half decades have witnessed a fast expanding chemistry of transition metal complexes containing more than one metal atom. Such complexes are generally referred to as "transition metal clusters." Several definitions have been proposed for the term "cluster," the one

most widely accepted being that given by Cotton (1). For the purpose of the present review, we define a transition metal cluster according to Johnson (2) simply as a discrete molecular unit containing at least three metal atoms, in which metal-metal bonding is present. Thus important classes of related compounds are excluded, such as dinuclear transition metal complexes with or without metal-metal bond, oligonuclear transition metal complexes in which the metal atoms are held together by bridging ligands, and transition metal derivatives of main-group metal compounds.

The rapid development of transition metal cluster chemistry was mainly stimulated by the prospects of catalytic applications. There are very reasonable arguments as to why transition metal clusters should have a considerable potential as homogeneous catalysts: Multisite interactions between the substrate molecule and more than one, preferably adjacent, metal center can facilitate activation and transformation of the substrate. Furthermore, the high mobility of the ligands in transition metal clusters can promote reactions between several molecules bonded to a cluster framework. These two aspects imply that, at least in principle, it should be possible to tailor a "cluster-based catalyst to measure" for a given substrate and a given transformation. Transition metal clusters can be designed in various geometries, and different metals can be joined together to accommodate specific reactivity patterns.

Most transition metal clusters are soluble molecular compounds that react in a homogeneous phase with substrates and can be isolated and characterized like mononuclear metal complexes. On the other hand, metal clusters show typical phenomena known for polynuclear metal surfaces such as polycentric ligand-metal bonds and delocalized metal-metal bonds. Chini (3) was the first to realize the common features of metal cluster ligand shells and molecules chemisorbed on metal surfaces and to suggest metal clusters as models for catalytic reactions on metal surfaces. In 1975, Lewis and Johnson (4), Ugo (5), and Muetterties (6) pointed out with many examples the striking analogy between metal clusters and metal surfaces. Muetterties (7) formulated what is known as the "cluster-surface analogy" by considering metal clusters as tiny pieces of metal with chemisorbed species on the periphery. Consequently, one of the main interests in cluster chemistry arises from studying fundamental transformations of ligands on a cluster skeleton as models for steps discussed in heterogeneous catalysis.

As oligonuclear species, metal clusters can be placed between mononuclear metal complexes on the one hand and polynuclear metal surfaces on the other (Scheme 1). Because of this intermediary position between typical homogeneous and typical heterogeneous catalysts, transition metal clusters may not only provide models for heterogeneous catalysts, but they



SCHEME 1. Metal clusters in the no-man's land between metal complexes and metal surfaces.

may equally serve themselves as homogeneous catalysts. The potential of transition metal clusters as homogeneous catalysts was pointed out by Johnson and Lewis (8). Muetterties and Krause (9) were the first to claim unique catalytic properties for transition metal clusters, raising expectations that transition metal clusters might provide a new generation of soluble catalysts.

The implication of transition metal clusters in catalytic reactions has been addressed by several workers (10–15). The use of cluster compounds as homogeneous catalysts has already been reviewed in general (9,16–21), and special aspects have also been treated (22–29). There are also a considerable number of reviews on supported metal clusters as heterogeneous catalysts (17,29–38). The present review considers exclusively catalytic applications of transition metal clusters in a homogeneous phase.

The catalytic applications quoted in this article are regarded as cluster-based reactions as far as these reactions are catalyzed upon addition of a transition metal cluster; whether the cluster is a catalyst precursor or a catalytically active species is not a crucial point in our discussion. Criteria for identifying transition metal cluster-catalyzed reactions as opposed to those in which the cluster functions only as a catalyst precursor have been proposed by Laine (39), but the question of cluster disintegration throughout the reaction remains a debatable point, since in most catalytic reactions the mechanism is not clear. Furthermore, no distinction is made between homogeneous catalysis by mixed-metal clusters and homogeneous reactions catalyzed by mixtures of transition metal clusters because the nature of the synergistic effects involved has never been elucidated in a convincing way. The structure of this review follows only criteria of reaction typology.

One of the major problems encountered in reviewing catalytic applications of transition metal clusters is the need for comparable data describing the catalytic activity of the clusters employed. There is no consistency in the use of the term "catalytic turnover." Very often it means the number of catalytic cycles irrespective of the time; sometimes it is related to the time

unit. In general it is calculated on the basis of the product formed but sometimes on the basis of the starting material consumed, without taking into account side products. Several authors give only yields based on the organic starting material; in many cases the necessary data are missing completely. Throughout this text the term catalytic turnover is defined as "the number of moles of product per mole of catalyst." For continuous reactions, it is more useful to describe the activity by "the number of moles of product per mole of catalyst formed in unit time"; this is referred to as "catalytic turnover rate." Wherever possible, all published data have been recalculated to the unit moles of product per mole of catalyst (catalytic turnover, CT). The reaction time is given as complementary information.

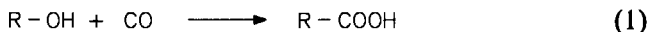
## II

### CATALYTIC REACTIONS INVOLVING CO

The vast majority of transition metal clusters contain carbonyl ligands, which have been shown in many cases to be fluxional on the metal skeleton of the cluster (40,41). Therefore, the most obvious reactions to be catalyzed by such clusters should be those involving carbon monoxide. In fact, catalytic carbonylations are frequently encountered with transition metal carbonyl cluster catalysts, but very often the carbonylation step is followed by a consecutive step, e.g., a hydrogenation step, to give an overall hydroformylation. Simple carbonylation reactions have nevertheless been observed for various structures.

#### A. Carbonylation of Alcohols, Amines, and Heterocycles

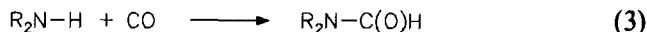
Alcohols are versatile building blocks for the synthesis of basic organic molecules. Thus the carbonylation of a primary alcohol can lead either to the corresponding acid or to the corresponding formyl ester:



The carbonylation of methanol to give acetic acid, according to Eq.(1), based on the catalyst  $[\text{Rh}(\text{CO})_2\text{I}_2]^-$ , is a major industrial process (Monsanto acetic acid process). However, ruthenium clusters as catalysts seem to favor the insertion of carbon monoxide into the O-H and not into the C-O bond, according to Eq.(2).  $\text{Ru}_3(\text{CO})_{12}$  in basic solution converts methanol to methyl formate with 90% selectivity (400–450 bar CO,

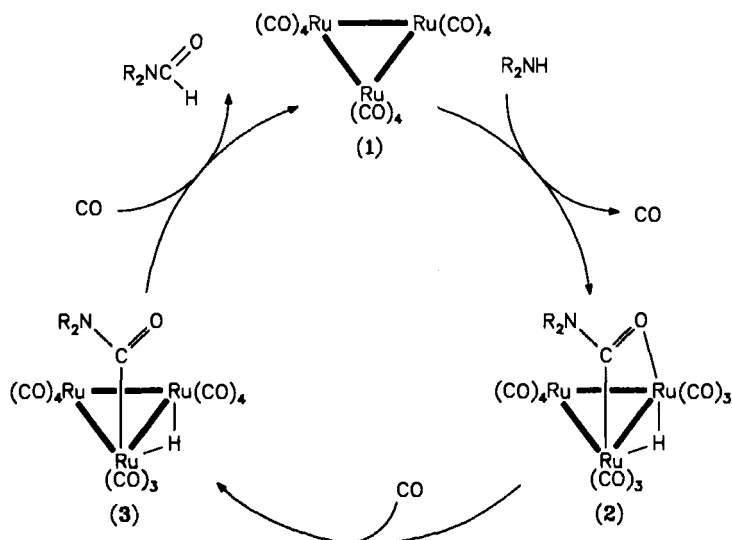
200°C, 2 hr, CT 1100). After the catalytic reaction, the cluster anion  $[\text{HRu}_3(\text{CO})_{11}]^-$  was detected in the reaction solution. It is also noteworthy that the mononuclear complex  $\text{RuCl}_2(\text{PPh}_3)_3$  has no catalytic effect (42). In the presence of iodine,  $\text{Ru}_3(\text{CO})_{12}$  converts ethanol mainly into ethyl acetate (2.5 ml EtOH, 0.117 mmol  $\text{Ru}_3(\text{CO})_{12}$ , 0.75 mmol  $\text{I}_2$ , 450 bar CO, 200°C, 2 hr, conversion 88%, selectivity 38%, CT 122) (43a). The cluster anion  $[\text{FeCo}_3(\text{CO})_{12}]^-$ , with methyl iodide as cocatalyst, is reported to catalyze the conversion of methanol into methyl acetate with 96% selectivity (toluene, 180°C, 270 bar CO, CT 4600) (43b). The carbonylation of methanol to give methyl formate, using  $\text{CO}_2$  and  $\text{H}_2$  as carbon monoxide source (implying the water-gas shift equilibrium, cf. Section V.A) is catalyzed by the cluster anions  $[\text{HFe}_3(\text{CO})_{11}]^-$  (175°C, 41 bar, 4 days, CT 6) (43c) or  $[\text{HRu}_3(\text{CO})_{11}]^-$  (125°C, 17 bar, 24 hr, CT 4) (43d).

Amines are carbonylated to give the corresponding formamides



in the presence of various ruthenium clusters.  $\text{Ru}_3(\text{CO})_{12}$  was reported to convert octyl amine into octyl formamide at 180°C and under a pressure of 39 bar CO (benzene, 6 hr, conversion 100%, selectivity 91%, CT 540), whereas the mononuclear complex  $\text{RuCl}_2(\text{PPh}_3)_3$  is inactive; the rhodium cluster  $\text{Rh}_6(\text{CO})_{16}$  catalyzes the same reaction with reduced conversion and reduced selectivity (44). Piperidine is converted specifically into the corresponding formamide by  $\text{Ru}_3(\text{CO})_{12}$  under mild conditions (neat, 1 bar CO, 75°C, CT 450) (45). Piperidine and other cyclic amines (3-methylpiperidine, pyrrolidine, heptamethyleneimine, morpholine) react with carbon monoxide to give the corresponding formamides in the presence of catalytic amounts of  $\text{Ru}_3(\text{CO})_{12}$ ,  $[\text{HRu}_3(\text{CO})_{11}]^-$ , or  $[\text{H}_3\text{Ru}_4(\text{CO})_{12}]^-$ . Interestingly, the carbonylation can be performed either with carbon monoxide or with a mixture of carbon dioxide and hydrogen. For instance, the reaction of piperidine with  $\text{Na}[\text{HRu}_3(\text{CO})_{11}]$  gives *N*-formylpiperidine under a CO pressure of 70 bar (THF, 190°C, 24 hr, conversion 97.3%, selectivity 99.9%, CT 1002), while the analogous reaction performed under a pressure of 60 bar  $\text{H}_2$  and 60 bar  $\text{CO}_2$  gave the same product with a catalytic turnover of 850 (140°C, 24 hr, conversion 92.8%, selectivity 99.9%) (46).

When the neutral cluster  $\text{Ru}_3(\text{CO})_{12}$  (**1**) was employed as the catalyst for the carbonylation of cyclic amines, the carbamoylato clusters of type **2** were isolated from the reaction mixture and characterized. In the case of piperidine, the corresponding carbamoylato cluster  $\text{HRu}_3(\text{CO})_{10}[\text{OCN}(\text{CH}_2)_5]$  (**2a**) was shown to have the same catalytic properties as **1**. On the basis of these findings, a catalytic cycle involving exclusively trinuclear ruthenium species has been proposed (Scheme 2): The amine is believed to attack a carbonyl ligand in **1**, which provokes the formation of



SCHEME 2. Proposed catalytic cycle for the carbonylation of amines catalysed by  $\text{Ru}_3(\text{CO})_{12}$  (46).

a  $\mu_2$ - $\eta^2$ -carbamoyl ligand, accompanied by CO elimination. The intermediate 2 is then converted into a  $\mu_1$ - $\eta^1$ -carbamoylato intermediate 3 by the action of carbon monoxide. Further reaction of CO leads to the elimination of the formamide and to the reconstitution of 1.

The regiospecific carbonylation of oxetanes and thietanes, resulting in a ring expansion



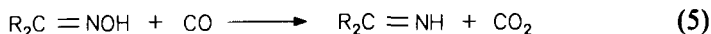
can be catalyzed by a mixture of  $\text{Ru}_3(\text{CO})_{12}$  and  $\text{Co}_2(\text{CO})_8$ ; the individual components of the binary catalyst system are also active, but to a lower extent. Oxetane is converted into  $\gamma$ -butyrolactone at  $190^\circ\text{C}$  under a CO pressure of 60 bar (DME,  $\text{Ru}_3(\text{CO})_{12}/\text{Co}_2(\text{CO})_8$  1 : 1, 2 days, CT 7) (47).

#### B. Carbon Monoxide-Mediated Deoxygenation of Oximes and Nitro Compounds

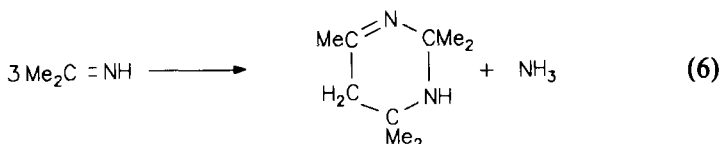
In a number of catalytic reactions, carbon monoxide can serve to eliminate oxygen from organic substrates. In particular, nitrogen-containing functions can be reduced in this way to give imine, amine, or even nitro functions. Accordingly, carbon dioxide is formed in these reactions.

Ketoximes have been found to give the corresponding ketimines accord-

ing to



in the presence of  $Ru_3(CO)_{12}$  as the catalyst (48,49): For instance, propiophenone oxime is converted into its imine with 100% conversion and 100% selectivity (benzene, 20 bar CO, 100°C, 4 hr, CT 50).  $Rh_6(CO)_{16}$  is less active and less selective than  $Ru_3(CO)_{12}$  (48). In the case of acetone oxime ( $R = Me$ ) the intermediary imine formed according to Eq.(5) spontaneously undergoes cyclocondensation to give 2,3,4,5-tetrahydro-2,2,4,4,6-pentamethylpyridine (acetone), thus providing a simple catalytic access to anhydrous acetone from acetone oxime and carbon monoxide



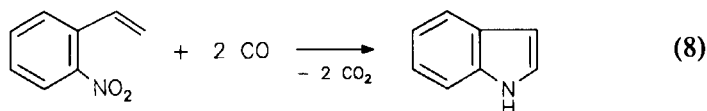
The reaction proceeds with  $Ru_3(CO)_{12}$  in cyclohexane at 100°C under a CO pressure of 50 bar; after 17 hr the conversion is 85%, corresponding to a catalytic turnover of 825 (49). The isolation of the dinuclear bisoximato complexes  $Ru_2(CO)_5(Me_2CNO)_2(Me_2CNOH)$  (49) and  $Ru_2(CO)_4(Me_2CNO)_2(Me_2CNOH)_2$  (50) suggests a catalytic cycle involving dinuclear intermediates.

Aldoximes react with CO in the presence of  $Rh_6(CO)_{16}$  to give the corresponding nitriles according to



Thus propanal oxime gives propionitrile in 73% yield together with 12% of propanol ( $H_2O$ /tetramethyl-1,3-propanediamine/ethoxyethanol, 8 bar CO, 40°C, 5 hr, CT 73) (51).

Another CO-mediated reaction was observed for *ortho*-nitrostyrenes: Both  $Ru_3(CO)_{12}$  and  $Rh_6(CO)_{16}$  catalyze independently the formation of the corresponding indoles

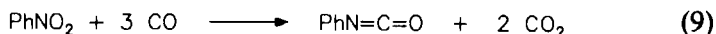


*ortho*-Aminostyrenes and other aromatics are formed as side products. Under a carbon monoxide pressure of 80 bar and 220°C in toluene,  $Ru_3(CO)_{12}$  gives 18% yield of indole (CT 9) and  $Rh_6(CO)_{16}$  gives 25% (CT 13) (52). The cluster  $Ru_3(CO)_{12}$  is also reported in a poorly organized



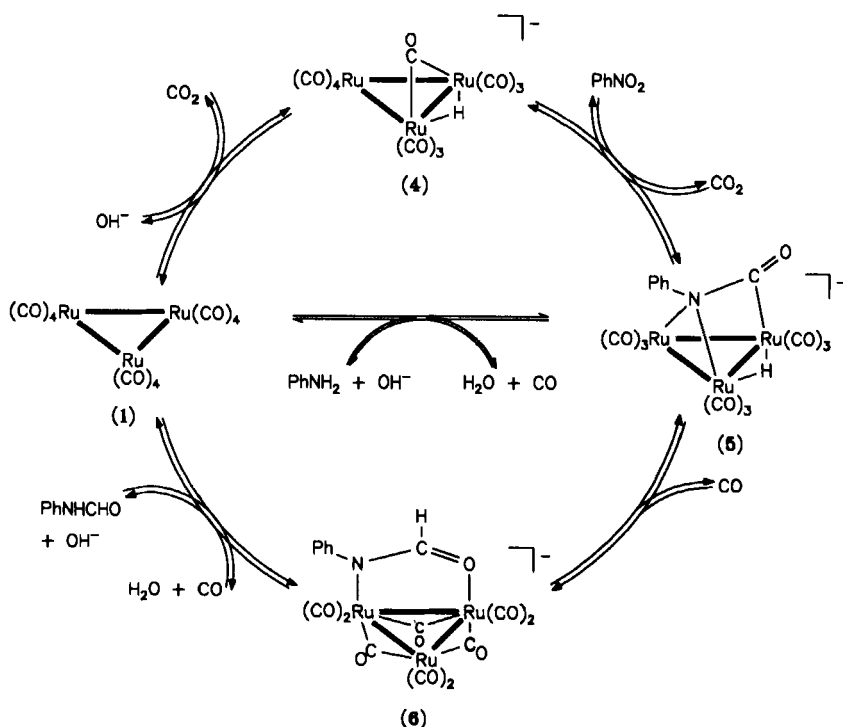
paper to catalyze the deoxygenation of *ortho*-nitrophenylallyl ether with CO to give a mixture of aromatic compounds, the composition of which is not entirely clear (53).

A very interesting deoxygenation reaction, in which carbon monoxide serves as both, a deoxygenating agent as well as a carbonylating agent, was found recently by Bhaduri *et al.*: The formation of phenyl isocyanate from nitrobenzene with carbon monoxide is catalyzed by trinuclear ruthenium clusters such as  $\text{Ru}_3(\text{CO})_{12}$  or  $[\text{HRu}_3(\text{CO})_{11}]^-$ :



In the latter case a conversion of 100% was observed in acetonitrile solution at  $140^\circ\text{C}$  under a CO pressure of 21 bar within 3 hr, the selectivity is 95% (with 5% aniline formed), and the catalytic turnover is 57 (54).

The synthesis and structural characterization (Scheme 3) of the cluster anions  $[\text{HRu}_3(\text{CO})_9(\text{PhNCO})]^-$  (5) (55) and  $[\text{HRu}_3(\text{CO})_{10}(\text{PhNCHO})]^-$  (6) (56a) and their tests for the catalytic reaction suggest the formation of



SCHEME 3. Proposed catalytic cycle for the deoxygenating carbonylation of nitrobenzene with water as promoter according to (56a).

formanilide and aniline along with phenyl isocyanate. On the basis of these findings, it has been proposed that the anionic catalyst **4** is transformed by nitrobenzene into anion **5**, which takes up carbon monoxide to give anion **6**. Hydrolysis in the presence of CO gives the neutral carbonyl and the intermediate  $\text{PhNHCHO}$ . Basic decarbonylation of **1** closes the catalytic cycle to **4** (Scheme 3) while formanilide undergoes dehydrogenation to give phenyl isocyanate (56a). In the absence of water and methanol, the catalytic reaction is believed to proceed through the intermediacy of only neutral trinuclear ruthenium clusters such as  $\text{Ru}_3(\text{CO})_{10}(\text{NPh})$ ,  $\text{H}_2\text{Ru}_3(\text{CO})_9(\text{NPh})$ , and  $\text{HRu}_3(\text{CO})_{10}(\text{PhNH})$  (56b).

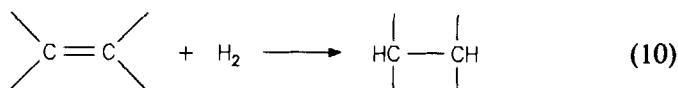
### III

#### CATALYTIC REACTIONS INVOLVING $\text{H}_2$

Hydrogenation reactions rank among the best studied processes in homogeneous catalysis. Numerous hydrogenation catalysts, both homogeneous and heterogeneous, are known, some of which are transition metal clusters. For several cases, special properties such as high selectivity have been observed with cluster compounds.

##### A. Hydrogenation of Olefins

A considerable number of transition metal clusters have been reported to catalyze the hydrogenation of olefins to alkanes:



Catalytic turnover and practicability vary a great deal; the details are presented in Table I (57–73).

Photocatalytic hydrogenation of olefinic carbon–carbon double bonds has also been studied with several transition metal clusters.  $\text{H}_4\text{Ru}_4(\text{CO})_{12}$  catalyzes the hydrogenation of ethylene to ethane in heptane at  $35^\circ\text{C}$ , the ethylene and hydrogen partial pressures being 0.13 bar; the catalytic turnover in these experiments was less than 1 (74). Kinetic studies indicate that photodissociation of CO from  $\text{H}_4\text{Ru}_4(\text{CO})_{12}$  is the first step of the catalytic cycle (75). The iron cluster  $\text{Fe}_3(\text{CO})_{10}(\text{NSiMe}_3)$  has been used for the photocatalytic hydrogenation of several olefins; the resulting cluster  $\text{H}_2\text{Fe}_3(\text{CO})_9(\text{NSiMe}_3)$  is assumed to act as the catalyst (76). In this fashion, methyl acrylate can be converted into methyl propionate in toluene

TABLE I  
HYDROGENATION OF ALKENES TO ALKANES BY VARIOUS TRANSITION METAL CLUSTERS

Substrate	Product (%)	Catalyst	Conditions	Time	Catalytic turnover	Remarks	References
Cyclohexene	Cyclohexane	$\text{Os}_3(\text{CO})_{12}$	Toluene, 150°C, 30 bar	10 hr	400	$\text{H}_4\text{Os}_4(\text{CO})_{12}$ formed	(57)
Cyclohexene	Cyclohexane	$[\text{N}(\text{PPh}_3)_2]\text{-}[\text{HOs}_3(\text{CO})_{11}]$	Toluene, 150°C, 30 bar	10 hr	30	Cluster unchanged	(57)
Cyclohexene	Cyclohexane	$\text{H}_4\text{Os}_4(\text{CO})_{12}$	Toluene, 150°C, 30 bar	10 hr	610	Cluster unchanged	(57)
Cyclohexene	Cyclohexane	$[\text{N}(\text{PPh}_3)_2]\text{-}[\text{H}_3\text{Os}_4(\text{CO})_{12}]$	Toluene, 150°C, 30 bar	10 hr	80	Cluster unchanged	(57)
Cyclohexene	Cyclohexane	$\text{H}_3\text{Os}_4(\text{CO})_{12}\text{I}$	Toluene, 150°C, 30 bar	10 hr	880	Cluster unchanged	(57)
g Cyclohexene	Cyclohexane	$\text{H}_3\text{Os}_4(\text{CO})_{12}(\text{NO})$	Toluene, 150°C, 30 bar	10 hr	480	$\text{H}_4\text{Os}_4(\text{CO})_{12}$ formed	(57)
Cyclohexene	Cyclohexane	$[\text{H}_3\text{Os}_4(\text{CO})_{12}\text{-}(\text{MeCN})_2][\text{BF}_4]$	Toluene, 150°C, 30 bar	10 hr	630	$\text{H}_4\text{Os}_4(\text{CO})_{12}$ formed	(57)
Cyclohexene	Cyclohexane	$\text{Ru}_3(\text{CO})_9(\text{PPh}_3)_3$	Cyclohexane, 70°C, 1.7 bar	5 hr	18	$\text{H}_4\text{Ru}_4(\text{CO})_{12-x}$ ( $\text{PPh}_3$ ) <sub>x</sub> formed	(58)
Cyclohexene	Cyclohexane	$\text{Ru}_3(\text{CO})_7(\text{PPh}_2)_2\text{-}(\text{C}_6\text{H}_4)$	No solvent, 70°C, 1.7 bar	5 hr	19	Cluster unchanged	(58)
Cyclohexene	Cyclohexane	$\text{H}_4\text{Ru}_4(\text{CO})_{12}$	THF, 80°C, 40 bar	NG <sup>a</sup>	c.t.r. 0.567 s <sup>-1</sup>	Cluster unchanged	(59)
Cyclohexene	Cyclohexane	$\text{H}_3\text{Ru}_4(\text{CO})_{10}\text{-}(\text{PhPCH}_2\text{PPh}_2)$	THF, 80°C, 40 bar	NG	c.t.r. 0.211 s <sup>-1</sup>	Cluster unchanged	(59)
Cyclohexene	Cyclohexane	$\text{H}_4\text{Ru}_4(\text{CO})_{10}\text{-}(\text{Ph}_2\text{PCH}_2\text{PPh}_2)$	THF, 80°C, 40 bar	NG	c.t.r. 0.194 s <sup>-1</sup>	$\text{H}_3\text{Ru}_4(\text{CO})_{10}\text{-}(\text{PhPCH}_2\text{PPh}_2)$ formed	(59)
Cyclohexene	Cyclohexane	$\text{H}_2\text{Ru}_3(\text{O})(\text{CO})_5\text{-}(\text{DPPM})_2$	THF, 55°C, 7.5 bar	10 hr	708	Cluster unchanged, conversion 85%	(60)

Cyclohexene	Cyclohexane	$\text{H}_2\text{Ru}_3(\text{S})(\text{CO})_5\text{-(DPPM)}_2$	THF, 55°C, 7.5 bar	10 hr	647	Cluster unchanged, conversion 75%	(60)
Cyclohexene	Cyclohexane	$\text{Pt}_2\text{Ir}_2(\text{CO})_7\text{-(PPh}_3)_3$	No solvent, 70°C, 0.7 bar	5 hr	1600	Cluster unchanged	(61)
Cyclohexene	Cyclohexane	$\text{Pt}_2\text{Co}_2(\text{CO})_8\text{-(PPh}_3)_2$	Toluene, 50°C, 35 bar	40 hr	7	Cluster desinte- gration, conver- sion 6%	(62)
Cyclohexene	Cyclohexane	$\text{Rh}_6(\text{CO})_{12}\text{-[P(OPh)}_3]_4$	60°C	NG	NG	No details	(63)
Cyclohexene	Cyclohexane	$\text{Rh}_6(\text{CO})_{10}(\text{PPh}_3)_6$	Benzene, 25°C, 2 bar	1 hr	190	Cluster unchanged	(64)
Styrene	Ethylbenzene	$\text{H}_3\text{Os}_4(\text{CO})_{12}\text{I}$	Decalin, 100°C, 1 bar	2 hr	1166	Fragmentation probable	(65)
Styrene	Ethylbenzene	$\text{H}_4\text{Os}_4(\text{CO})_{12}$	Decalin, 100°C, 1 bar	2 hr	174	Fragmentation probable	(65)
Styrene	Ethylbenzene	$[\text{N}(\text{PPh}_3)_2]\text{-[H}_2\text{Os}_4(\text{CO})_{12}\text{I}]$	Decalin, 100°C, 1 bar	2 hr	126	Fragmentation probable	(65)
Styrene	Ethylbenzene	$[\text{N}(\text{PPh}_3)_2]\text{-[H}_3\text{Os}_4(\text{CO})_{12}]$	Decalin, 100°C, 1 bar	2 hr	104	Fragmentation probable	(65)
Styrene	Ethylbenzene (100)	$\text{Co}_2\text{Rh}_2(\text{CO})_{12}$	Neat, 27°C, 2 bar, $\text{P(OPh)}_3$	2 hr	967	$\text{Co}_4(\text{CO})_{12}$ inactive	(66)
Styrene	Ethylbenzene (100)	$\text{Co}_3\text{Rh}(\text{CO})_{12}$	Neat, 27°C, 2 bar, $\text{P(OPh)}_3$	2 hr	NG	$\text{Co}_4(\text{CO})_{12}$ inactive	(66a)
Styrene	Ethylbenzene (100)	$\text{HCoRu}_2(\text{CO})_5\text{-(PMe)}$	Cyclohexane, 60°C, 80 bar	45 hr	2719	Cluster unchanged	(66b)
Hex-1-ene	Hexane	$\text{H}_3\text{Ni}_4(\text{C}_3\text{H}_5)_4$	No solvent, 40°C, 1 bar	40 hr	≈ 300	Quantitative	(67)
Hex-2-ene	Hexane	$\text{H}_3\text{Ni}_4(\text{C}_3\text{H}_5)_4$	No solvent, 40°C, 1 bar	40 hr	≈ 150	Conversion 60%, Z isomer reacts faster	(67)
3,3-Dimethylbut- 1-ene	2,2-Dimethylbutan	$[\text{N}(\text{PPh}_3)_2][\text{Ru}_3\text{-(CO)}_{10}(\text{NCO})]$	THF, 25°C, 0.75 bar	18 min	104		(68)

(continued)

TABLE I (continued)

	Substrate	Product (%)	Catalyst	Conditions	Time	Catalytic turnover	Remarks	References
	3,3-Dimethylbut-1-ene	2,2-Dimethylbutan	$\text{CpNiOs}_3\text{H}_3(\text{CO})_9$	<i>n</i> -Octane, 110°C, 1 bar	8 hr	1440	$\text{Cp}_3\text{Ni}_3\text{Os}_3(\text{CO})_9$ formed, conversion 43%	(69)
	Pent-1-ene	Pentane	$\text{H}_3\text{Ni}_4(\text{C}_5\text{H}_5)_4$	No solvent, 40°C, 1 bar	15 hr	≈ 300	Quantitative	(67)
	Cyclohex-1-en-2-one	Cyclohexanone, Cyclohexanol (1.45:1)	$\text{Ru}_3(\text{CO})_9(\text{PPh}_3)_3$	Cyclohexane, 70°C, 1.7 bar	5 hr	17	$\text{Ru}_3(\text{CO})_7(\text{PPh}_2)_2-(\text{C}_6\text{H}_4)$ formed	(58)
58	Cyclohex-1-en-2-one	Cyclohexanone, Cyclohexanol (13:1)	$\text{Ru}_3(\text{CO})_7(\text{PPh}_2)_2-(\text{C}_6\text{H}_4)$	Cyclohexane, 70°C, 1.7 bar	5 hr	70	Cluster unchanged	(58)
	Propene	Propane	$\text{Co}_3(\text{CO})_6(\text{PBu}_3)_3$	Heptane, 65°C, 15 bar	NG	NG	Substrate/cluster ratio 50	(70)
	( <i>Z</i> )-Penta-1,3-diene	( <i>E</i> )-Pent-2-ene (18), ( <i>Z</i> )-pent-2-ene (13), pent-1-ene (7), pentane (1)	$\text{CpNiOs}_3\text{H}_3(\text{CO})_9$	<i>n</i> -Octane, 120°C, 1 bar	20 min	226 <sup>b</sup>	Cluster decomposition 40%, conversion 41%	(71a)
	( <i>Z</i> )-Penta-1,3-diene	( <i>E</i> )-Pent-2-ene (48), ( <i>Z</i> )-pent-2-ene (12), pent-1-ene (7), pentane (1)	$\text{Ru}_3(\text{CO})_{12}$	Toluene, 80°C, 1 bar	16 hr	27 <sup>b</sup>	Conversion 68%	(72)
	( <i>Z</i> )-Penta-1,3-diene	( <i>E</i> )-Pent-2-ene (28), ( <i>Z</i> )-pent-2-ene (21), pent-1-ene (25), pentane (1)	$\text{CpNiOs}_3\text{H}_3(\text{CO})_8-(\text{PPh}_2\text{H})$	<i>n</i> -Octane, 120°C, 0.9 bar	4 hr	337 <sup>b</sup>		(62, 71b)

(Z)-Penta-1,3-diene	(E)-Pent-2-ene (28), (Z)-pent-2-ene (21), pent-1-ene (15), pentane (1)	CpNiOs <sub>3</sub> H <sub>3</sub> (CO) <sub>9</sub>	<i>n</i> -Octane, 120°C, 0.9 bar	6 hr	247 <sup>b</sup>		(71b,c)
(E)-Penta-1,3-diene	(E)-Pent-2-ene (44), (Z)-pent-2-ene (12), pent-1-ene (2), pentane (7)	Ru <sub>3</sub> (CO) <sub>12</sub>	Toluene, 80°C, 1 bar	16 hr	26 <sup>b</sup>	Conversion 65%	(72)
Penta-1,3-diene (E/Z mixture)	(E)-Pent-2-ene (55), (Z)-pent-2-ene (16), pent-1-ene (2), pentane (27)	[Pd <sub>4</sub> (SnCl <sub>2</sub> ) <sub>2</sub> - (SnCl <sub>3</sub> ) <sub>8</sub> ] <sup>3-</sup> c	EtOH/H <sub>2</sub> O/HCl 60°C, 50 bar	2 hr	196 <sup>b</sup>	Conversion 98%	(73)
Penta-1,4-diene	(Z)-Penta-1,3-diene (25), pent-1-ene (12), pentane (3)	CpNiOs <sub>3</sub> H <sub>3</sub> (CO) <sub>7</sub> - (PEt <sub>3</sub> ) <sub>2</sub>	<i>n</i> -Octane, 120°C, 1 bar	4 hr	139 <sup>b</sup>	Cluster decompo- sition 90%, conversion 60%	(71d)
Cycloocta-1,5-diene	Cycloocta-1,3-diene (24), cycloocta-1,4-diene (7), cyclooctene (41), cyclooctane (17)	Cp <sub>2</sub> Pt <sub>2</sub> W <sub>2</sub> (CO) <sub>6</sub> - (PPh <sub>3</sub> ) <sub>2</sub>	THF, 60°C, 14 bar	5 hr	481 <sup>b</sup>		(66c)
Cycloocta-1,5-diene	Cycloocta-1,3-diene (32), cyclooctene (61), cyclooctane (7)	Cp <sub>2</sub> Pt <sub>2</sub> Mo <sub>2</sub> (CO) <sub>6</sub> - (PEt <sub>3</sub> ) <sub>2</sub>	THF, 60°C, 14 bar	3 hr	557 <sup>b</sup>		(66c)
Cycloocta-1,5-diene	Cycloocta-1,3-diene (24), cycloocta-1,4-diene (3), cyclooctene (70), cyclooctane (1)	Cp <sub>2</sub> Pt <sub>2</sub> Mo <sub>2</sub> (CO) <sub>6</sub> - (PEt <sub>3</sub> ) <sub>2</sub>	THF, 60°C, 14 bar	3 hr	580 <sup>b</sup>		(66c)

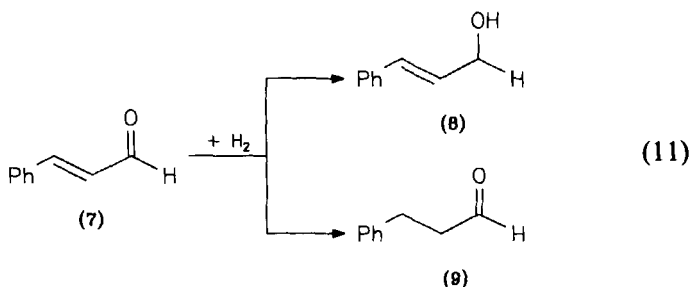
<sup>a</sup> NG, not given in the reference cited (all tables).

<sup>b</sup> Related to the total of hydrogenation products.

<sup>c</sup> Obscure solution containing excess SnCl<sub>2</sub>·2H<sub>2</sub>O.

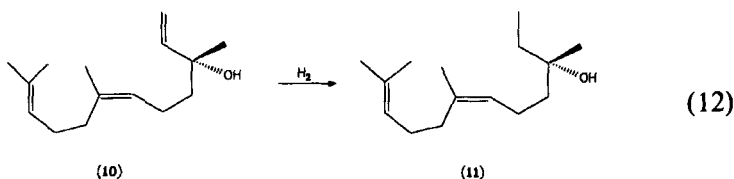
solution; the catalytic turnover is 100 after 106 hr, whereas without irradiation it is only 0.37 after 72 hr.

Examples in which transition metal clusters have been used as selective catalysts in the hydrogenation of complicated structures are rare, but there are reports on chemoselective and on regioselective applications.  $\text{Ru}_3(\text{CO})_{12}$  in the presence of phosphorous cocatalysts catalyzes the hydrogenation of  $\alpha,\beta$ -unsaturated aldehydes



The chemoselectivity is controlled by the catalyst/cocatalyst ratio: Cinnamaldehyde (7) is hydrogenated preferentially at the  $\text{C}=\text{O}$  function with a large excess of tri-*n*-butylphosphine to give cinnamic alcohol (8) ( $\text{Ru}_3(\text{CO})_{12}/\text{PBu}_3^n$  1 : 18, toluene, 30-bar  $\text{H}_2$ , 110°C, 9 hr conversion 96%, selectivity 87%, CT 660). Using a stoichiometric ratio of  $\text{Ru}_3(\text{CO})_{12}$  and  $\text{PBu}_3^n$ , the dominant hydrogenation product is 3-phenylpropanal (9), arising from the hydrogenation of the  $\text{C}=\text{C}$  function (toluene, 30-bar  $\text{H}_2$ , 110°C, 9 hr, conversion 100%, selectivity 56%, CT 440; side product: 3-phenylpropanol) (77).

The regioselectivity of cluster-based hydrogenation reactions is witnessed by the cluster anion  $[\text{HRu}_3(\text{CO})_{11}]^-$ , which catalyzes specifically the hydrogenation of the terminal  $\text{C}=\text{C}$  bond of *cis*-nerolidol (10); under mild conditions (DMF, 20°C, 40 bar) 11 is obtained exclusively with 51% conversion (78):



The tetranuclear cluster  $\text{H}_4\text{Ru}_4(\text{CO})_8(\text{R,R-DIOP})_2$ , in which the metal framework is modified by two chiral diphosphine ligands, is the main cluster candidate for asymmetric hydrogenation reactions (Scheme 4). This cluster catalyzes the enantioselective hydrogenation of mesaconic acid (12)

to methylsuccinic acid (**13**); the reaction proceeds in toluene–diethylether (2 : 1) at 20°C and a hydrogen pressure of 130 bar, giving 88.7% of **13** with an enantiomeric excess (ee) of 8.1% for the *S*-enantiomer, the catalytic turnover being 200. The hydrogenation of citraconic acid (**14**), the *E*-isomer of **12**, under the same conditions gives 83.3% of **13** with an optical purity of only 1.1% (79,80). Saturated and unsaturated lactones were observed in small yields as side products in this reaction. This example shows that the different steric arrangement of the carbonyl groups around the double bond in **12** and **14** plays a fundamental role in determining the extent of asymmetric induction.

Using the same catalyst, prochiral ketones and ketimines have been hydrogenated: Acetophenone (**15**) gives the corresponding alcohol (**16**) with an ee of 8.1% for the *S*-enantiomer. The best reaction conditions are toluene solution, 130°C, 100 bar, and 5 hr. The conversion is 40%, corresponding to a catalytic turnover of 280; it is essential that the chiral ligand *R,R*-DIOP is present in excess (81).

For the hydrogenation of 2-phenylbut-1-ene (**17**) to 2-phenylbutane (**18**),  $\text{H}_4\text{Ru}_4(\text{CO})_8(\text{R,R-DIOP})_2$  was used at 80°C and 100 bar to give **18** with 74% yield (catalytic turnover 203) and an optical purity of 4.5% (*S*-enantiomer) (82).  $\alpha$ -Methylcinnamic acid (**19**) was hydrogenated in toluene–ethanol (1 : 1) at 100°C and 130 bar to give preferentially the *S*-enantiomer of **20**; with  $\text{H}_4\text{Ru}_4(\text{CO})_8(\text{R,R-DIOP})_2$  as the catalyst, the ee is 58%; and with a cluster formulated as  $\text{Ru}_6(\text{CO})_{18}(\text{R,R-DIOP})_3$  the ee is 45 or 61% with trimethylamine present (83). The hydrogenation of tiglic acid (**21**) was used to study the enantiomeric discrimination by a tetranuclear carboxylato complex: In toluene–ethanol (1 : 1) at 80°C and 130 bar,  $\text{Ru}_4(\text{CO})_8(\text{OOCCH}_2\text{COO})_2(\text{R,R-DIOP})_2$  gives (*S*)-2-methylbutanoic acid (**22**) with a conversion of 99% after 65 hr and an optical purity of 41% (catalytic turnover 248) (84). With  $\text{Ru}_4(\text{CO})_8(\text{OOCCH}_2\text{CH}_2\text{CH}_2\text{COO})_2(\text{R,R-DIOP})_3$ , tiglic acid (**21**) was converted quantitatively into **22** giving an optical purity of 43% for the *S*-enantiomer of **22** (toluene–ethanol 1 : 1, 60°C,  $\text{H}_2$  pressure not given, 24 hr, CT 4000) (85). There is also a report that  $\text{Ru}_3(\text{CO})_{12}$  has been used as enantioselective hydrogenation catalyst precursor in the presence of chiral diphosphinites without isolating or characterizing the modified clusters; with glucophenite, **19** can be converted to **20** in 85% yield and ee 38% (THF, 120°C, 40 bar, 100 hr, CT 62); for the conversion of **21** to **22** the yield is 74% with an optical purity of 11% (CT 34) (86).

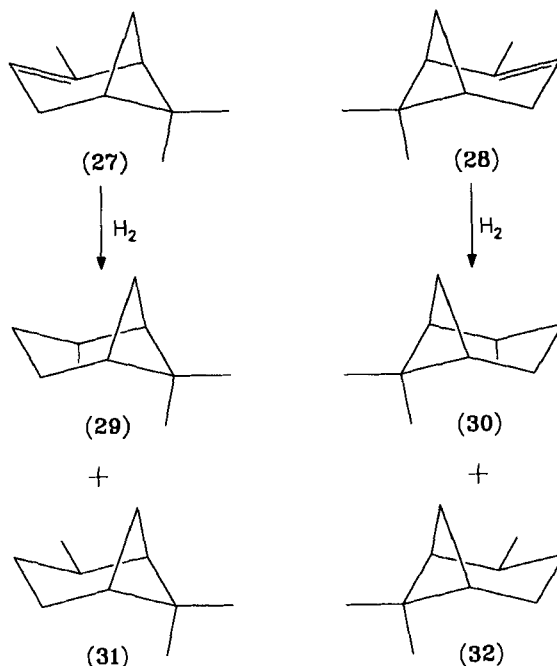
Rhodium clusters modified with chiral diphosphines have been reported to catalyze the enantioselective hydrogenation of prochiral dehydroamino acids (Scheme 4). In ethanol, **23** is hydrogenated by  $\text{Rh}_6(\text{CO})_{10}(\text{R,R-DIOP})_3$  (80°C, 1 bar, 24 hr) giving the *R*-enantiomer of **24** with 47% yield





citronellal (**26**) in toluene at ambient temperature and normal pressure. The conversion is quantitative with a catalytic turnover of ca.120. For the hexanuclear cluster, the enantiomeric excess was determined to be 59%, and for the tetranuclear cluster, 66%; use of the (–)-enantiomeric ligand leads to (*S*)-**26**, whereas the (+)-enantiomer produces predominantly (*R*)-**26** (89). In all the cases where rhodium clusters have been used with chiral ligands, the asymmetric hydrogenation could also be performed using the mononuclear complex  $\text{HRh}(\text{CO})(\text{PPh}_3)_3$  and the same ligand with even better results, suggesting that the tetra- or hexanuclear cluster is only a precursor for the formation of a mononuclear catalytic species (87–89).

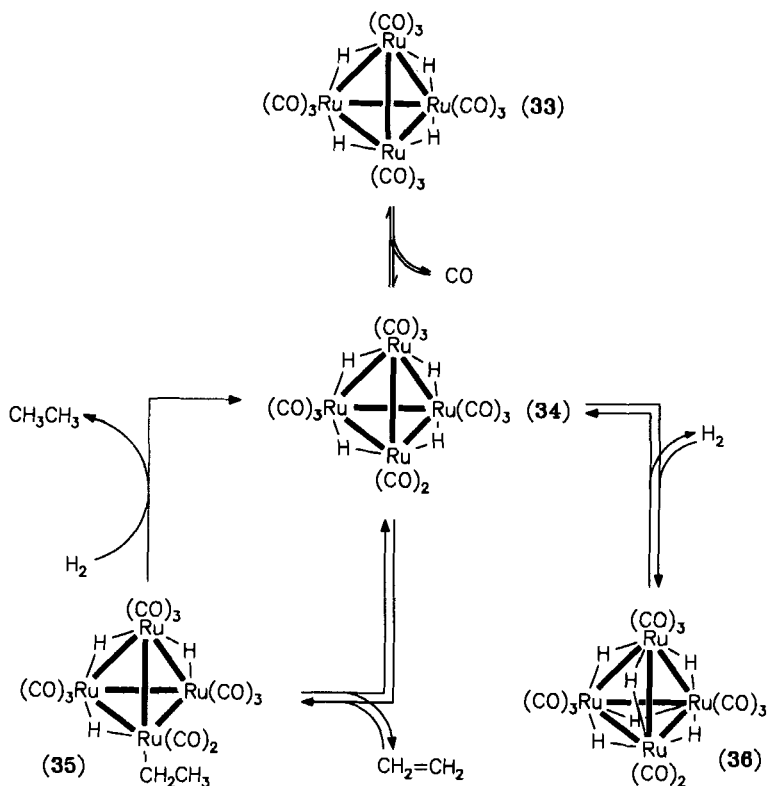
Chirally modified ruthenium clusters have also been used for a kinetic resolution of enantiomers in the catalytic hydrogenation of non-functionalized terpene olefins (Scheme 5): The hydrogenation of  $\alpha$ -pinene (1*R*,5*R*: **27**; 1*S*,5*S*: **28**) leads in principle to the *cis*- and *trans*-pinanes (1*R*,2*S*,5*R*: **29**; 1*S*,2*R*,5*S*: **30**; 1*R*,2*R*,5*R*: **31**; 1*S*,2*S*,5*S*: **32**). When a racemic mixture of both  $\alpha$ -pinene enantiomers (**27** and **28**) is hydrogenated in the presence of the (1*S*,2*S*,3*S*,5*R*)-isopinocampheyl cluster  $\text{HRu}_3(\text{CO})_9[\mu_3, \eta^2\text{-NEt-}$



SCHEME 5. Enantiomer discrimination in the hydrogenation of olefins by chirally modified cluster catalysts.

COO-(1*S*,2*S*,3*S*,5*R*)-C<sub>10</sub>H<sub>17</sub>] (THF, 50 bar H<sub>2</sub>, 68°C), only the *cis*-pinanes are formed, the enantiomeric excess of the (1*S*,2*R*,5*S*)-pinane (**30**) being 49%. The catalytic turnover related to **30** was found to be 74 and that related to **29** only 24 after 10 hr, thus resulting in a remarkable kinetic enantiomer discrimination (*90*).

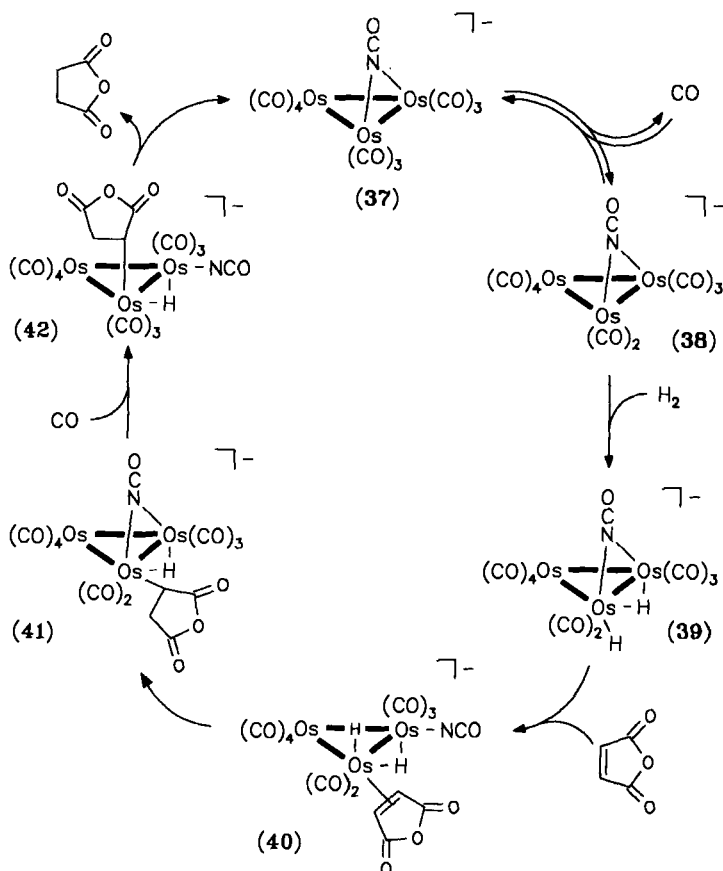
Although there is no direct proof for the implication of intact transition metal clusters in these hydrogenation reactions, in some cases experimental evidence is consistent with mechanistic proposals based on intact cluster intermediates. Kinetic data were employed for the mechanistic interpretation: The kinetics of the catalytic ethylene hydrogenation by H<sub>4</sub>Ru<sub>4</sub>(CO)<sub>12</sub> (**33**) (heptane, 72°C, 0.13 bar H<sub>2</sub>, 0.13 bar C<sub>2</sub>H<sub>4</sub>) have been studied (Scheme 6) (*91a*). The data are consistent with the formation of the



SCHEME 6. Proposed mechanism for the hydrogenation of ethylene catalyzed by H<sub>4</sub>Ru<sub>4</sub>(CO)<sub>12</sub> according to (*91a*). [From G. Süß-Fink and F. Neumann, in "The Chemistry of the Metal-Carbon Bond" (F. R. Hartley, ed.), Vol. 5, p. 306. Wiley, New York, 1989. Reprinted by permission of John Wiley & Sons, Ltd.]

unsaturated cluster **34** by loss of CO in an initial equilibrium. Further reaction is assumed to involve an ethyl cluster (**35**) (the ethyl ligand could also be bridging), which on reaction with hydrogen eliminates ethane, regenerating **34**. The rapid H–D exchange between  $\text{H}_2$  and  $\text{D}_4\text{Ru}_4(\text{CO})_{12}$  was rationalized in terms of an equilibrium between **34** and **36** (91a).

Another strategy for the elucidation of a catalytic cycle has been successfully applied: Since no intermediates could be isolated from the  $\text{Ru}_3(\text{CO})_{12}/\text{NCO}^-$  system active for alkene hydrogenation (91b), the corresponding osmium system was examined. In this case, the homologous



SCHEME 7. Modelling the catalytic cycle of the maleic anhydride hydrogenation catalyzed by  $[\text{Ru}_3(\text{CO})_{11}(\text{NCO})]^-$ , according to (91c). [From G. Süß-Fink and F. Neumann, in "The Chemistry of the Metal–Carbon Bond" (F. R. Hartley, ed.), Vol. 5, p. 304. Wiley, New York, 1989. Reprinted by permission of John Wiley & Sons, Ltd.]

intermediates were stable (93). After having established that the anionic ruthenium cluster  $[\text{Ru}_3(\text{CO})_{11}(\text{NCO})]^-$  was the active catalyst (91d), the osmium anion  $[\text{Os}_3(\text{CO})_{11}(\text{NCO})]^-$  (37) was prepared from  $\text{Os}_3(\text{CO})_{12}$  and  $[\text{N}(\text{PPh}_3)_2][\text{N}_3]$  (Scheme 7). In refluxing THF, 37 loses CO to give 38, the homolog of  $[\text{Ru}_3(\text{CO})_{11}(\text{NCO})]^-$ , characterized by IR spectroscopy. Molecular hydrogen reacts with 38 (52°C, 3.5 bar) to give 39, isolated as the bis(triphenylphosphine)iminium salt (91c). Reaction with maleic anhydride at 25°C gives 41 in quantitative yield; the intermediate is presumably 40. Cluster 41 was structurally characterized, and it represents the first characterization of a terminally bonded alkyl ligand on a metal carbonyl cluster (91c). The final step is the reductive elimination of the C–H bond; heating 41 under CO pressure (THF, 3.4 bar, 75°C) gives succinic anhydride and 37; and cluster 42 is a possible intermediate.

### B. Hydrogenation of Acetylenes

Most of the catalytic systems derived from transition metal clusters catalyze the hydrogenation of acetylenes to give predominantly olefins



the corresponding alkane being only a side product [Table II (69,72,78,92–104)].

Since most of the clusters used for hydrogenation also catalyze the double bond shift (cf. Section VI.A), the situation is complicated by isomerization; for acetylenes with an internal  $\text{C} \equiv \text{C}$  unit an *E/Z* problem also arises. The examples reported demonstrate that carbon–carbon triple bonds are more readily reduced than carbon–carbon double bonds. However, in most cases further hydrogenation and isomerization lead to complex product mixtures.

The hydrogenation potential of a large number of ruthenium, osmium, and mixed metal clusters for various acetylenes has been studied systematically by E. Sappa *et al.*; in some cases experimental observations suggest catalysis by intact clusters (69,98,99,104). A complete catalytic cycle for the hydrogenation of an alkyne to an alkene by a trinuclear osmium cluster has been proposed (105) and demonstrated by a trifluoromethyl-substituted substrate (Scheme 8). The hydrido cluster  $\text{H}_2\text{Os}_3(\text{CO})_{10}$  adds bis(trifluoromethyl)acetylene to give cluster 43, which itself takes up carbon monoxide ( $\text{CH}_2\text{Cl}_2$ , reflux) to give a 1:1 mixture of the alkene complexes 44 and 45. These complexes can be reacted separately with CO (octane, reflux) to generate  $\text{Os}_3(\text{CO})_{12}$  quantitatively with loss of the corresponding (*E*)- and (*Z*)-alkane. The cycle is completed by the known (106) hydro-

TABLE II  
HYDROGENATION OF ALKYNES CATALYZED BY VARIOUS TRANSITION METAL CLUSTERS

Substrate	Products (%)	Catalyst	Conditions	Time	Catalytic turnover	Remarks	References
Pent-1-yne	Pent-1-ene (84), pent-2-ene (10), pentane (3)	$\text{Cp}_4\text{Fe}_4(\text{CO})_4$	Benzene, 120°C, 7.2 bar	88 hr	340	Cluster unchanged	(92)
Pent-1-yne	Pent-1-ene (6), ( <i>E</i> )-pent-2-ene (2), ( <i>Z</i> )-pent-2-ene (2)	$\text{H}_4\text{Ru}_4(\text{CO})_{11}\text{-P}(\text{OEt})_3$	Toluene, 80°C, 1 bar	5.5 hr	14	No effect of CO	(93)
Pent-1-yne	Pent-1-ene (19), ( <i>E</i> )-pent-2-ene (4), ( <i>Z</i> )-pent-2-ene (4)	$\text{H}_4\text{Ru}_4(\text{CO})_9\text{-[P}(\text{OEt})_3\text{]}_3$	Toluene, 80°C, 1 bar	5.5 hr	42	Suppression by CO	(93)
Pent-1-yne	Pent-1-ene (7), ( <i>E</i> )-pent-2-ene (40), ( <i>Z</i> )-pent-2-ene (22), pentane (22)	$\text{Ru}_3(\text{CO})_{12}$	Toluene, 80°C, 1 bar	16 hr	28 <sup>a</sup>		(72)
Pent-2-yne	Pent-1-ene (3), ( <i>E</i> )-pent-2-ene (69), ( <i>Z</i> )-pent-2-ene (25), pentane (2)	$\text{H}_4\text{Ru}_4(\text{CO})_{12}$	Toluene, 80°C, 1 bar	15 hr	10		(94)
Pent-2-yne	Pent-1-ene (4), ( <i>E</i> )-pent-2-ene (4), ( <i>Z</i> )-pent-2-ene (10)	$\text{H}_4\text{Ru}_4(\text{CO})_9\text{-[P}(\text{OEt})_3\text{]}_3$	Toluene, 80°C, 1 bar	5.5 hr			(93)
Pent-2-yne	Pent-1-ene (2), ( <i>E</i> )-pent-2-ene (17), ( <i>Z</i> )-pent-2-ene (64), pentane (12)	$\text{Rh}_4(\text{CO})_{12}$	Toluene, 80°C, 1 bar	3 hr	NG	Supporting on $\text{Al}_2\text{O}_3$ increases pentane formation	(95)

(continued)

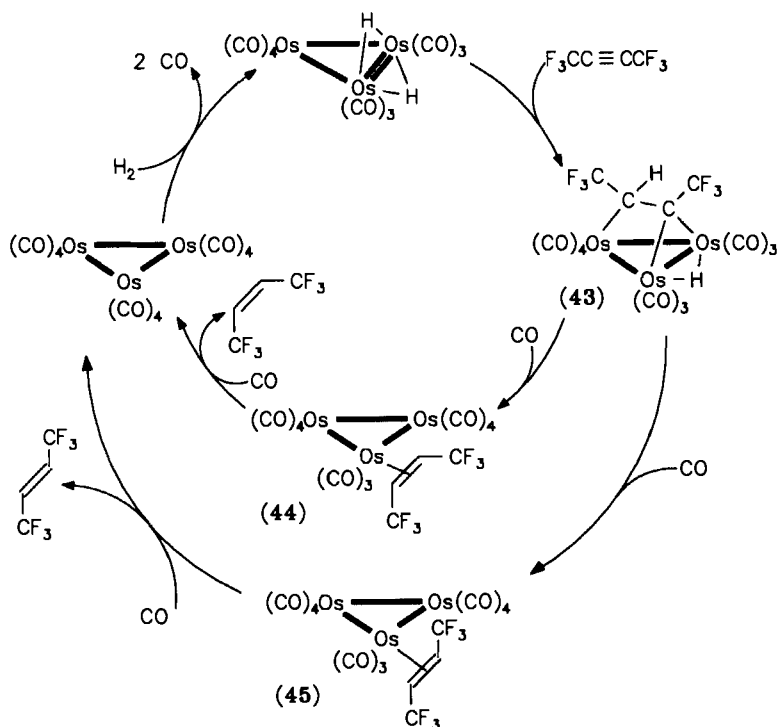
TABLE II (continued)

Substrate	Products (%)	Catalyst	Conditions	Time	Catalytic turnover	Remarks	References
Pent-2-yne	Pent-1-ene (2), ( <i>E</i> )-pent-2-ene (68), ( <i>Z</i> )-pent-2-ene (16), pentane (13)	$\text{Ru}_3(\text{CO})_{12}$	Toluene, 80°C, 1 bar	16 hr	40 <sup>a</sup>		(72)
But-2-yne	( <i>Z</i> )-But-2-ene (presumably 2–5%)	$\text{Ni}_4(\text{NCBu}^t)_7$	Benzene, 20°C, 3 bar	72 hr	NG	Report imprecise	(96, 97)
Hex-3-yne	( <i>E</i> )-Hex-3-ene, ( <i>Z</i> )-hex-3-ene, hexane (3–5%, rel. ratio 1:128:3)	$\text{Ni}_4(\text{NCBu}^t)_7$	Benzene, 3 bar	1–6 days	33–50	Report imprecise	(96, 97)
Hex-3-yne	( <i>Z</i> )-Hex-3-ene (4)	$\text{Cp}_4\text{Fe}_4(\text{CO})_4$	Benzene, 100°C, 6.9 bar	11 hr	16	Selectivity 100%	(92)
Hex-3-yne	( <i>E</i> )-Hex-3-ene (90), ( <i>Z</i> )-hex-3-ene (1)	$\text{HRu}_3(\text{CO})_9$ $\text{PPh}_2$	<i>n</i> -Octane, 120°C, 0.9 bar	45 min	17 <sup>a</sup>	Conversion 7%	(98)
3,3-Dimethylbut-1-yne	3,3-Dimethylbut-1-ene (56), 2,2-dimethylbutane (11)	$\text{Cp}_3\text{Ni}_3\text{Os}_3(\text{CO})_9$	<i>n</i> -Octane, 120°C, 1 bar	36 hr	2253 <sup>a</sup>	Cluster unchanged	(69)
3,3-Dimethylbut-1-yne	3,3-Dimethylbut-1-ene (97), 2,2-dimethylbutane (3)	$\text{HRu}_3(\text{CO})_7$ - $(\text{PPh}_2)_3$	<i>n</i> -Octane, 120°C, 0.9 bar	1 hr	99 <sup>a</sup>	Conversion 29%	(99)
Oct-1-yne	Oct-1-ene (55), octane (43)	$\text{Pt}_2\text{Co}_2(\text{CO})_8$ - $(\text{PPh}_3)_2$	Toluene, 50°C, 50 bar	20 hr	37 <sup>a</sup>		(100, 101)
Phenylacetylene	Styrene (3), ethylbenzene (53), oligomers (44)	$\text{Pt}_5(\text{CO})_6(\text{PPh}_3)_4$	Toluene, 50°C, 50 bar	20 hr	61 <sup>a</sup>		(100)
1-Phenylprop-1-yne	1-Phenyl-prop-2-ene	$\text{HRu}_3(\text{CO})_9$ - [NPh(C <sub>5</sub> H <sub>4</sub> N)]	NG	NG	NG		(102)

Diphenylacetylene	(Z)-Stilbene (50), (E)-stilbene (3), diphenylethane (2)	$\text{Pt}_3(\text{CO})_6(\text{PPh}_3)_4$	Toluene, 50°C, 50 bar	20 hr	63 <sup>a</sup>		(100)
Diphenylacetylene	(Z)-Stilbene, (E)-stilbene, 1,2-diphenylethane (11%; rel. ratio 6:100:3805)	$\text{Ru}_4(\text{CO})_{12}-$ ( $\text{C}_2\text{Ph}_2$ )	Heptane, 120°C, 0.9 bar	24 hr	NG		(103)
Diphenylacetylene	(Z)-Stilbene, (E)-stilbene, 1,2-diphenylethane (15%; rel. ratio 19:100:3541)	$\text{Fe}_3(\text{CO})_9(\text{C}_2\text{Ph}_2)$	Heptane, 120°C, 0.9 bar	18 hr	NG		(103)
Diphenylacetylene	(E)-Stilbene (96)	$\text{Na}[\text{HRu}_3(\text{CO})_{11}]$	DMF, 100°C, 50 bar	15 hr	38	Selectivity 100%	(78)
Diphenylacetylene	(Z)-Stilbene (22), (E)-stilbene (1), 1,2-diphenylethane (1)	$\text{Pt}_2\text{Co}_2(\text{CO})_8-$ ( $\text{PPh}_3$ ) <sub>2</sub>	Toluene, 50°C 50 bar	20 hr	26 <sup>a</sup>		(100, 101)
Diphenylacetylene	(Z)-Stilbene, (E)-stilbene, 1,2-diphenylethane (12%, rel. ratio 18:100:1030)	$\text{Cp}_2\text{Ni}_2\text{Fe}_2(\text{CO})_6-$ ( $\text{C}_2\text{Ph}_2$ )	Heptane, 120°C, 0.9 bar	12 hr	NG		(103)
Diphenylacetylene	(Z)-Stilbene, (E)-stilbene, 1,2-diphenylethane (40%, rel. ratio 18:1400:830)	$\text{Cp}_2\text{Ni}_2\text{Fe}(\text{CO})_3-$ ( $\text{C}_2\text{Ph}_2$ )	Heptane, 120°C, 0.9 bar	12 hr	NG		(103)
Diphenylacetylene	(Z)-Stilbene (20), (E)-stilbene (80)	$\text{H}_2\text{Fe}_3(\text{CO})_9-$ (P- <i>p</i> -tolyl)	<i>n</i> -Octane, 80°C, 0.9 bar	75 min	6 <sup>a</sup>	Conversion 10%	(104)

<sup>a</sup> Related to the total of hydrogenation products.





SCHEME 8. Proposed mechanism for the hydrogenation of bis(trifluoromethyl)acetylene catalyzed by  $\text{H}_2\text{Os}_3(\text{CO})_{10}$ . [From G. Süß-Fink and F. Neumann, in "The Chemistry of the Metal-Carbon Bond" (F. R. Hartley, ed.), Vol. 5, p. 302. Wiley, New York, 1989. Reprinted by permission of John Wiley & Sons, Ltd.]

genation of  $\text{Os}_3(\text{CO})_{12}$  to  $\text{H}_2\text{Os}_3(\text{CO})_{10}$  in refluxing octane. All these clusters are isolated compounds; **43** (107) and **45** (105) are fully characterized. The structure of **44** (105) has been established by a single-crystal X-ray structure analysis.

### C. Hydrogenation of Carbonyl Compounds

Several rhodium and ruthenium clusters are reported to catalyze the reduction of carbonyl compounds [Table III (70,108–112c)]. The hydrogenation of aldehydes and ketones yields the corresponding primary and secondary alcohols

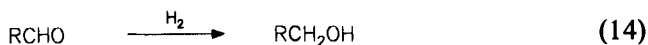
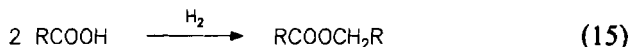


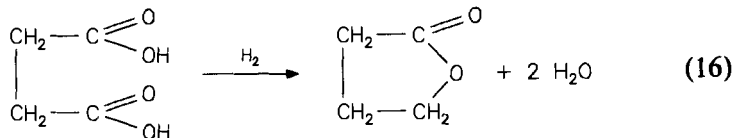
TABLE III  
HYDROGENATION OF CARBONYL COMPOUNDS BY VARIOUS TRANSITION METAL CLUSTERS

Substrate	Products (%)	Catalyst	Conditions	Time (hr)	Catalytic turnover	Remarks	References
Benzaldehyde	Benzyl alcohol	$\text{Rh}_6(\text{CO})_{16}$	Methanol, 110°C, 14-bar $\text{H}_2$ , 55-bar CO, $\text{NaHCO}_3$	1	110	$\text{NaHCO}_3$ and CO required	(108)
Butanal	Butan-1-ol	$\text{Rh}_4(\text{CO})_{12}$	Hexane, 160°C, 115-bar $\text{H}_2$ , 55-bar CO	3.6	701	Formation of $\text{HRh}(\text{CO})_3$ as active species	(109)
2-Ethyl-hex-2-enal	2-Ethylhexanal (58), 2-ethylhexanol (16)	$\text{Co}_3(\text{CO})_8(\text{PBu}_3)_3$	Heptane, 80°C, 150-bar $\text{H}_2$	12	8	Reduction unselective	(70)
Cyclohexanone	Cyclohexanol	$\text{H}_4\text{Ru}_4(\text{CO})_{12}$	THF, 100°C, 100-bar $\text{H}_2$	6	880	Conversion 60%	(110)
Cyclohexanone	Cyclohexanol	$\text{H}_4\text{Ru}_4(\text{CO})_{10}-(\text{PPh}_3)_2$	THF, 100°C, 100-bar $\text{H}_2$	6	125	Conversion 9%	(110)
Cyclohexanone	Cyclohexanol	$\text{H}_4\text{Ru}_4(\text{CO})_9-(\text{PPh}_3)_3$	THF, 100°C, 100-bar $\text{H}_2$	6	200	Conversion 14%	(110)
Cyclohexanone	Cyclohexanol	$\text{H}_4\text{Ru}_4(\text{CO})_8-(\text{PPh}_3)_4$	THF, 100°C, 100-bar $\text{H}_2$	6	800	Conversion 54%	(110)
Cyclohexanone	Cyclohexanol	$\text{Ru}_3(\text{CO})_8(\text{PPh}_2)-[\text{PPh}(\text{C}_5\text{H}_4\text{N})]$	THF, 120°C, 40-bar $\text{H}_2$	2	151	Conversion 77%	(111)
Dimethyl oxalate	Methyl glycolate	$\text{H}_4\text{Ru}_4(\text{CO})_8-(\text{PBu}_3)_4$	Benzene, 20°C, 130-bar $\text{H}_2$	39	156	Conversion 100%	(112a)
Dimethyl succinate	$\gamma$ -Butyrolactone	$\text{H}_4\text{Ru}_4(\text{CO})_8-(\text{PBu}_3)_4$	Benzene, 180°C, 130-bar $\text{H}_2$	144	160	Conversion 7%, selectivity 100%	(112a)
Succinic acid	$\gamma$ -Butyrolactone	$\text{H}_4\text{Ru}_4(\text{CO})_8-(\text{PBu}_3)_4$	Dioxane, 180°C, 130-bar $\text{H}_2$	22	263	Conversion 83%	(112b)
Acetic acid	Ethyl acetate	$\text{H}_4\text{Ru}_4(\text{CO})_8-(\text{PBu}_3)_4$	Dioxane, 180°C, 130-bar $\text{H}_2$	48	2285	No ethanol obtained	(112c)
Propionic acid	Propyl acetate (97), propanol (3)	$\text{H}_4\text{Ru}_4(\text{CO})_8-(\text{PBu}_3)_4$	Dioxane, 180°C, 130-bar $\text{H}_2$	48	1625		(112c)

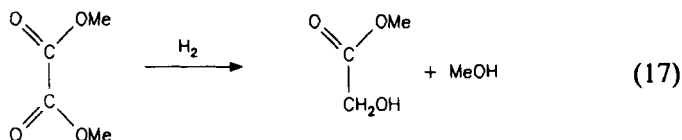
In the case of carbonic acids, the reduction of the alcohol is often followed by the esterification of the alcohol with unreacted acid



A special case is lactone formation after the partial reduction of a dicarboxylic acid

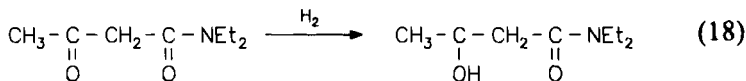


Esters of dicarboxylic acids are partially reduced with the elimination of alcohol; in this fashion methyl glycolate is obtained from dimethyl oxalate



The fact that carbon monoxide is required for the hydrogenation of aldehydes catalyzed by  $\text{Rh}_6$  and  $\text{Rh}_4$  clusters (108,109) has been interpreted in terms of a cluster breakdown to give the mononuclear complex  $\text{HRh}(\text{CO})_3$ , which is the active catalyst. This hypothesis is supported by kinetic studies (109).

In some cases, ruthenium clusters have been found to catalyze selectively the hydrogenation of a  $\text{C}=\text{O}$  bond next to a  $\text{C}=\text{C}$  double bond [Eq.(11), cf. Section III.A (77)] or the hydrogenation of one of two  $\text{C}=\text{O}$  bonds in a given molecule: Thus, acetoacetic diethylamide is hydrogenated in the presence of  $[\text{H}_3\text{Ru}_4(\text{CO})_{12}]^-$  selectively in the keto function according to

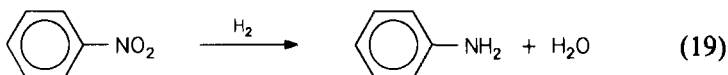


(THF, 120°C, 40 bar, 20 hr, CT 124) (112d).

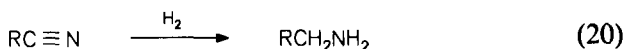
A particular case is the hydrogenation of orthoesters:  $\text{Rh}_4(\text{CO})_{12}$  has been found to catalyze the reduction of ethyl orthoformate  $\text{HC}(\text{OEt})_3$  to give  $\text{CH}_2(\text{OEt})_2$ ; the reaction is conducted under a combined  $\text{H}_2/\text{CO}$  pressure (solvent not mentioned, 150°C, 40 bar  $\text{H}_2$ , 40 bar  $\text{CO}$ , conversion 55%, selectivity 100%, CT 2200). After the catalytic run,  $\text{Rh}_6(\text{CO})_{16}$  separated from the reaction mixture, and the infrared spectrum of the resultant solution indicated the presence of  $[\text{Rh}_5(\text{CO})_{15}]^-$  (112e).

#### D. Hydrogenation of Nitrogen-Containing Functions

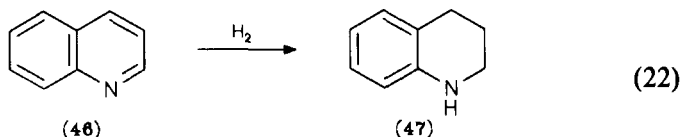
Whereas trinuclear iron clusters have been used in stoichiometric reduction of aromatic nitro compounds, the tetranuclear iron cluster  $\text{Cp}_4\text{Fe}_4(\text{CO})_4$  can be used for the catalytic hydrogenation of nitrobenzene to aniline [Table IV (92,96,113–116)].



The hydrogenation of nitriles and isonitriles



has been achieved with a tetranuclear nickel cluster, but the reduction is not very efficient (Table IV). Quinoline (**46**) was found to give tetrahydroquinoline (**47**) on pressurizing with hydrogen in the presence of trinuclear osmium clusters (114,115):



The two clusters isolated from this reaction,  $\text{HOs}_3(\text{CO})_{10}(\text{NC}_9\text{H}_8)$  and  $\text{HOs}_3(\text{CO})_{10}(\text{NC}_9\text{H}_6)$ , are regarded as intermediates (117).

#### E. Hydrogen Transfer Reactions

Catalytic hydrogen transfer from a hydrogen donor molecule to an unsaturated substrate sometimes presents advantages over hydrogenation by molecular hydrogen. This type of reaction can be catalyzed by a number of ruthenium or rhodium catalysts. Cycloocta-1,5-diene and hexa-1,5-diene can be selectively reduced to cyclooctene and a mixture of hexenes, respectively, by  $\text{Rh}_6(\text{CO})_{16}$  via hydrogen transfer from isopropanol. The reaction proceeds at 145°C and a CO pressure of 45 bar. For cycloocta-1,5-diene

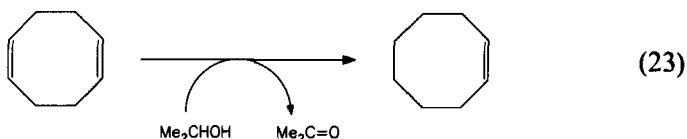


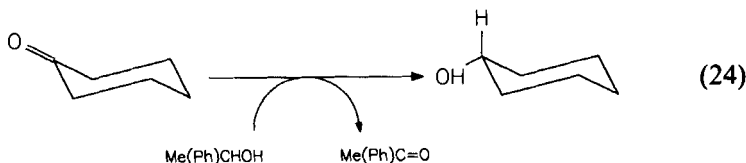
TABLE IV  
HYDROGENATION OF NITROGEN-CONTAINING FUNCTIONS BY VARIOUS TRANSITION METAL CLUSTERS

Substrate	Products (%)	Catalyst	Conditions	Time (hr)	Catalytic turnover	Remarks	References
Nitrobenzene	Aniline	$\text{Cp}_4\text{Fe}_4(\text{CO})_4$	Benzene, 130°C, 21 bar	24	126	Conversion 31%	(92)
Acetonitrile	Ethylamine	$\text{Ni}_4(\text{CNBu}')_7$	Neat, 90°C, 1 bar	NG	NG	Report imprecise	(96, 113)
<i>tert</i> -Butyl-isonitrile	<i>tert</i> -Butylmethyl-amine	$\text{Ni}_4(\text{CNBu}')_7$	Toluene, 90–120°C, 1–3 bar	NG	NG	Report imprecise	(96)
Quinoline	Tetrahydroquinoline	$\text{Os}_3(\text{CO})_{12}$	Heptane, 145°C, 41 bar	24	1200	Intermediates isolated	(114, 115)
Quinoline	Tetrahydroquinoline	$\text{H}_2\text{Os}_3(\text{CO})_{10}$	Methanol, 145°C, 41 bar	24	2088	Intermediates isolated	(114, 115)
<i>N</i> -Benzylidene aniline	<i>N</i> -Benzylaniline	$\text{Ru}_3(\text{CO})_{12}$	<i>N</i> -Isopropylpyrrolidinone, 130°C, 100 bar <sup>a</sup>	16	594	Conversion 100%, selectivity 99%	(116)
<i>N</i> -Benzylidene aniline	<i>N</i> -Benzylaniline	$[\text{N}(\text{PPh}_3)_2]\text{[HRu}_3(\text{CO})_{11}]$	<i>N</i> -Isopropylpyrrolidinone, 100°C, 100 bar <sup>a</sup>	16	546	Conversion 94% selectivity 97%	(116)

<sup>a</sup> CO/H<sub>2</sub> mixture (1 : 1).

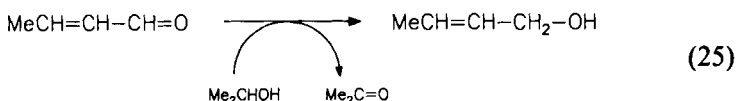
the conversion is 99% after 23 hr (catalytic turnover 150), and for hexa-1,5-diene the conversion is 97% after 55 hr (catalytic turnover 162) (118).

Cyclohexanone can be reduced to cyclohexanol by using 1-phenylethanol as a hydrogen donor in the presence of  $\text{Fe}_3(\text{CO})_{12}$



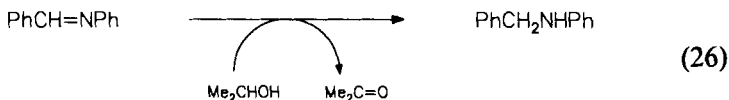
The reaction proceeds under phase-transfer conditions (benzyltriethylammonium chloride and 18-crown-6) at 28°C. After 2.5 hr, cyclohexanol is formed with 78% conversion (catalytic turnover 20) (119). With  $\text{Ru}_3(\text{CO})_{12}$ , methanol can be used as the hydrogen source for the cyclohexanone reduction; a large excess of triphenylphosphine increases the conversion considerably. After 18 hr at 150°C, 44% of cyclohexanol was formed, corresponding to a catalytic turnover of 44 (120).

Cyclohex-1-en-2-one can be reduced to give cyclohexanol via cyclohexanone using the isopropanol/acetone hydrogen transfer couple in the presence of  $\text{Ru}_3(\text{CO})_{12}$  (cyclohexane, 80°C, 16 hr, conversion 100%, catalytic turnover 100). The clusters  $\text{Ru}_3(\text{CO})_{10}(\text{C}_6\text{H}_8\text{O})$  and  $\text{Ru}_4(\text{CO})_{12}(\text{C}_6\text{H}_6\text{O})$  have been isolated from the reaction mixture and are believed to be active intermediates in the catalytic process (121). A selective transfer hydrogenation of  $\alpha,\beta$ -unsaturated aldehydes, using isopropanol as the hydrogen source, was observed with the cluster  $\text{H}_4\text{Ru}_4(\text{CO})_8(\text{P}^t\text{Bu}_3)_4$ : Crotonaldehyde is converted into crotyl alcohol



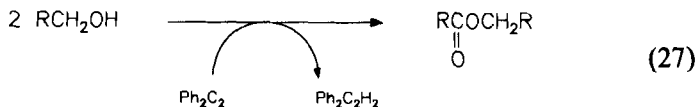
with 90% selectivity and 75% conversion (82°C, 16 hr, CT 90) (122).

In a similar fashion, Schiff bases can be reduced by a transfer hydrogenation with isopropanol to give the corresponding secondary amines:  $\text{Ru}_3(\text{CO})_{12}$  converts *N*-benzylidene aniline into *N*-benzylaniline



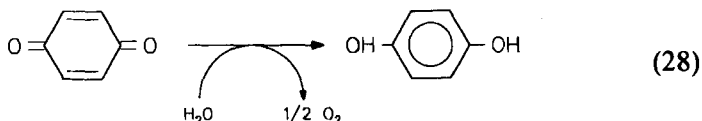
with 80% conversion (82°C, 5 hr, CT 80). The isolation and characterization of the cluster  $\text{HRu}_3(\text{CO})_9(\text{PhNCPh})$  is suggestive of a catalytic reaction taking place at the intact  $\text{Ru}_3$  metal skeleton (123).

Ruthenium carbonyl catalyzes the oxidative coupling of alcohols to esters via hydrogen transfer to diphenylacetylene, chalcone, or maleic anhydride



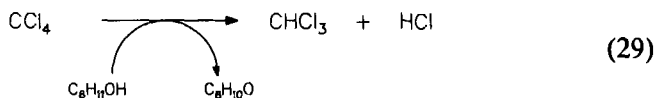
For instance, propanol is converted into propyl propionate (conversion 93%, selectivity 98%) in acetone at 145°C with  $\text{Ru}_3(\text{CO})_{12}$  and diphenylacetylene, the catalytic turnover being 140 (124,125). This reaction can be extended to other alcohols with excellent yields and selectivity (125). The intermediacy of the unsaturated mononuclear complex  $\text{Ru}(\text{CO})_2(\text{C}_4\text{Ph}_4\text{CO})$  seems to be the key step in this catalysis (126); 1,4- and 1,5-diols give rise to lactones while 1,6- and 1,10-diols are polymerized in this reaction (127).

Water can be used as the hydrogen source in reduction of *p*-benzoquinone to *p*-dihydroxybenzene in the presence of the anionic platinum cluster  $[\text{Pt}_{12}(\text{CO})_{24}]^{2-}$



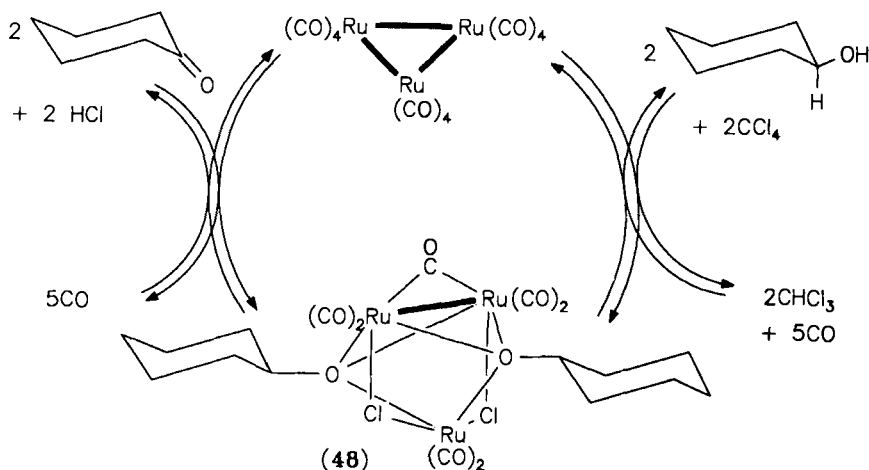
The reaction proceeds in acetonitrile at 30°C; after 5 hr, ca. 50% of the quinone is converted, corresponding to a catalytic turnover of 25. The interesting point is that molecular oxygen is derived from water in this reaction (128,129). Spectroscopic data suggest the involvement of  $[\text{Pt}_9(\text{CO})_{18}]^{2-}$  and  $[\text{Pt}_{12}(\text{CO})_{24}]^{2-}$  as active intermediates in the catalytic process (129).

Tetrachloromethane



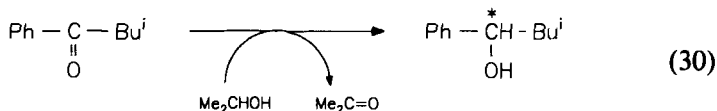
and tetrabromomethane can be reduced using the cyclohexanol/cyclohexanone hydrogen transfer couple to give chloroform or bromoform, respectively, in the presence of  $\text{Ru}_3(\text{CO})_{12}$  (82°C, 34 bar CO, CT 2100). The mechanism proposed for this hydrogen transfer catalysis (Scheme 9) is based on the isolation and structural characterization of the active intermediate  $\text{Ru}_3(\text{CO})_7\text{Cl}_2(\text{OC}_6\text{H}_{11})_2$  (48) (130).

Hydrogen transfer reactions have also been carried out in an asymmetric



SCHEME 9. Supposed mechanism for the transfer hydrogenation of tetrachloromethane, as (erroneously) proposed in (130).

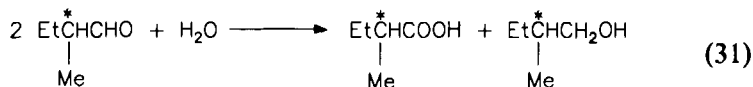
variant using the chiral cluster  $\text{H}_4\text{Ru}_4(\text{CO})_8(\text{R,R-DIOP})_2$  at the catalyst. A racemic mixture of 1-phenylethanol can be used as hydrogen donor for the reduction of isobutyl phenyl ketone to give 1-phenyl-3-methylbutan-1-ol with the *S*-configuration in an optical purity of 6.8%. The reaction takes place at  $120^\circ\text{C}$  with 18% conversion after 112 hr (catalytic turnover 244) (131). With isopropanol as hydrogen donor, isobutyl phenyl ketone gives under the same conditions 1-phenyl-3-methylbutan-1-ol



with an enantiomeric excess of 9.8% (*S*-enantiomer) and the yield being 37% after 86 hr (the catalytic turnover was not given) (132).

For the asymmetric reduction of tiglic acid (**21**) to 2-methylbutanoic acid (**22**), isopropanol can also be used as the hydrogen source. In the presence of  $\text{H}_4\text{Ru}_4(\text{CO})_8(\text{R,R-DIOP})_2$  at  $120^\circ\text{C}$ , 42% of **21** was converted after 227 hr, giving *R*-**22** (catalytic turnover 210) with 5.4% optical purity (cf. Scheme 4) (133).

If the Cannizzaro reaction of racemic 2-methylbutanal is catalyzed by  $\text{H}_4\text{Ru}_4(\text{CO})_8(\text{R,R-DIOP})_2$ , an enantiomeric selection takes place for 2-methylbutanoic acid



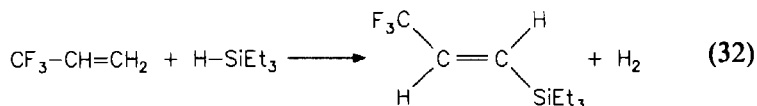


The *S*-configuration is preferred with an enantiomeric excess of 1.7%. The alcohol formed, however, is found to be racemic. The reaction proceeds in dioxane at 120°C over 103 hr with a conversion of 18%, corresponding to a catalytic turnover of 296 (134). The different discriminating ability of the catalyst in the dehydrogenation and hydrogenation steps of the reaction on the same substrate may be explained by assuming that the molecule that is dehydrogenated is the hydrated form of the substrate. The substrate may then enter as a bidentate ligand in the intermediate complex while the hydrogen acceptor acts as monodentate ligand.

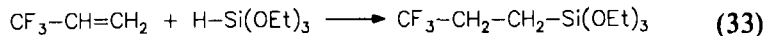
#### F. Related Reactions

Not only molecular hydrogen, but also silanes of the type  $\text{HSiR}_3$  can be added to an unsaturated substrate. Thus considering  $\text{HSiR}_3$  formally as derivatives of the  $\text{H}_2$  molecule, hydrosilylation reactions are strictly related to hydrogenation processes. Several transition metal clusters have been reported to catalyze the hydrosilylation of  $\text{C}=\text{C}$ ,  $\text{C}\equiv\text{C}$ , and  $\text{C}=\text{O}$  functions.

Ruthenium carbonyl is reported to catalyze both the hydrosilylation (addition) and the dehydrogenating hydrosilylation (substitution) of olefins. With trifluoromethylethylene, the ratio of hydrosilylation and dehydrogenating hydrosilylation depends on the nature of the silane:  $\text{HSiEt}_3$  gives specifically (*E*)-1-triethylsilyl-2-trifluoromethylethylene



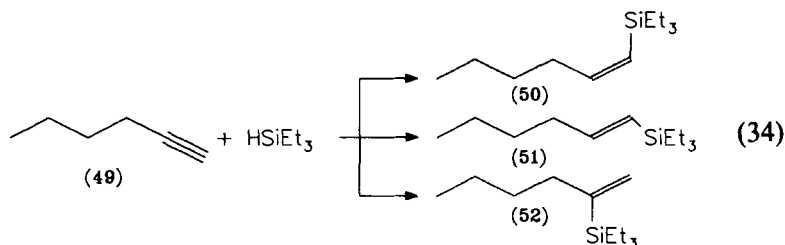
(70°C, 6 hr, conversion 78%, catalytic turnover 210), whereas  $\text{HSi(OEt)}_3$  yields exclusively the saturated product 1-triethoxysilyl-2-trifluoromethylethane



(150°C, 24 hr, conversion 52%, CT 140) (135). Styrene reacts with triethylsilane to give (*E*)-2-triethylsilylstyrene in 96% yield ( $\text{Ru}_3(\text{CO})_{12}$ , benzene, 80°C, 5 hr, CT 186) (136,137). Dehydrogenating hydrosilylation of trimethylsilylethylene, catalyzed by  $\text{Ru}_3(\text{CO})_{12}$ , leads to (*E*)-1,2-disilylenes: With triethylsilane, the reaction gives 67% of (*E*)- $\text{Me}_3\text{SiCH=CHSiEt}_3$  (benzene, 70°C, 5 hr, CT 268); the "disproportionation product" (*E*)- $\text{Me}_3\text{SiCH=CHSiMe}_3$  is formed as a side product (25%)

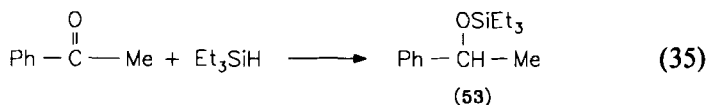
(138). The cluster anion  $[\text{HRu}_3(\text{CO})_{10}(\text{SiEt}_3)_2]^-$  catalyzes the reaction of triethylsilane with ethylene to give both vinyltriethylsilane (52%) and tetraethylsilane (22%); the reaction proceeds in  $\text{CH}_2\text{Cl}_2$  at  $100^\circ\text{C}$  with an initial ethylene pressure of 5 bar (total catalytic turnover 280) (139).

Several transition metal clusters are reported to catalyze the hydrosilylation of hex-1-yne (49) to give the corresponding silylhexenes

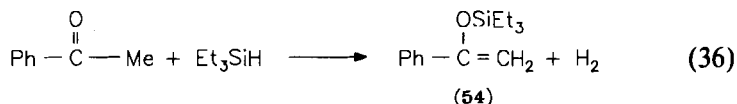


Under comparable conditions (toluene,  $20^\circ\text{C}$ , 72 hr)  $\text{Rh}_4(\text{CO})_{12}$  gives 90% of **50**, 5% of **51**, and 5% of **52** (conversion 100%, CT 1000),  $\text{Co}_2\text{Rh}_2(\text{CO})_{12}$  gives 95% of **50**, 2.5% of **51**, and 2.5% of **52** (conversion 100%, CT 1000), whereas  $\text{Co}_3\text{Rh}(\text{CO})_{12}$  yields 96% of **50**, 2% of **51**, and 2% of **52** (conversion 100%, CT 1000) (139).

A number of mixed-metal clusters catalyze the hydrosilylation as well as the dehydrogenating hydrosilylation of acetophenone induced by UV irradiation: The reaction



was of special interest because a prochiral ketone is hydrosilylated; the use of a transition metal cluster representing framework chirality as a chiral catalyst would provide an unambiguous proof for catalysis by intact clusters. The cluster enantiomer (+)- $\text{CpMoFeCo}(\text{S})(\text{CO})_8$ , however, gave only racemic **53** (16%) along with 48% of **54**



The cluster itself was also recovered in a racemic form (140). This result means that the photo-induced racemization of the chiral catalyst is faster than the hydrosilylation, and it may be used as an argument for or against cluster integrity throughout the catalytic process.

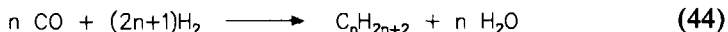
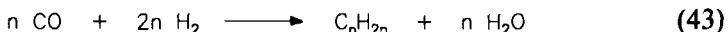
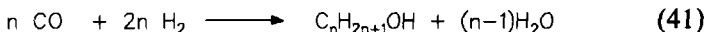
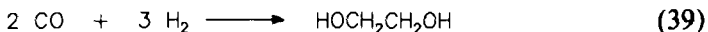
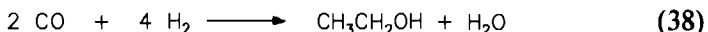
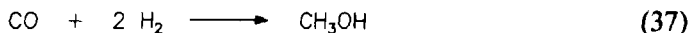
## IV

CATALYTIC REACTIONS INVOLVING CO AND H<sub>2</sub>

One of the fundamental strategies for the systematic build-up of organic molecules uses carbon monoxide and hydrogen as reactants. Transition metal clusters, especially those containing carbonyl and hydride ligands, are particularly suited to catalyze such reactions. Classical examples of this synthetic strategy are syngas reactions, hydroformylation reactions, and homologation reactions.

## A. Syngas Reactions

A series of reactions involving carbon monoxide and hydrogen (synthesis gas) as building blocks for basic organic chemicals are commonly referred to as "syngas reactions." These reactions, based on the catalytic hydrogenation of carbon monoxide, involve the formation of oxygenates, mainly methanol, ethanol, ethylene glycol, and methyl formate, and hydrocarbons, mainly methane, higher alkanes, and olefins



The catalytic synthesis of hydrocarbons from syngas is also represented by the Fischer-Tropsch process (141).

With the exception of the methanol synthesis, which is a major industrial process, heterogeneously catalyzed syngas reactions are very unselective and yield a variety of products. Much effort has therefore been invested in a homogeneous process to produce mainly ethanol and ethylene glycol with high selectivity. Metal clusters are thought to play a key role in these reactions. Syngas chemistry is of less interest for organic synthesis, but of great commercial potential, particularly since the oil crisis has revealed the need for basic chemical feedstocks independent of primary

resources. The generation of ethylene glycol and ethanol from syngas has been reviewed in great detail (142,143). The potential of metal carbonyl clusters in the catalytic hydrogenation of carbon monoxide has also been reviewed (26), and the industrial aspects of cluster chemistry with regard to syngas reactions have been summarized (144–146). Therefore, only a few typical examples have been selected in this section.

Most of the catalytic systems used for syngas reactions are based on rhodium or ruthenium, but there are also some reports on the use of cobalt and, to a lesser extent, platinum clusters [Table V (147–181)]. Of special interest is the selective synthesis of ethylene glycol, which has attracted intense industrial activity. Several patents describing a high-pressure ethylene glycol synthesis using rhodium carbonyl catalysts were disclosed in the 1970s (182–186). A process based on the procedure of Pruett and Walker (182) reached the stage of a pilot plant (187) and operates with rhodium clusters. The reactor is charged with the mononuclear complex  $\text{Rh}(\text{CO})_2(\text{acac})$ , which is converted into various rhodium clusters depending on the reaction conditions. Infrared studies of the catalyst solution under pressures of 550–1030 bar and temperatures up to 200°C suggested the presence of anionic rhodium clusters. The  $\nu(\text{CO})$  IR bands were initially assigned to an anionic species described as  $[\text{Rh}_{12}(\text{CO})_{\sim 34}]^{2-}$  (188,189), which is in a CO-pressure-dependent equilibrium with the isolated and structurally characterized anion  $[\text{Rh}_{12}(\text{CO})_{30}]^{2-}$  (190). Later studies by high-pressure IR spectroscopy (144,191) and high-pressure  $^{13}\text{C}$  NMR spectroscopy (192) showed that the species present under the catalytic conditions is  $[\text{Rh}_5(\text{CO})_{15}]^-$ , which finally could be isolated at low temperatures (193). However, the presence of other anionic rhodium clusters at conditions generally employed for catalytic experiments cannot be excluded. In particular,  $[\text{H}_3\text{Rh}_{13}(\text{CO})_{24}]^{2-}$ ,  $[\text{H}_2\text{Rh}_{13}(\text{CO})_{24}]^{3-}$ ,  $[\text{Rh}_4(\text{CO})_{25}]^{4-}$ , and  $[\text{Rh}_{15}(\text{CO})_{27}]^{3-}$  are under discussion (142). Up to now the role of these anionic rhodium clusters remained uncertain; because of the labile fragmentation and rearrangement processes, the identity of the active species is not apparent.

A particularly broad potential for application in syngas reactions is shown by ruthenium carbonyl clusters. Iodide promoters seem to favor ethylene glycol (155,156); the formation of  $[\text{HRu}_3(\text{CO})_{11}]^-$  and  $[\text{Ru}(\text{CO})_3\text{I}_3]^-$  was observed under the catalytic conditions. These species possibly have a synergistic effect on the catalytic process. Imidazole promoters have been found to increase the catalytic activity for both methanol and ethylene glycol formation (158–160). Quaternary phosphonium salt melts have been used as solvents; in these cases the anion  $[\text{HRu}_3(\text{CO})_{11}]^-$  was detected in the mixture (169). Cobalt iodide as cocatalyst in molten  $[\text{PBu}_4]\text{Br}$  directs the catalytic synthesis toward acetic acid (163). With

TABLE V  
HYDROGENATION OF CARBON MONOXIDE CATALYZED BY VARIOUS TRANSITION METAL CLUSTERS

	Catalyst	Products (%)	Conditions (bar H <sub>2</sub> /bar CO)	Time	Catalytic turnover	Remarks	References
	Co <sub>3</sub> (CO) <sub>9</sub> (CMe)	Methanol (52), ethanol (25), propanol (15), methyl formate (4), ethyl formate (3)	Dioxane, 200°C (100/100)	7 days	6 <sup>a</sup> 3 <sup>b</sup> 2 <sup>c</sup>	HCo(CO) <sub>4</sub> formation	(147)
	Co <sub>4</sub> (CO) <sub>10</sub> (PPh) <sub>2</sub>	Methanol (42), ethanol (30), propanol (9), methyl formate (14), ethyl formate (5)	Dioxane, 185°C (100/100)	7 days	3 <sup>a</sup> 2 <sup>b</sup>	HCo(CO) <sub>4</sub> formation	(147)
	Ru <sub>3</sub> (CO) <sub>12</sub>	Methanol (62), methyl formate (22), ethanol (1), ethylene glycol formate (1), methyl acetate (1)	<i>N</i> -Methylpyrrolidone, 230°C (1000/1000)	2 hr	NG	Conversion 25%	(148, 149)
76	Ru <sub>3</sub> (CO) <sub>12</sub>	Methane (81), ethane (3), propane (2), C <sub>4</sub> –C <sub>30</sub> alkanes (13)	Heptane, 300°C (50/50)	20 hr	84 <sup>d</sup>	Probably erroneous (151, 152)	(150)
	Ru <sub>3</sub> (CO) <sub>12</sub> or H <sub>4</sub> Ru <sub>4</sub> (CO) <sub>12</sub>	Methanol (75), methyl formate (24)	THF, 268°C (520/780)	3 hr	75 <sup>a</sup> 24 <sup>e</sup>	Ru(CO) <sub>5</sub> formation	(151, 152)
	Ru <sub>3</sub> (CO) <sub>12</sub>	Methanol (45), dimethyl ether (6), acetone (4), methyl formate (2)	2-Methoxyethanol, 180°C (120/60)	48 hr	49 <sup>a</sup>	Conversion 60%	(153)
	Ru <sub>3</sub> (CO) <sub>12</sub>	Methyl acetate (99), ethylene glycol diacetate (1)	Acetic acid, 260°C (170/170)	2 hr	177 <sup>f</sup>		(154)
	Ru <sub>3</sub> (CO) <sub>12</sub>	Ethylene glycol (52), methanol (44), ethanol (4)	Sulfolane, 180°C (425/425), I <sub>2</sub> promoter	3 hr	≈ 1 <sup>g</sup> ≈ 1 <sup>a</sup>	[HRu <sub>3</sub> (CO) <sub>11</sub> ] <sup>−</sup> and [Ru(CO) <sub>3</sub> I <sub>3</sub> ] <sup>−</sup> formed	(155, 156)
	Ru <sub>3</sub> (CO) <sub>12</sub>	Ethanol (62), methanol (34), ethylene glycol (<4)	230°C (430/430), Pr <sub>3</sub> PO, I <sub>2</sub> promoter	1 hr	146 <sup>b</sup> 81 <sup>a</sup>	[HRu <sub>3</sub> (CO) <sub>11</sub> ] <sup>−</sup> and [Ru(CO) <sub>3</sub> I <sub>3</sub> ] <sup>−</sup> formed	(157)
	Ru <sub>3</sub> (CO) <sub>12</sub>	Methanol (74), ethylene glycol (10)	<i>N</i> -Methylpyrrolidone, 240°C (250/250), benzimidazole promoter	2 hr	938 <sup>a</sup> 322 <sup>g</sup>		(158–160)

77	$\text{Ru}_3(\text{CO})_{12}$	Methanol (90), ethylene glycol (10)	1,3-Dimethylimidizolidin-2-one, $[\text{N}(\text{PPh}_3)_2]^+$ promoter	1 hr	313 <sup>a</sup> 34 <sup>s</sup>		(161)
	$\text{Ru}_3(\text{CO})_{12}$	Methanol (50), ethanol (36), ethylene glycol monoesters (9), ethylene glycol (5)	$[\text{PBu}_4]\text{Br}$ melt, 220°C (215/215)	6–18 hr	188 <sup>a</sup> 135 <sup>b</sup>		(162)
	$\text{Ru}_3(\text{CO})_{12}$	Acetic acid (57), methane (18), ethyl acetate (17), propyl acetate (3), methyl acetate (2), propionic acid (2)	$[\text{PBu}_4]\text{Br}$ melt, 220°C (241/241), $\text{CoI}_2$ cocatalyst	18 hr	87 <sup>h</sup>	$[\text{Ru}(\text{CO})_3\text{I}_3]^-$ and $[\text{Ru}(\text{CO})_4]^-$ formed	(163)
	$\text{Ru}_3(\text{CO})_{12}$	Methanol (85), ethylene glycol (7), ethanol (7)	<i>N</i> -Methylpyrrolidine, 240°C, $[\text{NMe}_4]\text{Cl}$ (250/250)	2 hr	690 <sup>a</sup>	$[\text{HRu}_3(\text{CO})_{11}]^-$ formed	(164)
	$\text{Ru}_3(\text{CO})_{12}$	Ethylene glycol (61), methanol (38)	Tetraglyme, 240°C, 1-methylbenzimidazol (250/250)	2 hr	120 <sup>s</sup>	$[\text{HRu}_3(\text{CO})_{11}]^-$ formed	(165)
	$\text{Ru}_3(\text{CO})_{12}$	Ethylene glycol (41), methanol (34), glycerine (14)	THF, 1-methyl-3-ethylbenzimidazoliumbromide, $\text{NEt}_3$ , 150°C (50/50)	3 hr	Not specified	$[\text{HRu}_3(\text{CO})_{11}]^-$ formed	(166)
	$\text{Ru}_3(\text{CO})_{12}$	Ethanol (62), propanol (7), methanol (5), methane (5), acetic acid (20)	$[\text{N}(\text{PPh}_3)_2]\text{Br}$ , $\text{Ph}_2\text{O}$ , $\text{Me}_3\text{PO}_4$ , 240°C (200/200)	21 hr	4240 <sup>b</sup>	Continuous reactor	(167)
	$\text{Ru}_3(\text{CO})_{12}$	Methanol (56), glycol aldehyde (25), formaldehyde (10), ethylene glycol (9)	$[\text{N}(\text{PPh}_3)_2]\text{Br}$ , <i>N</i> -methylpyrrolidine, 180°C (160/160)	3 hr	4 <sup>a</sup>	Catalyst concentration unclear	(168)
	$[\text{PBu}_4]-[\text{HRu}_3(\text{CO})_{11}]$	Methanol (48), ethanol (37), ethylene glycol (8), ethylene glycol monoesters (8)	$[\text{PBu}_4]\text{Br}$ melt, 220°C (215/215)	6–18 hr	178 <sup>a</sup> 138 <sup>b</sup>		(169)
	$[\text{PBu}_4]-[\text{Ru}_6(\text{CO})_{18}]$	Methanol (86), ethanol (7), ethylene glycol (5), ethylene glycol monoesters (2)	$[\text{PBu}_4]\text{Br}$ melt, 220°C (215/215)	6–18 hr	105 <sup>a</sup>		(169)

(continued)

TABLE V (continued)

Catalyst	Products (%)	Conditions (bar H <sub>2</sub> /bar CO)	Time	Catalytic turnover	Remarks	References
Rh <sub>4</sub> (CO) <sub>12</sub>	Ethylene glycol (68), methanol (31), methyl formate (1)	Dimethylimidazolidone, 220°C (270/270)	2 hr	20 <sup>a</sup>		(170)
Rh <sub>4</sub> (CO) <sub>12</sub>	Ethylene glycol (66), methanol (22), glycerine (9), methyl formate (2)	THF, NBU <sub>3</sub> , 230°C (900/900)	1 hr	92 <sup>a</sup>	Catalyst concentra- tion unclear	(171)
(MeCN) <sub>2</sub> - Cu <sub>2</sub> Ru <sub>6</sub> C(CO) <sub>16</sub>	Methanol (84), methyl formate (11)	THF, 275°C (600/600)	5 hr	680 <sup>a</sup>		(172)
[N(PPh <sub>3</sub> ) <sub>2</sub> ]- [PtRh <sub>5</sub> (CO) <sub>15</sub> ]	Ethylene glycol (38), methanol (14), methyl formate (2), ethanol (15), ethyl formate (2)	THF, 230°C, 2-hydroxy- pyrrolidine (1000/1000)	4 hr	475 <sup>a</sup>		(173)
[N(PPh <sub>3</sub> ) <sub>2</sub> ]- [PtRh <sub>4</sub> (CO) <sub>12</sub> ]	Ethylene glycol (13), methanol (13), methyl formate (1), ethanol (21)	THF, 230°C (1000/1000)	4 hr	130 <sup>a</sup>		(173)
Ru <sub>3</sub> (CO) <sub>12</sub> / Rh(CO) <sub>2</sub> (acac) (6:1)	Methanol (50), ethylene glycol (50)	N-Methylpyrrolidine, NaI, 230°C (43/43)	1 hr	1000 <sup>a</sup>		(174)
Ru <sub>3</sub> (CO) <sub>12</sub> / Co <sub>2</sub> (CO) <sub>8</sub> (1:1)	Ethanol (40), methanol (18), propanol (13), ethyl acetate (15), propyl ace- tate (7), methyl acetate (6)	[PBu <sub>4</sub> ]Br melt, 220°C (217/217)	6 hr	≈ 85 <sup>b</sup>		(176)
Ru <sub>3</sub> (CO) <sub>12</sub> /CoI <sub>2</sub> (1:3)	Acetic acid (70), ethyl acetate (21), propyl acetate (4), methyl acetate (2), propionic acid (3)	[PBu <sub>4</sub> ]Br melt, 220°C, (241/241)	18 hr	87 <sup>a</sup>		(177)

$\text{Ru}_3(\text{CO})_{12}/\text{Re}_2(\text{CO})_{10}$ (1:3.5)	Methanol (74), ethylene glycol (19), ethanol (6)	<i>N</i> -Methylpyrrolidone, 230°C, $[\text{N}(\text{PPh}_3)_2]\text{Cl}$ (150/150)	2 hr	328 <sup>a</sup>	Catalyst concentration unclear	(178)
$\text{Ru}_3(\text{CO})_{12}/\text{Co}_2(\text{CO})_8$ (2:1)	Acetic acid (77), ethanol (3), methane (10)	Toluene, 220°C, <i>n</i> -heptyl-triphenylphosphoniumbromide, $\text{P}(\text{OPh})_3$ (645/645)	3 hr	44 <sup>b</sup>		(179)
$\text{Ru}_3(\text{CO})_{12}/\text{Co}_2(\text{CO})_8$ (2:3)	Methanol (50), ethylene glycol (24), methyl formate (26)	Toluene, $\text{PPr}_3$ , 270°C (1333/667)	1 hr	394 <sup>a</sup>		(180)
$\text{Ru}_3(\text{CO})_{12}/\text{Co}_2(\text{CO})_8$ (1.8:1)	Methanol (81), ethanol (18), <i>n</i> -propanol (1)	<i>N</i> -Methylpyrrolidone, KI, 220°C (425/425)	4 hr	113 <sup>a</sup>		(181)
$\text{Ru}_3(\text{CO})_{12}/\text{Rh}_4(\text{CO})_{12}$ (4:1)	Methanol (43), ethylene glycol (26), glycol aldehyde (28)	<i>N</i> -Methylpyrrolidone, 200°C, CsI (170/170)	3 hr	19 <sup>a,i</sup>	Catalyst concentration unclear	(168)

<sup>a</sup> Related to methanol.

<sup>b</sup> Related to ethanol.

<sup>c</sup> Related to propanol.

<sup>d</sup> Related to methane.

<sup>e</sup> Related to methyl formate.

<sup>f</sup> Related to methyl acetate.

<sup>g</sup> Related to ethylene glycol.

<sup>h</sup> Related to acetic acid.

<sup>i</sup> Based on the minor cluster component.

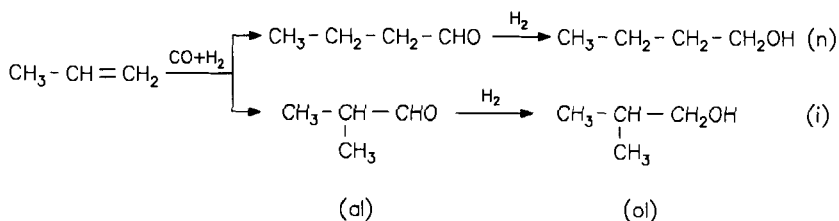


cobalt catalysts, the clusters seem to break down to mononuclear species (147,149). It is believed that in these cases clusters are of no importance (149).

### B. Hydroformylation Reactions

Hydroformylation refers to the addition of hydrogen and carbon monoxide to unsaturated systems. The hydroformylation of olefins is also known as the "oxo synthesis" or the "Roelen reaction" in honor of its inventor. It is one of the major industrial processes. Technical plants use cobalt- or rhodium-based catalysts; the active species are supposed to be mononuclear complexes (194). The most desired oxo product is butanal, generated by the hydroformylation of propylene (195).

The hydroformylation of olefins yields predominantly aldehydes. In the case of terminal olefins, there are two selectivity problems, which are illustrated for propene in Scheme 10. The carbon-carbon coupling can occur at either  $C_1$  or  $C_2$  of the olefin to give the *n*- or the *iso*aldehyde. Many hydroformylation catalysts catalyze also the hydrogenation of the aldehydes formed to give the corresponding alcohols. The ratio of aldehydes to alcohols (al/ol ratio) describes the chemoselectivity of the catalysis. The regioselectivity can be expressed as the ratio of linear to branched products (*n*/*i* ratio). The technical processes based on cobalt catalysts usually yield a mixture of about 80%  $C_4$ -aldehydes, 10% butanols, and 10% other products; the *n*/*i* ratio is 3:1 (195). With rhodium catalysts in combination with phosphine cocatalysts, the *n*/*i* ratio is adjustable within the range 8:1 to 16:1 (195). In contrast to the technical catalysts, most of the transition metal clusters reported as hydroformylation catalysts show a very high chemoselectivity for aldehydes, some of them even being chemospecific [Table VI (196-230)]. The regioselectivity, however, depends markedly on the cluster. A very high *n*/*i* ratio for the hydroformylation of propene was observed with the cluster anion  $[\text{HRu}_3(\text{CO})_{11}]^-$ : In diglyme



SCHEME 10. Chemoselectivity (al/ol ratio) and regioselectivity (*n*/*i* ratio) in the hydroformylation of propene.

TABLE VI  
HYDROFORMYLATION OF OLEFINS CATALYZED BY VARIOUS TRANSITION METAL CLUSTERS

Alkene	Products (%)	Catalyst	Conditions (bar H <sub>2</sub> /bar CO)	Time (hr)	Catalytic turnover <sup>a</sup>	Remarks	References
Ethylene	Propanal (74), ethane (traces)	[NEt <sub>4</sub> ][HRu <sub>3</sub> (CO) <sub>11</sub> ]	DMF, 100°C (13/26), 13-bar C <sub>2</sub> H <sub>4</sub>	5	355	No alcohols observed, catalyst recoverable	(196)
Propene	Butanal (37), 2-methylpropanal (0.5)	[NEt <sub>4</sub> ][HRu <sub>3</sub> (CO) <sub>11</sub> ]	Diglyme, 75°C (1.7/3.3), 5-bar C <sub>3</sub> H <sub>6</sub>	66	57	No alcohols observed, catalyst recoverable	(197)
Propene	Butanal (28), 2-methylpropanal (13), propane (20)	Ru <sub>3</sub> (CO) <sub>12</sub>	Toluene, 150°C (63/98)	1.5	250	No alcohols observed	(198)
But-1-ene	Pentanal (38), 2-methylbutanal (12), butane (26)	Ru <sub>3</sub> (CO) <sub>12</sub>	Toluene, 150°C (45/29)	2.5	155	No alcohols observed	(198)
Pent-1-ene	Hexanal (19), 2-methylpentanal (5)	Rh <sub>4</sub> (CO) <sub>12</sub> /PPh <sub>3</sub> (1:4)	Benzene, 25°C (0.5/0.5)	6	67	No comments on alcohol formation	(198)
Pent-1-ene	Hexanal (78), 2-methylpentanal (21)	Rh <sub>4</sub> (CO) <sub>12</sub> /PPh <sub>3</sub> (1:5)	Benzene, 25°C (0.5/0.5)	6	237	No comments on alcohol formation	(198)
Pent-1-ene	Hexanal (27), 2-methylpentanal (1)	Rh <sub>4</sub> (CO) <sub>12</sub> /P(OPh) <sub>3</sub> (1:4)	Benzene, 25°C (0.5/0.5)	24	74	No comments on alcohol formation	(198)
Pent-1-ene	Hexanal (4), 2-methylpentanal (0.2)	[AsPh <sub>4</sub> ][H <sub>3</sub> Ru <sub>4</sub> (CO) <sub>12</sub> ]	THF, 150°C (10/62)	0.25	19	No comments on alcohol formation	(199)
Pent-1-ene	Hexanal (49), 2-methylpentanal (23)	Co <sub>4</sub> (CO) <sub>10</sub> (PPh) <sub>2</sub>	Toluene, 140°C (110/110)	6	20	No comments on alcohol formation, catalyst recoverable	(200)
Pent-1-ene	C <sub>6</sub> -Aldehydes (61), C <sub>6</sub> -alcohols (0.1), pentane (2), pent-2-enes (23)	[N(PPh <sub>3</sub> ) <sub>2</sub> ]- [HRu <sub>3</sub> (CO) <sub>11</sub> ]	DMF, 150°C (150/150)	16.5	364	Conversion 91%, linearity 95%	(201)
Pent-1-ene	Hexanal (74), 2-methylpentanal (26)	CpMoCo <sub>2</sub> (CMe)(CO) <sub>7</sub> [P(OMe) <sub>3</sub> ]	THF, 130°C (21/21)	24	230	Conversion 25%	(202)

(continued)

TABLE VI (continued)

Alkene	Products (%)	Catalyst	Conditions (bar H <sub>2</sub> /bar CO)	Time (hr)	Catalytic turnover <sup>a</sup>	Remarks	References
Pent-1-ene	Hexanal (76), 2-methylpentanal (24)	Fe <sub>2</sub> Co <sub>2</sub> (CO) <sub>11</sub> (PPh) <sub>2</sub>	Benzene, 130°C (14/14)	168	900	Conversion 50%	(203)
Pent-1-ene	Hexanal (2), 2-methylpentanal (1)	Co <sub>2</sub> Rh <sub>2</sub> (CO) <sub>12</sub> /PPh <sub>2</sub> H (1:3)	Benzene, 25°C (0.5/0.5)	1	6	No side-products measured	(204)
Pent-1-ene	Hexanal (51), 2-methylpentanal (19), pent-2-ene (30)	[N(PPh <sub>3</sub> ) <sub>2</sub> ]- [Fe <sub>2</sub> RhC(CO) <sub>10</sub> ]	CH <sub>2</sub> Cl <sub>2</sub> , 100°C (30/30)	24	NG		(205)
Pent-1-ene	Hexanal (50), 2-methylpentanal (50)	Fe <sub>4</sub> Rh <sub>2</sub> C(CO) <sub>16</sub>	CH <sub>2</sub> Cl <sub>2</sub> , 100°C (30/30)	6	608		(205)
Pent-1-ene	Hexanal (47), 2-methylpentanal (18), pentenes (35)	[PPh <sub>4</sub> ][Fe <sub>4</sub> RhC(CO) <sub>14</sub> ]	CH <sub>2</sub> Cl <sub>2</sub> , 100°C (30/30)	24	395		(205)
Pent-1-ene	Hexanal (50), 2-methylpentanal (50)	[PPh <sub>4</sub> ][Fe <sub>3</sub> Rh <sub>3</sub> C(CO) <sub>15</sub> ]	CH <sub>2</sub> Cl <sub>2</sub> , 100°C (30/30)	5	608		(205)
Pent-1-ene	Hexanal (47), 2-methylpentanal (23)	HFe <sub>3</sub> Rh(CO) <sub>11</sub> - (CCHPh)	Benzene, 60°C (10/10)	5	175		(206)
Pent-1-ene	Hexanal (63), 2-methylpentanal (15), hexan-1-ol (7)	Pt <sub>2</sub> Co <sub>2</sub> (CO) <sub>8</sub> (PPh <sub>3</sub> ) <sub>2</sub>	Benzene, 100°C (28/28)	17	703		(207)
Pent-1-ene	Hexanal (26), 2-methylpentanal (4), hexan-1-ol (1)	Fe <sub>3</sub> (CO) <sub>12</sub> /Ru <sub>3</sub> (CO) <sub>12</sub> (1:1)	MeOH, KOH, H <sub>2</sub> O, 150°C (0/55)	0.5	110		(208, 209)
Pent-1-ene	Hexanal (12), 2-methylpentanal (6), hexan-1-ol (8), 2-methylpentan-1-ol (2)	Rh <sub>6</sub> (CO) <sub>16</sub> /Fe <sub>3</sub> (CO) <sub>12</sub> (1:1)	MeOH, KOH, H <sub>2</sub> O, 150°C (0/55)	0.5	65		(208)
Hex-1-ene	Heptanal (38), 2-methylhexanal (12)	Ru <sub>3</sub> (CO) <sub>12</sub> /Co <sub>2</sub> (CO) <sub>8</sub> (2:3)	Benzene, 110°C (40/40)	1.5	579		(209)

Hex-1-ene	Heptanal (54), 2-methylhexanal (44), 2-ethylpentanal (2)	$\text{Rh}_4(\text{CO})_{12}$	Benzene, 50°C (50/50)	NG	88822	Conversion >98%, catalyst addition of 0.5 mg(!)	(210)
Hex-1-ene	Heptanal (44), 2-methylhexanal (44), 2-ethylpentanal (12)	$\text{Rh}_6(\text{CO})_{16}$	Toluene, 50°C (11/11)	22.5	9588	Conversion 100%, aldehyde selectivity 97%	(211–214)
Hex-1-ene	Heptanal (74), 2-methylhexanal (26), 2-ethylpentanal (1)	$\text{Rh}_4(\text{CO})_{12}$	Toluene, $\text{PPhMe}_2$ (large excess), 125°C (11/11)	21	8000	Conversion 100%, aldehyde selectivity 100%	(213)
Hex-1-ene	Heptanal (18), internal $\text{C}_7$ -aldehydes (5)	$\text{Co}_3(\text{CO})_9(\text{CPh})$	Toluene, 100°C (69/69)	22	55	No comments on alcohol formation	(215)
Hept-1-ene	Octanal, presumably 2-methylheptanal	$\text{Rh}_4(\text{CO})_{12}$	<i>n</i> -Hexane, 75°C (44/46)	1	962	No alcohols observed, <i>n/i</i> ratio ng, $\text{HRh}(\text{CO})_3$ formed	(216, 217)
Oct-1-ene	Nonanal (31), nonan-1-ol (23), branched $\text{C}_9$ -aldehydes (5), branched $\text{C}_9$ -alcohols (2)	$\text{Ru}_3(\text{CO})_{12}$	$[\text{PBu}_4^+]\text{I}^-$ melt, 160°C, 2,2'-bipyridine (55/27)	4	36	$[\text{HRu}_3(\text{CO})_{11}]^-$ formed, conversion 81%	(218)
Octene (mixture)	$\text{C}_9$ -aldehydes (1), $\text{C}_9$ -alcohols (99)	$\text{Ru}_3(\text{CO})_{12}$	$[\text{PBu}_4^+]\text{I}^-$ melt, 180°C (55/27)	4	65 <sup>b</sup>	$[\text{HRu}_3(\text{CO})_{11}]^-$ formed, yield 66%, linearity 42%	(219)
Cyclohexene	Formylcyclohexane (23), cyclohexane (5)	$\text{Ru}_3(\text{CO})_{12}$	Toluene, 150°C (55/20)	2	145	No alcohols observed	(198)
Cyclohexene	Formylcyclohexane (97)	$\text{Rh}_6(\text{CO})_{16}$	Dioxane, 150°C	3	NG	No comments on alcohol formation, contradictory data	(220)
Cyclohexene	Formylcyclohexane (100)	$\text{Ru}_3(\text{CO})_{12}/\text{Co}_2(\text{CO})_8$ (10:1)	THF, 100°C (40/40)	4	400		(221)
Cyclohexene	Formylcyclohexane (27)	$[\text{NEt}_4][\text{FeCo}_3(\text{CO})_{12}]$	THF, 110°C (40/40)	4	108		(221)

(continued)

TABLE VI (continued)

Alkene	Products (%)	Catalyst	Conditions (bar H <sub>2</sub> /bar CO)	Time (hr)	Catalytic turnover <sup>a</sup>	Remarks	References
Cyclohexene	Formylcyclohexane	Ru <sub>3</sub> (CO) <sub>12</sub> /Co <sub>2</sub> (CO) <sub>8</sub> (20:3)	THF, 110°C (40/40)	NG	121	Yield 100%	(222)
Norbornene	Formylnorbornane <sup>c</sup> (55), lactones (15)	Ru <sub>3</sub> (CO) <sub>12</sub> /Co <sub>2</sub> (CO) <sub>8</sub> (20:3)	Benzene, 90°C (40/40)	4	17	Conversion 99%	(223)
Styrene	2-Phenylpropanal (98), 3-phenylpropanal (2)	Rh <sub>4</sub> (CO) <sub>12</sub>	Benzene, 20°C (25/85)	15	717	Conversion 100%	(224a)
Styrene	2-Phenylpropanal (60), 3-phenylpropanal (40)	SCo <sub>3</sub> (CO) <sub>7</sub> (CH <sub>3</sub> C=NC <sub>6</sub> H <sub>11</sub> )	THF, 130°C (60/60)	8	127	Conversion 25%, <i>n</i> / <i>i</i> = 2:3	(224b)
3,3,3-Trifluoropropene	2-Methyl-3,3,3-trifluoropropanal (96), 4,4,4-trifluorobutanal (4)	Rh <sub>6</sub> (CO) <sub>16</sub>	Toluene, 80°C (55/55)	5	7056	Conversion 98%, <i>n</i> / <i>i</i> = 4:96	(225)
Pentafluorostyrene	2-Methyl-2-pentafluorophenylethanal (97), 3-pentafluorophenylpropanal (3)	Rh <sub>6</sub> (CO) <sub>16</sub>	Benzene, 90°C (40/40)	3	30000	Conversion 100%, <i>n</i> / <i>i</i> = 3:97	(226)

Methylmethacrylate	Methyl 2-formyl-2-methylpropionate (97)	$\text{Rh}_4(\text{CO})_{12}$	Toluene, 120°C (55/55)	78	NG	Conversion 62%	(227)
<i>N</i> -Allylacetamide	2-Methyl-3-(acetylamino)propanal (79), 1-acetylpyrrolidine (21)	$\text{Co}_2\text{Rh}_2(\text{CO})_{12}$	THF, 80°C (41/41)	18	160	Conversion 80%	(228)
Dimethylitaconate	Dimethyl 2-formylmethylsuccinate (34), dimethyl 2-formyl-2-methylsuccinate (8), dimethyl methylsuccinate (58)	$\text{Rh}_4(\text{CO})_{12}$	Toluene, 100°C (40/40)	17	> 7360	Conversion > 92%	(229)
Dimethylitaconate	Dimethyl 2-formylmethylsuccinate (9), dimethyl 2-formyl-2-methylsuccinate (42), dimethyl methylsuccinate (45)	$\text{Rh}_4(\text{CO})_{12}$	Toluene, $\text{PPh}_3$ (large excess), 100°C (40/40)	7	> 7360	Conversion > 92%	(229)
<i>N,N</i> -Diethylmethacrylamide	<i>N,N</i> -Diethyl-2-methyl-4-hydroxybutyramide (24)	$\text{Rh}_4(\text{CO})_{12}$	Toluene, 100°C (40/40)	53	72	Several side products, conversion 90%	(230)

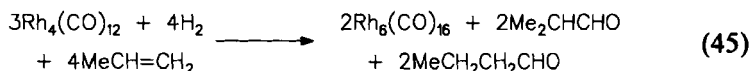
<sup>a</sup> Related to the total of aldehydes.

<sup>b</sup> Related to the total of alcohols.

<sup>c</sup> Unstable, isolated as alcohol upon treatment with  $\text{NaBH}_4$ .

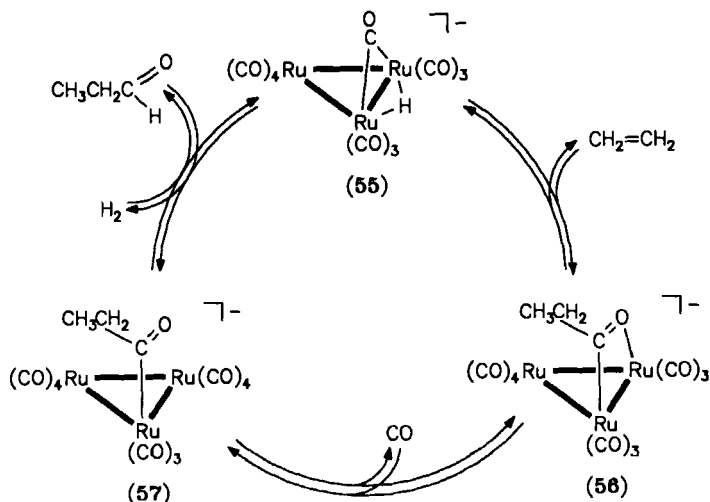
at 75°C under a total pressure of 10 bar, 98.6% of butanal and only 1.4% of 2-methylpropanal are formed (197). This catalysis is almost specific for the formation of butanal.

With rhodium clusters the nuclearity of the species involved is doubtful. Chini *et al.* (231) showed in a clean stoichiometric reaction that propene is converted into a 1:1 mixture of butanal and 2-methylpropanal by  $\text{Rh}_4(\text{CO})_{12}$  and hydrogen; the hexanuclear cluster  $\text{Rh}_6(\text{CO})_{16}$  is formed quantitatively:



The reaction is not catalytic, but it becomes catalytic with excess of tri-phenylphosphine. It appears, however, that in catalytic reactions the unsaturated mononuclear species  $\text{HRh}(\text{CO})_3$  is formed (232,233).

In the case of the cluster anion  $[\text{HRu}_3(\text{CO})_{11}]^-$  as hydroformylation catalyst, indirect evidence has been put forward for catalysis by intact trinuclear ruthenium clusters. The catalytic cycle proposed for the hydroformylation of ethylene by this cluster anion (55) is based on the isolation of the protonation product of the intermediate 56 in addition to isotope labeling studies (234) (Scheme 11). It is assumed that 55 is attacked by ethylene at the bridging carbon atom, possibly via an intermediary  $\eta^2$ -eth-



SCHEME 11. Catalytic cycle proposed for the hydroformylation of ethylene, catalyzed by the cluster anion  $[\text{HRu}_3(\text{CO})_{11}]^-$ , according to (234). [From G. Süss-Fink and F. Neumann, in "The Chemistry of the Metal-Carbon Bond" (F. R. Hartley, ed.), Vol. 5, p. 305. Wiley, New York, 1989. Reprinted by permission of John Wiley & Sons, Ltd.]

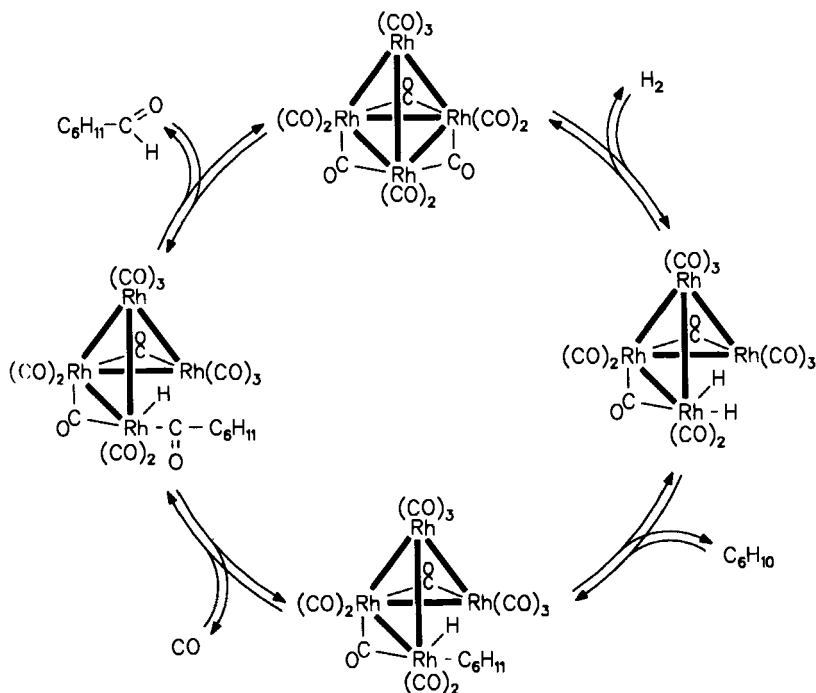
ylene complex, to give the  $\mu_2\text{-}\eta^2(\text{C,O})$ -propionyl complex **56**. Acidification of the reaction solution with  $\text{CF}_3\text{COOH}$  produces the known (235) neutral cluster  $\text{HRu}_3(\text{CO})_{10}(\text{OCCH}_2\text{Me})$ , the crystal structure of which proves the presence of the  $\mu_2\text{-}\eta^2$ -propionyl ligand. The transfer of the hydrido ligand from the metal skeleton in **56** was demonstrated by acidification with  $\text{CF}_3\text{COOD}$ ; the resulting deuterated cluster  $\text{DRu}_3(\text{CO})_{10}(\text{OCCH}_2\text{Me})$  was isolated and characterized (234). While the intermediate **57** could not be trapped by protonation, the mechanism of Scheme 11 is further supported by deuterioformylation of ethylene, giving the expected deuterium distribution in the catalytic product (234).

In the presence of alkali metal halides or iodine as promoters for the hydroformylation of ethylene catalyzed by  $[\text{HRu}_3(\text{CO})_{11}]^-$ , however, kinetic studies indicate that mono- and dinuclear species are responsible for the catalytic activity under these conditions (236). This is in line with reactivity studies involving  $[\text{HRu}_3(\text{CO})_{11}]^-$ ,  $[\text{HRu}(\text{CO})_4]^-$ ,  $[\text{Ru}(\text{CO})_3\text{I}]^-$ , and  $\text{Ru}(\text{CO})_4\text{I}_2$  (237).

For  $\text{Rh}_4(\text{CO})_{12}$  as hydroformylation catalyst, several mechanistic studies including isotope labeling and kinetics have been undertaken. Thus, the deuterioformylation of 2,3,3-trimethylbut-1-ene and of styrene in the presence of  $\text{Rh}_4(\text{CO})_{12}$  have been studied: In the first case, the 3,4,4-trimethylpentanal formed was found to be deuterated exclusively in the formyl position (238). In the latter case, the aldehydes formed were deuterated in the formyl and in the corresponding  $\alpha$ -position; (*E*)- and (*Z*)- $\text{PhCH}=\text{CHD}$  and  $\text{PhCH}=\text{CD}_2$  were also observed (239). The mechanistic implications of these findings are not entirely clear. However, a kinetic study of the  $\text{Rh}_4(\text{CO})_{12}$ -catalyzed low-pressure cyclohexene hydroformylation provides some evidence in favor of intact cluster catalysis: A mechanism proposed on the basis of these findings includes fission of one Rh–Rh bond, whereby the tetranuclear cluster framework remains intact (Scheme 12) (240).

Mixed-metal clusters and mixtures of clusters have also been used as catalysts for the hydroformylation of olefins. No remarkable selectivity has been observed in comparison with monometallic systems; synergistic effects concern only the activity (Table VI). Of particular interest are the metal framework transformations observed for mixed iron–rhodium carbido clusters under hydroformylation conditions. For example the catalyst precursor  $[\text{Fe}_5\text{RhC}(\text{CO})_{16}]^-$  evolves a mixture of  $[\text{Fe}_4\text{Rh}_2\text{C}(\text{CO})_{16}]$  and  $[\text{Fe}_4\text{RhC}(\text{CO})_{16}]^-$ . The latter cluster anion further transforms to  $[\text{Fe}_3\text{Rh}_3\text{C}(\text{CO})_{15}]^-$  under hydroformylation conditions (205). Obviously the carbido ligand stabilizes the cluster skeleton, but a redistribution of the metals around the interstitial carbon atom cannot be avoided during the catalysis. In contrast to these findings, suggesting the catalytic reaction





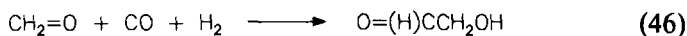
SCHEME 12. Proposed mechanism for the  $\text{Rh}_4(\text{CO})_{12}$ -catalyzed hydroformylation of cyclohexene, adapted from (240).

proceeds at intact clusters, the synergism observed for  $\text{Ru}_3(\text{CO})_{12}$ – $\text{Co}_2(\text{CO})_8$  mixtures has been explained in terms of a “hand-to-hand” cooperation of the individual metals; cobalt carbonyl species seem to perform the carbonylation step, whereas the hydrogenation step is assisted by hydridoruthenium species (222).

Chiral hydroformylation reactions have been studied using the tetranuclear ruthenium cluster  $\text{H}_4\text{Ru}_4(\text{CO})_8(\text{R},\text{R-DIOP})_2$ . The hydroformylation of bicyclo[2.2.2]oct-2-ene (toluene,  $140^\circ\text{C}$ , 100 bar,  $\text{CO}/\text{H}_2=1$ ) yields bicyclo [2.2.2.]octane-2-carbaldehyde with 51% conversion in an optical purity of 1.2% for the *R*-enantiomer (the catalytic turnover was not given) (241). The enantioselectivity is inferior to that reported for the same reaction using the mononuclear system  $\text{HRh}(\text{CO})(\text{PPh}_3)_3$ -*R,R*-DIOP (242). The cluster  $\text{Rh}_4(\text{CO})_{12}$  has also been used with chiral diphosphines as cocatalysts for the enantioselective hydroformylation of styrene (*R,R*-DIOP, benzene,  $40^\circ\text{C}$ , 6-bar  $\text{H}_2$ , 6-bar CO, 96 hr, conversion 70%, CT 1120, *n*/*i* 0.6, ee 18% (*R*)); it is believed, however, that the catalytic

species is the mononuclear complex  $\text{HRh}(\text{CO})_2(\text{R,R-DIOP})$  (243a). With the tetracyclohexyl-modified DIOP ( $\text{R,R-CYDIOP}$ ) as chiral cocatalyst,  $\text{Rh}_4(\text{CO})_{12}$  catalyzes the hydroformylation of (*E*)-2-butene to give predominantly the corresponding branched aldehyde in an optical purity of 2.3% (*S*) (benzene, 80°C, 40-bar CO, 40-bar  $\text{H}_2$ , 24 hr, conversion 60%, *n*/*i* 3:97, CT 1648) (243b).

In addition to the olefin hydroformylation, the hydroformylation of formaldehyde has become particularly interesting since it provides access to ethylene glycol from syngas without involving ethylene. The hydroformylation of formaldehyde, normally employed as polymer (paraformaldehyde), yields glycolaldehyde



which is then hydrogenated to ethylene glycol. The scope and the potential of this reaction have been reviewed recently (244).

There are several reports on transition metal clusters as active catalysts in this reaction. With  $[\text{N}(\text{PPh}_3)_2][\text{Rh}_5(\text{CO})_{15}]$  and  $\text{PPh}_3$ , the reaction proceeds in acetone at 110°C under a pressure of 95 bar ( $\text{H}_2/\text{CO}=1$ ); after 2 hr the paraformaldehyde is completely consumed. The yield of glycolaldehyde is 43% (CT 42); side products are methanol (47%), ethylene glycol (10%), and methyl formate (1%) (245). The proportion of glycolaldehyde can be increased to 88% by using a synergistic system of  $[\text{Rh}_5(\text{CO})_{15}]^-$ ,  $[\text{Rh}(\text{CO})_2\text{Cl}_2]^-$ , and  $\text{PPh}_3$  (245). The tetranuclear rhodium cluster  $\text{Rh}_4(\text{CO})_{12}$ , in the presence of tetrabutylammonium halides as promoters, also converts paraformaldehyde predominantly into glycolaldehyde (acetone, 110°C, 67-bar CO, 67-bar  $\text{H}_2$ , conversion 71%, selectivity 75%, CT 210). Spectroscopic monitoring of the depressurized catalytic solution indicates the presence of  $[\text{Rh}_5(\text{CO})_{15}]^-$ ,  $[\text{Rh}(\text{CO})_2\text{Cl}_2]^-$ , and  $[\text{Rh}_5(\text{CO})_{14}\text{Cl}]^{2-}$  (246).

With a mixture of  $\text{Co}_2(\text{CO})_8$  and  $\text{Ru}_3(\text{CO})_{12}$  (10:1), ethylene glycol was obtained directly (57%), together with 26% methanol (toluene, phenol, 140°C, 450-bar  $\text{H}_2$ , 50-bar CO, 2 hr, CT 98) (247).

The remarkable difference between mixed-metal clusters and an adequate mixture of related clusters is demonstrated by using  $\text{Co}_2\text{Rh}_2(\text{CO})_{12}$  or  $\text{Co}_4(\text{CO})_{12}/\text{Rh}_4(\text{CO})_{12}$  as the catalyst for the hydroformylation of paraformaldehyde. In the first case, 41% of glycolaldehyde was obtained, along with 45% of methanol and 7% of ethylene glycol, while in the latter case the reaction gave 79% of methanol and only 0.3% of glycolaldehyde, but 18% of ethylene glycol (248). So, while the reactivity remained almost the same, the selectivity dropped considerably by going from the cobalt–rhodium cluster to the mixture of cobalt and rhodium clusters.

### C. Homologation Reactions

There is a considerable interest in building up basic organic substrates such as alcohols, carboxylic acids, and esters from their lower-molecular-weight homologs using synthesis gas



The elongation of the carbon chain of these molecules by a  $\text{CH}_2$  unit derived from  $\text{CO}/\text{H}_2$  is called "homologation." Without any doubt, the syngas homologation of methanol to ethanol, once achieved on an industrial scale, would have enormous commercial potential, since it represents the key step in a syngas route to ethylene (249).

Several transition metal clusters, mainly ruthenium compounds, are known to catalyze homologation reactions [Table VII (43b,175,250–261)]. One of the intrinsic problems with this type of reaction is the formation of several higher homologs since the homologation product itself is accessible to homologation catalysis. However, it appears that substrates become less active with increasing carbon chain length. A special application is the conversion of acetic acid into ethylene glycol diacetate with syngas (257), but methyl acetate is the dominant reaction product in this case.

The synergistic effect of two different metals seems to be especially large for reactions with synthesis gas. Accordingly, mixed-metal clusters and mixtures of clusters represent catalysts particularly favorable for homologation processes using  $\text{CO}/\text{H}_2$  for the generation of a  $\text{CH}_2$  building unit. Hidai *et al.* (252) showed that in a given experiment the mixed-metal clusters  $[\text{RuCo}_3(\text{CO})_{12}]^-$  and  $[\text{Ru}_3\text{Co}(\text{CO})_{13}]^-$  convert 18 and 11 mmol of methanol into ethanol, respectively, whereas the conversion with the individual components  $\text{Co}_4(\text{CO})_{12}$  and  $\text{Ru}_3(\text{CO})_{12}$  is only 0.6 and 3 mmol, respectively. The cluster anion  $[\text{FeCo}_3(\text{CO})_{12}]^-$  in the presence of methyl iodide as promoter has been found to convert methanol predominantly into acetaldehyde and its dimethylacetal; at  $180^\circ\text{C}$  and a pressure of 120 bar ( $\text{H}_2/\text{CO}=2$ ), the catalytic turnover is 1395 after 2.5 hr (252). Under a pressure of 270 bar ( $\text{H}_2/\text{CO}=1$ ), a catalytic turnover of 2435 after 1 hr was reported (254a) (Table VII).

Another homologation reaction extensively studied with bimetallic catalysts is the conversion of methyl acetate into ethyl acetate. The most active and also most selective system is composed of  $\text{Ru}_3(\text{CO})_{12}$  and  $\text{Co}_2(\text{CO})_8$  (1:9) in acetic acid with lithium acetate–methyltriphenylphosphonium iodide promoters; yields of 71% product with a catalytic turnover of 2505 in less than 1 hr are reported (260).

TABLE VII  
HOMOLOGATION OF ALCOHOLS, ACIDS, ESTERS, AND HALIDES CATALYZED BY VARIOUS TRANSITION METAL CLUSTERS

Substrate	Products	Catalyst	Conditions (bar H <sub>2</sub> /bar CO)	Time (hr)	Catalytic turnover	References
Methanol	Ethanol (26 mmol), methane (26 mmol)	Ru <sub>3</sub> (CO) <sub>12</sub> /1-methylpiperidine (5:2)	Neat, 200°C (50/150)	3.4	3.3	(250, 251)
Methanol	Ethanol (19%), methoxymethane (16%), methoxyethane (8%), methyl acetate (4%)	[PPh <sub>4</sub> ][RuCo <sub>3</sub> (CO) <sub>12</sub> ]	Neat, 180°C, MeI promoter (80/40)	2.5	144 <sup>a</sup>	(252)
Methanol	Ethanol (15%), methoxymethane (23%), methoxyethane (9%), methyl acetate (3%)	HRuCo <sub>3</sub> (CO) <sub>12</sub>	Neat, 180°C, MeI promoter (80/40)	2.5	116 <sup>a</sup>	(252)
Methanol	Ethanol (11%), methoxymethane (14%), methoxyethane (9%), methyl acetate (3%)	[NEt <sub>4</sub> ][Ru <sub>3</sub> Co(CO) <sub>13</sub> ]	Neat, 180°C, MeI promoter (80/40)	2.5	88 <sup>a</sup>	(252, 253)
Methanol	Acetaldehyde (40%), <sup>a</sup> methyl acetate (6%), ethanol (1%)	[NBu <sub>4</sub> ][FeCo <sub>3</sub> (CO) <sub>12</sub> ]	Neat, 180°C, MeI promoter (135/135)	1	2435	(254a)
Methanol	Ethanol (73%), acetaldehyde (10%)	[NBu <sub>4</sub> ][FeCo <sub>3</sub> (CO) <sub>12</sub> ]	Neat, 220°C, MeI promoter (135/135)	6	2370	(43b)
Methanol	Ethanol (68%), methyl acetate (17%), ethyl acetate (12%)	[(PPh <sub>3</sub> ) <sub>2</sub> Au][RuCo <sub>3</sub> (CO) <sub>12</sub> ]	Neat, 180°C, MeI/KI promoter (65/65)	3	1165 <sup>a</sup>	(254b)
Acetic acid	Propionic acid (25%), butyric acids (7%), valeric acids (3%)	Ru <sub>3</sub> (CO) <sub>12</sub>	Neat, 220°C, MeI promoter (135/135)	18	145	(255, 256)
Acetic acid	Propionic acid (34%), butyric acids (5%)	H <sub>4</sub> Ru <sub>4</sub> (CO) <sub>12</sub>	Neat, 220°C, MeI promoter (135/135)	18	87	(255, 256)
Acetic acid	Methyl acetate (25 mmol), ethylene glycol acetate (0.7 mmol), ethyl acetate (0.5 mmol)	Ru <sub>3</sub> (CO) <sub>12</sub>	Neat, 220°C (215/215)	6	13	(257)

(continued)

TABLE VII (continued)

Substrate	Products	Catalyst	Conditions (bar H <sub>2</sub> /bar CO)	Time (hr)	Catalytic turnover	References
Acetic acid	Methyl acetate (18 mmol), ethyl acetate (12 mmol)	Ru <sub>3</sub> (CO) <sub>12</sub> /PBU <sub>3</sub> (1:6)	Neat, 220°C (215/215)	6	15	(257)
Acetic acid	Methyl acetate (18 mmol), ethyl acetate (4 mmol), glycol acetate (1 mmol)	Ru <sub>3</sub> (CO) <sub>12</sub> /NaRe(CO) <sub>5</sub> (1:3)	Neat, 240°C (150/150)	4	135	(175)
Methyl propionate	Ethyl propionate (127 mmol), <i>n</i> -propyl propionate (12 mmol), acetic acid (19 mmol)	Ru <sub>3</sub> (CO) <sub>12</sub>	Neat, 200°C (138/138)	8	207	(258)
Methyl acetate	Ethyl acetate (21%), acetic acid (22%), ethanol (9%), ethers <sup>b</sup> (7%)	[NEt <sub>4</sub> ][RuCo <sub>3</sub> (CO) <sub>12</sub> ]	Neat, 180°C, MeI promoter (60/60)	18	265 <sup>c</sup>	(259)
Methyl acetate	Ethyl acetate (33%), acetic acid (26%), ethanol (10%), ethers <sup>b</sup> (16%)	[NEt <sub>4</sub> ][Ru <sub>3</sub> Co(CO) <sub>13</sub> ]	Neat, 180°C, MeI promoter (60/60)	18	285 <sup>c</sup>	(259)
Methyl acetate	Ethyl acetate (71%), methanol (15%), ethanol (11%), acetaldehyde (3%)	Ru <sub>3</sub> (CO) <sub>12</sub> /Co <sub>2</sub> (CO) <sub>8</sub> (1:9)	Acetic acid, 215°C, LiOOCCH <sub>3</sub> , [PPh <sub>3</sub> Me]I promot- ers (93/47)	0.7	2505 <sup>c</sup>	(260)
Benzylchloride	2-Phenylethanol (88%), phenylacetaldehyde (3%), toluene (3%)	Rh <sub>4</sub> (CO) <sub>12</sub> /Co <sub>2</sub> (CO) <sub>8</sub> (1:4)	CH <sub>3</sub> CN, Na <sub>2</sub> CO <sub>3</sub> , 110°C (100/150)	3	124	(261)

<sup>a</sup> Related to ethanol.<sup>b</sup> Methoxymethane, methoxyethane.<sup>c</sup> Related to ethyl acetate.<sup>d</sup> Including the corresponding dimethylacetal.

#### D. Miscellaneous and Related Reactions

In contrast to aliphatic carboxylic acids that undergo homologation with syngas in the presence of a suitable catalyst, aryl carboxylic acids are reported to undergo reduction instead of homologation. Diphenylacetic acid is converted into diphenylmethane under a syngas pressure of 435 bar ( $\text{CO}/\text{H}_2=2$ ) using a catalytic system composed of  $\text{Ru}_3(\text{CO})_{12}$  and  $\text{MeI}$  ( $220^\circ\text{C}$ , 16 hr) with 30% yield, corresponding to a catalytic turnover of 7.5 (262).

Formamides can be obtained from ammonia and syngas using ruthenium catalysts:



In molten  $[\text{PBU}_4]\text{I}$ ,  $\text{Ru}_3(\text{CO})_{12}$  yields predominantly methyl- and dimethylformamide ( $220^\circ\text{C}$ , 215-bar  $\text{H}_2$ , 215-bar  $\text{CO}$ , 4 hr, CT 180) (263,264), while with  $\text{Ru}_3(\text{CO})_{12}$  in sulfolane, the main product is formamide ( $204^\circ\text{C}$ , 170-bar  $\text{H}_2$ , 170-bar  $\text{CO}$ , 3.5 hr, CT 645) (265).

Nitrobenzene is reduced to aniline by synthesis gas in the presence of  $\text{Ru}_3(\text{CO})_{12}$

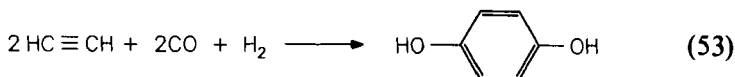


The reaction proceeds without solvent at  $140^\circ\text{C}$  under a pressure of 200 bar ( $\text{CO}/\text{H}_2=1$ ). After 6 hr, 66% of the nitrobenzene is converted to aniline, the catalytic turnover being 800 (266). In contrast to this reduction, nitrobenzene is reduced by synthesis gas to give phenylformamide, if a catalytic system composed of  $\text{Ru}_3(\text{CO})_{12}$  and  $\text{NaOMe}$  is used ( $\text{THF}$ ,  $60^\circ\text{C}$ , 1 bar, 12 hr, 29% yield, CT 4) (267):



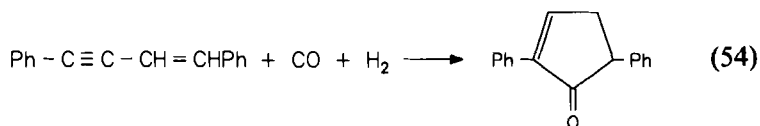
If  $\text{Fe}_3(\text{CO})_{12}$  is used in place of  $\text{Ru}_3(\text{CO})_{12}$ , *N*-phenyl-*O*-methylurethane (61% yield, CT 8) is the predominant product.

Ruthenium carbonyl,  $\text{Ru}_3(\text{CO})_{12}$ , has been reported to catalyze the cyclohydrocarbonylation of acetylene to give hydroquinone:



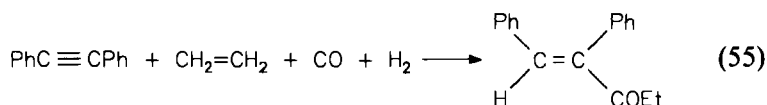
The reaction proceeds in  $\text{THF}$  at  $220^\circ\text{C}$  (127-bar  $\text{CO}$ , 5-bar  $\text{H}_2$ ); after 170 min, 59% of the acetylene is converted into hydroquinone (CT 449) (268). A similar reaction has been described in a patent, giving lower yields of hydroquinone at lower temperature (269). Cyclic enones can be synthe-

sized by hydrocarbonylation of enynes, according to

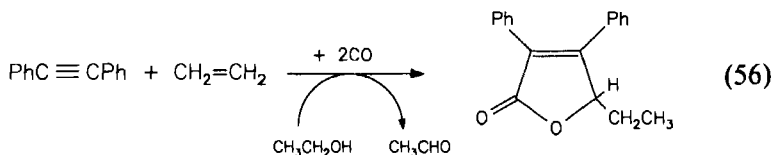


with  $\text{Rh}_4(\text{CO})_{12}$  as the catalyst (benzene, 100-bar  $\text{H}_2$ , 100-bar  $\text{CO}$ ,  $60^\circ\text{C}$ , 6 hr, conversion 91%, selectivity 23%, CT 38) (270).

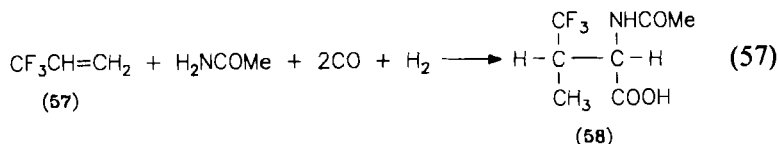
A few reactions in which four components are reacted together in the presence of a transition metal cluster as the catalyst are known. These reactions involve an acetylene, an olefin, carbon monoxide and hydrogen, or a hydrogen donor and are catalyzed by the rhodium cluster  $\text{Rh}_4(\text{CO})_{12}$ . In a typical experiment, an acetone solution of diphenylacetylene is pressurized with ethylene (25 bar),  $\text{CO}$  (30 bar), and  $\text{H}_2$  (5 bar) at  $150^\circ\text{C}$  for 6 hr; the reaction



gives 1,2-diphenylpent-1-en-3-one in 60% yield, the catalytic turnover being 120 (271,272). In contrast, 5-ethyl-3,4-diphenylfuran-2(5H)-one was obtained from an ethanol solution of diphenylacetylene pressurized with ethylene (20 bar) and  $\text{CO}$  (30 bar) at  $180^\circ\text{C}$  for 6 hr, the yield being 73% (CT 292) (273,274):

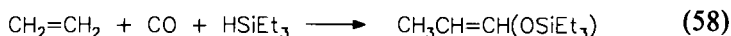


A regioselective hydroformylation–amidocarbonylation process of a fluoroolefin is reported for cobalt–rhodium bimetallic catalyst systems: With  $\text{Rh}_6(\text{CO})_{16}$  and  $\text{Co}_2(\text{CO})_8$  (1:50) in dioxane, 3,3,3-trifluoropropene (57) reacts with acetamide under hydroformylation conditions to give 58 with 94% selectivity (80-bar  $\text{CO}$ , 50-bar  $\text{H}_2$ ,  $120^\circ\text{C}$ , 10 hr, CT 821) (226,275):



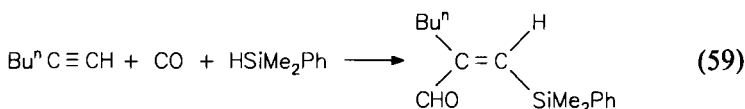
The dinuclear complex  $\text{CoRh}(\text{CO})_7$  is believed to be the active catalyst (276).

When organosilanes of the type  $\text{R}_3\text{SiH}$  are employed instead of molecular hydrogen, catalytic reactions closely related to the hydroformylation process, such as silacarbonylation and silylformylation, can be observed. The cluster anion  $[\text{HRu}_3(\text{CO})_{10}(\text{SiEt}_3)_2]^-$  (or  $[\text{HRu}_3(\text{CO})_{11}]^-$ ) catalyzes the silacarbonylation of ethylene and propene. Ethylene is converted with CO and  $\text{Et}_3\text{SiH}$  at  $100^\circ\text{C}$  in THF into the *Z*-(29%) and *E*-isomers (21%) of 1-(triethylsiloxy)prop-1-ene, the catalytic turnover being 280 after 20 hr (139):



The analogous reaction of hex-1-ene with CO and  $\text{HSiEt}_2\text{Me}$  has been studied with various catalysts. With  $\text{Ru}_3(\text{CO})_{12}$ , the reaction in benzene ( $140^\circ\text{C}$ , 50 bar, 20 hr) yields 40% of the four expected silacarbonylation products (CT 10); the composition of this mixture is (*Z*)-1-diethylmethylsiloxyhept-1-ene 44%, (*E*)-1-diethylmethylsiloxyhept-1-ene 45%, (*Z*)-1-diethylmethylsiloxy-2-methylhex-1-ene 4%, and (*E*)-1-diethylmethylsiloxy-2-methylhex-1-ene 7% (277).

Silylformylation of hex-1-yne was observed with carbon monoxide and dimethylphenylsilane



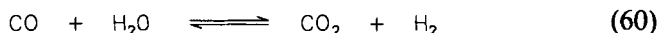
using  $\text{Co}_2\text{Rh}_2(\text{CO})_{12}$  as the catalyst (toluene,  $25^\circ\text{C}$ , 10 bar, 24 hr, conversion 92%, selectivity 100%, CT 720) (278). Similarly, dimethylacetylene reacts with CO and  $\text{Me}_2\text{PhSiH}$  in the presence of  $\text{Rh}_4(\text{CO})_{12}$  (benzene,  $\text{NEt}_3$ ,  $100^\circ\text{C}$ , 30 bar) to give 2-methyl-3-(dimethylphenylsilyl)-but-2-enal (*Z:E* 80:20, conversion 99%, CT 99) (279).

## V

### CATALYTIC REACTIONS INVOLVING CO AND $\text{H}_2\text{O}$

#### A. Water-Gas Shift Reaction

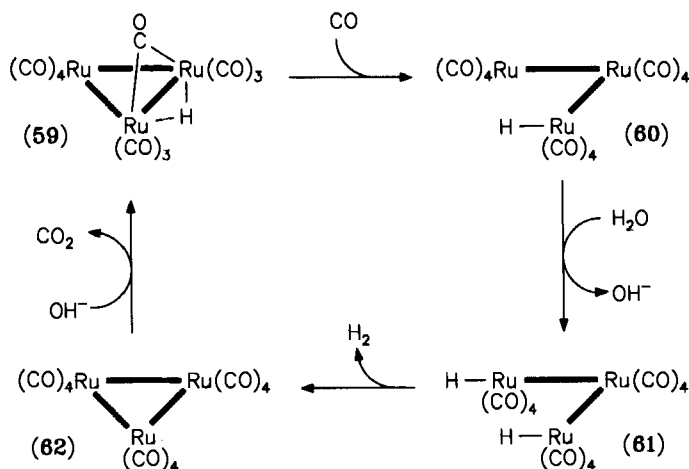
The term "water-gas shift reaction" denotes the conversion of carbon monoxide and water into carbon dioxide and hydrogen





This reaction is of considerable commercial interest because the hydrogen content of synthesis gas can be increased by this equilibrium. Current methods for effecting this reaction involve heterogeneous catalysis at high temperature. The homogeneous catalyst systems for this reaction have been reviewed by Laine and Crawford (280).

Several metal clusters are reported to catalyze this conversion in the homogeneous phase. Most of the reports focus on ruthenium clusters. Ford and co-workers (281) used alkaline solutions of  $\text{Ru}_3(\text{CO})_{12}$  in ethoxyethanol and water, stirred at  $100^\circ\text{C}$  under 1 bar of CO. Over a period of 30 days, the total hydrogen produced by this system corresponded to a catalytic turnover of 150 mol of  $\text{H}_2$  per mole of  $\text{Ru}_3(\text{CO})_{12}$ . In later studies, it was found that alkaline aqueous ethoxyethanol solutions of  $\text{Ru}_3(\text{CO})_{12}$  contain the two known cluster anions  $[\text{HRu}_3(\text{CO})_{11}]^-$  and  $[\text{H}_3\text{Ru}_4(\text{CO})_{12}]^-$  as the principle species present under catalytic conditions (282). These two cluster anions were regarded as the active species for which feasible catalytic cycles have been proposed (282,285). At first it was speculated that  $[\text{HRu}_3(\text{CO})_{11}]^-$  can be protonated by water to give  $\text{H}_2\text{Ru}_3(\text{CO})_{11}$ , which on reaction with CO yields  $\text{Ru}_3(\text{CO})_{12}$  and  $\text{H}_2$ . Ruthenium carbonyl is then reconverted into  $[\text{HRu}_3(\text{CO})_{11}]^-$  by attack of  $\text{OH}^-$  accompanied by the elimination of  $\text{CO}_2$  (282). Because of the instability of  $\text{H}_2\text{Ru}_3(\text{CO})_{11}$  in alkaline solutions, this proposal has been dropped in favor of a cycle depicted in Scheme 13. It is assumed that



SCHEME 13. Proposed catalytic cycle for the implication of  $\text{Ru}_3(\text{CO})_{12}$  and  $[\text{HRu}_3(\text{CO})_{11}]^-$  in the water-gas shift reaction. [From G. Süß-Fink and F. Neumann, in "The Chemistry of the Metal-Carbon Bond" (F. R. Hartley, ed.), Vol. 5, p. 273. Wiley, New York, 1989. Reprinted by permission of John Wiley & Sons, Ltd.]

$[\text{HRu}_3(\text{CO})_{11}]^-$  (**59**) takes up carbon monoxide to give the open-chain anion  $[\text{HRu}_3(\text{CO})_{12}]^-$  (**60**), which is protonated by water to give the neutral  $\text{H}_2\text{Ru}_3(\text{CO})_{12}$  (**61**). With elimination of  $\text{H}_2$ , **61** gives ruthenium carbonyl (**62**), from which **59** is recycled by  $\text{OH}^-$  (283,284). This view is supported by the synthesis of the osmium analog with an open  $\text{Os}_3$  chain,  $\text{H}_2\text{Os}_3(\text{CO})_{12}$  (286). A similar cycle has been proposed for the second anionic species detected in the catalytic solution, the tetranuclear  $[\text{H}_3\text{Ru}_4(\text{CO})_{12}]^-$ . This anion has been assumed to react with CO with elimination of  $\text{H}_2$  to give  $[\text{HRu}_4(\text{CO})_{13}]^-$ , which in turn adds water to give  $[\text{H}_3\text{Ru}_4(\text{CO})_{12}(\text{CO}_2)]^-$ . This species would decarboxylate to regenerate  $[\text{H}_3\text{Ru}_4(\text{CO})_{12}]^-$  (282,283). Careful studies by Shore *et al.* (287*a,b*), however, demonstrated that the tetranuclear cluster anion is formed as a side product of  $[\text{HRu}_3(\text{CO})_{11}]^-$  and  $\text{Ru}_3(\text{CO})_{12}$  under hydrogen pressure; it does not seem to be a catalytic species in the water–gas shift reaction. The equilibrium between tetra- and trinuclear species explains that the trinuclear combination **59**–**62** plays the major role in the catalytic water–gas reaction, irrespective of whether the reaction is initiated by tri- or tetranuclear ruthenium carbonyl complexes (287*a,b*). Using  $^{13}\text{CO}$ , the kinetics of the CO exchange in  $[\text{HRu}_3(\text{CO})_{11}]^-$  established a dissociative pathway that is first order in anion and zero order in CO, to dominate the exchange process. With increasing CO concentration, an associative step that is first order in anion and first order in CO (as proposed in Scheme 13) becomes increasingly significant (287*c*,288).

A catalytic system for the water–gas shift reaction based on  $\text{Ru}_3(\text{CO})_{12}$  in aqueous acetic acid–diglyme solution has also been described (289) [Table VIII (289–296*a*)]. The reaction proceeds in diglyme with  $\text{H}_2\text{SO}_4$  and  $\text{H}_2\text{O}$  added at  $100^\circ\text{C}$  and a partial pressure of CO of 0.9 bar. After an induction period of 6–10 hr, the activity rises to a maximum level and remains constant for about 120 hr; the catalytic turnover is  $\sim 1200$  with respect to hydrogen. After 6–7 days, the catalytic activity drops substantially owing to the limited lifetime of the catalyst. In contrast to alkaline media,  $\text{Ru}_3(\text{CO})_{12}$  seems to form dinuclear species in acidic solutions, and a mechanism based on cationic  $\text{Ru}_2$  clusters has been proposed (289). An aqueous methanol solution of  $\text{Ru}_3(\text{CO})_{12}$  containing sodium sulfide has been reported as a sulfur-tolerant homogeneous catalyst for the water–gas shift reaction (292).

A very pronounced synergistic effect is found for binary ruthenium–iron carbonyl catalysts in the water–gas shift reaction. Both mixed ruthenium–iron clusters and mixtures of ruthenium clusters with iron complexes are considerably more active in basic solutions. Whereas the water–gas shift activity (moles of  $\text{H}_2$  per mole of complex per day) of alkaline aqueous ethoxyethanol solutions of  $\text{Ru}_3(\text{CO})_{12}$  and  $\text{Fe}(\text{CO})_5$  is

TABLE VIII  
HYDROGEN FORMATION BY THE WATER-GAS SHIFT REACTION CATALYZED BY VARIOUS TRANSITION METAL CLUSTERS

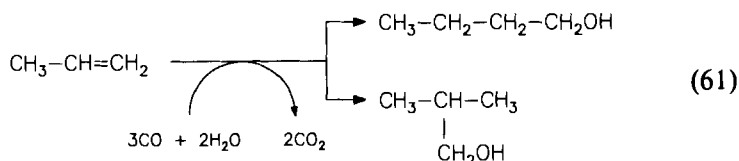
Catalyst	Conditions	Time (hr)	Catalytic turnover	Remarks	References
$\text{Ru}_3(\text{CO})_{12}$	THF, $\text{H}_2\text{O}$ , $\text{NEt}_3$ , $150^\circ\text{C}$ , 24 bar	10	3300		(290)
$\text{H}_4\text{Ru}_4(\text{CO})_{12}$	THF, $\text{H}_2\text{O}$ , $\text{NEt}_3$ , $150^\circ\text{C}$ , 24 bar	10	3400		(290)
$\text{Ru}_3(\text{CO})_{12}$	$\text{AcOH}$ , $\text{H}_2\text{O}$ , Diglyme, $\text{H}_2\text{SO}_4$ , $100^\circ\text{C}$ , 0.9 bar	120	1200	Continuous system, catalyst lifetime 6–7 days	(289)
$\text{Ru}_3(\text{CO})_{12}$	2,2'-Bipyridine, $\text{H}_2\text{O}$ , $150^\circ\text{C}$ , 0.8 bar	24	4400		(291a)
$\text{Ir}_4(\text{CO})_{12}$	$\text{EtOH}$ , $\text{H}_2\text{O}$ , $\text{KOH}$ , $100^\circ\text{C}$ , 0.9 bar	7	60		(291b)
$\text{Ru}_3(\text{CO})_{12}$	$\text{MeOH}$ , $\text{H}_2\text{O}$ , $\text{KOH}$ , $160^\circ\text{C}$ , 27 bar	24	870	Sulfur-tolerant catalyst	(292)
$\text{Rh}_6(\text{CO})_{16}$	THF, $\text{H}_2\text{O}$ , $\text{NMe}_3$ , $150^\circ\text{C}$ , 24 bar	10	1700		(290)
$\text{Rh}_6(\text{CO})_{16}$	2-Ethoxyethanol, $\text{H}_2\text{O}$ , ethylenediamine, $100^\circ\text{C}$ , 0.9 bar	4	98		(293)
$\text{H}_2\text{FeRu}_3(\text{CO})_{13}$	2-Ethoxyethanol, $\text{H}_2\text{O}$ , $\text{KOH}$ , $100^\circ\text{C}$ , 0.9 bar	24	10	Continuous system	(294)
$\text{H}_4\text{Ru}_4(\text{CO})_{12}/\text{Fe}(\text{CO})_5$	2-Ethoxyethanol, $\text{H}_2\text{O}$ , $\text{KOH}$ , $100^\circ\text{C}$ , 0.9 bar	24	30	Continuous system	(294)
$\text{FeRu}_2(\text{CO})_{12}$	Pyridine, $100^\circ\text{C}$ , $\approx 0.4$ bar	24	220	Continuous system	(295, 296a)
$\text{Fe}_2\text{Ru}(\text{CO})_{12}$	Pyridine, $100^\circ\text{C}$ , $\approx 0.4$ bar	24	250	Continuous system	(295, 296a)

reported to be 2.8 and 1.0, respectively, the activity of the mixture  $\text{Ru}_3(\text{CO})_{12}\text{-Fe}(\text{CO})_5$  is 7.4 (208,294). For the mixed-metal cluster  $\text{H}_2\text{FeRu}_3(\text{CO})_{13}$ , the catalytic activity is reported as high as 10.3 (100°C, 0.9-bar CO) (294). A similar increase is found in piperidine-ethoxyethanol solutions under the same conditions ( $\text{H}_4\text{Ru}_4(\text{CO})_{12}$  8.0,  $\text{Fe}(\text{CO})_5$  0.9,  $\text{H}_4\text{Ru}_4(\text{CO})_{12}\text{-Fe}(\text{CO})_5$  30.0) (294). A more dramatic effect has been shown in a different study: A pyridine solution of  $\text{Fe}_3(\text{CO})_{12}$  shows activity 0, the same solution of  $\text{Ru}_3(\text{CO})_{12}$  15, whereas the activities of the mixed clusters  $\text{FeRu}_2(\text{CO})_{12}$  and  $\text{Fe}_2\text{Ru}(\text{CO})_{12}$  were found to be 220 and 250, respectively (100°C, 0.42 to 0.47-bar CO) (295,296a).

The water-gas shift reaction has been applied to the catalytic exchange of deuterium for hydrogen (296b) and for hydroformylation reactions using carbon monoxide and water in the place of molecular hydrogen (199,290). These reactions are discussed in the following section.

### B. Hydroformylation Reactions Using Water as the Hydrogen Source

Hydrogen can be generated from water with carbon monoxide by the water-gas shift reaction (cf. Section V,A). Therefore, water can be used in the place of molecular hydrogen for the oxo synthesis. This modification, which converts olefins predominantly into alcohols, is generally called "hydrohydroxymethylation":



The only industrial application, the synthesis of butanol from propene (Reppe synthesis), was not very successful (297). This reaction is catalyzed by iron carbonyls in the presence of tertiary ammonium salts; the trinuclear cluster anion  $[\text{HFe}_3(\text{CO})_{11}]^-$  detected in the reaction mixture has been discussed as the active species (298). Spectroscopic studies under CO pressure, however, showed the trinuclear anion  $[\text{HFe}_3(\text{CO})_{11}]^-$  to be converted into the mononuclear species  $[\text{HFe}(\text{CO})_4]^-$  (299), and this anion is now assumed to be the catalyst in the Reppe reaction (290).

In most cases, hydroformylation employing the water-gas shift reaction

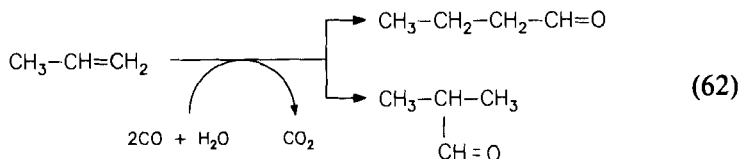


TABLE IX  
HYDROHYDROXYMETHYLATION INCLUDING HYDROFORMYLATION OF OLEFINS WITH CO/H<sub>2</sub> CATALYZED  
BY VARIOUS TRANSITION METAL CLUSTERS

Substrate	Products	Catalyst	Conditions	Time (hr)	al/ol	<i>n</i> / <i>i</i>	Catalytic turnover	References
Propene	Butanal, 2-methylpropanal, butan-1-ol, butan-2-ol, propane	Rh <sub>6</sub> (CO) <sub>16</sub>	THF, H <sub>2</sub> O, NEt <sub>3</sub> , 125°C, 10-bar C <sub>3</sub> H <sub>6</sub> , 24-bar CO	10	40	1.4	300 <sup>a</sup>	(290)
Propene	Butanal, 2-methylpropanal, butan-1-ol, butan-2-ol	Ru <sub>3</sub> (CO) <sub>12</sub>	THF, H <sub>2</sub> O, 100°C, 10-bar C <sub>3</sub> H <sub>6</sub> , 24-bar CO	10	43	11.5	47 <sup>a</sup>	(290)
Propene	Butanal, 2-methylpropanal, butan-1-ol, butan-2-ol	H <sub>4</sub> Ru <sub>4</sub> (CO) <sub>12</sub>	THF, H <sub>2</sub> O, 100°C, 10-bar C <sub>3</sub> H <sub>6</sub> , 24-bar CO	10	37	11	79 <sup>a</sup>	(290)
Propene	Butanal, 2-methylpropanal, butan-1-ol, butan-2-ol, propane	Os <sub>3</sub> (CO) <sub>12</sub>	THF, H <sub>2</sub> O, 180°C, 10-bar C <sub>3</sub> H <sub>6</sub> , 24-bar CO	10	6.6	1.9	13 <sup>a</sup>	(290)
Propene	Butanal, 2-methylpropanal, butan-1-ol, butan-2-ol, propane	H <sub>2</sub> Os <sub>3</sub> (CO) <sub>10</sub>	THF, H <sub>2</sub> O, 180°C, 10-bar C <sub>3</sub> H <sub>6</sub> , 24-bar CO	10	300	1.2	6 <sup>a</sup>	(290)
Propene	Butanal, 2-methylpropanal, butan-1-ol, butan-2-ol, propane	H <sub>4</sub> Os <sub>4</sub> (CO) <sub>12</sub>	THF, H <sub>2</sub> O, 180°C, 10-bar C <sub>3</sub> H <sub>6</sub> , 24-bar CO	10	300	1.4	9 <sup>a</sup>	(290)

Propene	Butanal, 2-methylpropanal, butan-1-ol, butan-2-ol	$\text{Ir}_4(\text{CO})_{12}$	THF, $\text{H}_2\text{O}$ , $125^\circ\text{C}$ , 10-bar $\text{C}_3\text{H}_6$ , 24-bar CO	10	300	1.8	250 <sup>a</sup>	(290)
Propene	Butanal, 2-methylpropanal, butan-1-ol, butan-2-ol	$\text{Co}_3(\text{CO})_9(\text{CMe})$	THF, $\text{H}_2\text{O}$ , DPPE, $135^\circ\text{C}$ , 9-bar $\text{C}_3\text{H}_6$ , 12-bar CO	17	90	NG	5	(300)
Propene	Butanal, 2-methylpropanal, butan-1-ol, butan-2-ol	$[\text{HNEt}_3][\text{HFe}_3(\text{CO})_{11}]$	DMF, $\text{H}_2\text{O}$ , $150^\circ\text{C}$ , 8-bar $\text{C}_3\text{H}_6$ , 20-bar CO	2	10	2	4.5	(301–304)
Pent-1-ene	Hexanal, 2-methylpentanal, hexan-1-ol, hexan-2-ol	$\text{Fe}_3(\text{CO})_{12}$	MeOH, $\text{H}_2\text{O}$ , KOH, $150^\circ\text{C}$ , 55-bar CO	0.5	11.4	1.7	1.1 52 <sup>b</sup>	(305)
Pent-1-ene	Hexanal, 2-methylpentanal, hexan-1-ol, hexan-2-ol	$\text{Ru}_3(\text{CO})_{12}$	MeOH, $\text{H}_2\text{O}$ , KOH, $150^\circ\text{C}$ , 55-bar CO	0.5	$\infty$	48	1.1 55 <sup>b</sup>	(305)
Pent-1-ene	Hexanal, 2-methylpentanal, hexan-1-ol, hexan-2-ol	$\text{H}_4\text{Ru}_4(\text{CO})_{12}$	MeOH, $\text{H}_2\text{O}$ , KOH, $150^\circ\text{C}$ , 55-bar CO	0.5	$\infty$	48	NG	(305)
Pent-1-ene	Hexanal, 2-methylpentanal, hexan-1-ol, hexan-2-ol	$\text{Rh}_6(\text{CO})_{16}$	MeOH, $\text{H}_2\text{O}$ , KOH, $150^\circ\text{C}$ , 55-bar CO	0.5	2.2	2.8	2.7 130 <sup>b</sup>	(305)

<sup>a</sup> Absolute yields not given.

<sup>b</sup> After 24 hr.

dominates hydrohydroxymethylation [Table IX (290,300–305)]. A catalytic system composed of  $\text{Fe}_3(\text{CO})_{12}$ ,  $\text{NEt}_3$ ,  $\text{NaOH}$ ,  $\text{H}_2\text{O}$ , and  $\text{MeOH}$  has been reported to catalyze the hydroformylation and hydrogenation of styrene at  $140^\circ\text{C}$  and 100-bar  $\text{CO}$ ; the products are 2-phenylpropanol (22%) and ethylbenzene (24%), and the catalytic turnover does not exceed 3 (306)

### C. Hydrogenation Reactions Using Water as the Hydrogen Source

There are numerous examples in which  $\text{H}_2\text{O}$  and  $\text{CO}$  were used as hydrogenating agent, taking advantage of the water–gas shift equilibrium, which generates  $\text{H}_2$  and  $\text{CO}_2$  from the water and carbon monoxide feedstock (cf. Section V,A).

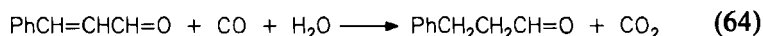
Nitroaryls can be reduced to anilines not only with hydrogen (cf. Section III,D) or synthesis gas (cf. Section IV,D), but also with carbon monoxide and water:



A fairly large number of transition metal clusters have been reported to be active for this conversion [Table X (307–313)].

The  $\text{CO}/\text{H}_2\text{O}$  reduction of aromatic nitrogroups, catalyzed by  $\text{Rh}_4(\text{CO})_{12}$  with 9,10-diaminophenanthrene as cocatalyst, proceeds also with remarkable high selectivities: 1-Nitroanthraquinone is reduced to the corresponding 1-aminoanthraquinone without reduction of the carbonyls (2-methoxyethanol,  $\text{H}_2\text{O}$ ,  $\text{NaOH}$ , 1-bar  $\text{CO}$ ,  $25^\circ\text{C}$ , 10 hr,  $\text{CT} > 250$ ) (312b). On the other hand, with this catalytic system, aromatic nitrofunctions are reduced both with electron-withdrawing or electron-pushing substituents on the aromatic ring: The catalytic turnover varies from 128 for *p*-nitrotoluene over 140 for *p*-nitroanisole and 158 for *p*-chloronitrobenzene to 250 for *p*-nitroaniline (312a).

Some reports concern selective catalytic hydrogenations using  $\text{CO}$  and  $\text{H}_2\text{O}$  in the presence of catalytically active metal clusters. Selective reduction at the  $\text{C}=\text{C}$  double bond occurs for  $\alpha,\beta$ -unsaturated aldehydes, ketones, and nitriles with  $\text{Rh}_6(\text{CO})_{16}$ . As a typical example,  $\beta$ -phenylacrolein is converted into  $\beta$ -phenylpropion-aldehyde in THF at  $130^\circ\text{C}$  and 100 bar; after 20 hr the yield is 74% with 100% selectivity ( $\text{CT} 1190$ ) (314):



In contrast, with  $\text{CO}$  and  $\text{H}_2\text{O}$  the aldehyde function of acrolein is selectively reduced to the alcohol function without reducing the  $\text{C}=\text{C}$  double bond by a catalytic system composed of  $\text{Rh}_6(\text{CO})_{16}$  and 1,3-bis(dimethylamino)propane ( $80^\circ\text{C}$ , 10 bar, 24 hr, yield 94%,  $\text{CT} 56$ ) (315):

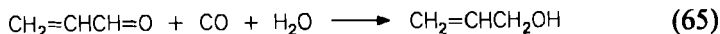
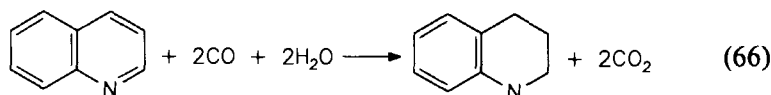


TABLE X  
REDUCTION OF NITROBENZENE TO ANILINE WITH CO/H<sub>2</sub>O CATALYZED BY VARIOUS TRANSITION METAL CLUSTERS

Catalyst	Solvent/promoter	Conditions (bar CO)	Time	Conversion (%)	Catalytic turnover	References
Ru <sub>3</sub> (CO) <sub>12</sub>	Et <sub>3</sub> N-H <sub>2</sub> O	100°C (35)	2	71	710	(307, 308)
H <sub>4</sub> Ru <sub>4</sub> (CO) <sub>12</sub>	Et <sub>3</sub> N-H <sub>2</sub> O	100°C (35)	2	73	730	(307, 308)
Os <sub>3</sub> (CO) <sub>12</sub>	Et <sub>3</sub> N-H <sub>2</sub> O	180°C (35)	1	100	1000	(307, 308)
H <sub>2</sub> Os <sub>3</sub> (CO) <sub>10</sub>	Et <sub>3</sub> N-H <sub>2</sub> O	180°C (35)	1	100	1000	(307, 308)
H <sub>4</sub> Os <sub>4</sub> (CO) <sub>12</sub>	Et <sub>3</sub> N-H <sub>2</sub> O	180°C (35)	1	100	1000	(307, 308)
Ir <sub>4</sub> (CO) <sub>12</sub>	Et <sub>3</sub> N-H <sub>2</sub> O	125°C (35)	1	100	1000	(307, 308)
[NBu <sub>4</sub> ] <sub>2</sub> [Pt <sub>3</sub> (CO) <sub>6</sub> ] <sub>5</sub>	Et <sub>3</sub> N-H <sub>2</sub> O	125°C (35)	10	18	180	(307, 308)
Rh <sub>6</sub> (CO) <sub>16</sub>	Et <sub>3</sub> N-H <sub>2</sub> O	125°C (35)	1	100	1000	(307, 308)
Rh <sub>6</sub> (CO) <sub>16</sub>	H <sub>2</sub> O-Me <sub>2</sub> N(CH <sub>2</sub> ) <sub>2</sub> NMe <sub>2</sub>	80°C (0.9)	4	100	30	(309)
Rh <sub>6</sub> (CO) <sub>16</sub>	H <sub>2</sub> O-H <sub>2</sub> N(CH <sub>2</sub> ) <sub>2</sub> NH <sub>2</sub>	80°C (0.9)	10	34	10	(309)
Rh <sub>6</sub> (CO) <sub>16</sub>	THF, H <sub>2</sub> O, Me <sub>2</sub> NC <sub>6</sub> H <sub>4</sub> CH <sub>2</sub> NH <sub>2</sub>	120°C (24)	8	90	315	(310)
Rh <sub>6</sub> (CO) <sub>16</sub>	EtOH, H <sub>2</sub> O, 3,4,7,8-tetrameth- ylphenanthroline	165°C (30)	2	100	6000	(311)
Rh <sub>4</sub> (CO) <sub>12</sub>	2-Methoxyethanol, H <sub>2</sub> O, NaOH	25°C (1)	3	NG	93	(312a)
Rh <sub>4</sub> (CO) <sub>12</sub>	2-Methoxyethanol, H <sub>2</sub> O, NaOH, DPPM	25°C (1)	3	NG	199	(312a)
Rh <sub>4</sub> (CO) <sub>12</sub>	2-Methoxyethanol, H <sub>2</sub> O, NaOH, 9,10-diaminophenanthrene	25°C (1)	3	NG	610	(312b)
Co <sub>3</sub> (CO) <sub>9</sub> (CPh)	Benzene, H <sub>2</sub> O, NaOH, cetyltri- methylammoniumbromide	20°C (1)	18	81	8	(313)



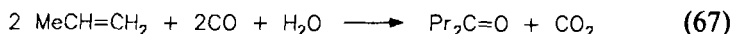
Quinoline is hydrogenated selectively in the nitrogen-containing ring by means of carbon monoxide and water



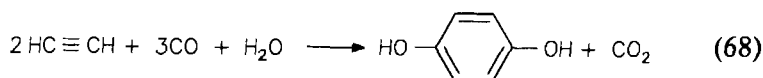
in the presence of catalytic amounts of  $\text{Rh}_6(\text{CO})_{16}$  (2-methoxyethanol,  $150^\circ\text{C}$ , 56 bar CO, 24 hr, yield 97%, CT 117). Substituted quinolines react similarly, but isoquinolines give the corresponding *N*-formyl-1,2,3,4-tetrahydroisoquinolines (316,317).

#### D. Miscellaneous and Related Reactions

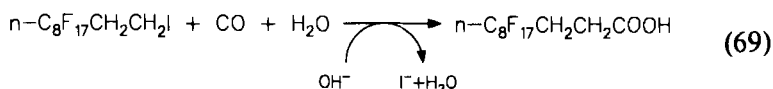
Cobalt clusters in the presence of 1,2-bis(diphenylphosphino)ethane catalyze the hydrocarbonylation of propene with  $\text{CO}/\text{H}_2\text{O}$  to give a mixture of the isomeric dipropyl ketones:



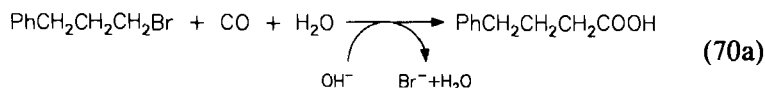
With  $\text{Co}_3(\text{CO})_9(\text{CMe})$ , the yield is 53%, the catalytic turnover being 12 (dioxane,  $165^\circ\text{C}$ , 100 bar) (318). The cyclohydrocarbonylation of acetylene to give hydroquinone has also been performed with  $\text{CO}/\text{H}_2\text{O}$  using  $\text{Ru}_3(\text{CO})_{12}$  as the catalyst (THF,  $190^\circ\text{C}$ , 175 bar, conversion 60%, CT 435) (268):

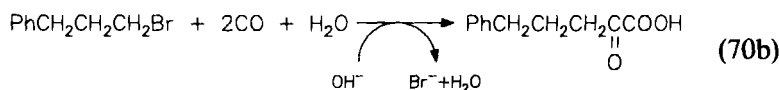


1-Perfluoroalkyl substituted 2-iodoalkanes can be converted with water and carbon monoxide, in the presence of base and  $\text{Rh}_6(\text{CO})_{16}$ , into the corresponding carboxylic acids:



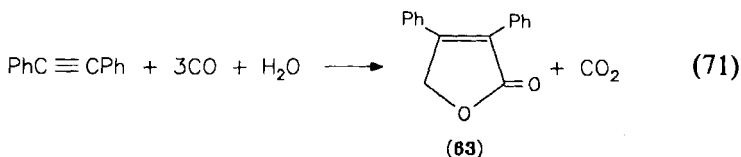
For the perfluorooctyl substituent, the reaction yields 60% of the acid (*tert*-butanol,  $\text{H}_2\text{O}$ ,  $\text{Ca}(\text{OH})_2$ ,  $120^\circ\text{C}$ , 50-bar CO, 24 hr, CT 75) (319a). Alkyl halides react with carbon monoxide and aqueous lithium hydroxide to give carboxylic acids and  $\alpha$ -keto carboxylic acids according to





With the bimetallic cluster  $\text{HFeCo}_3(\text{CO})_{12}$  in *tert*-butanol ( $80^\circ\text{C}$ , 36-bar CO, 2 hr), the conversion is 69%, giving 33% of the acid (CT 20) and 16% of the  $\alpha$ -keto acid (CT 10) (319b).

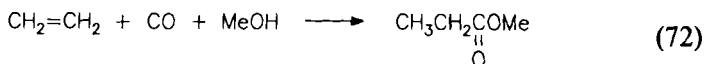
Substituted acetylenes can be converted under water-gas conditions into furan-2(5H)-ones, using  $\text{Rh}_4(\text{CO})_{12}$  as the catalyst. Thus, diphenylacetylene gives 63



with 83% yield (THF,  $\text{H}_2\text{O}$ ,  $\text{NEt}_3$ , 100-bar CO,  $100^\circ\text{C}$ , 5 hr, CT 149) (320).

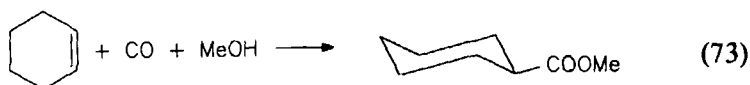
The same cluster catalyzes in the presence of HI the reaction of isoprene with CO and  $\text{H}_2\text{O}$  to give pyroterebic acid and  $\gamma,\gamma$ -dimethyl- $\gamma$ -butyrolactone [ $\text{Rh}_4(\text{CO})_{12}$ , HI,  $\text{H}_2\text{O}$ , THF, 50-bar CO,  $120^\circ\text{C}$ , yield 88%, CT 44, acid/lactone 0.05]; the stoichiometry of the overall reaction is not clear (321). The cluster  $\text{Rh}_6(\text{CO})_{16}$  catalyzes the reaction of pyridine with carbon monoxide and water ( $150^\circ\text{C}$ , 55 bar, 20 hr) to give a series of products, among which the dominant species are 1,5-di(*N*-piperidyl)pentane (55%) and *N*-piperidyl aldehyde (14%). The total catalytic turnover is about 330, but the reaction is not very clear (322).

Strictly related to catalytic reactions involving CO and  $\text{H}_2\text{O}$  are reactions in which CO and alcohols, ROH, or CO and amines,  $\text{R}_2\text{NH}$ , are used as building blocks. The catalytic addition of carbon monoxide and an alcohol to an olefin yields carboxylic esters (hydroesterification). Thus, the synthesis of methyl propionate from ethylene, CO, and methanol using a catalytic system composed of  $\text{Ru}_3(\text{CO})_{12}$  and  $[\text{PPh}_4]\text{I}$  ( $190^\circ\text{C}$ , 20 bar  $\text{C}_2\text{H}_4$ , 45 bar CO, 2.5 hr, yield 74%, CT 1000) has been reported (323):

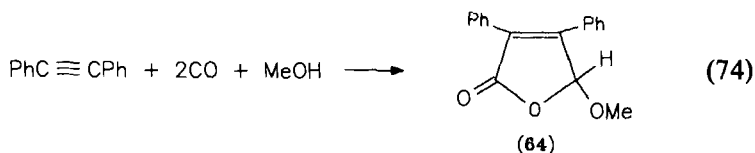


The reaction works also with  $\text{Ru}_3(\text{CO})_{12}$  alone, but the yield and the catalytic turnover are considerably lower. The iodide promoter seems to generate the two anionic species  $[\text{HRu}_3(\text{CO})_{11}]^-$  and  $[\text{Ru}(\text{CO})_3\text{I}_3]^-$ , and a combination of these anions increases the activity and selectivity of the reaction (323). Propylene undergoes hydroesterification with CO and

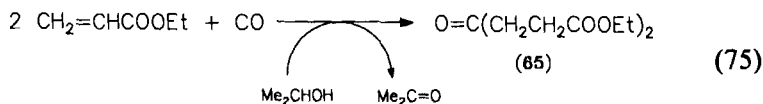
methanol to give *n*- and *i*-methylbutyrate (*n*:*i* = 1:1) in the presence of a binary catalytic system composed of  $\text{Ru}_2\text{Fe}(\text{CO})_{12}$  and  $\text{CuCl}_2$  (*n*-hexane, methanol,  $\text{H}_2\text{O}$ , 8-bar  $\text{C}_3\text{H}_6$ , 20-bar  $\text{CO}$ ,  $180^\circ\text{C}$ , 5 hr, CT 174) (324a). The same reaction is also catalyzed by  $\text{Ru}_3(\text{CO})_{12}$  (benzene, methanol,  $\text{H}_2\text{O}$ , 8-bar  $\text{C}_3\text{H}_6$ , 20-bar  $\text{CO}$ ,  $180^\circ\text{C}$ , 5 hr, CT 540, *n*:*i* = 1:1) (324b). The mixture  $\text{Co}_2(\text{CO})_8$ - $\text{Ru}_3(\text{CO})_{12}$  (3:2) catalyzes the hydroesterification of cyclohexene with carbon monoxide and methanol ( $150^\circ\text{C}$ , 50 bar, 24 hr, 53% yield, catalytic turnover 633) (324c):



In a similar reaction, internal acetylenes can be converted with CO and alcohols into furanones using  $\text{Rh}_4(\text{CO})_{12}$  as the catalyst in combination with a sodium acetate promoter; 5-ethoxy-3,4-diphenylfuran-2(5*H*)-one (64) can be obtained in 87% yield (CT 348) from diphenylacetylene, CO, and methanol ( $125^\circ\text{C}$ , 50 bar, 6 hr) (325,326):

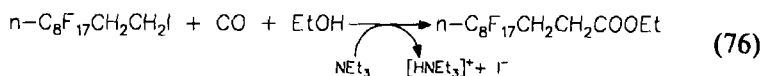


The tetranuclear rhodium cluster  $\text{Rh}_4(\text{CO})_{12}$  has also been reported to catalyze the hydrocarbonylation of acrylic acid derivatives with isopropanol as hydrogen donor. As a typical example, ethyl acrylate reacts with CO and isopropanol



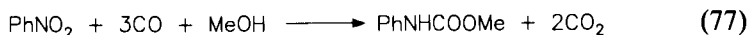
to give diethyl- $\gamma$ -ketopimelate (65) in 60% yield (CT 2400) and acetone ( $180^\circ\text{C}$ , 95 bar, 6 hr); ethyl propionate is formed as side product (327).

In the presence of triethylamine and  $\text{Rh}_6(\text{CO})_{16}$ , 1-perfluoroalkyl substituted 2-iodoalkanes can be converted with CO and alcohols into the corresponding carboxylic esters



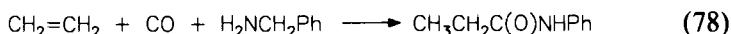
For the perfluorooctyl substituent, the reaction yields 66% of the ester after 24 hr (50-bar  $\text{CO}$ ,  $100^\circ\text{C}$ , CT 35) (319a).

The trinuclear  $\text{Ru}_3(\text{CO})_{12}$  can be used in combination with  $[\text{NEt}_4]\text{Cl}$  to catalyze the selective reductive carbonylation of aromatic nitro compounds to carbamates. Thus, nitro benzene reacts in toluene with CO and methanol ( $160-170^\circ\text{C}$ , 82 bar, 5 hr) to give methyl *N*-phenylcarbamate in 93% yield, the catalytic turnover being 92:

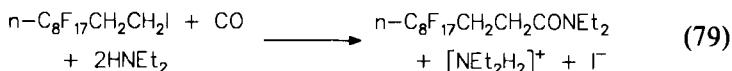


A small amount of aniline (6%) was formed (328,329). The same reaction is also catalyzed by  $\text{Rh}_6(\text{CO})_{16}$  in the presence of 2,2'-bipyridine (toluene, MeOH,  $170^\circ\text{C}$ , 60-bar CO, 1.5 hr, conversion 88%, selectivity 81%, CT 162) (330).

Hydroamidation of olefins can be catalyzed by  $\text{Ru}_3(\text{CO})_{12}$ : The reaction of ethylene and benzylamine (benzene, 17-bar  $\text{C}_2\text{H}_4$ , 40-bar CO,  $150^\circ\text{C}$ , 4 hr) gives *N*-phenylpropioamide



in 51% yield, corresponding to a catalytic turnover of 340 (44). 1-Perfluorooctyl-2-iodoethane reacts with carbon monoxide and diethylamine to give the amide according to



The reaction is catalyzed by  $\text{Rh}_6(\text{CO})_{16}$  (heptane,  $100^\circ\text{C}$ , 50-bar CO, 15 hr, yield 19%, CT 6) (331).

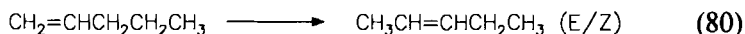
## VI

### OTHER CATALYTIC REACTIONS

After having discussed catalytic reactions involving carbon monoxide, hydrogen, carbon monoxide and hydrogen, as well as carbon monoxide and water, this section is dedicated mainly to isomerization and rearrangement reactions and to carbon-carbon and carbon-nitrogen coupling reactions.

#### A. Isomerization and Rearrangement Reactions

The isomerization of terminal olefins to a mixture of internal olefins



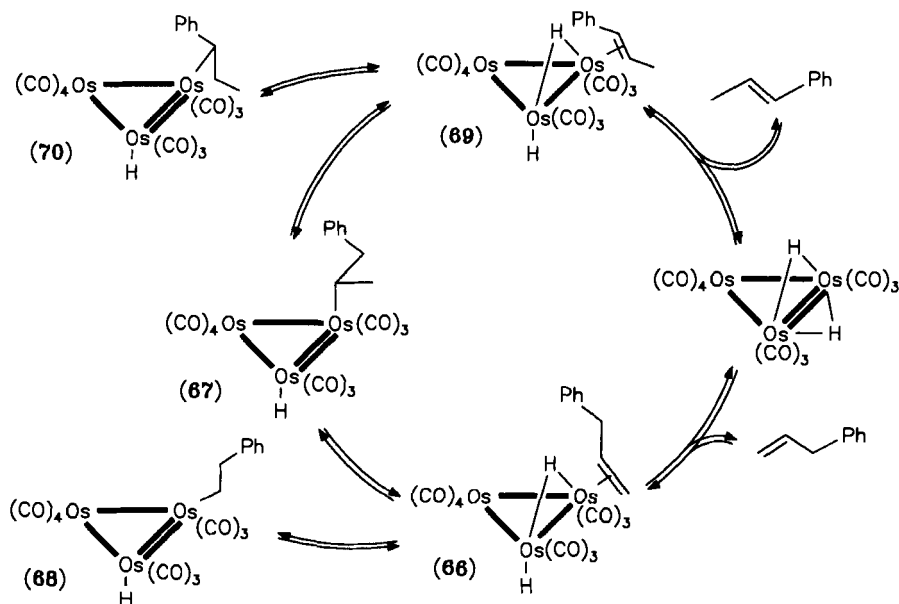
has been studied mainly with ruthenium and osmium clusters.

TABLE XI  
ISOMERIZATION OF OLEFINS AND DIENES CATALYZED BY VARIOUS TRANSITION METAL CLUSTERS

Substrate	Products (%)	Catalyst	Conditions	Time	Catalytic turnover	Remarks	References
Pent-1-ene	( <i>E</i> )-Pent-2-ene (74), ( <i>Z</i> )-pent-2-ene (23)	$\text{Ru}_3(\text{CO})_{12}$	<i>n</i> -Hexane, 70°C	A few hours	NG	Equilibrium composition	(332)
Pent-1-ene	( <i>E</i> )-Pent-2-ene, ( <i>Z</i> )-pent-2-ene	$\text{H}_4\text{Ru}_4(\text{CO})_{12}$	Toluene, 70°C	NG	NG	Product composition NG	(333)
Pent-1-ene	( <i>E</i> )-Pent-2-ene (52), ( <i>Z</i> )-pent-2-ene (48)	$\text{H}_4\text{Ru}_4(\text{CO})_{11}$ - [P(OPh) <sub>3</sub> ] P(OEt) <sub>3</sub>	Toluene, 70°C,	3 hr	20	Conversion 20%	(334)
Pent-1-ene	( <i>E</i> )-Pent-2-ene (51), ( <i>Z</i> )-pent-2-ene (18)	$\text{H}_3\text{Ru}_4(\text{CO})_{12}$ - (AuPPh <sub>3</sub> )	$\text{CH}_2\text{Cl}_2$ , 35°C, 1-bar $\text{H}_2$	24 hr	19	Conversion 71%	(335)
Hex-1-ene	( <i>E</i> )-Hex-2-ene (76), ( <i>Z</i> )-hex-2-ene (24)	$\text{H}_2\text{FeRu}_3(\text{CO})_{13}$	Neat, reflux	2 hr	9000	No hex-3-enes detected	(336)
Hex-1-ene	( <i>E</i> )-Hex-2-ene (66), ( <i>Z</i> )-hex-2-ene (25)	[Pd <sub>4</sub> (SnCl <sub>2</sub> ) <sub>2</sub> - (SnCl <sub>3</sub> ) <sub>8</sub> ] <sup>2-</sup>	EtOH, $\text{H}_2\text{O}$ , HCl, 50-bar $\text{H}_2$	2 hr	146	Excess SnCl <sub>2</sub>	(73)
Hept-1-ene	( <i>E</i> )-Hept-2-ene (40), ( <i>Z</i> )-hept-2-ene (14), ( <i>E</i> )-hept-3-ene (35), ( <i>Z</i> )-hept-3-ene (9)	[NEt <sub>4</sub> ][HRu <sub>3</sub> (CO) <sub>11</sub> ]	Dioxane, 90°C	15 hr	104	Conversion 98%	(337)
Oct-1-ene	Oct-2-ene (60), oct-3-ene (40)	[PPh <sub>4</sub> ][Fe <sub>3</sub> Rh <sub>2</sub> - (CO) <sub>13</sub> (MeCCCH <sub>2</sub> )]	$\text{CH}_2\text{Cl}_2$ , 60°C, 10-bar $\text{H}_2$	24 hr	216	Isomerization 75%	(338)
Oct-1-ene	Octenes <sup>a</sup>	$\text{Pt}_2\text{Co}_2(\text{CO})_8(\text{PPh}_3)_2$	Toluene, 50°C, 33-bar $\text{H}_2$	40 hr	47	Isomerization 43%, conversion 47%	(62)
Penta-1,4-diene	( <i>Z</i> )-Penta-1,3-diene	$\text{Ru}_3(\text{CO})_{12}$	<i>n</i> -Octane, 120°C, 0.9-bar $\text{H}_2$	40 min	113	Yield 39%	(71a)
Penta-1,4-diene	( <i>Z</i> )-Penta-1,3-diene	$\text{Ru}_3(\text{CO})_9(\text{PEt}_3)_3$	<i>n</i> -Octane, 120°C, 0.9-bar $\text{H}_2$	40 min	253	Yield 62%	(71d)
Cycloocta-1,5-diene	Cycloocta-1,4-diene (23), cycloocta-1,3-diene (27)	$\text{Ru}_3(\text{CO})_{12}$	<i>n</i> -Octane, 125°C	30 min	100		(339)
1,2-Dicarbethoxy- 1,2,3,6-tetrahy- dropyridazine	1,2-Dicarbethoxy-1,2,3,4- tetrahydropyridazine	$\text{H}_4\text{Ru}_4(\text{CO})_{12}$	Neat, 100°C	72 hr	117	Conversion 90%	(340)

<sup>a</sup> Product composition not specified.

Pent-1-ene is converted into (*E*)-pent-2-ene and (*Z*)-pent-2-ene when refluxed in hexane with  $\text{Ru}_3(\text{CO})_{12}$ ; the equilibrium is reached within a few hours (332) [Table XI (62,71a,71d,73,332–340)]. Similar results were obtained with  $\text{H}_4\text{Ru}_4(\text{CO})_{12}$  (333) and the phosphorus derivatives  $\text{H}_4\text{Ru}_4(\text{CO})_{11}\text{L}$ , where the isomerization rate decreases in the sequence  $\text{L} = \text{P}(\text{OEt})_3 > \text{P}(\text{OPh})_3 > \text{PPh}_3 > \text{CO}$  (334). The influence of the solvent on the isomerization rate decreases in the order chlorobenzene > benzene > toluene > cyclohexane > mesitylene (341). The catalytic turn-overs were not given. The same isomerization was also studied with  $\text{H}_2\text{Ru}_4(\text{CO})_{13}$ ,  $\text{HRu}_3(\text{CO})_9(\text{C}_6\text{H}_9)$  (342), and  $\text{Os}_3(\text{CO})_{12}$  (343). By comparing several metals, the *Z/E* ratio was found to vary from 0.4–0.5 for  $\text{Os}_3(\text{CO})_{12}$  (343), 0.3–0.4 for  $\text{Ru}_3(\text{CO})_{12}$  (332), 0.35 for  $\text{Fe}_3(\text{CO})_{12}$  (344) to 0.26 with  $\text{Co}_3(\text{CO})_6(\text{PBU}_3)_3$  (345). The isomerization of pent-1-ene using  $\text{Fe}_3(\text{CO})_{12}$ ,  $\text{Ru}_3(\text{CO})_{12}$ ,  $\text{Ru}_3(\text{CO})_9(\text{PPh}_3)_3$  (346) or  $\text{H}_4\text{Ru}_4(\text{CO})_{12}$  (347) has also been studied under photolytic conditions. By comparison with the mononuclear catalysts  $\text{Fe}(\text{CO})_5$  and  $\text{Ru}(\text{CO})_4\text{PPh}_3$  under photolytic conditions, the *Z/E* ratio of the pent-2-enes formed was shown to be substantially different, suggesting different active species (346).

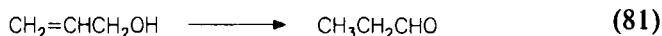


SCHEME 14. Proposed catalytic cycle for the isomerization of olefins catalyzed by  $\text{H}_2\text{Os}_3(\text{CO})_{10}$ , according to (348). [From G. Süss-Fink and F. Neumann, in "The Chemistry of the Metal–Carbon Bond" (F. R. Hartley, ed.), Vol. 5, p. 303. Wiley, New York, 1989. Reprinted by permission of John Wiley & Sons, Ltd.]

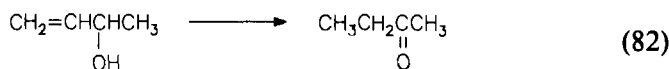
A catalytic cycle for the isomerization of olefins by the unsaturated cluster  $\text{H}_2\text{Os}_3(\text{CO})_{10}$  has been proposed by Deeming and Hasso (Scheme 14): It is assumed that  $\text{H}_2\text{Os}_3(\text{CO})_{10}$  adds to the alkene to give the  $\eta^2$ -alkene complex **66**, phosphine analogs of which have been synthesized and characterized (348). Complex **66** can react with hydrogen transfer from the metal framework to the coordinated olefin to give the hydridoalkyl complexes **67** or **68**. With diethyl fumarate or dimethyl maleate, a hydridoalkyl cluster of the type  $\text{HOs}_3(\text{CO})_{10}[\text{CH}(\text{CH}_2\text{COOEt})(\text{COOEt})]$ , in which the ester function helps to stabilize the system, could be characterized (348). The reverse hydrogen transfer from **67** gives **69**, from which the isomerized alkene can be eliminated.

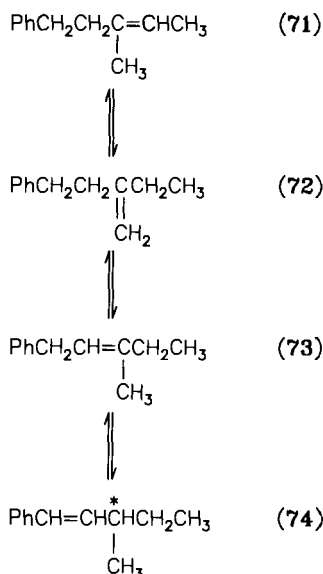
There are only a few reports on synthetic applications of the double bond isomerization reaction. Methyl linoleate (*Z,Z*-isomer) has been isomerized to a mixture of the *Z,E*- and *E,E*-isomers with a number of ruthenium, iron, osmium, and cobalt clusters (349,350). The highest conversion was observed with  $\text{H}_4\text{Ru}_4(\text{CO})_{12}$ , but there was a substantial amount of the hydrogenation product, methyl oleate. Readily obtained by Diels-Alder cycloaddition of buta-1,3-diene to azodicarboxylates, *N*-protected 1,2,3,6-tetrahydropyridazines can be transformed almost quantitatively and with complete chemoselectivity into the corresponding 1,2,3,4-tetrahydropyridazines; the double bond shift is catalyzed by the cluster  $\text{Ru}_3(\text{CO})_{12}$  (Table XI) or by the mononuclear complex  $\text{Ru}(\text{PPh}_3)_4\text{Cl}_2$  (340). An *enantio*-face discriminating isomerization process has been reported with the chiral cluster  $\text{H}_4\text{Ru}_4(\text{CO})_8(\text{R,R-DIOP})_2$  (Scheme 15) (351). The prochiral substrate **71** was heated with  $\text{H}_4\text{Ru}_4(\text{CO})_8(\text{R,R-DIOP})_2$  at 80°C under 130 bar of hydrogen. After 23 hr, the reaction mixture contained 12% of the *E*-isomer of the chiral olefin **74**; its optical purity was 0.5% (351).

The isomerization of olefinic bonds can lead to a refunctionalization of the molecule if it contains the appropriate substituents. In this fashion, allyl alcohol is not isomerized to methylvinyl alcohol but to propionaldehyde:



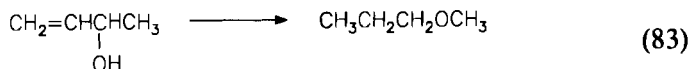
This reaction can be catalyzed (32°C) by the osmium cluster  $\text{H}_2\text{Os}_3(\text{CO})_{10}$  (352). The effect of substituents on the isomerization has also been studied: But-2-en-1-ol and but-3-en-2-ol react similarly to give butanal and butanone, respectively,





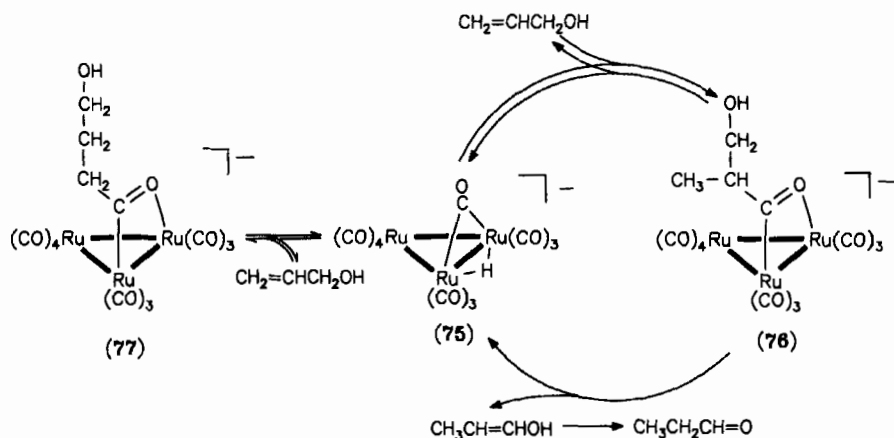
SCHEME 15. Enantioselective isomerization of 3-methyl-5-phenyl-pent-2-ene (71). [From G. Süss-Fink and F. Neumann, in "The Chemistry of the Metal-Carbon Bond" (F. R. Hartley, ed.), Vol. 5, p. 255. Wiley, New York, 1989. Reprinted by permission of John Wiley & Sons, Ltd.]

but 2-methylprop-2-en-1-ol does not react; substituents at C<sub>2</sub> lead to a complete suppression of the isomerization. The isomerization of mono-deuterated allyl alcohol, CH<sub>2</sub>=CHCH<sub>2</sub>OD, leads to CH<sub>3</sub>CHDCHO, thus demonstrating the shift of the alcoholic hydrogen (352). By using Rh<sub>6</sub>(CO)<sub>16</sub> as the catalyst, but-3-en-2-ol is isomerized to give not butan-2-one but methyl propyl ether (353):



The cluster anion [HRu<sub>3</sub>(CO)<sub>11</sub>]<sup>−</sup> also catalyzes the conversion of allyl alcohol into propionaldehyde, according to Eq.(81). The reaction proceeds in THF solution at 20°C, giving a catalytic turnover of 1100 (354). Isotope labeling and kinetic studies suggest a catalytic cycle depicted in Scheme 16. Allyl alcohol is assumed to attack the bridging carbonyl in 75, with transfer of the hydride from the metal framework to the incoming substrate. The isomeric clusters 76 or 77 are formed. While 77 can only undergo back reaction with elimination of allyl alcohol, 76 can react back to 75 by either allyl alcohol elimination or by elimination of the vinylog

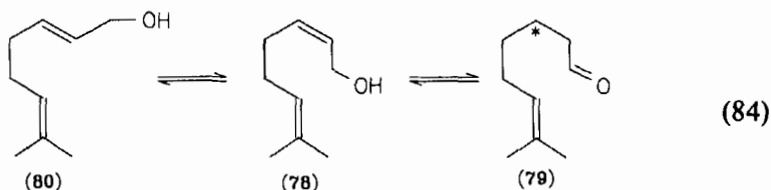




SCHEME 16. Proposed mechanism for the conversion of allyl alcohol into propionaldehyde catalyzed by  $[\text{HRu}_3(\text{CO})_{11}]^-$  according to (354).

$\text{CH}_3-\text{CH}=\text{CH}-\text{OH}$ , which is known to undergo spontaneous isomerization to propionaldehyde (354).

The chirally modified cluster  $\text{HRu}_3(\text{CO})_{10}(\overline{R\text{-OCNCH}_2\text{CH}_2\text{CH}_2\text{CHCH}_2\text{OCH}_3)$  catalyzes the conversion of the prochiral allylic alcohol nerol (78) into the chiral aldehyde citronellal (79)



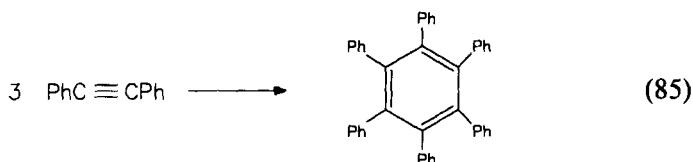
The reaction proceeds at  $60^\circ\text{C}$  in THF and also yields geraniol (80), the *trans*-isomer of 79. Both catalytic turnover (41 mol 79/mol catalyst) and optical purity (ee 12%) are rather modest (355).

The disproportionation of 1,3-cyclohexadiene to a near 1:1 mixture of cyclohexene and benzene is reported to be catalyzed quite effectively by  $\text{Ir}_4(\text{CO})_{12}$ . The reaction proceeds at  $160^\circ\text{C}$ ; further experimental details and the catalytic turnover are not communicated (356).

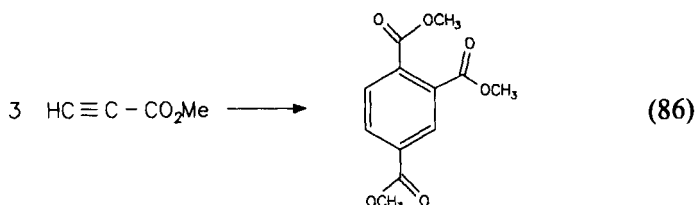
### B. Carbon-Carbon Coupling Reactions

Carbon-carbon coupling reactions represent the key step in the build-up of more sophisticated organic structures. C-C coupling reactions of

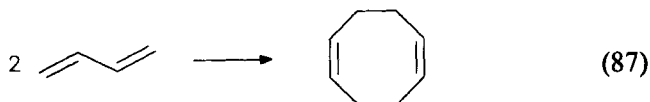
special interest are cyclizations. The cyclotrimerization of diphenylacetylene to give hexaphenylbenzene



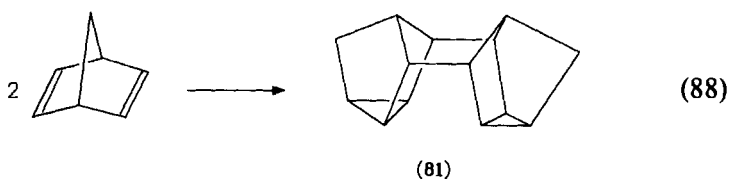
has been reported with  $\text{Fe}_3(\text{CO})_{12}$  as the catalyst (neat, 266–280°C, seconds, 75% yield, CT 3–4) or with  $\text{Co}_4(\text{CO})_{10}(\text{C}_2\text{Ph}_2)$  (dioxane, 100°C, 1 hr, yield 80%, CT 26) (357). The parent acetylene is cyclotrimerized to give benzene at 17°C in the presence of the nickel cluster  $\text{Ni}_4(\text{CNBu}^t)_7$ ; details are not reported (358). Methyl propiolate can be cyclotrimerized in the same way using  $\text{Ru}_3(\text{CO})_{12}/\text{PPh}_3$  as the catalyst, where the main product is the 1,2,4-isomer (neat, 130°C, sealed tube, 20 hr, CT 574) (359):



Another important class of reactions is the cyclodimerization of dienes. Thus, cycloocta-1,5-diene is accessible from buta-1,3-diene

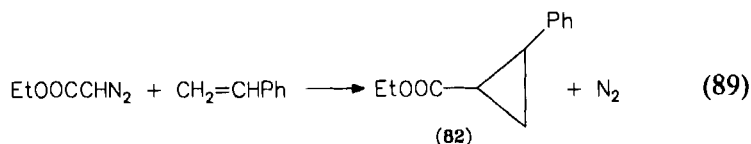


in the presence of  $\text{Ni}_4(\text{CNBu}^t)_7$ . The reaction takes place at 20°C, and after 27 hr the solution contains 76% of the 1,5-isomer and 4% of the 1,3-isomer, corresponding to a catalytic turnover of 33 (358,360). Probably the first example of a new organic molecule catalytically generated by a transition metal cluster is *endo,endo*-heptacyclo [5.3.1.1<sup>2,6</sup>.1<sup>4,12</sup>.1<sup>9,11</sup>.0<sup>3,5</sup>.0<sup>8,10</sup>]tetradecan (Binor-S) (81). This compound is accessible by the stereospecific fusion of two norbornadiene molecules



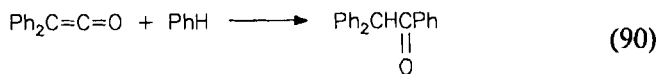
The process is catalyzed by a number of cobalt and rhodium clusters (361). Anionic clusters such as  $[\text{FeCo}_3(\text{CO})_{12}]^-$  and  $[\text{Co}_6(\text{CO})_{15}]^-$  show greater catalytic activity than would be expected from neutral clusters of the same size (361). Other mixed-metal clusters, such as  $\text{Zn}_2\text{Co}_4(\text{CO})_{15}$  (362) and  $\text{Pt}_3\text{Co}_2(\text{CO})_9(\text{PPh}_3)_3$  (363), have also been reported to be active for the stereospecific dimerization of norbornadiene to give **81**. In the presence of  $\text{BF}_3 \cdot \text{Et}_2\text{O}$ ,  $\text{Pt}_3\text{Co}_2(\text{CO})_9(\text{PPh}_3)_3$  converts norbornadiene into **81** with 100% yield and 100% selectivity (20°C, 30 min, CT 31).

Cyclopropanation reactions are catalyzed by rhodium clusters. Styrene reacts with ethyl diazoacetate to give the cyclopropane derivative **82**, catalyzed by  $\text{Rh}_6(\text{CO})_{16}$  (25°C, conversion 87%, CT 174) (364):

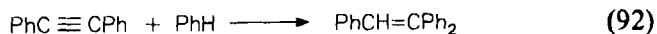
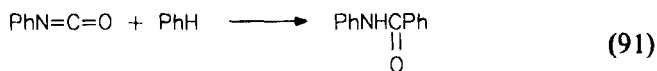


The analogous reaction at 83°C with cyclohexene produces the corresponding bicycle in 43% yield (*anti/syn* ratio = 3), the catalytic turnover being 430 (365).

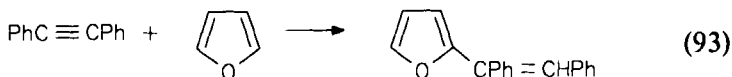
A number of C–C coupling reactions involving the activation of aromatic C–H bonds have been reported with the rhodium clusters  $\text{Rh}_4(\text{CO})_{12}$  and  $\text{Rh}_6(\text{CO})_{16}$  as catalysts. Thus, benzene can be reacted with diphenyl ketene, according to



to give diphenyl acetophenone. Similarly, benzene reacts with isocyanates or with acetylenes to give the products according to

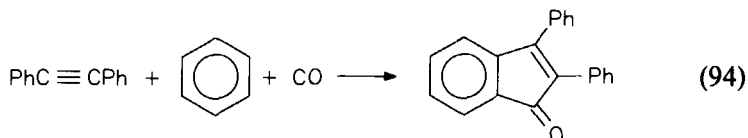


These reactions are carried out at temperatures between 180 and 220°C and under a pressure of carbon monoxide (20–30 bar); exact data for calculating the catalytic turnovers were not reported (366). In a similar reaction, furans have been added to acetylenes to give furylethylenes using  $\text{Rh}_4(\text{CO})_{12}$  as catalyst



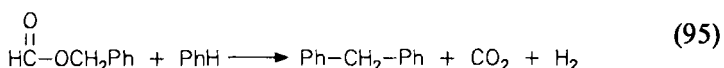
The reaction requires a pressure of 25-bar CO in order to suppress the trimerization of the acetylene. The products are formed within 7 hr at 220°C, giving yields up to 86% (CT up to 1000) (367).

Rhodium carbonyl,  $\text{Rh}_4(\text{CO})_{12}$ , catalyzes the cyclocarbonylation of acetylenes with benzene to give indenones. For example 2,3-diphenyl-indenone is obtained from diphenyl acetylene and benzene in 10% yield, corresponding to a catalytic turnover of 11 (220°C, 25 bar, 7 hr)

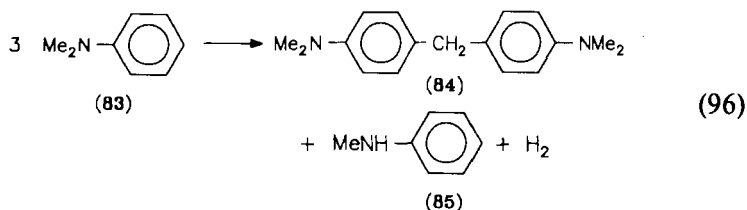


The reaction is not very selective; triphenyl-ethylene (45%), 1-benzylidene-2,3-diphenylindene (8%), *trans*-stilbene (12%), and 2,3,4,5-tetraphenylcyclopentenone (16%) are further reaction products (368). In a similar fashion, benzene and CO can be added to diphenylketene in the presence of  $\text{Rh}_4(\text{CO})_{12}$  to give small amounts of 1-diphenylmethylene-3-phenylindene (3% yield, CT 6). The main product of the reaction (200°C, 30 bar, 5 hr), however, is 2,2-diphenylacetophenone (68%) (369).

The benzylation of arenes with benzyl formate is catalyzed by  $\text{Ru}_3(\text{CO})_{12}$ : Benzene is shown to give diphenylmethane according to

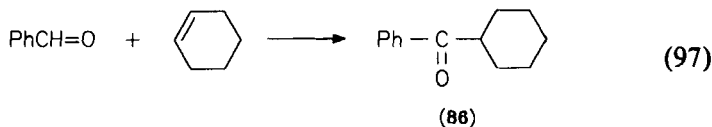


(200°C, 6 hr, yield 22%, CT 11) (370). A carbon-carbon coupling of aromatic amines has been reported to occur in the presence of  $\text{Os}_3(\text{CO})_{12}$  or  $\text{H}_4\text{Os}_4(\text{CO})_{12}$ . *N,N*-Dimethylaniline (**83**) is converted into bis (*p*-*N,N*-dimethylaminophenyl)methane (**84**) and *N*-methylaniline (**85**)



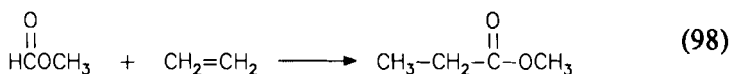
The fate of the hydrogen eliminated in this reaction is not clear, the stoichiometry of the reaction not being precisely established (358). The catalytic reaction proceeds in pure refluxing *N,N*-dimethylaniline (140°C); after 36 hr the catalytic turnover is 742 mol of **84** per mole of  $\text{Os}_3(\text{CO})_{12}$ . The reaction is inhibited by CO pressure (358).

Apart from arenes, most carbon-carbon coupling reactions involve olefins. Ruthenium carbonyl,  $\text{Ru}_3(\text{CO})_{12}$ , catalyzes the addition of aldehydes to olefins according to



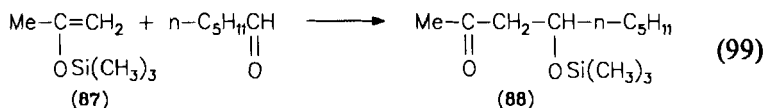
For example, benzaldehyde reacts with cyclohexene to give the corresponding phenone **86** in 50% yield (neat,  $200^\circ\text{C}$ , 48 hr, 20-bar CO, CT 50) (371,372). Allylic acetates as the olefin component, however, react with aldehydes to give homoallylic alcohols. For instance,  $\text{PhCH(OH)CH}_2\text{CH=CH}_2$  is accessible from allyl acetate and benzaldehyde with 87% yield ( $\text{Ru}_3(\text{CO})_{12}$ ,  $\text{NEt}_3$ , THF,  $120^\circ\text{C}$ , 10-bar CO, 24 hr, CT 87) (373).

Alkyl formates react with olefins to give the corresponding esters. The hydroesterification reaction is catalyzed by ruthenium clusters. Thus, methyl propionate is accessible from methyl formate and ethylene

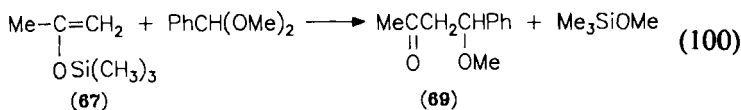


(toluene,  $\text{Ru}_3(\text{CO})_{12}$ , 90-bar  $\text{C}_2\text{H}_4$ ,  $230^\circ\text{C}$ , 20 hr, yield 92%, CT 4600) (374). Similar hydroesterification reactions with other alkyl formates and higher olefins have also been reported using  $\text{Ru}_3(\text{CO})_{12}/\text{PBu}_3$  (375) or  $\text{Ru}_3(\text{CO})_{12}/\text{Me}_3\text{NO}$  (376) as the catalytic systems. In the same way, formamides can be reacted with olefins to give the corresponding carbonic amides, catalyzed by  $\text{Ru}_3(\text{CO})_{12}$  under a slight carbon monoxide pressure (377).

Cross aldol-type reactions are catalyzed by  $\text{Rh}_4(\text{CO})_{12}$ : The trimethylsilyl enolether **87** reacts with hexanal to give **88**



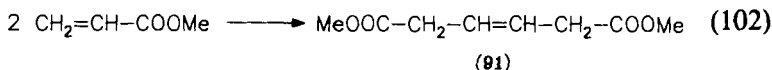
(benzene,  $100^\circ\text{C}$ , 21 hr, yield 71%, CT 172) (378), and with benzaldehyde dimethylacetal to give **89**



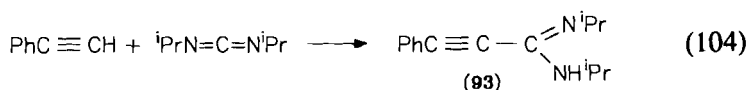
(benzene,  $100^\circ\text{C}$ , 15 hr, yield 58%, CT 29) (379). The analogous derivative **90** is also accessible from methyl vinyl ketone, benzaldehyde, and the

$$\begin{array}{c} \text{MeCCH=CH}_2 + \text{HCPH} + \text{Et}_2\text{MeSiH} \longrightarrow \text{Me}-\text{C}-\text{CH}(\text{Me})-\text{CHPh} \\ \parallel \qquad \qquad \parallel \qquad \qquad \qquad \qquad \parallel \qquad \qquad \qquad | \\ \text{O} \qquad \qquad \text{O} \qquad \qquad \qquad \text{O} \quad \text{MeEt}_2\text{SiO} \end{array} \quad (101)$$

Ruthenium carbonyl,  $\text{Ru}_3(\text{CO})_{12}$ , has been found to be active for the catalytic dimerization of methyl acrylate to give predominantly the *trans*-isomer of 91


$$\text{Ph}-\text{CH}=\text{CH}_2 + \text{C}_6\text{H}_{11}\text{NC} + \text{H}_2 \longrightarrow \text{Ph}-\underset{\text{(92)}}{\text{CHMe}}-\text{CH}=\text{NC}_6\text{H}_{11} \quad (103)$$

As far as alkynes are concerned, C-C coupling reactions have been reported to be catalyzed by rhodium or ruthenium clusters. Phenylacetylene can be coupled to diisopropyl carbodiimide to give **93**

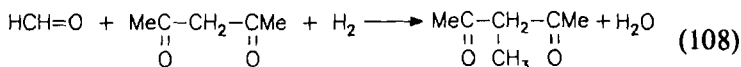

$$\begin{array}{ccc} \text{PhC}\equiv\text{CH} + 3\text{CO} & \longrightarrow & \text{PhCHCH}_2\text{CMe} + \text{CO}_2 + \text{I}^- \\ + \text{H}_2\text{O} + \text{MeI} + \text{OH}^- & & \begin{array}{c} | \qquad \qquad || \\ \text{HOOC} \qquad \text{O} \end{array} \end{array} \quad (105)$$
$$\text{HC}\equiv\text{C}-\text{CH}_2\text{OH} + \text{CO} + \text{Me}_2\text{PhSiH} \longrightarrow \begin{array}{c} \text{H} \qquad \text{CH}_2\text{OH} \\ \diagdown \quad \diagup \\ \text{C}=\text{C} \\ \diagup \quad \diagdown \\ \text{Me}_2\text{PhSi} \quad \text{CHO} \end{array} \quad (106)$$

in the presence of  $\text{Rh}_4(\text{CO})_{12}$  and  $\text{NEt}_3$ ; **94** is formed with 83% yield (benzene,  $100^\circ\text{C}$ , 15–40 bar, 2 hr, CT 830). Methyl-substituted propargylic alcohols, however, give the corresponding  $\beta$ -lactones (384).

Carbon–carbon coupling reactions involving formaldehyde have been observed with trinuclear ruthenium clusters. Thus, a THF solution containing  $\text{Ru}_3(\text{CO})_{12}$ , 1-methyl-3-ethylbenzimidazolinium bromide and  $\text{NEt}_3$  was active for the reductive coupling of formaldehyde to itself to give glycol aldehyde. Under syngas conditions, the glycol aldehyde is converted into ethylene glycol



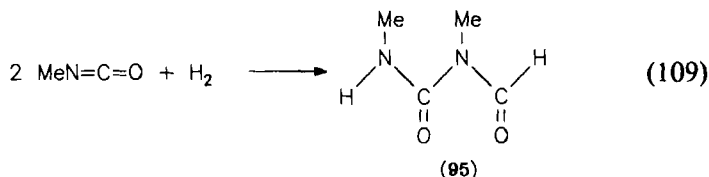
The use of  $^{13}\text{C}$ formaldehyde resulted in the formation of 80% of the dilabeled ethylene glycol, indicating that the ethylene glycol formation proceeds preferentially via reductive carbon–carbon coupling over hydroformylation of formaldehyde; the catalytic turnover is not given (166).  $\text{Ru}_3(\text{CO})_{12}$  was also found to catalyze the reductive alkylation of active methylene compounds with formaldehyde under synthesis gas. For example, pentan-2,4-dione is converted into 3-methylpentan-2,4-dione



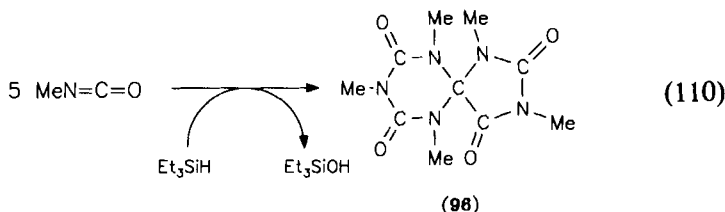
with 85% yield (DMF,  $150^\circ\text{C}$ , 100 bar,  $\text{CO}/\text{H}_2=1$ , 16 hr, CT 500) (385).

### C. Carbon–Nitrogen Coupling Reactions

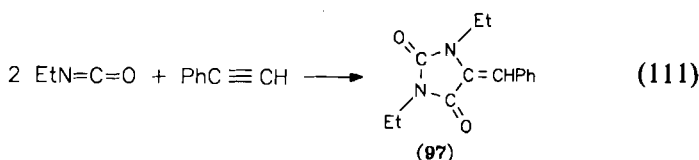
Several examples of novel catalytic reactions involving C–N coupling steps have been found with anionic ruthenium clusters as catalysts (386). The tetranuclear cluster anion  $[\text{H}_3\text{Ru}_4(\text{CO})_{12}]^-$  is reported to catalyze a reaction termed “hydrocoupling of alkyl isocyanates.” Here two isocyanate molecules are coupled together with uptake of hydrogen and C–N bond formation; astonishingly, the dialkyl carbamyl–formamides of the type **95** had not been made by conventional methods before. The reaction of methyl isocyanate is carried out in THF at  $120^\circ\text{C}$  under a hydrogen pressure of 40 bar, and the yield of **95** after 200 hr is 46% corresponding to a catalytic turnover of 230 (387):



The trinuclear cluster anion  $[\text{HRu}_3(\text{CO})_{10}(\text{SiEt}_3)_2]^-$  catalyzes a process best described as "silane-assisted spirocyclization of alkyl isocyanates," giving a surprisingly simple access to a new series of [4,5]-spiroheterocycles. No less than five isocyanate molecules are coupled together, one of them losing its oxygen atom to provide the spirocarbon atom of the product. The methyl derivative **96** is obtained in 40% yield (CT 400) in THF on heating at 150°C for 25 hr (388):

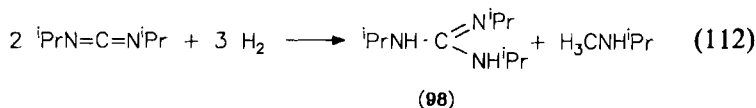


The formation of some new (*E*)- and (*Z*)-benzylidenehydantoin such as **97** from alkyl isocyanates and phenylacetylene



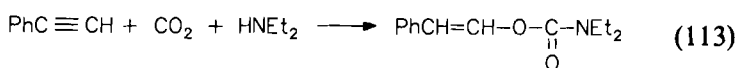
is catalyzed by the cluster dianion  $[\text{Ru}_3(\text{CO})_{11}]^{2-}$ , generated from various precursors (THF, 120°C, 224 hr, yield of (*Z*)-**97** 9% and of (*E*)-**97** 1%, CT 49) (389).

Several ruthenium clusters catalyze the synthesis of some new *N,N',N''*-trialkylguanidines from the corresponding carbodiimides and hydrogen. For the isopropyl derivative **98**



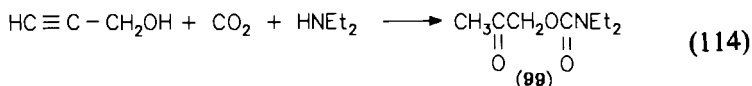
the best results are obtained with the cluster anion  $[\text{H}_3\text{Ru}_4(\text{CO})_{12}]^-$  as the catalyst (THF, 120°C, 40 bar  $\text{H}_2$ , 29 hr, yield 14%, CT 136) (390).

Vinyl carbamates are accessible from carbon dioxide, amines, and alkynes. The reaction is catalyzed by  $\text{Ru}_3(\text{CO})_{12}$ . As a typical example, phenylacetylene,  $\text{CO}_2$ , and  $\text{HNEt}_2$  are converted into the isomeric phenylvinylcarbamates (toluene, 140°C, 50 bar, 20 hr, yield 36%, CT 18) (391,392):



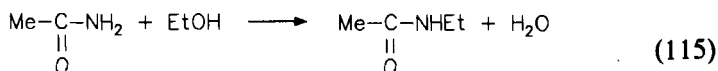


Similarly, 2-oxoalkylcarbamates have been synthesized in one step and in moderate yields by the reaction of carbon dioxide, secondary amines, and propargylic alcohols. For instance, **99** is accessible from propargyl alcohol,  $\text{HNEt}_2$ , and  $\text{CO}_2$  according to

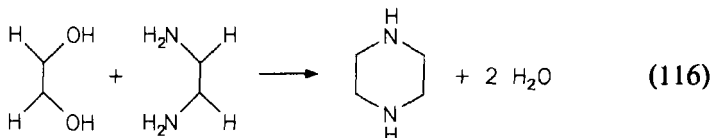


(acetonitrile, 50 bar,  $80^\circ\text{C}$ , 20 hr, yield 54%, CT 54) (393,394).

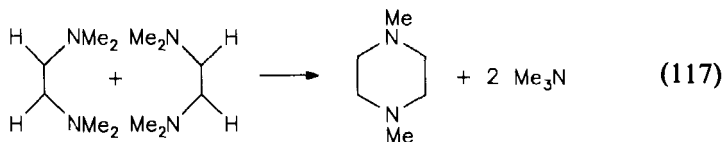
Among other ruthenium catalysts, the cluster  $\text{Ru}_3(\text{CO})_{12}$  has been found to efficiently catalyze the N-alkylation of amides, imides, and lactams by alcohols. Acetamide can be converted into *N*-ethylacetamide with ethanol, according to



in the presence of  $\text{Ru}_3(\text{CO})_{12}$  and  $\text{PBU}_3$  (neat,  $210^\circ\text{C}$ , 10 hr, 100% conversion, 45% selectivity, CT 80) (395). Vicinal diamines can be condensed with vicinal diols to give the corresponding piperazines; e.g., ethylene glycol and ethylene diamine give piperazine according to

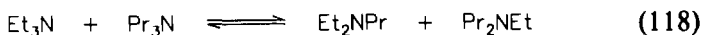


The reaction is catalyzed by  $\text{Ru}_3(\text{CO})_{12}$  and  $\text{PBU}_3$  (dioxane,  $220^\circ\text{C}$ , 5 hr, 88% yield, CT 1144) (396). *N,N'*-Dimethylpiperazine is also accessible by transalkylation of 1,2-bis(dimethylamino)-ethane according to



The reaction is catalyzed by a mixture of  $\text{Ru}_3(\text{CO})_{12}$  and  $\text{Fe}(\text{CO})_5$  (ethanol,  $160^\circ\text{C}$ , 34-bar CO, 120 hr, conversion 53%, CT 70) (397).

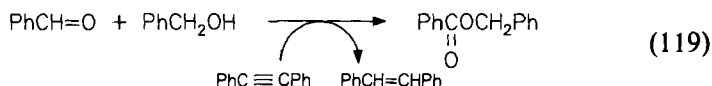
Catalytic transalkylation reactions of tertiary amines have been described with  $\text{Os}_3(\text{CO})_{12}$  (398–400),  $\text{Ru}_3(\text{CO})_{12}$  (398–401),  $\text{Ir}_4(\text{CO})_{12}$  (398), and  $\text{Os}_3(\text{CO})_{10}\text{S}$  (402). In the catalytic alkyl exchange between triethylamine and tripropylamine



$\text{Os}_3(\text{CO})_{10}\text{S}$  catalyzes the formation of 25%  $\text{Et}_2\text{NPr}$  and 27%  $\text{EtNPr}_2$  (methanol,  $143^\circ\text{C}$ , 16 hr, CT 150) (402).

#### D. Miscellaneous Reactions

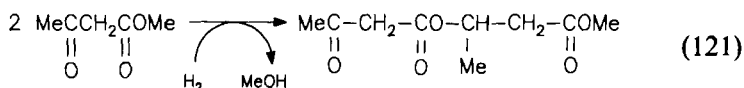
The selective formation of carboxylic esters from aldehydes and alcohols in the presence of a hydrogen acceptor such as diphenylacetylene is catalyzed by  $\text{Ru}_3(\text{CO})_{12}$ . For instance, benzyl benzoate is obtained from benzaldehyde and benzyl alcohol in 72% yield (CT 54) after 2 hr, when the reaction is carried out without solvent at  $147^\circ\text{C}$  (403):



The reaction of  $\text{CO}_2$  with hydrogen and methanol to give methyl formate

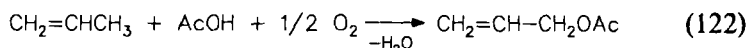


is catalyzed by either  $[\text{N}(\text{PPh}_3)_2][\text{HFe}_3(\text{CO})_{11}]$  ( $175^\circ\text{C}$ , 41 bar, 4 days, CT 6) (404) or  $[\text{N}(\text{PPh}_3)_2][\text{HRu}_3(\text{CO})_{11}]$  ( $125^\circ\text{C}$ , 17 bar, 24 hr, CT 4) (405). It has been reported that  $\beta$ -ketoesters undergo a C–O coupling under hydrogen pressure and in the presence of  $[\text{H}_3\text{Ru}_4(\text{CO})_{12}]^-$ : With methyl acetoacetate the reaction proceeds in THF at  $120^\circ\text{C}$  under a hydrogen pressure of 40 bar



(20 hr, yield 5%, CT 45) (406).

Palladium clusters have been reported to catalyze the oxidative acetoxylation of alkenes: Propene reacts with acetic acid and oxygen to give allyl acetate according to

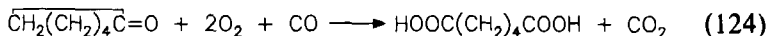


$(\text{Pd}_4(\text{CO})_4(\text{OAc})_4 \cdot 2\text{AcOH})$ , 1,10-phenanthroline, neat,  $90^\circ\text{C}$ , 1 hr, CT 8) (407). The anionic palladium–molybdenum cluster  $[\text{Pd}_4(\text{CpMo}(\text{CO})_3)_4]^{2-}$  was found to catalyze at  $20$ – $50^\circ\text{C}$  the dehydration of alcohols, presumably according to



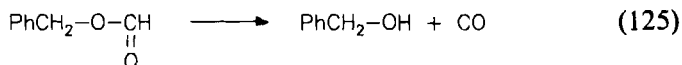
In the case of benzylalcohol, *trans*-stilbene is obtained; details are not given. The reaction products formed with methanol, ethanol, and isopropanol are not mentioned (408). There is also a report, unfortunately

lacking clarity, on the oxidation of ketones to carboxylic acids by oxygen and carbon monoxide, which is catalyzed by  $\text{Rh}_6(\text{CO})_{16}$ . Thus, cyclohexanone gives adipic acid at  $100^\circ\text{C}$  (34 bar,  $\text{O}_2/\text{CO}=3$ , 24 hr)



The catalytic turnover claimed is 1000 (409).

Several reports concern the decarbonylation of formic esters catalyzed by  $\text{Ru}_3(\text{CO})_{12}$ . Benzyl formate gives benzyl alcohol



with  $\text{Ru}_3(\text{CO})_{12}$  and  $\text{Me}_2\text{NO} \cdot 2\text{H}_2\text{O}$  in benzene at  $200^\circ\text{C}$ ; after 6 hr, the yield is 74%, corresponding to a catalytic turnover of 37 (370). The same reaction can be catalyzed by  $\text{Ru}_3(\text{CO})_{12}/\text{PBu}_3$ . In this variant also methyl formate can be decarbonylated to methanol (diglyme,  $180^\circ\text{C}$ , 8 hr, selectivity 49%, CT 60) (410a,b).

## VII

### CONCLUSIONS

The past two decades have seen much excitement in the area of transition metal cluster chemistry, which was stimulated, at least to a large extent, by the catalytic perspectives of these species. Twenty years of intensive research have demonstrated the versatile catalytic potential of clusters. However, it seems that clusters are not very likely to replace soon well-established conventional catalysts in large-scale industrial production. The challenge in cluster catalysis appears to reside in the search for novel catalytic reactions and for highly selective catalytic processes, making use of the unique polymetallic coordination sites in soluble organometallic molecules.

### REFERENCES

1. F. A. Cotton, *Q. Rev. Chem. Soc.* **20**, 389 (1966).
2. B. F. G. Johnson, in "Transition Metal Clusters" (B. F. G. Johnson, ed.), p. 2. Wiley, Chichester, England, 1980.
3. P. Chini, *Inorg. Chim. Acta Rev.* **2**, 31 (1968).
4. J. Lewis and B. F. G. Johnson, *Pure Appl. Chem.* **44**, 43 (1975).
5. R. Ugo, *Catal. Rev. Sci. Eng.* **11**, 225 (1975).
6. E. L. Muetterties, *Bull. Soc. Chim. Belg.* **84**, 959 (1975); E. L. Muetterties, *Bull. Soc. Chim. Belg.* **85**, 451 (1976).

7. E. L. Muetterties, *Science* (Washington, D.C.) **196**, 839 (1977).
8. B. F. G. Johnson and J. Lewis, *Colloq. Int. C.N.R.S.* **281**, 101 (1977).
9. E. L. Muetterties and H. J. Krause, *Angew. Chem.* **95**, 135 (1983); E. L. Muetterties and H. J. Krause, *Angew. Chem. Int. Ed. Engl.* **22**, 135 (1983).
10. J. Lewis and B. F. G. Johnson, *Gazz. Chim. Ital.* **109**, 271 (1979).
11. A. L. Robinson, *Science* (Washington, D.C.) **194**, 1150 (1976).
12. C. U. Dittman, Jr., and R. C. Ryan, *CHEMTECH* **8**, 170 (1978).
13. J. R. Shapley, *Strem Chem.* **4**, 3 (1978).
14. G. Huttner, *Nachr. Chem. Tech. Lab.* **27**, 261 (1979).
15. P. Braunstein, *Nouv. J. Chim.* **10**, 366 (1986).
16. A. K. Smith and J. M. Basset, *J. Mol. Catal.* **2**, 229 (1977).
17. R. Whyman, in "Transition Metal Clusters" (B. F. G. Johnson, ed.), p. 545. Wiley, Chichester, England, 1980.
18. L. Markó and A. Vizi-Orosz, in "Metal Clusters in Catalysis" (B. C. Gates, L. Guzzi, and H. Knözinger, eds.) p. 89. Elsevier, Amsterdam, The Netherlands, 1986.
19. G. Süß-Fink and F. Neumann, in "The Chemistry of the Metal-Carbon Bond" (F. R. Hartley, ed.), Vol. 5, p. 231. Wiley, Chichester, England, 1989.
20. B. Walther, *Z. Chem.* **29**, 117 (1989).
21. W. L. Gladfelter and K. J. Roesselet, in "The Chemistry of Metal Cluster Complexes" (D. F. Shriver, H. D. Kaesz, and R. D. Adams, eds.), p. 329. VCH, Weinheim, Germany, 1990.
22. D. V. Korolkov, *Izv. Sib. Otd. Akad. Nauk SSSR Ser. Khim. Nauk* **9**, 54 (1982).
23. M. Castiglioni, R. Giordano, and E. Sappa, *J. Organomet. Chem.* **258**, 217 (1983).
24. R. Ugo and R. Psaro, *J. Mol. Catal.* **20**, 53 (1983).
25. R. D. Adams, *Acc. Chem. Res.* **16**, 67 (1983).
26. J. Zwart and R. Snel, *J. Mol. Catal.* **30**, 305 (1985).
27. G. Süß-Fink, *Nachr. Chem. Tech. Lab.* **36**, 1110 (1988).
28. S. Bhaduri, K. R. Sharma, and H. I. Khwaja, *Proc. Indian Acad. Sci. Chem. Sci.* **101**, 195 (1989).
29. P. Braunstein, in "Chemical Bonds—Better Ways to Make Them and Breake Them" (I. Bernal, ed.), p. 3. Elsevier, Amsterdam, The Netherlands, 1989.
30. Y. I. Ermakov, L. N. Arzamaskova, and V. L. Kuznetsov, *Koord. Khim.* **10**, 877 (1984).
31. A. Brenner, in "Metal Clusters" (M. Moskovits, ed.), p. 249. Wiley, New York, 1986.
32. B. C. Gates, in "Metal Clusters" (Moskovits, ed.), p. 283. Wiley, New York, 1986.
33. B. C. Gates, in "Metal Clusters in Catalysis" (B. C. Gates, L. Guzzi, and H. Knözinger, eds.), p. 497. Elsevier, Amsterdam, The Netherlands, 1986.
34. G. Maire, in "Metal Clusters in Catalysis" (B. C. Gates, L. Guzzi, and H. Knözinger, eds.), p. 509. Elsevier, Amsterdam, The Netherlands, 1986.
35. B. C. Gates and H. Knözinger, in "Metal Clusters in Catalysis" (B. C. Gates, L. Guzzi, and H. Knözinger, eds.), p. 531. Elsevier, Amsterdam, The Netherlands, 1986.
36. L. Guzzi, in "Metal Clusters in Catalysis" (B. C. Gates, L. Guzzi, and H. Knözinger, eds.), p. 547. Elsevier, Amsterdam, The Netherlands, 1986.
37. L. N. Arzamaskova and Y. I. Ermakov, *Zh. Vses. Khim. Ova. im. D. I. Mendeleeva* **32**, 75 (1987).
38. B. C. Gates, in "Metal-Metal Bonds and Clusters in Chemistry and Catalysis" (J. P. Fackler, Jr., ed.), p. 127. Plenum, New York, 1990.
39. R. M. Laine, *J. Mol. Catal.* **14**, 137 (1982).
40. B. F. G. Johnson and R. E. Benfield, in "Transition Metal Clusters" (B. F. G. Johnson, ed.), p. 471. Wiley, Chichester, England, 1980.
41. R. E. Benfield and B. F. G. Johnson, *Transition Met. Chem.* (London) **6**, 131 (1981).

42. G. Jenner and G. Bitsi, *J. Mol. Catal.* **45**, 235 (1988).
- 43a. G. Jenner and G. Bitsi, *J. Mol. Catal.* **40**, 71 (1987).
- 43b. G. Doyle, U. S. Patent 4,408,069 (1983); G. Doyle, *Chem. Abstr.* **95**, 114 784a (1981).
- 43c. G. O. Evans and C. J. Newell, *Inorg. Chim. Acta* **31**, L387 (1978).
- 43d. D. J. Darensbourg, C. Ovalles, and M. Pala, *J. Am. Chem. Soc.* **105**, 5937 (1983).
44. Y. Tsuji, T. Ohsumi, T. Kondo, and Y. Watanabe, *J. Organomet. Chem.* **309**, 333 (1986).
45. J. J. Byerby, G. L. Rempel, and N. Takebe, *J. Chem. Soc. Chem. Commun.*, 1482 (1971).
46. G. Süss-Fink, M. Langenbahn, and T. Jenke, *J. Organomet. Chem.* **368**, 103 (1989).
47. M. Wang, S. Calet, H. Alper, *J. Org. Chem.* **54**, 21 (1989).
48. M. Akazome, Y. Tsuji, and Y. Watanabe, *Chem. Lett.*, 635 (1990).
49. M. Langenbahn, H. Stoeckli-Evans, and G. Süss-Fink, *Helv. Chim. Acta* **74**, 549 (1991).
50. M. Langenbahn, H. Stoeckli-Evans, and G. Süss-Fink, *J. Organomet. Chem.* **397**, 347 (1990).
51. K. Kaneda, K. Doken, and T. Imanoka, *Chem. Lett.*, 285 (1988).
52. C. Crotti, S. Cenini, B. Rindone, S. Tollari, and F. Demartin, *J. Chem. Soc. Chem. Commun.*, 784 (1986).
53. A. Bassoli, B. Rindone, S. Tollari, S. Cenini, and C. Crotti, *J. Mol. Catal.* **52**, L45 (1989).
54. A. Basu, S. Bhaduri, and H. Khwaja, *J. Organomet. Chem.* **319**, C28 (1987).
55. S. Bhaduri, H. Khwaja, P. G. Jones, *J. Chem. Soc. Chem. Commun.*, 194 (1988).
- 56a. S. Bhaduri, H. Khwaja, K. R. Sharma, and P. G. Jones, *J. Chem. Soc. Chem. Commun.*, 515 (1989).
- 56b. S. Bhaduri, H. Khwaja, N. Sapre, K. R. Sharma, A. Basu, P. G. Jones, and G. Carpenter, *J. Chem. Soc. Dalton Trans.*, 1313 (1990).
57. S. A. Sánchez-Delgado, J. Puga, and M. Rosales, *J. Mol. Catal.* **24**, 221 (1984).
58. A. Basu, S. Bhaduri, H. Khwaja, P. G. Jones, T. Schroeder, and G. M. Sheldrick, *J. Organomet. Chem.* **290**, C19 (1985).
59. C. Bergounhou, J.-J. Bonnet, P. Fompeyrine, G. Lavigne, N. Logun, and F. Mansilla, *Organometallics* **5**, 60 (1986).
60. C. Bergounhou, P. Fompeyrine, G. Commenges, and J.-J. Bonnet, *J. Mol. Catal.* **48**, 285 (1988).
61. S. Bhaduri, K. R. Sharma, W. Clegg, G. M. Sheldrick, and D. Stalke, *J. Chem. Soc. Dalton Trans.*, 2851 (1984).
62. A. Fusi, R. Ugo, R. Psaro, P. Braunstein, and J. Dehand, *Philos. Trans. R. Soc. London A* **308**, 125 (1982).
63. W. Abboud, Y. Ben Taarit, and J. M. Basset, *J. Organomet. Chem.* **220**, C15 (1981).
64. W. Reimann, W. Abboud, J. M. Basset, R. Mutin, G. L. Rempel, and A. K. Smith, *J. Mol. Catal.* **9**, 349 (1980).
65. S. A. Sánchez-Delgado, A. Audriollo, J. Puga, and G. Martin, *Inorg. Chem.* **26**, 1867 (1987).
- 66a. D. Labroue and R. Poilblanc, *J. Mol. Catal.* **2**, 329 (1979).
- 66b. D. Mani and H. Vahrenkamp, *J. Mol. Catal.* **29**, 305 (1985).
- 66c. C. U. Pittmann, Jr., W. Honnick, M. Absi-Halabi, M. G. Richmond, R. Bender, and P. Braunstein, *J. Mol. Catal.* **32**, 177 (1985).
67. J. Müller, B. Passon, and S. Schmitt, *J. Organomet. Chem.* **195**, C21 (1980).
68. J. L. Zuffa, M. L. Blohm, and W. L. Gladfelter, *J. Am. Chem. Soc.* **108**, 552 (1986).
69. M. Castiglioni, E. Sappa, M. Valle, M. Lafranchi, and A. Tiripicchio, *J. Organomet. Chem.* **241**, 99 (1983).

70. G. F. Pregaglia, A. Andreetta, G. F. Ferrari, G. Montrasi, and R. Ugo, *J. Organomet. Chem.* **33**, 73 (1971).
- 71a. M. Castiglioni, R. Giordano, and E. Sappa, *J. Organomet. Chem.* **319**, 167 (1987).
- 71b. M. Castiglioni, R. Giordano, E. Sappa, A. Tiripicchio, and M. Tiripicchio Camellini, *J. Chem. Soc. Dalton Trans.*, 23 (1986).
- 71c. M. Castiglioni, R. Giordano, E. Sappa, G. Predieri, and A. Tiripicchio, *J. Organomet. Chem.* **270**, C7 (1984).
- 71d. M. Castiglioni, R. Giordano, and E. Sappa, *J. Organomet. Chem.* **342**, 111 (1988).
72. P. Michelin Lausarot, G. A. Vaglio, and M. Valle, *J. Organomet. Chem.* **275**, 233 (1984).
73. N. V. Borunova, P. G. Antonova, N. V. Antseva, V. Z. Sharf, and Y. N. Kukushkin, *Zh. Obshch. Khim.* **57**, 265 (1987).
74. Y. Doi, S. Tamura, and K. Koshizuka, *Inorg. Chim. Acta* **65**, L63 (1982).
75. Y. Doi, S. Tamura, and K. Koshizuka, *J. Mol. Catal.* **19**, 213 (1983).
76. J. Fischler, R. Wagner, and E. A. Koerner von Gustdorf, *J. Organomet. Chem.* **112**, 155 (1976).
77. C. P. Lau, C. Y. Ren, M. T. Chu, and C. H. Yeung, *J. Mol. Catal.* **65**, 287 (1991).
78. G. Süss-Fink, unpublished results; cf., G. Süss-Fink, Habilitationsschrift, Universität Bayreuth, Bayreuth, Germany, 1983.
79. M. Bianchi, F. Piacenti, P. Frediani, U. Matteoli, C. Botteghi, S. Gladiali, and E. Benedetti, *J. Organomet. Chem.* **141**, 107 (1977).
80. M. Bianchi, F. Piacenti, G. Menchi, P. Frediani, U. Matteoli, C. Botteghi, S. Gladiali, and E. Benedetti, *Chim. Ind. (Milan)* **60**, 588 (1978).
81. C. Botteghi, M. Bianchi, E. Benedetti, and U. Matteoli, *Chimica* **29**, 256 (1975).
82. B. Bianchi, U. Matteoli, P. Frediani, G. Menchi, F. Piacenti, C. Botteghi, and M. Marchetti, *J. Organomet. Chem.* **252**, 317 (1983).
83. C. Botteghi, S. Gladiali, M. Bianchi, U. Matteoli, P. Frediani, P. G. Vergamini, and E. Benedetti, *J. Organomet. Chem.* **140**, 221 (1977).
84. U. Matteoli, G. Menchi, P. Frediani, M. Bianchi, and F. Piacenti, *J. Organomet. Chem.* **285**, 281 (1985).
85. M. Bianchi, G. Menchi, P. Frediani, F. Piacenti, A. Scrivanti, and U. Matteoli, *J. Mol. Catal.* **50**, 277 (1989).
86. T. H. Johnson, L. A. Siegle, and V. J. K. Chaffin, *J. Mol. Catal.* **9**, 307 (1980).
87. R. Mutin, W. Abbout, J. M. Basset, and D. Sinou, *J. Mol. Catal.* **33**, 47 (1985).
88. G. Balavoine, T. Dang, C. Eskenzai, and H. B. Kagan, *J. Mol. Catal.* **7**, 531 (1980).
89. T.-P. Dang, P. Aviron-Violet, Y. Colleuille, and J. Varagnat, *J. Mol. Catal.* **16**, 51 (1982).
90. T. Jenke and G. Süss-Fink, *J. Organomet. Chem.* **405**, 383 (1991).
- 91a. Y. Doi, K. Koshizuka, T. Keii, *Inorg. Chem.* **21**, 2732 (1982).
- 91b. J. L. Zuffa, M. L. Blohm, and W. L. Gladfelter, *J. Am. Chem. Soc.* **108**, 552 (1986).
- 91c. J. L. Zuffa and W. L. Gladfelter, *J. Am. Chem. Soc.* **108**, 4669 (1986).
- 91d. D. E. Fjare, J. A. Jensen, and W. L. Gladfelter, *Inorg. Chem.* **22**, 1774 (1983).
92. C. U. Pittmann, Jr., R. C. Ryan, J. McGee, and J. P. O'Conner, *J. Organomet. Chem.* **178**, C43 (1979).
93. P. Michelin Lausarot, G. A. Vaglio, and M. Valle, *Inorg. Chim. Acta* **36**, 213 (1979).
94. P. Michelin Lausarot, G. A. Vaglio, and M. Valle, *Inorg. Chim. Acta* **25**, L105 (1977).
95. P. Michelin Lausarot, G. A. Vaglio, and M. Valle, *J. Organomet. Chem.* **204**, 249 (1981).
96. E. L. Muetterties, E. Band, A. Kokorin, W. R. Pretzer, and M. G. Thomas, *Inorg. Chem.* **19**, 1552 (1980).

97. M. G. Thomas, W. R. Pretzer, B. F. Beier, F. J. Hirsekorn, and E. L. Muetterties, *J. Am. Chem. Soc.* **99**, 743 (1977).
98. M. Castiglioni, R. Giordano, and E. Sappa, *J. Organomet. Chem.* **369**, 419 (1989).
99. M. Castiglioni, R. Giordano, and E. Sappa, *J. Organomet. Chem.* **362**, 399 (1989).
100. A. Fusi, R. Ugo, R. Psaro, P. Braunstein, and J. Dehand, *J. Mol. Catal.* **16**, 217 (1982).
101. A. Fusi, R. Ugo, R. Psaro, P. Braunstein, and J. Dehand, *Philos. Trans. R. Soc. London A* **308**, 125 (1982).
102. N. Lugan, F. Laurent, G. Lavigne, T. P. Newcomb, E. W. Liimatta, J.-J. Bonnet, *J. Am. Chem. Soc.* **112**, 8607 (1990).
103. M. Castiglioni, R. Giordano, and E. Sappa, *J. Organomet. Chem.* **258**, 217 (1983).
104. M. Castiglioni, R. Giordano, and E. Sappa, *J. Organomet. Chem.* **407**, 377 (1991).
105. Z. Dawoodi, K. Henrick, and M. J. Mays, *J. Chem. Soc. Chem. Commun.*, 696 (1982).
106. S. A. R. Knox, J. W. Koepke, M. A. Andrews, and H. D. Kaesz, *J. Am. Chem. Soc.* **97**, 3942 (1975).
107. M. Laing, P. Somerville, Z. Dawoodi, M. J. Mays, and P. Wheatley, *J. Chem. Soc. Chem. Commun.*, 1035 (1978).
108. B. R. Cho and R. M. Laine, *J. Mol. Catal.* **15**, 383 (1982).
109. B. Heil and L. Markó, *Acta Chim. Acad. Sci. Hung.* **55**, 107 (1968).
110. P. Frediani, U. Matteoli, M. Bianchi, F. Piacenti, and G. Menchi, *J. Organomet. Chem.* **150**, 273 (1978).
111. N. Lugan, G. Lavigne, J.-J. Bonnet, R. Réan, D. Neibecker, and I. Tkatchenko, *J. Am. Chem. Soc.* **110**, 5369 (1988).
- 112a. U. Matteoli, M. Bianchi, G. Menchi, F. Frediani, and F. Piacenti, *J. Mol. Catal.* **22**, 353 (1984).
- 112b. U. Matteoli, G. Menchi, M. Bianchi, P. Frediani, and F. Piacenti, *Gazz. Chim. Ital.* **115**, 603 (1985).
- 112c. M. Bianchi, G. Menchi, F. Francalanci, F. Piacenti, U. Matteoli, P. Frediani, and C. Botteghi, *J. Organomet. Chem.* **188**, 109 (1980).
- 112d. G. F. Schmidt, J. Reiner, and G. Süss-Fink, *J. Organomet. Chem.* **355**, 379 (1988).
- 112e. A. M. Raspolli Galletti, G. Braca, and G. Sbrana, *J. Organomet. Chem.* **356**, 221 (1988).
113. E. Band, W. Pretzer, M. G. Thomas, and E. L. Muetterties, *J. Am. Chem. Soc.* **99**, 7380 (1977).
114. C. M. Giandomenico, A. Elsenstadt, M. F. Fredericks, A. S. Hirschon, and R. M. Laine, in "Catalysis of Organic Reactions" (R. L. Augustine, ed.), p. 73. Dekker, New York, 1985.
115. R. M. Laine, *Nouv. J. Chim.* **11**, 543 (1987).
116. T. Hayashi, F. Abe, T. Sakakura, and M. Tanaka, *J. Mol. Catal.* **58**, 165 (1990).
117. A. Eisenstadt, G. M. Giandomenico, M. F. Fredericks, A. S. Hirschon, and R. M. Laine, *Organometallics* **4**, 2033 (1985).
118. J. Kaspar, R. Spogliarich, and M. Graziani, *J. Organomet. Chem.* **281**, 299 (1985).
119. K. Jothimony, S. Vancheesan, and J. C. Kuriacose, *J. Mol. Catal.* **32**, 11 (1985).
120. T. A. Smith and P. M. Maitlis, *J. Organomet. Chem.* **289**, 385 (1985).
121. A. Basu, S. Bhaduri, K. R. Sharma, and P. G. Jones, *J. Organomet. Chem.* **328**, C34 (1987).
122. S. Bhaduri and K. R. Sharma, *J. Chem. Soc. Chem. Commun.*, 173 (1988).
123. A. Basu, S. Bhaduri, K. R. Sharma, and P. G. Jones, *J. Chem. Soc. Chem. Commun.*, 1126 (1987).
124. Y. Blum, D. Reshef, and Y. Shvo, *Tetrahedron Lett.* **22**, 1541 (1981).
125. Y. Blum and Y. Shvo, *J. Organomet. Chem.* **263**, 93 (1984).
126. Y. Blum and Y. Shvo, *J. Organomet. Chem.* **282**, C7 (1985).

127. Y. Shvo, Y. Blum, D. Reshef, and M. Menzin, *J. Organomet. Chem.* **226**, C21 (1982).
128. S. Bhaduri and K. R. Sharma, *J. Chem. Soc. Chem. Commun.*, 1412 (1983).
129. A. Basu, S. Bhaduri, and K. R. Sharma, *J. Chem. Soc. Dalton Trans.*, 2315 (1984).
130. S. Bhaduri, N. Y. Sapre, and K. R. Sharma, *J. Organomet. Chem.* **364**, C8 (1989).
131. M. Bianchi, U. Matteoli, P. Frediani, G. Menchi, and F. Piacenti, *J. Organomet. Chem.* **236**, 375 (1982).
132. M. Bianchi, U. Matteoli, G. Menchi, P. Frediani, S. Pratesi, F. Piacenti, and C. Botteghi, *J. Organomet. Chem.* **198**, 73 (1980).
133. M. Bianchi, U. Matteoli, G. Menchi, P. Frediani, F. Piacenti, and C. Botteghi, *J. Organomet. Chem.* **195**, 337 (1980).
134. M. Bianchi, U. Matteoli, G. Menchi, P. Frediani, and F. Piacenti, *J. Organomet. Chem.* **240**, 65 (1982).
135. J. Ojima, T. Fuchikami, and M. Yatabe, *J. Organomet. Chem.* **260**, 335 (1984).
136. Y. Seki, K. Takeshita, K. Kawamoto, S. Murai, and N. Sonoda, *Angew. Chem.* **92**, 974 (1980); Y. Seki, K. Takeshita, K. Kawamoto, S. Murai, and N. Sonoda, *Angew. Chem. Int. Ed. Engl.* **19**, 928 (1980).
137. Y. Seki, K. Takeshita, K. Kawamoto, S. Murai, and N. Sonoda, *J. Org. Chem.* **51**, 3890 (1986).
138. Y. Seki, K. Takeshita, and K. Kawamoto, *J. Organomet. Chem.* **369**, 117 (1989).
139. J. Ojima, N. Clos, R. J. Donovan, and P. Ingallina, *Organometallics* **9**, 3127 (1990).
140. C. U. Pittman, Jr., M. G. Richmond, M. Absi-Halabi, H. Beurich, F. Richter, and H. Vahrenkamp, *Angew. Chem. Int. Ed. Engl.* **21**, 786 (1982).
141. C. Masters, *Adv. Organomet. Chem.* **17**, 61 (1979).
142. B. D. Dombek, *Adv. Catal.* **32**, 325 (1983).
143. B. D. Dombek, *J. Organomet. Chem.* **372**, 151 (1989).
144. R. Whyman, *Philos. Trans. R. Soc. London A* **308**, 131 (1982).
145. R. L. Pruett, *Ann. N.Y. Acad. Sci.* **295**, 239 (1977).
146. S. Nakamura, *CHEMTECH* **20**, 556 (1990).
147. R. B. King, A. D. King, Jr., and K. Tanaka, *J. Mol. Catal.* **10**, 75 (1980).
148. W. Keim, M. Berger, A. Eisenbeis, J. Kadelka, and J. Schlupp, *J. Mol. Catal.* **13**, 95 (1981).
149. W. Keim, H. Berger, and J. Schlupp, *J. Catal.* **61**, 359 (1980).
150. C. Masters and J. A. van Doorn, German Offenlegung 2 644 185 (1975).
151. J. S. Bradley, *J. Am. Chem. Soc.* **101**, 7419 (1979).
152. J. Bradley, in "Fundamental Research in Homogeneous Catalysis" (M. Tsutsui, ed.), p. 165. Plenum, New York, 1979.
153. R. J. Daroda, J. R. Blackborow, and G. Wilkinson, *J. Chem. Soc. Chem. Commun.*, 1101 (1980).
154. B. D. Dombek, *J. Am. Chem. Soc.* **102**, 6855 (1980).
155. B. D. Dombek, *J. Am. Chem. Soc.* **103**, 6510 (1981).
156. B. D. Dombek, *J. Organomet. Chem.* **250**, 457 (1983).
157. B. K. Warren and B. D. Dombek, *J. Catal.* **79**, 334 (1983).
158. Y. Kiso and K. Saeki, *J. Organomet. Chem.* **309**, C26 (1986).
159. Y. Kiso and K. Saeki, *J. Organomet. Chem.* **303**, C17 (1986).
160. Y. Kiso and K. Saeki, *Bull. Chem. Soc. Jpn.* **60**, 617 (1987).
161. S.-I. Yoshida, S. Mori, H. Kinoshita, and Y. Watanabe, *J. Mol. Catal.* **42**, 215 (1987).
162. J. Knifton, *J. Am. Chem. Soc.* **103**, 3959 (1981).
163. J. Knifton, *Prepr. Am. Chem. Soc. Div. Pet. Chem.* **31**, 26 (1986).
164. Y. Kiso, M. Tanaka, H. Nakamura, T. Yamasaki, and K. Saeki, *J. Organomet. Chem.* **312**, 357 (1986).



165. Y. Kiso, K. Saeki, T. Hayashi, M. Tanaka, Y. Matsunaga, M. Ishino, M. Tamura, T. Deguchi, and S. Nakamura, *J. Organomet. Chem.* **335**, C27 (1987).
166. K. Murata, A. Matsuda, T. Masuda, Y. Kiso, and K. Saeki, *J. Mol. Catal.* **42**, 389 (1987).
167. H. Ono, K. Fujiwara, E. Sugiyama, and K. Yoshida, *Kagaku Kogaku Ronbunshu* **14**, 449 (1988).
168. M. Ishino, M. Tamura, T. Deguchi, and S. Nakamura, *J. Catal.* **105**, 478 (1987).
169. J. Knifton, *J. Am. Chem. Soc.* **103**, 3959 (1981).
170. Y. Ohgomori, S. Mori, S.-I. Yoshida, and Y. Watanabe, *J. Mol. Catal.* **40**, 223 (1987).
171. T. Masuda, K. Murata, and A. Matsuda, *Bull. Chem. Soc. Jpn.* **61**, 2865 (1988).
172. R. L. Pruett and J. S. Bradley, Eur. Patent 0037700 (1981).
173. M. Röper, M. Schieren, and A. Fumagalli, *J. Mol. Catal.* **34**, 173 (1986).
174. B. D. Dombek, *Organometallics* **4**, 1707 (1985).
175. Japanese Appl. 58-144 347 (1983); *Chem. Abstr.* **100**, 5877 (1984).
176. J. F. Knifton, R. A. Grigsby, Jr., and J. J. Lin, *Organometallics* **3**, 62 (1984).
177. J. F. Knifton, *J. Catal.* **96**, 439 (1985).
178. M. Tanaka, Y. Kiso, and K. Saeki, *J. Organomet. Chem.* **329**, 99 (1987).
179. H. Ono, M. Hashimoto, K. Fujiwara, E. Sugiyama, and K. Yoshida, *J. Organomet. Chem.* **331**, 387 (1987).
180. K. Murata, A. Matsuda, T. Masuda, M. Ishino, and M. Tamura, *Bull. Chem. Soc. Jpn.* **60**, 438 (1987).
181. R. A. Head and R. Whyman, *New. J. Chem.* **12**, 675 (1988).
182. R. L. Pruett and W. E. Walker, U.S. Patent 3,957,857 (1976).
183. R. L. Pruett and W. E. Walker, U.S. Patent 4,133,776 (1979).
184. R. L. Pruett and W. E. Walker, U.S. Patent 3,833,634 (1974).
185. L. Kaplan, U.S. Patent 3,944,588 (1976).
186. L. Kaplan, U.S. Patent 4,162,216 (1979).
187. R. L. Pruett, *Science* (Washington, D.C.) **211**, 11 (1981).
188. P. Chini and S. Martinengo, *Inorg. Chim. Acta* **3**, 299 (1969).
189. S. Martinengo and P. Chini, *Gazz. Chim. Ital.* **102**, 344 (1972).
190. P. Chini, G. Longoni, and V. G. Albani, *Adv. Organomet. Chem.* **14**, 285 (1976).
191. J. L. Vidal and W. E. Walker, *Inorg. Chem.* **19**, 896 (1980).
192. B. T. Heaton, J. Jones, T. Eguchi, and G. A. Hoffman, *J. Chem. Soc. Chem. Commun.*, 331 (1981).
193. A. Fumagalli, T. F. Koetzle, F. Takusagawa, P. Chini, S. Martinengo, and B. T. Heaton, *J. Am. Chem. Soc.* **102**, 1740 (1980).
194. B. Cornils, in "New Syntheses with Carbon Monoxide" (J. Falbe, ed.) p. 1. Springer-Verlag, Berlin, Germany, 1980.
195. K. Weissmehl and H. J. Arpe, "Industrielle Organische Chemie," p. 34. Verlag Chemie, Weinheim, Germany, 1978.
196. G. Süß-Fink, *J. Organomet. Chem.* **193**, C20 (1980).
197. G. Süß-Fink and G. Schmidt, *J. Mol. Catal.* **42**, 361 (1987).
198. G. Braca, G. Sbrana, F. Piacenti, and P. Pino, *Chim. Ind. (Milan)* **52**, 1091 (1970).
199. R. M. Laine, *J. Am. Chem. Soc.* **100**, 6451 (1978).
200. B.-H. Chang, *Inorg. Chim. Acta* **65**, L189 (1982).
201. T. Hayashi, Z. H. Gu, T. Sakakura, and M. Tanaka, *J. Organomet. Chem.* **352**, 373 (1988).
202. M. G. Richmond, M. Absi-Halabi, and C. U. Pittman, Jr., *J. Mol. Catal.* **22**, 367 (1984).
203. M. G. Richmond, *J. Mol. Catal.* **54**, 199 (1989).
204. A. Ceriotti, L. Garlaschelli, G. Longoni, M. C. Malatesta, D. Strumolo, A. Fumagalli, and S. Martinengo, *J. Mol. Catal.* **24**, 323 (1984).

205. M. K. Alami, F. Dahan, and R. Mathieu, *J. Chem. Soc. Dalton Trans.*, 1983 (1987).
206. S. Attali and R. Mathieu, *J. Organomet. Chem.* **291**, 205 (1985).
207. C. U. Pittmann, Jr., W. Honnick, M. Absi-Halabi, M. G. Richmond, R. Bender, and P. Braunstein, *J. Mol. Catal.* **32**, 177 (1985).
208. R. M. Laine, *J. Org. Chem.* **45**, 3370 (1980).
209. R. M. Laine, U.S. Patent 4,226,845 (1980).
210. R. Lazzaroni, P. Pertici, S. Bertozzi, and G. Fabrizi, *J. Mol. Catal.* **58**, 75 (1990).
211. M. E. Davis, P. M. Buttler, J. A. Rossin, and B. E. Hanson, *J. Mol. Catal.* **31**, 385 (1985).
212. R. J. Davis, J. A. Rossin, and M. E. Davis, *J. Catal.* **98**, 477 (1986).
213. M. E. Davis, J. Schnitzer, J. A. Rossin, P. Taylor, and B. E. Hanson, *J. Mol. Catal.* **39**, 243 (1987).
214. B. E. Hanson and M. E. Davis, *J. Chem. Educ.* **64**, 928 (1987).
215. H. P. Withers, Jr., and D. Seyferth, *Inorg. Chem.* **22**, 2931 (1983).
216. B. Heil and L. Markó, *Chem. Ber.* **101**, 2209 (1968).
217. G. Csontos, B. Heil, and L. Markó, *Ann. N.Y. Acad. Sci.* **239**, 47 (1974).
218. J. F. Knifton, *J. Mol. Catal.* **47**, 99 (1988).
219. J. F. Knifton, *J. Mol. Catal.* **43**, 65 (1987).
220. N. S. Imyanitov and D. M. Rudkovskii, *Zh. Prikl. Khim. (Leningrad)* **39**, 1948 (1967).
221. M. Hidai, A. Fukuoda, Y. Koyasu, and Y. Uchida, *J. Chem. Soc. Chem. Commun.*, 516 (1984).
222. M. Hidai and H. Matsuzaka, *Polyhedron* **7**, 2369 (1988).
223. Y. Ishii, M. Sato, H. Matsuzaka, and M. Hidai, *J. Mol. Catal.* **54**, L13 (1989).
- 224a. R. Lazzaroni, A. Raffaelli, R. Settambolo, S. Bertozzi, and G. Vitulli, *J. Mol. Catal.* **50**, 1 (1989).
- 224b. C. Mahe, E. Patin, J.-Y. Le Marouille, and A. Benoit, *Organometallics* **2**, 1051 (1983).
225. I. Ojima, K. Kato, M. Okabe, and T. Fuchikami, *J. Am. Chem. Soc.* **109**, 7714 (1987).
226. I. Ojima, *Chem. Rev.* **88**, 1011 (1988).
227. G. Consiglio, L. Kollar, and R. Kolliker, *J. Organomet. Chem.* **396**, 375 (1990).
228. I. Ojima and Z. Zhang, *J. Org. Chem.* **53**, 4422 (1988).
229. L. Kollár, G. Consiglio, and P. Pino, *Chimia* **40**, 428 (1986).
230. L. Kollár, G. Consiglio, and P. Pino, *J. Organomet. Chem.* **386**, 389 (1990).
231. P. Chini, S. Martinengo, and G. Garlaschelli, *J. Chem. Soc. Chem. Commun.*, 709 (1982).
232. B. Heil and L. Markó, *Chem. Ber.* **101**, 2209 (1968).
233. G. Csontos, B. Heil, and L. Markó, *Ann. N.Y. Acad. Sci.* **239**, 47 (1974).
234. G. Süß-Fink and G. Herrmann, *J. Chem. Soc. Chem. Commun.*, 735 (1985).
235. C. E. Kampe, N. M. Boag, and H. D. Kaesz, *J. Am. Chem. Soc.* **105**, 2896 (1983).
236. J. Evans, G. Jingxing, H. Leach, and A. C. Street, *J. Organomet. Chem.* **372**, 61 (1989).
237. G. Braca, A. M. R. Galletti, and G. Sbrana, *J. Mol. Catal.* **55**, 184 (1989).
238. G. Consiglio, *Organometallics* **7**, 778 (1988).
239. R. Lazzaroni, R. Settambolo, A. Raffaelli, S. Pucci, and G. Vitulli, *J. Organomet. Chem.* **339**, 357 (1988).
240. N. Rosas, C. Márquez, H. Hernández, R. Gómez, *J. Mol. Catal.* **48**, 59 (1988).
241. F. Piacenti, G. Menchi, P. Frediani, and U. Matteoli, *Chim. Ind. (Milan)* **60**, 808 (1978).
242. C. Botteghi, M. Branca, G. Micera, F. Piacenti, and G. Menchi, *Chim. Ind. (Milan)* **60**, 16 (1978).
- 243a. Y. Pottier, A. Mortreux, and F. Petit, *J. Organomet. Chem.* **370**, 333 (1989).
- 243b. G. Consiglio and F. Rama, *J. Mol. Catal.* **66**, 1 (1991).
244. G. A. Korneeva and S. M. Loktev, *Russ. Chem. Rev. (Engl. Transl.)* **58**, 73 (1989).

245. M. Marchionna and G. Longoni, *Organometallics* **6**, 606 (1987).  
246. M. Marchionna and G. Longoni, *J. Chem. Soc. Chem. Commun.*, 1097 (1987).  
247. K. Murata, A. Matsuda, and T. Masuda, *Bull. Chem. Soc. Jpn.* **61**, 325 (1988).  
248. M. Marchionna and G. Longoni, *J. Mol. Catal.* **35**, 107 (1986).  
249. H. Bahrmann and B. Cornils, in "New Syntheses with Carbon Monoxide" (J. Falbe, ed.), p. 266. Springer-Verlag, Berlin, Germany, 1980.  
250. M. J. Chen, H. M. Feder, and J. W. Rathke, *J. Mol. Catal.* **17**, 331 (1982).  
251. M. J. Chen, H. M. Feder, and J. W. Rathke, *J. Am. Chem. Soc.* **104**, 7346 (1982).  
252. M. Hidai, M. Orisaku, M. Ue, Y. Koyasu, T. Kodama, and Y. Uchida, *Organometallics* **2**, 292 (1983).  
253. M. Hidai, M. Orisaku, M. Ue, Y. Uchida, K. Yasufuku, and H. Yamazaki, *Chem. Lett.*, 143 (1981).  
254a. G. Doyle, *J. Mol. Catal.* **13**, 237 (1981).  
254b. J. Rose, Thèse de Doctorat, Université de Strasbourg, France, 1985.  
255. J. F. Knifton, *J. Chem. Soc. Chem. Commun.*, 41 (1981).  
256. J. F. Knifton, *J. Mol. Catal.* **11**, 91 (1981).  
257. J. F. Knifton, *J. Catal.* **76**, 101 (1982).  
258. J. R. Zoeller, *J. Mol. Catal.* **37**, 117 (1986).  
259. M. Hidai, Y. Koyasu, M. Yokota, M. Orisaku, and Y. Uchida, *Bull. Chem. Soc. Jpn.* **55**, 3951 (1982).  
260. J. Gauthier-Lafaye and R. Perron, *Eur. Patent* 0031784 (1981).  
261. M. Ishino and T. Deguchi, *J. Mol. Catal.* **52**, L17 (1989).  
262. J. F. Knifton and J. J. Lin, *C<sub>1</sub> Mol. Chem.* **1**, 387 (1986).  
263. J. F. Knifton, *J. Chem. Soc. Chem. Commun.*, 1412 (1985).  
264. J. F. Knifton and D. C. Alexander, *Isr. J. Chem.* **27**, 255 (1986).  
265. J. A. Marsella and G. P. Pez, *Prepr. Am. Chem. Soc. Div. Pet. Chem.* **31**, 22 (1986).  
266. F. L'Éplattenier, P. Matthys, and F. Calderazzo, *Inorg. Chem.* **9**, 343 (1970).  
267. H. Alper and K. E. Hashem, *J. Am. Chem. Soc.* **103**, 6514 (1981).  
268. P. Pino, G. Braca, G. Sbrana, and A. Cuccuru, *Chem. Ind. (London)*, 1732 (1968).  
269. B. W. Howk and J. C. Sauer, U.S. Patent 3,055,949 (1958).  
270. K. Doyama, T. Joh, T. Shiohara, and S. Takahashi, *Bull. Chem. Soc. Jpn.* **61**, 4353 (1988).  
271. T. Mise, P. Hong, and H. Yamazaki, *Chem. Lett.*, 401 (1982).  
272. P. Hong, T. Mise, and H. Yamazaki, *J. Organomet. Chem.* **334**, 129 (1987).  
273. P. Hong, T. Mise, and H. Yamazaki, *Chem. Lett.*, 989 (1981).  
274. T. Mise, P. Hong, and H. Yamazaki, *J. Org. Chem.* **48**, 238 (1983).  
275. I. Ojima, K. Hirai, M. Fujita, and T. Fuchikami, *J. Organomet. Chem.* **279**, 203 (1985).  
276. I. Ojima, M. Okabe, K. Kato, H. B. Kwon, I. T. Horvath, *J. Am. Chem. Soc.* **110**, 150 (1988).  
277. Y. Seki, S. Murai, A. Hidaka, and N. Sonoda, *Angew. Chem.* **89**, 919 (1977); Y. Seki, S. Murai, A. Hidaka, and N. Sonoda, *Angew. Chem. Int. Ed. Engl.* **16**, 881 (1977).  
278. I. Ojima, P. Ingallina, R. J. Donovan, and N. Clos, *Organometallics* **10**, 38 (1991).  
279. I. Matsuda, A. Ogiso, S. Sato, and Y. Izumi, *J. Am. Chem. Soc.* **111**, 2332 (1989).  
280. R. M. Laine and E. J. Crawford, *J. Mol. Catal.* **44**, 357 (1988).  
281. R. M. Laine, R. G. Rinker, and P. C. Ford, *J. Am. Chem. Soc.* **99**, 252 (1977).  
282. C. Ungermann, V. Landis, S. A. Moya, H. Cohen, H. Walker, R. G. Pearson, R. G. Rinker, and P. C. Ford, *J. Am. Chem. Soc.* **101**, 5922 (1979).  
283. P. C. Ford, *Acc. Chem. Res.* **14**, 31 (1981).  
284. P. C. Ford, *Prepr. Am. Chem. Soc. Div. Pet. Chem.* **29**, 567 (1984).  
285. P. C. Ford, C. Ungermann, V. Landis, S. A. Moya, R. C. Rinkler, and R. M. Laine, *Adv. Chem. Ser.* **173**, 81 (1979).

286. J. R. Moss and W. A. G. Graham, *J. Chem. Soc. Dalton Trans.*, 89 (1977).
- 287a. J. C. Bricker, C. C. Nagel, and S. G. Shore, *J. Am. Chem. Soc.* **104**, 1444 (1982).
- 287b. J. C. Bricker, C. C. Nagel, A. A. Bhattacharyya, and S. G. Shore, *J. Am. Chem. Soc.* **107**, 377 (1985).
- 287c. M. W. Payne, D. L. Leussing, S. G. Shore, *J. Am. Chem. Soc.* **109**, 617 (1987).
288. M. W. Payne, D. L. Leussing, S. G. Shore, *Organometallics* **10**, 574 (1991).
289. P. Yarrow, H. Cohen, C. Ungermann, D. Vandenberg, P. C. Ford, and R. G. Rinker, *J. Mol. Catal.* **22**, 239 (1983).
290. H. C. Kang, C. H. Mauldin, T. Cole, W. Slegeir, K. Cann, and R. Pettit, *J. Am. Chem. Soc.* **99**, 8323 (1977).
- 291a. T. Venäläinen, T. A. Pakkanen, T. T. Pakkanen, and E. Iiskola, *J. Organomet. Chem.* **314**, C49 (1986).
- 291b. D. M. Vandenberg, Ph.D. Thesis, University of California, Santa Barbara, California, 1986.
292. A. D. King, R. B. King, and D. B. Yang, *J. Chem. Soc. Chem. Commun.*, 529 (1980).
293. K. Kaneda, M. Hiraki, K. Sano, T. Imanaka, and S. Teranishi, *J. Mol. Catal.* **9**, 227 (1980).
294. P. C. Ford, R. G. Rinker, C. Ungermann, R. M. Laine, V. Landis, and S. A. Moya, *J. Am. Chem. Soc.* **100**, 4595 (1978).
295. T. Venäläinen, *Ann. Acad. Sci. Fenn. Ser. A2* **211**, 1 (1987).
- 296a. T. Venäläinen, E. Iiskola, J. Pursiainen, T. A. Pakkanen, and T. T. Pakkanen, *J. Mol. Catal.* **34**, 293 (1986).
- 296b. R. M. Laine, D. W. Thomas, L. W. Cary, and S. E. Buttrill, *J. Am. Chem. Soc.* **100**, 6527 (1978).
297. J. Falbe, *J. Organomet. Chem.* **94**, 213 (1975).
298. N. Kutepow and H. Kindler, *Angew. Chem.* **72**, 802 (1960).
299. F. Wada and T. Matsuda, *J. Organomet. Chem.* **64**, 365 (1973).
300. A. Eisenstadt, G. M. Giandomenico, M. F. Fredericks, A. S. Hirschon, and R. M. Laine, *Organometallics* **4**, 2033 (1985).
301. E. Z. Gildenberg and A. L. Lapidus, *Kinet. Katal.* **18**, 124 (1977).
302. E. Z. Gildenberg, V. P. Gulmyai, L. N. Valueva, and A. L. Lapidus, *Izv. Akad. Nauk SSSR Ser. Khim.*, 332 (1979).
303. Y. T. Eidus, A. L. Lapidus, and E. Z. Gildenberg, *Kinet. Katal.* **14**, 598 (1973).
304. A. L. Lapidus, E. Z. Gildenberg, and Y. T. Eidus, *Kinet. Katal.* **16**, 252 (1975).
305. R. M. Laine, *Ann. N.Y. Acad. Sci.* **333**, 124 (1980).
306. J. Palágyi and L. Markó, *J. Organomet. Chem.* **236**, 343 (1982).
307. K. Cann, T. Cole, W. Slegeir, and R. Pettit, *J. Am. Chem. Soc.* **100**, 3969 (1978).
308. R. Pettit, J. Cann, T. Cole, C. H. Mauldin, and W. Slegeir, *Adv. Chem. Ser.* **173**, 121 (1979).
309. K. Kaneda, M. Hiraki, T. Imanaka, and S. Teranishi, *J. Mol. Catal.* **12**, 385 (1981).
310. R. C. Ryan, G. M. Wilemon, M. P. Dalsanto, and C. U. Pittmann, Jr., *J. Mol. Catal.* **5**, 319 (1979).
311. E. Alessio, G. Zassinovich, and G. Mestroni, *J. Mol. Catal.* **18**, 113 (1983).
- 312a. K. Nomura, M. Ishino, M. Hazama, *J. Mol. Catal.* **65**, L5 (1991).
- 312b. K. Nomura, M. Ishino, M. Hazama, *J. Mol. Catal.* **66**, L1 (1991).
313. M. Miura, M. Shinohara, and M. Nomura, *J. Mol. Catal.* **45**, 151 (1988).
314. T. Kitamura, N. Sakamoto, and T. Joh, *Chem. Lett.*, 379 (1973).
315. K. Kaneda, T. Imanaka, and S. Teranishi, *Proc. Int. Congr. Catal.* **8**, V15 (1984).
316. S.-I. Murahashi, Y. Imada, and Y. Hirai, *Tetrahedron Lett.* **28**, 77 (1987).
317. S.-I. Murahashi, Y. Imada, and Y. Hirai, *Bull. Chem. Soc. Jpn.* **62**, 2968 (1989).
318. K. Murata and A. Matsuda, *Chem. Lett.*, 11 (1980).

- 319a. H. Urata, O. Kosukegawa, Y. Ishii, H. Yugari, and T. Fuchikami, *Tetrahedron Lett.* **30**, 4403 (1989).
- 319b. B. Fell, H. Chrobaczek, and W. Kohl, *Chem. Ztg.* **100**, 167 (1985).
320. K. Doyama, T. Joh, K. Onitsuka, T. Shiohara, and S. Takahashi, *J. Chem. Soc. Chem. Commun.*, 649 (1987).
321. L. Garlaschelli, M. Marchionna, M. Iapalucci, and G. Longoni, *J. Organomet. Chem.* **378**, 457 (1989).
322. R. M. Laine, D. W. Thomas, and L. W. Carey, *J. Org. Chem.* **44**, 4964 (1979).
323. M. Hidai, Y. Koyasu, K. Chikanari, and Y. Uchida, *J. Mol. Catal.* **40**, 243 (1987).
- 324a. E. Z. Gildenberg, L. L. Krasnova, S. D. Piroshkov, and A. L. Lapidus, *Kinet. Katal.* **21**, 810 (1980).
- 324b. A. L. Lapidus, E. Z. Gildenberg, S. D. Piroshkov, and L. L. Krasnova, *Izv. Akad. Nauk SSSR Ser. Khim.*, 2532 (1981).
- 324c. M. Hidai, A. Fukuoka, Y. Koyasu, and Y. Uchida, *J. Mol. Catal.* **35**, 29 (1986).
325. T. Mise, P. Hong, and H. Yamazaki, *Chem. Lett.*, 993 (1981).
326. T. Mise, P. Hong, and H. Yamazaki, *J. Org. Chem.* **48**, 238 (1983).
327. P. Hong, T. Mise, and H. Yamazaki, *Chem. Lett.*, 361 (1982).
328. S. Cenini, M. Pizzotti, C. Crotti, F. Porta, and G. La Monica, *J. Chem. Soc. Chem. Commun.*, 1286 (1984).
329. S. Cenini, C. Crotti, M. Pizzotti, and F. Porta, *J. Org. Chem.* **53**, 1243 (1988).
330. S. Cenini, M. Pizzotti, C. Crotti, F. Ragaini, and F. Porta, *J. Mol. Catal.* **49**, 59 (1988).
331. H. Urata, Y. Ishii, and T. Fuchikami, *Tetrahedron Lett.* **30**, 4407 (1989).
332. M. Castiglioni, L. Milone, D. Osella, G. A. Vaglio, and M. Valle, *Inorg. Chem.* **15**, 394 (1976).
333. M. Valle, D. Osella, and G. A. Vaglio, *Inorg. Chim. Acta* **20**, 213 (1976).
334. G. A. Vaglio and M. Valle, *Inorg. Chim. Acta* **30**, 161 (1978).
335. J. Evans and G. Jingxing, *J. Chem. Soc. Chem. Commun.*, 39 (1985).
336. J. R. Fox, W. L. Gladfelter, G. L. Geoffroy, I. Tavanaiepour, S. Abdel-Mequid, V. W. Day, *Inorg. Chem.* **20**, 3230 (1981).
337. G. Süss-Fink, Habilitationsschrift, Universität Bayreuth, Germany, 1984.
338. S. Attali, F. Dahan, and R. Mathieu, *Organometallics* **5**, 1376 (1986).
339. J. Kaspar, M. Graziani, A. Trovarelli, and G. Dolcetti, *J. Mol. Catal.* **55**, 229 (1989).
340. G. Menchi, U. Matteoli, A. Scrivanti, S. Paganelli, and C. Botteghi, *J. Organomet. Chem.* **354**, 215 (1988).
341. P. M. Lausarot, G. A. Vaglio, and M. Valle, *Transition Met. Chem. (London)* **4**, 39 (1979).
342. G. A. Vaglio, D. Osella, and M. Valle, *Transition Met. Chem. (London)* **2**, (1977).
343. R. P. Ferrari and G. A. Vaglio, *Inorg. Chim. Acta* **20**, 141 (1976).
344. D. Bingham, B. Hudson, D. E. Webster, and P. B. Wells, *J. Chem. Soc. Dalton Trans.*, 1521 (1974).
345. G. Pregaglia, A. Andreetta, G. Ferrari, and R. Ugo, *J. Organomet. Chem.* **33**, 73 (1971).
346. J. L. Graff, R. D. Sanner, and M. S. Wrighton, *J. Am. Chem. Soc.* **101**, 273 (1979).
347. J. L. Graff and M. S. Wrighton, *J. Am. Chem. Soc.* **102**, 2123 (1980).
348. A. J. Deeming and S. Hasso, *J. Organomet. Chem.* **114**, 313 (1976).
349. A. Basu and K. R. Sharma, *J. Mol. Catal.* **38**, 315 (1986).
350. A. Basu, S. Bhaduri, K. R. Sharma, *Adv. Catal. [Proc. Natl. Symp. Catal.]* **8**, 669 (1985).
351. U. Matteoli, M. Bianchi, P. Frediani, G. Menchi, C. Botteghi, and M. Marchetti, *J. Organomet. Chem.* **263**, 243 (1984).
352. A. J. Deeming and S. Hasso, *J. Organomet. Chem.* **114**, 313 (1976).
353. T. Kitamura, N. Sakamoto, and T. Joh, *Chem. Lett.*, 379 (1973).

354. M. Langenbahn, K. Bernauer, and G. Süss-Fink, *J. Organomet. Chem.* **379**, 167 (1989).
355. G. Süss-Fink, T. Jenke, H. Heitz, M. A. Pellinghelli, and A. Tiripicchio, *J. Organomet. Chem.* **379**, 311 (1989).
356. K. G. Caulton, M. G. Thomas, B. A. Sosinsky, and E. L. Muetterties, *Proc. Nat. Acad. Sci. U.S.A.* **73**, 4274 (1976).
357. W. Hübel and C. Hoogzand, *Chem. Ber.* **93**, 103 (1960).
358. C. C. Yin and A. J. Deeming, *J. Organomet. Chem.* **144**, 351 (1978).
359. C. Y. Ren, W. C. Cheng, W. C. Chan, C. H. Yeung, and C. P. Lau, *J. Mol. Catal.* **59**, L1 (1990).
360. V. W. Day, R. O. Day, J. S. Kristoff, F. J. Hirsekorn, and E. L. Muetterties, *J. Am. Chem. Soc.* **97**, 2571 (1975).
361. G. A. Catton, G. F. C. Jones, M. J. Mays, and J. A. S. Howell, *Inorg. Chim. Acta* **20**, L41 (1976).
362. J. M. Burlitch, S. E. Hayes, and J. T. Lemley, *Organometallics* **4**, 167 (1985).
363. J.-P. Barbier, Thèse de Doctorat, Université de Strasbourg, Strasbourg, France, 1978.
364. M. P. Doyle, W. H. Tambllyn, W. E. Buhro, and R. L. Dorow, *Tetrahedron Lett.* **22**, 1783 (1981).
365. M. P. Doyle, D. van Leusen, and W. H. Tambllyn, *Synthesis*, 787 (1981).
366. H. Yamazaki and P. Hong, *J. Mol. Catal.* **21**, 133 (1983).
367. P. Hong, B.-R. Cho, and H. Yamazaki, *Chem. Lett.*, 507 (1980).
368. P. Hong, B.-R. Cho, and H. Yamazaki, *Chem. Lett.*, 339 (1979).
369. P. Hong, H. Yamazaki, K. Sonogashira, and N. Hagihara, *Chem. Lett.*, 535 (1978).
370. T. Kondo, S. Tantayanon, Y. Tsuji, and Y. Watanabe, *Tetrahedron Lett.* **30**, 4137 (1989).
371. T. Kondo, Y. Tsuji, and Y. Watanabe, *Tetrahedron Lett.* **28**, 6229 (1987).
372. T. Kondo, M. Akazome, Y. Tsuji, and Y. Watanabe, *J. Org. Chem.* **55**, 1286 (1990).
373. Y. Tsuji, T. Mukai, T. Kondo, and Y. Watanabe, *J. Organomet. Chem.* **369**, C51 (1989).
374. W. Keim and J. Becker, *J. Mol. Catal.* **54**, 95 (1989).
375. E. M. Nahmed and G. Jenner, *J. Mol. Catal.* **59**, L15 (1990).
376. T. Kondo, S. Yoshii, Y. Tsuji, and Y. Watanabe, *J. Mol. Catal.* **50**, 31 (1989).
377. Y. Tsuji, S. Yoshii, T. Ohsumi, T. Kondo, and Y. Watanabe, *J. Organomet. Chem.* **331**, 379 (1987).
378. S. Sato, I. Matsuda, and Y. Izumi, *J. Organomet. Chem.* **352**, 223 (1988).
379. S. Sato, I. Matsuda, and Y. Izumi, *Tetrahedron Lett.* **28**, 6657 (1987).
380. I. Matsuda and K. Takahashi, *Tetrahedron Lett.* **31**, 5331 (1990).
381. M. Tanaka and T. Hayashi, *J. Mol. Catal.* **60**, L5 (1990).
382. G. Schmidt and G. Süss-Fink, *J. Organomet. Chem.* **356**, 207 (1988).
383. H. Alper and J. F. Petrignani, *J. Chem. Soc. Chem. Commun.*, 1154 (1983).
384. I. Matsuda, A. Ogiso, and S. Sato, *J. Am. Chem. Soc.* **112**, 6120 (1990).
385. F. Abe, T. Hayashi, and M. Tanaka, *Chem. Lett.*, 765 (1990).
386. G. Süss-Fink, G. Herrmann, and G. F. Schmidt, *Polyhedron* **7**, 2341 (1988).
387. G. Süss-Fink and G. Herrmann, *Angew. Chem.* **98**, 568 (1986); G. Süss-Fink and G. Herrmann, *Angew. Chem. Int. Ed. Engl.* **25**, 570 (1986).
388. G. Süss-Fink, G. Herrmann, and U. Thewalt, *Angew. Chem.* **95**, 899 (1983); G. Süss-Fink, G. Herrmann, and U. Thewalt, *Angew. Chem. Int. Ed. Engl.* **22**, 880 (1983).
389. G. Süss-Fink, G. Schmidt, and G. Herrmann, *Chem. Ber.* **120**, 1451 (1987).
390. G. F. Schmidt and G. Süss-Fink, *J. Organomet. Chem.* **356**, 207 (1988).
391. Y. Sasaki and P. H. Dixneuf, *J. Chem. Soc. Chem. Commun.*, 790 (1986).
392. R. Mahé, Y. Sasaki, C. Bruneau, and P. H. Dixneuf, *J. Org. Chem.* **54**, 1518 (1989).

- 393. Y. Sasaki and P. H. Dixneuf, *J. Org. Chem.* **52**, 4389 (1987).
- 394. C. Bruneau and P. H. Dixneuf, *Tetrahedron Lett.* **28**, 2005 (1987).
- 395. G. Jenner, *J. Mol. Catal.* **55**, 241 (1989).
- 396. G. Jenner, *J. Mol. Catal.* **45**, 165 (1988).
- 397. R. B. Wilson, Jr., and R. M. Laine, *J. Am. Chem. Soc.* **107**, 361 (1985).
- 398. Y. Shvo and R. M. Laine, *J. Chem. Soc. Chem. Commun.*, 756 (1980).
- 399. R. M. Laine, *Ann. N.Y. Acad. Sci.* **415**, 271 (1983).
- 400. R. M. Laine, *J. Mol. Catal.* **2**, 119 (1983).
- 401. R. M. Laine, D. W. Thomas, and L. W. Cary, *J. Am. Chem. Soc.* **104**, 1763 (1982).
- 402. R. D. Adams, H.-S. Kim, and S. Wang, *J. Am. Chem. Soc.* **107**, 6107 (1985).
- 403. Y. Blum, D. Reshef, and Y. Shvo, *Tetrahedron Lett.* **22**, 1541 (1981).
- 404. G. O. Evans and C. J. Newell, *Inorg. Chim. Acta* **31**, L387 (1978).
- 405. D. J. Darensbourg, C. Ovalles, and M. Pala, *J. Am. Chem. Soc.* **105**, 5937 (1983).
- 406. G. F. Schmidt, J. Reiner, and G. Süss-Fink, *J. Organomet. Chem.* **355**, 379 (1988).
- 407. I. P. Stolarov, M. N. Vargaftik, O. M. Nefedov, and I. I. Moiseev, *Kinet. Katal.* **23**, 376 (1982).
- 408. T. A. Stromnova, I. N. Busygina, S. B. Katser, A. S. Antsyshkina, M. A. Porai-Koshits, and M. A. Moiseev, *Izv. Akad. Nauk SSSR Ser. Khim.*, 1435 (1987).
- 409. G. D. Mercer, J. S. Shu, T. B. Rauchfuss, and D. M. Roundhill, *J. Am. Chem. Soc.* **97**, 1967 (1975).
- 410a. G. Jenner, E. M. Nahmed, and H. Leismann, *Tetrahedron Lett.* **30**, 6501 (1989).
- 410b. G. Jenner, E. M. Nahmed, and H. Leismann, *J. Organomet. Chem.* **387**, 315 (1990).

# **The Interplay of Alkylidyne and Carbaborane Ligands at Metal Centers**

## **II: Proton-Mediated Reactions<sup>1</sup>**

STEPHEN A. BREW and F. GORDON A. STONE

*Department of Chemistry  
Baylor University  
Waco, Texas 76798*

I.	Introduction . . . . .	135
II.	Protonations with $\text{HBF}_4 \cdot \text{Et}_2\text{O}$ in the Presence of Monodentate Lewis Bases . . . . .	142
III.	Protonations with $\text{HBF}_4 \cdot \text{Et}_2\text{O}$ in the Presence of Bidentate Phosphines . . . . .	149
IV.	Protonations with $\text{HX}$ ( $\text{X} = \text{Cl}$ or $\text{I}$ ) . . . . .	152
V.	Formation of Dimetal Compounds. . . . .	157
	A. Protonation of Mixtures Containing Two Distinct Alkylidyne-Metal Complexes . . . . .	157
	B. Protonations Involving 0.5 Mol Eq. of $\text{HBF}_4 \cdot \text{Et}_2\text{O}$ . . . . .	165
VI.	<i>Exo-nido</i> Metallacarboranes . . . . .	172
VII.	Spectroscopic and X-Ray Diffraction Analysis . . . . .	176
	A. NMR Spectroscopy . . . . .	176
	B. X-Ray Diffraction Analysis . . . . .	182
VIII.	Conclusions. . . . .	183
	References . . . . .	183

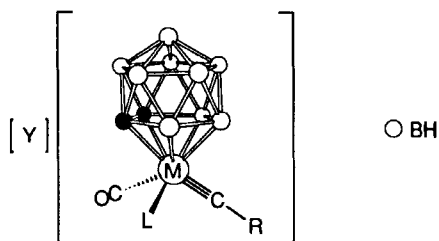
### I

### INTRODUCTION

This chapter surveys protonation reactions of the alkylidyne(carbaborane) complexes of the group 6 metals that are depicted in structural formulae 1–3. Many of the reactions described were carried out in the presence of donor substrate molecules, resulting in the observation of new B–C, P–C, C–C, and metal–metal bond-forming processes. Novel low-temperature polytopal rearrangements, cage degradation reactions, and metal–cage interactions have been discovered, as a consequence of the formation of molecules with unusual structures. The review follows another (1) in this series of volumes summarizing reactions of some of the species 1 and 2 with low-valent metal complexes, which afford polynuclear metal compounds containing bonds between different transition elements. The salts 1–3 contain both carbaborane cage fragments and alkylidyne

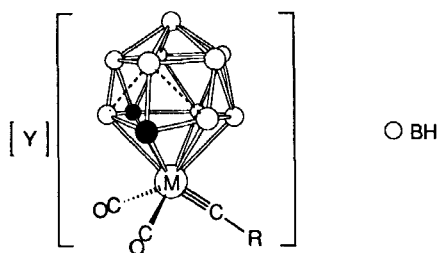
<sup>1</sup> For Part I, see Ref. (1).





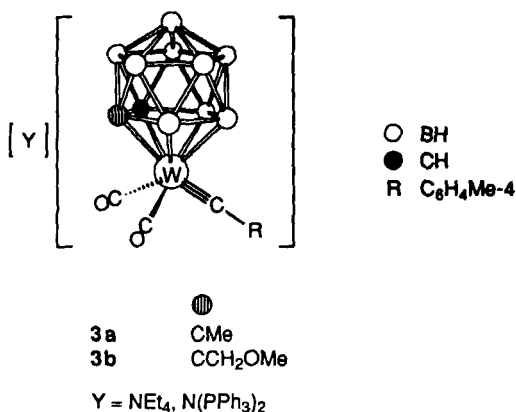
	M	L	R	●
1a	W	CO	C <sub>6</sub> H <sub>4</sub> Me-4	CMe
1b	W	CO	Me	CMe
1c	W	CO	C <sub>6</sub> H <sub>4</sub> Me-2	CMe
1d	W	CO	C <sub>6</sub> H <sub>3</sub> Me <sub>2</sub> -2,6	CMe
1e	W	CO	Ph	CMe
1f	W	CO	C <sub>6</sub> H <sub>4</sub> OMe-2	CMe
1g	W	CO	C <sub>6</sub> H <sub>4</sub> CH <sub>2</sub> OMe-2	CMe
1h	W	CO	C≡CBu <sup>t</sup>	CMe
1i	W	CO	C <sub>6</sub> H <sub>4</sub> Me-4	CH
1j	W	CO	Me	CH
1k	W	CO	C≡CBu <sup>t</sup>	CH
1l	Mo	CO	C <sub>6</sub> H <sub>4</sub> Me-4	CH
1m	Mo	CO	C <sub>6</sub> H <sub>4</sub> Me-4	CMe
1n	Mo	P(OMe) <sub>3</sub>	C <sub>6</sub> H <sub>4</sub> Me-4	CMe

Y = NEt<sub>4</sub>, PPh<sub>4</sub>, AsPh<sub>4</sub>, NMe<sub>3</sub>Ph, N(PPh<sub>3</sub>)<sub>2</sub>, etc.



	M	R	●
2a	W	C <sub>6</sub> H <sub>4</sub> Me-4	CMe
2b	W	Me	CMe
2c	W	C <sub>6</sub> H <sub>3</sub> Me <sub>2</sub> -2,6	CMe
2d	W	C <sub>6</sub> H <sub>4</sub> Me-4	CH
2e	W	Me	CH
2f	Mo	C <sub>6</sub> H <sub>4</sub> Me-4	CMe

Y = NEt<sub>4</sub>, N(PPh<sub>3</sub>)<sub>2</sub>, NMe<sub>3</sub>Ph

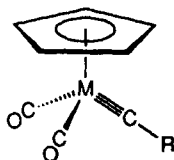


groups and thus form a bridge between two very active but hitherto quite separate domains of organometallic chemistry: the polyhedral metallacarbaboranes and the alkylidyne-metal complexes.

In the three decades since the icosahedral  $\text{C}_2\text{B}_{10}\text{H}_{12}$  species were first reported (2,3), polyhedral carbaborane chemistry has expanded in many different directions. Multitudinous studies have been carried out on metal-containing derivatives of the carbaboranes (4), since it was first recognized by Hawthorne and his co-workers (5) that the anionic species *nido*- $\text{C}_2\text{B}_9\text{H}_{11}^{2-}$  had ligating properties toward transition elements resembling those of the ubiquitous  $\text{C}_5\text{H}_5^-$  anion, both being able to coordinate to *d*- or *f*-metal centers in a penta-hapto-manner. Hydrogenation catalysts (6) and boron-neutron-capture therapy agents, which may be both tumor-specific and cytotoxic (7), are but two recent developments in research on the metallacarbaboranes that are of potential practical benefit. However, studies in this area have most frequently been stimulated by the desire of chemists to synthesize new, theoretically challenging, and aesthetically pleasing structures, a desire that this class of compound has shown an extraordinary capacity to satisfy.

Most metallacarbaborane complexes so far reported have generally displayed reactivity patterns involving the carbaborane cage, rather than the ligands attached to the metal vertices, the metal-bound exopolyhedral ligands usually remaining inert. Hence, the synthesis of metallacarbaborane complexes in which the metal bears a reactive alkylidyne ( $\equiv\text{CR}$ ) moiety, likely to interact with B—H groups on the periphery of the cage, was an exciting goal for us. It resulted from recognition of an isobal mapping (8) of the alkylidyne-carbaborane metal salts  $[\text{Y}][\text{M}(\equiv\text{CR})(\text{CO})_2(\eta^5\text{-C}_2\text{B}_9\text{H}_9\text{R}'_2)]$  ( $\text{Y} = \text{NEt}_4, \text{PPh}_4, \text{AsPh}_4, \text{N}(\text{PPh}_3)_2$ ,

$\text{NMe}_3\text{Ph}$ , etc.;  $\text{M} = \text{W}$  or  $\text{Mo}$ ;  $\text{R} = \text{alkyl, aryl, or alkynyl}$ ;  $\text{R}' = \text{H}$  or  $\text{Me}$ ) **1** with the neutral complexes  $[\text{M}(\equiv\text{CR})(\text{CO})_2(\eta\text{-C}_5\text{H}_5)]$  **4**, which them-



	M	R
4a	W	$\text{C}_6\text{H}_4\text{Me-4}$
4b	W	Me
4c	W	$\text{C}_6\text{H}_4\text{Me-2}$
4d	W	$\text{C}_6\text{H}_3\text{Me}_2\text{-2,6}$
4e	W	$\text{C}_6\text{H}_4\text{OMe-2}$
4f	W	$\text{C}_6\text{H}_4\text{CH}_2\text{OMe-2}$
4g	W	$\text{C}\equiv\text{CBu}^t$
4h	W	$\text{C}\equiv\text{CC}_6\text{H}_4\text{Me-4}$
4i	Mo	$\text{C}_6\text{H}_4\text{Me-4}$

selves have proven useful synthons for the rational synthesis of metal clusters (9). This concept was later extended to include syntheses of the complex salts **2** and **3**, which contain as ligands the *nido* 12-vertex cages  $[\eta^6\text{-C}_2\text{B}_{10}\text{H}_{10}\text{R}'_2]^{2-}$  ( $\text{R}' = \text{H}$  or  $\text{Me}$ ) and the asymmetric 11-vertex *nido* cages  $[\eta^5\text{-C}_2\text{B}_9\text{H}_9\text{R}'\text{R}'']^{2-}$  ( $\text{R}' = \text{H}$ ;  $\text{R}'' = \text{Me}$  or  $\text{CH}_2\text{OMe}$ ), respectively.

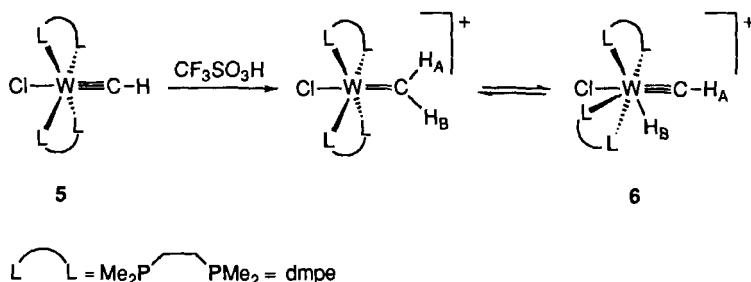
In the initial work (10) involving the use of some of the salts **1** as precursors to metal clusters, it was conceptually useful to regard these reagents as alkylidyne-metal complexes bearing *nido* carbaborane ligands, thus relating them to cyclopentadienylmetal compounds. However, although the early results supported the use of this formalism, the majority of polynuclear metal complexes subsequently discovered have involved both carbaborane and carbyne functionalities acting in concert, so that the  $\eta^5\text{-C}_2\text{B}_9\text{H}_9\text{R}'_2$  or  $\eta^6\text{-C}_2\text{B}_{10}\text{H}_{10}\text{R}'_2$  cages adopt a noninnocent role (1). This feature, together with the chemistry surveyed in this article, has led to more emphasis being placed on the alternative view that they be regarded as *closo*-metallacarbaborane cluster complexes, with the added spice of a reactive and indeed interactive alkylidyne ligand on the periphery of the cage. This is reflected in our use of the line formula  $[\text{Y}][\text{closo-1,2-Me}_2\text{-3-(}\equiv\text{CC}_6\text{H}_4\text{Me-4)-3,3-(CO)}_2\text{-3,1,2-WC}_2\text{B}_9\text{H}_9]$  to describe the salt **1a**, instead of the alternative description  $[\text{Y}][\text{W}(\equiv\text{CC}_6\text{H}_4\text{Me-4})(\text{CO})_2(\eta^5\text{-7,8-C}_2\text{B}_9\text{H}_9\text{Me}_2)]$ . However, representation of the carbon-boron cage frameworks as  $\eta^5$ - or  $\eta^6$ -ligands is advantageous in some respects, particularly when describing dimetal species. Thus, a formula such as  $[\text{closo-1,2-}$

$\text{Me}_2\text{-8-(CH}_2\text{C}_6\text{H}_4\text{Me-4)-3,3-(CO)}_2\text{-3-(}\mu\text{-CMe)-3-(W(CO)(}\eta^5\text{-C}_5\text{H}_5\text{))-4-(}\mu\text{-H)-3,1,2\text{-WC}_2\text{B}_9\text{H}_7\text{]}$  is excessively cumbersome, compared with  $[\text{W}_2(\mu\text{-CMe})(\text{CO})_3(\eta^5\text{-C}_2\text{B}_9\text{H}_8(\text{CH}_2\text{C}_6\text{H}_4\text{Me-4})\text{Me}_2)(\eta\text{-C}_5\text{H}_5)]$  for the same compound. For this reason, both systems of nomenclature are used in this review as appropriate.

The chemistry of alkylidyne-metal complexes, species containing  $\text{M}\equiv\text{C}$  triple bonds, has developed at a rate equally dramatic to that of the metallocarbaboranes in the two decades since the first examples were reported (11). Indeed, their significance is such that three reviews of the chemistry of alkylidyne-metal compounds have appeared in *Advances in Organometallic Chemistry* (12a-c), a book has been published on the subject (13), and personal accounts have been given by Fischer (14) and by Schrock (15), the individuals responsible for pioneering work in this area. A key interest in this class of compound has been their relevance to catalytic alkyne metathesis (13,16,17). However, much research has been spurred purely by their unique properties that have opened up new vistas in organometallic chemistry, including their use as precursors in metal cluster synthesis (1,9,18). Such has been the scope of this area that carbyne- or alkylidyne-metal complexes are now known for the transition elements of groups 5 to 10 inclusive.

Alkylidyne-metal complexes have traditionally been divided into two categories, according to the oxidation state of the metals, in a manner directly analogous to the classification of the very large number of known alkylidene-metal species (19a,b). Hence "Fischer-type" alkylidyne complexes involve metals in low oxidation states, while "Schrock-type" complexes generally involve more electropositive metals with higher oxidation states (13). However, the properties of some of the numerous carbyne-metal complexes that have been characterized since the early days have in many cases blurred the distinction between the two classes (12a).

Since this article is concerned with protonation reactions, some mention of earlier related work on the more classical alkylidyne-metal complexes is appropriate. The proton has proved a popular experimental probe for examining the reactivity of alkylidyne-metal complexes in studies attempting to establish the nature of the  $\text{M}\equiv\text{C}$  bonding interaction. Calculations by Kostić and Fenske (20) on Fischer-type alkylidynes suggest that the metal-carbon bond is generally polarized  $\text{M}^{\delta+}-\text{C}^{\delta-}$ , but that the lowest unoccupied molecular orbital (LUMO) is not always based on the  $\text{M}\equiv\text{C}$  fragment. Protonation studies were expected to reveal the most nucleophilic sites within these molecules and hence whether charge or frontier orbital effects control their reactivity toward electrophiles. However, although many novel complexes have resulted from these studies, the initial site of attack by the proton is frequently obscured by rapid

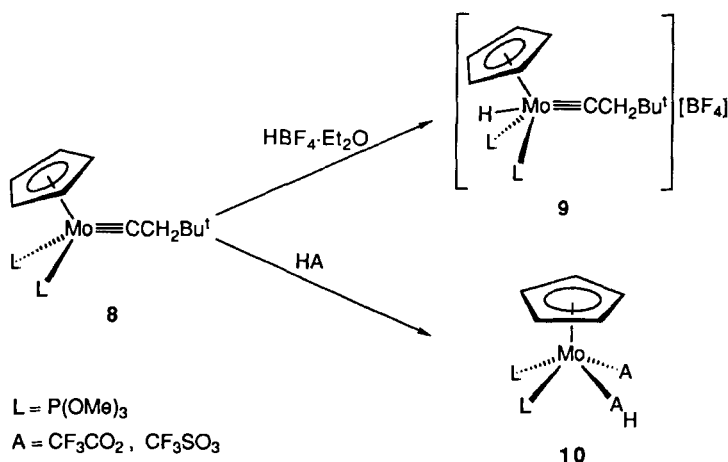


SCHEME 1.

secondary reactions and rearrangements of the products. This has been demonstrated, for instance, by Holmes and Schrock (21) who treated  $[\text{W}(\equiv\text{CH})(\text{Cl})(\text{dmpe})_2]$  **5** ( $\text{dmpe} = \text{Me}_2\text{P}(\text{CH}_2)_2\text{PMe}_2$ ) with  $\text{CF}_3\text{SO}_3\text{H}$  and obtained the alkylidyne-hydride complex  $[\text{W}(\equiv\text{CH})(\text{H})(\text{Cl})(\text{dmpe})_2][\text{CF}_3\text{SO}_3]$  **6** (Scheme 1). Rapid exchange, on the NMR time scale, of the alkylidyne- and metal-bound protons ( $\text{H}_\text{A}$  and  $\text{H}_\text{B}$ ) of **6** implicates the existence, in solution, of an equilibrium with an alkylidene complex carrying both protons. In certain cases, alkylidene complexes have been isolated following protonation, as described below. However, the resulting electron deficiency of the metal can lead to a distortion of the alkylidene-carbon atom geometry, implying interaction of the metal with the electron pair of one C—H bond. Hence in the solid state structure of  $[\text{W}(\equiv\text{C}(\text{H})\text{Ph})(\text{Cl})_2(\text{CO})(\text{PMe}_3)_2]$  **7** the alkylidene group shows a  $\text{W}-\text{C}-\text{C}'(\text{Ph})$  angle of  $164.6^\circ$  and a  $\text{W}-\text{C}-\text{H}$  angle of  $74.6^\circ$  (22).

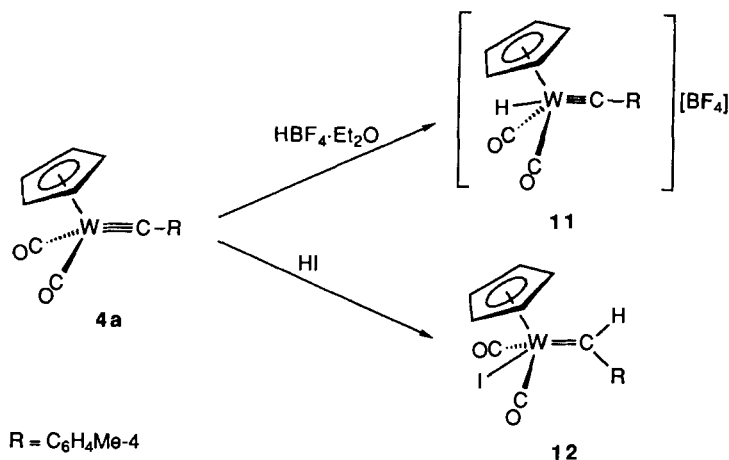
Protonation reactions of the alkylidyne(cyclopentadienyl)metal complexes **4** and related species have been studied by several research groups. Published results have consistently shown that the choice of acid is often critical in determining the reaction pathway, as the primary products are often electrophilic and are subject to further transformations. This has been demonstrated, for example, by Green *et al.* (23) (Scheme 2). Thus when protonating the alkylidyne-molybdenum species  $[\text{Mo}(\equiv\text{CCH}_2\text{Bu}^t)(\text{P}(\text{OMe})_3)_2(\eta\text{-C}_5\text{H}_5)]$  **8** with  $\text{HBF}_4 \cdot \text{Et}_2\text{O}$ , a terminal alkylidyne-hydride salt  $[\text{Mo}(\text{H})(\equiv\text{CCH}_2\text{Bu}^t)(\text{P}(\text{OMe})_3)_2(\eta\text{-C}_5\text{H}_5)][\text{BF}_4]$  **9** is formed. In contrast, when using the acids  $\text{HA}$  ( $\text{A} = \text{CF}_3\text{CO}_2$  or  $\text{CF}_3\text{SO}_3$ ), the  $\text{M}\equiv\text{C}$  bond is cleaved and the alkylidyne ligand replaced by a molecule each of acid ( $\text{HA}$ ) and its conjugate base ( $\text{A}^-$ ), forming  $[\text{Mo}(\text{A})(\text{AH})(\text{P}(\text{OMe})_3)_2(\eta\text{-C}_5\text{H}_5)]$  **10**.

The explanation for the differing nature of the products is that protonation initially yields a terminal alkylidene intermediate that will rearrange, if

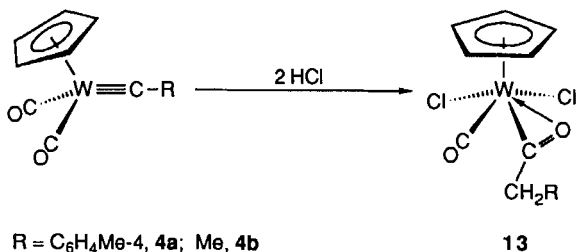


SCHEME 2.

allowed, to the thermodynamically favorable alkylidyne-hydrido complex **9**. However, in the presence of nucleophiles such as  $\text{CF}_3\text{CO}_2^-$  or  $\text{CF}_3\text{SO}_3^-$ , the alkylidyne ligand is displaced, and the metal coordination sphere subsequently completed by a molecule of associated acid acting as an electron-pair donor. The nucleophilic displacement of alkylidyne ligands from transition metals has been reported (24), but clearly cannot apply to the very weak nucleophile  $\text{BF}_4^-$ .



SCHEME 3.



SCHEME 4.

The species  $[W(\equiv CC_6H_4Me-4)(CO)_2(\eta-C_5H_5)]$  **4a**, which is related to **8**, showed comparable reactivity when treated with 1 mole equivalent of  $HBf_4 \cdot Et_2O$  (Scheme 3),<sup>2</sup> yielding  $[W(H)(\equiv CC_6H_4Me-4)(CO)_2(\eta-C_5H_5)][BF_4]$  **11** (25). However, when treated with HI, the complex  $[W(I)(=C(H)C_6H_4Me-4)(CO)_2(\eta-C_5H_5)]$  **12** was isolated and characterized by an X-ray diffraction study. This confirmed the existence of the alkylidene-metal intermediate, implicated by preceding results, which had been effectively trapped in **12** by coordination of the iodide ligand to the metal.

Independent simultaneous studies by Kreissl and his co-workers (26) showed that treatment of the complexes **4a** or **4b** with 2 equivalents of the halo-acid HCl produced the  $\eta^2$ -acyl-ligated species  $[WCl_2(\eta^2-C(O)CH_2R)(CO)(\eta-C_5H_5)]$  **13** (R = Me, C<sub>6</sub>H<sub>4</sub>Me-4) by migration of an alkyl group (CH<sub>2</sub>R) onto one carbonyl ligand (Scheme 4). This alkyl group clearly derives from protonation of the carbene ligand in an intermediate species of the type  $[W(X)(=C(H)R)(CO)_2(\eta-C_5H_5)]$  (X = Cl), akin to **12**.

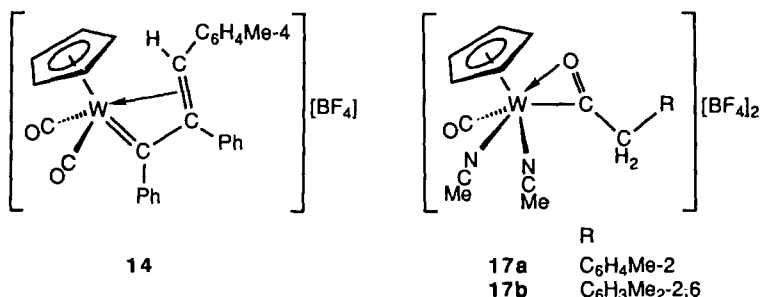
## II

### PROTONATIONS WITH $HBf_4 \cdot Et_2O$ IN THE PRESENCE OF MONODENTATE LEWIS BASES

The addition of Lewis base substrate molecules to solutions containing alkylidyne-metal species prior to treatment with acid introduces a new dimension in the protonation reactivity of these complexes. This was

<sup>2</sup> The final products of protonations with  $HBf_4 \cdot Et_2O$  depend critically on the stoichiometry of this reaction. As the results of employing different ratios of reactants are directly related to the products from similar reactions of the salts **1** and **2**, they are described in later sections.

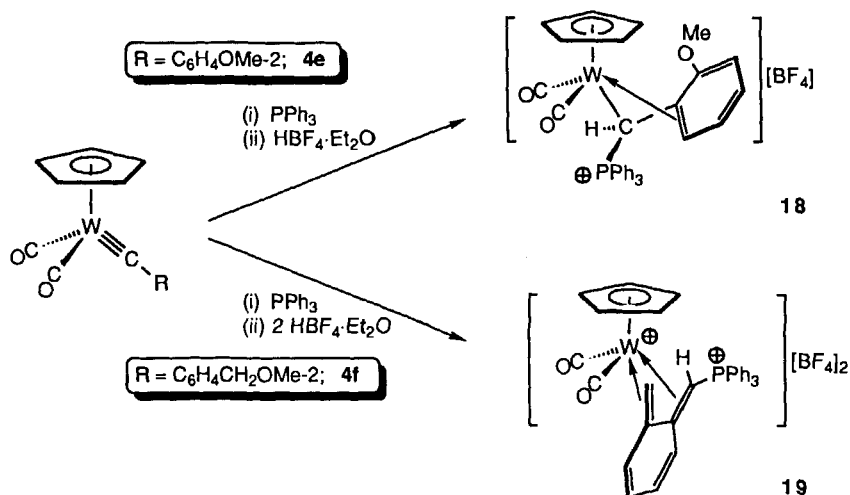
first demonstrated by Geoffroy *et al.* (27) who protonated the cyclopentadienyl-tungsten complex **4a** in the presence of alkynes. The resulting vinyl-carbene-metal salt,  $[W(=C(Ph)C(Ph)C(H)C_6H_4Me-4)(CO)_2(\eta-C_5H_5)][BF_4]$  **14** obtained from  $PhC\equiv CPh$  derives essentially from insertion of the alkyne into the  $M=C$  bond of an initially formed alkylidene-metal species arising from the protonation step. When protonations of **4a** or **4d** with  $HBf_4 \cdot Et_2O$  are carried out in the presence of  $MeC\equiv CMe$  and CO, a naphthol-coordinated compound  $[W(C_{13}H_{14}O)(CO)_2(\eta-C_5H_5)][BF_4]$  **15** and a diene-ligated salt  $[W(C_{14}H_{16}O)(CO)_2(\eta-C_5H_5)][BF_4]$  **16**, respectively, are formed by cyclic oligomerization processes. Such processes are typical of reactions between alkynes and group 6 metal carbene complexes (28).



A related reactivity pattern is observed when the complexes **4c** or **4d** are protonated with  $HBf_4 \cdot Et_2O$ , using the donor molecule NCMe as a solvent (29). In this instance, a dication results as the carbyne ligand is transformed into an  $\eta^2$ -acyl group in a stepwise process such as described earlier (Scheme 4). The coordination sphere of the metal is filled by two NCMe molecules, yielding the salts  $[W(CO)(NCMe)_2(\eta^2-COCH_2R)(\eta-C_5H_5)][BF_4]_2$  ( $R = C_6H_4Me-2$ , **17a**;  $R = C_6H_3Me_2-2,6$ , **17b**).

The diversity of species attainable by this methodology is illustrated by the following two reactions of closely related alkylidyne(cyclopentadienyl)metal complexes, when protonated with 1 equivalent of  $HBf_4 \cdot Et_2O$  in the presence of triphenylphosphine (Scheme 5). Treatment of **4e** in this manner affords  $[W(\sigma, \eta^2-CH(PPh_3)C_6H_4OMe-2)(CO)_2(\eta-C_5H_5)][BF_4]$  **18**, in which a proton and a  $PPh_3$  group have added to the ligated carbon atom of the alkylidyne group in the precursor (29). A single crystal X-ray diffraction study of this product revealed an asymmetric  $\sigma, \eta^2$ -rather than an allylic  $\eta^3$ -bonding mode of the organic fragment to the metal atom, the carbon atom  $\sigma$ -bonded to tungsten having appreciable  $sp^3$  geometry. Nevertheless, it is interesting to note that such a conformation is preferred over one in which the  $\eta^2$ -olefinic group is replaced by donation of





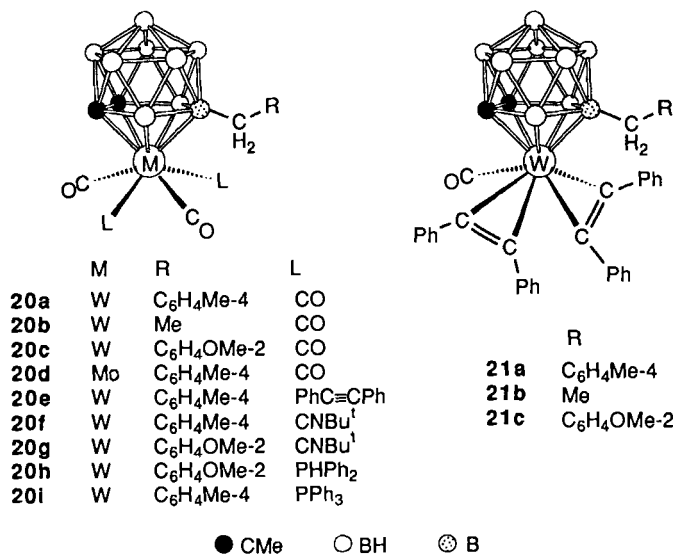
SCHEME 5.

an electron pair from the oxygen atom of the OMe substituent. Such a conformation would be readily attained by rotation about the  $C_\alpha-C_\beta$  bond, yet no evidence for such a species could be obtained.

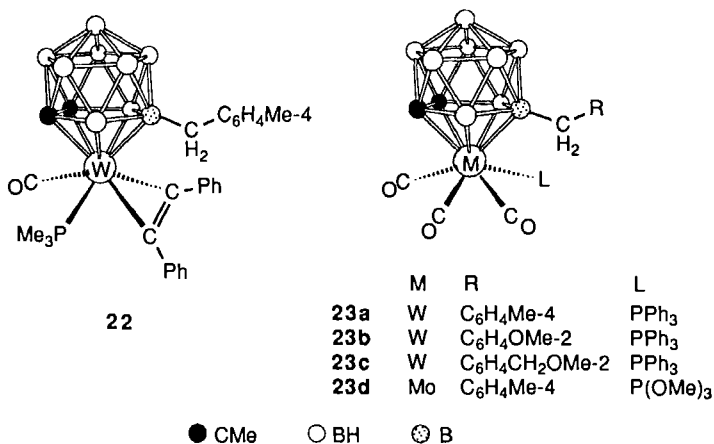
When the same reaction was performed on **4f** using 2 equivalents of acid, the substantially different product  $[W(CO)_2(\eta^4-C_6H_4(CH_2)-[CH(PPh_3)]-1,2)(\eta-C_5H_5)][BF_4]_2$  **19** resulted. However, this difference in reactivity was found not to be attributable to the reaction stoichiometry (30). In this case, an OMe group has been eliminated, presumably as methanol, and the tungsten atom is  $\eta^4$ -ligated by a diene fragment carrying a  $PPh_3$  group in an *exo*-position. An X-ray diffraction study of complex **19** confirmed that all four carbon atoms of the diene ligand showed  $sp^2$  geometry, contrasting with the ligating carbon atoms of complex **18**. The proposed pathway for formation of the salt **19** includes an intermediate analogous to complex **18**, carrying a  $CH_2OMe$  substituent in the *ortho*-position. By this means, the stereochemistry of  $PPh_3$  addition to the alkylidyne carbon atom after protonation may be preserved during its transformation to the final butadiene product **19**.

In contrast, when the alkylidyne(carbaborane)tungsten complexes of type **1** are protonated with  $HBF_4 \cdot Et_2O$  in a similar manner in the presence of donor molecules (L), notably different species result (31,32). In this case the metal atom in each of the products  $[closo-1,2-Me_2-8-(CH_2R)-3,3-(CO)_2-3,3-(L)_2-3,1,2-MC_2B_9H_8]$  **20** is ligated on one side by two CO molecules and by two of the 2e donor molecules L, while maintaining its position as a vertex of a 3,1,2- $MC_2B_9$  carbaborane cage. However, one

boron atom adjacent to the tungsten, and in a  $\beta$ -position with respect to the cage carbon vertices, now bears a  $\text{CH}_2\text{R}$  substituent. A similar reactivity pattern is shown by the molybdenum salt **1m**, which affords **20d** on treatment with  $\text{HBF}_4 \cdot \text{Et}_2\text{O}$  in the presence of CO (33). The products **20** are presumed to derive from an intermediate [*closo*-1,2- $\text{Me}_2$ -3,3-(CO) $_2$ -3-(C(H)R)-3,1,2- $\text{MC}_2\text{B}_9\text{H}_9$ ], the alkylidene ligand of which inserts into the B–H bond of the neighboring vertex, the  $\beta$ -site apparently being activated by the cage CMe groups. The coordinatively unsaturated metal center captures two donor molecules (L) from the mixture to yield as products, species with  $\text{M}(\text{CO})_2(\text{L})_2$  groups. If no donor molecules are added to solutions of the reagents **1** prior to treatment with acid, the only products isolated are the tetracarbonyl metal complexes **20a**–**20d**, in low yield. These are formed by scavenging of CO molecules from the solutions.



While complexes **20a**–**20d** are reasonably stable in solutions of organic solvents at room temperature, the remaining species **20** undergo a variety of transformations (31,32). Dichloromethane solutions of **20e** release CO if warmed above  $-20^\circ\text{C}$ , cleanly affording complex **21a**. The analogous products **21b** and **21c** are the only species isolable from protonation of the reagents **1b** or **1f**, respectively, in the presence of  $\text{PhC}\equiv\text{CPh}$ , although the fleeting existence of dicarbonyl species akin to **20e** was indicated by the IR spectrum of each reaction mixture. Treatment, at low temperature, of **20e** with  $\text{PMe}_3$ , yielded the monoalkyne complex **22**. Complexes **20e**, **21**, and **22** thus represent a series in which diphenylacetylene acts, respectively, as a



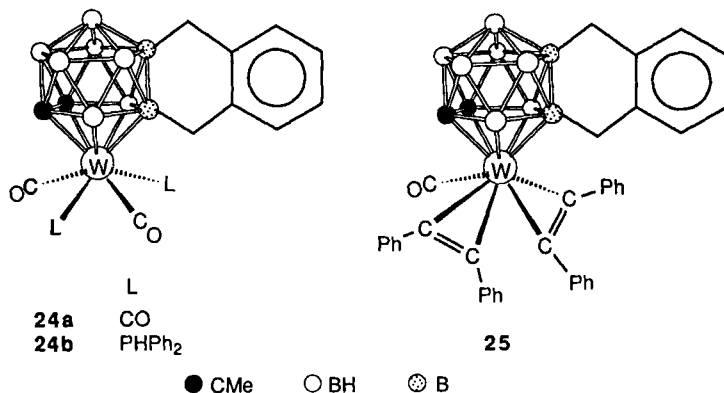
formal two-, three-, and four-electron donor to a metal center (34). The isocyanide complexes **20f** and **20g** by contrast are quite stable, but exist in both cases as mixtures of interchanging *cisoid* and *transoid* isomers. For the sake of simplicity, only the latter have been shown diagrammatically.

Upon protonating salts **1a** and **1f** in the presence of monodentate phosphines, an interesting balance of reactivity was observed. When using the secondary phosphine PHPH<sub>2</sub> the expected bis-phosphine product **20h** was obtained from protonation of **1f** (32). Simply replacing this phosphine in the reaction mixture with the tertiary phosphine PPh<sub>3</sub> afforded complex **23b**, in which only one substrate molecule is present, CO having been scavenged from the solution. A similar product **23c** was isolated from the reaction between **1g**, PPh<sub>3</sub>, and HBF<sub>4</sub>·Et<sub>2</sub>O. In contrast, the less sterically demanding C<sub>6</sub>H<sub>4</sub>Me-4 carbyne substituent present in **1a** results in the latter, yielding a mixture of **20i** and **23a** when protonated in the presence of PPh<sub>3</sub> (31). These two complexes interconvert slowly by a disproportionation process, with gradual decomposition evident after several hours in solution. Examination of space-filling models of **20i** and **23b**, using data obtained from X-ray diffraction studies, reveal that the ligands are very crowded at the metal centers. This supports the assertion that the observed reactivity trend is attributable primarily to steric requirements within the molecules. The related molybdenum phosphite complex **23d** has been obtained by protonating a CO-saturated solution of **1n**, which carries the P(OMe)<sub>3</sub> ligand, with HBF<sub>4</sub>·Et<sub>2</sub>O (33).

Despite these subtle differences in reactivity, all the compounds **20** to **23** have in common an identical 3,1,2-MC<sub>2</sub>B<sub>9</sub> (M = W or Mo) icosahedral cage framework, with the carbyne-derived CH<sub>2</sub>R fragment attached to the

B(8) site (the  $\beta$ -boron atom with respect to the C atoms of the cage).<sup>3</sup> That the alkylidene fragment may migrate from the metal to an adjacent cage vertex is the key factor in allowing the synthesis of species of this type, a process not open to the cyclopentadienyl-bearing alkylidyne-metal species **4**. Furthermore, the carbaborane cage is a fully three-dimensional structure that offers more varied reaction possibilities than its "two-dimensional" cyclopentadienyl analog.

This feature is well demonstrated by syntheses of the complexes [*closo*-1,2-Me<sub>2</sub>-8,9-(CH<sub>2</sub>C<sub>6</sub>H<sub>4</sub>CH<sub>2</sub>-2)-3,3-(CO)<sub>2</sub>-3,3-(L)<sub>2</sub>-3,1,2-WC<sub>2</sub>B<sub>9</sub>H<sub>7</sub>] **24** and [*closo*-1,2-Me<sub>2</sub>-8,9-(CH<sub>2</sub>C<sub>6</sub>H<sub>4</sub>CH<sub>2</sub>-2)-3-(CO)-3,3-( $\eta$ -PhC<sub>2</sub>Ph)<sub>2</sub>-3,1,2-

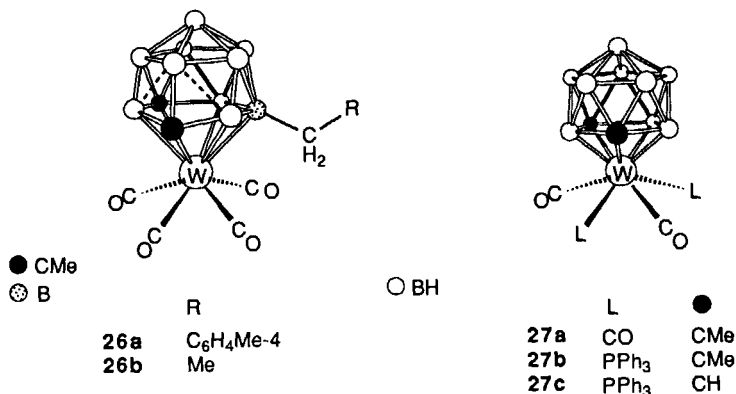


WC<sub>2</sub>B<sub>9</sub>H<sub>7</sub>] **25** (**35**). These products are formed via protonation of the reagent **1g**, in which tungsten bears the  $\equiv$ CC<sub>6</sub>H<sub>4</sub>CH<sub>2</sub>OMe-2 ligand, in the presence of CO, PPh<sub>2</sub>, or PhC $\equiv$ CPh, respectively. In these compounds, the metal-ligating groups are exactly as those of the complexes discussed above, but the "upper" pentagonal ring of the carbaborane cage is exopolyhedrally linked to the lower. This arises from elimination of MeOH between the *ortho*-CH<sub>2</sub>OMe group and a B—H vertex. Thus a second exopolyhedral B—C bond is formed between the cage and the *ortho*-substituted aryl group derived from the alkylidyne ligand present in the precursor. Such a process may well be promoted by steric crowding of the metal-bound ligands as discussed in relation to the species **20i** and **23b**. This would encourage a BCH<sub>2</sub>C<sub>6</sub>H<sub>4</sub>CH<sub>2</sub>OMe-2 group present in the likely intermediate to swing away from the metal center and into the vicinity of the B—H bond of B(9). It is interesting to note, however, that when a

<sup>3</sup> According to conventional numbering of the cage atoms, this boron is vertex number 8 in a 3,1,2-MC<sub>2</sub>B<sub>9</sub> icosahedron.

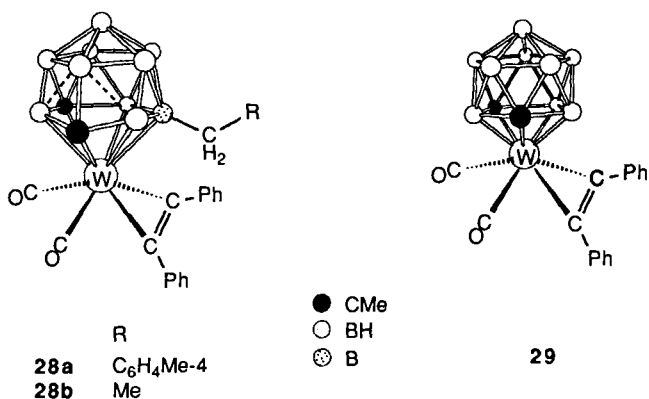
single molecule of the bulkier  $\text{PPh}_3$  ligand is present as in complex **23c**, the elimination step does not occur. This is apparently also due to conformational restraints imposed by the steric requirements of these large groups.

A natural extension of the above studies involved similar experiments with the 13-vertex cage system present in the salts **2**. Thus CO saturated solutions of **2a** or **2b** afford, upon treatment with  $\text{HBF}_4 \cdot \text{Et}_2\text{O}$ , mixtures of tetra-carbonyl tungsten complexes (**36**). The former reagent yields a mixture of **26a** and **27a**, while the latter affords **26b** and **27a**. Both of the species **26** mutate slowly into compound **27a** in dichloromethane solu-



tions by extrusion of their respective  $\text{BCH}_2\text{R}$  fragments. This process is an extremely novel degradation of the docosahedral cage system in which one boron vertex is expelled. The product contains the icosahedral core structure, which is fundamental in boron chemistry, with a 2,1,7- $\text{WC}_2\text{B}_9$  arrangement of atoms. The stability of this structural unit is apparently a sufficient driving force for these reactions to occur at room temperature. The precise nature of the extruded fragment, which is empirically  $\text{BCH}_2\text{R}$ , is unknown and currently under investigation. However, it is interesting to note that in the absence of carbon monoxide, treatment of **2a** or **2b** with  $\text{HBF}_4 \cdot \text{Et}_2\text{O}$  affords only **27a** (~40% yield) by scavenging of CO ligands from solution. The implications of this observation for the mechanism of cage degradation are presently unclear.

Similar behavior is observed when **2a** or **2b** are protonated in the presence of  $\text{PhC}\equiv\text{CPh}$ . In these circumstances, mixtures containing **28a** or **28b**, respectively, together with **29**, are obtained. The compounds **28** also decompose in solution with loss of  $\text{BCH}_2\text{R}$  groups to yield **29**. In addition to this novel degradation of the cage, it may be noted that the formulation of the diphenylacetylene complexes **28** or **29** contrasts with those of the species **20e** and **21**. In the last pair two alkyne molecules are coordinated to the metal, as opposed to one in each of the complexes **28** and **29**. However, this difference is found not to be a function of the stoichiometry of the



reaction mixtures concerned. Thus it is evident that although broadly similar in their effects on the metal vertex, the icosahedral and dicosahedral cage systems, of the salts **1** and **2**, confer tangibly different steric and electronic requirements on their respective metal centers. Interestingly, treatment of **27a** with  $\text{PhC}\equiv\text{CPh}$  leads directly to **29** by the displacement of two carbonyl ligands.

Contrasting with these results involving formation of  $\text{PhC}\equiv\text{CPh}$  complexes, are the protonations of **2a** or **2b**, containing CMe cage vertices, and those of **2d** or **2e**, with CH vertices, in the presence of  $\text{PPh}_3$ . These reactions yield the icosahedral complexes **27b** and **27c**, respectively, the 13-vertex intermediate species of structural type **26** evidently being too unstable for isolation. It is reasonable to suggest, on the basis of earlier discussion concerning the related species **23**, that this is an effect of the sterically demanding  $\text{PPh}_3$  groups, facilitating ejection of the  $\text{BCH}_2\text{R}$  fragment.

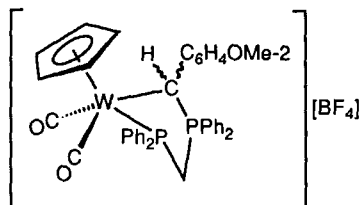
Products resulting from protonations of the 13-vertex metallacarborane carbyne salts **2** are thus characterized by initial retention of the dicosahedral structure bearing a  $\text{CH}_2\text{R}$  substituent, which subsequently loses this group along with the boron atom cage vertex to which it is attached. The relative stability of the 12-vertex over the 13-vertex cage is, however, significantly affected by the exopolyhedral groups (L) ligating the metal vertex.

### III

#### PROTONATIONS WITH $\text{HBF}_4 \cdot \text{Et}_2\text{O}$ IN THE PRESENCE OF BIDENTATE PHOSPHINES

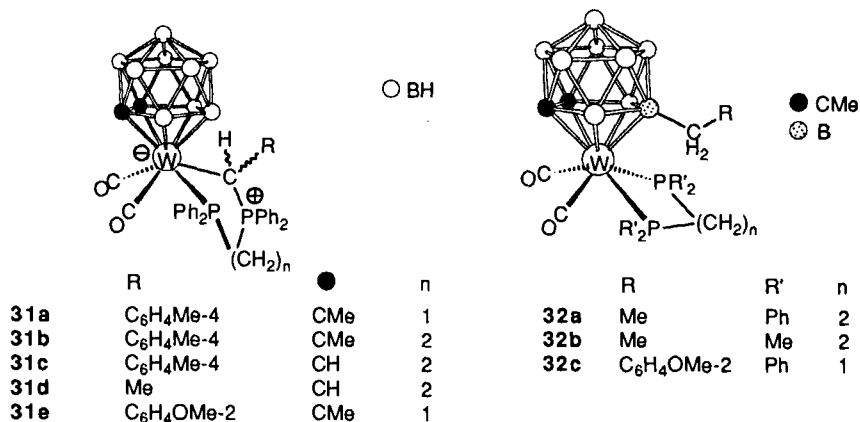
Given that the majority of the products from protonations described in the preceding section contain two Lewis base substrate molecules ligating the metal, it was of interest to study such reactions in the presence of

bidentate species. When treated with  $\text{HBF}_4 \cdot \text{Et}_2\text{O}$  in the presence of bis(diphenylphosphino)methane (dppm), the alkylidyne(cyclopentadienyl)metal complex **4e** yields the cationic ylid species in the salt  $[\text{W}(\text{CH}(\text{C}_6\text{H}_4\text{OMe}-2)_2\text{PPh}_2\text{CH}_2\text{PPh}_2)(\text{CO})_2(\eta\text{-C}_5\text{H}_5)]^+[\text{BF}_4]^-$  **30** (29). Complex **30** may be

**30**

viewed as a product in which the initially formed alkylidene ligand is trapped and thereby prevented from undergoing further transformation such as a second protonation followed by CO insertion, as discussed earlier in the context of formation of the complexes **13** and **17**. Evidently, this is due to the ability of dppm to bridge the  $\text{C}=\text{W}$  bond in the initially formed alkylidene species, thereby stabilizing it. Reactions between alkylidene-metal complexes and monodentate phosphines in which thermo-labile ylid structures are formed have long been known (37).

Similar protonation treatment of the alkylidyne(carbaborane) salts of type **1** yields two types of product, depending on the cage-carbon atom substituents, the particular phosphine, and the substituent on the alkylidyne-carbon atom. Hence the ylid zwitterion complexes **31** and the chelated species **32** are produced as follows (38). Protonation of **1a** with  $\text{HBF}_4 \cdot \text{Et}_2\text{O}$  in the presence of dppm yields [*closo*-1,2- $\text{Me}_2$ -3,3-(CO)<sub>2</sub>-3,3-{P(Ph)<sub>2</sub>CH<sub>2</sub>P(Ph)<sub>2</sub>C(H)(C<sub>6</sub>H<sub>4</sub>Me-4))-3,1,2-WC<sub>2</sub>B<sub>9</sub>H<sub>9</sub>}] **31a**, while simi-

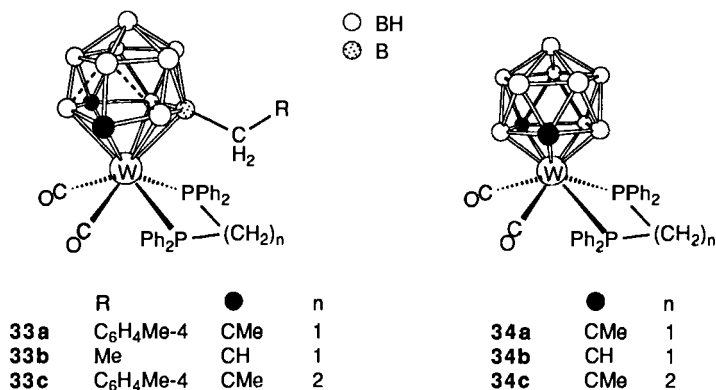


lar treatment of **1a**, **1i**, or **1j** in the presence of dppe (bis(diphenylphosphino)ethane) gives **31b**, **31c**, or **31d**, respectively. A single-crystal X-ray diffraction study of **31a** showed the tungsten atom fusing a 12-vertex  $WC_2B_9$  icosahedron with a five-membered WCPCP ring. In accord with the expected geometries of each, the latter is bent away from the former [ $W-C-P$ ,  $109.5(4)^\circ$ ,  $W-P-C$ ,  $105.4(3)^\circ$ ].

By contrast, protonation of **1b** in the presence of dppe or dmpe (bisdimethylphosphinoethane) gives only the chelate complexes [*closo*-1,2- $Me_2$ -8-Et-3,3-(CO) $_2$ -3,3-( $PR'_2(CH_2)_2PR'_2$ )-3,1,2- $WC_2B_9H_8$ ] **32a** or **32b**, respectively. In these compounds the metallacarborane cage displays its more familiar involvement in the protonation reactivity of the reagents **1**, by adopting the  $CH_2R$  substituent discussed earlier. The coordination sphere of the metal vertex is thus open to chelation by the bis-phosphine ligands.

It appears from these results that formation of ylid structures is favored starting from those reagents **1** containing  $W\equiv CC_6H_4Me$ -4 groups. However, whether CH or CMe fragments are present in the  $C_2B_9$  cages also influences the nature of the product. Thus, formation of the ylid complex **31d** versus the chelated molecule **32a** reflects an apparent activation of the B(8)—H bond by methyl substitution of the cage-carbon vertices. Interestingly, treatment of **1f** with dppm and  $HBF_4 \cdot Et_2O$  yielded a separable mixture of the ylid complex **31e** and the chelated species **32c**, in which the former was found to be by far the major component (**32**).

Preliminary results (**36**) of related protonation reactions employing the  $C_2B_{10}$  alkylidyne(carbaborane)metal salts **2** have yielded only chelated species. These are formed as chromatographically separable mixtures of the compounds **33**, containing docosahedral cages bearing  $CH_2R$  substituents, and the species **34**, featuring the icosahedral cage with a 2,1,7- $WC_2B_9$  arrangement of atoms. In solution, the former all collapse to give the latter,





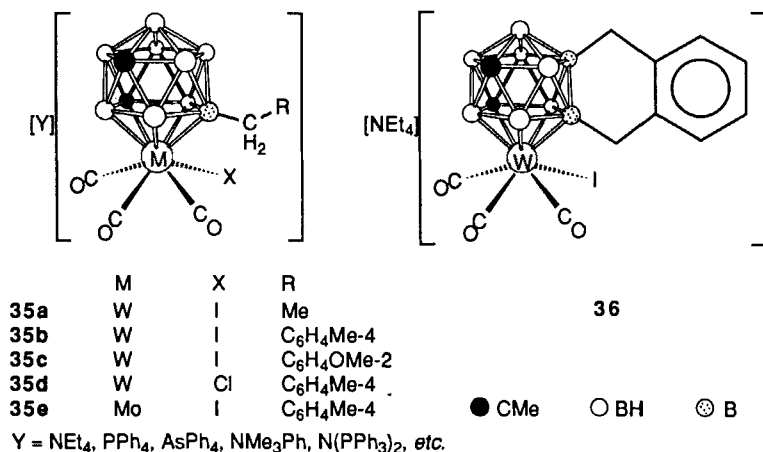
with formal loss of  $\text{BCH}_2\text{R}$ , in a manner similar to that of the species **26** and **28** described in the preceding section.

#### IV

#### PROTONATIONS WITH $\text{HX}$ ( $\text{X} = \text{Cl}$ or $\text{I}$ )

Treatment of the alkylidyne(cyclopentadienyl)metal species **4** with haloacids ( $\text{HX}$ ;  $\text{X} = \text{Cl}$ ,  $\text{Br}$ ,  $\text{I}$ ) has been described in Section I. The carbene- or acyl-ligated metal complexes so formed are stabilized by coordination to the metal of the halide ion intrinsically involved in the protonation reaction, thus highlighting the important difference between employing  $\text{HX}$  and  $\text{HBF}_4 \cdot \text{Et}_2\text{O}$  in the protonations.

This difference in behavior is even more pronounced when the metalla-carbaborane salts **1** are protonated with  $\text{HX}$  acids, as once again the polyhedral cage becomes intimately involved in the reactivity. Thus, treatment of dichloromethane solutions of **1b**, **1a**, or **1f** with aqueous  $\text{HI}$  yields, within seconds, the salts  $[\text{Y}][\text{closo-1,8-Me}_2\text{-11-(CH}_2\text{R)-2-I-2,2,2-(CO)}_3\text{-2,1,8-WC}_2\text{B}_9\text{H}_9]$  ( $\text{R} = \text{Me}$ , **35a**;  $\text{C}_6\text{H}_4\text{Me-4}$ , **35b**;  $\text{C}_6\text{H}_4\text{OMe-2}$ , **35c**) (32,39). The salt **35d** was likewise prepared from **1a** and aqueous (or dry



gaseous)  $\text{HCl}$  (Fig. 1). Complex **36** resulted from similar treatment of **1g** with  $\text{HI}$ , and shows the exopolyhedral aryl substituent seen in earlier protonation reactions of this salt (**35**), but is otherwise analogous to the species **35**. In all of these products an icosahedral  $\text{WC}_2\text{B}_9$  cage bears one halide and three carbonyl ligands on the metal vertex and a  $\text{CH}_2\text{R}$  substituent on an adjacent boron vertex, as in the  $\text{HBF}_4 \cdot \text{Et}_2\text{O}$  reactions described

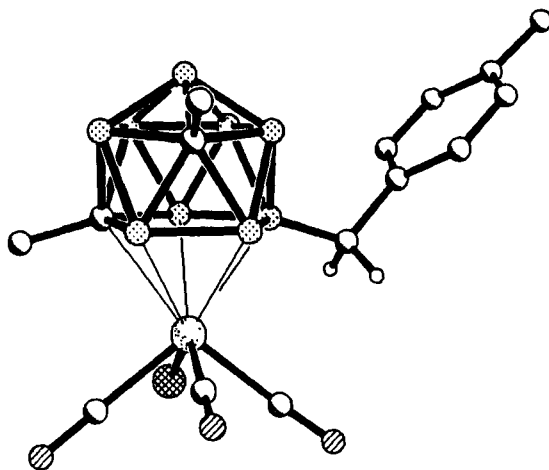
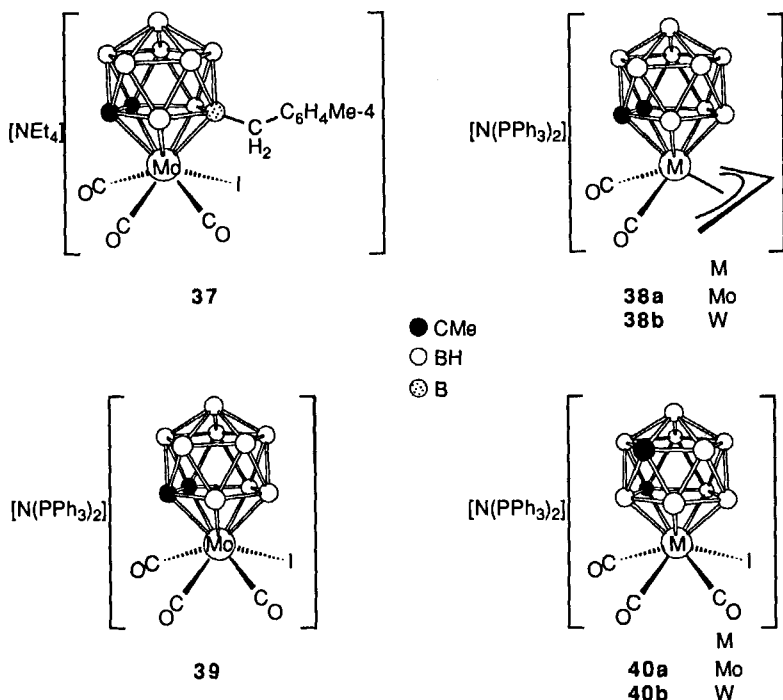


FIG. 1. Structure of the anion of salt 35d.

earlier. However, the most striking feature of the anions of **35** and **36** is that the carbon-atom vertices of the icosahedron are no longer adjacent, so that there is now only one metal-carbon connectivity. Thus the metallacarborane species have undergone a remarkably facile polytopal rearrangement to give a 2,1,8-WC<sub>2</sub>B<sub>9</sub> core structure, rather than the 3,1,2-WC<sub>2</sub>B<sub>9</sub> cage system existing in the precursors and found in the products of the HBF<sub>4</sub>·Et<sub>2</sub>O reactions. This rearrangement may be regarded as a 120° rotation of one C—B—B triangular face of the WC<sub>2</sub>B<sub>9</sub> cage (**40**).

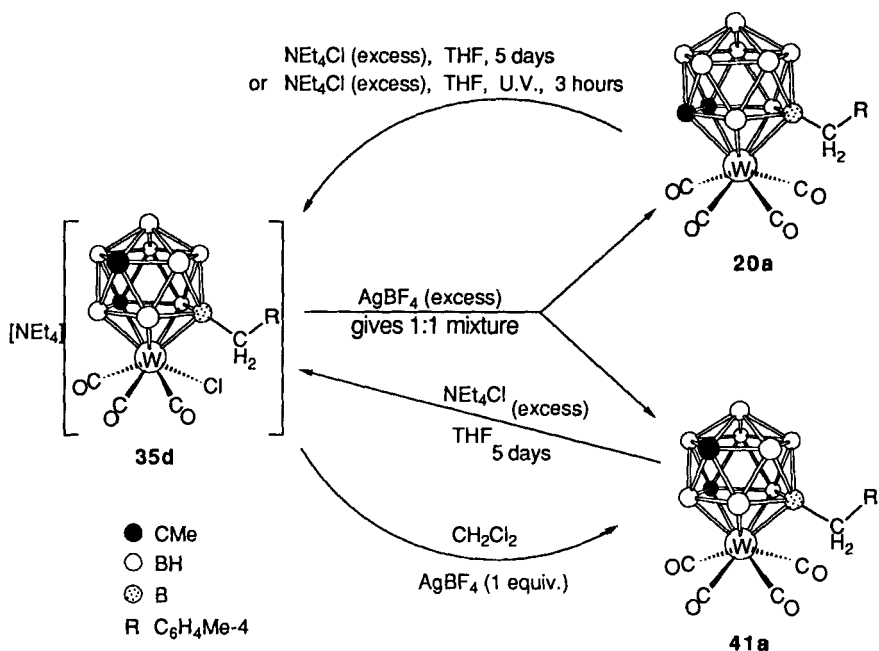
To test the ease with which this process may occur, a dichloromethane solution of **1a** was cooled to −78°C prior to treatment with HI. Under these conditions, complex **35b** was again formed, the reaction being complete within 10 min (**39**). Although polytopal isomerizations of metallacarborane cages are common, appreciably higher temperatures are generally required. Nevertheless, a handful of such rearrangements have previously been reported at temperatures as low as 0°C (**41**). However, **35b** is formed at a temperature significantly lower than any previously reported for the rearrangement of a carbametallaborane polyhedron.

Interestingly, treatment of the molybdenum-alkylidyne salt **1m** (Y = NEt<sub>4</sub>) with HI allows the discrete observation of both the protonation and the rearrangement processes. The first-formed product is [NEt<sub>4</sub>][*closo*-1,2-Me<sub>2</sub>-8-(CH<sub>2</sub>C<sub>6</sub>H<sub>4</sub>Me-4)-3-I-3,3,3-(CO)<sub>3</sub>-3,1,2-MoC<sub>2</sub>B<sub>9</sub>H<sub>8</sub>] **37**, which exhibits via its NMR spectra a plane of symmetry and retains the cage topology of its precursor. However, within 18 hr, solutions of **37** isomerize quantitatively into **35e** at ambient temperatures (**42**). This type of behavior is also observed when the allyl-molybdenum complex **38a** is treated with HI in the presence of carbon monoxide. Propene is liberated and the metal



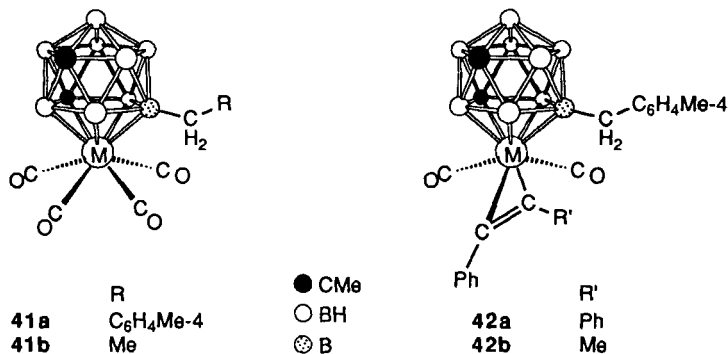
coordination sphere completed by the iodide ion, and a molecule of CO, yielding  $[N(PPh_3)_2][closo-1,2-Me_2-3-I-3,3,3-(CO)_3-3,1,2-MoC_2B_9H_9]$  **39** as the product (42). The cage topology is unchanged, making the anions of the salts **37** and **39** identical but for the absence in the latter of a  $CH_2C_6H_4Me-4$  substituent. However, complex **39** also isomerizes if stirred in solution for several days, to produce  $[N(PPh_3)_2][closo-1,8-Me_2-2-I-2,2,2-(CO)_3-2,1,8-MoC_2B_9H_9]$  **40a**. When similarly protonated, the allyl-tungsten complex **38b** rapidly yields the salt **40b**, containing the rearranged 2,1,8- $WC_2B_9$  cage, as the only isolable product. Why the cage rearrangement in both systems is so much slower for the molybdenum species than for the tungsten is unknown.

The divorce of the rearrangement process from the protonation step is further emphasized by the reaction of the tetracarbonyl complex **20a** with  $NEt_4Cl$ . This reaction affords **35d** ( $Y = NEt_4$ ) in high yield, either by stirring in THF at ambient temperature for 5 days or by ultraviolet irradiation of solutions for  $\sim 3$  hr (Scheme 6). Remarkably, the process is partially reversible (39). Treatment of a CO-saturated solution of **35d** with an excess of  $AgBF_4$  affords a 1 : 1 mixture of the polytopal isomers  $[closo-1,2-Me_2-8-(CH_2C_6H_4Me-4)-3,3,3,3-(CO)_4-3,1,2-WC_2B_9H_8]$  **20a** and  $[closo-1,8-Me_2-$



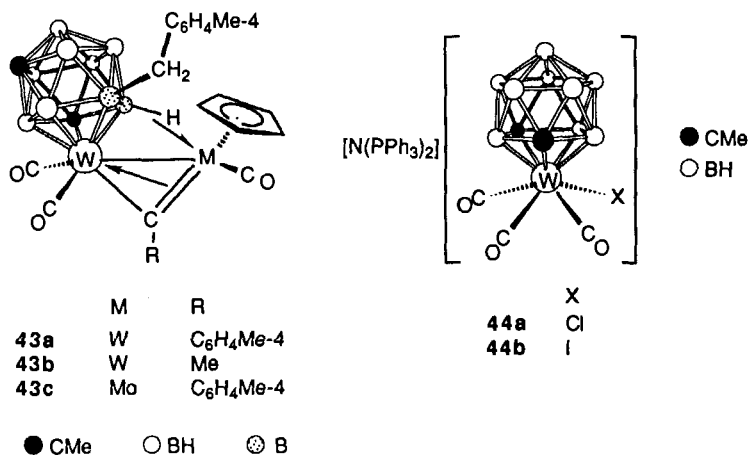
SCHEME 6.

11-( $\text{CH}_2\text{C}_6\text{H}_4\text{Me-4}$ )-2,2,2,2-(CO) $_4$ -2,1,8-WC $_2$ B $_9$ H $_8$ ] **41a**. Similar treatment of **35a**, bearing the Et substituent, yields a mixture of **20b** and **41b**. However, if only 1 mol eq. of AgBF $_4$  is used in each case, the complexes **41**, having the 2,1,8-WC $_2$ B $_9$  cage, are the only isomers obtained. It is interesting to note that treatment of the tetracarbonyl species **41a** with NEt $_4$ Cl simply yielded **35d** and did not lead to a product in which a second polytopal rearrangement had occurred. These reactions are also summarized in Scheme 6.



The synthetic utility of the salts **35** is further demonstrated by treatment of **35b** with the alkynes  $\text{PhC}\equiv\text{CR}'$  ( $\text{R}' = \text{Ph}$  or  $\text{Me}$ ), followed by addition of  $\text{AgBF}_4$ . These reactions afford the complexes  $[\text{closo-1,8-Me}_2\text{-11-(CH}_2\text{C}_6\text{H}_4\text{Me-4)-2-(}\eta\text{-PhC}_2\text{R')-2,2-(CO)}_2\text{-2,1,8-WC}_2\text{B}_9\text{H}_8]$  ( $\text{R}' = \text{Ph}$ , **42a**;  $\text{Me}$ , **42b**), respectively, by abstraction of the halide and coordination of the alkyne to the metal vertex of the polyhedron (**39**). This vertex also loses a molecule of  $\text{CO}$  leaving the alkyne to act as a 4e donor to the metal, but the icosahedron is otherwise unaltered. This synthesis may also be used to generate dimetal species, by substitution of the alkyne molecule with an alkylidyne-metal complex in the reaction (**43**). Thus the products obtained by treating **35b** ( $\text{Y} = \text{NMe}_3\text{Ph}$  or  $\text{AsPh}_4$ ) with **4a**, **4b**, or **4i**, respectively, followed by addition of  $\text{AgBF}_4$  or  $\text{TIBF}_4$ , are the electronically unsaturated dimetal compounds **43**.

By now the reader is aware that protonation reactions of the docosahe-dral (13-vertex) salts **2** and the icosahedral (12-vertex) complexes **1** follow broadly similar routes with respect to the metal vertex, but frequently differ in the form of the polyhedra found in the products. Protonations of the reagents **2** with  $\text{HX}$  are no exception. Thus treatment of **2a** [ $\text{Y} = \text{N}(\text{PPh}_3)_2$ ] with  $\text{HX}$  ( $\text{X} = \text{Cl}$ ,  $\text{I}$ ) afforded  $[\text{N}(\text{PPh}_3)_2][\text{closo-1,7-Me}_2\text{-2-X-2,2,2-(CO)}_3\text{-2,1,7-WC}_2\text{B}_9\text{H}_9]$  **44a** and **44b**, respectively, after stirring



overnight at room temperature (**39**). This reaction is considerably slower than corresponding reactions of the salts **1**. The products **44** contain an icosahedral carbaborane cage with the 2,1,7-WC<sub>2</sub>B<sub>9</sub> arrangement of the core atoms observed earlier in the products **27** from protonations of the salts **2** with  $\text{HBF}_4 \cdot \text{Et}_2\text{O}$ . The metal vertex of this cage bears the halide and three carbonyl ligands just as observed in the species **35**. Complex **44b** is

therefore an isomer of complex **40b**, which has a 2,1,8- $WC_2B_9$  cage topology. The former is generated by degradation of a dicosahedral cage and loss of an alkylidene ligand, formed by protonation of an alkylidyne group. The latter is produced by rearrangement of an icosahedral cage after loss of a propene ligand, formed by protonation of an allyl group.

Thus the effect of haloacids and  $HBF_4 \cdot Et_2O$  on the 13-vertex framework is identical, a feature distinguishing the behavior of salts **1** from salts **2**. This is ratified by the observation that treatment of **44b** with  $TiBF_4$ , as a halide abstracting agent, in the presence of excess  $PPh_3$  yields **27b** as the only product (36). This product was originally obtained directly by protonation of **2a** with  $HBF_4 \cdot Et_2O$ , in the presence of  $PPh_3$ .

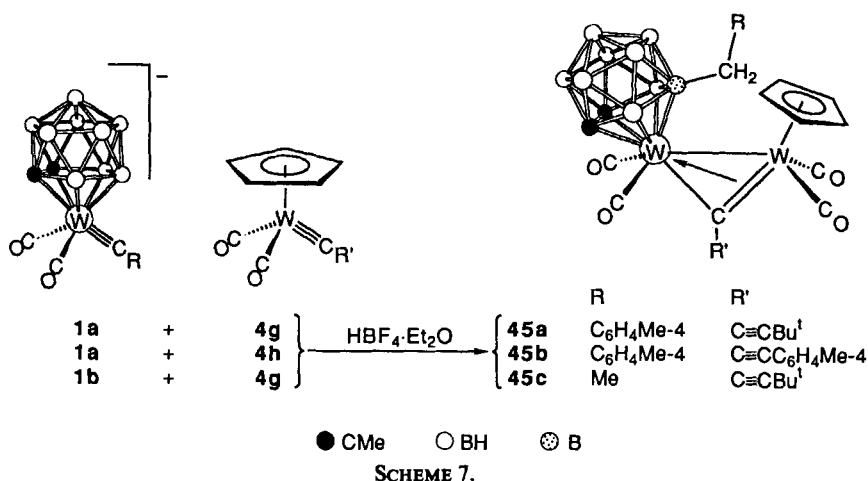
## V

### FORMATION OF DIMETAL COMPOUNDS

By employing protonation reactions, it is possible to use the compounds **1** or **2** as precursors to a variety of dimetal complexes with unusual structures. Two different methodologies are available. In method **A**, mixtures containing one or other of the reagents **1** or **2** together with one of the neutral alkylidyne(cyclopentadienyl)metal complexes **4** are protonated. Because protonation of the salts **1** or **2** generates an electronically and coordinatively unsaturated alkylidene-metal species, the latter can bind a molecule of type **4** to generate a metal-metal bond. This process is formally similar to the protonation of the salts **1** or **2** in the presence of alkynes, described in Section II, since the latter are isolobal with the compounds **4**. Method **B** depends on the fact that if one of the salts **1** or **2** is treated with half a molar equivalent of acid, the electronically and coordinatively unsaturated alkylidene-metal species so formed is present in a mixture with unreacted salt, the anion of which contains an  $M \equiv C$  group able to complex with the alkylidene-metal intermediate. This also generates a metal-metal bond, but the product is now a salt.

#### *A. Protonation of Mixtures Containing Two Distinct Alkylidyne-Metal Complexes*

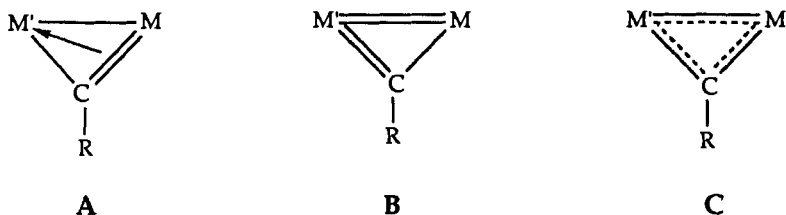
Several types of dimetal product have been obtained by this method. Thus, treatment of equimolar mixtures of the (alkynyl-alkylidyne)metal complexes **4g** or **4h** and the alkylidyne(carbaborane)metal salts **1a** or **1b**, with  $HBF_4 \cdot Et_2O$  in the combinations shown in Scheme 7, yields the compounds **45** (44). In these products, the icosahedral cage from the precursors **1** adopts the form familiar from protonation reactions described



SCHEME 7.

earlier. Thus, atom B(8) bears a  $CH_2R$  substituent while the tungsten vertex retains its ligated carbonyl ligands. The coordination sphere of the metal is completed by a molecule of the neutral species **4**, bound in a manner analogous to that of a 4e-donor acetylene molecule. The isolobal mapping of [*closo*-1,7-Me<sub>2</sub>-2-( $\eta$ -PhC<sub>2</sub>Ph)-2,2-(CO)<sub>2</sub>-2,1,7-WC<sub>2</sub>B<sub>9</sub>H<sub>9</sub>] **29** with the species **45** is thus apparent. It should be noted, however, that the cage in the former does not have a  $CH_2R$  substituent and that the cage in the latter has a 3,1,2- rather than a 2,1,7-WC<sub>2</sub>B<sub>9</sub> core structure.

Dimetal complexes in which an  $RC\equiv ML_n$  moiety formally acts as a four-electron donor to a metal (M') as in the products **45** are electronically unsaturated species with a cluster-valence-electron (c.v.e.) count of 32. The three-membered rings may be depicted in a number of ways, the most relevant of which are shown below.



Representation A most clearly indicates the origin of the bridging alkyldi-nyne ligand, while the schematic B may be considered a more faithful indication of the observed bond lengths in certain X-ray structures (**45**). The fully delocalized structure C may be preferred in cases where the

alkylidyne ligand is known to bridge the metal-metal bond symmetrically (46). The best description of a given compound is often found only by detailed analysis of the structural parameters obtained from an X-ray diffraction study, or of *ab initio* molecular orbital calculations. The 32 c.v.e. dimetal complexes presented in this chapter are represented by the structure A, the intention being to emphasize the origins of the fragments forming the products and the isolobal relationship of the  $C\equiv M$  groups in the precursors with 4e donor alkynes, rather than to make a precise structural statement.

When a THF solution of **45a** is heated at reflux temperature for 2 hr, carbon monoxide is liberated and complex **46a**, with a three-center-two-electron ( $3c-2e$ ) B-H $\rightarrow$ W bridge bond, is formed, thereby maintaining the valence electron count at the metal center bearing the cyclopentadienyl group (44). Complex **46a** is thus the thermodynamic product of protonating a mixture of **1a** and **4g** with  $HBF_4 \cdot Et_2O$ .

Compound **46a** is structurally related to complexes **46b**–**46e** (Fig. 2), which are obtained directly by protonating the combinations of reagents indicated in Scheme 8. In these syntheses (43,47), intermediates analogous to the tetracarbonyl dimetal complexes **45** are clearly implicated, but none were detected. However, complex **46e** reacts with  $PMe_3$  to yield a product  $[W_2(\mu-CMe)(CO)_3(PMe_3)(\eta^5-7,8-C_2B_9H_8-10-Et-7,8-Me_2)(\eta-C_5H_5)]$  in

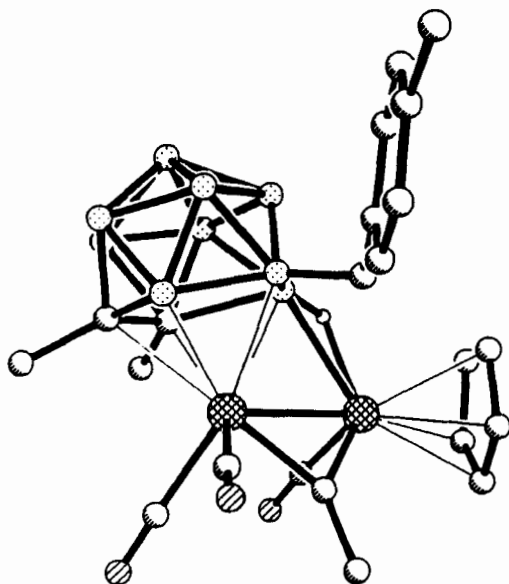
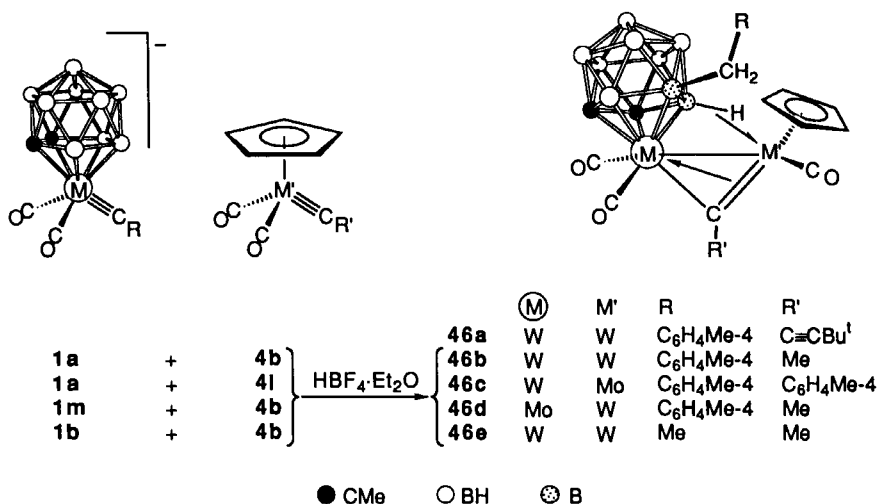


FIG. 2. Molecular structure of complex **46b**.

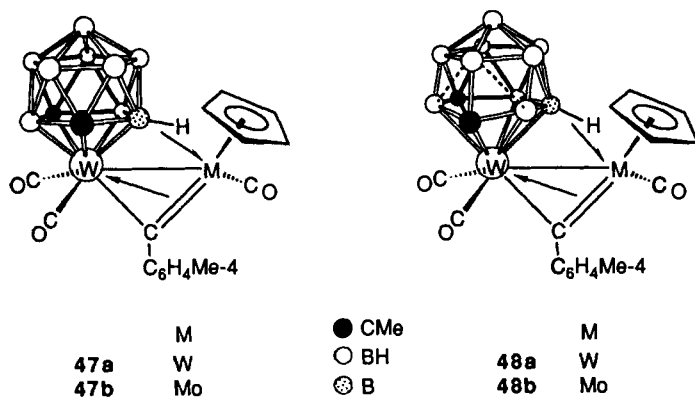




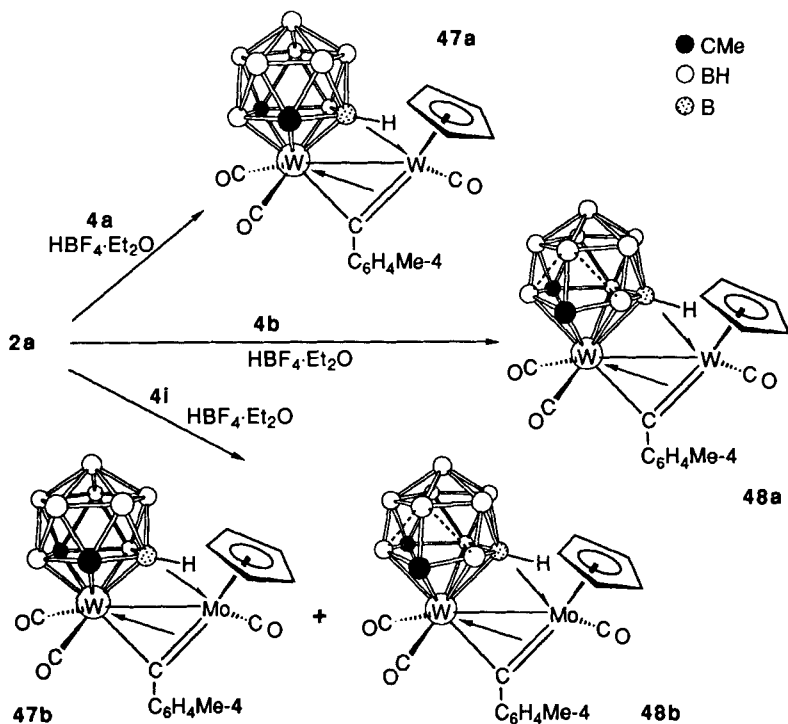
SCHEME 8.

which the B-H→W interaction has been lifted (43), and hence this PMe<sub>3</sub> complex is structurally akin to the species 45. Furthermore, a sizeable family of 32-c.v.e. dimetal complexes related to the compounds 46 have now been characterized. These complexes have resulted from treatment of the salts 1a, 1l, or 1m with ML<sub>n</sub> fragments such as [M(CO)<sub>2</sub>(NCMe)<sub>2</sub>(η<sup>5</sup>-C<sub>9</sub>H<sub>7</sub>)] [BF<sub>4</sub>] (M = Mo or W; C<sub>9</sub>H<sub>7</sub> = indenyl) or [Mo(CO)<sub>2</sub>(NCMe)(η<sup>7</sup>-C<sub>7</sub>H<sub>7</sub>)] [BF<sub>4</sub>] (46, 48). However, despite the probable existence of an intermediate containing all four carbonyl ligands in every case, no such compound has been detected, implying that the replacement of a CO ligand by a B-H→M bridge is highly favorable. It therefore appears that the alkynyl-alkylidyne group is perhaps responsible for stabilizing the intermediate species 45.

When similar protonation studies were conducted using mixtures of the 13-vertex salts 2 and the neutral alkylidyne(cyclopentadienyl)metal complexes 4, subtly different species were produced. Thus, two types of compound were identified, differing in both the topology and geometry of the cage structures, as exemplified by compounds 47 and 48 (47). The combinations of reagents leading to these products, which contain, respectively, an icosahedral cage and a framework based on a docosahedron, are detailed in Scheme 9. This shows that the type of product isolated is dependent on the nature of the cyclopentadienyl(alkylidyne)metal reagent used. Thus protonation of an equimolar mixture of the tungsten compounds 2a and 4a affords 47a as the only product, whereas when the cyclopentadienyl-molybdenum complex 4i is employed with 2a, a mix-



ture of the two product classes results. On the other hand, mixtures of **2a** and **4b**, which bears the  $\equiv\text{CMe}$  group, yield only complex **48a** upon protonation (**47**). The overall form of the dimetal species **47** and **48** is related to the species **46**, however, unlike the latter compound, no  $\text{CH}_2\text{R}$

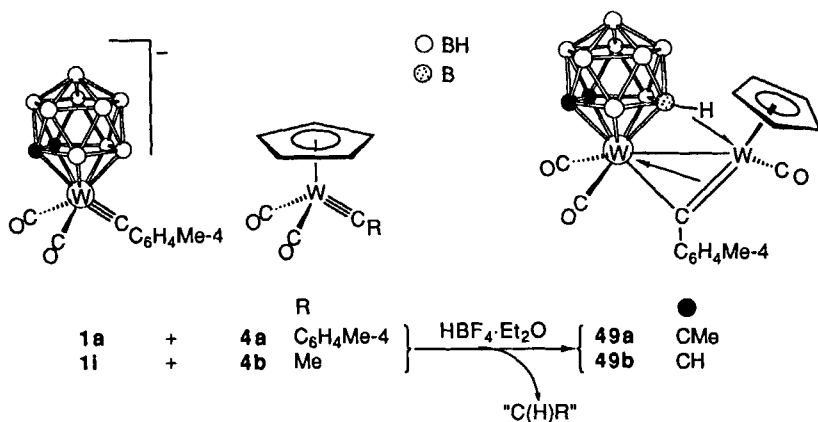


SCHEME 9.

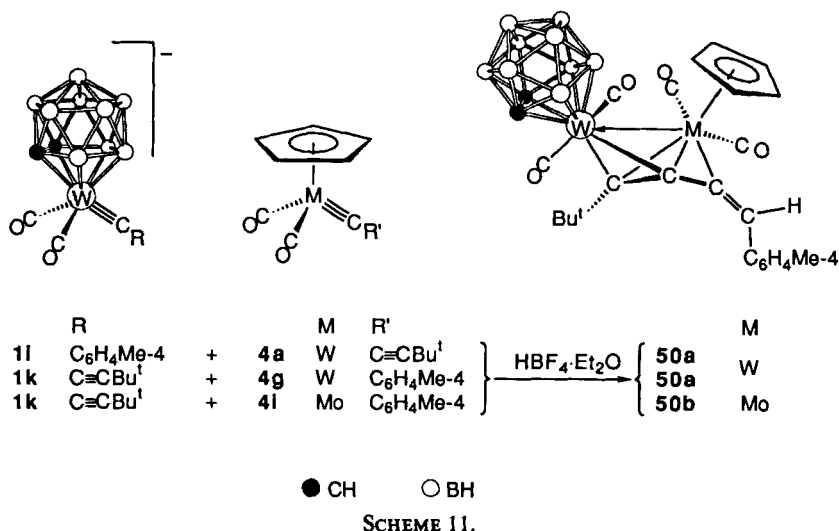
boron-cage substituent is observed in the products from **2a**. The compounds **47** are formed by ejection of a boron vertex along with an alkylidyne fragment, in a manner familiar from earlier sections. The resulting 12-vertex cage having the 2,1,7- $\text{MC}_2\text{B}_9$  topology is thus identical to that of the species **29** or **44**. On the other hand, formation of the species **48** involves the loss only of the alkylidene fragment. This is an unusual feature of the protonations of these particular combinations of reagents, as the less stable 13-vertex cage structure is retained in the products **48**.

Two particular combinations of reagents starting from the icosahedral salts **1a** or **1i** yielded the closely related yet unexpected products **49**, shown in Scheme 10 (**47,49**). These are structurally similar to the compounds **47** in every respect, except that they exhibit a 3,1,2- $\text{WC}_2\text{B}_9$  arrangement of atoms in the cage. This also implies loss of the alkylidene fragment  $\text{C(H)R}$  at some stage in the reaction profile. Indeed compounds **47a** and **49a** are polytopal isomers, the former having a 2,1,7- $\text{WC}_2\text{B}_9$  cage structure and the latter a 3,1,2- $\text{WC}_2\text{B}_9$  arrangement. Interestingly, the thermodynamically favorable isomer **47a**, in which the carbon atoms are separated, is formed quantitatively upon heating a toluene solution of **49a** at  $\sim 80^\circ\text{C}$  for 3 hr (**47**).

The reasons for these variations in reactivity patterns are presently unclear; however, unpredictable and subtle differences in reactivity are a feature of the compounds **46–49** and analogs reported elsewhere. This is perhaps not surprising as they constitute an assembly of reactive ligands around an unsaturated dimetalla–cyclopropene core, each group exerting its own specific electronic and steric influence. This has previously been observed to result in coupling of a variety of ligands with the bridging



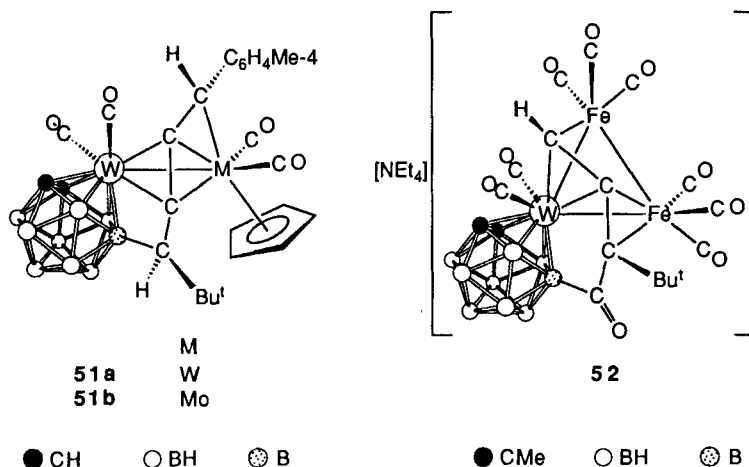
SCHEME 10.



alkylidyne group and/or the carbaborane cage, leading to B—C and/or C—C bond-forming reactions (1). Such coupling may be proton-mediated, as when the alkylidyne-metal complex mixtures shown in Scheme 11 are treated with  $HB F_4 \cdot Et_2O$  (50).

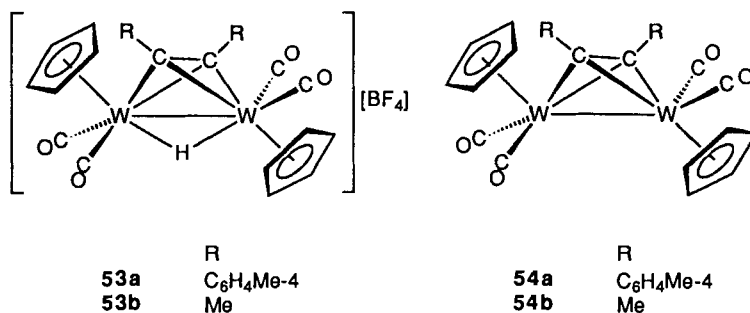
The products **50** are noteworthy in several respects. They are apparently formed by the union of alkylidyne and alkylidene ligands. Moreover, compound **50a** is the product no matter which combination of precursors (**1i** and **4a**, or **1k** and **4g**) is used. Thus the acid-derived proton reaches its preferred site on the tolyl-bearing carbon atom. A probable pathway is shown in Scheme 12, in which the first step involves protonation of the alkylidyne(carbaborane)metal complexes **1i** or **1k**, to yield the alkylidene intermediates **A** or **A'**, respectively. Addition of the  $C\equiv W$  groups of the neutral molecules **4g** or **4a**, followed by metal-metal and C—C bond formation would give the  $\mu$ -vinyl intermediates **B** and **B'**. The reversible isomerizations of **B** into **D** and of **B'** into **D'** involve the pivoting of these  $\mu$ -vinyl groups at dimetal centers, which is a well-established process, facilitated in 32 valence electron dimetal species of this type (51). However, any of these  $\mu$ -vinyl species may be converted to any other via the  $\mu$ -hydrido( $\mu$ -alkyne)ditungsten intermediate **C**. Such a process has been observed previously in the facile interconversion of  $\mu-C(H)=C(H)C_6H_4Me-4$  into  $\mu-C(C_6H_4Me-4)=CH_2$  groups at W—Fe dimetal centers (52). Moreover, in symmetric systems, complexes analogous to intermediate **C** are the stable products of related protonation reactions (25). These will be detailed in the following subsection. The



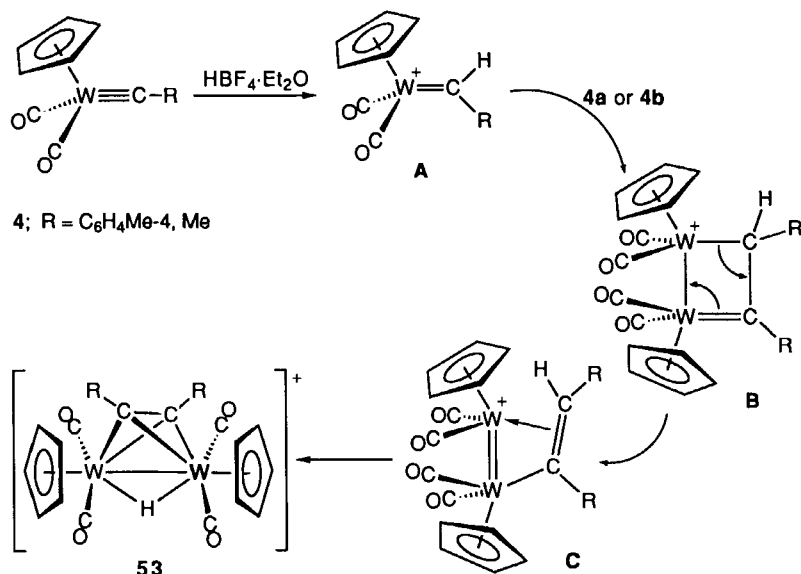


### B. Protonations Involving 0.5 Mol Eq. of $\text{HBF}_4 \cdot \text{Et}_2\text{O}$

Dimetal complexes may equally well be obtained from the reagents **1**, **2**, or **4** alone, by treatment with 0.5 mol eq. of acid, as mentioned in the introduction to this section. With this stoichiometry, a mixture is effectively created upon protonation, containing alkylidyne- and alkylidene-metal species in equal proportions. The validity of this methodology was first demonstrated in 1985 during protonation studies of the reagents **4a** and **4b** (25). In practice, it was found that 0.4 mol eq. of  $\text{HBF}_4 \cdot \text{Et}_2\text{O}$  produced the best results by ensuring that the alkylidyne-metal species remained in excess. Thus, from **4a** and **4b**, the ditungsten complexes **53**



were isolated and identified by their characteristic NMR signals, most notably high field signals in their  $^1\text{H}$  spectra. Hence the bridging proton resonates at  $\delta - 17.00$  (**53a**) or  $\delta - 18.50$  (**53b**), with a pattern of  $^{183}\text{W}$  satellites (0.04:1:6:1:0.04) indicating coupling to 2 equivalent tungsten

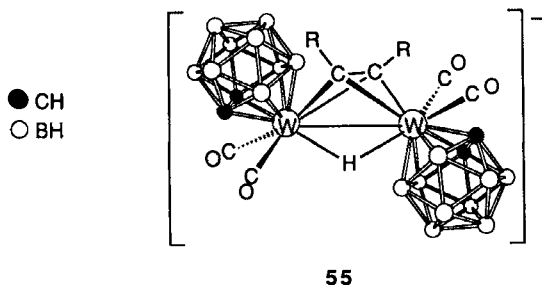


SCHEME 13.

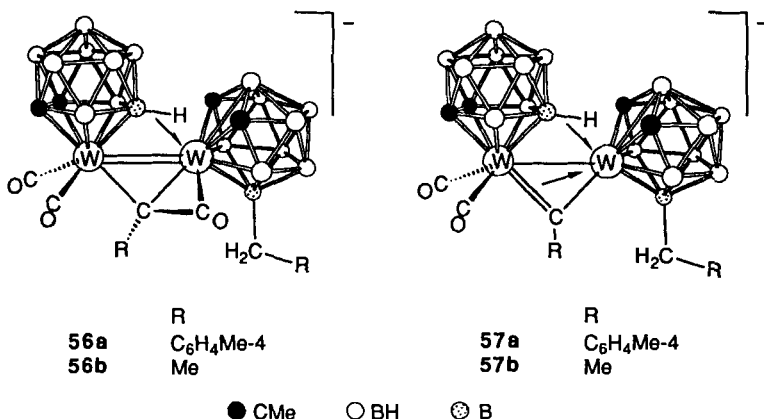
centers. Deprotonations with PMe<sub>3</sub> or K[BH(CHMeEt)<sub>3</sub>] yield the neutral alkyne-bridged species **54**, a process reversible by treatment with HBF<sub>4</sub>·Et<sub>2</sub>O.

The proposed mechanism for formation of the ditungsten species **53** involves the coupling of an alkyldiene-metal intermediate formed by protonation, with unreacted alkyldiene-ligated starting material (Scheme 13). Thus W-W and C-C bonds are formed, and the observed product results from intramolecular transfer of the proton into a metal-metal bond-bridging position. The reagent **1i** containing the WC<sub>2</sub>B<sub>9</sub>H<sub>11</sub> cage follows a similar pathway leading to the anionic species **55** upon treatment with 0.5 equivalent of HBF<sub>4</sub>·Et<sub>2</sub>O (**54**).

Contrasting with these results are protonation studies of the WC<sub>2</sub>B<sub>9</sub>H<sub>9</sub>Me<sub>2</sub> cage systems of **1a** and **1b** or the MC<sub>2</sub>B<sub>10</sub> polyhedra of the



salts **2**, using 0.4 mol eq. of  $\text{HBF}_4 \cdot \text{Et}_2\text{O}$ . Although dimetal species are again formed as expected, interactions of the metallacarborane cages with the rest of the cluster are not limited to the metals alone. Thus, treatment of **1a** or **1b** with 0.4 mol eq. of  $\text{HBF}_4 \cdot \text{Et}_2\text{O}$  affords the  $\mu\text{-}\sigma, \eta^2$  ketenyl species **56a** and **56b**, respectively (55). In both cages in each



product the  $\beta$ -boron atom [B(8)] exhibits “noninnocent” behavior, being involved either in a  $\text{B}-\text{H}\rightarrow\text{M}$  interaction or  $\text{BCH}_2\text{R}$  group formation. Furthermore, the polyhedron bearing the latter group exhibits pronounced distortion arising from a formal deficiency of one electron pair. This is thus recognized as a *hyper-closo* cage structure, with no connectivity between the two carbon vertices.<sup>4</sup> The two metallacarborane cluster fragments are linked by the aforementioned  $\text{B}-\text{H}\rightarrow\text{M}$  interaction and by a formal double bond between the metal vertices. This bond is supported by the bridging  $\text{C(R)C(O)}$  ketenyl group. However, after solutions of these salts are heated, CO is expelled from the ketenyl ligand to form the  $\mu$ -alkylidyne bridged compounds **57** (Fig. 3).

Protonations of the dicosahedral salts **2** in the mole ratio 2:1 (carbyne:acid) yield the products **58** (36), which are similar but not directly analogous to the complexes **56**. Thus the X-ray-determined structure of the

<sup>4</sup> The term *hyper-closo* (56) has been invoked to describe polyhedral structures with  $n$  vertices but having fewer than the  $n + 1$  skeletal electron pairs demanded by skeletal electron pair theory. For a 12-vertex icosahedral structure the availability of 12 rather than 13 electron pairs causes a distortion of the cage, as observed for the compounds **56**. The tungsten vertex associated with the  $\text{C}_2\text{B}_9\text{H}_8(\text{CH}_2\text{C}_6\text{H}_4\text{Me-4})\text{Me}_2$  cage and its associated ligand set would contribute three orbitals and zero electrons for cluster bonding [ $\text{W(0)} d^6$ ]. An alternative view (57) is to define such structures as *iso-closo*, suggesting that the electron deficiency in the core is relieved by donation of an additional electron pair from the metal valence shell [ $\text{W(II)} d^4$ ], with the metal employing four orbitals rather than three for cluster bonding. However, theoretical treatment has favored the *hyper-closo* interpretation (58).



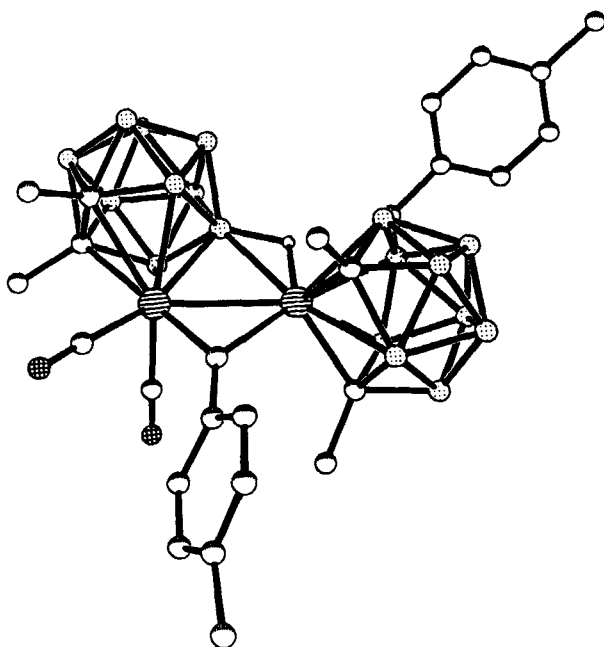
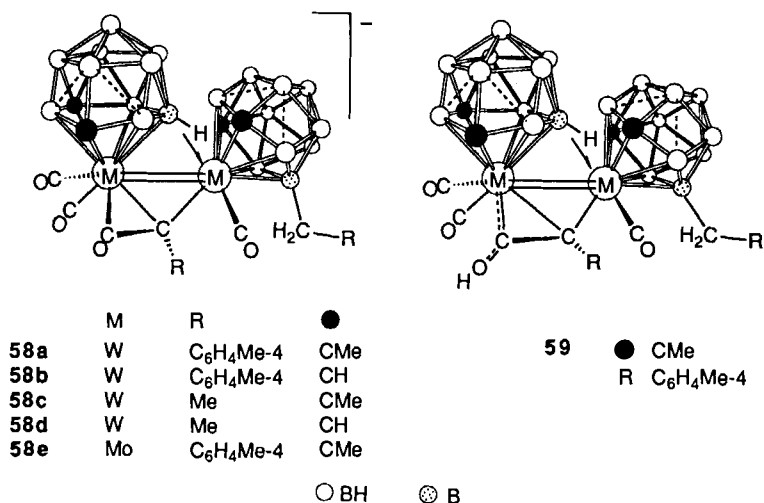


FIG. 3. Structure of the anion of salt 57a.

anion of 58c (Fig. 4) shows two 13-vertex metallacarborane cages linked both by a metal-metal double bond and by a B-H $\rightarrow$ M 3c-2e interaction. The second cage again bears a BCH<sub>2</sub>R fragment, while the metal-metal bond is spanned by the  $\mu$ - $\sigma$ , $\eta^2$  ketenyl ligand. However, the already



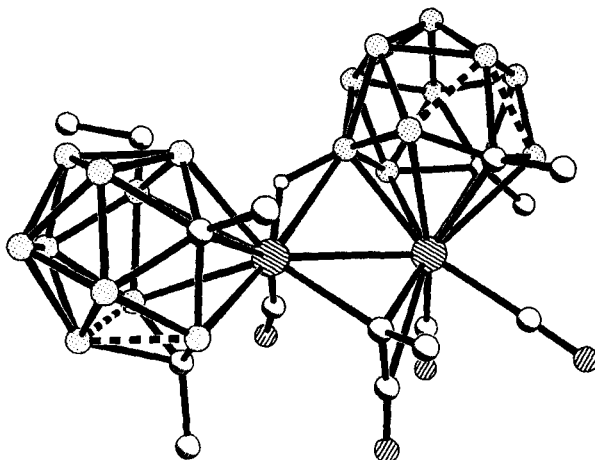
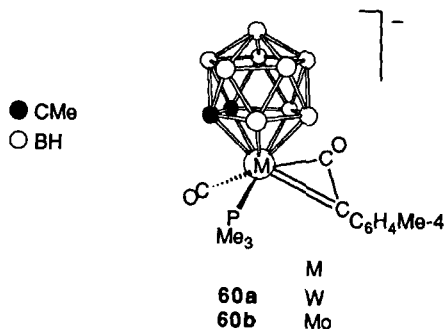


FIG. 4. Structure of the anion of salt 58c.

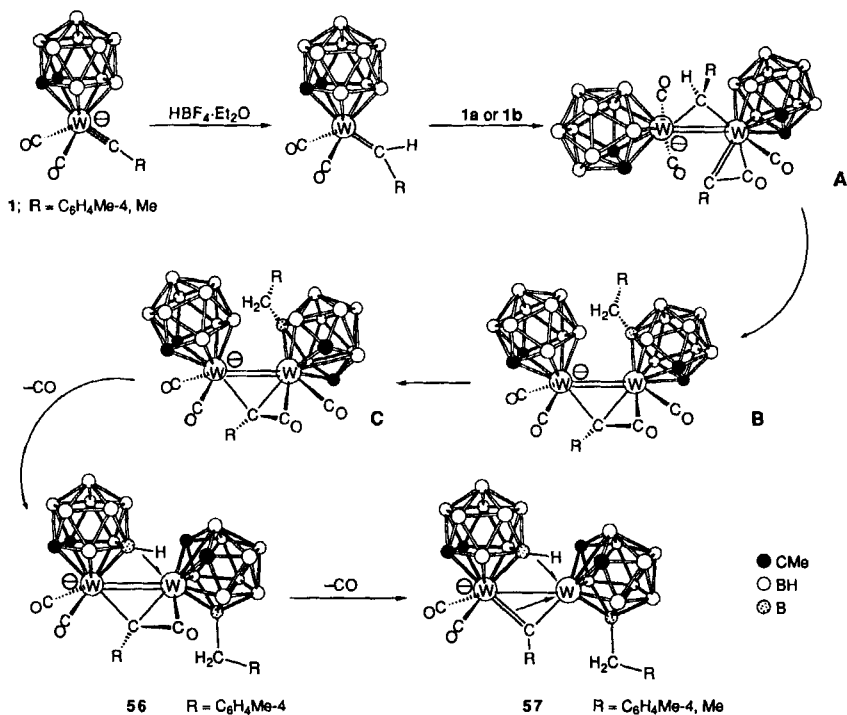
strained 13-vertex cage system is apparently unable to adopt a *hyper-closo* configuration, and a third carbonyl ligand is retained to donate the required electron pair to the cluster. This necessitates a transfer of the ketenyl ligand such that in the solid state it becomes  $\sigma$ -bonded to the metal vertex of the cage bearing the  $\text{BCH}_2\text{R}$  substituent and  $\eta^2$ -bonded to the metal vertex of the cage involved in the  $\text{B}-\text{H} \rightarrow \text{M}$  interaction. However, NMR and IR spectroscopy firmly indicate that solutions of the salts **58** in organic solvents adopt the alternative  $\mu\text{-}\eta^1$  bonding mode in which the ketenyl oxygen atom carries a formal positive charge. Unlike the related species **56**, the salt **58a** may be protonated slowly to yield the  $\mu$ -alkyne compound **59**. The hydroxy-alkyne ligand in this molecule adopts a relatively rare asymmetric bonding mode in which the  $\text{C}-\text{C}$  bond is twisted with respect to the metal-metal vector (**59**).

The mechanism for formation of these ketenyl complexes is subject to speculation, presently based on the observation that  $\text{PMe}_3$ , a strong nu-



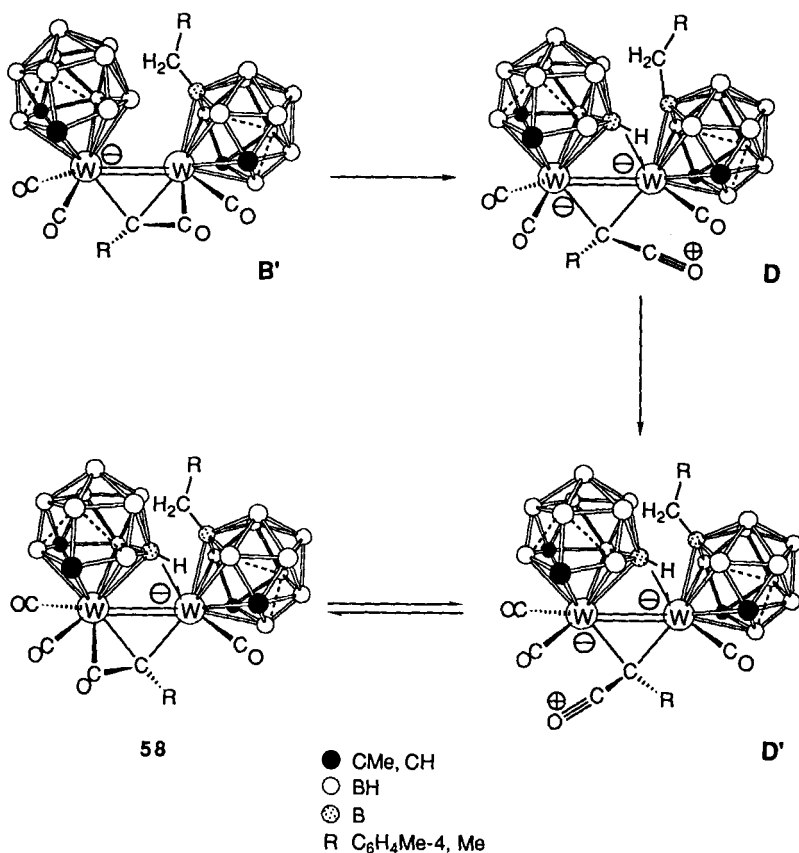
cleophile, reacts rapidly with **1a** at  $-30^{\circ}\text{C}$  to produce the ketenyl complex **60a** (**54**) or with **1m** at room temperature to yield **60b** (**33**). This reaction is also well known for the cyclopentadienyl complexes **4** (**60**). The proposed route for syntheses of the complexes **56** and **57** is shown in Scheme 14. Thus a dimetal intermediate **A**, with a bridging alkylidene group and a terminal ketenyl ligand, might be produced by attack of the carbene-metal complex, initially formed by protonation, on the unreacted carbyne reagent **1**. Insertion of the carbene group into a B-H bond as commonly observed would allow the ketenyl ligand to bridge the M-M vector (**B**), whereupon B-H $\rightarrow$ M formation with concomitant elimination of CO would yield complex **56**, with further elimination of CO subsequently producing **57**.

A critical stage of this pathway is the cage distortion from **B**, in which both cages are *closo*, but one metal formally has only 16 valence electrons. Intermediate **C** contains one *hyper-closo* cage, both metals thus attaining a formal 18-electron valence shell by effectively delocalizing the electron-pair deficiency throughout this cage. The docosahedral cage system present in anions of the salts **2** cannot undergo such a distortion and so must find



SCHEME 14.

an alternative means of alleviating electron shortage in the pathway to the products **58**. Such a means is proposed in Scheme 15, starting from an intermediate **B'** which may be formed in a manner directly analogous to that of the aforementioned species **B** of Scheme 14. Formation of a B-H→W bridge would achieve 18-valence-electron configurations at both metal centers in **D** but apparently imposes sufficient driving force, presumed to be sterically based, for the ketenyl ligand to rotate across to the other metal center, perhaps in the manner shown. The two different bonding modes of ketenyl groups in the intermediates in Schemes 14 and 15 have ample precedent in other dimetal complexes (60-62). Furthermore, the  $\mu\text{-}\sigma,\eta^2$  bonding mode adopted by **58c** in the solid state is readily transformed to the  $\mu\text{-}\eta^1$  conformation (**D'**) in solution as previously mentioned.



SCHEME 15.

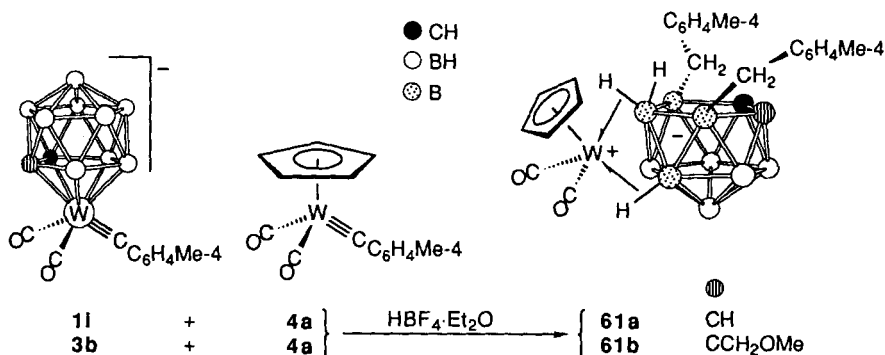
Protonations of the alkylidyne-metal complexes **1-4** involving half molar equivalents of  $\text{HBF}_4 \cdot \text{Et}_2\text{O}$  thus follow essentially two pathways, leading to the  $\mu$ -alkyne complexes **53** and **55** (Scheme 13) or the ketenyl complexes **56** and **58** (Schemes 14 and 15). The former pathway involves addition of an initially formed alkylidene-metal complex across the  $\text{M}\equiv\text{C}$  bond of the related alkylidyne species. The latter involves nucleophilic attack of the alkylidene-metal complex upon the metal center in the unreacted alkylidyne reagent. This subtle difference appears to be key to the sharply contrasting nature of the products obtained from these reactions. The reasons for the distinction between these reactivity patterns are not clear; however, the former (Scheme 13) is favored by those alkylidyne-metal species bearing cyclopentadienyl or  $\eta^5\text{-C}_2\text{B}_9\text{H}_{11}$  ligands. These groups thus appear to have similar electronic properties, which are distinct from those of the alkylidyne(carbaborane)metal reagents containing  $\text{MC}_2\text{B}_9\text{H}_9\text{Me}_2$  or  $\text{MC}_2\text{B}_{10}$  polyhedra. Further inferences about the relative electronic effects within these compounds are restricted by the fact that the alkylidene- and alkylidyne-metal species reacting in the critical stage of these pathways are not independently variable.

## VI

### EXO-NIDO METALLACARBABORANES

As mentioned in the Introduction, the *nido* 11-vertex carbaborane cages used for syntheses of the salts **1** have long been recognized as isolobal analogs of the ubiquitous cyclopentadienyl ligands  $\eta^5\text{-C}_5\text{R}_5$  ( $\text{R} = \text{H}$  or  $\text{Me}$ ). However, the dazzling variety of options open to metallacarbaborane species, in terms of their structures, bonding modes, and electronic or steric influences on metal-ligand clusters, has more recently served to distance the complexes **1** and **2** from their neutral cyclopentadienyl-bearing counterparts **4**. Syntheses of *exo-nido* metallacarbaborane complexes in Scheme 16, formed serendipitously from protonation reactions of certain alkylidyne-metal complex mixtures, emphasize the comparative ease with which radically different bonding modes can be adopted.

Thus treatment of an equimolar mixture of **1i** and **4a** with 1 mol eq. of  $\text{HBF}_4 \cdot \text{Et}_2\text{O}$  at ambient temperature does not yield a dimetal species analogous to those described in Section V,A, but rather the unusual *exo-nido* monotungsten product [*exo-nido*-9,11- $(\text{CH}_2\text{C}_6\text{H}_4\text{Me-4})_2$ -5,10- $\{\text{W}(\text{CO})_2(\eta\text{-C}_5\text{H}_5)\}$ -5,10- $(\mu\text{-H})_2$ -7,8- $\text{C}_2\text{B}_9\text{H}_8$ ] **61a** (Scheme 16) (49). The related compound **61b** has been similarly obtained from **3b** and **4a** (42). The contrasting species [*exo-nido*-7,8- $\text{Me}_2$ -9,10- $\{\text{W}(\text{CO})_2(\eta\text{-C}_5\text{R}'_5)\}$ -9,10-

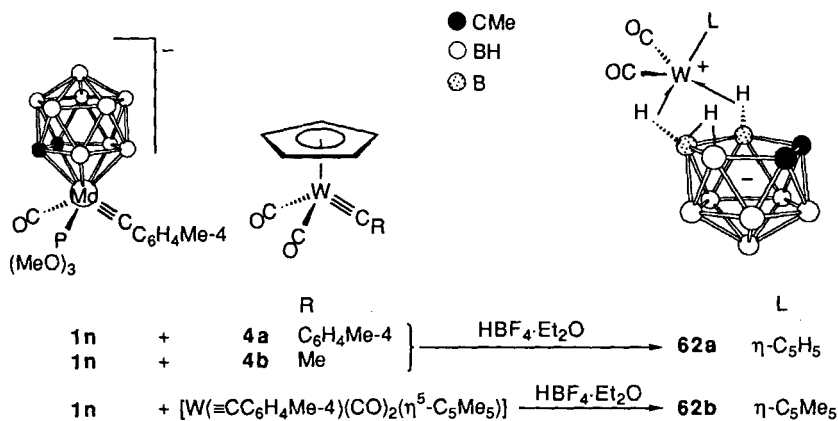


SCHEME 16.

$(\mu-H)_2-7,8-C_2B_9H_8]$  ( $R' = H, Me$ ; **62**) were obtained by protonating mixtures containing the molybdenum carbaborane salt **1n**, as shown in Scheme 17 (49).

Thus the complexes **61** and **62** represent two distinct types of *exo-nido* tungstacarbaborane, in which *nido*-7,8- $C_2B_9$  anions formally donate four electrons to  $[W(CO)_2(\eta-C_5R'_5)]^+$  ( $R' = H, Me$ ) cations via two B-H $\rightarrow$ W 3c-2e interactions. These species may therefore conveniently be regarded as zwitterionic. But this may exaggerate the degree of charge separation, as an X-ray diffraction study of **62b** (Fig. 5) clearly shows the  $\eta-C_5Me_5$  ring tending toward  $\eta^3$ - rather than  $\eta^5$ -coordination to the tungsten atom (49). A similar effect is noticed for the  $\eta-C_5H_5$  ligand of **61a** (Fig. 5) but is statistically less significant owing to imperfect diffraction data.

It is noteworthy that the *nido* carbaborane cages of the products **61**



SCHEME 17.

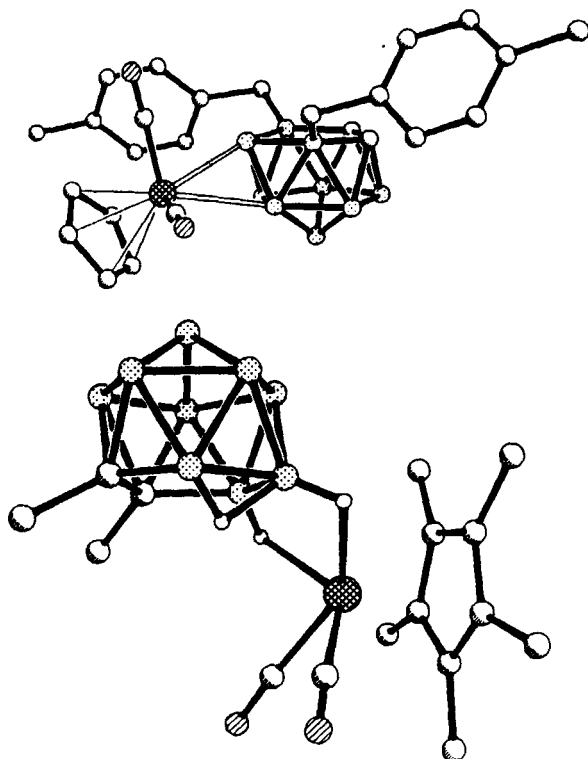
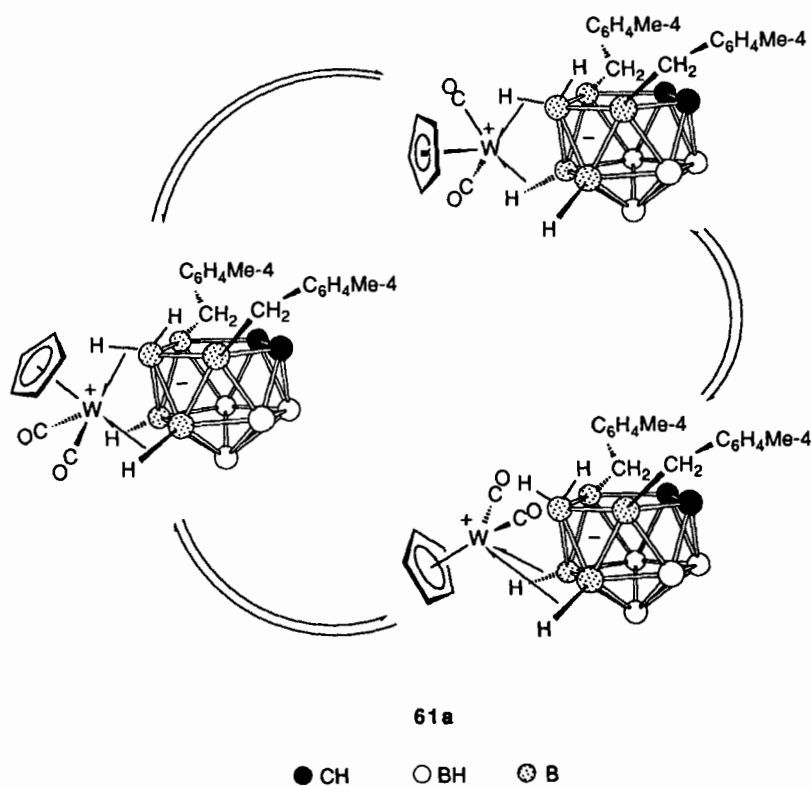
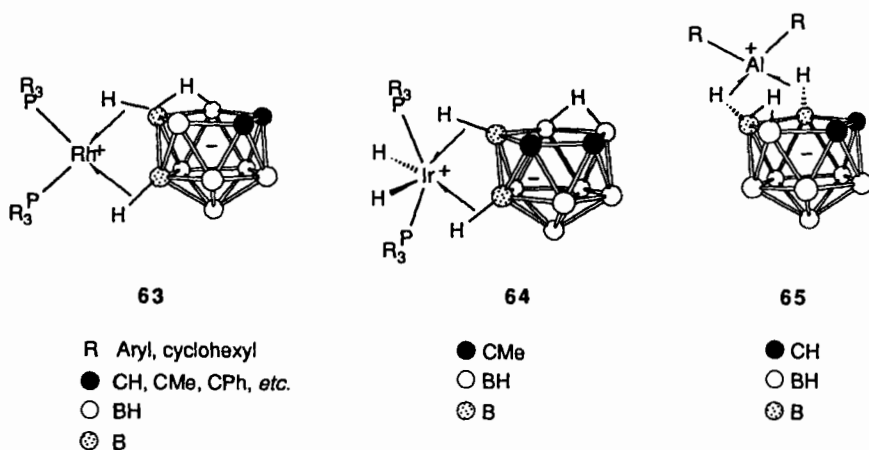


FIG. 5. Molecular structures of complexes **61a** (top) and **62b** (bottom).

utilize B–H bonds from separate pentagonal layers, whereas the species **62** form these linkages from two boron atoms in the single open pentagonal face of the cage. This difference may be due, in large part, to the presence in the former complexes of two  $\text{CH}_2\text{C}_6\text{H}_4\text{Me}$ -4 substituents. These bulky groups reduce the number of exopolyhedral B–H bonds from this pentagonal ring to one, thus enforcing a conformation such as that observed. This conformation is not necessarily unfavorable, however, having been observed earlier by Hawthorne and co-workers (63), in rhoda- and iridacarbaborane complexes such as **63** and **64**. The alternative bonding geometry exhibited by the complexes **62** has also been observed for the aluminum and gallium *exo-nido* complexes [*exo-nido*-9,10-( $\text{EMe}_2$ )-9,10-( $\mu\text{-H}$ ) $_2$ -7,8- $\text{C}_2\text{B}_9\text{H}_{10}$ ] (E = Al, Ga; **65**), as long ago as 1971 (64).

*Exo-nido* metallacarbaborane complexes are at present comparatively rare, but are nevertheless a clear bonding option by which a number of metal–ligand fragments may interact with a  $\text{C}_2\text{B}_9$  cage system. However, the species **62** are singled out from all other known examples by having



SCHEME 18.



"static" structures, on the NMR time scale, in solutions at ambient temperature. With this exception, all the above *exo-nido* complexes exhibit extremely facile fluxional processes. Proposed mechanisms for this fluxionality include site exchange of metal-ligand ( $ML_n$ ) fragments with *endo*-B-H protons or of *exo*- with *endo*-protons, and mobility of the  $ML_n$  group between various pairs of B-H vertices. The suggested mechanism by which compound **61a** achieves a time-averaged plane of symmetry, displayed via solution NMR spectra recorded as low as  $-80^\circ\text{C}$ , is shown in Scheme 18 (49). Thus the  $W(CO)_2(\eta-C_5H_5)^+$  fragment rotates by stepping around a triangular face of the  $C_2B_9$  cage. The apparent inflexibility of the complexes **62**, on the other hand, has made them excellent subjects for NMR correlation experiments (49). These studies have shown that the boron nuclei of the B-H $\rightarrow$ W interactions exhibit the highest and lowest chemical shifts in the  $^{11}\text{B}$  NMR spectra, a difference of almost 80 ppm for compound **62a**, emphasizing the unusual electronic shielding effects in these structures.

## VII

### SPECTROSCOPIC AND X-RAY DIFFRACTION ANALYSIS

Characterizations of the metallacarbaborane species described in this review and in our earlier article (1) would not have been possible without modern tools of analysis. Of crucial importance to this work are high-field multinuclear magnetic resonance spectroscopy and single-crystal X-ray diffraction analysis, two cornerstones of synthetic organometallic chemistry. It is therefore appropriate to highlight certain diagnostic features that are essential to the successful application of these techniques.

#### A. NMR Spectroscopy

The chemical shift ranges covering the majority of examples of the most important functional groups are shown in three figures in this section and are discussed further below. However, it is important to stress that both the chemical shifts and the profiles of the spectral peaks are powerful indicators of chemical structure. This is due largely to the presence in these molecules of at least nine quadrupolar boron nuclei ( $^{11}\text{B}$ ,  $I = \frac{3}{2}$ , 80%;  $^{10}\text{B}$ ,  $I = \frac{3}{2}$ , 20%), which can be both a hindrance and an invaluable aid to structural characterization.

### 1. Proton NMR

Terminal B-H protons generally appear as broad unresolved signals in the range  $\delta$  0 to +3, but may be observed as low as  $\delta$  -2. They cannot be assigned without the aid of a broadband  $^{11}\text{B}$  decoupling signal and/or two-dimensional correlation experiments. For the work described herein they are of no diagnostic value, simply impeding the accurate measurement of the integrated intensities of other peaks in this range and frequently masking weak signals such as cage CH proton resonances, which are also somewhat broad owing to the quadrupolar boron nuclei. The methylene protons of a  $\text{BCH}_2\text{R}$  ( $\text{R} = \text{Aryl}$ ) group are often observed as an [AB] pattern, approximately 1.5 ppm higher in frequency than the corresponding multiplet for those of a  $\text{BCH}_2\text{Me}$  fragment (Fig. 6). Through-bond relaxation by the boron nuclei does not extend through a second 2c-2e bond; hence cage CMe proton signals are usually sharp peaks, often indistinguishable from other methyl groups within the molecule, such as that of the *p*-tolyl group.

The most valuable region of the  $^1\text{H}$  NMR spectrum in applicable cases is the area to high field of  $\text{SiMe}_4$ , where  $\text{B-H} \rightarrow \text{M}$  resonances are observed. These signals are invariably extremely broad quartet resonances with direct  $^1\text{J}(^{11}\text{B}-^1\text{H})$  couplings measurable in the range  $\sim 60$ – $90$  Hz. Hence they cannot be mistaken for other groups with high-field resonances, such as terminal or bridging metal hydrides. The  $\text{B-H} \rightarrow \text{M}$  signals fall across a wide frequency range ( $\delta \sim -5$  to  $-11$ ) even when involving a particular metal, perhaps indicating the variable extent to which this type of 3c-2e interaction may occur. Unfortunately, unfavorable circumstances, particularly molecular fluxionality, occasionally broaden these  $\text{B-H} \rightarrow \text{M}$  signals to such an extent that  $^{11}\text{B}-^1\text{H}$  coupling is not detectable or the resonances

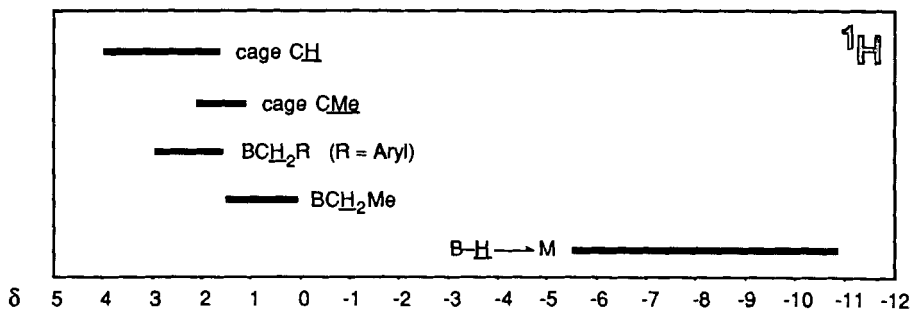


FIG. 6. Diagnostic chemical shift ranges in the  $^1\text{H}$  NMR spectra from metallacarborane complexes of the types described herein.

simply cannot be observed. However, these groups may be identified from  $^{11}\text{B}$  NMR spectra, as discussed later.

## 2. Carbon-13 NMR

Despite its low natural abundance and poor magnetic susceptibility, carbon-13 NMR spectroscopy has developed, through technological advances, into an indispensable element of spectroscopic analysis for the compounds described herein. High-field, high-resolution spectrometers make possible the routine observation of broad and weak signals that would have passed unnoticed only a few years ago. Moreover, it is precisely these signals that convey the most significant structural information. Once again, the profiles of the resonances are as significant as their frequencies.

Thus, exopolyhedral substituents  $\text{CH}_2\text{R}$  are characterized in  $^{13}\text{C}\{-^1\text{H}\}$  NMR spectra by an extremely broad quartet in the ranges  $\delta \sim 25\text{--}40$  ( $\text{R} = \text{Aryl}$ ) or  $\delta \sim 15\text{--}25$  ( $\text{R} = \text{Me}$ ) corresponding to the  $\text{BCH}_2$  nucleus (Fig. 7). When the spectral resolution permits measurement of the  $^{11}\text{B}\text{--}^{13}\text{C}$  coupling constant, it is found to be in the region of 80 Hz. In contrast, the  $^{13}\text{C}$  nuclei of cage  $\text{CH}$  or  $\text{CMe}$  groups appear as singlets, coupling to several boron nuclei being unresolved. Indeed, the resonances of cage  $\text{CMe}$  nuclei are sharp and, but for their relatively high chemical shift, indistinguishable from other methyl groups in the molecule. It is noteworthy that the average chemical shift of  $\text{CMe}$  nuclei in  $\text{MC}_2\text{B}_{10}$  cages is approximately 5 ppm higher than of those in  $\text{MC}_2\text{B}_9$  systems, although this feature alone cannot unequivocally define the cage structure. However, the cage-carbon vertex signals themselves do allow distinction between  $\text{MC}_2\text{B}_9$  and  $\text{MC}_2\text{B}_{10}$  complexes, as discussed below.

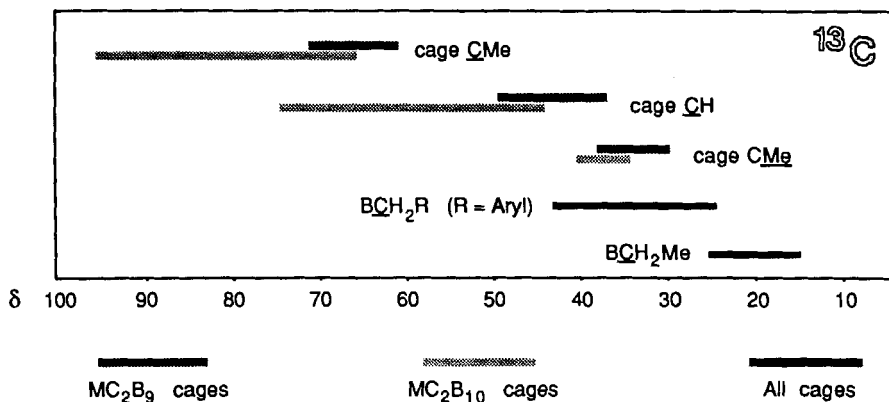


FIG. 7. Diagnostic chemical shift ranges in the  $^{13}\text{C}\{-^1\text{H}\}$  NMR spectra from metallocarborane complexes of the types described herein.

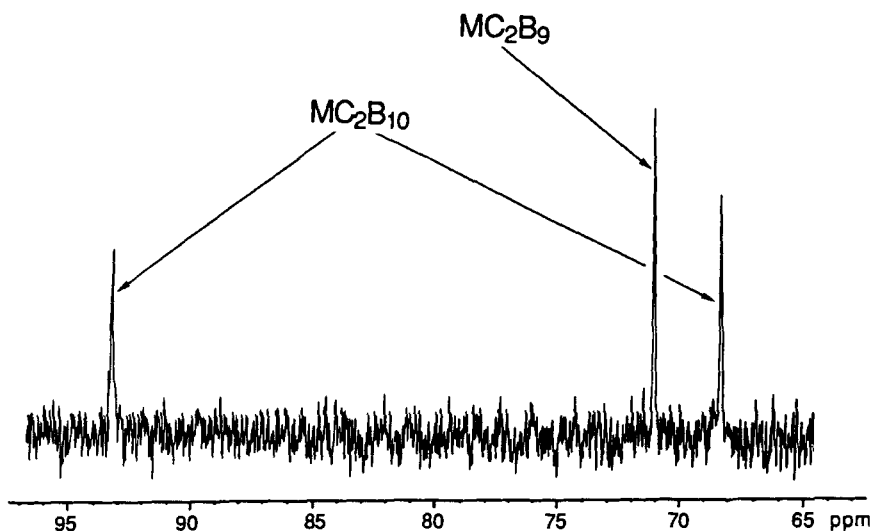


FIG. 8. Typical  $^{13}\text{C}\{-^1\text{H}\}$  NMR spectrum of related  $\text{MC}_2\text{B}_9\text{Me}_2$  and  $\text{MC}_2\text{B}_{10}\text{Me}_2$  complexes, showing the cage-carbon resonances.

Although noticeably broader and significantly weaker than primary or secondary carbon atom signals, the resonance intensities of cage CMe or CH nuclei are of the same order of magnitude as those of M–C–O groups and are thus readily observed under normal circumstances. These signals provide powerful evidence for both the structure and the topology of the metallocarbaborane cage concerned. Structural information is provided by chemical shift, which, for *closo*- $\text{MC}_2\text{B}_9$  cages with CMe groups, falls in the range  $\delta \sim 60\text{--}75$ . Docosahedral *closo*- $\text{MC}_2\text{B}_{10}\text{Me}_2$  cage resonances, on the other hand, appear in the range  $\delta \sim 65\text{--}95$  (Fig. 7). Furthermore, the two cage-carbon atom signals in the latter structures are generally separated by at least 20 ppm.<sup>5</sup> This is illustrated in Fig. 8, showing the CMe resonances of a mixture in which a typical  $\text{MC}_2\text{B}_{10}$  cage, bearing a  $\text{CH}_2\text{R}$  substituent, is slowly converting to the corresponding  $\text{MC}_2\text{B}_9$  icosahedron via loss of a  $\text{BCH}_2\text{R}$  fragment as discussed in Sections II and III. A directly comparable trend is observed in comparing icosahedral or docosahedral structures having CH vertices (Fig. 7). The  $^{13}\text{C}\{-^1\text{H}\}$  NMR chemical shift of cage-carbon atoms is also a useful indicator of more unusual cage structures. For example, the CMe nuclei of *hyper-closo* 12-vertex cages (Section V, B)

<sup>5</sup> Docosahedral  $\text{MC}_2\text{B}_{10}$  cages contain a puckered 6-membered BBBCBC ring that flexes, in solutions at ambient temperature, on the NMR time scale (1). Spectra of the “static” structure, in which the carbon vertices necessarily have different environments with respect to the metal center, may generally be obtained by cooling to  $\sim -20^\circ\text{C}$ .

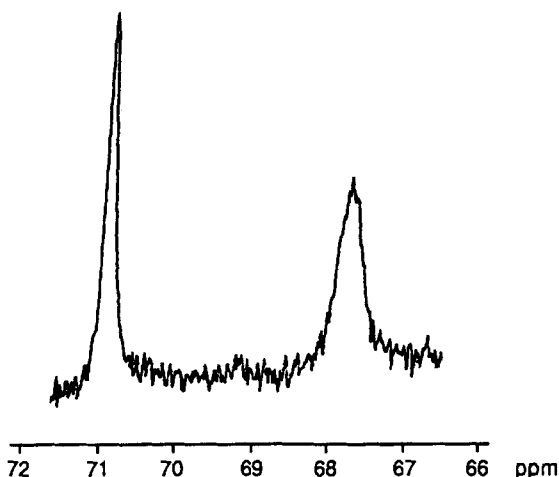


FIG. 9. Typical  $^{13}\text{C}\{-^1\text{H}\}$  NMR spectrum, showing the cage-carbon resonances, of a 12-vertex metallocarbaborane complex having a 2,1,8- $\text{MC}_2\text{B}_9$  arrangement of atoms.

resonate in the range  $\delta \sim 170\text{--}180$  (55,65), while “slipped”  $\eta^3\text{-MC}_2\text{B}_9\text{H}_9\text{Me}_2$  cage structures may be suggested by the appearance of cage-carbon resonances in the range  $\delta \sim 70\text{--}80$  (66).

The topological arrangement of cage atoms, on the other hand, is indicated by the profiles of these carbon vertex resonances. Thus, cages in which both carbon atoms have the same numbers of B–C, C–C, and C–M connectivities, i.e., 3,1,2- $\text{MC}_2\text{B}_9$  or 2,1,7- $\text{MC}_2\text{B}_9$ , display two CMe resonances of approximately equal width and intensity, provided there is no molecular symmetry. But the “rearranged” 2,1,8- $\text{MC}_2\text{B}_9$  cage topology described for several compounds in Section IV shows distinctively contrasting peak profiles in its  $^{13}\text{C}\{-^1\text{H}\}$  NMR spectra. A typical example, showing one broad and one relatively sharp signal, is shown in Fig. 9. This feature is attributed to the different number of B–C connectivities, and therefore the different nuclear relaxation rates, for each carbon vertex.

The  $^{13}\text{C}\{-^1\text{H}\}$  NMR spectrum is thus extremely powerful in determining the structures of metallocarbaboranes of the types described herein. Its value is further increased as the information it holds is often not provided in either  $^1\text{H}$  or  $^{11}\text{B}$  spectra.

### 3. Boron-11 NMR

Very short relaxation times and the presence of 20% boron-10 ( $I = \frac{3}{2}$ ) combine to make the peaks in any  $^{11}\text{B}$  NMR spectrum broad. These factors are exacerbated in metallocarbaborane complexes such as those

described in this chapter, by the bulk of the molecules, and by the electric field gradient imposed across them due to the metal, both of which aid spin-lattice relaxation processes still further. Nevertheless, useful information is available from  $^{11}\text{B}$  NMR spectra with the aid of a high-field spectrometer, particularly when proton-coupled and -decoupled spectra are compared. The chemical shift ranges for three types of "noninnocent" cage interaction are shown in Fig. 10, along with the range of terminal, or "innocent," B-H nuclear resonances. As these ranges are generally quite distinct, chemical shift alone is often sufficient to identify the type of exopolyhedral interaction. Moreover, cases of potential ambiguity are avoided by measuring a fully coupled  $^{11}\text{B}$  spectrum. In this mode, B-M and  $\text{BCH}_2\text{R}$  nuclei remain as singlets as they have no attached protons. In contrast, boron nuclei involved in  $\text{B-H}\rightarrow\text{M}$  3c-2e linkages give rise to doublet signals, with  $J(\text{HB}) \sim 70$  Hz. This value is significantly smaller than the 2c-2e  $J(\text{HB})$  coupling of terminal B-H groups at  $\sim 130$  Hz. A similar trend in C-H coupling constants has been recognized as a feature of the related "agostic"  $\text{C-H}\rightarrow\text{M}$  3c-2e interaction (67). Occasionally, the small B-H coupling of the  $\text{B-H}\rightarrow\text{M}$  moiety is not resolved, and thus greater reliance is placed on the distinctive signal produced in the  $^1\text{H}$  spectrum by this fragment, discussed above.

It should be noted that the terminal BH signals themselves provide no valuable structural information in *closo* systems owing to their close proximity and broad linewidths. Indeed, the integrated intensities of this region are often not sufficiently accurate to distinguish reliably between  $\text{B}_9$  and  $\text{B}_{10}$  systems, hence the importance of the  $^{13}\text{C}\{-^1\text{H}\}$  spectrum in this respect. Furthermore, two-dimensional correlation experiments (COSY) provide connectivity maps only in exceptional circumstances (e.g., compounds 62), as the peaks in most of the complexes described are not sufficiently resolved.

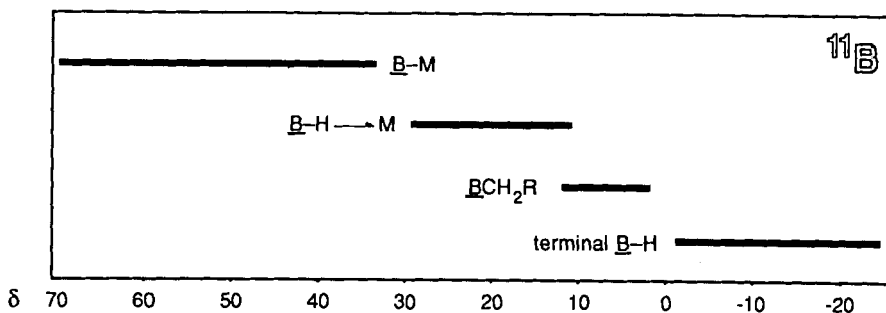


FIG. 10. Diagnostic chemical shift ranges in the  $^{11}\text{B}\{-^1\text{H}\}$  NMR spectra from metallacarborane complexes of the types described herein.

### B. X-Ray Diffraction Analysis

Despite the wealth of information provided by NMR spectroscopy, the importance of X-ray crystallography in placing these results on firm foundations cannot be overemphasized. Single-crystal diffraction analysis has thus been utilized extensively for characterizations of the complexes described herein. Examples of selected structures have been included throughout this chapter, and a comprehensive list of structurally characterized metallocarborane species among the compounds **1** to **63** is given in Table I.

One noteworthy factor affects the determination of metallocarborane complex structures by X-ray diffraction techniques: the distinction in an electron-density map between cage-carbon and boron atoms. It is possible, given a good data set, to distinguish between these two elements purely on the basis of thermal displacement coefficients. Nevertheless, in practice, interatomic separations must also be taken into consideration, as C–C distances are generally 1.65 Å or less, while B–C or B–B connectivities are 1.70 Å or more. Isomers of the 12- and 13-vertex cages, used throughout this work, which have no C–C connectivity, could therefore be subject to some structural ambiguity, were it not for the methyl substituents attached to the cage-carbon atoms. Indeed, these groups were initially introduced simply to aid the structural and spectroscopic identification of various

TABLE I  
REFERENCES TO X-RAY DIFFRACTION STUDIES  
ON CARBATORANE–METAL COMPLEXES

Formula	Reference	Formula	Reference
<b>1a</b> <sup>a</sup>	(68)	<b>46b</b>	(47)
<b>2c</b> <sup>b</sup>	(69)	<b>47a</b>	(47)
<b>20i</b>	(31)	<b>48b</b> <sup>d</sup>	(47)
<b>23b</b>	(32)	<b>50b</b>	(50)
<b>24b</b>	(35)	<b>52<sup>b</sup></b>	(53)
<b>31a</b>	(38)	<b>57a</b> <sup>b</sup>	(55)
<b>35d</b> <sup>c</sup>	(39)	<b>58c</b> <sup>e</sup>	(36)
<b>36<sup>b</sup></b>	(35)	<b>61a</b>	(49)
<b>42b</b>	(39)	<b>62b</b>	(49)

<sup>a</sup> PPh<sub>4</sub><sup>+</sup> salt.

<sup>b</sup> NEt<sub>4</sub><sup>+</sup> salt.

<sup>c</sup> N(PPh<sub>3</sub>)<sub>2</sub><sup>+</sup> salt.

<sup>d</sup> Study made on a PMe<sub>3</sub> derivative containing a Mo(PMe<sub>3</sub>)(η-C<sub>5</sub>H<sub>5</sub>) group.

<sup>e</sup> Au(PPh<sub>3</sub>)<sub>2</sub><sup>+</sup> salt.

reaction products. However, as has become abundantly clear, the presence of cage CMe vertices has a profound effect on the pathways followed by the reagents **1** and **2**, in a widely diverse range of reactions.

## VIII

### CONCLUSIONS

The potential of metallacarbaborane complexes bearing reactive alkylidyne functionalities is proving to reach far beyond what was imaginable at the time of their initial synthesis (8). Although there are areas of overlap with their alkylidyne(cyclopentaidenyl)metal counterparts, the chemistry of these polyhedral salts extends into boundless new territory, limited only by the imagination of its discoverers. The complexes summarized in this chapter demonstrate how the proton, perhaps the simplest of all chemical reagents, can be used to unlock the potential of alkylidyne(carbaborane)metal complexes.

The scope of this area of investigation is illustrated by the observation that numerous primary journal articles have stemmed from the study of essentially two types of cage system (12- and 13-vertex), utilizing only two metals (W and Mo). Extensions of the research into synthetic methods for alkylidyne(carbaborane)metal complexes based on alternative metal centers and/or new cage systems would appear to offer the prospect of dramatic new developments in future years.

### ACKNOWLEDGMENTS

We thank the Robert A. Welch Foundation for support.

### REFERENCES

1. F. G. A. Stone, *Adv. Organomet. Chem.* **31**, 53 (1991).
2. M. M. Fein, J. Bobinski, N. Mayes, N. Schwartz, and M. S. Cohen, *Inorg. Chem.* **2**, 1111 (1963); T. L. Heying, J. W. Ager, S. L. Clark, D. J. Mangold, H. L. Goldstein, M. Hillman, R. J. Polak, and J. W. Szymanski, *Inorg. Chem.* **2**, 1089 (1963); L. I. Zakharkin, V. I. Stanko, V. A. Brattsev, Yu. A. Chapovskii, and Yu. T. Struchkov, *Izv. Akad. Nauk SSSR Ser. Khim.*, 2069 (1963).
3. T. Onak, in "Comprehensive Organometallic Chemistry" (G. Wilkinson, E. W. Abel, and F. G. A. Stone, eds.), Vol. 1, p. 411. Pergamon, Oxford, England, 1982.
4. K. P. Callahan and M. F. Hawthorne, *Adv. Organomet. Chem.* **14**, 145 (1976); R. N. Grimes, in "Comprehensive Organometallic Chemistry" (G. Wilkinson, E. W. Abel, and F. G. A. Stone, eds.), Vol. 1, p. 459. Pergamon, Oxford, England, 1982.
5. M. F. Hawthorne, D. C. Young, T. D. Andrews, D. V. Howe, R. L. Pilling, A. D. Pitts, M. Reintjes, J. F. Warren, and P. A. Wegner, *J. Am. Chem. Soc.* **90**, 879 (1968).



6. J. A. Belmont, J. Soto, R. E. King III, A. J. Donaldson, J. D. Hewes, and M. F. Hawthorne, *J. Am. Chem. Soc.* **111**, 7475 (1989), and references cited therein; M. F. Hawthorne, in "Advances in Boron and the Boranes" (J. Liebman and A. Greenberg, eds.), Chapter 10, p. 225. VCH, New York, 1988.
7. M. F. Hawthorne, A. Varadarajan, C. B. Knobler, S. Chakrabarti, R. J. Paxton, B. G. Beatty, and F. L. Curtis, *J. Am. Chem. Soc.* **112**, 5365 (1990); Y. Yamamoto, T. Seko, H. Nakamura, H. Nemoto, H. Hojo, N. Mukai, and Y. Hashimoto, *J. Chem. Soc. Chem. Commun.*, 157 (1992).
8. M. Green, J. A. K. Howard, A. P. James, C. M. Nunn, and F. G. A. Stone, *J. Chem. Soc. Chem. Commun.*, 1114 (1984).
9. F. G. A. Stone, *ACS Symp. Ser.* **211**, 383 (1983); F. G. A. Stone, *Pure Appl. Chem.* **58**, 529 (1986); F. G. A. Stone, *Angew. Chem. Int. Ed. Engl.* **23**, 89 (1984).
10. M. Green, J. A. K. Howard, A. P. James, C. M. Nunn, and F. G. A. Stone, *J. Chem. Soc. Dalton Trans.*, 61 (1987).
11. E. O. Fischer, G. Kreis, C. G. Kreiter, J. Müller, G. Huttner, and H. Lorenz, *Angew. Chem. Int. Ed. Engl.* **12**, 564 (1973).
12. (a) M. A. Gallop and W. R. Roper, *Adv. Organomet. Chem.* **25**, 121 (1986);  
(b) H. P. Kim and R. J. Angelici, *Adv. Organomet. Chem.* **27**, 51 (1987);  
(c) A. Mayr and H. Hoffmeister, *Adv. Organomet. Chem.* **32**, 227 (1991).
13. H. Fischer, P. Hofmann, F. R. Kreissl, R. R. Schrock, U. Schubert, and K. Weiss, "Carbyne Complexes." VCH, Weinheim, Germany, 1988.
14. E. O. Fischer, *Adv. Organomet. Chem.* **14**, 1 (1976).
15. R. R. Schrock, *J. Organomet. Chem.* **300**, 249 (1986).
16. R. H. Grubbs, in "Comprehensive Organometallic Chemistry" (G. Wilkinson, E. W. Abel, and F. G. A. Stone, eds.), Vol. 8, p. 499. Pergamon, Oxford, England, 1982.
17. J. Sancho and R. R. Schrock, *J. Mol. Catal.* **15**, 75 (1982); R. R. Schrock, *Science* **219**, 13 (1983).
18. H. Vahrenkamp, *Adv. Organomet. Chem.* **22**, 169 (1983); R. D. Adams, in "The Chemistry of Metal Cluster Complexes" (D. F. Shriver, H. D. Kaesz, and R. D. Adams, eds.), Chapter 3, p. 121. VCH, New York, 1990.
19. (a) U. Schubert, ed., "Advances in Metal Carbene Chemistry." Kluwer, Dordrecht, The Netherlands, 1989;  
(b) S. W. Kirtley, in "Comprehensive Organometallic Chemistry" (G. Wilkinson, E. W. Abel, and F. G. A. Stone, eds.), Vol. 3, p. 783 and p. 1255. Pergamon, Oxford, England, 1982.
20. N. M. Kostić and R. F. Fenske, *J. Am. Chem. Soc.* **103**, 4677 (1981); N. M. Kostić and R. F. Fenske, *Organometallics* **1**, 489 (1982).
21. S. J. Holmes and R. R. Schrock, *J. Am. Chem. Soc.* **103**, 4599 (1981).
22. A. Mayr, M. F. Asaro, M. A. Kjelsberg, K. S. Lee, and D. van Engen, *Organometallics* **6**, 432 (1987); A. Mayr, M. A. Kjelsberg, K. S. Lee, M. F. Asaro, and T. C. Hsieh, *Organometallics* **6**, 2610 (1987).
23. M. Bottrill and M. Green, *J. Am. Chem. Soc.* **99**, 5795 (1977); M. Bottrill, M. Green, A. G. Orpen, D. R. Saunders, and I. D. Williams, *J. Chem. Soc. Dalton Trans.*, 511 (1989).
24. R. P. A. Sneed, "Organochromium Compounds." Academic Press, New York, 1975; H. Werner and H. Rascher, *Inorg. Chim. Acta* **2**, 181 (1968).
25. J. A. K. Howard, J. C. Jeffery, J. C. V. Laurie, I. Moore, F. G. A. Stone, and A. Stringer, *Inorg. Chim. Acta* **100**, 23 (1985).
26. F. R. Kreissl, W. J. Sieber, M. Wolfgruber, and J. Riede, *Angew. Chem. Int. Ed. Engl.* **23**, 640 (1984); F. R. Kreissl, W. J. Sieber, H. Keller, J. Riede, and M. Wolfgruber, *J. Organomet. Chem.* **320**, 83 (1987).

27. K. E. Garrett, J. B. Sheridan, D. B. Pourreau, W. C. Feng, G. L. Geoffroy, D. L. Staley, and A. L. Rheingold, *J. Am. Chem. Soc.* **111**, 8383 (1989).
28. W. D. Wulff, in "Comprehensive Organic Synthesis" (B. M. Trost and I. Fleming, eds.), Vol. 5, p. 1065. Pergamon, Oxford, England, 1991; K. H. Dötz, *Angew. Chem. Int. Ed. Engl.* **23**, 587 (1984); see also K. H. Dötz in Ref. 19a, pp. 199–210.
29. J. A. K. Howard, J. C. Jeffery, S. Li, and F. G. A. Stone, *J. Chem. Soc. Dalton Trans.*, 627 (1992).
30. J. C. Jeffery, S. Li, and F. G. A. Stone, *J. Chem. Soc. Dalton Trans.*, 635 (1992).
31. S. A. Brew, D. D. Devore, P. D. Jenkins, M. U. Pilotti, and F. G. A. Stone, *J. Chem. Soc. Dalton Trans.*, 393 (1992).
32. J. C. Jeffery, S. Li, D. W. I. Sams, and F. G. A. Stone, *J. Chem. Soc. Dalton Trans.*, 877 (1992).
33. M. D. Mortimer, Ph.D. Thesis, Bristol University, Bristol, England, 1991.
34. J. L. Templeton, *Adv. Organomet. Chem.* **29**, 1 (1989).
35. J. C. Jeffery, S. Li, and F. G. A. Stone, *Organometallics* **11**, 1902 (1992).
36. N. Carr and F. G. A. Stone, *Organometallics* **12**, 1131 (1993).
37. F. R. Kreissl and W. Held, *Chem. Ber.* **110**, 799 (1977); H. Fischer, *J. Organomet. Chem.* **170**, 309 (1979).
38. S. A. Brew, P. D. Jenkins, J. C. Jeffery, and F. G. A. Stone, *J. Chem. Soc. Dalton Trans.*, 401 (1992).
39. S. A. Brew, N. Carr, J. C. Jeffery, M. U. Pilotti, and F. G. A. Stone, *J. Am. Chem. Soc.* **114**, 2203 (1992).
40. G. M. Edverson and D. F. Gaines, *Inorg. Chem.* **29**, 1210 (1990).
41. M. F. Hawthorne, K. P. Callahan, and R. J. Wiersema, *Tetrahedron* **30**, 1795 (1974); L. F. Warren, Jr., and M. F. Hawthorne, *J. Am. Chem. Soc.* **92**, 1157 (1970).
42. S. Li and F. G. A. Stone, unpublished results.
43. S. A. Brew and F. G. A. Stone, *J. Chem. Soc. Dalton Trans.*, 867 (1992).
44. G. C. Bruce and F. G. A. Stone, *Polyhedron* **11**, 1607 (1992).
45. S. J. Dossett, A. F. Hill, J. C. Jeffery, F. Marken, P. Sherwood, and F. G. A. Stone, *J. Chem. Soc. Dalton Trans.*, 2453 (1988).
46. M. Green, J. A. K. Howard, A. P. James, A. N. de M. Jelfs, C. M. Nunn, and F. G. A. Stone, *J. Chem. Soc. Dalton Trans.*, 81 (1987).
47. S. A. Brew, N. Carr, M. D. Mortimer, and F. G. A. Stone, *J. Chem. Soc. Dalton Trans.*, 811 (1991).
48. S. J. Dossett, I. J. Hart, and F. G. A. Stone, *J. Chem. Soc. Dalton Trans.*, 3481 (1990).
49. S. A. Brew, J. C. Jeffery, M. D. Mortimer, and F. G. A. Stone, *J. Chem. Soc. Dalton Trans.*, 1365 (1992).
50. G. C. Bruce, D. F. Mullica, E. L. Sappenfield, and F. G. A. Stone, *J. Chem. Soc. Dalton Trans.*, 2685 (1992).
51. J. R. Shapley, S. I. Richter, M. Tachikawa, and J. B. Keister, *J. Organomet. Chem.* **94**, C43 (1975); A. F. Dyke, S. A. R. Knox, M. J. Morris, and P. J. Naish, *J. Chem. Soc. Dalton Trans.*, 1417 (1983); P. O. Nubel and T. L. Brown, *J. Am. Chem. Soc.* **106**, 644 (1984); C. P. Casey, S. R. Marder, and B. R. Adams, *J. Am. Chem. Soc.* **107**, 7700 (1985); M. E. Garcia, N. H. Tran-Huy, J. C. Jeffery, P. Sherwood, and F. G. A. Stone, *J. Chem. Soc. Dalton Trans.*, 2201 (1987).
52. E. Delgado, J. Hein, J. C. Jeffery, A. L. Ratermann, F. G. A. Stone, and L. J. Farrugia, *J. Chem. Soc. Dalton Trans.*, 1191 (1987); J. C. Jeffery, M. J. Parrott, and F. G. A. Stone, *J. Chem. Soc. Dalton Trans.*, 3017 (1988).
53. N. Carr, S. J. Dossett, and F. G. A. Stone, *J. Organomet. Chem.* **413**, 223 (1991).
54. A. P. James and F. G. A. Stone, *J. Organomet. Chem.* **310**, 47 (1986); see also Ref. 49.

55. N. Carr, D. F. Mullica, E. L. Sappenfield, and F. G. A. Stone, *Organometallics* **11**, 3697 (1992).
56. R. T. Baker, *Inorg. Chem.* **25**, 109 (1986); C. W. Jung, R. T. Baker, and M. F. Hawthorne, *J. Am. Chem. Soc.* **103**, 810 (1981); C. W. Jung, R. T. Baker, C. B. Knobler, and M. F. Hawthorne, *J. Am. Chem. Soc.* **102**, 5782 (1980).
57. J. D. Kennedy, *Inorg. Chem.* **25**, 111 (1986); J. E. Crook, M. Erlington, N. N. Greenwood, J. D. Kennedy, M. Thornton-Pett, and J. D. Woolins, *J. Chem. Soc. Dalton Trans.*, 2407 (1985), and references cited therein.
58. R. L. Johnston and D. M. P. Mingos, *Inorg. Chem.* **25**, 3321 (1986).
59. F. Muller, G. van Koten, M. J. A. Kraakman, K. Vrieze, D. Heijdenrijk, and M. Zoutberg, *Organometallics* **8**, 1331 (1989); E. Cabrera, J.-C. Daran, Y. Jeannin, O. Kristiansson, *J. Organomet. Chem.* **310**, 367 (1986); El. Amin, J. C. Jeffery, and T. M. Walters, *J. Chem. Soc. Chem. Commun.*, 170 (1990); S. A. Brew, S. J. Dossett, J. C. Jeffery, and F. G. A. Stone, *J. Chem. Soc. Dalton Trans.*, 3017 (1988).
60. G. L. Geoffroy and S. L. Bassner, *Adv. Organomet. Chem.* **28**, 1 (1988); J. C. Jeffery, C. Sambale, M. Schmidt, and F. G. A. Stone, *Organometallics* **1**, 1597 (1982).
61. J. C. Jeffery, M. A. Ruiz, and F. G. A. Stone, *J. Organomet. Chem.* **355**, 231 (1988); J. Martin-Gil, J. A. K. Howard, R. Navarro, and F. G. A. Stone, *J. Chem. Soc. Chem. Commun.*, 1168 (1979); O. Orama, U. Schubert, F. R. Kreissl, and E. O. Fischer, *Z. Naturforsch. B: Anorg. Chem. Org. Chem.* **35**, 82 (1980).
62. L. J. Farrugia, J. C. Jeffery, C. Marsden, P. Sherwood, and F. G. A. Stone, *J. Chem. Soc. Dalton Trans.*, 51 (1987), and references cited therein.
63. J. A. Doi, R. G. Teller, and M. F. Hawthorne, *J. Chem. Soc. Chem. Commun.*, 80 (1980); J. A. Long, T. B. Marder, P. E. Behnken, and M. F. Hawthorne, *J. Am. Chem. Soc.* **106**, 2979 (1984); C. B. Knobler, T. B. Marder, E. A. Mizusawa, R. G. Teller, J. A. Long, P. E. Behnken, and M. F. Hawthorne, *J. Am. Chem. Soc.* **106**, 2990 (1984).
64. D. A. T. Young, R. J. Wiersma, and M. F. Hawthorne, *J. Am. Chem. Soc.* **93**, 5687 (1971); M. R. Churchill and A. H. Reiss, *J. Chem. Soc. Dalton Trans.*, 1314 (1972).
65. M. J. Attfield, J. A. K. Howard, A. N. de M. Jelfs, C. M. Nunn, and F. G. A. Stone, *J. Chem. Soc. Dalton Trans.*, 2219 (1987).
66. J. C. Jeffery, P. A. Jelliss, and F. G. A. Stone, *J. Chem. Soc. Dalton Trans.*, 1083 (1993).
67. M. Brookhart and M. L. H. Green, *J. Organomet. Chem.* **250**, 395 (1983).
68. O. Johnson, J. A. K. Howard, M. Kapan, and G. M. Reisner, *J. Chem. Soc. Dalton Trans.*, 2903 (1988).
69. S. J. Crennell, D. D. Devore, S. J. B. Henderson, J. A. K. Howard, and F. G. A. Stone, *J. Chem. Soc. Dalton Trans.*, 1363 (1989).

# Di- and Trinuclear Metal Complexes of Diboraheterocycles

WALTER SIEBERT

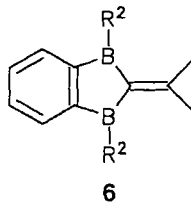
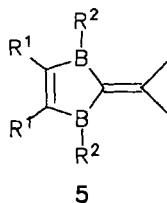
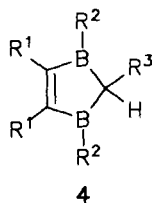
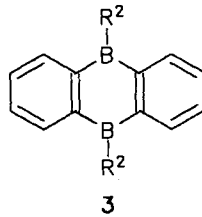
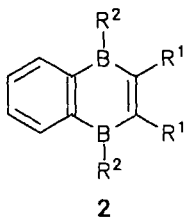
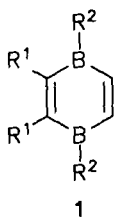
Anorganisch-Chemisches Institut der Universität Heidelberg  
W-6900 Heidelberg, Germany

I.	Introduction . . . . .	187
II.	1,4-Diboracyclohexadiene Metal Complexes . . . . .	191
III.	1,4-Dihydro-1,4-Diboranaphthalene Metal Complexes . . . . .	194
IV.	9,10-Dihydro-9,10-Diboraanthracene Metal Complexes . . . . .	197
V.	2,3-Dihydro-1,3-Diborolyl Metal Complexes . . . . .	202
VI.	1,3-Diborafulvene Metal Complexes . . . . .	205
VII.	Concluding Remarks . . . . .	208
	References . . . . .	209

## I

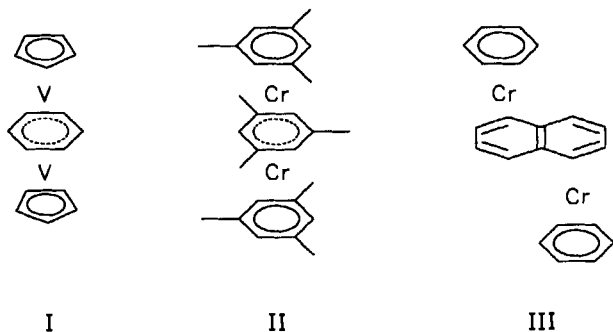
### INTRODUCTION

The donor and acceptor properties of the heterocycles 1,4-diboracyclohexadiene (**1**), 1,4-diboracyclohexene ( $1H_2$ ), 1,4-dihydro-1,4-diboranaphthalene (**2**), 9,10-dihydro-9,10-diboraanthracene (**3**), as well as the five-membered heterocycles 2,3-dihydro-1,3-diborol (**4**) and the 1,3-dihydro-1,3-diborafulvenes (**5** and **6**), allow the formation of mono-, di-, and trinuclear complexes. Usually the metals are anti-facially coordinated to



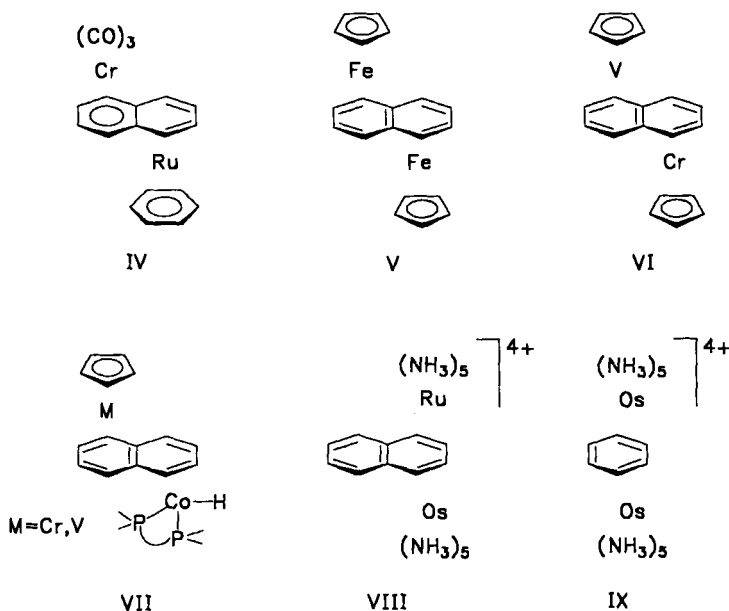
the bridging ligand, resulting in a regular or a slipped triple-decker arrangement. The two metal moieties should at least be connected via two-ring atoms of the bridging ligand and share its  $\pi$ -electrons. When each of the metals has its own 18 VE configuration, the anti-dinuclear compound does not belong to the family of triple-decker complexes. The boron heterocycles **1–6** ( $R^1 = \text{Et}$ ,  $R^2 = \text{Me}$ ) have  $2\pi$  electrons less than their parent carbacyclic compounds benzene, naphthalene, anthracene, cyclopentadiene, and fulvene. Due to the high acceptor capabilities of the two alkylboron groups, unique ligand properties of these heterocycles are observed. Several reviews on the synthesis and reactivity of diboraheterocycles are available (1–9); this article summarizes results on di- and trinuclear complexes.

The organic  $\pi$ -ligands have played the leading role in the development of organometallic  $\pi$ -complex chemistry (10). However, examples of di- and trinuclear complexes of the carbacyclic  $\pi$ -systems have only been synthesized in the last decade. First, a short survey on di- and trinuclear metal complexes of hydrocarbon  $\pi$ -ligands is given; detailed information is in reviews of Wadepohl (11) and Jonas (12). The chemistry of  $\mu$ -arene triple-decker compounds was initiated by Jonas' group (13), who synthesized the remarkable 26 VE triple-decker sandwich bis( $\eta^5$ -cyclopentadienyl)vanadium( $\mu_6$ -benzene) (**I**). The paramagnetic complex easily undergoes an



exchange reaction of the bridging arene ligand. On the basis of PE spectra, an MO scheme for **I** that indicates four unpaired electrons was calculated (14). This was confirmed by magnetic measurements. The dichromium-trimesitylene complex (**II**) reported by Lamanna and co-workers (15) is a closed-shell species, which fits the 30/34 VE rule of Hoffmann *et al.* for triple-decker complexes (16).

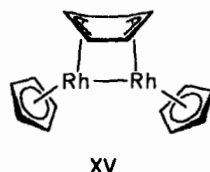
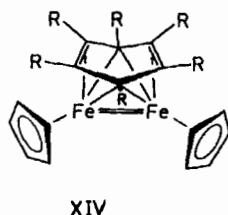
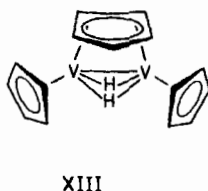
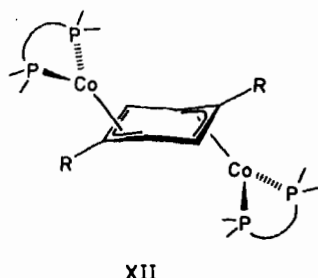
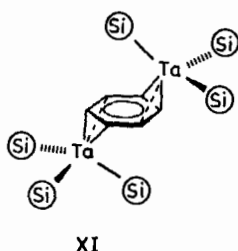
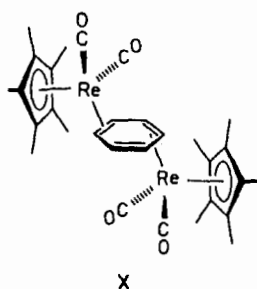
The dichromium- $\mu$ -naphthalene compound (**III**) of Lagowski *et al.* (17) is a slipped triple-decker sandwich, in which the metals share two  $\pi$ -electrons of the bridging carbon atoms (C9,10 of naphthalene) and thus complete their 18e shell. In the dinuclear CrRu- $\mu$ -naphthalene complex



(IV) of Hull, Jr., and Gladfelter (18), each metal has a filled 18e shell. Jonas (12) contributed the interesting complexes V to VII to the growing number of dinuclear  $\mu$ -naphthalene compounds. In V, the  $(C_5H_5)Fe$  moieties are attached to the doubly folded bridging naphthalene: The four outer carbon atoms are complexed diene-like to an iron atom [Fe-C 2.018(2) to 2.111(2) Å], whereas the bridging carbon atoms are bonded to both iron atoms [Fe-C 2.457(2), 2.466(2) Å]. Mössbauer data indicate that the iron atoms are identical. V has 36 and VI has 31 VE. In the complexes VII with  $M = Cr$  a total of 35 VE and  $M = V$ , 34 VE are present.

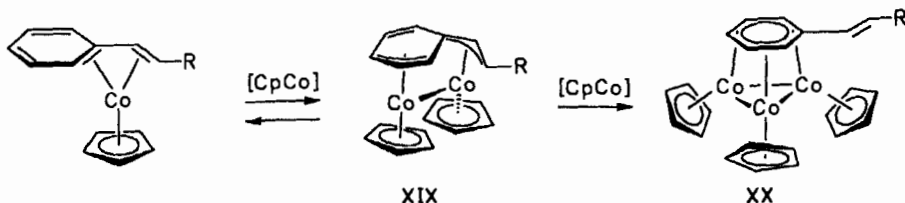
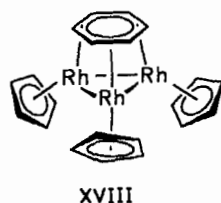
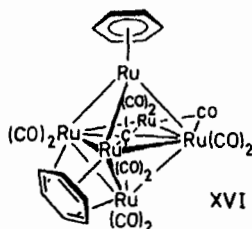
Binuclear complexes of naphthalene (VIII) and of benzene (IX) with  $[Os(NH_3)_5]^{2+}$  and  $[Ru(NH_3)_5]^{2+}$  moieties were reported by Taube *et al.* (19), in which anti- $(\mu-1,2-\eta^2:3,4-\eta^2)$  coordination of the arene is present. This bonding mode was first observed by Pasman *et al.* (20) in the binuclear Rhenium complex X. Wolczanski *et al.* (21) obtained complex XI from the mononuclear complex  $[Ta(O-Si^tBu_3)_3(\eta^2-(N,C)\text{-pyridine})]$  and benzene. Each tantalum atom is bound unsymmetrically to one C=C bond of benzene with a weak interaction to a third carbon atom; the bonding may be described as a distorted  $\eta^3$ -enyl. In the dinuclear cobalt complex XII, the xylene functions as a bis(enyl)-ligand (12,22).

Whenever two metal moieties are syn-facially coordinated, a metal-metal bond is observed. In XIII and XIV, reported by Jonas *et al.* (23,24),



all arene carbon atoms are bonded to the  $M_2$  unit. **XIII** is obtained from  $[K(Cp_2V)]$  and cyclohexadiene via dehydrogenation, and **XIV** is formed from  $[CpFe(C_8H_{12})]$  and alkynes via cyclotrimerization.

Müller *et al.* (25) have obtained the complex **XV** with  $\text{syn}(1-3\eta:4-6\eta)$ -bonded  $\mu_2$ -benzene by irradiating  $[CpRh(C_2H_4)_2]$  and benzene in hexane. On longer irradiation the trinuclear  $\text{syn}$ -complex, **XVIII** is formed, in

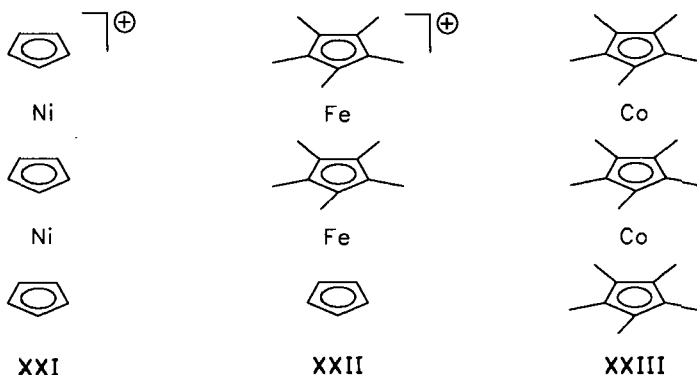


which the arene ligand coordinates to three metals. The first example of a  $(\mu\text{-arene})M_3$  complex is **XVI**, reported by Lewis and co-workers (26) in 1985. In the octahedral cluster, one benzene ring interacts with three

ruthenium atoms, and the other benzene molecule functions as an  $\eta^6$ -ligand to a single Ru center. Two examples of the type **XVII** were also synthesized by the Cambridge groups: Three Os(CO)<sub>3</sub> and three Ru(CO)<sub>3</sub> fragments are connected via metal-metal bonds (27).

Wadepohl *et al.* (11,28) developed a new method of synthesizing trico-balt clusters with face-capping arene ligands: 1-alkenyl benzenes react with the Jonas reagent CpCo(C<sub>2</sub>H<sub>4</sub>)<sub>2</sub> (29) or with CpCo(C<sub>6</sub>H<sub>6</sub>) to give via the proposed dinuclear complexes **XIX** the [(CpCo)<sub>3</sub>( $\mu_3$ -arene)] clusters **XX**. The 1-alkenyl group acts as a "landing strip" for the first CpCo fragment; benzene and alkylbenzenes do not form clusters of the type **XX**.

As an introduction to five-membered heterocyclic ligands, a brief summary of bifacially coordinated cyclopentadienyl ligands is given. The first triple-decker sandwich was reported in 1972 by Werner and Salzer (30), who obtained the diamagnetic Cp<sub>3</sub>Ni<sub>2</sub><sup>+</sup> cation (**XXI**) by reacting nickeloc-



cene with HBF<sub>4</sub>. Its closed-shell configuration has 34 VE. Hoffman *et al.* (16) first reported the electronic structure of triple-decker compounds and thus initiated an increasing interest in this field. However, it took 15 years from the synthesis of **XXI** until the FeFe triple-decker cation **XXII** (30 VE) along with the [RuRu]<sup>+</sup> and [OsOs]<sup>+</sup> analogs were prepared by Rybinskaya *et al.* (31). Very recently Schneider *et al.* (32) reported the neutral CoCo triple-decker **XXIII** (33 VE).

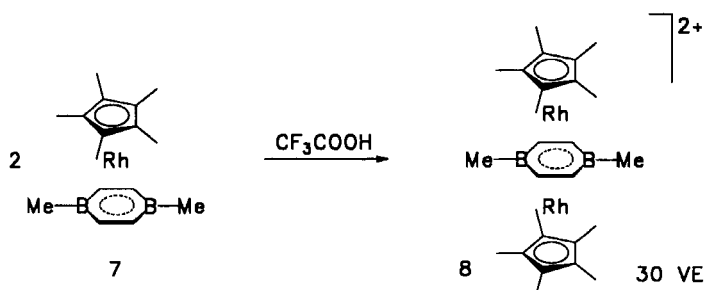
## II

### 1,4-DIBORACYCLOHEXADIENE METAL COMPLEXES

B-Alkyl derivatives of the 1,4-diboracyclohexadiene (**1**) (R<sup>2</sup> = Me, Et) are labile and rearrange to nido carboranes with the C<sub>4</sub>B<sub>2</sub> framework,

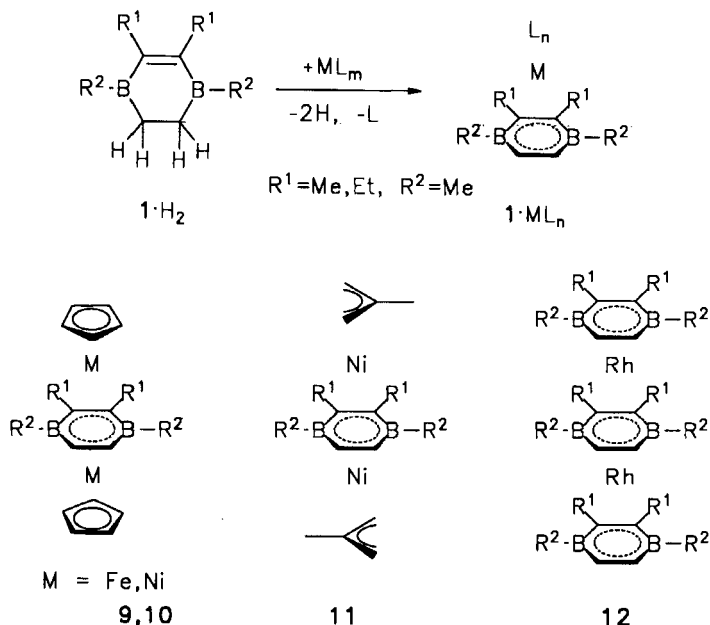


whereas the B-methyl derivatives of the 1,4-dihydro-1,4-diboranaphthalene (**2**) and of the 9,10-dihydro-9,10-diboraanthracene (**3**) are stable, due to the aromatic character of the annelated carbacycles. Timms *et al.* (33) and Herberich (3) have prepared several complexes of **1** with the electron-donating substituents  $R^2 = \text{F, OMe, (C}_5\text{H}_4\text{)FeC}_5\text{H}_5\text{)}$ , which prevent its rearrangement to carboranes. Substitution of  $R^2 = \text{OMe}$  in  $(\text{C}_5\text{Me}_5)\text{Rh}$  (**1**) with  $\text{MeMgI}$  leads to the corresponding dimethyl derivative **7**, which reacts with  $\text{CF}_3\text{COOH}$  to give the first triple-decker **8** with the 1,4-dimethyl-1,4-

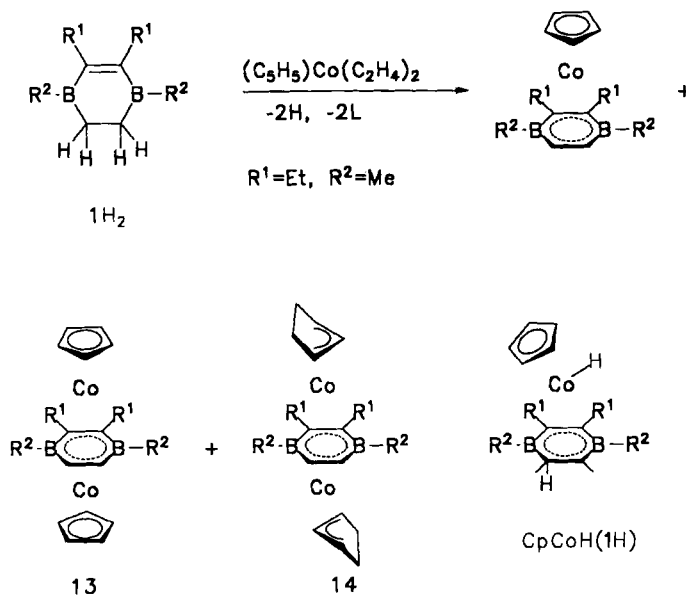


diboracyclohexadiene as  $\mu, \eta^6, \eta^6$ -ligand (34). This triple-decker dication has 30 VE (closed shell).

Recently we reported the synthesis of the 1,4-diboracyclohexene derivatives ( $1\text{H}_2$ ) ( $R^1 = \text{Et, } R^2 = \text{Me}$ ), which allow the formation of mono- and



dinuclear 1,4-diboracyclohexadiene complexes (**35**). Via dehydrogenation of  $1H_2$  ( $R^1 = R^2 = Me$ ) during complexation (C–H activation by the metal) the Lewis-acid 18 VE complexes ( $1$ ) $ML_n$  are formed. Attack of a further metal complex fragment  $ML_n$  at the complexed boron heterocycle leads to anti-facial coordination. The obtained triple-decker sandwich complexes **9** (30 VE) and **10** (34 VE) are closed-shell species (**36**). The 30 VE bis(methallyl)-nickel triple-decker **11** is formed as a mixture of *cis*-/*trans*-isomeres (of the methallyl groups). The 30 VE complex **12** is entirely composed of the ligand **1** and is obtained from the reaction of  $1H_2$  with  $[(C_2H_4)_2RhCl]_2$ . The reaction of  $1H_2$  with  $(C_5H_5)Co(C_2H_4)_2$  yields the expected sandwich, the 32 VE triple-decker **13**, and, surprisingly, the bis(cyclopentenylcobalt) triple-decker **14** with 28 VE (**37**). Both dinuclear



complexes are paramagnetic, and **14** exhibits a temperature-dependent  $^1H$  NMR spectrum. The constitution of **14** was confirmed by X-ray structure analysis (Fig. 1). It is formed by hydrogenation of both cyclopentadienyl ligands during complexation: The hydrogen of the activated C–H bond of the ligand  $1H_2$  is transferred via the cobalt atom to the cyclopentadienyl ligand. The expected intermediate  $(C_5H_5)Co(H)(1H)$ , in which one hydrogen in  $(C_5H_5)Co(1H_2)$  has moved to the cobalt atom, could be identified by  $^1H$  NMR; however, the signal for Co–H was not found.

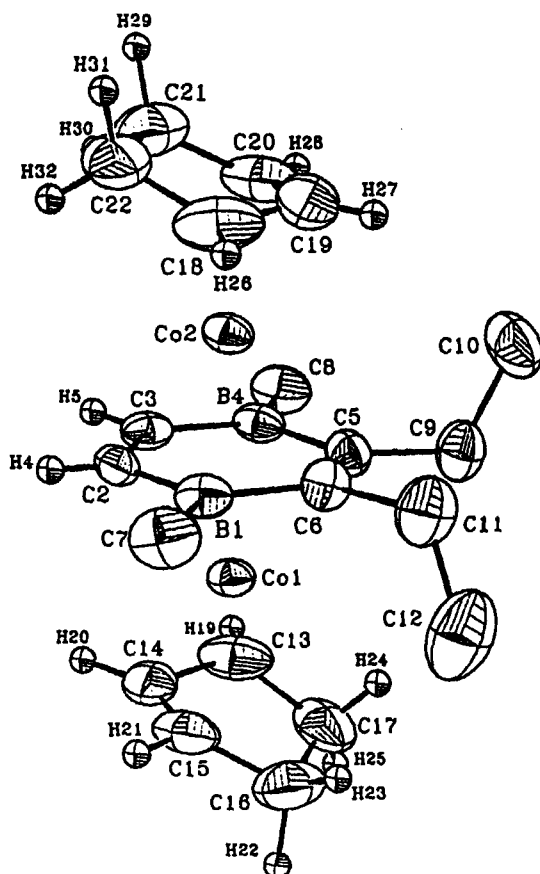
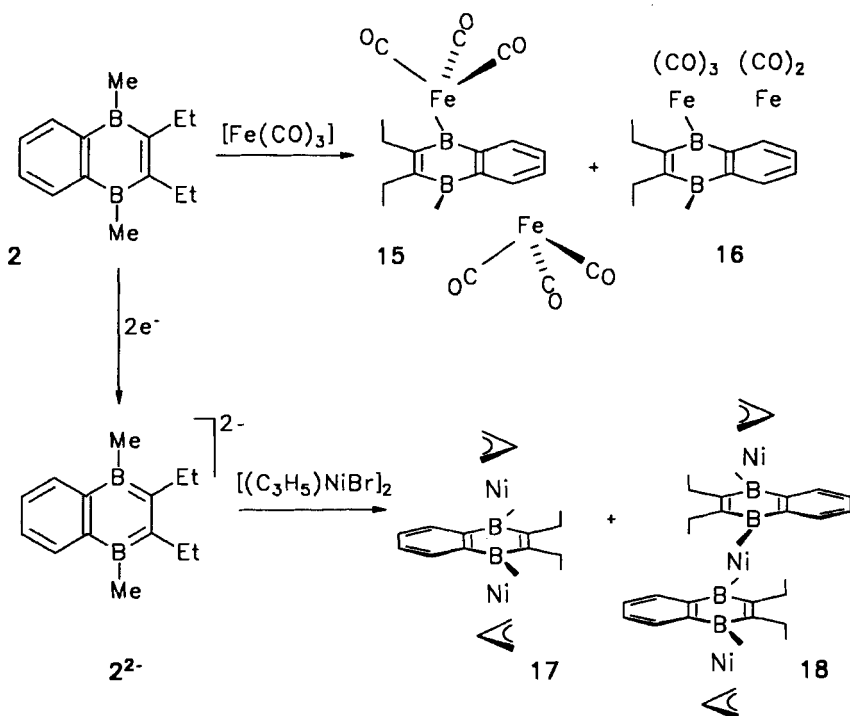


FIG. 1. Molecular structure of anti- $((\eta^3\text{-C}_5\text{H}_7)\text{Co})_2(\mu, \eta^6, \eta^6\text{-(EtC)}_2(\text{MeB})_2(\text{CH})_2)$  (**14**).

### III

#### 1,4-DIHYDRO-1,4-DIBORANAPHTHALENE METAL COMPLEXES

The 2,3-diethyl-1,4-dihydro-1,4-dimethyl-1,4-diboranaphthalene (**2**) (**38**) reacts with  $(\text{CO})_3\text{Fe}(\text{C}_8\text{H}_{14})_2$  to give the orange anti-dinuclear complex **15** and the cherry-red syn-complex **16** (**39**). Its formation occurs via the mononuclear complex  $(\text{2})\text{Fe}(\text{CO})_3$ , which is attacked by the second  $\text{Fe}(\text{CO})_3$  moiety at the diene of the  $\eta^2$ -complexed benzo-ring. Obviously the anti-complex **15** (43%) is favored over the syn-product **16** (14%). In **16** a weak iron-iron interaction (2.98 Å) is present. On the basis of the 18 VE



rule, two electrons must be shared by both iron centers, since only five CO ligands are attached to the iron atoms. The X-ray structure analysis of 16 reveals an unexpected structural feature: The  $\text{Fe}(\text{CO})_3$  group of the heterocycle in (2) $\text{Fe}(\text{CO})_3$  is shifted from  $\eta^6$ - to  $\eta^4$ -bonding upon coordination of the  $\text{Fe}(\text{CO})_2$  group, which binds to the benzo-ring in  $\eta^6$ -fashion. As shown in Fig. 2, the 1,4-diboranaphthalene in 16 is almost planar, and in 15 a considerable bending of the benzo-ring occurs as observed in many diene-tricarbonyliron complexes. The isomer of 16 with the  $\text{Fe}(\text{CO})_3$  and  $\text{Fe}(\text{CO})_2$  groups anti-facially coordinated at the heterocycle would have a 30 VE triple-decker structure. However, the electron-accepting CO ligands do not allow the formation of the regular triple-decker arrangement.

When 2 is reacted with  $[(\text{C}_3\text{H}_5)\text{FeC}_8\text{H}_{12}]_2\text{Zn}$  at  $160^\circ\text{C}$  in mesitylene, the formation of the green, 30 VE triple-decker sandwich  $[(\text{C}_3\text{H}_5)_2\text{Fe}]_2-\mu^6-(2)$  occurs. The 13 VE  $\text{CpFe}$  moieties are anti-bound to the 1,4-diboracyclohexadiene of 2 in remarkable difference to the 14 VE  $(\text{CO})_3\text{Fe}$  complex fragments (Fig. 3). Similarly, with the  $\text{Ni}(\text{C}_3\text{H}_5)$  group—isolobal with

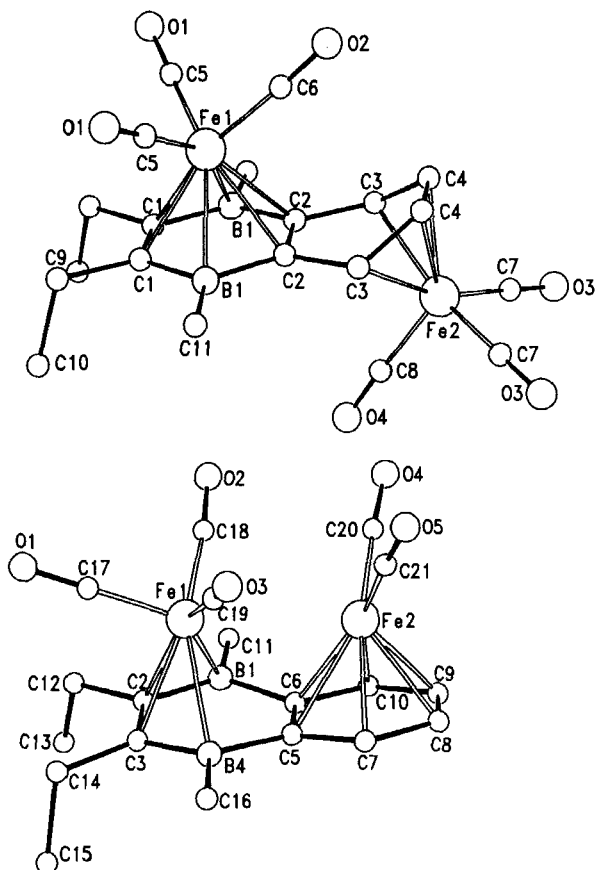


FIG. 2. Molecular structures of anti-(CO)<sub>3</sub>Fe(μ,η<sup>6</sup>,η<sup>4</sup>-(EtC)<sub>2</sub>(MeB)<sub>2</sub>C<sub>6</sub>H<sub>4</sub>)Fe(CO)<sub>3</sub> (15) and syn-(CO)<sub>3</sub>Fe(μ,η<sup>4</sup>,η<sup>6</sup>-(EtC)<sub>2</sub>(MeB)<sub>2</sub>C<sub>6</sub>H<sub>4</sub>)Fe(CO)<sub>2</sub> (16).

Fe(C<sub>3</sub>H<sub>5</sub>) — the triple-decker 17 is preferred: The dianion 2<sup>2-</sup> reacts with [(C<sub>3</sub>H<sub>5</sub>)NiBr]<sub>2</sub> to give red 17 (36%) and in low yield the diamagnetic tetradecker complex 18 (40). This trinuclear species has 44 VE and should be paramagnetic for a regular tetradecker. The X-ray structural data (Fig. 3) prove the slipped arrangement around the central nickel atom: It is only tetrahapto-bonded to each of the 1,4-diboracyclohexadiene ligand, whereas the (C<sub>3</sub>H<sub>5</sub>) Ni groups are η<sup>6</sup>-coordinated. The formation of the centrosymmetric 18 most likely occurs via (2)Ni(C<sub>6</sub>H<sub>10</sub>), obtained from 2 and Ni(C<sub>3</sub>H<sub>5</sub>)<sub>2</sub>.

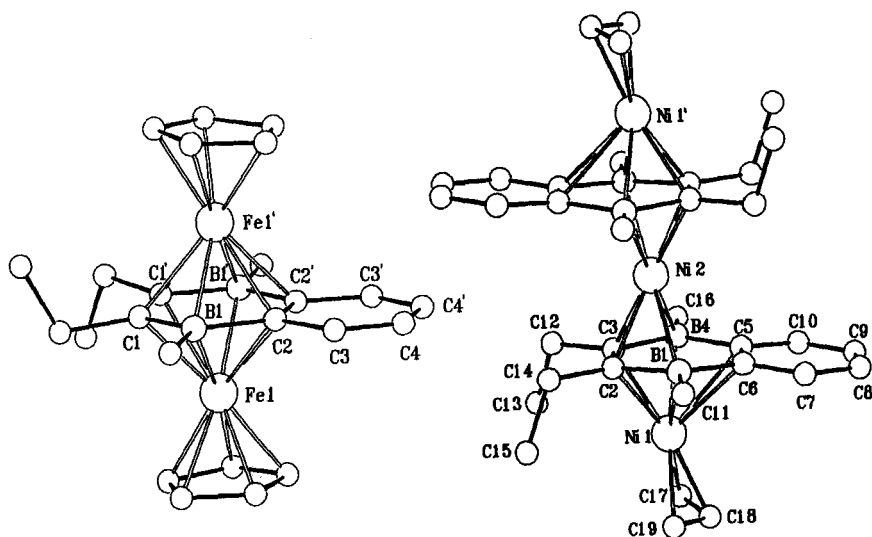


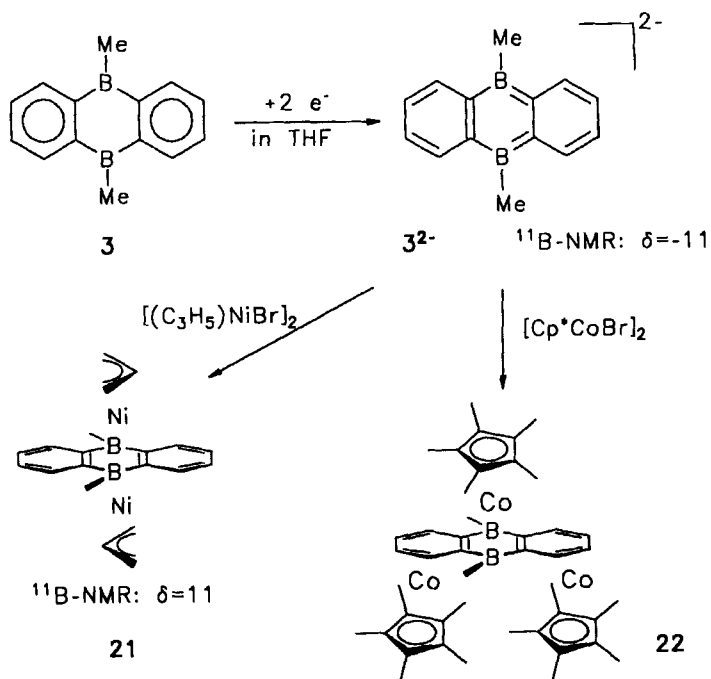
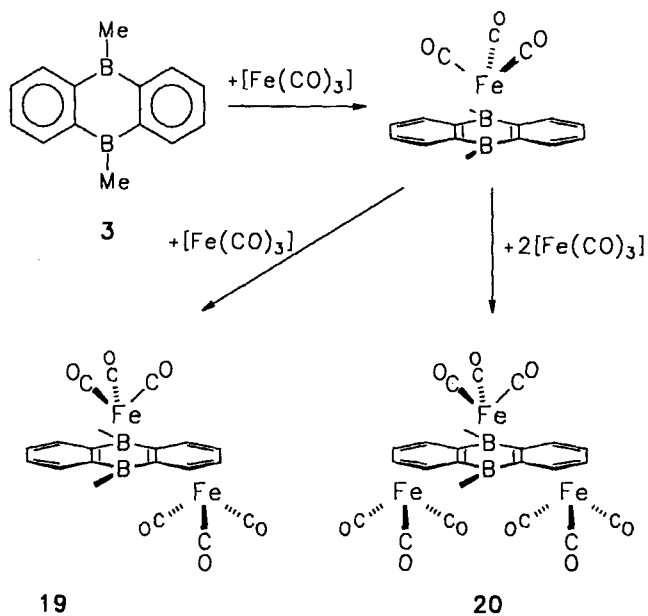
FIG. 3. Molecular structures of anti- $\{(\eta^3\text{-C}_3\text{H}_5)\text{Fe}\}_2(\mu, \eta^6, \eta^6\text{-(EtC)}_2(\text{MeB})_2\text{C}_6\text{H}_4)$  and anti- $\{(\eta^3\text{-C}_3\text{H}_5)\text{Ni}(\mu, \eta^6, \eta^4\text{-(EtC)}_2\text{C}_6\text{H}_4)\}_2\text{Ni}$  (18).

#### IV

#### 9,10-DIHYDRO-9,10-DIBORAANTHRACENE METAL COMPLEXES

Reaction of 9,10-dihydro-9,10-dimethyl-9,10-diboraanthracene (3) with  $(\text{CO})_3\text{Fe}(\text{C}_8\text{H}_{14})_2$  gives green  $(\text{CO})_3\text{Fe}(\eta^6\text{-(3)})$ , red  $[(\text{CO})_3\text{Fe}]_2(\eta^4, \eta^6\text{-(3)})$  (19), and orange  $[(\text{CO})_3\text{Fe}]_3(\eta^4, \eta^4, \eta^6\text{-(3)})$  (20). The constitutions of these complexes are derived from NMR, IR, and MS data and confirmed by X-ray structure analyses (Fig. 4). 19 and 20 are formed from planar  $(\text{CO})_3\text{Fe}(\eta^6\text{-(3)})$  by complexation of the diene of one and both benzo-rings *anti*- to the  $\eta^6$ -bonded  $\text{Fe}(\text{CO})_3$  group (41). These complexes are obtained even when the ration 3: $(\text{CO})_3\text{Fe}(\text{C}_8\text{H}_{14})_2$  is 1:1. An excess of the iron carbonyl exclusively yields 20. Figure 4 shows the molecular structures of 19 and 20.

In  $(\text{CO})_3\text{Fe}(\eta^6\text{-(3)})$ , 19 and 20, the iron atoms are  $\eta^6$ -bonded and are 1.71–1.73 Å from the plane of the heterocycle. The distances are Fe1–B 2.31–2.34 Å and Fe1–C 2.21–2.32 Å with Fe–C11(C12) (average 2.29 Å) longer than Fe–C5(C6) (average 2.24 Å). This indicates a small slippage of Fe<sub>1</sub> from the midpoint, which is caused by a stronger bonding of C5–C6 to the iron center. The noncomplexed carbacycle lies in the plane of the heterocycle. In 19 and 20, the iron atoms are 1.66–1.68 Å away from the C<sub>4</sub> plane, which forms an angle with the plane of the



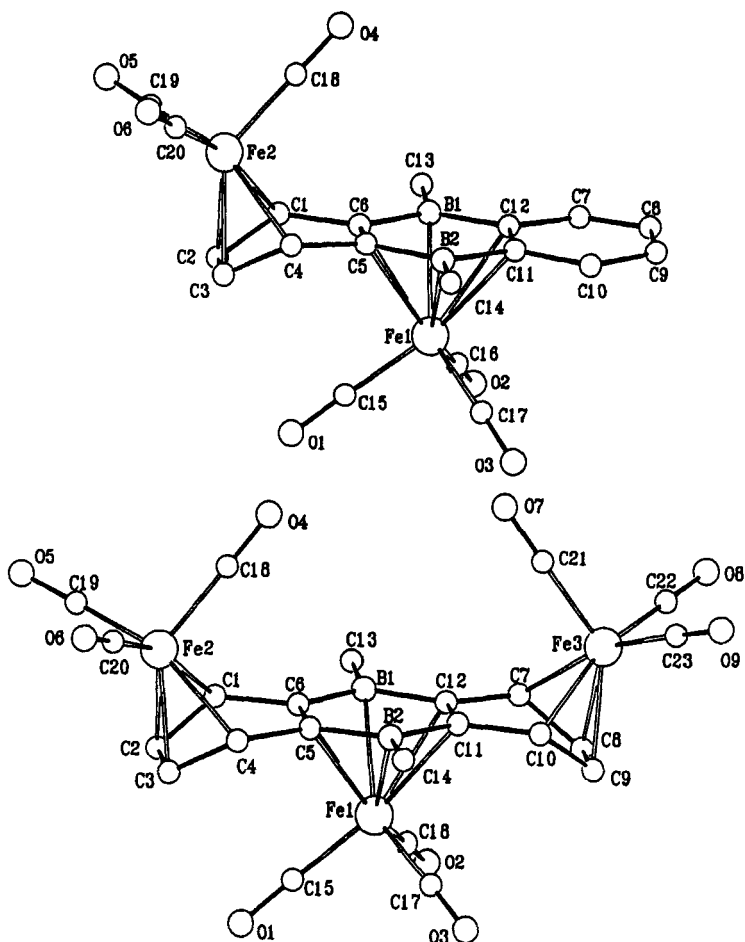


FIG. 4. Molecular structures of anti-(CO)<sub>3</sub>Fe(μ,η<sup>6</sup>,η<sup>4</sup>-(C<sub>6</sub>H<sub>4</sub>)<sub>2</sub>(MeB)<sub>2</sub>)Fe(CO)<sub>3</sub> (**19**) and anti-(CO)<sub>3</sub>Fe(μ,η<sup>6</sup>,η<sup>4</sup>,η<sup>4</sup>-(C<sub>6</sub>H<sub>4</sub>)<sub>2</sub>(MeB)<sub>2</sub>)(Fe(CO)<sub>3</sub>)<sub>2</sub> (**20**).

heterocycle ( $\angle 30-38^\circ$ ). The distances between iron and the outer C atoms of the formed butadiene systems are 2.14–2.18 Å, whereas the inner C atoms are closer (2.05–2.06 Å). The center C—C bond (C2—C3, C8—C9, average 1.39 Å) is shorter than the outer C—C bonds (average 1.42 Å). In the noncomplexed carbacycles the inner C—C (1.395 Å) is longer than the outer C—C (1.355 Å), as in many butadiene complexes (42).

The dihydrodiboranthracene **3** easily forms the dianion  $3^{2-}$ , which reacts with the corresponding organometal halides to give the bis(allylnickel) triple-decker **21** and the trinuclear Cp\*Co complex **22** (where Cp\*



is  $\eta^5\text{-C}_5\text{Me}_5$ ), which is isoelectronic with **20**. The constitution of **21** and **22** follows from NMR and MS data, and it is confirmed by X-ray structure analyses (43). The plots of **21** and **22** in Fig. 5 show that **21** has a planar diboraanthracene ligand **3** analogous to  $(\text{CO})_3\text{Fe}(\eta^6\text{-(3)})$ . As in the tetra-decker **18**, the two nickelallyl groups are  $\eta^6$ -coordinated in the 30 VE triple-decker **21**. The tricobalt complex **22** is isostructural with the triiron complex **20**; the cobalt atoms Co2 and Co2' are each  $\eta^4$ -coordinated to the diene systems of the benzo-rings. This result indicates that the  $\text{Cp}^*\text{Co}$

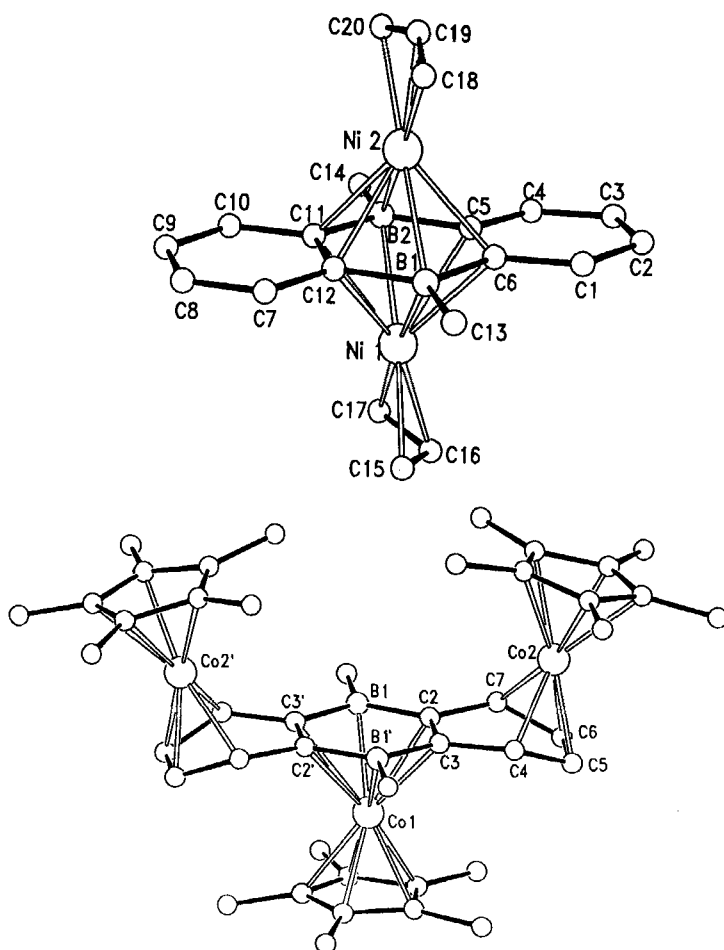
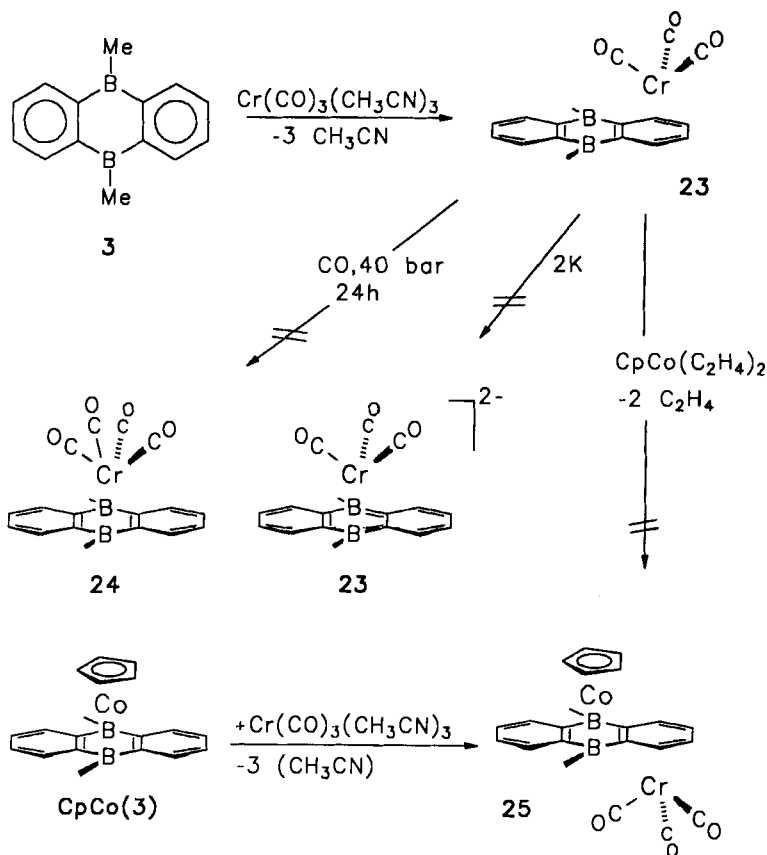


FIG. 5. Molecular structures of anti- $\{(\eta^5\text{-C}_5\text{H}_5)\text{Ni}\}_2(\mu\text{-}\eta^6,\eta^6\text{-(C}_6\text{H}_4)_2(\text{MeB})_2\}$  (**21**) and anti- $\{(\eta^5\text{-C}_5\text{Me}_5)\text{Co}(\mu\text{-}\eta^6,\eta^4,\eta^4\text{-(C}_6\text{H}_4)_2(\text{MeB})_2\{(\eta^5\text{-C}_5\text{Me}_5)\text{Co}\}_2\}$  (**22**).

moiety avoids the formation of the 32 VE triple-decker  $(\text{Cp}^*\text{Co})_2(\mu, \eta^6\text{-(3)})$  with a triplet groundstate, although the corresponding  $(\text{CpCo})_2\text{-(}\mu, \eta^6\text{-(1))}$  (**13**) is known.

The reaction between **3** and  $(\text{CO})_3\text{Cr}(\text{NCCH}_3)_3$  leads to a surprising result: The attack of the chromium moiety does not occur at the heterocycle, but at the benzo-ring to yield **23**. Our attempts failed to form **24** by

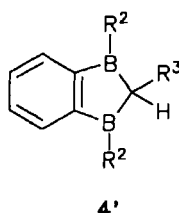
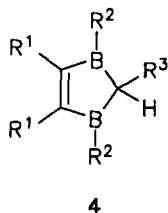


applying CO pressure on **23**; also the formation of the dianion of **23** with slippage of the  $(\text{CO})_3\text{Cr}$  group to the heterocycle did not occur. Surprisingly, **23** could not be stacked with the  $\text{CpCo}$  group to yield **25**, a slipped triple decker (34 VE), in which the metals share two  $\pi$ -electrons. However, the formation of **25** was achieved by reacting  $(\text{CpCo})(\eta^6\text{-(3)})$  with  $(\text{CO})_3\text{Cr}(\text{NCCH}_3)_3$  (**44**).

## V

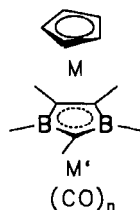
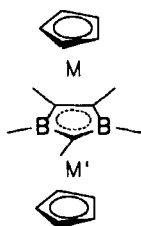
## 2,3-DIHYDRO-1,3-DIBOROLYL METAL COMPLEXES

In the past decade we have studied the ligand properties of the 2,3-dihydro-1,3-diborole (**4**), and the results are described in several reviews (6–9). The benzo-1,3-diborole (**4'**) with hydrogen atoms in two-position exhibits



a reduced stability: Two molecules **4'** undergo a condensation reaction to form the diboraanthracene **3** (**45**). Recently Herberich *et al.* (**46**) have synthesized the 4-methylene-1,2-diborolane, deprotonated it to the corresponding dianion, and protonated it to yield the 4-methyl-1,2-diborole. The dianion reacts with  $[(C_8H_{12})RhCl]_2$  to give the slipped triple-decker  $[(C_8H_{12})Rh]_2(\mu, \eta^4, \eta^5\text{-4,5-diborafulvene})$  (**47**) (Section VI).

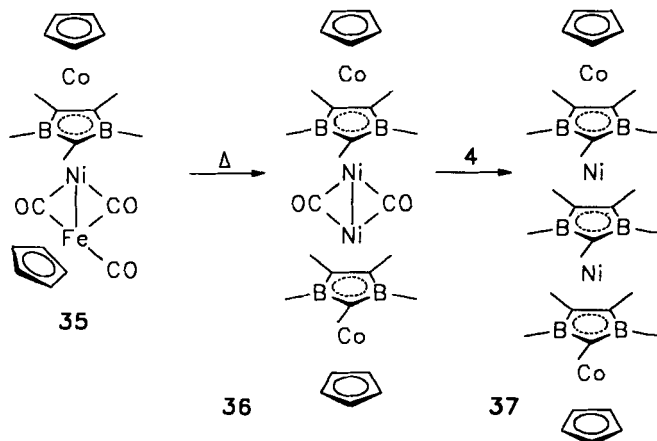
The 1,3-diborolyl ligand (**4-H**) functions as a 3e donor and as a good electron acceptor (formally 3e), which allowed the formation of the first complete family of triple-decker sandwich complexes (**26**<sup>+</sup>–**30**<sup>–</sup>) (**6**) ranging from FeFe<sup>+</sup> cation (28 VE) to NiNi<sup>–</sup> anion (34 VE). In addition, the unsymmetrical triple-decker **31**–**34** have been reported; however, we did not succeed in the synthesis of any triple-decker with CO ligands in both terminal decks. The complexes **26**–**34** exhibit an interesting redox behavior and reactivity. The paramagnetic triple-decker **29** and **30** react with



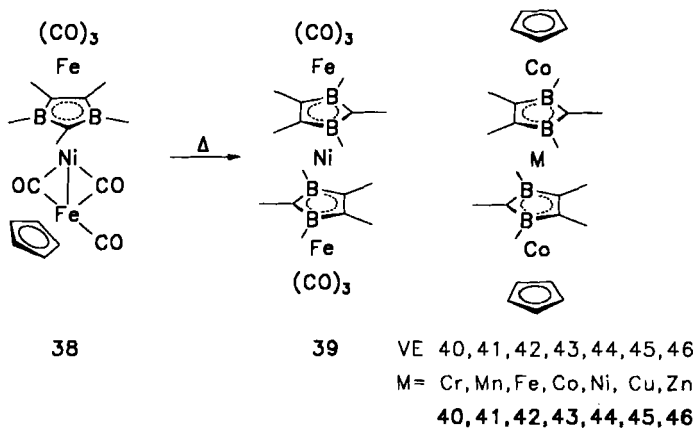
M	Fe	Fe	Co	Co	Ni	Ni <sup>1–</sup>
M'	Fe	Co	Co	Ni	Ni	Ni
VE	29	30	31	32	33	34
	26	27	28	29	30	30 <sup>–</sup>

M	Fe	Co	Ni	Co
M'	Fe	Fe	Fe	Co
	(CO) <sub>3</sub>	(CO) <sub>3</sub>	(CO) <sub>3</sub>	(CO) <sub>2</sub>
	31	32	33	34

$\text{Fe}_2(\text{CO})_9$  to give products resulting either from replacement of an  $(\eta^5\text{-C}_5\text{H}_5)\text{Ni}$  fragment by  $\text{Fe}(\text{CO})_3$  or insertion of  $\text{Fe}(\text{CO})_3$  into the  $(\eta^5\text{-C}_5\text{H}_5)\text{—Ni}$  bond (48). Thus, the reaction of **29** with  $\text{Fe}_2(\text{CO})_9$  proceeds via  $\text{Fe}(\text{CO})_3$  insertion into the  $(\eta^5\text{-C}_5\text{H}_5)\text{—Ni}$  bond to yield the trinuclear carbonyl-bridged complex **35** and subsequently by heating the tetranuclear complex **36**, in which the CO groups could be substituted for the 2,3-dihydro-1,3-diborolyl ligand to yield the first pentadecker sandwich complex **37** (49). The constitution of paramagnetic **37** was derived from MS and

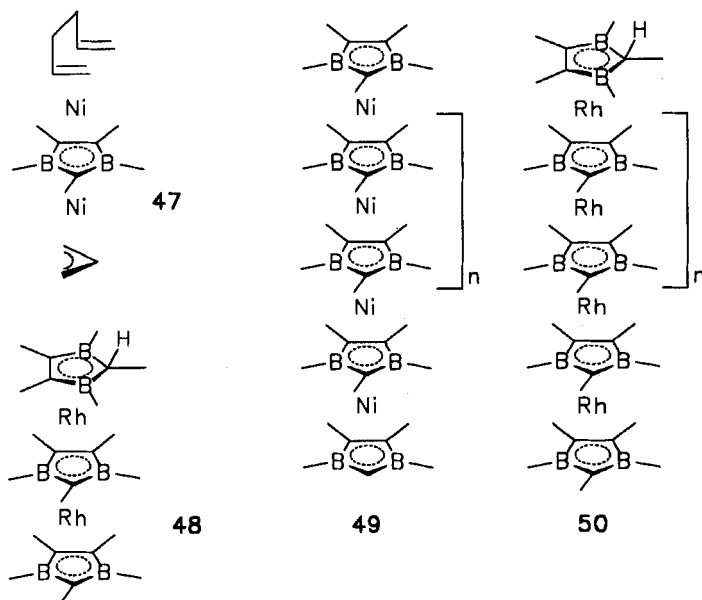


NMR data and confirmed by an X-ray structure analysis. **30** reacts with  $\text{Fe}_2(\text{CO})_9$  to give initially the triple-decker **33**. Subsequent reactions lead to the carbonyl-bridged **38**, the tetradecker **39**, and the triple-decker **31**. The unsymmetrical triple-decker **33** have been made independently by stacking the sandwich  $(\eta^5\text{-C}_5\text{H}_5)\text{Ni}[(4\text{-H})]$  with an  $\text{Fe}(\text{CO})_3$  fragment.



The paramagnetic 44 VE FeNiFe tetradecker **39** has six terminal CO ligands; this result demonstrates that opposite to the nonexistent hexacarbonyl triple-decker, this and related tetradecker are stable, because each  $(\text{CO})_3\text{Fe}$  group is attached only to one ligand (**4-H**). A designed synthesis by reacting the sandwich anion  $[(\text{C}_5\text{H}_5)\text{Co}(\text{4-H})]^-$  with the cations  $\text{Cr}^{2+}$  to  $\text{Zn}^{2+}$  led to the tetradecker sandwich complexes **40–46** (6), in which two CpCo fragments are the terminal groups. Interestingly, all but **46** are paramagnetic species with high-spin configuration in **40–43**. The Zn complex **46** has a closed shell of 46 VE. These findings proved that two 1,3-diborolyl–metal stacking units can be connected, which finally led also to pentadecker, hexadecker, and polydecker complexes.

Black polymers of the type **49** (8) were obtained by thermal polycondensation reactions of trisallyl-dinickel- $\mu$ -1,3-diborolyl triple-decker or its hexadiene-allyl-dinickel- $\mu$ -1,3-diborolyl isomer **47** (50), and **50** was



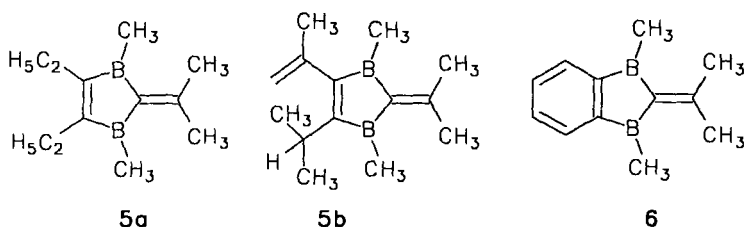
formed by heating the dirhodium triple-decker **48**, which eliminates the terminal 1,3-diborole **4**.

The amorphous, air-sensitive products were studied by EXAFS, which revealed Ni–Ni distances in the range 3.40 Å as in the corresponding triple-decker complexes and Rh–Rh distances of 3.60 Å. The conductivity measurements showed **49** to be a semiconductor ( $10^{-2} \text{ S cm}^{-1}$ , 330 K) and **50** to be an insulator ( $10^{-10} \text{ S cm}^{-1}$ ).

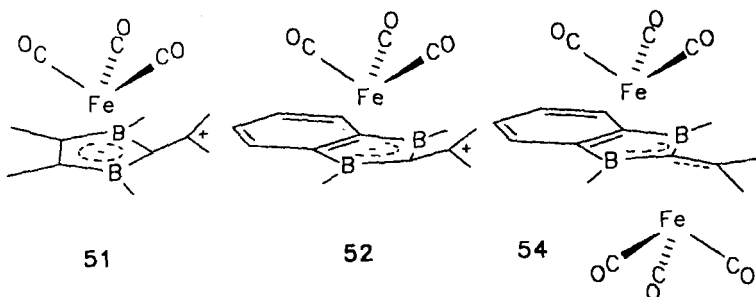
## VI

## 1,3-DIBORAFULVENE METAL COMPLEXES

The 1,3-dihydro-1,3-diborifulvene **5** and its benzo-derivative **6** are the structural isomers of the 1,4-diboracyclohexadiene **1** and the 1,4-dihydro-1,4-diboranaphthalene **2**. The air-sensitive 1,3-diborifulvenes **5a,b** (51) and **6** (38) do not rearrange to nido-carboranes at room temperature;



however, heating of **5a** under nitrogen atmosphere to 120°C yields a carborane as shown by its  $^{11}\text{B}$  NMR signals ( $\delta = -45.4$  and  $+16.6$ ). Reactions of **5a,b** and **6** with  $(\text{CO})_3\text{Fe}(\text{C}_3\text{H}_{14})_2$  lead via the mononuclear complexes **51** and **52** to the violet dinuclear complexes **53** and **54**, which



possess slipped triple-decker structures (**52**). The X-ray structure analyses reveal that one  $\text{Fe}(\text{CO})_3$  group is pentahapto-coordinated to the 1,3-diborole frame of the  $\text{C}_2\text{B}_2\text{C}=\text{C}$ , whereas the other interacts with the Y-shaped  $\text{B}_2\text{C}=\text{C}$  unit. The latter resembles the interaction of  $\text{Fe}(\text{CO})_3$  with trimethylenemethane. The umbrella-like coordination of  $\text{Fe}2$  in **53b** and **54** (Fig. 6) is documented by short  $\text{Fe}2-\text{C}2$  bonds (1.905, 1.918 Å) and longer  $\text{Fe}2-\text{C}6$  bonds (2.118, 2.103 Å), as well as by  $\text{Fe}2-\text{B}1/\text{B}3$  (2.436, 2.424, 2.375, 2.401 Å). The differences in the  $\text{Fe}1-\text{C}4/5$  distances (2.139, 2.156 Å in **53b** and 2.236, 2.227 Å in **54**) are caused by the weaker donor properties of the  $\text{C}4/5$  atoms of the benzo-ring in comparison to the  $\text{C}=\text{C}$

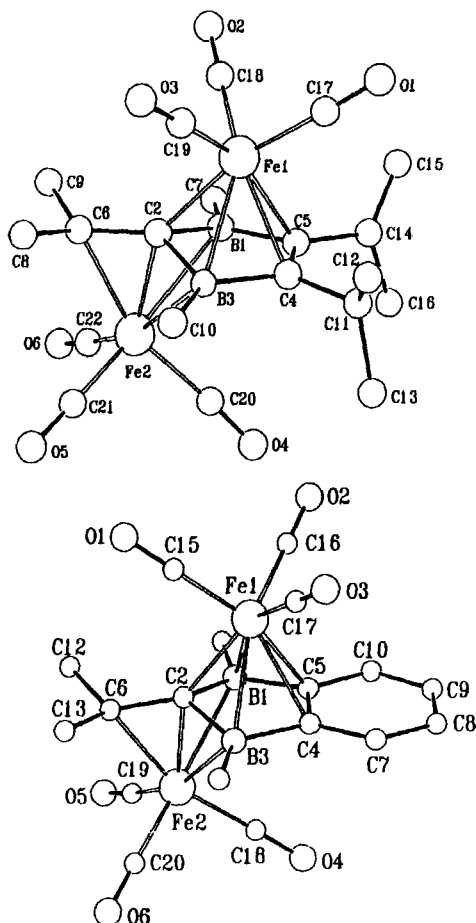
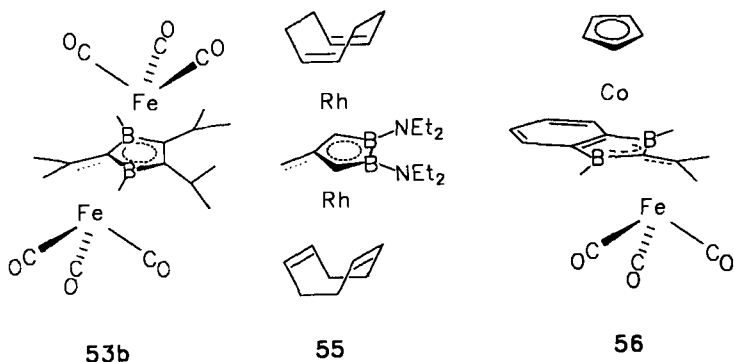


FIG. 6. Molecular structures of anti-(CO)<sub>3</sub>Fe( $\mu$ ,  $\eta^4$ ,  $\eta^5$ -Me<sub>2</sub>C=C(MeB)<sub>2</sub>(CC<sub>3</sub>H<sub>7</sub>)(CC<sub>3</sub>H<sub>3</sub>)) Fe(CO)<sub>3</sub> (**53b**) and anti-(CO)<sub>3</sub>Fe( $\mu$ ,  $\eta^4$ ,  $\eta^5$ -Me<sub>2</sub>C=C(MeB)<sub>2</sub>(C<sub>6</sub>H<sub>4</sub>)) Fe(CO)<sub>3</sub> (**54**).

bond in **5b**. The folding along B1—B3 increases from 9.9° in **6** to 16.3° in **54**. An MO calculation indicates that the formation of **53** and **54** occurs by distortion of **51** and **52**; the slippage of Fe(CO)<sub>3</sub> from  $\eta^5$ - to  $\eta^4$ -bonding is followed by  $\eta^5$ -coordination of the second Fe(CO)<sub>3</sub> group. When **6** is reacted with (CO)<sub>3</sub>Fe(C<sub>8</sub>H<sub>14</sub>)<sub>2</sub> and (C<sub>5</sub>H<sub>5</sub>)Co(C<sub>2</sub>H<sub>4</sub>)<sub>2</sub> in a 1 : 1 : 1 ratio, the diamagnetic slipped triple-decker **56** is obtained, which is also formed when **52** is stacked with the Co(C<sub>5</sub>H<sub>5</sub>) fragment (**53**).

The X-ray structure analysis reveals that the Co(C<sub>5</sub>H<sub>5</sub>) moiety is  $\eta^5$ -coordinated to the 1,3-diborole ring, and the Fe(CO)<sub>3</sub> group interacts with the Y-shaped B<sub>2</sub>C=C unit. It is similar to that of **54**; the folding of the



diborole along B1—B3 has increased to 20°. The C<sub>2</sub> atom lies 0.25 Å above and the Fe1 atom 1.66 Å below the plane through B1, B3, and C6. Because of the umbrella-like bonding of the B<sub>2</sub>C=C to the iron, the B—C<sub>2</sub> distance (1.67 Å) is longer than in diborolyl rings (1.56 Å). It is to compare with the B—C<sub>2</sub> bond in 1,3-diborole complexes, in which the C<sub>2</sub> atom between the boron atoms is pentacoordinated as in **53**, **54**, and **56**. The two metals in **56** form stronger bonds to C<sub>2</sub> than in other 1,3-diborolyl metal complexes. An MO calculation indicates that the formation of **56** occurs by distortion of **52** ( $\eta^5$ -  $\rightarrow$   $\eta^4$ -bonding of the Fe(CO)<sub>3</sub> group) and  $\eta^5$ -complexation of the Co(C<sub>5</sub>H<sub>5</sub>) fragment (Fig. 7). **56** is 16 kcal/mol

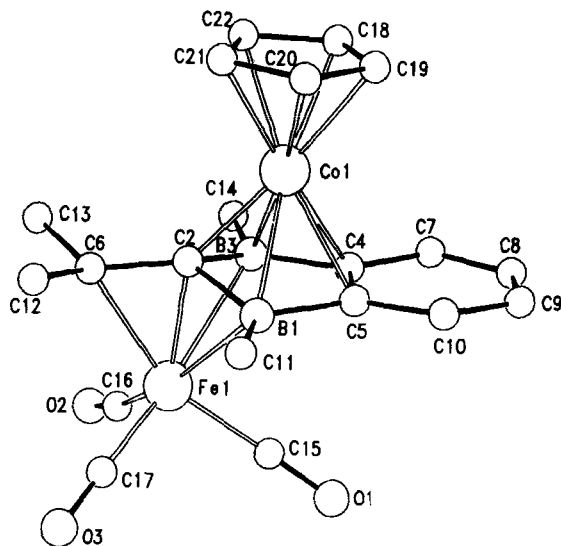


FIG. 7. Molecular structure of anti-(CO)<sub>3</sub>Fe( $\mu$ , $\eta^4$ , $\eta^5$ -Me<sub>2</sub>C=C(MeB)<sub>2</sub>(C<sub>6</sub>H<sub>4</sub>))Co(C<sub>5</sub>H<sub>5</sub>) (**56**).



more stable than its structural isomer, in which  $\text{Fe}(\text{CO})_3$  is  $\eta^5$ , and  $\text{Co}(\text{C}_3\text{H}_3)$  is  $\eta^4$  bonded (53).

The first dinuclear complex of a diborifulvene was reported by Herberich *et al.* (47). They reacted the 3,4-diboratafulvene derivative  $\text{Li}_2[\text{H}_2\text{C}(\text{CHBNEt}_2)_2]$  with  $[\text{RhCl}(\text{COD})]_2$  and obtained the 3,4-diborifulvene complex 55. The complexes 53b and 55 are almost isostructural; however, they have 32 and 30 VE, respectively.

## VII

### CONCLUDING REMARKS

In the past decade,  $\pi$ -organoboron heterocycles and carborane ligands with the frame atoms  $\text{C}_3\text{B}_2$  and  $\text{C}_2\text{B}_3$  (1) have contributed much to the development of stacked sandwich compounds. Whereas the carbacyclic  $\pi$ -systems benzene and cyclopentadienyl only allowed the formation of triple-decker complexes, the unsaturated organoboranes 1,2,5-thiadiborole (2) and 1,3-diborole (4) were first used for the construction of tetradeccker complexes (6). The unique properties of the  $\text{C}_3\text{B}_2$  ligand (4) made it also possible to synthesize pentadecker, hexadecker, and polydecker complexes, as well as to construct triple-decker (54) and tetradeccker complexes (55), which incorporate the  $\text{C}_3\text{B}_2$  and the  $\text{C}_2\text{B}_3$  carboranyl ligand. These results demonstrate that mixed-ligand complexes are stable, and most likely these di- and trinuclear "hybrid" complexes may be used for the formation of novel oligo- and polydecker complexes. The oligodecker complex chemistry of six-membered diboraheterocycles has only one example; the slipped tetradeccker 18 with 2 as bridging ligand could be obtained. It is obvious that the number of VE and the ring size is important for the formation of stacked organometallic complexes. A combination of five- and six-membered unsaturated organoboranes and/or carborane ligands should result in interesting products.

### ACKNOWLEDGMENTS

I thank my co-workers for their valuable contributions and their enthusiastic collaboration. Our research was generously supported by the Deutsche Forschungsgemeinschaft (SFB 247), the Fonds der Chemischen Industrie, the State of Baden-Württemberg, the BASF AG, and Degussa.

## REFERENCES

1. R. N. Grimes, *Coord. Chem. Rev.* **28**, 47 (1979); R. N. Grimes in "Comprehensive Organometallic Chemistry" (G. Wilkinson, F. G. A. Stone, and E. W. Abel, eds.), Vol. 1, p. 459. Pergamon, Oxford, England, 1982.
2. W. Siebert, *Adv. Organomet. Chem.* **18**, 301 (1980).
3. G. E. Herberich in "Comprehensive Organometallic Chemistry" (G. Wilkinson, F. G. A. Stone, and E. W. Abel, eds.), Vol. 1, p. 381. Pergamon, Oxford, England, 1982.
4. W. Siebert, in "Transition Metal Chemistry" (A. Müller and E. Diemann, eds.), p. 161. Verlag Chemie, Weinheim, Germany, 1981.
5. G. Schmid and R. Köster *Methoden Org. Chem.* 4th Ed. (Houben-Weyl) **13/3c**, 1 (1984).
6. W. Siebert, *Angew. Chem.* **97**, 924 (1985); *Angew. Chem. Int. Ed. Engl.* **24**, 943 (1985).
7. W. Siebert, *Pure Appl. Chem.* **59**, 947 (1987).
8. W. Siebert, *Pure Appl. Chem.* **60**, 1345 (1988).
9. W. Siebert, *Usp. Khim.* **60**, 1553 (1991).
10. Ch. Elschenbroich and A. Salzer, "Organometallics." VCH, Weinheim, Germany, 1989.
11. H. Wadepohl, *Angew. Chem.* **104**, 253 (1992); *Angew. Chem. Int. Ed. Engl.* **31**, 247 (1992).
12. K. Jonas, *Pure Appl. Chem.* **62**, 1169 (1990).
13. A. W. Duff, K. Jonas, R. Goddard, H.-J. Krauss, and C. Krüger, *J. Am. Chem. Soc.* **105**, 5479 (1983); K. Angermund, K. H. Klaus, R. Goddard, and C. Krüger, *Angew. Chem.* **97**, 241 (1985); *Angew. Chem. Int. Ed. Engl.* **24**, 237 (1985).
14. P. T. Chesky and M. B. Hall, *J. Am. Chem. Soc.* **106**, 5186 (1984).
15. W. M. Lamanna, *J. Am. Chem. Soc.* **108**, 2096 (1986); W. M. Lamanna, W. B. Gleason, and D. Britton, *Organometallics* **6**, 1583 (1987).
16. J. W. Lauher, M. Elian, R. H. Summerville, and R. Hoffmann, *J. Am. Chem. Soc.* **98**, 3219 (1976).
17. B. F. Bush, V. M. Lynch, and J. J. Lagowski, *Organometallics* **6**, 1267 (1987).
18. J. W. Hull, Jr., and W. L. Gladfelter, *Organometallics* **3**, 605 (1984).
19. W. D. Harman and H. Taube, *J. Am. Chem. Soc.* **109**, 1883 (1987); W. D. Harman, M. Gebhard, and H. Taube, *Inorg. Chem.* **29**, 567 (1990).
20. H. van der Heijden, A. G. Orpen, and P. Pasman, *J. Chem. Soc. Chem. Commun.* 1567 (1989).
21. D. R. Neithamer, L. Párkányi, J. F. Mitchell, and P. T. Wolczanski, *J. Am. Chem. Soc.* **110**, 4421 (1988).
22. K. Jonas, *J. Organomet. Chem.* **400**, 165 (1990).
23. K. Jonas, V. Wiskamp, Y.-H. Tsay, and C. Krüger, *J. Am. Chem. Soc.* **105**, 5480 (1983).
24. K. Jonas, G. Koepe, L. Schieferstein, R. Mynott, C. Krüger, and Y.-H. Tsay, *Angew. Chem.* **95**, 637 (1983); *Angew. Chem. Int. Ed. Engl.* **22**, 620 (1985).
25. J. Müller, private communication (1991); P. Escarpa Gaede, C. Hirsch, J. Müller, K. Qiao, and R. Schubert, *XV Int. Conf. Organomet. Chem.*, Abstr. 049, Warsaw, Poland, 1992.
26. M. P. Gomez-Sal, B. F. G. Johnson, J. Lewis, P. R. Raithby, and A. H. Wright, *J. Chem. Soc. Chem. Commun.*, 1682 (1985).
27. B. F. G. Johnson, J. Lewis, M. Martinelli, A. H. Wright, D. Braga, and F. Grepioni, *J. Chem. Soc. Chem. Commun.*, 364 (1990); D. Braga, F. Grepioni, B. F. G. Johnson, J. Lewis, C. E. Housecroft, and M. Martinelli, *Organometallics* **10**, 1260 (1991).
28. H. Wadepohl, K. Büchner, and H. Pritzkow, *Angew. Chem.* **99**, 1294 (1987); *Angew. Chem. Int. Ed. Engl.* **26**, 1259 (1987); H. Wadepohl, K. Büchner, M. Herrmann, and H. Pritzkow, *Organometallics* **10**, 861 (1991).

29. K. Jonas and C. Krüger, *Angew. Chem.* **92**, 513 (1980); *Angew. Chem. Int. Ed. Engl.* **19**, 520 (1980).
30. H. Werner and A. Salzer, *Synth. React. Inorg. Met. Org. Chem.* **2**, 239 (1972); H. Werner, *Angew. Chem.* **89**, 1 (1977); *Angew. Chem. Int. Ed. Engl.* **16**, 1 (1977).
31. A. R. Kudinov, M. I. Rybinskaya, Y. T. Struchkov, and A. I. Yanovskii, *J. Organomet. Chem.* **336**, 187 (1987).
32. J. J. Schneider, R. Goddard, S. Werner, and C. Krüger, *Angew. Chem.* **103**, 1145 (1991); *Angew. Chem. Int. Ed. Engl.* **30**, 1130 (1991).
33. P. S. Maddren, A. Modinos, P. L. Timms, and P. Woodward, *J. Chem. Soc. Dalton Trans.* 1272 (1975).
34. G. E. Herberich, B. Hessner, G. Huttner, and L. Zsolnai, *Angew. Chem.* **93**, 471 (1981); *Angew. Chem. Int. Ed. Engl.*, **20**, 472 (1981).
35. J. K. Uhm, H. Römich, H. Wadepohl, and W. Siebert, *Z. Naturforsch. B: Chem. Sci.* **43B**, 306 (1988); K.-F. Wörner and W. Siebert, *Z. Naturforsch.*, **44B**, 1211 (1989).
36. K. F. Wörner, J.-K. Uhm, H. Pritzkow, and W. Siebert, *Chem. Ber.* **123**, 1239 (1990).
37. J. K. Uhm, Ph.D. Dissertation, Universität Heidelberg, Heidelberg, Germany, 1987.
38. A. Feßenbecker, H. Schulz, H. Pritzkow, and W. Siebert, *Chem. Ber.* **123**, 2273 (1990).
39. H. Schulz, H. Pritzkow, and W. Siebert, *Chem. Ber.* **125**, 987 (1992).
40. H. Schulz, H. Pritzkow, and W. Siebert, *Chem. Ber.* **125**, 993 (1992).
41. H. Schulz, H. Pritzkow, and W. Siebert, *Chem. Ber.* **124**, 2203 (1991).
42. A. J. Deeming, in "Comprehensive Organometallic Chemistry" (G. Wilkinson, F. G. A. Stone, and E. W. Abel, eds.), Vol. 4, p. 377. Pergamon, Oxford, England, 1982.
43. P. Müller, H. Pritzkow, and W. Siebert, unpublished results.
44. P. Müller and W. Siebert, unpublished results.
45. H. Schulz, Ph.D. Dissertation, Universität Heidelberg, Heidelberg, Germany, 1991.
46. G. E. Herberich, C. Ganter, L. Wesemann, and R. Boese, *Angew. Chem.* **102**, 914 (1990); *Angew. Chem. Int. Ed. Engl.* **29**, 912 (1990).
47. G. E. Herberich, C. Ganter, L. Wesemann, and R. Boese, *J. Organomet. Chem.* **394**, C1 (1990).
48. J. Edwin, M. W. Whiteley, W. Herter, and W. Siebert, *J. Organomet. Chem.* **394**, 329 (1990).
49. M. W. Whiteley, H. Pritzkow, U. Zenneck, and W. Siebert, *Angew. Chem.* **94**, 464 (1982); *Angew. Chem. Int. Ed. Engl.* **21**, 453 (1982).
50. W. Siebert and U. Fenner, unpublished results.
51. V. Schäfer, H. Pritzkow, and W. Siebert, *Angew. Chem.* **100**, 272 (1988); *Angew. Chem. Int. Ed. Engl.* **27**, 299 (1988); *Chem. Ber.* **122**, 401 (1989).
52. A. Feßenbecker, M. Enders, H. Pritzkow, W. Siebert, I. Hyla-Kryspin, and R. Gleiter, *Chem. Ber.* **124**, 1505 (1991).
53. Z. Nagy-Magos, A. Feßenbecker, H. Pritzkow, W. Siebert, I. Hyla-Kryspin, and R. Gleiter, *Chem. Ber.* **124**, 2685 (1991).
54. A. Feßenbecker, M. D. Attwood, R. F. Bryan, R. N. Grimes, M. K. Woode, M. Stephan, U. Zenneck, and W. Siebert, *Inorg. Chem.* **29**, 5157 (1990).
55. A. Feßenbecker, M. D. Attwood, R. N. Grimes, M. Stephan, H. Pritzkow, U. Zenneck, and W. Siebert, *Inorg. Chem.* **29**, 5164 (1990).

# Trifluoromethyl-Containing Transition Metal Complexes

JOHN A. MORRISON

Department of Chemistry  
University of Illinois at Chicago  
Chicago, Illinois 60680

I. Scope of the Review . . . . .	211
II. Early Studies . . . . .	212
III. Transition Metal Trifluoromethyl Chemistry of the Past Decade . . . . .	218
A. Trifluoromethyl Derivatives of Group 3–5 Metals . . . . .	218
B. Trifluoromethyl Derivatives of Group 6 Metals . . . . .	218
C. Trifluoromethyl Derivatives of Group 7 Metals . . . . .	221
D. Trifluoromethyl Derivatives of Group 8 Metals . . . . .	223
E. Trifluoromethyl Derivatives of Group 9 Metals . . . . .	227
F. Trifluoromethyl Derivatives of Group 10 Metals . . . . .	230
G. Trifluoromethyl Derivatives of Group 11 Metals . . . . .	231
H. Trifluoromethyl Derivatives of Group 12 Metals . . . . .	233
IV. Synopsis of Trifluoromethyl Metal Structural Data . . . . .	234
V. Prospects . . . . .	235
References . . . . .	237

## I

### SCOPE OF THE REVIEW

The purpose of the present review is to examine the current status of the chemistry of trifluoromethyl-containing transition metal compounds where the term transition metal had been defined to include the metals of groups 3–12. The early studies in this area have been discussed previously several times (1–4), and there has been no effort to provide a comprehensive literature coverage of the  $\text{CF}_3$ –metal chemistry that was reported prior to 1980.

While there are a number of other fluorine-containing ligands with interesting properties, including those used for MOCVD studies and ring-opening metathesis polymerization reactions, here the intent is to focus solely upon transition metal species that are substituted by  $\text{CF}_3$  ligands, thus metal species containing, e.g.,  $\text{C}_2\text{F}_5$ ,  $\text{C}_3\text{F}_7$ ,  $\text{C}_6\text{F}_5$ ,  $\eta^2\text{-C}_2\text{F}_4$ , and fluorinated or trifluoromethylated cyclopentadienyl ligands are not included. Recent reviews on related topics include those on transition metal fluorides (5), on dihalocarbene ligands (6), and on complexes of the octafluorocyclooctatetraene ligand (7).

The first portion of this summary is an overview of some of the early results that were reported in the trifluoromethyl transition metal area (Section II). That survey is followed by a discussion of more recent studies, which is presented by group of the periodic table (Section III). Section IV is a précis of the X-ray crystallographic data that have been obtained, while Section V indicates some aspects of the importance of trifluoromethyl transition metal chemistry and its future.

## II

### EARLY STUDIES

Unlike many ligands that can be found readily in nature or can be generated easily from the materials found in nature, the trifluoromethyl group is wholly synthetic. One of the first  $\text{CF}_3$  precursors,  $\text{CF}_3\text{I}$ , was initially separated by Emeleus and his students from the products of the reaction between  $\text{Cl}_4$  and  $\text{IF}_5$  (8). They then went on to examine the reactivity of  $\text{CF}_3\text{I}$  toward elemental mercury and several group 5A and 6A (15 and 16) elements. One of the more significant findings of their studies was that  $\text{CF}_3\text{I}$  would oxidize Hg to  $\text{Hg}(\text{CF}_3)_2$ , but only if the mercury had been previously amalgamated with magnesium, copper, silver, or cadmium, the last being particularly effective (9). Bis(trifluoromethyl)mercury and  $\text{HgI}(\text{CF}_3)$  were the first trifluoromethylated organometallic compounds prepared. Emeleus also observed that in many of its reactions, the  $\text{CF}_3$  group could be likened more to a pseudohalide than to a methyl group (8), and that the decomposition temperature of  $\text{Hg}(\text{CF}_3)_2$ , ca.  $170^\circ\text{C}$ , is substantially lower than that of the perhydrogenated analog  $\text{Hg}(\text{CH}_3)_2$ , which begins to decompose near  $300^\circ\text{C}$  (9).

The first trifluoromethyl-containing derivative of a *d* block element was formed when  $\text{Mn}(\text{CO})_5(\text{COCF}_3)$  was thermally decarbonylated to give  $\text{Mn}(\text{CO})_5(\text{CF}_3)$  (10):



Trifluoromethyl migrations were later found to generate a number of trifluoromethylated transition metal complexes, but the success of this method is dependent upon the ability of the metal center to provide a chemically and energetically accessible vacant coordination site to which the  $\text{CF}_3$  group can migrate at a temperature that does not decompose the product. In practice, successful conversions of  $\text{CF}_3\text{CO}$  ligands to  $\text{CF}_3$  substituents have been largely restricted to derivatives of low-valent, late transition metals, and typically these have been compounds of the 3*d*

metals that also have thermally labile CO ancillary ligands (1). One exception is the Pt(II) derivative  $\text{Pt}(\text{Cl})(\text{PMePh}_2)_2(\text{CF}_3)$ , which can be generated by the thermolysis of  $\text{Pt}(\text{Cl})(\text{PMePh}_2)_2(\text{COCF}_3)$ , but this reaction requires temperatures of  $210^\circ\text{C}$  to proceed (11).

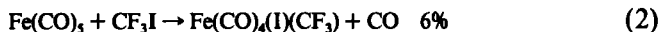
One important property of  $\text{CF}_3$ -transition metal complexes became apparent almost immediately when all of the low-valent, late transition metal trifluoromethylated compounds then known were found to be significantly more thermally and oxidatively stable than the analogous methylated species. Tetracarbonyl(trifluoromethyl)cobalt(I), for example, was isolated by distillation at  $91^\circ\text{C}$ , whereas the hydrocarbyl  $\text{Co}(\text{CO})_4(\text{CH}_3)$  decomposes at subambient temperatures (12). Additionally, while the reverse of the decarbonylation reaction, CO insertion, is commonly observed in methylated transition metal species, these reactions are essentially unknown for trifluoromethyl metal complexes (13). Prior to 1980, evidence for CO insertion into an  $\text{M}-\text{CF}_3$  bond had been reported in only one case. That reaction employed the photolysis of  $\text{Mn}(\text{CO})_5(\text{CF}_3)$  in an argon matrix at 17 K, and the identity of the product was not determined (14). The clear implication of the above results is that  $\text{MCF}_3$  metal-carbon bonds are significantly less reactive and thus presumably stronger than  $\text{MCH}_3$  metal-carbon bonds.

This finding has been rationalized by invoking backbonding from the filled metal  $d$  orbitals into the nominally unoccupied  $\text{C}-\text{F}$  antibonding orbitals, a type of bonding that is not available to  $\text{MCH}_3$  derivatives or compounds like  $\text{CF}_3\text{I}$  (15). The backbonding contribution was assumed to augment the  $\text{M}-\text{C}$  bond length decrease that is expected to result from the higher positive charge on the metal that arises because the  $\text{CF}_3$  group electronegativity is so much greater than that of the  $\text{CH}_3$  group (16).

Others, however, have argued that the enhanced stability of  $\text{M}-\text{CF}_3$  bonds is almost exclusively derived from effects within the  $\sigma$ -bonding manifold (17) and that in addition to the increased ionic character of the metal-carbon bond in the trifluoromethyl derivatives, the substitution of fluorine atoms for the hydrogen atoms in a methyl ligand ultimately results in a larger amount of  $s$  character in the bonding orbital directed from the carbon atom toward the metal atom (18). The anticipated result is a somewhat shorter, stronger  $\text{M}-\text{C}$  bond for  $\text{MCF}_3$  compounds than that found in the analogous  $\text{MCH}_3$  compounds. Regardless of the reasons, it was soon experimentally apparent that in typical fluoroalkyl complexes, the metal-carbon bond lengths are appreciably shorter (by ca.  $0.05 \text{ \AA}$ ) than the metal-carbon bond lengths of similar hydroalkyl organometallic compounds (19).

At approximately the same time that the thermal decarbonylation method was under intense study, Stone (3) began to develop the second

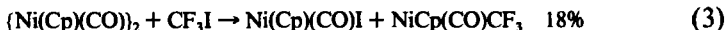
major route to the formation of transition metal trifluoromethyl compounds. The initial experiments in this area utilized oxidative additions of  $\text{CF}_3\text{I}$  (and other perfluoroalkyl halides) to complexes of low-valent transition metals, and a typical example is shown:



In this reaction iron pentacarbonyl was found to add  $\text{CF}_3\text{I}$  to form the first (trifluoromethyl)iron derivative reported (20). The oxidative-addition route has proven to be successful in a number of systems in which  $d^8$  or  $d^{10}$  metal complexes have been employed as reagents, but ineffective with substrates in which the metal had an alternative  $d$  electron count (1–4).

In some instances, the  $\text{CF}_3\text{I}$  reactions resulted in products in which the trifluoromethylated metal was found to be in the same formal oxidation state as the reagent. For example, the interaction of  $\text{Pt}(\text{COD})(\text{CH}_3)_2$  with  $\text{CF}_3\text{I}$  yielded  $\text{Pt}(\text{COD})(\text{CF}_3)_2$  along with  $\text{Pt}(\text{I})(\text{CH}_3)_3$ . Although the  $\text{Pt}-\text{CF}_3$  compound most probably resulted from sequential  $\text{CF}_3\text{I}$  oxidative additions followed by  $\text{CH}_3\text{I}$  reductive eliminations, the possibility of radical reactions involving  $\text{Pt}(\text{II})-\text{CH}_3$  bond cleavages followed by trifluoromethylation of the  $\text{Pt}(\text{I})$  center remaining could not be ruled out (21). Clark and Manzer also isolated the  $\text{Pt}(\text{IV})$  complex  $\text{Pt}(\text{PMe}_2\text{Ph})_2(\text{I})_2(\text{CF}_3)_2$  from the reaction of  $\text{Pt}(\text{PMe}_2\text{Ph})_2(\text{CF}_3)_2$  with  $\text{I}_2$  in good yield (82%) (21). The  $d^6$   $\text{Pt}(\text{IV})$  complexes were (and are) the highest known oxidation state of a transition metal that is also bonded to a trifluoromethyl group.

Albeit with less overall success, trifluoromethyl iodide has also been employed to effect oxidative trifluoromethylations of elemental copper and a few chromium and cobalt coordination complexes and to oxidatively cleave metal—metal bonds in complexes like  $\text{Ni}_2(\text{CO})_2(\text{Cp})_2$ ,  $\text{Co}_2(\text{CO})_8$ , and  $\text{GeMe}_3\text{Fe}(\text{CO})_2\text{Cp}$ . One of the first examples of this type of reaction is (22)



Aside from the fact that the  $\text{CF}_3\text{I}$  oxidative additions and oxidative cleavages require that the metal substrate possess two stable oxidation states that differ by two or one units, respectively, the inherent difficulties of these reactions arise from the fact that  $\text{CF}_3\text{I}$  is a relatively poor oxidizing agent, one that is generally less effective than  $\text{I}_2$ . The overall result is that typically the substrate to which the  $\text{CF}_3\text{I}$  is to be added must be quite electron rich (easily oxidized) or the metal—metal bond to be cleaved must be weak, as in the case of the  $\text{Ni}-\text{Ni}$  bond shown in Eq. (3).

The third general approach that was devised to form transition metal trifluoromethyl compounds relied upon the use of metal atom techniques of the type originally developed by Timms and Skell. In one set of experi-

ments, Klabunde examined the reactions of a number of metal atoms, including Pd, Ni, Zn, and Ag, with, e.g.,  $\text{CF}_3\text{I}$  or  $\text{CF}_3\text{COCl}$ , which were cocondensed with the metal upon the walls of a reactor (23). In some cases, the trifluoromethylated products, e.g.,  $\text{PdI}(\text{CF}_3)$ , could be trapped by the subsequent addition of excess phosphine at low temperatures. In others, the product identity was established by hydrolysis of the matrix and separation of the  $\text{CF}_3\text{H}$  formed. Among other findings, these studies resulted in the isolation of some of the first Pd— $\text{CF}_3$  compounds, species like  $\text{PdI}(\text{CF}_3)(\text{PEt}_3)_2$ , and the somewhat surprising observation that the formally two-coordinate  $\text{PdI}(\text{CF}_3)$  was air stable at ambient temperature even in the absence of added phosphine (24).

During approximately the same time period, Lagow had begun to study the reactions of a number of metal and metalloid halides with the  $\text{CF}_3$  radicals that are generated in the radiofrequency discharge of  $\text{C}_2\text{F}_6$  (2). The first applications of this methodology to transition metal chemistry involved the cocondensation of  $\text{CF}_3$  radicals with Ni and Pd atoms. The presumed bis(trifluoromethyl)nickel and palladium intermediates were then trapped by the addition of excess  $\text{PMe}_3$  to the metal/fluorocarbon matrix, which resulted in  $\text{Ni}(\text{CF}_3)_2(\text{PMe}_3)_3$  and *trans*- $\text{Pd}(\text{CF}_3)_2(\text{PMe}_3)_2$ ; the products ultimately separated (25). Later, the generality of the scheme was established when  $\text{Zn}(\text{SiF}_3)_2\text{py}_2$ , for example, was generated from zinc atoms and the products of an  $\text{Si}_2\text{F}_6$  discharge (26).

Although these methods did result in the preparation of a number of then new compounds, they are inherently limited by the fact that the amount of material afforded by a typical reaction is often only in the tens of milligrams range, which is ample for product characterization but insufficient for a reasonably thorough examination of the chemistry of the new compounds. Additionally, while metal atom reactions have been successfully utilized on the elements of groups 10–12 (see below), the synthesis, isolation, and characterization of trifluoromethyl derivatives of the elements from earlier periods of the periodic table is yet to be established.

By means of the three general synthetic approaches outlined above, a fairly large number of trifluoromethylated transition metal complexes were synthesized during the period 1959–1980. Several studies had indicated that ancillary ligand exchanges, e.g.,  $\text{PPh}_3$  for CO or Cl for Br, could be carried out either thermally or photochemically and that the removal of  $\text{CF}_3$  groups (which is commonly carried out by hydrolysis) could also be achieved as (27)



Somewhat like the nonbarking dog in the Sherlock Holmes story, however, one of the most interesting facets of the  $\text{CF}_3$ -transition metal chemistry known at that time was that several synthetic approaches commonly



employed to generate  $\text{CH}_3$ -containing metal species had not been successfully adapted to the preparation of the trifluoromethylated derivatives.

For example, one well-tested method for the formation of a  $\text{CH}_3$ —metal bond is the interaction of  $\text{CH}_3\text{I}$  with a metallate anion. However, although several early studies had shown that while the reactions of  $\text{CF}_3\text{I}$  with a number of main group anions like  $\text{GeH}_3^-$  do result in trifluoromethylated products like  $\text{CF}_3\text{GeH}_3$  (28), the corresponding reactions of  $\text{CF}_3\text{I}$  with transition metal anions yielded the metal iodide instead (1–4).

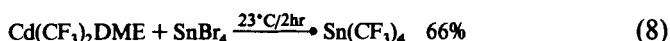
Another extremely useful method for preparing methylated species employs the reactions of selected main group alkyls like  $\text{Hg}(\text{CH}_3)_2$ ,  $\text{Cd}(\text{CH}_3)_2$ ,  $\text{Zn}(\text{CH}_3)_2$ ,  $\text{Al}(\text{CH}_3)_3$ ,  $\text{CH}_3\text{MgX}$ , or  $\text{LiCH}_3$  with an appropriate halide. Much of the power of the method is derived from the fact that there is an entire series of reagents from which to choose; thus one can match the alkylating power of a particular reagent with the difficulty of alkylating the substrate of interest. One excellent example of the beneficial results that can arise by the judicious selection of reagents is found in the synthesis of  $\text{W}(\text{CH}_3)_6$ , a compound that is easily prepared with  $\text{Al}(\text{CH}_3)_3$ , but only obtained with great difficulty when  $\text{LiCH}_3$  is utilized.

In 1980 the situation with respect to reagents that could potentially be used to deliver a  $\text{CF}_3$  group to a metal by a ligand exchange process was much different from that of the alkyls. The only readily available trifluoromethyl derivatives were the mercurials  $\text{HgI}(\text{CF}_3)$  and  $\text{Hg}(\text{CF}_3)_2$ , and these compounds had been repeatedly described as ineffective toward ligand interchanges of the type characteristic of  $\text{Hg}(\text{CH}_3)_2$ . A more recent examination of the reactions of  $\text{Hg}(\text{CF}_3)_2$  with main group halides like  $\text{GeBr}_4$  and  $\text{SnBr}_4$  at elevated temperatures had shown that in fact  $\text{GeCF}_3$ - and  $\text{SnCF}_3$ -containing compounds could be formed from the mercurial (29), but a detailed study of the  $\text{SnBr}_4/\text{Hg}(\text{CF}_3)_2$  interaction indicated that the activation energies for ligand exchange preclude the use of  $\text{Hg}(\text{CF}_3)_2$  in all but the most labile (or thermally robust) systems (30). Clearly, if the ligand exchange approach was to be successful, a more powerful trifluoromethylating agent needed to be developed.

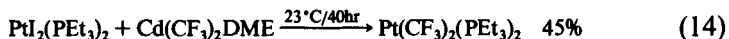
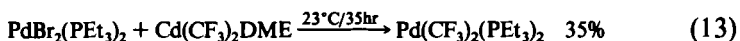
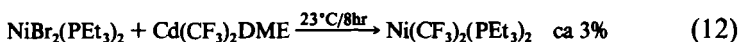
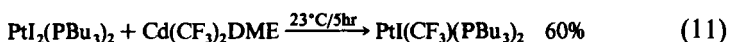
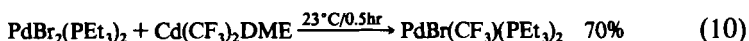
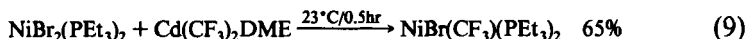
Based in part on the observations of Emeleus and Haszeldine on the  $\text{Hg}/\text{CF}_3\text{I}$  reaction (9), our initial approaches to preparing a more reactive trifluoromethylating reactant were centered upon the chemistry of cadmium. At least to us, it seemed most plausible that the synthesis and separation of the first characterized  $\text{CdCF}_3$  compounds might well simultaneously result in a trifluoromethylating agent more powerful than  $\text{Hg}(\text{CF}_3)_2$ . The preparation of  $\text{Cd}(\text{CF}_3)_2(\text{DME})$  (where DME is  $\text{CH}_3\text{OCH}_2\text{CH}_2\text{OCH}_3$ ) was carried out by exposing  $\text{Cd}(\text{CH}_3)_2$  to  $\text{Hg}(\text{CF}_3)_2$  in DME. The separation of the reagent is based upon the fact that of all of the  $\text{CH}_3/\text{CF}_3$  derivatives of Hg and Cd,  $\text{Cd}(\text{CF}_3)_2$  is the strongest Lewis

acid; thus its adduct with DME is the most thermally stable. In fact,  $\text{Cd}(\text{CF}_3)_2\text{DME}$  is the only compound formed in this system that is not dissociated by prolonged pumping at ambient temperature. The yield of  $\text{Cd}(\text{CF}_3)_2\text{DME}$  is ca. 60%, and it can be stored at  $-78^\circ\text{C}$  indefinitely (31).

Once  $\text{Cd}(\text{CF}_3)_2\text{DME}$  had been isolated, the first experiments with the reagent were devoted to comparing the reactivity of the new compound with that of  $\text{Hg}(\text{CF}_3)_2$  in ligand substitution reactions of main group metalloids. The results shown in Eqs. (5)–(8) clearly indicated that at least with Ge and Sn halides, the cadmium-based trifluoromethylating reagent was much superior to the mercurial (31):



The second set of experiments was focused upon whether the reagent could be employed to generate trifluoromethyl derivatives of representative transition metal coordination complexes, and for this study the group 10 dihalide diphosphines were selected as typical substrates (32). These results,



demonstrated that while the first trifluoromethyl substitution proceeded reasonably efficiently, the second step [Eqs. (11)–(14)] was much slower and required as long as 40hr to proceed to completion. Although  $\text{Pt}(\text{CF}_3)_2(\text{PEt}_3)_2$  could be separated in reasonable amounts (45%) from these reactions, for  $\text{Ni}(\text{CF}_3)_2(\text{PEt}_3)_2$ , the least thermally stable of the  $\text{M}(\text{CF}_3)_2(\text{PEt}_3)_2$  complexes, the rate of decomposition of the compound was comparable to its rate of formation. Ultimately, alternative reaction

conditions under which the  $\text{CF}_3$  ligand substitutions were more facile would need to be devised.

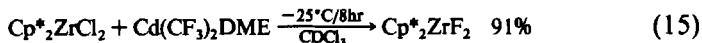
### III

#### TRANSITION METAL TRIFLUOROMETHYL CHEMISTRY OF THE PAST DECADE

While the period 1960–1970 could fairly be characterized as a time in which the generation of new metal— $\text{CF}_3$  derivatives was emphasized, during the decade immediately past, more attention has been given to determining the reactivity of these trifluoromethyl compounds. In particular, the preparation, characterization, and reactions of species containing difluorocarbene ligands has drawn the interest of several investigators. In the following section, newly reported syntheses and reactions of metal— $\text{CF}_3$  compounds are presented by group of the periodic table. Structural studies are summarized in Section IV.

##### A. Trifluoromethyl Derivatives of Group 3–5 Metals

Although several reactions that were designed to provide  $\text{CF}_3$  derivatives of these metals have been reported, to date no successful experiments of this type have been described. The results of one reaction that was directed toward the formation of a  $\text{Hf—CF}_3$  bond are



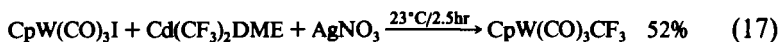
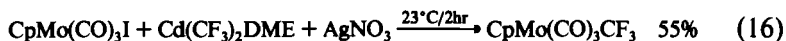
During this reaction, the results of which are quite typical of those obtained from very early (electron poor) transition metal substrates, the only product isolated was the fluoride, which was separated in good yield. The only evidence for the existence of a  $\text{Hf—CF}_3$  intermediate was a small transient  $^{19}\text{F}$  NMR signal in the  $\text{M—CF}_3$  chemical shift region (33).

##### B. Trifluoromethyl Derivatives of Group 6 Metals

###### 1. $\text{CpMo}(\text{CO})_3\text{CF}_3$ and $\text{CpW}(\text{CO})_3\text{CF}_3$

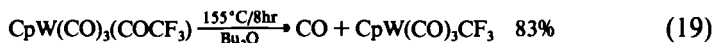
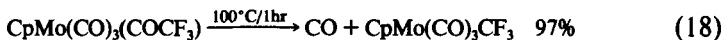
The original preparation of a group 6 trifluoromethyl complex was reported by King and Bisnette (34) who thermally decarbonylated  $\text{CpMo}(\text{CO})_3(\text{COCF}_3)$  at  $120^\circ\text{C}$  to give  $\text{CpMo}(\text{CO})_3\text{CF}_3$  in yields that varied from 24 to 60%. Neither thermal nor photolytic decarbonylation of the analogous tungsten compound,  $\text{CpW}(\text{CO})_3(\text{COCF}_3)$ , was successful (34).

When we initially set about to prepare  $\text{CpMo}(\text{CO})_3\text{CF}_3$  and  $\text{CpW}(\text{CO})_3\text{CF}_3$  by reactions with  $\text{Cd}(\text{CF}_3)_2\text{DME}$ , the results were sorely disappointing since in  $\text{CH}_2\text{Cl}_2$  the *best* yields obtained were ca. 15% for  $\text{CpW}(\text{CO})_3\text{CF}_3$  (from the chloride) after 2 hr at  $90^\circ\text{C}$  and only ca. 3% for  $\text{CpMo}(\text{CO})_3\text{CF}_3$  (from  $\text{CpMo}(\text{CO})_3\text{CH}_3$ ) using a high-pressure Hg lamp to photolyze the reaction (35). Later, an alternative, more productive procedure was developed when it was found that the addition of an equimolar amount of silver salts into the reaction milieu greatly accelerated the rate of the trifluoromethylation reactions (36):



Alternatively, if the reactions are carried out in DMSO, after several days the  $\text{MoCF}_3$  and  $\text{WCF}_3$  products can be obtained in 54 and 27% yields, respectively (37).

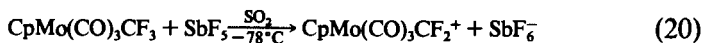
The most efficient syntheses of these compounds of which we are aware, however, employ the thermal decarbonylations of the trifluoroacyl derivatives under slightly different conditions than those originally reported by King. As shown in Eqs. (18) and (19), if the reactions are carried out in sealed vessels with aprotic solvents present, both of the  $\text{COCF}_3$  complexes can be cleanly decarbonylated, and the trifluoromethyl derivatives can then be separated in very high yields (35):



Both of these bright yellow complexes are very sensitive to light, but in the dark they are reasonably thermally stable. For example, if maintained in the dark in a sealed vial, the half-life of  $\text{CpMo}(\text{CO})_3\text{CF}_3$  at ambient temperature is a little over 2 years.

## 2. $\text{CpMo}(\text{CO})_3\text{CF}_3$ Difluorocarbene Derivatives

The initial experiments that indicated that difluorocarbene ligands could be generated from trifluoromethyl groups were reported by Reger who abstracted fluoride ions from compounds like  $\text{CpMo}(\text{CO})_3\text{CF}_3$  with strong Lewis acids. The  $\text{CpMo}(\text{CO})_3\text{CF}_2^+$  ion produced,



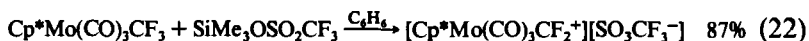
could be characterized spectroscopically, but it was not stable enough to isolate (38).

Somewhat later, Richmond and Shriver (39) demonstrated that the trifluoromethyl ligand in  $\text{CpMo}(\text{CO})_3\text{CF}_3$  could be converted into a trichloromethyl or tribromomethyl substituent merely by adding  $\text{BCl}_3$  or  $\text{BBR}_3$ , as shown for the  $\text{BCl}_3$  reaction.



Although unproven, the mechanism of the halogen interchange was presumed to involve the transient formation of dihalocarbenes and, e.g.,  $\text{BCl}_3\text{F}^-$  (39).

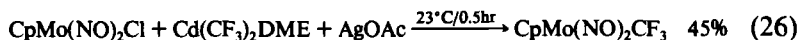
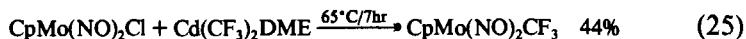
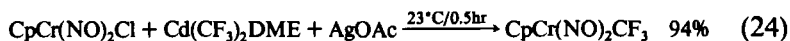
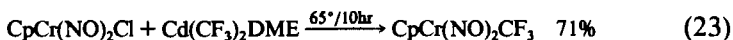
The first group 6 difluorocarbene-containing complex that was sufficiently stable for characterization by X-ray crystallography was recently reported by Koola and Roddick (40) who utilized  $\text{SiMe}_3\text{OSO}_2\text{CF}_3$  as the fluoride abstracting agent. Both  $\text{CpMo}(\text{CO})_3\text{CF}_2^+$  and  $\text{Cp}^*\text{Mo}(\text{CO})_3\text{CF}_2^+$  were formed by reactions like that shown in Eq. (22)



and the structures of  $\text{Cp}^*\text{Mo}(\text{CO})_3\text{CF}_3$  and  $[\text{Cp}^*\text{Mo}(\text{CO})_3\text{CF}_2^+][\text{SO}_3\text{CF}_3^-]$  were ascertained. The reaction of the difluorocarbene with ethylene glycol resulted in a product tentatively identified as  $\text{Cp}^*\text{Mo}(\text{CO})_3\text{C}(\text{OCH}_2)_2^+$  but in general, this difluorocarbene appears to be less amenable to study than the difluorocarbenes ligated to the later (more electron-rich) metals that are described below.

### 3. $\text{CpCr}(\text{NO})_2\text{CF}_3$ and $\text{CpMo}(\text{NO})_2\text{CF}_3$

Since no group 6 compounds that contained both NO and  $\text{CF}_3$  substituents had been prepared and since  $\text{Cr}(0)$  and  $\text{Mo}(0)$  trifluoromethyl compounds were also unknown, we investigated the reactivities of  $\text{CpCr}(\text{NO})_2\text{Cl}$ ,  $\text{CpMo}(\text{NO})_2\text{Cl}$ , and  $\text{CpW}(\text{NO})_2\text{Cl}$  with  $\text{Cd}(\text{CF}_3)_2\text{DME}$ . Although the reactions in  $\text{CH}_2\text{Cl}_2$  at ambient temperature were slow, by either raising the temperature to  $65^\circ\text{C}$  or adding silver salts into the mixture, the new compounds  $\text{CpCr}(\text{NO})_2\text{CF}_3$  and  $\text{CpMo}(\text{NO})_2\text{CF}_3$  could be generated in reasonable amounts. Equations (23)–(26) provide a comparison of the efficiency of the two methods:



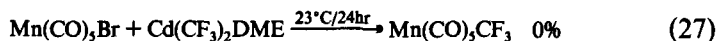
The addition of CuBr to these reactions was also investigated, but the yields were lower, 54% for the Cr species and 35% for CpMo(NO)<sub>2</sub>CF<sub>3</sub>. The tungsten analog was not observed in any of the similar reactions that were carried out with CpW(NO)<sub>2</sub>Cl (36,41).

The chromium complex is exceptionally oxidatively and thermally stable. It can be exposed to the atmosphere for 6 months without change and in Bu<sub>2</sub>O at 115°C, the half-life of the compound is ca 400 hr; even after 1100 hr at 115°C, 2% of the material remains. The molybdenum derivative, however, is much less stable since sealed samples begin to decompose within 10 hr and upon exposure to air, brown fumes are evolved immediately. As anticipated, the NO stretching frequencies are very high for both compounds, slightly higher than those of the chloride in both cases (16,41). The X-ray crystal structure of CpCr(NO)<sub>2</sub>CF<sub>3</sub> is discussed below.

### C. Trifluoromethyl Derivatives of Group 7 Metals

#### 1. Synthesis of Mn(CO)<sub>5</sub>CF<sub>3</sub>

The reaction of Cd(CF<sub>3</sub>)<sub>2</sub>DME with Mn(CO)<sub>5</sub>Br is very slow at ambient temperature, but if AgNO<sub>3</sub> is added in a 1 : 1 mole ratio with the cadmium reagent, the silver-assisted reaction is complete within 15 min. The addition of CuBr to Cd(CF<sub>3</sub>)<sub>2</sub>DME trifluoromethylations of Mn(CO)<sub>5</sub>Br, however, is ineffective (36). The results of the AgNO<sub>3</sub> comparison are



The role of the silver salt is not known with certainty, but two possibilities are most plausible. One is that first the AgNO<sub>3</sub> is trifluoromethylated by the cadmium reagent and then the more reactive, but much less thermally stable, AgCF<sub>3</sub> (see below) trifluoromethylates the organometallic halide. An alternative possibility is that the silver may remove halide from the substrate, leaving a more reactive, coordinatively unsaturated metal that is then trifluoromethylated by Cd(CF<sub>3</sub>)<sub>2</sub>DME.

#### 2. Mn(CO)<sub>5</sub>CF<sub>3</sub> Ligand Exchange with Boron Trihalides

Richmond and Shriver (39) have examined the reactivity of Mn(CO)<sub>5</sub>-CF<sub>3</sub> and Mn(CO)<sub>5</sub>COCF<sub>3</sub> with the boron trihalides. The interaction of Mn(CO)<sub>5</sub>CF<sub>3</sub> with BCl<sub>3</sub> in CH<sub>2</sub>Cl<sub>2</sub> generated Mn(CO)<sub>5</sub>CCl<sub>3</sub> (91%) and BF<sub>3</sub>, but the products from the BBr<sub>3</sub> and BI<sub>3</sub> reactions were less stable. The

reaction of  $\text{Mn}(\text{CO})_5\text{COCF}_3$  with, e.g.,  $\text{BCl}_3$ , did not result in halide interchange. These results appear to be general in that the fluorine substituents of an alkyl carbon directly bonded to a transition metal are commonly much more labile than those bonded to a nonadjacent alkyl carbon. These results were interpreted to signify that halogenated carbon atoms adjacent to transition metals have an enhanced ability to form transient carbenes (39).

### 3. $\text{Mn}(\text{CO})_5\text{CF}_3$ Carbonylation and $\text{Mn}(\text{CO})_5\text{COCF}_3$ Decarbonylation

Calorimetric measurements that were carried out upon reactions (e.g., halogenations) of a number of  $\text{Mn}(\text{CO})_5\text{R}$  compounds resulted in estimated bond dissociation enthalpies of 41.1 kcal/mol for the  $\text{Mn}-\text{CF}_3$  bond in  $\text{Mn}(\text{CO})_5\text{CF}_3$  and 36.6 kcal/mol for the  $\text{Mn}-\text{CH}_3$  bond in  $\text{Mn}(\text{CO})_5\text{CH}_3$  (42). Within the experimental uncertainty, the difference between the two  $\text{M}-\text{C}$  alkyl bond energies is the same as that derived for the  $\text{Mn}-\text{C}$  bond dissociation enthalpies of the analogous acyl compounds, 35.1 kcal/mol for  $\text{Mn}(\text{CO})_5\text{COCF}_3$  and 30.8 kcal/mol for  $\text{Mn}(\text{CO})_5\text{COCH}_3$  (42). Clearly, the effects that strengthen the  $\text{Mn}-\text{CF}_3$  bond relative to the  $\text{Mn}-\text{CH}_3$  bond extend to the trifluoroacetyl derivative as well.

Shin and Beauchamp (43) have compared the gas-phase infrared  $\text{C}-\text{F}$  stretching frequencies of  $\text{Mn}(\text{CO})_5\text{CF}_3$  with those of the  $\text{Mn}(\text{CO})_4\text{CF}_3^-$  and  $\text{Mn}(\text{CO})_3(\text{NO})\text{CF}_3^-$  anions that were produced by the infrared multiphoton-induced dissociation of CO from the parent pentacarbonyl. The infrared evidence suggests that in the gas phase, the structure of  $\text{Mn}(\text{CO})_4\text{CF}_3^-$  is based on a square pyramid, whereas the structure of  $\text{Mn}(\text{CO})_3(\text{NO})\text{CF}_3^-$  is based on a trigonal bipyramid (43). In an experimentally similar study, the gas-phase decarbonylation of  $\text{Mn}(\text{CO})_5(\text{COCF}_3)$  has been examined. The results of the study were consistent with the generally accepted solution state mechanism (CO loss followed by  $\text{CF}_3$  migration) for this transformation. The activation energy estimated for the gas-phase decarbonylation of  $\text{Mn}(\text{CO})_5(\text{COCF}_3)$  is 36 kcal/mol, and that for the decarbonylation of  $\text{Mn}(\text{CO})_4\text{COCF}_3$  is 5–10 kcal/mol (44).

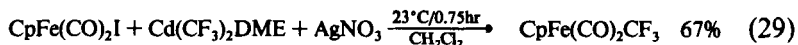
Calculations carried out at the extended CNDO level on the carbonylation reactions of the  $\text{Mn}(\text{CO})_5(\text{CF}_n\text{H}_{3-n})$ ,  $n = 0-3$ , compounds indicate that the charge on the alkyl carbon is positive for the trifluoromethyl derivative, but negative for the methyl and other fluoromethyl derivatives. Since the calculated charge densities of the carbon atoms of the CO groups *cis* to the alkyls are also all positive, the first step postulated for the "CO insertion" reaction, an intramolecular nucleophilic attack of the alkyl group upon a neighboring CO ligand, is greatly disfavored for  $\text{Mn}(\text{CO})_5\text{CF}_3$  relative to the methyl and other fluoroalkyl derivatives (45).

In a theoretical examination of the carbonylation reaction of  $\text{Mn}(\text{CO})_5\text{CF}_3$  and related species that was carried out at the PRDDO and ab initio levels, Marynick has examined the energies of the reagents and products, as well as those of three probable intermediates (46). These calculations indicated that the (computed) difference in the  $\text{Mn}-\text{CF}_3$  and  $\text{Mn}-\text{CH}_3$  bond strength is 30–40 kcal/mol and that the differences in the bonding MOs of the two types of  $\text{Mn}-\text{C}$  bonds are as previously described (18). The calculated  $\Delta E$ s for the carbonylation reaction (which generates  $\text{Mn}(\text{CO})_5(\text{COCF}_3)$  from  $\text{Mn}(\text{CO})_5\text{CF}_3$  and  $\text{CO}$ ) are +18 (PRDDO) and +29 (ab initio) kcal/mol relative to the methyl manganese carbonylation. The computed activation energies of the alkyl migration step, in which an  $\eta^2\text{-COR}$  transition state was assumed, were 15 kcal/mol more positive for the  $\text{Mn}(\text{CO})_5\text{CF}_3$  to  $\text{Mn}(\text{CO})_4(\text{COCF}_3)$  transformation than for the analogous methyl group migration (46).

#### D. Trifluoromethyl Derivatives of Group 8 Metals

##### 1. $\text{CpFe}(\text{CO})_2\text{CF}_3$ and Related Compounds

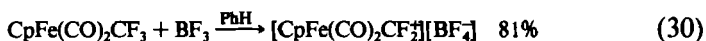
The preparation of  $\text{CpFe}(\text{CO})_2\text{CF}_3$  from  $\text{CpFe}(\text{CO})_2\text{I}$  and  $\text{Cd}(\text{CF}_3)_2\text{DME}$  has been examined at ambient temperature. In  $\text{CH}_2\text{Cl}_2$  with no  $\text{AgNO}_3$  added, the  $\text{CpFe}(\text{CO})_2\text{CF}_3$  resonance is not observed by  $^{19}\text{F}$  NMR even after 72 hr, but if an equimolar amount of  $\text{AgNO}_3$  is added to the reaction mixture, the desired product is generated in 67% yield;



in DME solvent, with  $\text{AgNO}_3$  added, the yield is 68% (36). Alternatively,  $\text{CpFe}(\text{CO})_2\text{CF}_3$  can be generated in 50–70% yield by the photolysis of the trifluoroacetyl derivative (39).

In  $\text{CH}_2\text{Cl}_2$  the reaction of 1 mol of  $\text{BCl}_3$  with  $\text{CpFe}(\text{CO})_2\text{CF}_3$  forms  $\text{CpFe}(\text{CO})_2\text{CCl}_3$  (71%) within 5 min (39). Similarly,  $\text{BBr}_3$  and  $\text{B}_2\text{H}_6$  apparently exchange ligands with  $\text{CpFe}(\text{CO})_2\text{CF}_3$  to give  $\text{CpFe}(\text{CO})_2\text{CBr}_3$  and  $\text{CpFe}(\text{CO})_2\text{CH}_3$ , but these compounds are much less stable under the reaction conditions. The interaction of  $\text{BCl}_3$  with  $\text{CpFe}(\text{CO})_2\text{C}_6\text{F}_5$ , a compound in which there are no fluorines attached to the  $\alpha$ -carbon, did not result in an interchange of F and Cl between the carbon and boron centers (39).

In benzene, the reaction of  $\text{CpFe}(\text{CO})_2\text{CF}_3$  with  $\text{BF}_3$  resulted in the precipitation of the difluorocarbene





in 81% yield. The reaction of 3 equivalents of  $\text{BCl}_3$  with  $\text{CpFe}(\text{CO})_2\text{CF}_3$  gave the less stable dichlorocarbene  $[\text{CpFe}(\text{CO})_2\text{CCl}_2][\text{BCl}_4]$  along with  $\text{BF}_3$  (47).

Although the  $\text{CpFe}(\text{CO})_2\text{CF}_2^+$  ion does readily hydrolyze to  $\text{CpFe}(\text{CO})_3^+$ , under anhydrous conditions the reaction of the electrophilic  $\text{CpFe}(\text{CO})_2\text{CF}_2^+$  cation with the electron-rich Ir(I) compound  $\text{Ir}(\text{CO})\text{Cl}(\text{PMe}_2\text{Ph})_2$  yields a very unusual product,  $[\text{Cp}(\text{CO})\text{Fe}(\mu_2\text{-CO})(\mu_2\text{-CF}_2)\text{Ir}(\text{CO})\text{Cl}(\text{PMe}_2\text{Ph})_2][\text{BF}_4]$  in 66% yield (48). Crystallography has shown that in the cation, both the CO and the  $\text{CF}_2$  bridge the Fe—Ir bond (48,49). The addition of the strong Lewis-acid  $\text{BCl}_3$  to the  $\text{BPh}_4^-$  salt of the Fe—Ir cation displaces the weaker acid, the difluorocarbene, from the Ir center, resulting in  $[\text{CpFe}(\text{CO})_2\text{CF}_2][\text{BPh}_4]$  and  $\text{Cl}_3\text{BIr}(\text{CO})\text{Cl}(\text{PMe}_2\text{Ph})_2$  (48). The related complexes  $[\text{CpFe}(\text{CO})(\text{PPh}_3)(\text{CF}_2)][\text{BF}_4]$  and  $[\text{CpFe}(\text{CO})_2(\text{CCl}_2)][\text{BCl}_4]$  have also been characterized by X-ray crystallography (50).

## 2. *Cis-Fe(CO)<sub>4</sub>(CF<sub>3</sub>)<sub>2</sub> and Related Compounds*

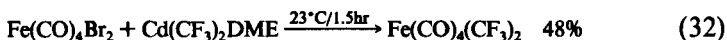
Several studies have been carried out to develop better syntheses of  $\text{Fe}(\text{CO})_4(\text{CF}_3)_2$ . The initial preparation of the compound involved refluxing  $\text{Fe}(\text{CO})_4(\text{COCF}_3)_2$  in heptane (98°C) for 2 hr. The yield of  $\text{Fe}(\text{CO})_4(\text{CF}_3)_2$  from this procedure was 55% (51). Because of the success of the  $\text{CpMo}(\text{CO})_3(\text{COCF}_3)$  and  $\text{CpW}(\text{CO})_3(\text{COCF}_3)$  decarbonylations discussed above, the thermal reaction of  $\text{Fe}(\text{CO})_4(\text{COCF}_3)_2$  in a sealed reactor using  $\text{CH}_2\text{Cl}_2$  as the solvent was investigated (36):



Naumann has studied the trifluoromethylation of the tetracarbonyliron dihalides with  $\text{Cd}(\text{CF}_3)_2\text{DME}$  and  $\text{Cd}(\text{CF}_3)_2(\text{CH}_3\text{CN})_2$  in several solvents under "polar" reaction conditions. Polar reaction conditions include the use of solvents of high Gutmann donor number, which are stated to favor the transfer of the softer  $\text{CF}_3^-$  anion rather than the harder  $\text{F}^-$  anion to the substrate (52).

In the iron tetracarbonyl dihalide reactions, however,  $\text{Fe}(\text{CF}_3)_3$  complexes were not formed even after months when py or dmf were the solvents, and in  $\text{CH}_3\text{CN}$ , CO was displaced by the solvent to yield  $\text{Fe}(\text{CF}_3)_3$  and  $\text{FeF}$  acetonitrile complexes;  $\text{Fe}(\text{CO})_4(\text{CF}_3)_2$  was not observed. In ether,  $\text{Fe}(\text{CO})_4(\text{CF}_3)_2$  was isolated from the reaction of  $\text{Fe}(\text{CO})_4\text{Br}_2$  with  $\text{Cd}(\text{CF}_3)_3\text{DME}$  after 21 hr at 37°C. After the product had been dried at  $-196^\circ\text{C}$  in high vacuum (52), the yield was 65%. In  $\text{CH}_2\text{Cl}_2$ , the reaction of the bromide with  $\text{Cd}(\text{CF}_3)_2(\text{CH}_3\text{CN})_2$  resulted in an explosion within minutes of the inception of the experiment.

In our own study, the interactions of  $\text{Fe}(\text{CO})_4\text{Br}_2$  and  $\text{Fe}(\text{CO})_4\text{I}_2$  with  $\text{Cd}(\text{CF}_3)_2\text{DME}$  were examined in  $\text{CH}_2\text{Cl}_2$  at ambient temperature. The reactions of the bromide are much faster than those of the iodide in that the former proceed to completion within 1.5 hr, whereas the latter require 24 hr. The isolated yields of *cis*- $\text{Fe}(\text{CO})_4(\text{CF}_3)_2$  from each of the reactions are similar, however, 45 and 48%, respectively (36):



The two isomers of  $\text{Fe}(\text{CO})_4\text{I}(\text{CF}_3)$  were readily isolated from the reaction of  $\text{Fe}(\text{CO})_4\text{I}_2$  with  $\text{Cd}(\text{CF}_3)_2\text{DME}$  since the *cis*-isomer (the kinetic product) is less soluble in polar solvents and the *trans*-isomer (the thermodynamic product) is more volatile. No evidence for *trans*- $\text{Fe}(\text{CO})_4(\text{CF}_3)_2$  was obtained.

Although the addition of  $\text{AgNO}_3$  into  $\text{Cd}(\text{CF}_3)_2\text{DME}/\text{Fe}(\text{CO})_4\text{I}_2$  reaction mixtures had no discernable effect, if small amounts (ca. 10 mol%) of the well-known radical trapping agent galvinoxyl were added into reactions of either the bromide or the iodide, no trifluoromethylation was observed by  $^{19}\text{F}$  NMR until the dark color of the radical scavenger had been discharged. We take this as evidence that at least in this reaction, the  $\text{CF}_3$  transfer proceeds by a radical rather than an ionic mechanism.

An alternative preparation of  $\text{Fe}(\text{CO})_4(\text{CF}_3)_2$  (32%) involves the reaction of  $\text{Fe}(\text{CO})_5$  with  $\text{CF}_3\text{ISO}_2\text{F}$ , which yields *cis*- and *trans*- $\text{Fe}(\text{CO})_4\text{I}(\text{CF}_3)$  (72%). Symmetrization of the iodo(trifluoromethyl)iron compound with  $\text{AgF}$  affords *cis*- $\text{Fe}(\text{CO})_4(\text{CF}_3)_2$  (53). Like  $\text{CpCr}(\text{NO})_2\text{CF}_3$ , *cis*- $\text{Fe}(\text{CO})_4(\text{CF}_3)_2$  is stable to air for months. When sealed into small vessels with  $\text{Bu}_2\text{O}$  and maintained at  $115^\circ\text{C}$ , however, the half-life of  $\text{Fe}(\text{CO})_4(\text{CF}_3)_2$  is only ca. 5 hr; thus this  $d^6$  Fe(II) compound is significantly less stable than the  $d^6$  Cr(0) compound  $\text{CpCr}(\text{NO})_2(\text{CF}_3)$  under similar conditions.

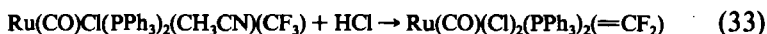
### 3. *Fe(diars)(CO)<sub>2</sub>I(COCF<sub>3</sub>)*

Since both experimental and computational results indicate that it should be extremely difficult to "insert" CO into an  $\text{MCF}_3$  bond, it is somewhat surprising that the reaction of  $\text{CF}_3\text{I}$  with  $\text{Fe}(\text{diars})(\text{CO})_3$ , where diars is  $1,2\text{-C}_6\text{H}_4(\text{AsMe}_2)_2$ , has been reported to form readily the trifluoroacyl derivatives *cis,cis*- and *cis,trans*- $\text{Fe}(\text{diars})(\text{CO})_2\text{I}(\text{COCF}_3)$  at temperatures as low as  $-78^\circ\text{C}$  and to yield the same products when galvinoxyl is present (54). Although less facile, the reaction of  $\text{CH}_3\text{I}$  with the iron substrate gave similar products, but the direct reaction of  $\text{CF}_3\text{COI}$  with  $\text{Fe}(\text{diars})(\text{CO})_3$  yielded  $[\text{Fe}(\text{diars})(\text{CO})_3(\text{COCF}_3)][\text{I}]$  rather than the dicarbonyl (54).

#### 4. Ruthenium(II) Trifluoromethyl and Difluorocarbene Compounds

Roper exploited a second type of reactivity that had been demonstrated for  $\text{Hg}(\text{CF}_3)_2$  when he oxidatively added the mercurial to  $\text{Ru}(\text{CO})_3(\text{PPh}_3)_2$  or  $\text{Ru}(\text{CO})_2(\text{PPh}_3)_3$ . Both reactions yielded  $\text{Ru}(\text{CO})_2(\text{PPh}_3)_2(\text{CF}_3)(\text{HgCF}_3)$  (55) (72%) (56). X-ray crystallography demonstrated that the compound is of the *cis,trans* configuration and that the CF bonds of the  $\text{HgCF}_3$  group are ca. 0.1 Å shorter than those of the Ru bound  $\text{CF}_3$  (55).

Chlorination removed the  $\text{HgCF}_3$  giving  $\text{Ru}(\text{CO})_2(\text{Cl})(\text{PPh}_3)_2(\text{CF}_3)$ , and treatment with  $\text{CH}_3\text{CN}$  displaced the CO *trans* to the  $\text{CF}_3$ . The  $\text{CF}_3$  can be converted to CO with  $\text{HClO}_4$ , but the more interesting reaction is



in which the addition of dry HCl simultaneously replaces the  $\text{CH}_3\text{CN}$  with  $\text{Cl}^-$  and removes  $\text{F}^-$  from the  $\text{CF}_3$  substituent forming a Ru(II) difluorocarbene (55). Exposure of  $\text{Ru}(\text{CO})_2(\text{Cl})(\text{PPh}_3)_2(\text{CF}_3)$  to  $\text{BCl}_3$  forms the dichlorocarbene  $\text{Ru}(\text{CO})(\text{Cl})_2(\text{PPh}_3)_2(=\text{CCl}_2)$  in high yields (56).

The Ru(II) difluorocarbene is very easily hydrolyzed and it also reacts with  $\text{HOCH}_2\text{CH}_2\text{OH}$  to form the  $=\text{C}(\text{OCH}_2)_2$  carbene. The reactions of the difluoride with  $\text{NMe}_2$  or  $\text{CH}_3\text{OH}$  give the monofluorocarbene ligands  $=\text{CF}(\text{NMe}_2)$  and  $=\text{CF}(\text{OMe})$ , respectively (55).

The reaction of  $\text{Ru}(\text{CO})_2(\text{PPh}_3)_2(\text{CF}_3)(\text{HgCF}_3)$  with  $\text{Br}_2$  in  $\text{CH}_2\text{Cl}_2$  yields  $\text{RuBr}(\text{CO})_2(\text{PPh}_3)_2(\text{CF}_3)$  (82%). The attempted preparation of the dibromocarbene complex by the reaction of the bromo Ru(II) compound with  $\text{BBr}_3$ , however, resulted in the separation of the bicyclic  $\text{RuBr}_2(\text{CO})[\text{=CC}_6\text{H}_4\text{PPh}_2]_2$  instead. The last product can be viewed as arising from the intramolecular elimination of 2 mol of HBr from the expected dibromocarbene complex (56).

#### 5. Ru(0) and Os(0) Trifluoromethyl and Difluorocarbene Compounds

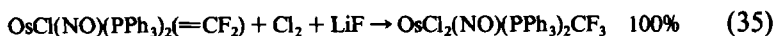
Because attempted oxidative additions of  $\text{Hg}(\text{CF}_3)_2$  to Os(0) compounds proved to be only marginally successful, the reactions of  $\text{Cd}(\text{CF}_3)_2\text{DME}$  were examined. As shown in



the reaction with  $\text{Ru}(\text{CO})_2(\text{PPh}_3)_3$  resulted in the direct formation of a Ru(0) difluorocarbene. In this product, the phosphines occupy the axial positions (57). Although  $\text{Cd}(\text{CF}_3)_2\text{DME}$  has been shown to be an effective  $\text{CF}_2$  source as well as a trifluoromethylating agent (31), the postulated mechanism of the reaction involves oxidative addition of the  $\text{Cd}(\text{CF}_3)_2$  in a manner similar to that of the  $\text{Hg}(\text{CF}_3)_2$  addition discussed above, followed by a 1,2 elimination of  $\text{CdF}(\text{CF}_3)$  from the  $\text{Ru}(\text{II})(\text{CF}_3)(\text{CdCF}_3)$  intermediate (57).

The difluorocarbene in this more electron-rich Ru(0) compound is much less reactive toward nucleophiles than the Ru(II) difluorocarbene, but it does interact with  $\text{NH}_2\text{CH}_3$  to generate the  $\text{RuCNMe}$  derivative, and with  $\text{Ag}^+$ . Dry  $\text{HCl}$  instantaneously adds across the  $\text{Ru}-\text{C}$  double bond to give  $\text{Ru}(\text{CO})_2\text{Cl}(\text{PPh}_3)_2(\text{CF}_2\text{H})$  from which  $\text{F}^-$  can be abstracted with a second mole of  $\text{HCl}$ . The product is the monofluorocarbene  $\text{Ru}(\text{CO})_2(\text{Cl})(\text{PPh}_3)_2(=\text{CFH})$  (57).

Osmium(0) complexes like  $\text{OsCl}(\text{NO})(\text{PPh}_3)_3$  react with  $\text{Cd}(\text{CF}_3)_2\text{DME}$  similarly to give, e.g.,  $\text{Os}(\text{Cl})(\text{NO})(\text{PPh}_3)_2(=\text{CF}_2)$  (80%) (58). In  $\text{CH}_2\text{Cl}_2$  the  $\text{Os}(0)$  difluorocarbene can be oxidized with  $\text{Cl}_2$  in the presence of  $\text{LiF}$  to form the  $\text{Os}(\text{II})$  trifluoromethyl compound.

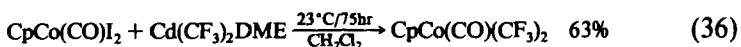


The reaction of  $\text{I}_2$  is similar (58,59).

### E. Trifluoromethyl Derivatives of Group 9 Metals

#### 1. Synthesis of $\text{CpCo}(\text{CO})(\text{CF}_3)_2$

Very soon after the reactivity of  $\text{Cd}(\text{CF}_3)_2\text{DME}$  toward main group halides (31) and group 10 dihalides (32) had been established, we set out to determine if the cadmium reagent was effective in trifluoromethylating representative organometallic compounds. One of the first substrates chosen was  $\text{CpCo}(\text{CO})\text{I}_2$ , which was selected because the mono-trifluoromethyl derivative was known, but the disubstituted compound was not. The results of this reaction are (60)



The very volatile  $\text{CpCo}(\text{CO})(\text{CF}_3)_2$  is stable toward air for months, and the half-life of sealed samples dissolved in  $\text{Bu}_2\text{O}$  is ca. 260 hr at  $115^\circ\text{C}$ . This  $d^6$   $\text{Co}(\text{III})$  compound is thus more stable thermally than the  $d^6$   $\text{Fe}(\text{II})$  compound  $\text{Fe}(\text{CO})_4(\text{CF}_3)_2$ , but less enduring than the  $d^6$   $\text{Cr}(0)$  species  $\text{CpCr}(\text{NO})_2\text{CF}_3$  discussed above. For comparison, the half-life of the methylated derivative,  $\text{CpCo}(\text{CO})(\text{CH}_3)_2$ , is ca. 11 hr at ambient temperature.

#### 2. Electrochemical Reduction of $\text{Co}(\text{III})-R_f$ Compounds

Few electrochemical studies have been carried out on perfluoroalkyl derivatives of transition metals, but polarographic and cyclic voltammetric measurements have been reported for a series of  $\text{Co}(\text{salen})\text{R}$  complexes in which  $\text{R}$  was  $\text{CF}_3$  and  $\text{CH}_3$ , among others (61). These studies indicated that in THF the reduction of  $\text{Co}(\text{salen})\text{CF}_3$  to  $\text{Co}(\text{salen})\text{CF}_3^-$  is 0.574 V easier (less negative) than the corresponding reduction of the methyl

Co(III) complex. These findings can be rationalized on the basis of the higher electronegativity of  $\text{CF}_3$ . The reduced product,  $\text{Co}(\text{salen})\text{CF}_3^-$  is much more stable in solution than the methyl analog, but it does slowly decompose. A second observed reduction, to  $\text{Co}(\text{salen})\text{CF}_3^{2-}$ , was irreversible (61).

### 3. Thermodynamics and Kinetics of Co(III)— $R_f$ Compounds

Studies of the relative binding energies of the sixth ligand to a series of  $\text{CF}_3$ - and  $\text{CH}_3$ -substituted Co(III) coordination complexes  $\text{RCoL}_4$ , where  $\text{L}_4$  is a tetradentate base, e.g., bis(acetylaceton)ethylenediimine(bae), found that the bond enthalpies for a typical monodentate ligand like pyridine at the sixth coordination site (*trans* to R) are higher for the  $\text{CF}_3$  derivatives than the  $\text{CH}_3$  derivatives, e.g., by 6 kcal/mol for bae. Similarly, fluorination of the  $\text{L}_4$  entity increases the Co—py bond enthalpy, but to a smaller extent, e.g., 2 kcal/mol for bae (62).

In addition, as part of a kinetic examination of the rates of ligand displacement by  $\text{H}_2\text{O}$  in trifluoromethyl cobaloximes, the  $\text{p}K_a$  of the  $\text{CF}_3$ —Co(III) aquo derivative ( $-1.36$ ) was found to be significantly lower than that of alkylcobaloximes ( $0.0$  to  $0.67$ ) (63). The differences between the results for the  $\text{CH}_3$  and  $\text{CF}_3$  substituents in both sets of experiments was attributed to the greater electron-withdrawing ability of the  $\text{CF}_3$  group. (Trifluoromethyl) cobaloxime was chosen for the second study because it is much more stable toward strong aqueous acids than the alkylcobaloximes (63).

### 4. $\text{Rh}(\text{CO})(\text{PPh}_3)_2(\text{CF}_3)$ and Related Compounds

Roper has shown that in refluxing benzene, the Rh(I) complex  $\text{Rh}(\text{H})\text{CO}(\text{PPh}_3)_3$  reacts with  $\text{Hg}(\text{CF}_3)_2$  to form a Rh(I) trifluoromethyl derivative  $\text{Rh}(\text{CO})(\text{PPh}_3)_2(\text{CF}_3)$  (77%) and that when treated similarly, the Rh(III) compound  $\text{Rh}(\text{Cl})_2(\text{H})(\text{PPh}_3)_3$  forms a mixture of  $\text{Rh}(\text{Cl})_2(\text{PPh}_3)_2(\text{CF}_3)$  (10%) and  $\text{Rh}(\text{Cl})_2(\text{PPh}_3)_2(\text{CF}_2\text{H})$  (38%) (64). The Rh(I) trifluoromethyl compound adds CO,  $\text{C}_2\text{H}_4$ , and  $\text{H}_2$  reversibly, and it can be halogenated to yield, e.g., *cis,trans*- $\text{Rh}(\text{CO})(\text{Cl})_2(\text{PPh}_3)_2(\text{CF}_3)$  in 84% yield. However, the attempted oxidative addition of  $\text{CH}_3\text{I}$  to  $\text{Rh}(\text{CO})(\text{PPh}_3)_2(\text{CF}_3)$  resulted in the formation of the acyl derivative  $\text{Rh}[\text{C}(\text{O})\text{CH}_3](\text{PPh}_3)_2\text{I}(\text{CF}_3)$  (70%) rather than the expected methyl species. Finally, the reaction of the Rh(I) trifluoromethyl compound with dry HCl gave the difluoromethyl Rh(III) product.



Carbonylation of the five-coordinate  $\text{Rh}(\text{Cl})_2(\text{PPh}_3)_2(\text{CF}_2\text{H})$  produced

above also yielded the product shown in Eq. (37) in 95% yield. In both cases, the conversion of the  $\text{CF}_3$  ligand to a  $\text{CF}_2\text{H}$  ligand was thought to involve the intermediacy of a Rh(III) difluorocarbene (64).

### 5. Trifluoromethyl Ir(III) Compounds

Reaction of  $\text{Ir}(\text{CO})(\text{Cl})(\text{PPh}_3)_2$  with  $\text{CF}_3\text{I}$  gave the previously known  $\text{Ir}(\text{CO})(\text{Cl})(\text{I})(\text{PPh}_3)_2\text{CF}_3$  (73%) from which the iodide (the ligand *trans* to  $\text{CF}_3$ ) can be removed with  $\text{Ag}^+$  in acetonitrile (65). By the addition of milder ( $\text{BEt}_3\text{H}^-$ ) or stronger ( $\text{BH}_4^-$ ) reducing agents, the cation,  $\text{Ir}(\text{CH}_3\text{CN})(\text{CO})(\text{Cl})(\text{PPh}_3)_2\text{CF}_3^+$ , can be reduced to either the mono (99%) or the dihydride (84%):



Attempts to deprotonate the dihydride were unsuccessful (65).

The reaction of  $\text{Ir}(\text{CO})(\text{Cl})_2(\text{PPh}_3)_2(\text{CF}_3)$ , formed from the cation in Eq. (33) above and  $\text{NaCl}$ , with 2 equivalents of  $\text{BCl}_3$  generated an unstable dichlorocarbene, but this compound immediately underwent intramolecular cyclization of the type discussed above for the Ru(II) analog (66).

### 6. The Trifluoromethyl Analog of Vaska's Complex

Roper has synthesized  $\text{Ir}(\text{CO})(\text{PPh}_3)_2\text{CF}_3$  by the double decarbonylation of  $\text{Ir}(\text{CO})_2(\text{PPh}_3)_2(\text{COCF}_3)$ , the reaction of  $\text{Hg}(\text{CF}_3)_2$  with  $\text{Ir}(\text{CO})_2\text{H}(\text{PPh}_3)_2$  followed by decarbonylation, and the direct reaction of  $\text{Ir}(\text{CO})(\text{H})(\text{PPh}_3)_3$  with  $\text{Hg}(\text{CF}_3)_2$  (67). This long sought derivative of Vaska's complex adds CO (98%),  $\text{Cl}_2$  (92%),  $\text{HCl}$  (92%),  $\text{H}_2$  (90%), and  $\text{CH}_3\text{I}$  (89%). In the six-coordinate products, both *cis*- and *trans*-adducts were found. The  $\text{CH}_3\text{I}$  adduct is a relatively rare case in which both  $\text{CH}_3$  and  $\text{CF}_3$  groups are attached to the same transition metal atom. The reaction of  $\text{Ir}(\text{CO})_2(\text{PPh}_3)_2\text{CF}_3$  with  $\text{C}_2\text{F}_4$  generated  $\text{Ir}(\text{CO})(\text{PPh}_3)_2(\text{C}_2\text{F}_4)(\text{CF}_3)$ , 92% (67).

The addition of  $\text{Cd}(\text{CF}_3)_2\text{DME}$  to  $\text{Ir}(\text{CO})_2(\text{PPh}_3)_2(\text{CF}_3)$ ,  $\text{Ir}(\text{CO})(\text{PPh}_3)_2(\text{CF}_3)$ , or  $\text{Ir}(\text{CO})(\text{Cl})(\text{PPh}_3)_2$  results in  $\text{Ir}(\text{CO})(=\text{CF}_2)(\text{PPh}_3)_2(\text{CF}_3)$ , the only known complex that contains both  $\text{CF}_2$  and  $\text{CF}_3$  ligands. The last reaction is unique in that  $\text{Cd}(\text{CF}_3)_2\text{DME}$  acts as both a trifluoromethylating agent and a difluorocarbene source simultaneously.

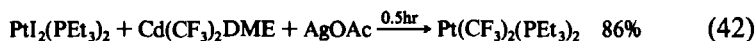
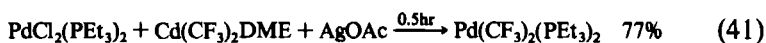


In the  $\text{Ir}(\text{CF}_2)(\text{CF}_3)$  derivative, the  $\text{CF}_3$  group is axial, and the  $\text{CF}_2$  group is equatorial, as might be expected. Treatment of  $\text{Ir}(\text{CO})(=\text{CF}_2)(\text{PPh}_3)_2(\text{CF}_3)$  with  $\text{H}_2\text{O}$  slowly hydrolyzes the  $\text{CF}_2$  ligand to CO, giving  $\text{Ir}(\text{CO})_2(\text{PPh}_3)_2(\text{CF}_3)$  (57%), while the addition of aqueous  $\text{HCl}$  results in  $\text{Ir}(\text{CO})(\text{Cl})(\text{H})(\text{PPh}_3)_2(\text{CF}_3)$  (59,67).

## F. Trifluoromethyl Derivatives of Group 10 Metals

### 1. Silver-Assisted Trifluoromethylations of Ni, Pd, and Pt Dihalides

In order to better assess the efficiency of the silver-assisted trifluoromethylations described earlier, we elected to reexamine the reactions of the group 10 diligand dihalides with  $\text{Cd}(\text{CF}_3)_2\text{DME}$ . The reactions were all carried out in  $\text{CH}_2\text{Cl}_2$  at ambient temperature with one equivalent of silver salt for each equivalent of the group 10 halide. The results of these reactions are



To more fully appreciate the benefits of the silver salt additions, the reaction conditions and the yields obtained from this study should be compared to those contained in Eqs. (12)–(14).

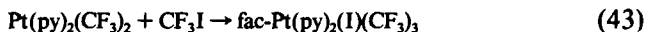
One of the most interesting aspects of these reactions was found in the trifluoromethylations of  $\text{NiCl}_2(\text{PMe}_3)_2$ . The expected product, *trans*- $\text{Ni}(\text{CF}_3)_2(\text{PMe}_3)_2$ , could be observed spectroscopically, but this compound clearly decomposed at ambient temperature ( $t_{1/2} \sim 1$  hr) into, among others,  $\text{Ni}(\text{CF}_3)_2(\text{PMe}_3)_3$ . If excess  $\text{PMe}_3$  was added to the reaction mixture after 10 min, however, the much more stable  $\text{Ni}(\text{CF}_3)_2(\text{PMe}_3)_3$  could be isolated in 24% yield (36). This is the same compound that was isolated by Firsich and Lagow from the metal atom reactions with  $\text{CF}_3$  radicals in 1981 (25).

In several of the Pd and Pt trifluoromethylations,  $\text{CuBr}$  was added to the reaction mixture rather than  $\text{AgOAc}$ . In those instances the trifluoromethylations proceeded even more rapidly, but the yields were somewhat lower, 71% for  $\text{Pd}(\text{CF}_3)_2(\text{PEt}_3)_2$  and 73% for  $\text{Pt}(\text{CF}_3)_2(\text{PEt}_3)_2$  (36).

### 2. Trifluoromethyl Platinum(II) and Platinum(IV) Compounds

The chemistry of trifluoromethylated platinum compounds continues to be an area of great interest. Lin and Klabunde have shown that platinum atoms react with  $\text{CF}_3\text{I}$ , but not  $\text{CF}_3\text{Br}$  or  $\text{CF}_3\text{Cl}$ , and that, in general, platinum atoms seem to be less reactive than those of Pd or Ni (68). The norbornadiene (NBD) ligand can be more easily displaced by weak bases like pyridine than COD, and the preparation and oxidations of a series of  $\text{Pt}(\text{CF}_3)_2$  compounds containing S-, N-, and O-donor ligands has been

examined. Under fluorescent light one of these compounds,  $\text{Pt}(\text{py})_2(\text{CF}_3)_2$ , oxidatively added  $\text{CF}_3\text{I}$  to generate  $\text{fac-PtI}(\text{py})_2(\text{CF}_3)_3$ , the first transition metal compound to contain three  $\text{CF}_3$  ligands (69–71):



In another study, the potentially tetradentate 2,2'-bipyrimidyl ligand (which contains four nitrogen atoms) was first coordinated to a  $\text{Pt}(\text{CF}_3)_2$  and then to a  $\text{PtMe}_2$  fragment, generating a molecule with a  $\text{Pt}(\text{CF}_3)_2$  group on one side and a  $\text{PtMe}_2$  group on the other (72).

Roundhill has shown that the  $\text{CF}_3$  group can be cleaved from *trans*- $\text{PtCl}(\text{PPh}_3)_2(\text{CF}_3)$  by  $\text{LiNMe}_2$  to give  $\text{NMe}_2(\text{CF}_3)$ . The proposed mechanism invokes direct attack of  $\text{NMe}_2^-$  on the  $\text{CF}_3$  ligand (73).

The Italian group has examined a series of  $\text{Pt}(\text{II})$  trifluoromethyl compounds that contain peroxo, hydrido, and alkoxy ligands along with the  $\text{CF}_3$  group (27,74). In several cases the  $\text{CF}_3$  (75) [or  $\text{CO}$  (76)] ligands have been converted into Fischer-type carbenes as



and in others the  $\text{CF}_3$  group serves as a spectator ligand (77).

Finally the UV–PES spectra of a number of *cis*- $\text{Pt}(\text{CF}_3)_2\text{L}_2$  complexes have been compared and contrasted with those of their dimethyl analogs. The assignments were made with the aid of  $\text{MS-X}\alpha$  calculations, which indicated that the  $\text{Pt}-\text{CF}_3$  bond has significant  $\text{C-}2s$  and  $\text{C-F}$  antibonding character (78).

### G. Trifluoromethyl Derivatives of Group 11 Metals

#### 1. Copper Trifluoromethyl Compounds

Copper trifluoromethyl has been synthesized by a number of techniques, including the reaction of  $\text{CuBr}$  with  $\text{Cd}(\text{CF}_3)_2\text{DME}$  in basic solvents, and by the reaction of  $\text{CuBr}$  with  $\text{CCl}_2\text{F}_2$  or  $\text{CBr}_2\text{F}_2$  and elemental cadmium in DMF (79,80). (Trifluoromethyl)copper, which exists in solution along with other  $\text{Cu}$  species including  $\text{Cu}(\text{CF}_3)_2^-$ , is thermally unstable and slowly decomposes into  $\text{CuC}_2\text{F}_5$  and  $\text{CuC}_3\text{F}_7$ . The addition of  $\text{PMe}_3$  into  $\text{CuCF}_3$ -containing solutions slows but does not stop the decomposition, presumably because  $\text{PMe}_3$  is not sufficiently strongly coordinated to  $\text{CuCF}_3$  to stabilize the complex (80). As yet, no simple derivative of  $\text{CuCF}_3$  has been isolated and characterized, but in an extensive series of investigations, Burton and co-workers have shown that  $\text{CuCF}_3$  can be generated *in situ* and then immediately utilized for the trifluoromethylation of organic substances (79,81).



Burton *et al.* have also isolated and characterized the very unusual Cu(III) trifluoromethyl compound  $\text{Cu}(\text{S}_2\text{CNET}_2)(\text{CF}_3)_2$  in which the coordination of the  $d^8$  Cu(III) ion is essentially square planar (82).

## 2. Silver Trifluoromethyl Compounds

Cocondensation of Ag atoms with  $\text{CF}_3$  radicals, followed by the addition of  $\text{PMe}_3$ , gave the very light-sensitive  $\text{Ag}(\text{PMe}_3)(\text{CF}_3)$  (24%) (83). This compound is also available in 36% yield from etherial solutions of  $\text{AgOAc}$  and  $\text{Cd}(\text{CF}_3)_2\text{DME}$  to which  $\text{PMe}_3$  was later added (80). In the absence of added  $\text{PMe}_3$ ,  $\text{AgCF}_3$  begins to decompose at  $-10^\circ\text{C}$  (83), and the products have been identified as  $\text{Ag}^\circ$  and the Ag(III)-containing  $\text{Ag}(\text{CF}_3)_4^-$  ion (86%), which are thought to arise from the disproportionation of the trifluoromethyl Ag(I) species (84).

## 3. Gold Trifluoromethyl Compounds

The Au(I) trifluoromethyl compounds  $\text{Au}(\text{PR}_3)(\text{CF}_3)$ ,  $\text{R}=\text{CH}_3$ ,  $\text{C}_2\text{H}_5$ , and  $\text{C}_6\text{H}_5$ , can all be formed in good yield from the interactions of the halides with  $\text{Cd}(\text{CF}_3)_2\text{DME}$  in  $\text{CH}_2\text{Cl}_2$  (80,85). Unlike the Au(I) alkyls, the trifluoromethyl derivatives can be halogenated with, e.g.,  $\text{Br}_2$  to form Au(III) trifluoromethyl dihalides (85).

The stability of the trivalent state of Au is quite sensitive to the nature of the ligands. For example,  $\text{CF}_3\text{I}$  [but not  $\text{CH}_3\text{I}$  (85)] oxidatively adds to  $\text{Au}(\text{PMe}_3)(\text{CF}_3)$  rapidly and quantitatively to generate *cis*- $\text{Au}(\text{I})(\text{PMe}_3)(\text{CF}_3)_2$  (80,85). The oxidative addition to the  $\text{PET}_3$  derivative, however, yields a mixture containing gold in both oxidation states (80). Trifluoromethyl iodide addition is not observed with the  $\text{PPh}_3$  compound (85). The  $\text{CF}_3\text{I}$  additions are quenched by the addition of galvinoxyl, an indication of a radical intermediate (80,85).

In the absence of  $\text{CF}_3\text{I}$ ,  $\text{Cd}(\text{CF}_3)_2\text{DME}$  is not an effective reagent for the trifluoromethylation of the Au(III) halides, but if  $\text{CF}_3\text{I}$  is added,  $\text{AuPMe}_3(\text{CF}_3)_3$  can be isolated in 80% yield (85). Metal atom reactions with cocondensed  $\text{CF}_3$  radicals have also resulted in  $\text{Au}(\text{PMe}_3)(\text{CF}_3)_3$  (20%), but in the absence of added ligand,  $\text{Au}(\text{CF}_3)_3$  begins to decompose at  $0^\circ\text{C}$  (83). Typically, the phosphine-stabilized trifluoromethyl gold compounds are reasonably air stable, and the  $\text{PMe}_3$  derivatives are noticeably more long lived than the  $\text{PET}_3$  compounds. In the absence of light, the thermal stability order of the trifluoromethyl group 11  $\text{PMe}_3$  compounds is  $\text{Au} > \text{Ag} > \text{Cu}$  (80).

Finally, the  $\text{Cd}(\text{CF}_3)_2\text{DME}$  trifluoromethylation of the gold ylide dimer  $[\text{Au}(\text{CH}_2)_2\text{PPh}_2]_2\text{Br}_2$  in  $\text{CH}_2\text{Cl}_2$  resulted in the formation of  $[\text{Au}(\text{CH}_2)_2\text{PPh}_2]_2(\text{CF}_3)_2$  (50%), the first Au(II) trifluoromethyl complex (86).

## H. Trifluoromethyl Derivatives of Group 12 Metals

### 1. Synthesis of $\text{Zn}(\text{CF}_3)_2\text{L}_2$ Compounds

Since  $\text{Cd}(\text{CF}_3)_2\text{DME}$  is ordinarily vastly superior to  $\text{Hg}(\text{CF}_3)_2$  as a trifluoromethylating agent, it seems only reasonable to assume that trifluoromethyl zinc compounds might well be even more effective. Diligand  $\text{Zn}(\text{CF}_3)_2$  complexes have been prepared by a number of routes, including the reactions of  $\text{Zn}(\text{CH}_3)_2$  with  $\text{Hg}(\text{CF}_3)_2$  (87) or  $\text{CF}_3\text{I}$  (88) in basic solvents like pyridine, dimethoxyethane, and acetonitrile.

In practice, however, the trifluoromethylating ability of the diligand  $\text{Zn}(\text{CF}_3)_2$  systems that have been investigated to date has been disappointing since the reactivity of the zinc compounds has been much less than that of the cadmium-based systems. As far as we are aware, the results of our study on the trifluoromethylation of  $\text{SnBr}_4$  are typical: The reactivity of the group 12 trifluoromethyl species examined falls in the order  $\text{Cd}(\text{CF}_3)_2\text{DME} \gg \text{Zn}(\text{CF}_3)_2(\text{py})_2 > \text{Zn}(\text{CF}_3)_2(\text{CH}_3\text{CN})_2 \gg \text{Hg}(\text{CF}_3)_2$  (33). As a result, at the present time the use of  $\text{Zn}-\text{CF}_3$  compounds is restricted to the preparation of fluorinated organic compounds, species that can easily withstand the thermal, ultrasound, or microwave excitation conditions that are generally required to induce reactions in the  $\text{Zn}(\text{CF}_3)_2\text{L}_2$  system.

Presumably, the difficulties associated with  $\text{Zn}(\text{CF}_3)_2\text{L}_2$  trifluoromethylations could be considerably reduced by utilizing a more weakly coordinating base. This alteration of the ligand, however, would almost surely reduce the thermal stability of the reagent. For example, in the weakly coordinating solvent  $\text{CH}_2\text{Cl}_2$ , the decomposition temperature of unligated  $\text{Zn}(\text{CF}_3)_2$  has been determined to be  $-40^\circ\text{C}$  (26).

### 2. $\text{Cd}(\text{CF}_3)_2\text{DME}$

Much of the inorganic chemistry of  $\text{Cd}(\text{CF}_3)_2\text{DME}$  has been recounted in the preceding sections where the diligand  $\text{Cd}(\text{CF}_3)_2$  complexes have been shown to be effective fluorinating agents (89), difluorocarbene sources, or trifluoromethyl donors, depending upon the nature of the substrate, the solvent, and the ligand. In one case,  $\text{Cd}(\text{CF}_3)_2\text{DME}$  served as a  $\text{CF}_2$  and  $\text{CF}_3$  donor simultaneously (67). In the absence of added base,  $\text{Cd}(\text{CF}_3)_2$  decomposes at  $0^\circ\text{C}$  in  $\text{CH}_2\text{Cl}_2$  (26).

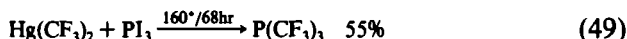
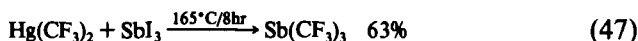
It should be noted here, however, that trifluoromethyl Cd compounds are becoming increasingly widely used in organic chemistry, particularly for the trifluoromethylation of organic (aryl) halides (90). One simple illustration of the versatility of the Cd reagent in carbon chemistry is that in  $\text{CH}_2\text{Cl}_2$ ,  $\text{Cd}(\text{CF}_3)_2\text{DME}$  fluorinates  $\text{PhC}(\text{O})\text{Cl}$  in 86% yield, and the liber-

ated  $\text{CF}_2$  can be trapped as  $\text{C}_2\text{F}_4$  in 40% yield (31). Alternatively, however, in pyridine, the reaction predominantly results in trifluoromethylation, and the ketone,  $\text{PhC(O)CF}_3$ , can be separated in 61% yield (91).

### 3. $\text{Hg}(\text{CF}_3)_2$

With the advent of the cadmium-based trifluoromethylating agents, the use of  $\text{Hg}(\text{CF}_3)_2$  in transition metal chemistry has become largely that of a compound useful for oxidative-addition reactions of electron-rich substrates, a type of reactivity that was first observed by Reutov *et al.* in  $\text{Pt(0)}$  systems (92). In main group chemistry,  $\text{Hg}(\text{CF}_3)_2$  can be used as either a fluorinating agent [with electron-poor species like the diboron tetrahalides (93)] or as a trifluoromethylating agent. For the latter function, the mercurial can be utilized somewhat more easily with main group substrates than with transition metal derivatives since trifluoromethyl containing main group compounds are often even more thermally stable than transition metal trifluoromethyl compounds.

For comparative purposes, some typical conditions that have been employed for ligand exchange reactions between  $\text{Hg}(\text{CF}_3)_2$  and group 5A(15) and group 6A(16) halides are



These, of course, are thermal conditions that very few transition metal organometallic compounds could withstand (94).

## IV

### SYNOPSIS OF TRIFLUOROMETHYL METAL STRUCTURAL DATA

Because the trifluoromethyl group has some of the attributes of a halogen and some of an alkyl, there are two obvious comparisons for the molecular structures of trifluoromethyl organometallic compounds. The first is to chlorides, compounds in which the  $\text{CF}_3$  group has replaced a halide of equivalent electronegativity (16). Recently, the structure of  $\text{CpCr(NO)}_2\text{CF}_3$  has been obtained, and within experimental uncertainty,

all but one of the parameters for the spectator ligands are unaffected by the  $\text{CF}_3$  for Cl substitution. The lone exception is the NO bond length, which is slightly longer in the  $\text{CF}_3$  compound (1.18 Å) (41) than in the chloride (1.14 Å) (95). The average C—F bond lengths (1.356 Å) and FCF bond angles (103.5°) are typical of those found in very thermally stable  $\text{CF}_3$  derivatives (41). For example, they are very similar to the 1.363 Å and 103.0° values found for the  $\text{CF}_3$  group in  $\text{Cp}^*\text{Mo}(\text{CO})_3\text{CF}_3$  (40) and near the 1.404 Å and 99.1° found in *trans*- $\text{PtH}(\text{PPh}_3)_2(\text{CF}_3)$  (75). The decrease from the tetrahedral bond angle can be explained by Bent's rule (1).

The M—C bond lengths decrease when the difluorocarbene cation is formed and the bond shortening is 0.28 Å in  $\text{Cp}^*\text{Mo}(\text{CO})_3\text{CF}_2^+$  (40). The C—F bond length is also shorter in the carbene by 0.05 Å, and the FCF angle is reduced to 98.2°. These last are very typical of the  $\text{CF}_2$  groups in  $\text{M}=\text{CF}_2$  compounds and comparable to those in  $\text{CpFe}(\text{CO})(\text{PPh}_3)(\text{CF}_2)^+$  (50). The FCF angle in  $\text{Ru}(\text{CO})_2(\text{PPh}_3)_2(=\text{CF}_2)$ , however, is only 88.7° (57). In the Fe—Ir complex (48), the C—F bond length of the bridging  $\text{CF}_2$  group is 1.367 Å and the FCF bond angle is 103.0°. The classic example of the differences in bond length between M— $\text{CF}_3$  and  $\text{M}=\text{CF}_2$  bonds, of course, is provided by Roper and co-workers' complex,  $\text{Ir}(\text{CO})(\text{PPh}_3)_2(=\text{CF}_2)(\text{CF}_3)$ , in which the bond lengths are 1.874 Å for the  $\text{Ru}=\text{CF}_2$  bond and 2.095 Å for the M— $\text{CF}_3$  bond (67).

Typically, the difference between the M— $\text{CH}_3$  and M— $\text{CF}_3$  bond lengths in similar complexes is ca. 0.05 Å with the latter expected to be the shorter. In  $\text{Ir}(\text{CO})\text{I}(\text{CH}_3)(\text{CF}_3)(\text{PPh}_3)_2$ , however, the reverse is true in that the Ir— $\text{CH}_3$  bond appears to be somewhat (ca. 0.03 Å) shorter than the Ir— $\text{CF}_3$  bond (67).

Finally, as noted above, in  $\text{Ru}(\text{CO})_2(\text{PPh}_3)_2(\text{CF}_3)(\text{HgCF}_3)$  the C—F bonds of the trifluoromethyl group attached to the mercury (1.29 Å) are shorter than those of the trifluoromethyl group attached to the Ru (1.38 Å) (55). This is in accord with the general expectation, but one interesting fact is that the corrected C—F bond distance (1.349 Å) in the parent mercurial,  $\text{Hg}(\text{CF}_3)_2$ , is longer by 0.06 Å than in the Ru derivative (96). Thus two-thirds of the difference between the two C—F bond lengths in the Ru compound comes from the contraction of the C—F bond length of the mercurial upon substitution.

## V

### PROSPECTS

The  $\text{CF}_3$  ligand is a highly desirable ligand for many applications in both organic and inorganic chemistry. As discussed above, in transitional metal organometallic chemistry, the substitution of a  $\text{CF}_3$  group for a  $\text{CH}_3$  group

commonly dramatically improves the thermal, oxidative, and hydrolytic stability of the product. Simultaneously, it provides an almost unique spectroscopic probe since the  $^{19}\text{F}$  NMR chemical shift range of trifluoromethyl metal compounds is in a region of the spectrum that is largely unencumbered by resonances derived from unrelated species. Similarly, the CF stretches in the IR (ca.  $1000\text{ cm}^{-1}$ ) are often well separated from the absorptions due to other chromophores.

On a second level, the introduction of a  $\text{CF}_3$  group in place of a  $\text{CH}_3$  substituent often has subtle effects on the remainder of the molecule. For example, due to the high *trans*-influence of  $\text{CF}_3$ , the bond lengths of other groups are often increased slightly with a concomitant increase in reactivity. The relative stability of the higher oxidation states of metals is often dramatically affected, which strongly influences reactions of the oxidative-addition type. An even longer-range effect can be found in some of Schrock's polymerization catalysts, which are much more efficient when partially fluorinated alcoxides are coordinated to the metal than when the comparable hydrogenated alcoxides are. Because of the unique nature of the  $\text{CF}_3$  ligand, a substituent not found in nature and first nurtured to life in Harry Emeleus' laboratory, there has been a steadily growing interest in chemistry of trifluoromethylated compounds. The present summary has presented much of the work that has been carried out during the past decade, but what of the future?

Obviously, to examine the chemistry of new compounds there must first be a preparative route to these species. During the past decade, considerable progress has been made in learning how to utilize the newer reagents that have been developed, and especially  $\text{Cd}(\text{CF}_3)_2\text{DME}$  in the presence of silver salts and as a  $\text{CF}_2$  transfer reagent; but many, if not most of the potential substrates, have not yet been examined. Beyond these studies, however, there remains a variety of interesting questions. One trivial example is, How does one make any trifluoromethyl derivative of any of the lanthanides or the actinides? A second example is, How does one selectively substitute organic species, especially biologically active compounds with a trifluoromethyl group? At least on the basis of the present knowledge, these types of questions will only be answered when reagents even more effective than the cadmium reagent have been developed.

#### ACKNOWLEDGMENTS

The financial assistance of the National Science Foundation is deeply appreciated, and the essential experimental contributions of Larry Krause, Cindy Ontiveros, Haridasan Nair, Ed Ganja, and Demetrakis (Jim) Loizau are gratefully acknowledged.

## REFERENCES

1. J. A. Morrison, *Adv. Inorg. Chem. Radiochem.* **27**, 293 (1983).
2. R. J. Lagow, and J. A. Morrison, *Adv. Inorg. Chem. Radiochem.* **23**, 177 (1980).
3. P. M. Treichel, and F. G. A. Stone, *Adv. Organomet. Chem.* **1**, 143 (1964).
4. R. E. Banks, "Fluorocarbons and Their Derivatives" Oldbourne, London, England, 1964; R. E. Banks, ed. "Fluorocarbon and Related Chemistry," Vols. 1–3. Chemical Society, London, England, 1971, 1974, 1976.
5. N. M. Doherty, and N. R. Hoffman, *Chem. Rev.* **91**, 553 (1991).
6. P. J. Brothers, and W. R. Roper, *Chem. Rev.* **88**, 1293 (1988).
7. R. P. Hughes, *Adv. Organomet. Chem.* **31**, 183 (1990).
8. H. J. Emeleus, "The Chemistry of Fluorine and its Compounds." Academic Press, New York, 1969.
9. H. J. Emeleus, and R. N. Haszeldine, *J. Chem. Soc.*, 2953 (1949).
10. T. H. Coffield, J. Kozikowski, and R. D. Closson, *Abstr. Proc. Int. Conf. Coord. Chem.*, 5th, p. 126. Chemical Society, London, England, 1959.
11. M. A. Bennett, H. Chee, and G. B. Robertson, *Inorg. Chem.* **18**, 1061 (1979).
12. W. R. McClellan, *J. Am. Chem. Soc.* **83**, 1598 (1961).
13. See, for example, R. B. King, A. D. King, M. Z. Iqbal, and C. C. Frazier, *J. Am. Chem. Soc.* **100**, 1687 (1978).
14. J. F. Ogilvie, *J. Chem. Soc. Chem. Commun.*, 323 (1970).
15. H. C. Clark, and J. H. Tsai, *J. Organomet. Chem.* **7**, 515 (1967); F. A. Cotton, and R. M. Wing, *J. Organomet. Chem.* **9**, 511 (1967).
16. In "Inorganic Chemistry, 3rd Ed." Harper and Row, New York, 1983, J. E. Huheey gives "best" group electronegativities of 2.3 for the  $\text{CH}_3$  group and 3.4 for the  $\text{CF}_3$  group. The electronegativities (Pauling) of F, Cl, and Br are 4.0, 3.2, and 3.0. The electronegativity of a  $\text{CF}_3$  group is thus at least as high as that of chlorine.
17. W. A. G. Graham, *Inorg. Chem.* **7**, 315 (1968).
18. M. B. Hall, and R. F. Fenske, *Inorg. Chem.* **11**, 768 (1972).
19. See, for example, M. R. Churchill, and J. P. Fennessey, *Inorg. Chem.* **6**, 1213 (1967); M. R. Churchill, *Perspect. Struct. Chem.* **3**, 91 (1970).
20. R. B. King, S. L. Stafford, P. M. Treichel, and F. G. A. Stone, *J. Am. Chem. Soc.* **83**, 3604 (1961).
21. H. C. Clark, and L. E. Manzer, *J. Organomet. Chem.* **59**, 411 (1973).
22. D. W. McBride, E. Dudek, and F. G. A. Stone, *J. Chem. Soc.*, 1752 (1964).
23. K. J. Klabunde, *Angew. Chem. Int. Ed. Engl.* **14**, 287 (1975).
24. K. J. Klabunde, B. B. Anderson, and K. Neuenschwander, *Inorg. Chem.* **19**, 3719 (1980).
25. D. W. Firsich, and R. J. Lagow, *J. Chem. Soc. Chem. Commun.*, 1283 (1981).
26. T. J. Juhlke, R. W. Braun, T. R. Bierschenk, and R. J. Lagow, *J. Am. Chem. Soc.* **101**, 3229 (1979); M. S. Guerra, T. R. Bierschenk, and R. J. Lagow, *J. Am. Chem. Soc.* **108**, 4103 (1986).
27. R. A. Michelin, U. Belluco, and R. Ros, *Inorg. Chim. Acta* **24**, L33 (1976).
28. L. C. Krisher, W. A. Watson, and J. A. Morrison, *J. Chem. Phys.* **61**, 3429 (1974).
29. R. J. Lagow, R. Eujen, L. L. Gerchman, and J. A. Morrison, *J. Am. Chem. Soc.* **100**, 1722 (1978).
30. L. J. Krause, and J. A. Morrison, *Inorg. Chem.* **19**, 604 (1980).
31. L. J. Krause, and J. A. Morrison, *J. Am. Chem. Soc.* **103**, 2995 (1981).
32. L. J. Krause, and J. A. Morrison, *J. Chem. Soc. Chem. Commun.*, 1282 (1981).
33. C. D. Ontiveros, Ph.D. Thesis, University of Illinois at Chicago, Chicago, Illinois, 1986.
34. R. B. King, and M. B. Bisnette, *J. Organomet. Chem.* **2**, 15 (1964).

35. E. A. Ganja, Ph.D. Thesis, University of Illinois at Chicago, Chicago, Illinois, 1988; E. A. Ganja, D. C. Loizou, and J. A. Morrison, *J. Organomet. Chem.*, submitted.
36. D. C. Loizou, Ph.D. Thesis, University of Illinois at Chicago, Chicago, Illinois, 1991.
37. D. Naumann, and H. Varbelow, *J. Fluorine Chem.* **41**, 415 (1988).
38. D. L. Reger, and M. D. Dukes, *J. Organomet. Chem.* **153**, 67 (1978).
39. T. G. Richmond, and D. F. Shriver, *Organometallics* **2**, 1061 (1983); **3**, 305 (1984).
40. J. D. Koola, and D. M. Roddick, *Organometallics* **10**, 591 (1991).
41. D. C. Loizou, J. Castillo, A. R. Oki, N. S. Hosmane, and J. A. Morrison, *Organometallics* **11**, 4189 (1992).
42. J. A. Connor, M. T. Zafarani-Moattar, J. Bickerton, N. I. El Saied, S. Suradi, R. Carson, G. Al Takhin, and H. A. Skinner, *Organometallics* **1**, 1166 (1982).
43. S. K. Shin, and J. L. Beauchamp, *J. Am. Chem. Soc.* **112**, 2066 (1990).
44. S. K. Shin, and J. L. Beauchamp, *J. Am. Chem. Soc.* **112**, 2057 (1990).
45. D. Saddei, H. J. Freund, and G. Hohlneicher, *J. Organomet. Chem.* **186**, 63 (1980).
46. F. U. Axe, and D. S. Marynick, *J. Am. Chem. Soc.* **110**, 3728 (1988).
47. T. G. Richmond, A. M. Crespi, and D. F. Shriver, *Organometallics* **3**, 314 (1984).
48. A. M. Crespi, M. Sabat, and D. F. Shriver, *Inorg. Chem.* **27**, 812 (1988).
49. An alternative approach to the synthesis of bridging CF<sub>2</sub> complexes has been reported in W. Schulze, H. Hartl, and K. Seppelt, *Angew. Chem. Int. Ed. Engl.* **25**, 185 (1986).
50. A. M. Crespi, and D. F. Shriver, *Organometallics* **4**, 1830 (1985).
51. D. W. Hensley, W. L. Wurster, and R. P. Stewart, *Inorg. Chem.* **20**, 645 (1981).
52. W. Dukat, and D. Naumann, *J. Chem. Soc. Dalton Trans.* 739 (1989).
53. I. I. Gerus, Yu. L. Yagupol'skii, and N. D. Volkov, *Zh. Org. Khim.* **18**, 1186 (1982).
54. C. R. Jablonski, *Inorg. Chem.* **20**, 3940 (1981).
55. G. R. Clark, S. V. Hoskins, and W. R. Roper, *J. Organomet. Chem.* **234**, C9 (1982).
56. L. M. Boyd, G. R. Clark, and W. R. Roper, *J. Organomet. Chem.* **397**, 209 (1990).
57. G. R. Clark, S. V. Hoskins, T. C. Jones, and W. R. Roper, *J. Chem. Soc. Chem. Commun.*, 719 (1983).
58. G. R. Clark, T. R. Greene, and W. R. Roper, *Aust. J. Chem.* **39**, 1315 (1986).
59. In addition to Ref. (6), the chemistry of these compounds has been summarized in M. A. Gallop, and W. R. Roper, *Adv. Organomet. Chem.* **25**, 121 (1986), and in W. R. Roper, *J. Organomet. Chem.* **300**, 167 (1986).
60. C. D. Ontiveros, and J. A. Morrison, *Organometallics* **5**, 1446 (1986).
61. D. J. Brockway, B. O. West, and A. M. Bond, *J. Chem. Soc. Dalton Trans.*, 1891 (1979).
62. D. G. Brown, and R. B. Flay, *Inorg. Chim. Acta* **57**, 63 (1982).
63. K. L. Brown, and T. Yang, *Inorg. Chem.* **26**, 3007 (1987).
64. A. K. Burrell, G. R. Clark, J. G. Jeffrey, C. E. F. Rickard, and W. R. Roper, *J. Organomet. Chem.* **388**, 391 (1990).
65. T. R. Greene, and W. R. Roper, *J. Organomet. Chem.* **299**, 245 (1986).
66. G. R. Clark, T. R. Greene, and W. R. Roper, *J. Organomet. Chem.* **293**, C25 (1985).
67. P. J. Brothers, A. K. Burrell, G. R. Clark, C. E. F. Rickard, and W. R. Roper, *J. Organomet. Chem.* **394**, 615 (1990).
68. S. T. Lin, and K. J. Klabunde, *Inorg. Chem.* **24**, 1961 (1985).
69. T. G. Appleton, R. D. Berry, J. R. Hall, and D. W. Neale, *J. Organomet. Chem.* **364**, 249 (1989).
70. T. G. Appleton, J. R. Hall, D. W. Neale, and M. A. Williams, *J. Organomet. Chem.* **276**, C73 (1984).
71. T. G. Appleton, R. D. Berry, J. R. Hall, and D. W. Neale, *J. Organomet. Chem.* **342**, 399 (1988).
72. V. F. Sutcliffe, and G. B. Young, *Polyhedron* **3**, 87 (1984).

73. S. Park, M. Pontier-Johnson, and D. M. Roundhill, *Inorg. Chem.* **29**, 2689 (1990).
74. R. A. Michelin, and R. Ros, *J. Chem. Soc. Dalton Trans.*, 1149 (1989).
75. R. A. Michelin, G. Facchin, and R. Ros, *J. Organomet. Chem.* **279**, C25 (1985); R. A. Michelin, R. Ros, G. Guadalupi, G. Bombieri, F. Benetollo, and G. Chapuis, *Inorg. Chem.* **28**, 840 (1989).
76. L. Zanotto, R. Bertani, and R. A. Michelin, *Inorg. Chem.* **29**, 3265 (1990).
77. R. A. Michelin, R. Bertani, M. Mozzon, L. Zanotto, F. Benetollo, and G. Bombieri, *Organometallics* **9**, 1449 (1990).
78. D. Yang, G. M. Bancroft, R. J. Puddephatt, and J. S. Tse, *Inorg. Chem.* **29**, 2496 (1990).
79. D. M. Wiemers, and D. J. Burton, *J. Am. Chem. Soc.* **108**, 832 (1986).
80. H. K. Nair, and J. A. Morrison, *J. Organomet. Chem.* **376**, 149 (1989).
81. J. G. MacNeil, and D. J. Burton, *J. Fluorine Chem.* **55**, 225 (1991), presents an alternative methodology for the formation of solvated  $\text{CuCF}_3$ .
82. M. A. Willert-Porada, D. J. Burton, and N. C. Baenziger, *J. Chem. Soc. Chem. Commun.*, 1633 (1989).
83. M. A. Guerra, T. R. Bierschenk, and R. J. Lagow, *J. Organomet. Chem.* **307**, C58 (1986).
84. W. Dukat, and D. Naumann, *Rev. Chim. Miner.* **23**, 589 (1986).
85. R. D. Sanner, J. H. Satcher, and M. W. Droege, *Organometallics* **8**, 1498 (1989).
86. H. H. Murray, J. P. Fackler, L. C. Porter, D. A. Briggs, M. A. Guerra, and R. J. Lagow, *Inorg. Chem.* **26**, 357 (1987).
87. E. K. S. Liu, *Inorg. Chem.* **19**, 266 (1980).
88. H. Lange, and D. Naumann, *J. Fluorine Chem.* **26**, 435 (1984).
89. In addition to the fluorinations of electron-poor metals described above, the fluorination of an Os(II) dichlorocarbene to give  $\text{Os}(\text{CO})(\text{Cl})_2(\text{PPh}_3)_2(=\text{CClF})$  has been described. S. V. Hoskins, R. A. Pauptit, W. R. Roper, and J. M. Waters, *J. Organomet. Chem.* **269**, C55 (1984).
90. In the reactions of the organic substrates, the trifluoromethyl cadmium reagents are generally prepared *in situ*. See, for example, P. L. Heinze, and D. J. Burton, *J. Fluorine Chem.* **29**, 359 (1985).
91. D. Naumann, M. Finke, H. Lange, W. Dukat, and W. Tyrre, *J. Fluorine Chem.* **56**, 215 (1992).
92. V. I. Sokolov, V. V. Bashilov, and O. A. Reutov, *J. Organomet. Chem.* **97**, 299 (1975).
93. D. A. Saulys, J. Castillo, and J. A. Morrison, *Inorg. Chem.* **28**, 1619 (1989).
94. E. A. Ganja, C. D. Ontiveros, and J. A. Morrison, *Inorg. Chem.* **27**, 4535 (1988).
95. O. L. Carter, A. T. McPhail, and G. A. Sim, *J. Chem. Soc. A*, 1095 (1966).
96. D. J. Brauer, H. Burger, and R. Eujen, *J. Organomet. Chem.* **135**, 281 (1977); H. Oberhammer, *J. Mol. Struct.* **48**, 389 (1978).



This Page Intentionally Left Blank

# ***Intramolecular Coordination in Organotin Chemistry<sup>1</sup>***

JOHANN T. B. H. JASTRZEBSKI and  
GERARD VAN KOTEN

*Department of Metal-Mediated Synthesis  
Debye Research Institute  
University of Utrecht  
3584 CH Utrecht  
The Netherlands*

I.	Introduction . . . . .	242
A.	Historical Perspective . . . . .	242
B.	Tin: Its Bonds and Valency . . . . .	242
C.	Principal Coordination Geometries at the Tin Center in Organotin Compounds. . . . .	244
D.	Outline . . . . .	246
II.	Divalent Organotin Compounds Containing a C,Y-Chelating Ligand . . . . .	247
A.	Introduction . . . . .	247
B.	Divalent Organotin Compounds Containing a Tin-Transition Metal Coordination Bond . . . . .	247
C.	Divalent Organotin Compounds Stabilized by Intramolecular Coordination . . . . .	249
D.	Reactivity of Divalent Organotin Compounds . . . . .	255
III.	Tetravalent Organotin Compounds Containing a C,Y-Chelating Ligand . . . . .	256
A.	General . . . . .	256
B.	Tetraorganotin Compounds Containing a C,Y-Chelating Ligand . . . . .	257
C.	Enhanced Reactivity of the Sn-C Bonds in Tetraorganotin Compounds as a Result of the Enforced Coordination of a Heteroatom-Containing Substituent . . . . .	261
D.	Triorganotin Halides Containing a C,Y-Chelating Ligand . . . . .	262
E.	Diorganotin Dihalides Containing a C,Y-Chelating Ligand . . . . .	279
F.	Monoorganotin Halides Containing a C,Y-Chelating Ligand . . . . .	286
IV.	Concluding Remarks . . . . .	288
	References . . . . .	290

<sup>1</sup> This article is dedicated to the 80th birthday of Prof. Dr. G. J. M. van der Kerk in recognition of his fine and pioneering contribution to organotin chemistry and its applications.

## I

## INTRODUCTION

*A. Historical Perspective*

The field of organotin chemistry has a long history that started as early as 1849, when Frankland isolated a specimen of diethyltin diiodide (1,2). In 1852, Löwich independently reported on the reaction of alkyl halides with a tin-sodium alloy giving alkyltin compounds (3). This last publication is usually considered to represent the beginning of organotin chemistry.

By 1935, about 200 publications concerning organotin chemistry had appeared in the literature. Important names in the development of organotin chemistry at that time were Krause in Germany, Kraus in the United States, and Kozeshkov in Russia [for a review, see Ref. (4)]. The discovery of industrial applications of organotin compounds as stabilizers against loss of HCl in polyvinyl chloride (5-7), as agrochemicals (8-11), as wood preservatives (12-16), and biocides (17-19) produced a renaissance of organotin chemistry. Particularly van der Kerk and his group in the Netherlands played a dominant role in this development [see Refs. (20) and (21) and references cited therein].

It was not until the early sixties that it was recognized that the tin atom in organotin compounds is capable of extending its coordination number beyond four. Based on colligative studies, a polymeric structure was proposed for trimethylpyrazolytin in apolar solvents with pentacoordinate tin centers; see Fig. 1a (22). Similarly, on the basis of IR spectroscopic studies, oligomeric structures with pentacoordinate tin centers were proposed for trimethyltin fluoride (23) and trimethyltin carboxylates (24-26) in which a fluoride or carboxylate group bridge trimethyl tin units; see Fig. 1b. However, the trimethyltin chloride pyridine adduct, Fig. 1c, was the first authenticated five-coordinate triorganotin halide complex for which the structure was proven by an X-ray crystal structure determination (27).

Although divalent inorganic tin compounds have been known for a long time,<sup>2</sup> it was in 1956 that the first example of a divalent organotin compound, i.e., bis(cyclopentadienyl)tin(II), was reported (29).

*B. Tin: Its Bonds and Valency*

In the periodic table of the elements, tin is listed in group 14, together with the elements carbon, silicon, germanium, and lead. The four electrons

<sup>2</sup> The first scientist who experimentally demonstrated the existence of two oxidation states of tin seems to have been B. Pelletier in 1792 (28).

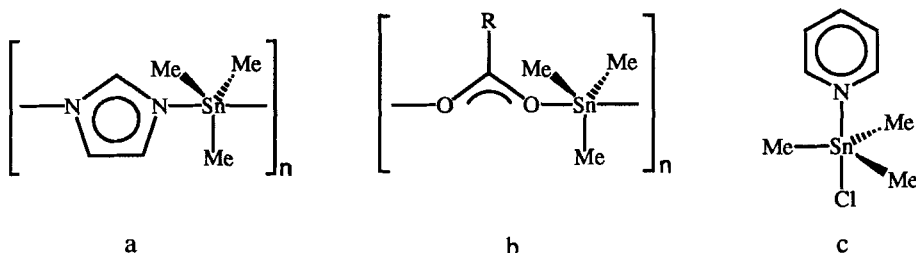


FIG. 1.

in the valence shell of the tin atom have the  $5s^25p^2$  electronic configuration. These valence electrons can undergo  $sp^3$  hybridization, and tetravalent tin atoms are therefore tetrahedral. The bonding of tin is almost entirely covalent, at least in crystalline solids, in nonpolar solvents and in the vapor phase. This is true even for tin—halogen bonds. The polarity that should follow from the difference in electronegativities is not observed, probably because of the large bond lengths.

Within group 14, the bond lengths to carbon increase considerably: C—C 1.54, C—Si 1.94, C—Ge 1.99, C—Sn 2.15, and C—Pb 2.29 Å. The increased bond length for tin is the cause of the increased reactivity and the related lower thermal stability of the tin alkyls compared with their C, Si, and Ge analogs. Long bonds naturally have low strength and also lessen the screening of the central atom by the ligands. Attacking reagents thus have easier access. This is particularly evident in organolead compounds (30).

Tin, like its congeners germanium and lead, can form compounds in the  $II^+$  formal oxidation state. Such compounds may be regarded as carbene analogs (31,32). Their main characteristics are that there are only six electrons in the valence shell and that one electron pair is nonbonding. This nonbonding electron pair may occupy one orbital with antiparallel spins (singlet,  $^1\sigma^2$ ) or two different orbitals with antiparallel (singlet,  $^1\sigma p$ ) or parallel spins (triplet,  $^3\sigma p$ ). In contrast to carbenes, the heavier analogs all have one property in common: The energetically most favorable electronic state is the singlet  $^1\sigma^2$  one (31). There are two ways to describe the structure of these singlet carbene analogs: (i) the nonbonding electron pair occupies an  $s$  orbital, the bonding electrons occupy  $p$  orbitals, and the third  $p$  orbital remains empty. The bond angles should then be strictly  $90^\circ$  (Fig. 2A), and (ii) both nonbonding and bonding electron pairs occupy  $sp^2$ -hybrid orbitals while again a  $p$  orbital is unoccupied. In this case, the bonding angle should be  $120^\circ$  (Fig. 2B).

When the experimentally determined bond angles of carbene analogs are compared, e.g., in  $MX_2$  ( $M = \text{Si, Ge, Sn, Pb}$ , and  $X = \text{F or Cl}$ ), the values

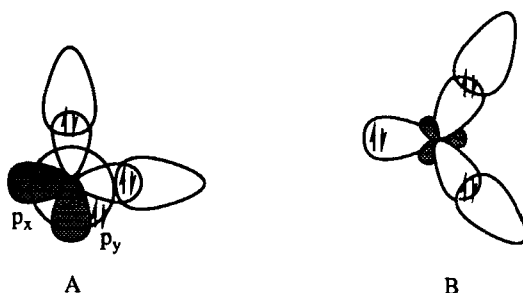


FIG. 2. The two possibilities to describe the structure of singlet carbene analogs.

are found to be between these two possibilities (31). With increasing atomic number of the central atom, the angles seem to approach  $90^\circ$ . The deviation from the angles predicted by the models A and B is accounted for by repulsion forces between the ligands (model A) or repulsion between the lone pair and the ligands in model B (valence-shell electron-pair repulsion theory) (33–35). For heavy elements, model A seems to be more important, and it is expected that divalent tin compounds have this geometry. For all inorganic divalent tin compounds known, so far this is the case (36). It should be noted that the nonbonding electron pair at the tin atom is not stereochemically active because it is located in a radially distributed *s* orbital. However, structures of solid tin(II) compounds often show the contrary (36). It is therefore assumed that the *s* orbital is mixed with energetically favorable orbitals, allowing a deviation from a spherical shape (37,38).

### C. Principal Coordination Geometries at the Tin Center in Organotin Compounds

Since empty *5d* orbitals of suitable energy also may be involved in the hybridization in divalent as well as in tetravalent tin, higher coordination numbers at tin are possible. In Fig. 3, the principal coordination geometries for both divalent and tetravalent tin are given, while it is assumed that in the case of divalent tin, the lone pair is also involved in the hybridization.

Some general trends for organotin coordination compounds [see Ref. (39) and references cited therein] have been well established. Based on the decreasing Lewis acidity with increasing number of organic groups present at tin, tetraorganotin compounds were regarded until recently as being unable to extend their coordination number due to the poor acceptor properties of the tin atom in these compounds. However, various examples showing that this assumption needs correction are now known.

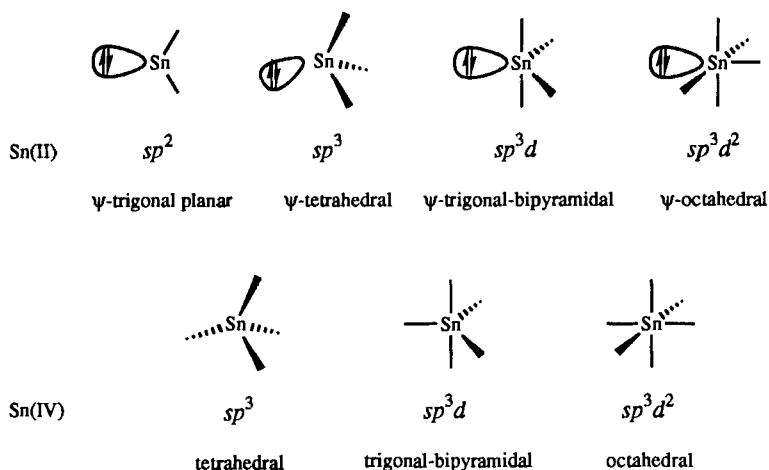
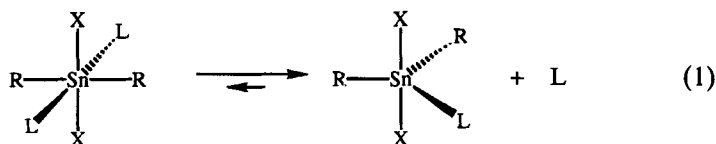


FIG. 3. The principal coordination geometries of divalent and tetravalent tin.

The preferred coordination geometry of the tin atom in triorganotin halides is trigonal bipyramidal with the carbon ligands at the equatorial sites and the more electronegative halide and donor atom at the axial positions (39).

Both trigonal bipyramidal and octahedral coordination geometries have been found for the tin atom in adducts of diorganotin dihalides with Lewis bases. The solid-state structures of complexes,  $\text{SnX}_2\text{R}_2 \cdot 2\text{L}$  ( $\text{L}$  = monobasic ligand), have generally two *trans*-oriented carbon ligands ( $\text{R}$ ), whereas the two halide and the two donor molecules can adopt either mutual *trans*- or *cis*-configurations, depending upon the nature of the substituent (40–48). In solution, these complexes exist as an equilibrium of a hexacoordinate and a pentacoordinate species, with the latter as the predominant one (49),



Little has been reported yet on the coordination chemistry of monoorganotin compounds. Coordination numbers of five to eight for the tin atom have been reported in such compounds (39,50,51). It has been suggested, however, that in solution a trigonal bipyramidal arrangement at tin is the most favorable one (49).

The coordination chemistry of divalent organotin compounds is a special case, since the tin atom can act both as an acceptor and as a donor, e.g., as in  $(\text{CO})_5\text{CrSn}(t\text{-Bu})_2 \cdot \text{pyridine}$  (52).

#### D. Outline

It has been well established that by using the properties of C,Y-chelating ligands (Y = heteroatom-containing substituent), organometallic compounds that have interesting properties and special reactivities can be isolated. It is therefore surprising that the concept of intramolecular coordination by the use of C,Y-chelating ligands has been little explored in organotin chemistry.

The first example of an organotin compound having C,Y-chelating ligands, i.e., bis[1, 2-bis(ethoxycarbonyl)ethyl]tin dibromide, was reported in 1968 for which the structure in the solid state was unambiguously established by an X-ray crystal structure determination (53). However, from 1976 a more systematic study of the properties of organotin halides containing C,N-chelating ligands was started (54).

It was recognized at an early stage of this research that the presence of an intramolecular coordinating substituent considerably increases the configurational stability of chiral triorganotin halides (54). Moreover, modern NMR techniques allowed a detailed interpretation of the fluxional processes operative in solution of these compounds. Furthermore, the penta-coordinate tin center in triorganotin halides may be considered as a model for the transition state of the  $\text{S}_{\text{N}}2$  substitution reaction at tetrahedral carbon centers, by which the intramolecular coordinating heteroatom may be regarded as the incoming nucleophile and the halogen atom as the leaving group.

It should be noted here that Corriu and co-workers have reported on organosilicon compounds containing C,N-chelating ligands in which the silicon atom is penta- or hexacoordinate (55–58). Such organosilicon compounds are models for the intermediates proposed for the activation of enoxysilanes by  $\text{F}^-$  leading to cross-aldolizations or Michael reactions (59).

In this account, we give an overview on organotin compounds containing C,Y-chelating ligands. Successively, the following type of compounds are discussed: (i) organotin(II) compounds, (ii) tetraorganotin(IV), (iii) triorganotin(IV), and (iv) di- and monoorganotin(IV) compounds. Special attention is given to (i) structures in the solid state, (ii) fluxional behavior in solution, and (iii) stereochemical aspects. Also attention is given to the enhanced reactivity of tin—carbon bonds in tetraorganotin compounds as result of intramolecular coordination.

## II

**DIVALENT ORGANOTIN COMPOUNDS CONTAINING A C,Y-CHELATING LIGAND***A. Introduction*

It was recognized fairly early that divalent organotin compounds  $\text{SnR}_2$  having covalent  $\text{Sn}-\text{C}$  bonds are unstable and polymerize readily (60–65). This was ascribed to the fact that the divalent tin atom in  $\text{SnR}_2$  compounds has both a doubly occupied and an empty orbital, which are accessible for  $\text{Sn}-\text{Sn}$  bond formation. This notion paved the way to methods that would lead to the stabilization of monomeric  $\text{SnR}_2$  species. It appeared that under certain conditions, organotin(II) compounds can be stabilized. These conditions, each of which may be sufficient by itself, are (i) the use of bulky organic groups as, e.g., in  $\text{Sn}[\text{CH}(\text{SiMe}_3)_2]_2$  (66), (ii) the coordination of the lone pair at tin to a suitable transition metal acceptor as, e.g., in  $(\text{CO})_5\text{CrSn}(t\text{-Bu})_2 \cdot \text{pyridine}$  (52), and (iii), the completion of the tin coordination sphere by the introduction in the organo-groups of substituents that are capable of intramolecular coordination. Since the first two approaches are beyond the scope of our account, only divalent organotin compounds that met the last condition are discussed. In general, it is now known that by using the steric and electronic properties of C,Y-chelating ligands, organometallic compounds that have interesting properties and special reactivities can be isolated. Special features of some of these compounds are: (i) stabilization of organometallic compounds in which the metal has an unusual oxidation number, e.g.,  $\text{Fe(III)}$  (67),  $\text{Co(II)}$  (68), and  $\text{Ni(III)}$  (69); (ii) the trapping of organometallic species that are supposed to be intermediates in reactions, e.g., organoplatinum compounds in which a diiodine molecule is coordinated end-on to platinum as a first step in oxidative-addition reactions (70); (iii) the use of a novel organonickel(II) compound as a catalyst in the selective Karasch addition of polyhaloalkanes to olefins (71); and (iv) the unexpected reactivity of organocopper compounds toward acetylenes (72). As discussed, these special effects of the C,Y-chelating ligand are also obvious in divalent organotin chemistry.

*B. Divalent Organotin Compounds Containing a Tin-Transition Metal Coordination Bond*

The earliest isolated organotin species in which the tin atom is in the  $\text{II}^+$  formal oxidation state are compounds in which the tin atom acts as a Lewis base that coordinates to a suitable transition metal fragment,



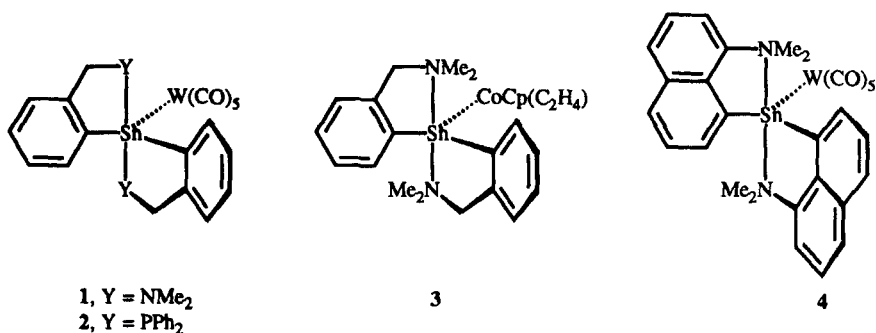
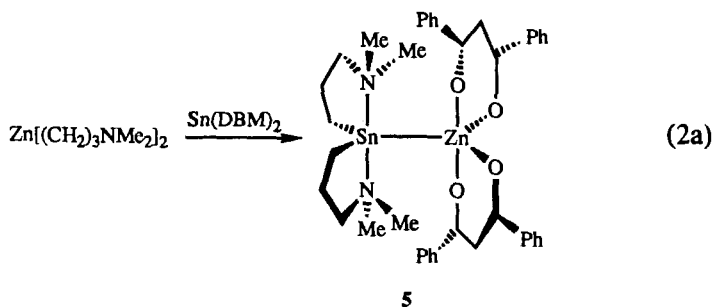


FIG. 4. Divalent organotin-transition metal compounds containing a C,Y-chelating ligand.

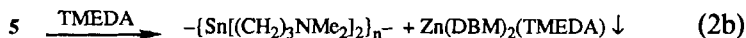
e.g., (CO)<sub>5</sub>CrSn(*t*-Bu)<sub>2</sub>·pyridine (52). It is therefore not surprising that the first reported divalent organotin compounds containing a C,Y-chelating ligand also contain a transition metal fragment, i.e., bis[2-[(dimethylamino)methyl]phenyl]tin tungsten pentacarbonyl, **1**; bis[2-[(diphenylphosphino)methyl]phenyl]tin tungsten pentacarbonyl, **2** (73); bis[2-[(dimethylamino)methyl]phenyl]tin cyclopentadienyl(ethylene)cobalt, **3** (74); and bis[8-(dimethylamino)-1-naphthyl]tin tungsten pentacarbonyl, **4** (75). It was found by X-ray crystallography that these compounds have closely related structures in which the tin centers have a trigonal bipyramidal coordination geometry, with the carbon ligands and the transition metal atom at the equatorial sites and both intramolecular coordinating heteroatoms at the axial positions; see Fig. 4.

A novel example of this type of SnR<sub>2</sub>·Lewis acid compound is the product obtained from the transmetalation reaction of bis[3-(dimethylamino)propyl]zinc with bis(dibenzoylmethanato)tin(II).



An X-ray crystal structure determination showed this compound to be a unique complex, **5**, in which an intramolecularly coordinated dialkyl-

tin(II) compound is acting as an electron donor to a zinc- $\beta$ -diketonate acceptor (76). The importance of the coordination of the  $\text{Sn}[(\text{CH}_2)_3\text{NMe}_2]_2$  tin lone pair to the  $\text{Zn}(\text{DBM})_2$  moiety for the stability of **5** becomes evident when **5** is reacted with 1 equivalent of tetramethylethylenediamine (TMEDA)



This reaction results in the quantitative formation of insoluble  $\text{Zn}(\text{DBM})_2(\text{TMEDA})$  and a soluble organotin oligomer. It is clear that in this reaction  $\text{Sn}[(\text{CH}_2)_3\text{NMe}_2]_2$  is liberated by a ligand-substitution reaction and undergoes the fast oligomerization reaction that is common for simple dialkyl- and diaryl-tin(II) compounds (77).

### C. Divalent Organotin Compounds Stabilized by Intramolecular Coordination

Recently the first examples of divalent organotin compounds in which intramolecular coordination as such is sufficient for stabilization were reported. These compounds are bis[2-[(dimethylamino)methyl]phenyl]tin(II), **6** (74); bis[2-[1-(dimethylamino)ethyl]phenyl]tin(II), **7** (78); bis[8-(dimethylamino)-1-naphthyl]tin(II), **8** (75); bis[[2-(dimethylamino)phenyl](trimethylsilyl)methyl]tin(II), **9** (78); and bis[(2-pyridyl)bis(trimethylsilyl)methyl]tin(II), **10** (79) and are schematically shown in Fig. 5.

According to X-ray crystal structure determinations of **6** and **8**, the best description of the coordination geometry of the tin center in these compounds is a  $\psi$ -trigonal bipyramidal one, with the carbon ligands and the lone pair at the equatorial sites and both intramolecular coordinating nitrogen atoms at the apical positions (74,75). Compound **10** has a square-pyramidal structure, with the lone pair at the apex of the pyramid. Most

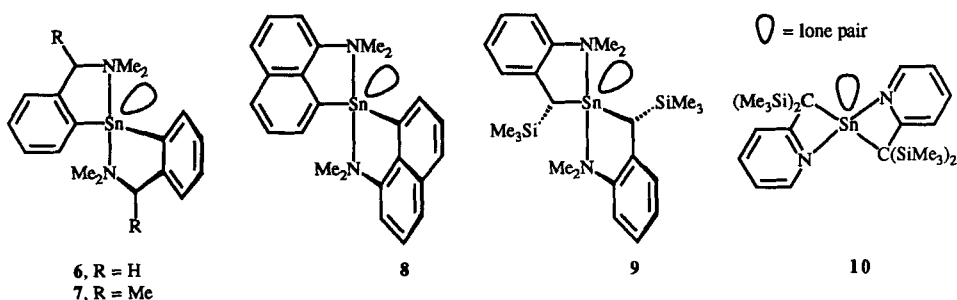


FIG. 5. Divalent organotin compounds stabilized by two C,N-chelating ligands.

likely, this latter geometry is the result of strain in the molecule due to the formation of two four-membered chelate rings (79).

The very acute C—Sn—C angles [100.5(1) and 93.8(5)° for **6** and **8**, respectively] seem to contrast with the values found for their corresponding W(CO)<sub>5</sub> adducts **1** and **4** [117.4(2) and 102.6(3)°, respectively]. However, the distorted  $\psi$ -trigonal bipyramidal arrangement in **6** and **8** is fully consistent with predictions using the VSEPR model (33–35) for discrete AX<sub>2</sub>Y<sub>2</sub>E species (A = central atom; E = lone pair; X, Y = ligands). In diorganotin N-donor complexes, repulsive forces between the Sn—C bonding electrons and the tin lone pair may be relieved either by a decrease in the C—Sn—C angle from 120° or by lengthening of the Sn—N bonds (35). In **6** and **8**, a reduction in the C—Sn—C angle is observed.

Based on the observed <sup>1</sup>H and <sup>13</sup>C NMR spectra of **7** and **9** at various temperatures, a  $\psi$ -trigonal bipyramidal coordination geometry at the tin center in these compounds was proposed also. <sup>1</sup>H and <sup>13</sup>C NMR spectroscopic studies of **6**–**10** showed that in solution, fluxional processes are operative. Although the coalescence of the diastereotopic NMe<sub>2</sub> resonances observed for **6** was explained in terms of a rapid “polytopal” rearrangement (74), studies on **7**, in which the chiral C<sub>6</sub>H<sub>4</sub>CH(Me)NMe<sub>2</sub>-2 ligand is present, showed unequivocal evidence for a process involving Sn—N dissociation/association (78).

As a consequence of the anticipated coordination geometry ( $\psi$ -trigonal bipyramidal) of the tin center in **9**, this atom becomes an additional chiral center. Since this compound is prepared starting from a racemic precursor, in principle three different diastereoisomers A, B, and C are expected (Fig. 6).

Structure C, in which the two chiral carbon atoms have opposite configurations, may be excluded on the basis of the low-temperature <sup>1</sup>H and <sup>13</sup>C NMR spectra. Here, the two organic groups are inequivalent and thus should give rise to two different resonance patterns, as was indeed observed for racemic bis[2-[1-(dimethylamino)ethyl]phenyl]tin(II) **7**, *vide infra*. However, **9** has only one resonance pattern to –80°C in the <sup>1</sup>H and <sup>13</sup>C NMR spectra. For steric reasons, structure A seems to be more likely than structure B, because the repulsion between the bulky SiMe<sub>3</sub> substituents in structure A will be considerable less than in B (cf. Fig. 6).

However, the existence of an equilibrium between A and B in solution, which lies predominantly to the side of A, may not be excluded, since this equilibrium would only require inversion of configuration at the Sn(II) center. Moreover, it was previously shown that for Sn(IV)Br[CH(SiMe<sub>3</sub>)C<sub>6</sub>H<sub>4</sub>NMe<sub>2</sub>-2]MePh in the solid state, as well as in solution, only one of the two possible diastereoisomers is present, i.e., the sterically most favorable one in which the SiMe<sub>3</sub> substituent and the phenyl group of tin lie at opposite sites of the molecule (80).

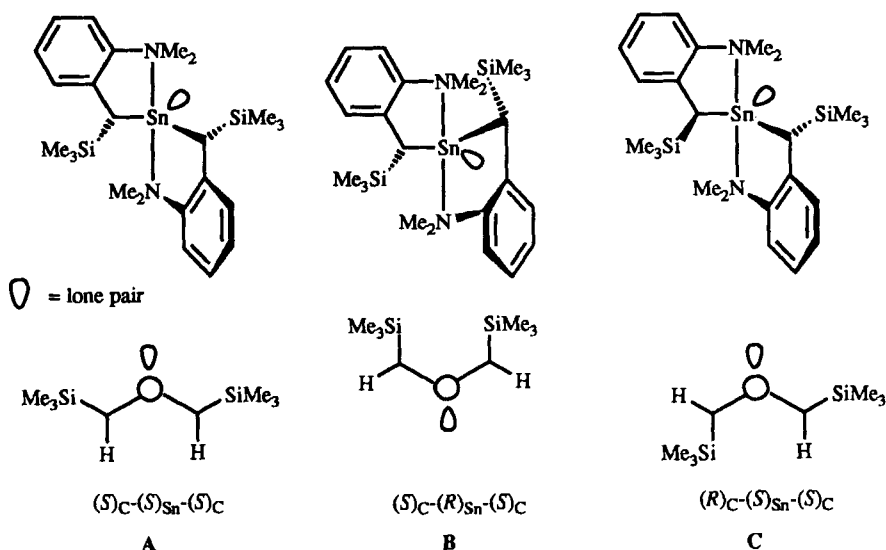


FIG. 6. Schematic representation of the three possible diastereoisomeric structures A, B, and C for **9**, together with a view along the axial vertex of the trigonal bipyramid, showing the relative positions of the bulky  $\text{Me}_3\text{Si}$  substituents.

The observation that only the diastereoisomer in which the two chiral carbon atoms have the same configuration is formed indicates that the reaction of racemic  $\text{Li}[\text{CH}(\text{SiMe}_3)(\text{C}_6\text{H}_4\text{NMe}_2-2)]$  with  $\text{SnCl}_2$  is diastereoselective. Most likely, the actual diastereoselection occurs in the second step of the reaction, i.e., during the reaction of the intermediate  $\text{SnCl}[\text{CH}(\text{SiMe}_3)(\text{C}_6\text{H}_4\text{NMe}_2-2)]$  with  $\text{Li}[\text{CH}(\text{SiMe}_3)(\text{C}_6\text{H}_4\text{NMe}_2-2)]$  to give **9**.

In contrast, the formation of two diastereoisomeric pairs of **7** in a 1 : 1 ratio from the reaction of racemic  $\text{Li}[\text{C}_6\text{H}_4\text{CH}(\text{Me})\text{NMe}_2-2]$  with  $\text{SnCl}_2$  is observed, indicating that this reaction is not diastereoselective. This is consistent with the rules for asymmetric induction (81–83) since in the diastereoselective step leading to the formation of **9**, the reaction center (the tin atom) is directly bonded to the chiral carbon atom, which controls the diastereoselectivity. In contrast, in the intermediate leading to **7**, the chiral center that could lead to diastereoselective induction is much farther away from the reaction center. Furthermore, in **7** the size of the substituents present at the chiral carbon atom is much smaller than that in **9** (Me versus  $\text{SiMe}_3$ ).

Finally, an interesting organotin compound is the product obtained from the reaction of 3 equivalents of (2-[(diphenylphosphino)methyl]phenyl)magnesium chloride with 2 equivalents of  $\text{SnCl}_2$  (84). For **11**, the

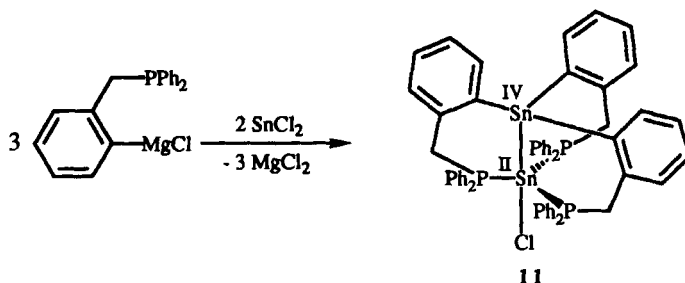


FIG. 7. Proposed structure for the product obtained from the reaction of 3 equivalents of (2-[(diphenylphosphino)methyl]phenyl)magnesium chloride with 2 equivalents of  $\text{SnCl}_2$ .

proposed structure, based on  $^1\text{H}$ ,  $^{31}\text{P}$ , and  $^{119}\text{Sn}$  NMR spectroscopy, is schematically shown in Fig. 7. In this compound the three C,P-chelating ligands bridge between a divalent and a tetravalent tin atom: A tin—tin bond between the two tin atoms is proposed.

The first examples of heteroleptic divalent organotin compounds authenticated by X-ray crystal structure determinations are: [2-pyridylbis(trimethylsilyl)methyl]tin chloride **12** and [2-pyridylbis(trimethylsilyl)methyl]bis(trimethylsilyl)amidotin **13**, for which the structures are schematically shown in Fig. 8 (73). The distorted trigonal pyramidal coordination geometry of the tin center in these compounds may be a result of the formation of a four-membered chelate ring.

It has been well established that the monoanionic terdentate 2,6-bis[(dimethylamino)methyl]phenyl ligand stabilizes otherwise unstable or transient organometallic species to such an extent that they become isolable (85). Especially in late transition metal chemistry, the three hard donor atoms of this ligand have been shown to enhance the nucleophilic character of  $\text{Ni(II)}$  and  $\text{Pt(II)}$  centers and, moreover, stabilize organometallic species in which the metal has an unusual oxidation number, e.g.,  $\text{Fe(III)}$ ,  $\text{Co(II)}$ , and  $\text{Ni(III)}$  (67–69) for an organometallic compound. Previously it was thought that this ligand enforces a coordination geometry to the

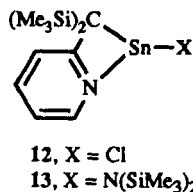
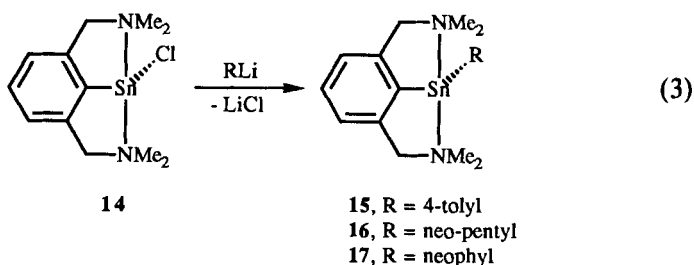


FIG. 8. The first examples of heteroleptic divalent organotin compounds.

metal in which the metal, the bound  $C_{ipso}$  atom, and the two coordinating nitrogen atoms are all in one plane. However, organotantalum compounds in which the tantalum atom has an octahedral coordination geometry containing a pseudo facially bonded 2,6-bis[(dimethylamino)methyl]phenyl ligand have been reported recently (86).

Previously, a Mössbauer spectroscopic study of  $SnCl[C_6H_3(CH_2NMe_2)_2-2,6]$  **14** and some related species that were assumed to be diaryltin(II) compounds were reported, but no further structural information on their structural features was given (87). Recently, the structural features of **14**, both in the solid state and in solution, have been reinvestigated (88). The X-ray structure determination of **14** showed the coordination geometry of this compound to be  $\psi$ -trigonal bipyramidal with the carbon ligand, the chlorine atom, and the lone pair at the equatorial sites and both coordinating nitrogen atoms at the axial positions, schematically shown in Eq. (3).



Remarkable is the acute  $C-Sn-Cl$  angle of  $95.0(3)^\circ$  in **14**, most probably for the same reason as found for the  $C-Sn-C$  angle in homoleptic divalent organotin compounds in which the tin center has a  $\psi$ -trigonal bipyramidal coordination geometry (*vide supra*).

Further reaction of the organotin(II) chloride **14** with 4-tolyl-, neopentyl-, or neophyllithium affords the unique corresponding mixed aryl-alkyltin(II) compounds **15**, **16**, and **17** respectively [Eq. (3)] (88).

The  $^1H$  and  $^{13}C$  NMR spectra of **14**–**17** show that in solution at low temperatures ( $-70^\circ C$  for **14** and  $-25^\circ C$  for **15**–**17**), these compounds have structures that are comparable to that found for **14** in the solid state, i.e., a  $\psi$ -trigonal bipyramidal coordination geometry at tin, with the nitrogen atoms at the axial positions and the remaining substituents and the lone pair in the equatorial plane.

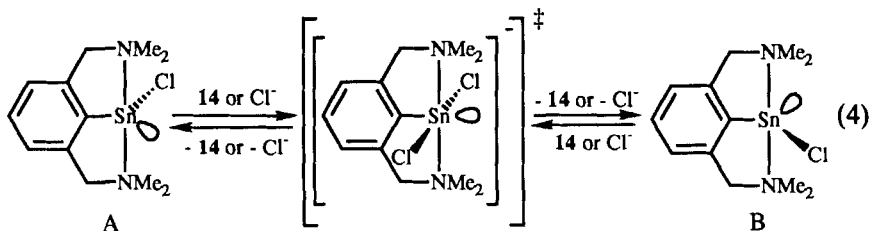
The observation of an AB pattern for the benzylic methylene resonances in the  $^1H$  NMR spectra indicates that the lone pair at tin is stereochemically active, and as a consequence the plane of the 2,6-bis[(dimethylamino)methyl]phenyl group is chiral. Furthermore, the observation of two

resonances for the  $\text{NMe}_2$  groups indicates that  $\text{Sn}-\text{N}$  coordination is inert at the NMR time scale at these temperatures.

A striking difference between the variable temperature NMR spectra of **14** and of **15-17** is observed. Although, in the heteroleptic diorganotin(II) compounds **15-17** coalescence occurs for the diastereotopic  $\text{NMe}_2$  resonances, the AB pattern of the benzylic methylene resonances remains intact up to  $+120^\circ\text{C}$  (the highest temperature studied). This points to a process involving  $\text{Sn}-\text{N}$  dissociation, while the  $\text{Sn}$  lone pair remains stereochemically active and rotation around the  $\text{C}_{\text{ipso}}-\text{Sn}$  bond is blocked. (Fast rotation around this bond would give rise to loss of the planar chirality and thus would render the diastereotopic benzylic methylene resonances homotopic.)

In the  $^1\text{H}$  NMR spectrum of **14**, however, simultaneous coalescence of both the  $\text{NMe}_2$  and  $\text{CH}_2$  resonances occurs, while the coalescence temperature  $T_c$  is strongly dependent on the concentration of **14** (16 mg/ml,  $T_c = -25^\circ\text{C}$ ; 180 mg/ml,  $T_c = -60^\circ\text{C}$ ). The coalescence of the AB pattern for the benzylic methylene protons indicates that the tin lone pair is no longer stereochemically active. The  $\Delta G^\ddagger$  values, calculated from the observed chemical shift differences and coalescence temperatures  $T_c$  for the benzylic methylene and  $\text{NMe}_2$  resonances, are 41.9 and 42.3 kJ/mol, respectively (concentration 180 mg/ml), indicating that both coalescence phenomena most probably result from the same process.  $\text{Sn}-\text{N}$  bond dissociation is most likely not involved in this process, as is shown by the presence in the  $^{13}\text{C}$  NMR spectrum of a two-bond  $^{117,119}\text{Sn}$  scalar coupling of 30 Hz to the  $\text{NMe}_2$  carbon atoms. This coupling does not change upon raising the temperature of the solution to  $120^\circ\text{C}$  (the highest temperature studied). Apparently, also at high temperature, i.e., in the coalesced situation,  $\text{Sn}-\text{N}$  coordination in **14** is inert at the NMR time scale. It is not unexpected that in **14**,  $\text{Sn}-\text{N}$  coordination is stronger than in **15-17**, since in **14** the  $\text{Sn}$  center has an increased Lewis acidity as a result of the presence of the chlorine atom.

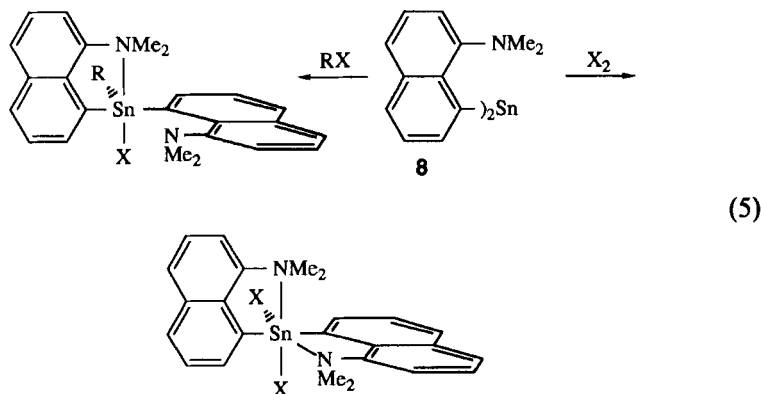
The simultaneous coalescence of the benzylic and  $\text{NMe}_2$  resonances in **14** indicates that on the NMR time scale a fast interconversion between structures A and B (inversion of configuration at tin) occurs.



The observation that the coalescence temperature is dependent on the concentration of **14** points to a bimolecular process. Furthermore, it appeared that addition of LiCl to a solution of **14** lowers the coalescence temperature of the NMe<sub>2</sub> and benzylic resonances. Therefore, ionic species, most probably resulting from initial dimerization of **14**, are proposed to be intermediates in the inversion of configuration at tin.

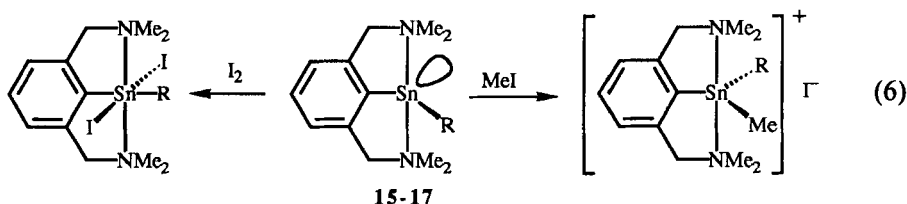
#### D. Reactivity of Divalent Organotin Compounds

It has been recognized that divalent organotin compounds easily undergo oxidative addition reactions (89). Similarly, **8** reacts with alkyl halides and dihalogen to give the corresponding oxidative addition products (75).



These interesting compounds are discussed in Section III.

Similarly, the heteroleptic diorganotin compounds **15–17** react with diiodine and methyl iodide



giving rise to the formation of hexacoordinate diorganotin diiodides and pentacoordinate triorganotin cations, respectively (88). These type of compounds are discussed in Section III.



## III

TETRAVALENT ORGANOTIN COMPOUNDS CONTAINING A C,Y-  
CHELATING LIGAND

## A. General

As a consequence of the increasing number of electronegative groups present at the tin atom in the series  $\text{SnR}_4$ ,  $\text{SnXR}_3$ ,  $\text{SnX}_2\text{R}_2$ ,  $\text{SnX}_3\text{R}$  ( $\text{X}$  = halide or pseudo halide), the Lewis acidity at the tin center increases down this series. Due to the poor acceptor properties of the tin atom in tetraorganotin compounds, for a long time these compounds were regarded as being unable to extend their coordination number beyond four. A few examples of tetraorganotin compounds in which the tin atom may be regarded as penta- or even hexacoordinate have now been reported. These compounds have in common that coordination is enforced as a result of the rigid arrangement of a potentially intramolecular substituent.

For triorganotin(pseudo)halides, coordination saturation seems to be reached at coordination number five, usually with the three carbon ligands at the equatorial sites and the (pseudo)halogen atom and the coordinating heteroatom at the axial sites of a trigonal bipyramid. This is also true for triorganotin halides containing a C,Y-chelating ligand, and in these compounds the C,Y-chelating ligand spans an equatorial-axial edge of a trigonal bipyramid.

Depending on the number (one or two) of C,Y-chelating ligands present in diorganotin dihalides, either trigonal bipyramidal or octahedral coordination geometries have been found for the tin center.

Only a very limited amount of data are available for monoorganotin halides containing a C,Y-chelating ligand. In the solid state, a trigonal bipyramidal coordination geometry for the tin center is preferred. However, in solution when external donor molecules are also present, hexacoordinate species may be formed.

Unambiguous structural information in the solid state on organotin compounds containing a C,Y-chelating ligands has been obtained by single-crystal X-ray structure determinations. Also  $^{119\text{m}}\text{Sn}$  Mössbauer spectroscopy provides information on the structure and the type of bonding of organotin compounds in the solid state (90-92).

Valuable information concerning the structures in solution of organotin compounds containing a C,N-chelating ligand is obtained from  $^1\text{H}$ ,  $^{13}\text{C}$ , and  $^{119}\text{Sn}$  NMR spectroscopic studies. Furthermore, these studies provide sometimes detailed information on the fluxional processes that are operative in solutions of these compounds. It appears that the  $^{119}\text{Sn}$  chemical

shift value depends on: (i) the type of substituents present at tin and (ii) the coordination number of tin. It is especially the latter property that may cause large changes in chemical shift values. When the coordination number at tin in a given compound is raised from four to five to six, the chemical shift value is shifted downfield by a few hundred parts per million (93). Recently we have reported the  $^{119}\text{Sn}$  spectroscopic parameters of a series of tetra-, tri-, and diorganotin compounds containing several C,N-chelating ligands (94). The observation of one-bond  $^{119}\text{Sn}-^{13}\text{C}$  and two bond  $^{119}\text{Sn}-^1\text{H}$  coupling constants in the  $^{13}\text{C}$  and  $^1\text{H}$  NMR spectra of organotin compounds provides detailed information on the hybridization of the tin atom in these compounds. The tin—carbon bonds in tetrahedral and trigonal bipyramidal and octahedral arrangements at tin, respectively, proceeds via  $sp^3$ -,  $sp^2$ -, and  $sp$ -like orbitals. As a result of the increasing  $s$ -electron participation in the tin—carbon bonds in this series, increasing magnitudes of the  $^{119}\text{Sn}-^{13}\text{C}$  and  $^{119}\text{Sn}-^1\text{H}$  coupling constants are observed in the  $^{13}\text{C}$  and  $^1\text{H}$  NMR spectra, respectively.

#### B. Tetraorganotin Compounds Containing a C,N-Chelating Ligand

The Mössbauer spectra of the 3-(2-pyridyl)-2-thienyl tetraorganotin derivatives, 18–22 (Fig. 9) indicate that the tin center in these compounds is pentacoordinate (95). For 18, this was unambiguously proven by an X-ray crystal structure determination. In this compound, the tin atom has a distorted trigonal-bipyramidal coordination geometry, with  $\text{C}_{\text{ipso}}$  of the thienyl group and two of the  $p$ -tolyl groups at approximately equatorial positions and the nitrogen atom and one of the  $p$ -tolyl groups at the axial sites. A similar coordination geometry was found for the tin center in

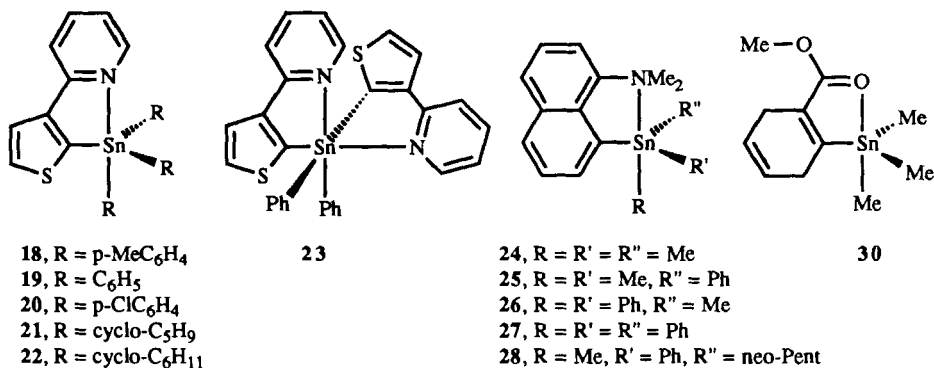


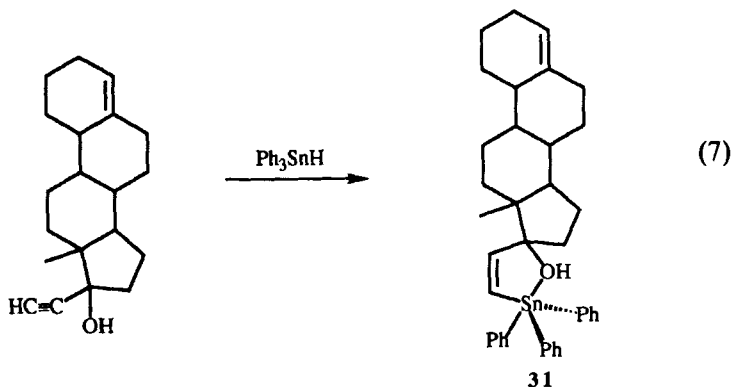
FIG. 9. Tetraorganotin compounds containing a C,N- or C,O-chelating ligand.

[8-(dimethylamino)-1-naphthyl]triphenyltin **27** (96). The Sn—N bond distances of 2.841(7) and 2.884(3) Å, for **18** and **27**, respectively, seem to be rather long, but are nevertheless shorter than those found in  $\text{SnCl}_2\text{Ph}_2 \cdot \text{pyrazine}$  (97), which amount to 2.782(11) and 2.965(11) Å, the latter distance being the longest one ascribed to Sn—N coordination. That in solution the tin centers in **18–22** and **24–28** are pentacoordinate was concluded from (i) the observation of an increase of the  $^1J(^{117,119}\text{Sn}—^{13}\text{C}_{\text{ipso}})$  value in the  $^{13}\text{C}$  NMR spectra and (ii) a high-field shift of the  $^{119}\text{Sn}$  resonance in the  $^{119}\text{Sn}$  NMR spectra (95,96).

An octahedral coordination geometry at the tin center was found by X-ray crystallography in bis[3-(2-pyridyl)-2-thienyl]diphenyltin, **23**; see Fig. 9 (98). The various groups at the tin center have an all-*cis* arrangement. The Sn—N distance of 2.560(2) Å is considerably shorter than that observed in **18**, *vide supra*. That the structure as found for **23** in the solid state is most likely retained in solution was concluded from the comparison of the  $^{119}\text{Sn}$  and  $^{13}\text{C}$  NMR spectra of solutions of **23**, with those of bis(2-thienyl)diphenyltin. Based on the  $^1\text{H}$ ,  $^{13}\text{C}$ , and  $^{119}\text{Sn}$  NMR spectral data of bis[8-(dimethylamino)-1-naphthyl]dimethyltin, **29**, a distorted octahedral coordination geometry for the tin center in this compound has also been proposed (96).

An X-ray crystal structure determination of (2-carbomethoxy-1,4-cyclohexadien-1-yl)trimethyltin, **30**, revealed that the tin center in this compound is pentacoordinate as a result of intramolecular Sn—O coordination; see Fig. 9 (99). The C(1) atom of the cyclohexadiene moiety and two of the methyl groups are at approximately equatorial positions, and the other methyl group and the coordinating oxygen atom [Sn—O distance 2.781(3) Å] are at the axial sites of a distorted trigonal bipyramid.

The reaction of 17-ethynyl-4-estren-17-ol with triphenyltin hydride



affords selectively the *cis*-addition product **31**, for which the X-ray struc-

ture unambiguously showed that the tin atom has a distorted trigonal bipyramidal coordination geometry, with two phenyl groups and the olefinic carbon atom at approximately equatorial positions, and the coordinating oxygen atom (Sn—O 2.77(1) Å) and one of the phenyl groups at the axial sites (100). It has been proposed that the preferred formation of the *Z*-isomer over the *E*-isomer, which generally are formed in these reactions, is a consequence of the presence of a potentially coordinating group.

The tetraorganotin compounds **18–31** all have in common that the coordinating heteroatom is part of a rather rigid skeleton, which keeps the potentially coordinating heteroatom in close proximity to the tin atom. It is probably this rigid ligand arrangement that enforces coordination of the heteroatom to tin.

Another class of tetraorganotin compounds for which pentacoordination of the tin atom was established are the diptych and triptych compounds, for which the proposed structures are schematically shown in Fig. 10.

That an Sn—Y interaction is present in the diptych compounds **32–34**, resulting in a trigonal-bipyramidal coordination geometry of the tin atom, was concluded from  $^1\text{H}$ ,  $^{13}\text{C}$ , and  $^{119}\text{Sn}$  NMR studies (101,102). The low-temperature  $^1\text{H}$  and  $^{13}\text{C}$  NMR spectra of **32** clearly showed the presence of an equatorial and an axial methyl group. The distinct difference between the equatorial and the axial substituent is furthermore illustrated by the observation of relatively large  $^1J(^{119}\text{Sn}—^{13}\text{C})$  and  $^2J(^{119}\text{Sn}—^1\text{H})$  values (377 and 54.5 Hz, respectively) for the equatorial methyl group compared with relatively small values for the axial methyl group (197 and 40.1 Hz, respectively). Most likely this is a result of the enhanced *s*-electron participation at the equatorial positions of the trigonal bipyramid.

That Sn—N coordination is present in the triptych compound **35** was unambiguously proven by an X-ray crystal structure determination of this compound (103). The tin atom in **35** has a distorted trigonal bipyramidal

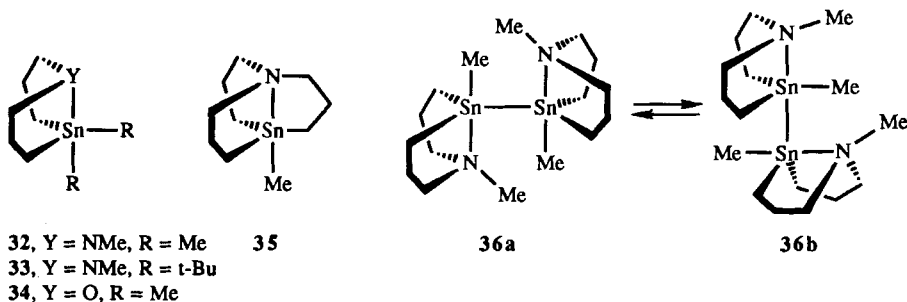


FIG. 10. Diptych and triptych tetraorganotin derivatives with intramolecular Sn—Y coordination.

coordination geometry, with the nitrogen atom (Sn—N distance 2.624(8) Å) and the methyl group at the axial positions.

Finally, in the diptych compound **36**, an intramolecular Sn—N interaction was proposed, based on the observed  $^1\text{H}$ ,  $^{13}\text{C}$ , and  $^{119}\text{Sn}$  NMR spectra (104). It appeared that in solution an equilibrium exists between at least three isomers for which the proposed structures of the two most abundant ones, **36a** and **36b** (70 and 27%, respectively) are shown in Fig. 10. Furthermore, 2D  $^{119}\text{Sn}$  EXSY spectroscopy (104) showed that these two isomers mutually isomerize via an uncorrelated rearrangement at the tin atom.

A rather unusual series of compounds, which may be regarded as tetraorganotin compounds containing a potentially C,N-chelating ligand, are the triorganotin hydrides **37–39** shown in Fig. 11 (105,106).

These compounds were obtained from the  $\text{LiAlH}_4$  reduction of the corresponding triorganotin bromides (*vide infra*). It should be noted that it is rather unexpected that these compounds are stable, since it is well known that amines catalyze the decomposition of organotin hydrides to ditin compounds and hydrogen (107).

The fact that these compounds were obtained as diastereoisomeric mixtures [the configuration of the (–)-menthyl unit is fixed, the configuration of the tin center may be either (*R*) or (*S*)], varying from 46:54 for **37** to 40:60 for **39** for the two diastereoisomers, indicates that the diastereoselection during the reduction step is small. Evidence for the anticipated intramolecular Sn—N coordination in **37** and **38** was obtained from the  $^1\text{H}$  and  $^{13}\text{C}$  NMR spectra of these compounds. The increased (compared to the values of menthylmethylnaphthyltin hydride)  $^1\text{J}(^{13}\text{C}—^{119}\text{Sn})$  and  $^1\text{J}(^1\text{H}—^{119}\text{Sn})$  values of the menthyl and hydride resonances, respectively, points to an increased *s*-orbital participation in these bonds, while the decreased (again compared to the values of menthylmethylnaphthyltin hydride)  $^1\text{J}(^{13}\text{C}—^{119}\text{Sn})$  and  $^2\text{J}(^1\text{H}—^{119}\text{Sn})$  values for the methyl resonance points to an decreased *s*-orbital participation in this bond. These

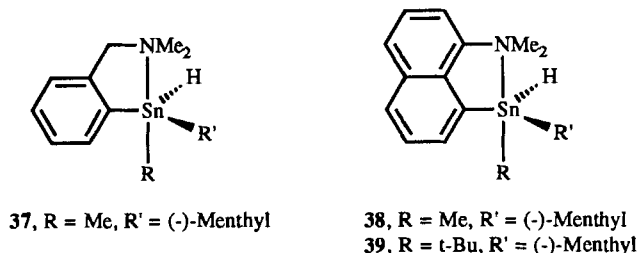
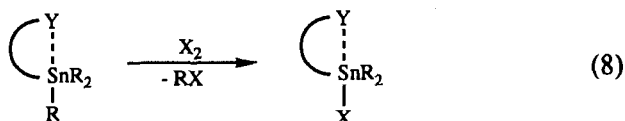


FIG. 11. Triorganotin hydrides containing a potentially C,N-chelating ligand and a chiral (–)-menthyl group.

observations suggest a distorted trigonal bipyramidal coordination geometry for the tin center in **37** and **38** with the menthyl group and hydride at equatorial positions and the methyl group at an axial site. An X-ray crystal structure determination unambiguously showed such a structure for **39** in which the menthyl group, the hydride and the naphthyl—C<sub>ipso</sub> are at the equatorial sites and the *tert*-butyl group and the coordinating nitrogen atom (Sn—N 2.885(3) and 2.931(3) Å for two independent molecules, respectively) at the axial positions.

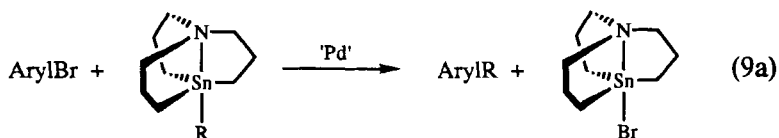
**C. Enhanced Reactivity of the Sn—C Bonds in Tetraorganotin Compounds as a Result of the Enforced Coordination of a Heteroatom-Containing Substituent**

Previously it has been suggested that the reversed reactivity sequence observed in halodemetalation reactions of mixed tetraorganotin compounds, in which a potentially coordinating group (Y) is present in the  $\gamma$ -position with respect to tin, is caused by intramolecular assistance of those groups (108,109):



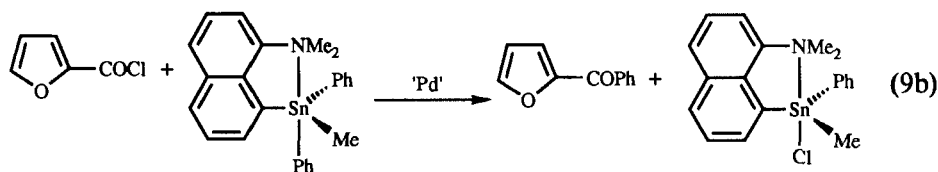
The presence of pentacoordinate tin in such tetraorganotin compounds was confirmed by the X-ray crystal structure determination of (2-carbomethoxy-1,4-cyclohexadien-1-yl)trimethyltin (**99**) *vide supra*. Furthermore, it was shown that tetraorganotin compounds containing the rigid C,N-chelating 8-(dimethylamino)-1-naphthyl ligand show an exceptional reactivity in the redistribution reaction with trimethyltin halide, resulting in the formation of tetramethyltin and a triorganotin halide containing the 8-(dimethylamino)-1-naphthyl ligand (96,110).

Recently it was shown that intramolecular coordination at tin in tetraorganotin compounds promotes the transfer of an organic group from tin to an organic halide in the Stille coupling reaction. In the presence of a Pd catalyst, the exocyclic alkyl group of 1-aza-5-alkyl-5-stannabicyclo[3.3.3]undecane selectively couples with aryl or alkenyl halides (111):



Furthermore, we have recently shown that the rate of the palladium-cata-

lyzed phenyl transfer from [8-(dimethylamino)-1-naphthyl]diphenylmethyltin to 2-furoyl chloride



is enhanced by a factor of  $10^2$  as a result of intramolecular assistance by the intramolecularly coordinating  $\text{NMe}_2$  group in the tetraorganotin compound (112).

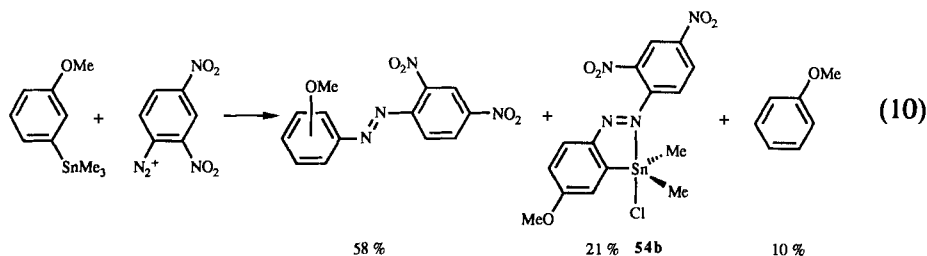
X-ray crystal structure determinations of different tetraorganotin compounds containing a C,Y-chelating ligand have shown that the  $\text{Sn}-\text{Y}$  coordination bonds are extremely long (*vide supra*). That these coordinating heteroatoms, however, have a considerable influence on the electronic situation at Sn is reflected in enlarged C—Sn bonds, *trans*-orientated with respect to the heteroatom. It is most likely that this *trans*-Sn—C bond shows an enhanced reactivity. Furthermore, it is interesting to note that these bond lengths fit very well in the theoretically deduced curve by Britton and Dunitz, of a  $\text{S}_{\text{N}}2$  pathway for substitution with inversion at tetrahedral tin (*vide infra*) (113).

#### D. Triorganotin Halides Containing a C,Y-Chelating Ligand

##### 1. Compounds Containing One Monoanionic C,N-Chelating Ligand

The triorganotin halides containing one monoanionic C,N-chelating ligand that has been studied are depicted in Fig. 12.

These compounds include the following type of C,N-chelating ligands: 2-[(dimethylamino)methyl]phenyl **40a–45** (54,114–117); [2-(dimethylamino)phenyl]methyl **46a–c**, **47a–c** (80); 8-dimethylamino-1-naphthyl **48–50** (110); (2-[(dimethylamino)methyl]phenyl)methyl **51,52** (118), 8-(dimethylamino)methyl-1-naphthyl, **53,54** (118), 2-(4,4-dimethyl-2-oxazoline)-5-(methyl)phenyl **55,56** (119); and 2-(phenylazo)phenyl **57a,57b** (120,121). For some representative examples, the structure was unambiguously proven by an X-ray crystal structure determination: **40c** (115), **41b** (114), **44b** (116), **47b** (80), **49** (96), **54** (118), **56** (119), **57a** (121), and **57b** (122). The last compound was obtained as an unexpected by-product from the reaction of 2,4-dinitrophenyldiazonium cation with (3-methoxyphenyl)trimethyltin (120):



All these compounds have in common that the tin center has a trigonal bipyramidal coordination geometry with the carbon ligands at the equatorial sites and the more electronegative nitrogen and halogen atom at the axial positions. Pentacoordination is attained by the formation of a five- or six-membered chelate ring spanning an equatorial-axial edge of the trigonal bipyramid.

Based on the  $^1\text{H}$ ,  $^{13}\text{C}$ , and  $^{119}\text{Sn}$  NMR data of these compounds, it is most likely that the structures as found in the solid state are retained in solution. It should be noted at this point that as a consequence of this geometry, the tin atom is stereogenic when different organic groups are present.

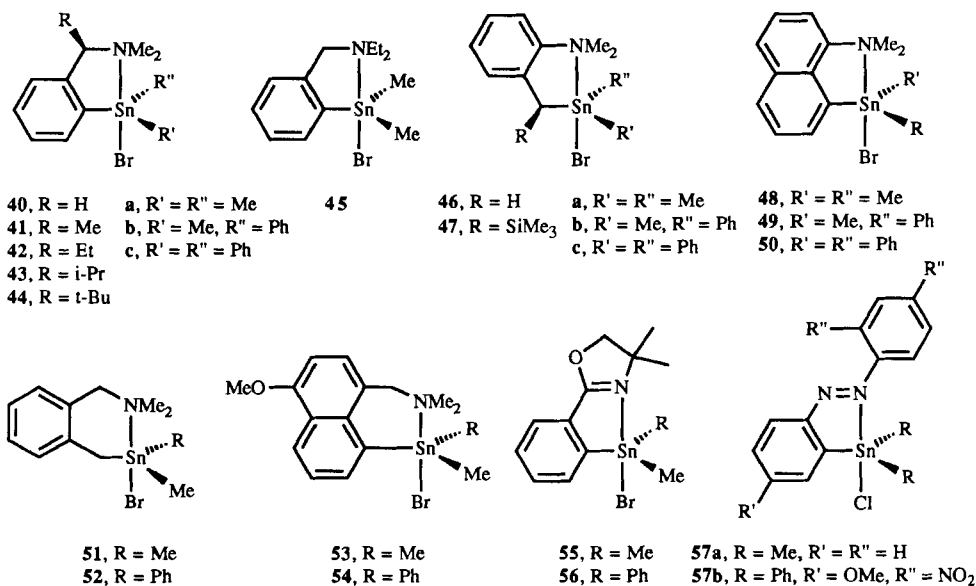


FIG. 12. Triorganotin halides containing one C,N-chelating ligand.



## 2. Stereochemical Aspects and Fluxional Processes at the Stereogenic Tin Centers in Triorganotin Halides Containing One Monoanionic C,N-Chelating Ligand

It has been well established that the configurational stability of the tin centers in triorganotin halides, which is usually very low, is enhanced to a considerable extent when intramolecularly coordinating substituents are present (123). The presence of a C,N-chelating ligand allows a detailed study concerning the fluxional processes that may be operative in solution. The two basic processes are (i) Sn—N dissociation/association and (ii) inversion of configuration of the tin center; see Fig. 13.

That these two processes are operative in solution was concluded by us from the observed  $^1\text{H}$  NMR spectra of chiral {2-[(dimethylamino)methyl]phenyl)methylphenyltin bromide **40b** at different temperature (54) (Fig. 14A). Below  $30^\circ\text{C}$ , the  $\text{NMe}_2$  and the benzylic  $\text{CH}_2$  groups are diastereotopic. Above this temperature, the two methyl resonances of the  $\text{NMe}_2$  group coalesce, indicating that a process involving Sn—N dissociation/association becomes fast on the NMR time scale [a similar conclusion was reached by a temperature-dependent lineshape analysis of the  $^1\text{H}$  resonances of the prochiral  $\text{NEt}_2$  group in **45** (117)]. In contrast, the AB pattern observed for the benzylic  $\text{CH}_2$  group remains unaltered up to at least  $125^\circ\text{C}$  (the highest temperature studied), indicating that configuration inversion of the chiral tin center does not occur or is still slow on the NMR time scale. Evidence that configuration inversion at the tin center does occur in such compounds was obtained by us from a study on triorganotin halides containing an additional, but configurationally stable, stereogenic center (chiral-labeling approach) (114,116).

When enantiomerically pure  $(R)_\text{C}(R)_\text{Sn}$  {2-[1-(dimethylamino)ethyl]phenyl)methylphenyltin bromide **41b** is dissolved in toluene, the  $^1\text{H}$  NMR spectrum at  $-30^\circ\text{C}$  shows the presence of only one diastereoisomer. However, at  $-13^\circ\text{C}$  an epimerization process starts, finally resulting in the formation of a 40:60 equilibrium mixture of the  $(R)_\text{C}(R)_\text{Sn}$  and  $(R)_\text{C}(S)_\text{Sn}$  diastereoisomers (114) (Fig. 14B).

This observation indicates that even at low temperature, i.e., when Sn—N coordination is inert at the NMR time-scale inversion of configura-



FIG. 13. The two basic fluxional processes operative in solutions of triorganotin halides containing a C,N-chelating ligand.

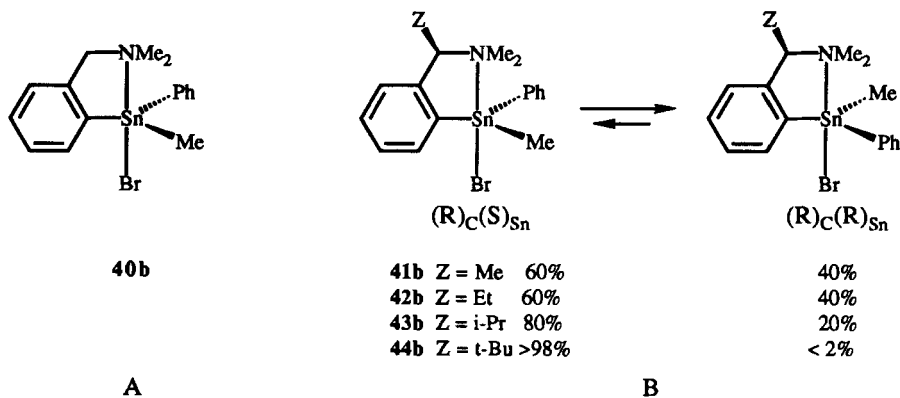


FIG. 14. Sn-chiral (A) and C,Sn-chiral (B) triorganotin halides.

tion of the tin center does occur. Furthermore it was shown that in solution the distribution between the two diastereoisomers is dependent on the bulk of the substituent present at the chiral benzylic carbon center (116), while for **14b** ( $Z = \text{Me}$ ) the  $(R)_C(S)_{\text{Sn}}:(R)_C(R)_{\text{Sn}}$  ratio is 60:40, and for **44b** ( $Z = t\text{-Bu}$ ) only the sterically less crowded  $(R)_C(S)_{\text{Sn}}$  diastereoisomer is present in solution; see Fig. 14B. Similarly, for [2-(dimethylamino)phenyl](trimethylsilyl)methyl]methylphenyltin bromide, **47b** (see Fig. 12), only one diastereoisomer is present in solution (80). It is obvious, since **47b** was prepared starting from a racemic precursor, that this must be an enantiomeric pair, most likely the same  $(R)_C(R)_{\text{Sn}}/(S)_C(S)_{\text{Sn}}$  pair as found in the solid state by X-ray diffraction (80), in which the bulky trimethylsilyl group and the phenyl—Sn group are at opposite sides of the molecule.

Also the size (five- or six-membered) and flexibility of the chelate ring has an important influence on the rate of the inversion of configuration process at tin. The latter effect was nicely illustrated by a recent study of the triorganotin bromides **58–61** (see Fig. 15) containing the chiral (–)-menthyl group as a chiral probe (105,106,124).

It appeared that crystalline **59** and **60** are diastereoisomerically pure, which was confirmed unambiguously by a crystal structure determination of **60** and showed the configuration of the tin center in **60** to be (*R*) (124). That epimerization of the tin center in these compounds does occur was shown by  $^1\text{H}$ ,  $^{13}\text{C}$ , and  $^{119}\text{Sn}$  NMR studies of these compounds, which show the presence of only one diastereoisomer in a freshly prepared solution and the appearance and a slow increase of the second diastereoisomer on standing to give eventually a 47:53 equilibrium mixture for **59** in 2.5 days and a 46:54 equilibrium mixture for **60** in 5 days. These observations

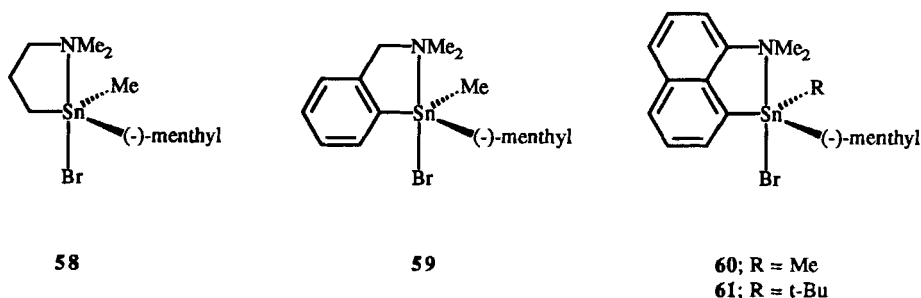


FIG. 15. Pentacoordinate triorganotin bromides containing the (–)-menthyl group as a chiral probe.

were furthermore confirmed by a linear increase of the  $[\alpha]_{20}^D$  values of **59** and **60**, from an initial value of  $-14.8^\circ$  to a constant value of  $-41.5^\circ$  after 2.5 days for **59** and from  $+2.9^\circ$  to a constant value of  $-37.9^\circ$  after 5 days for **60**. For **58**, however,  $^1\text{H}$ ,  $^{13}\text{C}$ , and  $^{119}\text{Sn}$  NMR studies showed the presence of only one resonance pattern at ambient temperature. At low temperature ( $-60^\circ\text{C}$ ), this single pattern tends to decoalesce in two resonance patterns for the two possible diastereoisomers. This observation indicates that in **58** the inversion of configuration process at tin must be very fast, even on the NMR time scale. Most likely this is a result of the much more flexible chelate ring present in **58** as compared to both **59** and **60**. Surprisingly,  $^1\text{H}$ ,  $^{13}\text{C}$ , and  $^{119}\text{Sn}$  NMR spectra of freshly prepared solutions of **61** showed the presence of two diastereoisomers in a constant 45:55 molar ratio. Most probably, due to (i) the rigid chelate ring and (ii) the steric constraints around the tin center in **61** (cf. *t*-Bu in **61** versus Me in **60**), the inversion of configuration process at the tin center in **61** is completely blocked, resulting in a constant ratio of the two diastereoisomers in the solid state as well as in solution. An alternative explanation could be the occurrence of an extremely fast epimerization process immediately after dissolution of solid **61**. However, with respect to the observations made for **60**, this seems highly unlikely.

In triorganotin bromides containing the 8-dimethylamino-1-naphthyl C,N-chelating ligand, i.e., **48–50** (Fig. 12) and **60–61** (Fig. 15), even at high temperature ( $125^\circ\text{C}$ ) Sn—N dissociation does not occur at the NMR time scale (*106,110,124*). Most likely this is the result of the fixed orientation of the N and C donor sites of the rigid 8-dimethylamino-1-naphthyl group, which holds the  $\text{NMe}_2$  substituent always in close proximity to the tin atom.

So far, it appears that triorganotin bromides containing a rigid five-membered chelate ring have a tin center that is configurationally stable on

the NMR time scale. In contrast,  $^1\text{H}$  NMR studies of triorganotin bromides containing a six-membered chelate-ring, i.e., **51**–**54** (see Fig. 12) revealed that both the Sn—N dissociation/association process and the process involving inversion of configuration of the tin center are operative (118). The  $^1\text{H}$  NMR spectrum of  $\{[2-[(\text{dimethylamino})\text{methyl}]\text{phenyl}]\text{methyl}\}\text{methylphenyltin}$  bromide **52** at  $-40^\circ\text{C}$  shows for both benzylic methylene groups AB patterns as well as two resonances for the  $\text{NMe}_2$  group, indicating that the Sn—N bonding and configuration of the tin center are stable on the NMR time scale. At  $-30^\circ\text{C}$  the two resonances of the  $\text{NMe}_2$  group coalesce while the two AB patterns remain unaltered up to  $0^\circ\text{C}$ , indicating that only the Sn—N dissociation/association process becomes fast at the NMR time scale. Finally, the coalescence of the two AB patterns to two singlets above  $0^\circ\text{C}$  indicates that now inversion of configuration of the tin center has become fast on the NMR time scale. Similar conclusions were drawn from the temperature-dependent  $^1\text{H}$  NMR spectra of **53** and **54** (118). An interesting feature of **54** is the presence in solution of two diastereoisomers as a result of the presence of the stereogenic Sn center in combination with an  $\alpha$ - or  $\beta$ -puckering of the six-membered chelate ring, as schematically shown in Fig. 16. As another consequence of this puckering for achiral **53**, at low temperature ( $-50^\circ\text{C}$ ), two  $\text{NMe}_2$  resonances and an AB pattern for the  $\text{CH}_2\text{N}$  group are observed in the  $^1\text{H}$  NMR spectrum.

That the dissociated form of triorganotin bromides that can form a six-membered chelate ring, i.e., a tetrahedral coordination geometry at the tin center, is abundantly populated at higher temperatures is indicated by the large temperature dependence of the  $^{119}\text{Sn}$  chemical shifts of **51**–**52** (94), e.g.,  $-49.4$  ppm for **51** at  $-85^\circ\text{C}$  versus  $-6.2$  ppm at  $100^\circ\text{C}$ . This conclusion is supported by the largely temperature-independent  $^{119}\text{Sn}$  chemical shift values of triorganotin bromides having a five-membered

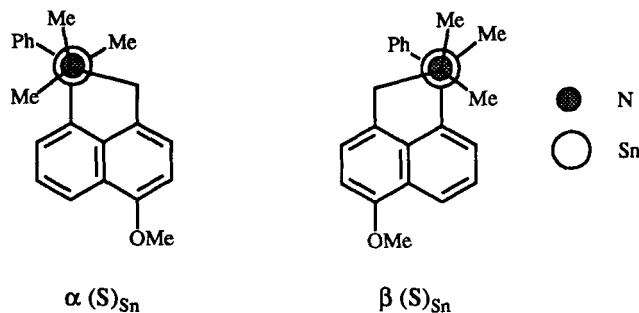


FIG. 16. Schematic projection along the N—Sn bond in **54** showing the two diastereoisomers as a consequence of the  $\alpha$ - or  $\beta$ -puckering of the six-membered chelate ring.

chelate ring (40–50,55,56) or a more rigid six-membered chelate ring (53,54), indicating that for these compounds the population of the dissociated form is infinitely small at higher temperatures (94).

### 3. Compounds Containing Miscellaneous C,N-Chelating Ligands

Interesting structural features are observed for triorganotin halides containing one quadridentate tris-anionic-, cf. 62, terdentate dianionic-, cf. 63,64, quadridentate dianionic-, cf. 70–72, terdentate monoanionic-, cf. 65–69, or two bidentate monoanionic ligands, cf. 73–75. The latter three types of ligands are potential candidates in enforcing hexacoordination in triorganotin halides.

An X-ray crystal structure determination of the triptych compound 62 revealed the trigonal bipyramidal coordination geometry, which is schematically shown in Fig. 17, with the three carbon atoms at the equatorial sites and the coordinating nitrogen atom and the chlorine atom at the axial positions. As a result of the fixed geometry of the quadridentate tris-anionic ligand, the Sn—N coordination bond (2.37(3) Å) is extremely short (125).

Based on  $^1\text{H}$ ,  $^{13}\text{C}$ , and  $^{119}\text{Sn}$  NMR spectroscopic studies a trigonal bipyramidal structure for the diptych compound 63 (102) has also been proposed; see Fig. 17.

The diptych compound 64 for which the structure was unambiguously proven by an X-ray crystal structure determination (104), consists of two enantiomorphous units connected via a Sn—Sn bond. In each unit, the tin atoms have trigonal bipyramidal coordination geometries with the two carbon ligands and the connecting Sn atom occupying equatorial sites. Based on  $^1\text{H}$ ,  $^{13}\text{C}$ , and  $^{119}\text{Sn}$  NMR spectroscopic studies, it is most likely that the structure as found in the solid state is retained in solution. At low temperature ( $-40^\circ\text{C}$ ), the  $^{13}\text{C}$  NMR spectrum of 64 shows inequivalent

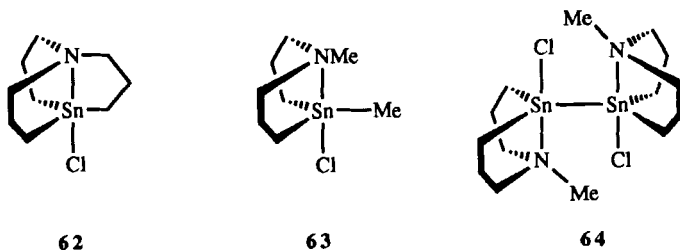


FIG. 17. Pentacoordinate triorganotin chlorides containing either quadridentate tris-anionic 62 or terdentate-dianionic 63 or 64 ligands.

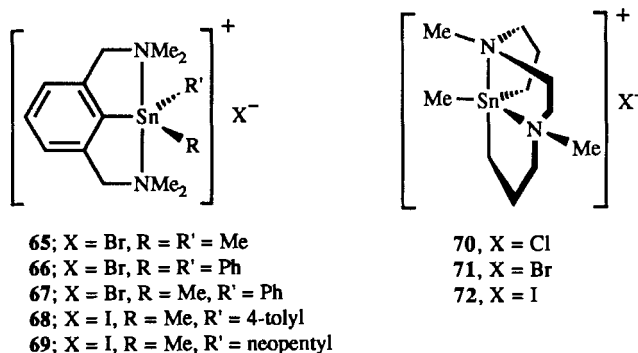


FIG. 18. Pentacoordinate triorganotin cations (stannonium ions) as a result of intramolecular coordination.

methylene carbon atoms in each unit, which was explained in terms of hindered rotation around the Sn—Sn bond (104).

A series of triorganotin halides containing the terdentate monoanionic 2,6-bis[(dimethylamino)methyl]phenyl ligand have been reported (88,126). As mentioned before, compounds **65–69** are potential candidates for hexacoordinate triorganotin halides. However, based on (i) the high solubility in polar solvents (even water), (ii) colligative studies, and (iii) conductivity measurements, it appeared that the presence of the 2,6-bis[(dimethylamino)methyl]phenyl ligand in these triorganotin halides promotes halogen displacement giving rise to the formation of stable ionic compounds **65–69**, which in fact are the first examples of triorganostannonium ions, as is shown schematically in Fig. 18. Moreover, in the case of **65**, the existence of such an ionic structure was unambiguously proven by an X-ray crystal structure determination (126). The observation of anisochronous resonances for the CH<sub>2</sub>N and NMe<sub>2</sub> groupings at temperatures below  $-10^{\circ}\text{C}$  in the <sup>1</sup>H NMR spectra of **67–69**, containing a chiral, trigonal plane, indicates that these compounds in solution have structures comparable to that found for **65** in the solid state. At higher temperatures, subsequent coalescence of the two resonances of the NMe<sub>2</sub> group and the AB pattern of the CH<sub>2</sub> group are observed. Based on the difference in coalescence temperature and difference in chemical shift values, it may be concluded that two different processes are operative: (i) a process involving Sn—N bond dissociation, followed by pyramidal inversion of the nitrogen atom, rotation around the CH<sub>2</sub>N bond, and finally reformation of the Sn—N bond; this process gives rise to the coalescence of the NMe<sub>2</sub> resonances, and (ii) a process that comprises Sn—N bond dissociation followed by rotation of the SnRR' group around the Sn—C bond to the



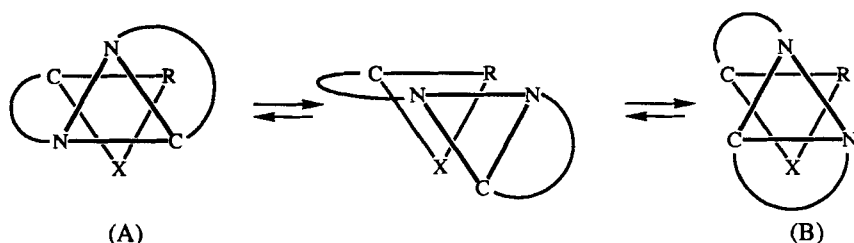


FIG. 20. Schematic representation visualizing the Bailar twist in 73–75.

distances in 73 do fit very well in the theoretically deduced curve; furthermore these distances predict a value of  $141^\circ$  for the  $C_{\text{ipso}}-\text{Sn}-C_{\text{ipso}}$  angle, which is very close to the value of  $140.0(5)^\circ$  found for 73!

$^1\text{H}$ ,  $^{13}\text{C}$ , and  $^{119}\text{Sn}$  NMR spectroscopic studies of 73–75 in solution indicated that at low temperature ( $-50^\circ\text{C}$ ) two distinctly different species are present. One has been attributed to structure (A), Fig. 19, as was established for 73 in the solid state, and the other to the isomeric structure (B), Fig. 19. The respective resonance patterns observed in the  $^1\text{H}$  and  $^{13}\text{C}$  NMR spectra could be assigned on the basis of the observed  $^1J(^{119}\text{Sn}-^{13}\text{C})$ ,  $^2J(^{119}\text{Sn}-^1\text{H})$  and  $^3J(^{119}\text{Sn}-^1\text{H})$  values. On the basis of these values, an enhanced *s*-electron participation in the  $C_{\text{ipso}}-\text{Sn}-C_{\text{ipso}}$  bonds in structure (A) and the linear  $C_{\text{ipso}}-\text{Sn}-C(\text{R})$  bonds in structure (B) was proposed. It is well established that in diorganotin compounds in which the tin atom has an octahedral coordination geometry, the *trans*-carbon atoms are bound to tin via *sp*-like orbitals at the tin center (39). At higher temperatures, a process becomes operative at the NMR time scale resulting in a fast interconversion between isomers (A) and (B). Such a stereoisomerization (Bailar twist), visualized in Fig. 20, is known for octahedral arrangements and proceeds via a trigonal prismatic transition state (131).

Alternatively the structures of 73–75 can also be seen as trigonal bipyramidal, with the carbon ligands at the equatorial sites, which undergo intramolecular nucleophilic attack at the tin atom by the noncoordinated nitrogen atom at the equatorial C—C edge opposite the methyl group. Recent *ab initio* calculations of related tin compounds have shown that such processes represent a lower energy reaction path.

It should be noted here that in isostructural silicon compounds, i.e., bis[8-(dimethylamino)-1-naphthyl]silicon dihydrides, difluorides, and hydride fluorides, the tetrahedral configuration at silicon is largely preserved. The hexacoordination at silicon can be seen best as that of a bicapped tetrahedron resulting from a twofold nucleophilic coordination (56).



#### 4. Triorganotin Halides Containing Other C,Y-Chelating Ligands

Although triorganotin halides containing a C,Y-chelating ligand in which Y = nitrogen atom containing substituents were the most intensively studied, compounds containing other heteroatom-containing substituents have also been reported. These substituents comprise: tertiary phosphine, **76–79**; phosphine oxide, **80–85**; carbonyl, **86–93**; and sulfoxide, **94–95** (see Fig. 21). Representative examples for which the structure in the solid state was established by X-ray crystallographic studies are **79** (*132*), **83** (*133*), **84** (*134*), **85** (*135*), **90–93** (*136*), **94**, and **95** (*137*), while for the other compounds **76–78** (*138*), **80–82** (*133*), and **86–89** (*139,140*), the structure was established on the basis of IR and Mössbauer spectroscopic studies. Like in the triorganotin halides containing a C,N-chelating ligand, also in these compounds the tin atom has a trigonal bipyramidal coordination geometry, as schematically shown in Fig. 21, with the three carbon atoms at equatorial positions and the more electronegative halogen and heteroatom at axial sites.

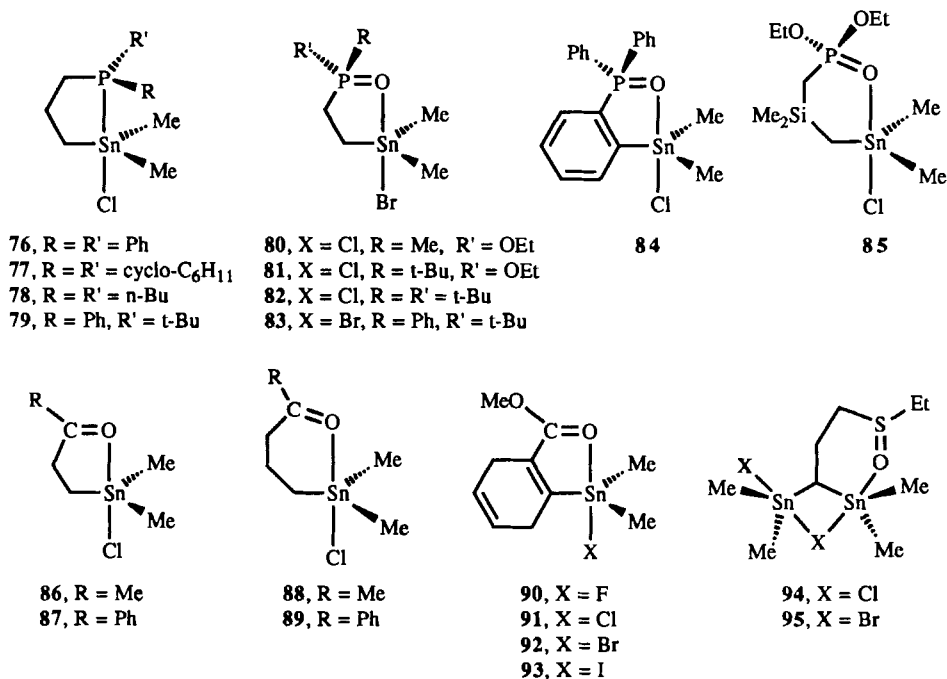
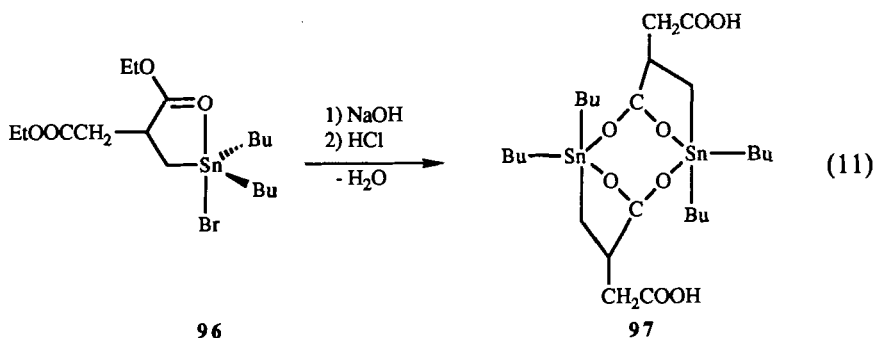


FIG. 21. Triorganotin halides containing an intramolecular coordinating phosphine, phosphine oxide, carbonyl, or sulfoxide ligand.

That the structures as found in the solid state are largely retained in solution could be concluded from  $^1\text{H}$ ,  $^{13}\text{C}$ , and  $^{119}\text{Sn}$  NMR spectroscopic studies. The  $\text{Sn}-\text{P}$  coordination in **76**–**79** is relatively weak as could be concluded from the observation that intermolecular coordination of external donor molecules like pyridine, HMPT, and DMF could compete with intramolecular  $\text{Sn}-\text{P}$  coordination (132). In contrast, intramolecular  $\text{Sn}-\text{O}$  coordination in the compounds with phosphine oxide ligands **80**–**85** appeared inert under these conditions.

Also in compounds **86**–**89**, intramolecular  $\text{Sn}-\text{O}$  coordination is relatively weak as was shown by replacement of the intramolecular coordinating oxygen atom by external ligands like pyridine (139,140).

A rather exotic example of a triorganotin compound in which penta-coordinate tin centers are proposed as a result of intramolecular coordination is the product **97**, obtained from the hydrolysis reaction of the ester-tin compound **96**. For the latter compound, the presence of a pentacoordinate tin center as a result of intramolecular  $\text{Sn}-\text{O}$  (carboxyl) coordination was proposed (141):



Nice examples of intramolecular  $\text{Sn}-\text{O}$  coordination are the six-membered carbocyclic tin compounds **98**–**100**; see Fig. 22 (142). The 1,3-diaxial conformation of these compounds is stabilized by the intramolecular  $\text{Sn}-\text{O}$  interaction.

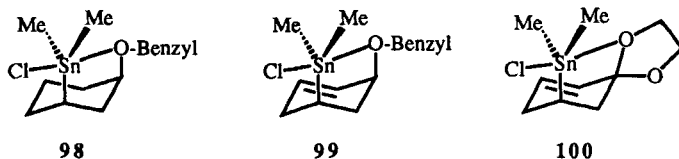
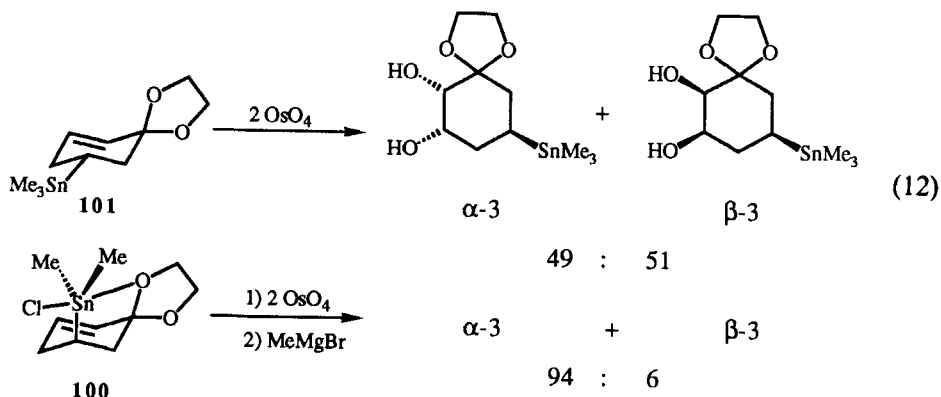


FIG. 22. Stabilization of 1,3-diaxial conformation in carbocyclic triorganotin chlorides by intramolecular  $\text{O}-\text{Sn}$  coordination.

In contrast, the corresponding trimethyltin derivatives (tetraorganotin compounds that lack O—Sn coordination) exist predominantly as diequatorial conformers, e.g., **101** in



As a result of the fixed geometry in, for example, **100**, the olefinic bond could be osmylated with very high stereoselectivity, in contrast to the corresponding trimethyltin derivative; see Eq. (12).

##### 5. The Inversion of Configuration Process at Tin Centers Having a Trigonal Bipyramidal Coordination Geometry

It was recognized long ago that the tin center in triorganotin halides is configurationally unstable, which makes the separation of chiral triorganotin halides into its enantiomers impossible [see Ref. (123) and references cited therein].

For simple triorganotin halides it has been established that the rate of the inversion process is accelerated if external nucleophiles, e.g., pyridine, are present (123). Based on the fact that the inversion process is second order in nucleophile, two possible mechanisms have been proposed: (i) addition of a nucleophile to the metal center, followed by addition of a second nucleophile and displacement of the halogen atom giving the achiral transition state (A) (see Fig. 23) or (ii) addition of two nucleophiles without loss of the halogen atom to give the achiral transition state (B), Fig. 23 (123).

For triorganotin halides containing a C,Y-chelating ligand, a different situation arises. It is obvious that triorganotin halides, containing a C,Y-chelating ligand, in which the heteroatom-containing substituent is already coordinated to the tin center, can never attain one of the transition-state structures (A) or (B), Fig. 23. This could explain why the configurational stability of triorganotin halides containing such a ligand is in-

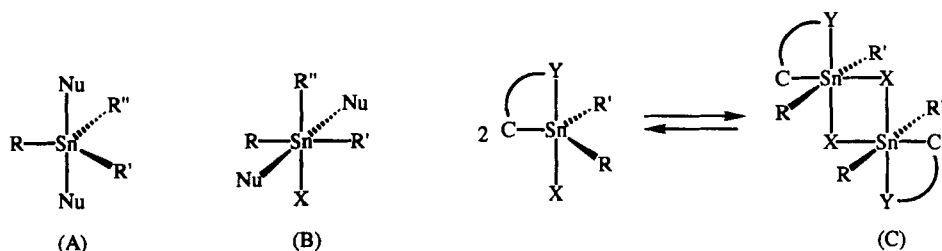


FIG. 23. Transition states (A) and (B) proposed for the inversion of configuration at tin.

creased to such an extent (114). It has been suggested that an alternative dimerization process may occur in solution, giving rise to structures shown schematically in Fig. 23C (114).

As has been mentioned before, the configurational stability of the tin center in pentacoordinate triorganotin halides is enhanced considerably by the formation of a five-membered chelate ring, but inversion of configuration at the tin center does occur at the laboratory time scale, as was shown for chiral {2-[(dimethylamino)methyl]phenyl)methylphenyltin bromide **41b** (114,116), *vide supra*. Therefore, it is most likely that this process proceeds via an intermediate, probably (A) or (B) in Fig. 23, in which the potentially intramolecular coordinating group is not coordinated to the tin center. As it was shown that the epimerization process at the tin center already occurs at low temperature, i.e., when Sn—N coordination is inert at the NMR time scale, it must be assumed that an infinite small population of the dissociated form is present. That at higher temperatures also, i.e., when a process involving Sn—N dissociation/association becomes fast on the NMR time scale, the population of the dissociated form is infinitely small was concluded from the observed temperature-independent  $^{119}\text{Sn}$  chemical shift values (94). Further evidence for such a process is the observation that the Sn center in triorganotin halides containing a six-membered chelate ring is configurationally less stable (118), indicating an increased population of the dissociated form. The latter conclusion is supported by the observation of temperature dependence of the  $^{119}\text{Sn}$  chemical shift values for this type of compound (94).

Alternatively, inversion of configuration at the pentacoordinate tin center involving a Berry pseudorotation mechanism seems to be energetically unfavorable in view of (i) the strong site preference of the electronegative halogen and nitrogen atoms for axial positions (143) and (ii) the geometric constraints of the five-membered chelate ring.

# 6. Structural Correlation of Triorganotin Halides Containing a C,Y-Chelating Ligand

Previously, Britton and Dunitz (113) and van Koten *et al.* (114) recognized that the axial arrangement of substituents X and Y in pentacoordinate triorganotin compounds of general formula  $C_3SnXY$  can be seen as a "snapshot" of a  $S_N2$  pathway for substitution with inversion at tetrahedral tin. Britton and Dunitz have correlated the structural features of about 50 of these triorganotin compounds. Two correlations were found: As the Sn—Y distance  $d_y$  becomes shorter, the Sn—X distance  $d_x$  tends to become longer and the average X—Sn—C angles tend to become smaller.

A theoretical curve showing these bond distance variations could be deduced using the simple relationship between bond length and bond order proposed by Pauling (144), where  $d(n)$  is the bond length,  $d(1)$  is the single bond length, and  $c$  depends on the type of bond:

$$\Delta d(n) = d(n) - d(1) = -c \log n \quad (13)$$

The value of  $c$  for any particular Sn(IV) ensemble could be obtained from

$$\sum n = \sum 10^{-\Delta d/c} = 4 \quad (14)$$

by assuming that the sum of the bond orders is constant.

The second correlation, between distance and angle, can be expressed in terms of the average C—Sn—X angle ( $\alpha_x$ ). For the dependence of bond order on bond angle, Bürgi (145) proposed

$$n_x = (1 - 3 \cos \alpha_x)/2 \quad (15a)$$

$$n_y = (1 + 3 \cos \alpha_x)/2 \quad (15b)$$

so that  $n_x = 1$  when  $\alpha_x$  is the tetrahedral angle and  $n_x = \frac{1}{2}$  when  $\alpha_x$  is  $90^\circ$ .

It is remarkable that the experimental data of the structures investigated by Britton and Dunitz fit so well with the calculated values using these simple models.

In Table I, the experimental data, obtained from X-ray crystal structure determinations of all triorganotin halides known so far in which the tin atom has a trigonal bipyramidal coordination geometry as a result of intramolecular coordination, are compiled (also the data for pentacoordinate tetraorganotin compounds are included). Figure 24 shows the interdependence of the derived  $\Delta d_x$  and  $\Delta d_y$  values of these compounds, while in Fig. 25, the interdependence of the  $\Delta d$  values and the averaged C—Sn—X ( $\alpha_x$ ) and C—Sn—Y ( $\alpha_y$ ) angles are given. The experimental data fit the theoretically deduced curves very well, the only exceptions being the  $\alpha_x$  and  $\alpha_y$  values of 62 and the  $\alpha_y$  value of 35. Probably this is a

TABLE I  
STRUCTURAL FEATURES OF TETRAORGANOTIN COMPOUNDS AND TRIORGANOTIN HALIDES  
HAVING A TRIGONAL BIPYRAMIDAL COORDINATION GEOMETRY AS A RESULT OF  
INTRAMOLECULAR COORDINATION.<sup>a</sup>

Compound	Sn—Y	Sn—X	$\Delta dy$	$\Delta dx$	C—Sn—Y <sup>b</sup>	C—Sn—X <sup>c</sup>
40c	2.511 (Sn—N)	2.630 (Sn—Br)	0.53	0.18	84.9	95.1
41b	2.476 (Sn—N)	2.683 (Sn—Br)	0.50	0.23	86.7	93.7
44b	2.552 (Sn—N)	2.673 (Sn—Br)	0.57	0.22	86.8	94.2
47b	2.492 (Sn—N)	2.663 (Sn—Br)	0.51	0.21	84.8	95.3
49	2.496 (Sn—N)	2.667 (Sn—Br)	0.52	0.22	85.3	95.0
54	2.401 (Sn—N)	2.739 (Sn—Br)	0.42	0.29	88.3	91.7
56	2.414 (Sn—N)	2.678 (Sn—Br)	0.43	0.23	85.0	94.9
57a	2.560 (Sn—N)	2.445 (Sn—Cl)	0.58	0.16	82.7	97.0
57b	2.674 (Sn—N)	2.433 (Sn—Cl)	0.69	0.15	81.8	98.5
60 (A) <sup>d</sup>	2.55 (Sn—N)	2.641 (Sn—Br)	0.57	0.19	85.3	95.3
60 (B) <sup>d</sup>	2.55 (Sn—N)	2.630 (Sn—Br)	0.57	0.18	85.2	95.2
62	2.372 (Sn—N)	2.613 (Sn—Cl)	0.39	0.32	80.5	99.5
64	2.448 (Sn—N)	2.560 (Sn—Cl)	0.47	0.27	86.3	93.7
83	2.324 (Sn—O)	2.684 (Sn—Br)	0.42	0.23	85.7	94.4
85	2.371 (Sn—O)	2.518 (Sn—Cl)	0.47	0.23	86.7	93.3
90	2.52 (Sn—O)	1.974 (Sn—F)	0.62	0.14	83.4	96.8
91	2.470 (Sn—O)	2.432 (Sn—Cl)	0.57	0.14	81.2	98.8
92	2.470 (Sn—O)	2.588 (Sn—Br)	0.57	0.14	80.8	99.2
93	2.391 (Sn—O)	2.830 (Sn—I)	0.49	0.14	81.1	98.9
94	2.301 (Sn <sub>2</sub> —O)	2.572 (Sn <sub>2</sub> —Cl <sub>1</sub> )	0.40	0.28	89.3	90.7
	2.925 (Sn <sub>1</sub> —Cl <sub>1</sub> )	2.478 (Sn <sub>2</sub> —Cl <sub>2</sub> )	0.63	0.18	82.7	97.3
95	2.287 (Sn <sub>2</sub> —O)	2.748 (Sn <sub>2</sub> —Br <sub>1</sub> )	0.39	0.30	89.5	90.5
	3.065 (Sn <sub>1</sub> —Br <sub>1</sub> )	2.626 (Sn <sub>2</sub> —Br <sub>2</sub> )	0.62	0.18	83.7	96.3
98	2.720 (Sn—O)	2.438 (Sn—Cl)	0.82	0.15	81.9	98.2
18 <sup>e</sup>	2.841 (Sn—N)	2.183 (Sn—C)	0.86	0.08	76.5	103.8
27 <sup>e</sup>	2.884 (Sn—N)	2.183 (Sn—C)	0.78	0.08	78.4	102.1
30 <sup>e</sup>	2.781 (Sn—O)	2.150 (Sn—C)	0.88	0.05	74.7	105.4
31 <sup>e</sup>	2.770 (Sn—O)	2.190 (Sn—C)	0.87	0.09	77.0	104.0
35 <sup>e</sup>	2.624 (Sn—N)	2.214 (Sn—C)	0.64	0.11	74.7	105.2
39 <sup>e</sup> (A) <sup>d</sup>	2.931 (Sn—N)	2.212 (Sn—C)	0.95	0.11	74.7	106.0
39 <sup>e</sup> (B) <sup>d</sup>	2.885 (Sn—N)	2.212 (Sn—C)	0.91	0.11	73.4	107.1

<sup>a</sup> Data of all known structures so far (July 1992).

<sup>b</sup> Averaged value of the three C—Sn—Y angles.

<sup>c</sup> Averaged value of the three C—Sn—X angles.

<sup>d</sup> Two molecules in the asymmetric unit.

<sup>e</sup> Tetraorganotin compounds.

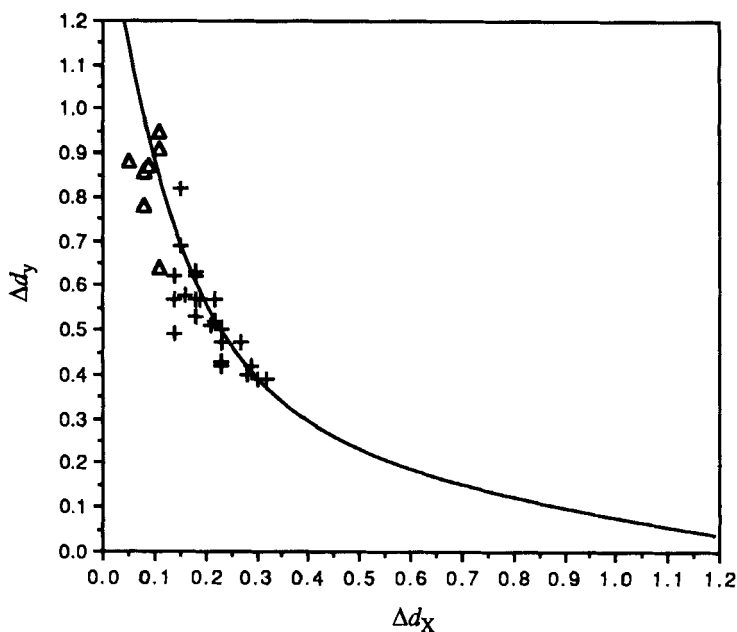


FIG. 24.  $\Delta d_x$  vs  $\Delta d_y$  for the triorganotin halides (+) and tetraorganotin compounds ( $\Delta$ ) having a trigonal bipyramidal arrangement at the tin center as a result of intramolecular coordination. The curve shows the bond order conservation function  $10^{-\Delta d_x/c} + 10^{\Delta d_y/c} = 1$ , with  $c = 1.20 \text{ \AA}$ .

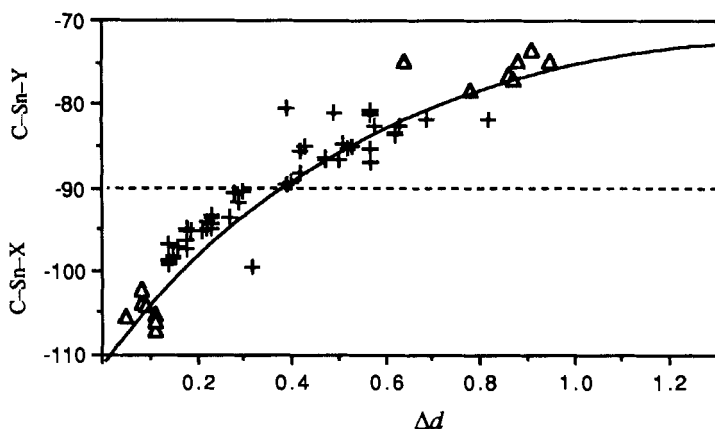


FIG. 25.  $C-Sn-X$  ( $\alpha_x$ ) and  $C-Sn-Y$  ( $\alpha_y$ ) vs  $\Delta d_x$  and  $\Delta d_y$  for the triorganotin halides (+) and tetraorganotin compounds ( $\Delta$ ) having a trigonal bipyramidal arrangement at the tin center as a result of intramolecular coordination. The curve gives the combination of Eqs. (13), (14), and (15) with  $c = 1.20 \text{ \AA}$ .

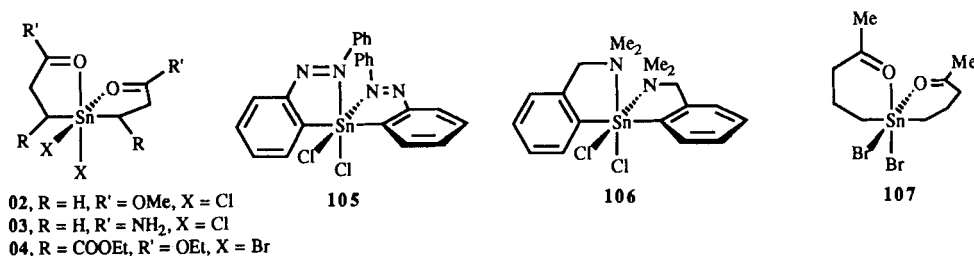


FIG. 26. Diorganotin dihalides having an octahedral arrangement at the tin atom.

consequence of the prefixed geometry of the tris-anionic tetradentate ligand present in these compounds, causing extremely short intramolecular Sn—N distances (see Table I). It is remarkable that the data for the pentacoordinate *tetra*-organotin compounds **18**, **27**, **30**, **31**, **35**, and **39** in which a carbon atom is in *trans*-position with respect to the intramolecular coordinating heteroatom fit so well.

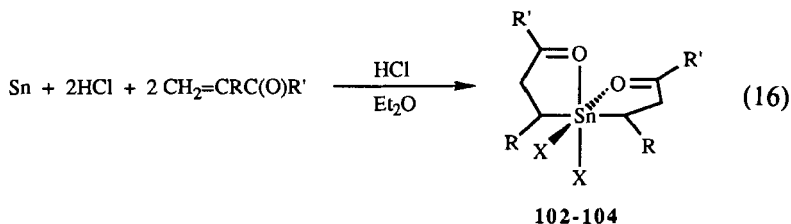
#### E. Diorganotin Dihalides Containing a C,Y-Chelating Ligand

##### 1. Compounds Having an Octahedral Arrangement at the Tin Atom

The structures of diorganotin dihalides containing two C,Y-chelating ligands are given schematically in Fig. 26. The structures of compounds **102**, **103** (146), **104** (147), and **105** (148) were unambiguously proven by X-ray crystal structure determinations. The tin centra have a distorted octahedral coordination geometry, with the two carbon ligands in *trans*-position and both coordinating heteroatoms and the two halogen atoms in *cis*-position.

On the basis of <sup>1</sup>H NMR spectroscopic data for **106** (149) and Mössbauer spectroscopic data for **107** (139), similar structures for these two compounds were proposed.

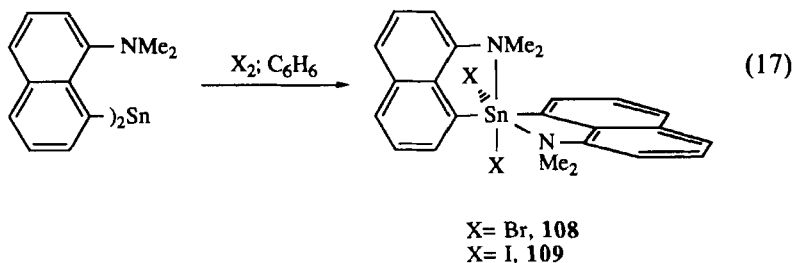
It is interesting to note that the functionally substituted organotin compounds **102**–**104** are easily prepared by direct methods starting from tin powder and an  $\alpha,\beta$ -unsaturated carbonyl compound (150).





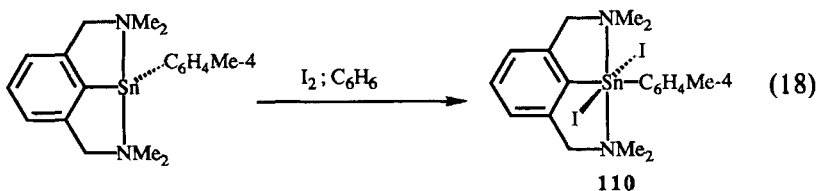
No catalyst is required for this reaction and it is likely to proceed via a solvated chlorostannane intermediate of the type  $\text{H}^+\text{SnCl}_3^- \cdot 2\text{Et}_2\text{O}$  (151).

Addition of dibromine or diiodine to the divalent organotin compound bis[8-(dimethylamino)-1-naphthyl]tin(II) affords in a quantitative oxidative-addition reaction bis[8-(dimethylamino)-1-naphthyl]tin dibromide **108** and diiodide **109**, respectively (152)



An X-ray crystal structure determination of **108** revealed an octahedral arrangement at the tin center, with the two carbon ligands in *trans*-position and both coordinating nitrogen and bromine atoms in *cis*-position.

Similarly the oxidative addition of diiodine to {2,6-bis[(dimethylamino)methyl]phenyl}(4-tolyl)tin(II) gives {2,6-bis[(dimethylamino)methyl]phenyl}(4-tolyl)tin(IV) diiodide **110**



Its X-ray crystal structure determination showed the tin center to be hexacoordinate, with the two carbon ligands, both coordinating nitrogen atoms, and both iodine atoms in *trans*-position (152).

The formation of a *trans*-oxidative-addition product in this case contrasts with the formation of a *cis*-oxidative-addition product when diiodine is reacted with {2,6-bis[(dimethylamino)methyl]phenyl}(4-methylphenyl)platinum(II). It has been argued that in the latter case, *trans*-oxidative-addition cannot take place for steric reasons (85). However, it may not be excluded that the initial step in the oxidative addition is also the formation of a *cis*-oxidative-addition product, which rapidly rearranges to the more stable *trans*-product **110**.

X-ray crystal structure determinations of **111** and **112**, schematically shown in Fig. 27, revealed structures in which, as a result of the formation

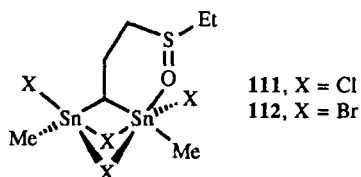
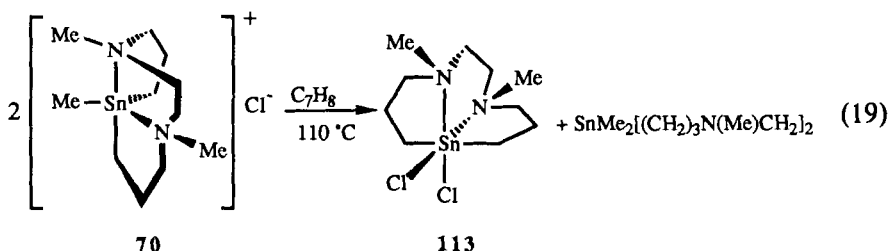


FIG. 27. Diorganotin dihalides containing one octahedral and trigonal bipyramidal coordinated tin center.

of two intramolecular halogen bridges and intramolecular coordination of the oxygen sulfoxide atom, one of the tin atoms has a trigonal bipyramidal and the other tin atom an octahedral coordination geometry (137).

Finally, the disproportionation reaction of the triorganotin chloride **70** into the novel diorganotin dichloride **113** has been reported. On the basis of its  $^1\text{H}$  and  $^{13}\text{C}$  NMR spectra, an octahedral coordination geometry has been proposed, schematically shown in Eq. (19)



for the tin atom that carries *trans*-carbon ligands (127).

## 2. Compounds Having a Trigonal Bipyramidal Arrangement at the Tin Atom

X-ray crystal structure determinations of **114–116**, cf. Fig. 28, have shown that in the solid state the tin atom in these compounds has a trigonal bipyramidal coordination geometry, with the two carbon ligands and one of the chlorine atoms at equatorial positions, while the other

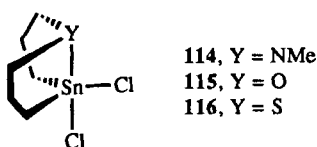
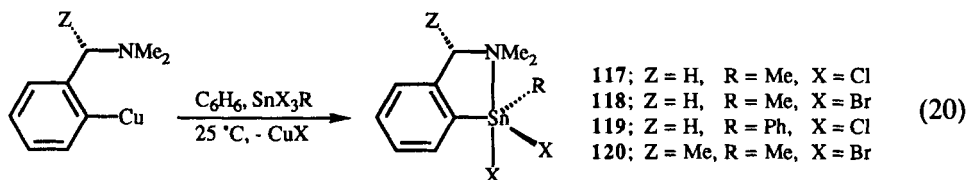


FIG. 28. Diorganotin dihalides containing a tridentate bis-anionic ligand resulting in a trigonal bipyramidal coordination geometry at the tin centers.

chlorine atom and the heteroatom occupy the axial sites. Furthermore, the solid-state investigations reveal that **114**, **115**, and **116** adopt a boat-chair, a chair-chair, and a boat-boat eight-membered ring conformation, respectively (102). In solution, however, a much more complicated situation arises because equilibria between these different conformations must be considered. A  $^{13}\text{C}$  NMR spectroscopic study of **114**–**116** showed both five-membered rings in each compound symmetry equivalent (at least on the NMR time scale), as was indicated by the observation of only one resonance for each type of methylene group.

A series of diorganotin dihalides containing the potentially intramolecularly coordinating 2-[(dimethylamino)methyl] group have been studied. It is well known that the direct alkyl or arylation of tin(IV) halides to organotin halides may be achieved with many organometallic reagents ( $\text{MgXR}$ ,  $\text{LiR}$ ,  $\text{NaR}$ ,  $\text{AlR}_3$ , etc.), but that, even when precise reaction stoichiometries are used, a mixture of the three possible halides  $\text{R}_n\text{SnX}_{4-n}$  usually results (107). It was shown however, that aryl-copper compounds are much more selective arylating agents (153).

The diorganotin dihalides **117**–**120** are formed quantitatively starting from the parent organocopper compounds (149).



Because diorganotin dihalides generally are stronger Lewis acids than triorganotin halides (39), the intramolecular  $\text{Sn}-\text{N}$  coordination that was observed in the corresponding triorganotin halides containing the 2-[(dimethylamino)methyl]phenyl group (*vide supra*) must also be expected to occur in **117**–**120**. The observed molecular weight data in solution (**117**–**120** are monomers) exclude the possibility of intermolecular  $\text{Sn}$ –halogen coordination (143). On this basis, the  $\text{Sn}$  atom in **117**–**120** is pentacoordinate. Additional evidence for pentacoordinate tin centers in these compounds are (i) the observed absolute  $^{119}\text{Sn}$  NMR chemical shift values (*vide infra*) and (ii) the magnitude of the  $^2J(^{119}\text{Sn}-^1\text{H})$  coupling constants of about 80 Hz for the methyltin derivatives **117**, **118**, and **120**. A trigonal bipyramidal coordination geometry at tin in which the aryl and R groups reside in the equatorial plane is most likely. The bite of the  $\text{C}_6\text{H}_4\text{CH}(\text{Z})\text{NMe}_2$ -2 ligand dictates that the amino ligand will occupy an axial position, leaving one equatorial and one axial position for the two halogen atoms as schematically shown in Eq. (20).

The occurrence of intramolecular Sn—N coordination has been unambiguously deduced from the observation that the  $^1\text{H}$  NMR spectrum of the C-chiral compound  $\text{SnBr}_2\text{Me}[\text{C}_6\text{H}_4\text{CH}(\text{Me})\text{NMe}_2\text{-(S)-2}]$ , **120**, at  $25^\circ\text{C}$  shows two resonances for the  $\text{NMe}_2$  group. The  $\text{NMe}_2$  methyl groups are only diastereotopic when the nitrogen center is a stable pyramidal assembly. This will only be the case when inversion of configuration is blocked by Sn—N coordination.

Since the diorganotin dihalide,  $\text{SnBr}_2\text{Me}[\text{C}_6\text{H}_4\text{CH}(\text{Me})\text{NMe}_2\text{-(S)-2}]$  **120**, contains two chiral centers, in principle two different diastereoisomers should exist (Fig. 29). The configuration of the chiral benzylic carbon atom is fixed (*S*), the configuration of the chiral tin center may be either (*S*) or (*R*).

The observation of only one resonance pattern in the  $^1\text{H}$  NMR spectrum of **120** over the whole temperature range studied ( $-80$  to  $100^\circ\text{C}$ ) may be caused by two reasons: (i) the energy difference between these two diastereoisomers is so large that in solution only one of them is present or (ii) a process is operative that results in inversion of configuration at tin, which is fast on the NMR time scale, even at very low temperature. It is most likely that the latter process is operative, since single resonances are also observed for the  $\text{NCH}_2$  group, as well as for the Me resonances of the  $\text{NMe}_2$  group in the  $^1\text{H}$  NMR spectra of **117–119**, evidently, as the result of the same process. If the Sn center in **117–119** would be configurational stable, an AB pattern for the  $\text{NCH}_2$  group and two resonances for the  $\text{NMe}_2$  group would be expected. It has been proposed that a mechanism resulting in inversion of configuration at the tin center in these compounds takes place in an achiral dimeric intermediate with hexacoordinate tin centers (Fig. 30) (114).

Additional evidence for such an intermediate was obtained from  $^1\text{H}$  NMR studies of a mixture of the diorganotin dichloride, **117**, and the diorganotin dibromide, **118**. The  $^1\text{H}$  NMR spectrum of a mixture of **117** and **118** in toluene- $d_8$  shows only one resonance pattern, of which the Sn—Me resonance appears at 0.90 ppm, a value in between those of the pure compounds, 0.80 and 1.00 ppm, respectively. Below  $-80^\circ\text{C}$ , the

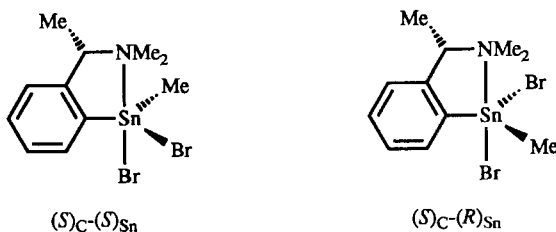


FIG. 29. The two possible diastereoisomers of **120**.

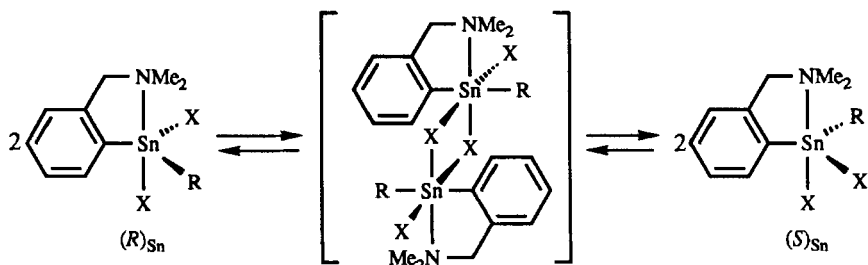


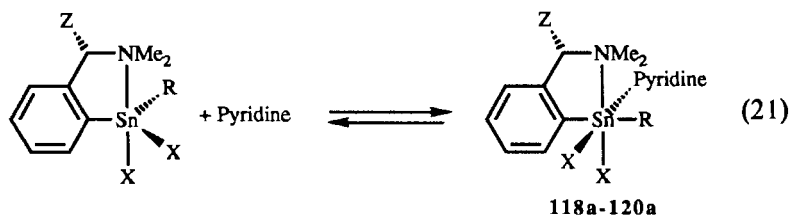
FIG. 30. Proposed mechanism for the inversion of configuration at tin in pentacoordinate-diorganotin dihalides.

Sn—Me resonance splits up into two resonances at positions of the pure compounds. Moreover, at this temperature the  $\text{NMe}_2$  and  $\text{NCH}_2$  resonances start to split up, which indicates that under these conditions the tin center is becoming configurationally stable on the NMR time scale.

In view of the well-documented tendency of diorganotin dihalides to form complexes in which the tin center has an octahedral coordination geometry (39,107), an  $^1\text{H}$  and  $^{119}\text{Sn}$  NMR study of compounds **118–120** in the presence of donor molecules was carried out (94).

When half an equivalent of pyridine is added to a toluene- $d_8$  solution of one of the diorganotin dihalides **118–120**, the  $^1\text{H}$  NMR spectra at  $25^\circ\text{C}$  remain unchanged as compared to those of the pure diorganotin dihalides. However, at  $-40^\circ\text{C}$  the  $^1\text{H}$  NMR spectra of these solutions show the presence of two resonance patterns in a one-to-one ratio; one pattern is identical to that of the original pentacoordinate diorganotin dihalide while the second resonance pattern has been ascribed to the pyridine adduct (**118a**, **119a** and **120a**, respectively) of the corresponding diorganotin dihalide.

From these observations it was concluded that in solution in the presence of pyridine the diorganotin dihalides **118–120** are in equilibrium with their respective pyridine adducts. At room temperature the equilibrium lies completely to the side of the pentacoordinate species, while at  $-40^\circ\text{C}$ , this equilibrium has shifted completely to the side of a hexacoordinate pyridine adduct, for which the structure is schematically shown in Eq. (21).



The tin center in these pyridine adducts **118a–120a** is hexacoordinate, which is not the result of a simple ligand displacement of the intramolecularly coordinating amino substituent by a pyridine molecule. This is reflected by the observation of two resonances for the  $\text{NMe}_2$  group in the  $^1\text{H}$  NMR spectrum of C-chiral  $\text{SnBr}_2\text{Me}[\text{C}_6\text{H}_4\text{CH}(\text{Me})\text{NMe}_2\text{-(S)-2}]$ , **118a**, indicating that coordination of the amino substituent to tin is inert on the NMR time scale (*vide supra*).

Further evidence for hexacoordinate tin in **118a–120a** is the increase in the value of the  $^2J(^{117,119}\text{Sn}-^1\text{H})$  from approximately 78 Hz in the methyltin compounds **118** and **120** to about 105 Hz in **118a** and **120a**. This increase in coupling constant is indicative for an increase in the coordination number at tin (143). The  $^{119}\text{Sn}$  NMR spectra of the pyridine adducts **118a–120a** show a 150 ppm shift to higher field compared to the values of **118–120** (94). This high-field shift is also indicative of an increase in the coordination number at tin (93). Furthermore the observed absolute  $^{119}\text{Sn}$  chemical shift values obtained for **118a–120a** (–293.8, –339.7, and –290.5 ppm, respectively) are in the same range as that observed for other diorganotin dihalides, for which hexacoordination at tin was established independently (*vide supra*).

Although in principle the pyridine adducts **118a–120a** can exist as various geometrically different isomers, those isomers having a *cis*-geometry of the two organic groups can be excluded. (It has been well established that the two organic groups in  $\text{R}_2\text{SnX}_2 \cdot 2\text{L}$  complexes are invariably, to date, anyway *trans*.) The two halide and the two donor molecules, however, can adopt either *cis*- or *trans*-configuration [see Ref. (39) and references cited therein], thus leaving three possible different geometrical isomers A–C, which are shown schematically in Fig. 31.

As has been outlined above, in structures A and B the two organic groups are in *trans*-position, while both coordinating nitrogen atoms and both halogen atoms have a *cis*-arrangement. In structure C, the two nitrogen atoms, and as a consequence the two halogen atoms, are in *trans*-position.

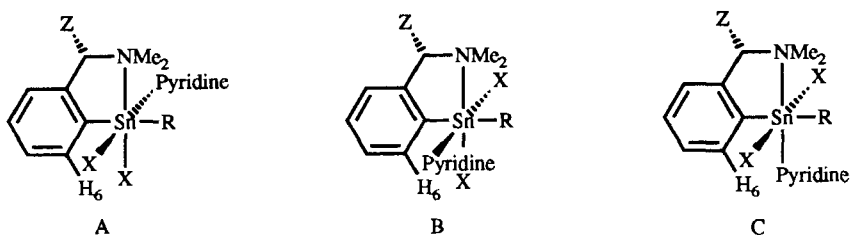


FIG. 31. The three possible different geometrical isomers of **118a–120a**.

Based on  $^1\text{H}$  NMR spectra of **118a**–**120a**, structure A or B (if  $Z = \text{H}$ , **118a** and **119a**, A and B are identical; see Fig. 31) seems to be most likely for these complexes. When the  $^1\text{H}$  NMR spectra of these pyridine adducts are compared with those of **118**–**120**, it appeared that major changes in chemical shift have occurred for the protons present in the  $\text{CH}(\text{Z})\text{NMe}_2$  substituent, as well as for those in the  $\text{Me}-\text{Sn}$  group in **118a** and **120a**. Most likely these changes in chemical shift are caused by the anisotropy of the pyridine ring, present in *cis*-position with respect to both the substituted phenyl group and the  $\text{Me}-\text{Sn}$  group, (cf. Fig. 31A and 31B). This is furthermore supported by the observation that the chemical shift values of the  $\text{H}_6$  protons in **118a**–**120a** are almost identical to those in **118**–**120**. A pyridine group present in *trans*-position with respect to the coordinating  $\text{CH}(\text{Z})\text{NMe}_2$  group, cf. Fig. 31C, would have had a major effect on the chemical shift of the  $\text{H}_6$  proton, while it would have little effect on the chemical shift values of the protons in the  $\text{CH}(\text{Z})\text{NMe}_2$  substituent. Based on the observed  $^1\text{H}$  NMR data of **120** and **120a**, it is not possible to conclude which structure, A or B, is correct for **120a**; however, for steric reasons structure B seems to be more likely.

#### F. Monoorganotin Halides Containing a C,Y-Chelating Ligand

Only a few examples of monoorganotin trihalides in which a C,Y-chelating ligand is present are known. Because of their importance as precursors for PVC stabilizers, some structural investigations on ester—tin trihalides have been carried out.

X-ray crystal structure determinations of **121** (146), **123** (154), and **128** (155) show that the tin centers in these compounds have a trigonal bipy-

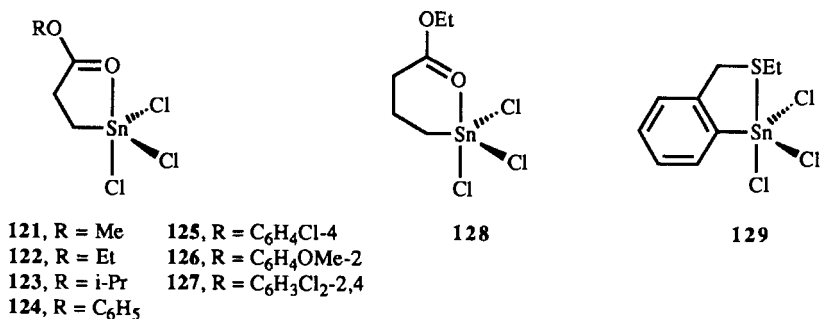
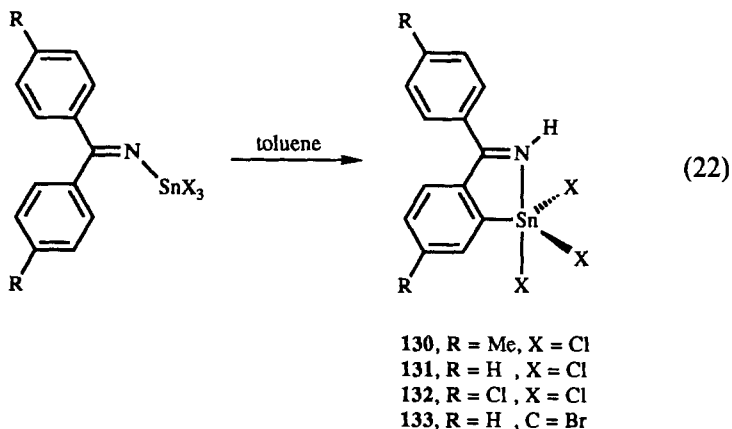


FIG. 32. Monoorganotin halides containing a C,Y-chelating ligand.

ramidal coordination geometry as a result of intramolecular coordination of the carbonyl oxygen atom (cf. Fig. 32). On the basis of IR spectroscopic studies of **122** and **124–127**, a similar structure was proposed (*154*). These compounds form 1 : 1 adducts with bidentate donor molecules like bipyridine; i.e., in these complexes, intramolecular Sn—O coordination is no longer present. However, with monodentate ligands like pyridine, an equilibrium exists between a 1 : 1 adduct, in which intramolecular coordination is still present, and a 1 : 2 adduct (*154,155*). Furthermore it was shown that Sn—O coordination in the compounds in which a five-membered chelate ring is present (**121–127**) is much stronger than that in **128** in which a six-membered chelate ring is present.

In the thioether compound **129**, Sn—S coordination was established on the basis of a temperature-dependent lineshape analysis of the  $^1\text{H}$  NMR resonances of the diastereotopic SEt group (*156*).

Wade *et al.* have found that ketaminotin trihalides  $\text{SnX}_3\text{N}=\text{CR}_2$  spontaneously rearrange to form a product in which a tin—carbon bond is formed.

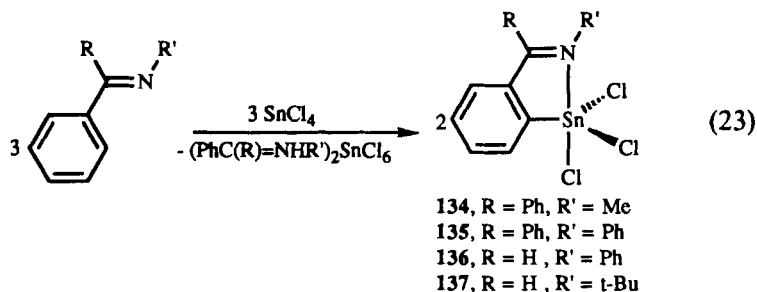


In fact, this was the first example of an orthometallation reaction in organotin chemistry (*157*).

In this way, compounds **130–133** were prepared. An X-ray crystal structure determination of **130** showed that the tin center has a distorted trigonal-bipyramidal coordination geometry as a result of intramolecular Sn—N coordination. On the basis of similarities in their IR and Mössbauer spectroscopic data, comparable structures for **131–133** have been proposed.



As an extension of this work, the same authors recently reported the direct orthometallation of several Schiff's bases according to (158):



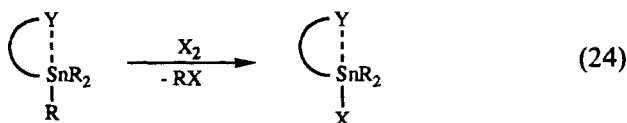
An X-ray crystal structure determination of **134** showed that these compounds have structural features that are comparable to those of **130**.

#### IV

#### CONCLUDING REMARKS

It has been shown that C,Y-chelating ligands can stabilize divalent organotin compounds to such an extent that these compounds can be isolated as well-defined monomeric species. It is very likely that as result of intramolecular coordination, the tin atom is shielded in such a way that polymerization is prevented. Application of bis-orthochelating aryldiamine ligands allowed the synthesis of stable mixed diaryl tin(II) compounds.

Despite the low Lewis acidity of the tin atom in tetraorganotin compounds, it has been demonstrated that by making use of rigid or cage-like C,Y-chelating ligands, it is possible to enforce coordination of the heteroatoms to tin, resulting in penta- or even hexacoordinate tin. This enforced coordination has been proposed to be responsible for the changes in the reactivity sequence observed in halodemetalation reactions of mixed tetraorganotin compounds, in which potentially coordinating groups (Y) are present in the  $\gamma$ -position with respect to the tin. It is thought that intramolecular assistance by those groups facilitates the cleavage of tin—carbon bonds *trans* to them:



It is anticipated that this concept of intramolecular assistance by heteroatom-tin coordination will be shown to be extremely useful in reactions comprising metal-mediated group transfer from tin to an organic substrate by C—C bond formation (111,112). In this context similar reactivity of tetraorganosilicon compounds with intramolecular heteroatom coordination can be expected.

In triorganotin halides containing a C,Y-chelating ligand, normally the tin atom has a trigonal bipyramidal coordination geometry, as a result of intramolecular coordination. The carbon ligands are at the equatorial sites, while the more electronegative halogen atom and the coordinating heteroatom reside at axial positions. This class of compounds are excellent model compounds for a study of the inversion process at the tin atom and chiral triorganotin halides. Our study on triorganotin halides containing the C,N-chelating 2-[(dimethylamino)methyl]phenyl ligand was the first example in which this was demonstrated (54). In triorganotin halides containing two potentially coordinating heteroatoms either halogen displacement occurs, resulting in the formation of pentacoordinate triorganostannonium cations, or a species is formed in which the coordination geometry of the tin atom may be regarded as distorted octahedral.

In diorganotin dihalides, the tin atom may be either pentacoordinate or hexacoordinate, depending on the number (one or two) of C,Y-chelating ligands present in the molecule. Furthermore, it was shown that in compounds in which only one C,Y-chelating ligand is present, in solution, when additional donor ligands are present, a temperature-dependent equilibrium exists between penta- and hexacoordinate species. In hexacoordinate species, the carbon ligands are always in *trans*-position of an octahedral arrangement.

The tin atom in monoorganotin trihalides in which a C,Y-chelating ligand is present have a trigonal bipyramidal coordination geometry in the solid state. However, in solution when external donor molecules are also present, hexacoordinate species may be formed.

#### ACKNOWLEDGMENTS

Thanks are due to the excellent practical work of a large number of graduate and undergraduate students participating in our research project concerning organotin compounds containing potentially intramolecular coordinating substituents. The X-ray crystallographers, Drs. A. L. Spek, C. H. Stam, and K. Goubitz and Professor J. Kroon are thanked for the continued interest in our studies and generous support with invaluable information concerning the structures of organometallic compounds in the solid state. Drs. J. Boersma and D. M. Grove are kindly acknowledged for their interest in this part of the research of the Utrecht group. The Netherlands Foundation for Chemical Research (SON), the Netherlands Organization for Scientific Research (NWO), and the Universities of Amsterdam (1977–1985) and Utrecht (1986–1992) are thanked for financial support.

## REFERENCES

1. E. Frankland, *Liebigs Ann. Chem.* **71**, 171 (1849).
2. E. Frankland, *J. Chem. Soc.* **2**, 267 (1850).
3. C. Löwich, *Liebigs Ann. Chem.* **84**, 308 (1852).
4. E. Krause and A. von Gosse, "Die Chemie der Metallorganischen Verbindungen." Verlag Sändig, Wiesbaden, Germany, 1965.
5. D. Lannigan, "Proceedings of the International Conference on PVC processing." Plastics and Rubber Institute, London, England, 1978.
6. P. Klimsch, *Plaste Kautsch.* **24**, 380 (1977).
7. G. Ayrey, B. C. Head, and R. C. Poller, *Macromol. Rev.* **8**, 1 (1974).
8. M. H. Gitlitz, *Adv. Chem. Ser.* **157**, 167 (1976).
9. C. J. Evans, *Tin Its Uses* **86**, 7 (1970).
10. V. G. Kumar Das, *Planter (Kuala Lumpur)* **51**, 355 (1975).
11. B. Sugavanam, *Tin Its Uses* **126**, 4 (1980).
12. S. King, *Tin Its Uses* **124**, 13 (1980).
13. A. J. Crowe, R. Hill, and P. J. Smith, "Tributyltin Wood Preservatives." International Tin Research Institute, London, England, 1978.
14. A. J. Crowe, R. Hill, P. J. Smith, and T. R. G. Cos, *Int. J. Wood Preserv.* **1**, 119 (1979).
15. B. A. Richardson, "Record of British Wood Preserving Association Annual Convention," p. 37. Cambridge, England, 1970.
16. T. Hof, *J. Inst. Wood Sci.* **4**, 19 (1969).
17. S. King, *Pigm. Resin Technol.* **9**, 8 (1980).
18. C. J. Evans and P. J. Smith, *J. Oil Colour Chem. Assoc.* **58**, 160 (1975).
19. R. H. Chandler and J. Chandler, "Fungicides, Preservatives and Antifouling Agents for Paints." Bibliog. Paint Technol. No. 29. Chandler, Braintree, England, 1977.
20. G. J. M. van der Kerk and J. G. A. Luijten, *J. Appl. Chem.* **4**, 314 (1954).
21. G. J. M. van der Kerk, J. G. A. Luijten, and J. G. Noltes, *Angew. Chem.* **70**, 298 (1958).
22. M. J. Janssen, J. G. A. Luijten, and G. J. M. van der Kerk, *J. Organomet. Chem.* **1**, 286 (1964).
23. I. R. Beattie and T. Gilson, *J. Chem. Soc.*, 2582 (1961).
24. G. J. M. van der Kerk, J. G. A. Luijten, and M. J. Janssen, *Chimia* **16**, 10 (1962).
25. R. Okawara, D. E. Webster, and E. G. Rochow, *J. Am. Chem. Soc.* **82**, 3287 (1960).
26. R. Okawara and H. Sati, *J. Inorg. Nucl. Chem.* **16**, 204 (1961).
27. R. Hulme, *J. Chem. Soc.*, 1524 (1963).
28. H. Kopp, "Geschichte der Chemie," Vol. 4, p. 129 Vieweg, Braunschweig, Germany, 1843.
29. E. O. Fischer and H. Grubert, *Z. Naturforsch. B: Anorg. Chem. Org. Chem. Biochem. Biophys. Biol.* **11**, 423 (1956).
30. L. C. Willemsen and G. J. M. van der Kerk, "Investigations in the Field of Organolead Chemistry." International Lead Zinc Research Organisation, Inc., Utrecht, The Netherlands, 1965.
31. O. M. Nefedov, S. P. Kolesnikov, and A. I. Ioffe, *J. Organomet. Chem. Libr.* **5**, 181 (1981).
32. W. Kirmse, "Carbene Chemistry." Academic Press, New York, 1971.
33. R. J. Gillespie, *J. Chem. Educ.* **47**, 18 (1970).
34. R. J. Gillespie, *J. Chem. Soc.*, 4672 (1963).
35. R. J. Gillespie, *Can. J. Chem.* **39**, 318 (1961).
36. M. Veith and O. Recktenwald, *Top. Curr. Chem.* **104**, 3 (1982).
37. L. E. Orgel, *J. Chem. Soc.*, 3815 (1959).
38. M. J. Tricker and J. D. Donaldson, *Inorg. Chim. Acta* **31**, L445 (1978).

39. P. G. Harrison, "Comprehensive Coordination Chemistry" (G. Wilkinson, R. D. Gillard, and J. A. McCleverty, eds.), Vol. 7, Chapter 26, p. 183. Pergamon, Oxford, England, 1987.
40. L. A. Aslanov, V. M. Ionov, M. W. Attiya, and A. B. Permin, *J. Struct. Chem.* (Engl. Transl.) **19**, 166 (1978).
41. L. A. Aslanov, V. M. Ionov, M. W. Attiya, A. B. Permin, and V. S. Petrosyan, *J. Organomet. Chem.* **144**, 39 (1978).
42. A. E. Blom, B. R. Penfold, and W. T. Robinson, *J. Chem. Soc. A*, 913, (1969).
43. L. Randaccio, *J. Organomet. Chem.* **55**, C58 (1973).
44. N. W. Isaacs and C. H. L. Kennard, *J. Chem. Soc. A*, 1257 (1970).
45. S. L. Chadha, P. G. Harrison, and K. C. Molloy, *J. Organomet. Chem.* **202**, 247 (1980).
46. P. G. Harrison, T. J. King, and J. A. Richards, *J. Chem. Soc. Dalton Trans.*, 1723 (1974).
47. L. Coghi, C. Pelizzi, and G. Pelizzi, *Gazz. Chim. Ital.* **104**, 873 (1974).
48. P. Ganis, V. Peruzzo, and G. Valle, *J. Organomet. Chem.* **256**, 245 (1983).
49. C. H. Yoder, D. Mokrynka, S. M. Coley, J. C. Otter, R. E. Haines, A. Grushow, L. J. Ansel, J. W. Hovick, J. Mikus, M. A. Shermak, and J. N. Spencer, *Organometallics* **6**, 1679 (1987).
50. H. H. Anderson, *Inorg. Chem.* **3**, 912 (1964).
51. G. S. Brownlee, A. Walker, S. C. Nyburg, and J. J. Szymanski, *J. Chem. Soc. Chem. Commun.*, 1073 (1971).
52. M. D. Brice and F. A. Cotton, *J. Am. Chem. Soc.* **95**, 4529 (1973).
53. M. Yoshida, T. Ueki, N. Yasuoka, N. Kasai, M. Kakudo, I. Omae, S. Kikkawa, and S. Matsuda, *Bull. Chem. Soc. Jpn.* **41**, 1113 (1968).
54. G. van Koten and J. G. Noltes, *J. Am. Chem. Soc.* **98**, 5393 (1976).
55. R. J. P. Corriu, *Pure Appl. Chem.* **60**, 99 (1988).
56. C. Brelière, F. Carré, R. J. P. Corriu, M. Poirier, G. Royo, and J. Zwecker, *Organometallics* **8**, 1831 (1989).
57. C. Brelière, R. J. P. Corriu, M. Poirier, G. Royo, and J. Zwecker, *Organometallics* **8**, 1834 (1989).
58. C. Brelière, R. J. P. Corriu, M. Poirier, C. Royo, W. W. C. Wong Chi Man, and J. Zwecker, *Organometallics* **9**, 2633 (1990).
59. R. Noyori, I. Nishida, and J. Sakata, *J. Am. Chem. Soc.* **105**, 1598 (1983).
60. E. Krause and R. Becker, *Ber. Dtsch. Chem. Ges.* **54**, 173 (1920).
61. R. F. Chambers and P. C. Scherer, *J. Am. Chem. Soc.* **48**, 1054 (1926).
62. H. G. Kuivila, A. K. Sawyer, and A. G. Armour, *J. Org. Chem.* **26**, 1426 (1961).
63. H. G. Kuivila and E. Jakusik, *J. Org. Chem.* **26**, 1430 (1961).
64. W. P. Neuman, in "The Organometallic and Coordination Chemistry of Germanium, Tin and Lead" (M. Gielen and P. G. Harrison, eds.). Freund, Tel-Aviv, Israel, 1978.
65. D. H. Olsen and F. E. Rundle, *Inorg. Chem.* **2**, 1310 (1963).
66. P. J. Davidson and M. F. Lappert, *J. Chem. Soc. Chem. Commun.*, 317 (1973).
67. A. de Koster, J. A. Kanters, A. L. Spek, A. A. H. van der Zeijden, G. van Koten, and K. Vrieze, *Acta Crystallogr. Sect. C: Cryst. Struct. Commun.* **C41**, 893 (1985).
68. A. A. H. van der Zeijden and G. van Koten, *Inorg. Chem.* **25**, 4723 (1986).
69. D. M. Grove, G. van Koten, R. Zoet, N. W. Murrall, and A. J. Welch, *J. Am. Chem. Soc.* **105**, 1379 (1983).
70. J. A. M. van Beek, G. van Koten, W. J. J. Smeets, and A. L. Spek, *J. Am. Chem. Soc.* **108**, 5010 (1986).
71. D. M. Grove, G. van Koten, and A. H. M. Verschuuren, *J. Mol. Catal.* **45**, 169 (1988).
72. E. Wehman, G. van Koten, M. Knotter, H. Spelten, D. Heijdenrijk, A. N. S. Mak, and C. H. Stam, *J. Organomet. Chem.* **325**, 293 (1987).

73. H. P. Abicht, K. Jurkschat, A. Tzschach, K. Peters, E. M. Peters, and H. G. von Schnering, *J. Organomet. Chem.* **326**, 357 (1987).
74. K. Angermund, K. Jonas, C. Krüger, J. L. Latten, and Y.-H. Tsay, *J. Organomet. Chem.* **353**, 17 (1988).
75. J. T. B. H. Jastrzebski, P. A. van der Schaaf, J. Boersma, G. van Koten, D. Heijdenrijk, K. Goubitz, and D. J. A. de Ridder, *J. Organomet. Chem.* **367**, 55 (1989).
76. J. T. B. H. Jastrzebski, H. A. J. Sytkens, F. J. A. des Tombe, P. A. van der Schaaf, J. Boersma, G. van Koten, A. L. Spek, and A. J. M. Duisenberg, *J. Organomet. Chem.* **396**, 25 (1990).
77. M. Veith and O. Recktenwald, *Top. Curr. Chem.* **104**, 1 (1982).
78. J. T. B. H. Jastrzebski, P. van der Schaaf, J. Boersma, and G. van Koten, *New J. Chem.* **15**, 301 (1991).
79. L. M. Engelhardt, B. S. Jolly, M. F. Lappert, C. L. Raston, and A. H. White, *J. Chem. Soc. Chem. Commun.*, 336 (1988).
80. J. T. B. H. Jastrzebski, G. van Koten, C. T. Knaap, A. M. M. Schreurs, J. Kroon, and A. L. Spek, *Organometallics* **5**, 1551 (1986).
81. D. J. Cram and F. A. A. Elhafez, *J. Am. Chem. Soc.* **74**, 5828 (1952).
82. J. D. Morrison and H. S. Mosher, in "Asymmetric Organic Reactions." Prentice-Hall, Englewood Cliffs, New Jersey, 1971.
83. Y. Izumi and A. Tai, in "Stereo Differentiating Reactions." Academic Press, New York, 1977.
84. K. Jurkschat, H. P. Abicht, A. Tzschach, and B. Mahieu, *J. Organomet. Chem.* **309**, C47 (1986).
85. G. van Koten, *Pure Appl. Chem.* **61**, 1681 (1989).
86. H. C. L. Abbenhuis, N. Feiken, D. M. Grove, J. T. B. H. Jastrzebski, H. Kooijman, P. van der Sluis, W. J. J. Smeets, A. L. Spek, and G. van Koten, *J. Am. Chem. Soc.*, **114**, 9773 (1992).
87. M. P. Bigwood, P. J. Corvan, and J. J. Zuckerman, *J. Am. Chem. Soc.* **103**, 7643 (1981).
88. J. T. B. H. Jastrzebski, P. A. van der Schaaf, J. Boersma, G. van Koten, M. C. Zoutberg, and D. Heijdenrijk, *Organometallics* **8**, 1373 (1989).
89. J. D. Cotton, P. J. Davidson, and M. F. Lappert, *J. Chem. Soc. Dalton Trans.*, 2276 (1976).
90. P. J. Smith, *Organomet. Chem. Rev., Sect. A* **5**, 373 (1970).
91. J. N. R. Ruddick, *Rev. Silicon Germanium Tin Lead Compd.* **2**, 115 (1976).
92. R. Barbieri, A. Silvestry, G. van Koten, and J. G. Noltes, *Inorg. Chim. Acta* **40**, 267 (1980).
93. B. Wrackmeyer, in "Annual Reports on NMR Spectroscopy" (G. A. Webb, ed.), Vol. 16, p. 291. Academic Press, London, England, 1985.
94. J. T. B. H. Jastrzebski, D. M. Grove, J. Boersma, G. van Koten, and J.-M. Ernsting, *Magn. Reson. Chem.* **29**, S25 (1991).
95. V. G. Kumar Das, L. K. Mun, C. Wei, S. J. Blunden, and T. C. W. Mak, *J. Organomet. Chem.* **322**, 163 (1987).
96. J. T. B. H. Jastrzebski, J. Boersma, P. M. Esch, and G. van Koten, *Organometallics* **10**, 930 (1991).
97. J. C. Slater, *J. Chem. Phys.* **41**, 3199 (1964).
98. V. G. Kumar Das, L. K. Mun, C. Wei, and T. C. W. Mak, *Organometallics* **6**, 10 (1987).
99. B. Jousseau, P. Villeneuve, M. Dräger, S. Roller, and J. M. Chezeau, *J. Organomet. Chem.* **349**, C1 (1988).
100. H. Pan, R. Willem, J. Meunier-Piret, and M. Gielen, *Organometallics* **9**, 2199 (1990).
101. A. Tzschach and K. Jurkschat, *Pure Appl. Chem.* **58**, 639 (1986).

102. K. Jurkschat, J. Schilling, C. Mügge, A. Tzschach, J. Meunier-Piret, M. van Meerssche, M. Gielen, and R. Willem, *Organometallics* **7**, 38 (1988).
103. K. Jurkschat, A. Tzschach, and J. Meunier-Piret, *J. Organomet. Chem.* **315**, 45 (1986).
104. K. Jurkschat, A. Tzschach, C. Mügge, J. Piret-Meunier, M. van Meerssche, G. van Binst, C. Wynants, M. Gielen, and R. Willem, *Organometallics* **7**, 593 (1988).
105. H. Schumann, B. C. Wasserman, and F. E. Hahn, *Organometallics* **11**, 2803 (1992).
106. B. C. Wasserman, Ph.D. Thesis, Technischen Universität Berlin, Berlin, Germany, 1992.
107. A. G. Davies and P. J. Smith, in "Comprehensive Organometallic Chemistry" (G. Wilkinson, F. G. A. Stone, and E. W. Abel, eds.), Vol. 2, Chapter 26, p. 519. Pergamon, Oxford, England, 1982.
108. D. Sanders, S. D. Rosenberg, E. Debreczeni, and E. L. Weinberg, *J. Am. Chem. Soc.* **81**, 972 (1959).
109. B. Jousseau and P. Villeneuve, *J. Chem. Soc. Chem. Commun.*, 513 (1987).
110. J. T. B. H. Jastrzebski, C. T. Knaap, and G. van Koten, *J. Organomet. Chem.* **255**, 287 (1983).
111. E. Vedejs, A. R. Haight, and W. O. Moss, *J. Am. Chem. Soc.* **114**, 6556 (1992).
112. J. M. Brown, M. Pearson, J. T. B. H. Jastrzebski, and G. van Koten, *J. Chem. Soc. Chem. Commun.*, 1440 (1992).
113. D. Britton and J. D. Dunitz, *J. Am. Chem. Soc.* **103**, 2971 (1981).
114. G. van Koten, J. T. B. H. Jastrzebski, J. G. Noltes, W. M. G. F. Pontenagel, J. Kroon, and A. L. Spek, *J. Am. Chem. Soc.* **100**, 5021 (1978).
115. G. van Koten, J. G. Noltes, and A. L. Spek, *J. Organomet. Chem.* **118**, 183 (1976).
116. J. T. B. H. Jastrzebski, J. Boersma, and G. van Koten, *J. Organomet. Chem.* **413**, 43 (1991).
117. M. Oki and M. Ohira, *Chem. Lett.*, 1267 (1982).
118. G. van Koten, J. T. B. H. Jastrzebski, J. G. Noltes, G. J. Verhoecks, A. L. Spek, and J. Kroon, *J. Chem. Soc. Dalton Trans.*, 1352 (1980).
119. J. T. B. H. Jastrzebski, E. Wehman, J. Boersma, G. van Koten, K. Goubitz, and D. Heijdenrijk, *J. Organomet. Chem.* **409**, 157 (1991).
120. W. P. Neumann and C. Wicenc, *J. Organomet. Chem.* **420**, 171 (1991).
121. J. Vicente, M. T. Chiote, M. del C. Ramirez-de-Arellano, and P. G. Jones, *J. Organomet. Chem.* **394**, 77 (1990).
122. H. Preut, C. Wicenc, and W. P. Neumann, *Acta Crystallogr. Sect. C: Cryst. Struct. Commun.* **C47**, 2214 (1991).
123. M. Gielen, *Top. Curr. Chem.* **104**, 57 (1982).
124. H. Schumann, B. C. Wasserman, and J. Pickardt, in "Chemistry and Technology of Silicon and Tin" (V. G. Kumar Das, S. W. Ng, and M. Gielen, eds.), pp. 532-543. Oxford University Press, Oxford, England, 1992.
125. K. Jurkschat, A. Tzschach, J. Meunier-Piret, and M. van Meerssche, *J. Organomet. Chem.* **290**, 285 (1985).
126. G. van Koten, J. T. B. H. Jastrzebski, J. G. Noltes, A. L. Spek, and J. C. Schoone, *J. Organomet. Chem.* **148**, 233 (1978).
127. K. Jurkschat, J. Kalbitz, M. Dargatz, E. Kleinpeter, and A. Tzschach, *J. Organomet. Chem.* **347**, 41 (1988).
128. B. K. Nicholson, *J. Organomet. Chem.* **265**, 153 (1984).
129. J. T. B. H. Jastrzebski, P. A. van der Schaaf, J. Boersma, G. van Koten, D. J. A. de Ridder, and D. Heijdenrijk, *Organometallics* **11**, 1521 (1992).
130. D. Cunningham, T. Higgins, and P. McArdle, *J. Chem. Soc. Chem. Commun.*, 833 (1984).

131. J. C. Bailar, Jr., *J. Inorg. Nucl. Chem.* **8**, 165 (1958).
132. H. Weichmann, J. Meunier-Piret, and M. van Meersche, *J. Organomet. Chem.* **309**, 267 (1986).
133. H. Weichmann, C. Mügge, A. Grand, and J. B. Robert, *J. Organomet. Chem.* **238**, 343 (1982).
134. H. Hartung, D. Petrick, C. Schmoll, and H. Weichmann, *Z. Anorg. Allg. Chem.* **550**, 148 (1987).
135. U. Kolb, M. Dräger, E. Fischer, and K. Jurkschat, *J. Organomet. Chem.* **423**, 339 (1992).
136. U. Kolb, M. Dräger, and B. Jousseau, *Organometallics* **10**, 2737 (1991).
137. K. Swami, J. P. Hutchinson, H. G. Kuivila, and J. A. Zubietta, *Organometallics* **3**, 1687 (1984).
138. H. Weichman, *J. Organomet. Chem.* **262**, 279 (1984).
139. S. Z. Abbas and R. C. Poller, *J. Chem. Soc. Dalton Trans.*, 1769 (1974).
140. H. G. Kuivila, J. E. Dixon, P. L. Maxfield, N. M. Scarpa, T. M. Topka, K. H. Tsai, and K. R. Wursthorn, *J. Organomet. Chem.* **86**, 89 (1975).
141. I. Omae, S. Onishi, and S. Matsuda, *J. Organomet. Chem.* **22**, 623 (1970).
142. M. Ochiai, S. Iwaki, T. Ukita, Y. Matsuura, M. Shiro, and Y. Nagao, *J. Am. Chem. Soc.* **110**, 4606 (1988).
143. B. Y. K. Ho and J. J. Zuckerman, *J. Organomet. Chem.* **49**, 1 (1973).
144. L. Pauling, *J. Am. Chem. Soc.* **69**, 542 (1947).
145. H. B. Bürgi, *Inorg. Chem.* **12**, 2321 (1973).
146. P. G. Harrison, T. J. King, and M. A. Healy, *J. Organomet. Chem.* **182**, 17 (1979).
147. M. Yoshida, T. Ueki, N. Yasuoka, N. Kasai, M. Kakudo, I. Omae, S. Kikkawa, and S. Matsuda, *Bull. Chem. Soc. Jpn.* **41**, 1113 (1968).
148. J. L. Briansó, X. Solans, and J. Vecente, *J. Chem. Soc. Dalton Trans.*, 169 (1983).
149. G. van Koten, J. T. B. H. Jastrzebski, and J. G. Noltes, *J. Organomet. Chem.* **177**, 283 (1979).
150. D. Lanigan, in "Proceedings of the International Conference on PVC Processing." Plastics and Rubber Institute, London, England, 1978.
151. E. J. Bulten and J. W. G. van den Hurk, *J. Organomet. Chem.* **162**, 161 (1978).
152. J. T. B. H. Jastrzebski, P. A. van der Schaaf, J. Boersma, M. de Wit, Y. Wang, D. Heijdenrijk, and C. H. Stam, *J. Organomet. Chem.* **407**, 301 (1991).
153. G. van Koten, C. A. Schaap, and J. G. Noltes, *J. Organomet. Chem.* **99**, 157 (1975).
154. R. A. Howie, E. S. Patterson, J. L. Wardell, and J. W. Burley, *J. Organomet. Chem.* **304**, 301 (1986).
155. R. A. Howie, E. S. Patterson, J. L. Wardell, and J. W. Burley, *J. Organomet. Chem.* **259**, 71 (1983).
156. M. Oki, *Pure Appl. Chem.* **61**, 699 (1989).
157. B. Fitzsimmons, D. G. Othen, H. M. M. Shearer, K. Wade, and G. Whitehead, *J. Chem. Soc. Chem. Commun.*, 215 (1977).
158. W. Clegg, C. J. M. Grievson, and K. Wade, *J. Chem. Soc. Chem. Commun.*, 969 (1987).

# Index

## A

- A-frame compounds, 15–19, 21, 24
- Alkylidyne ligands, metal centers, *see* Alkylidyne–metal complexes
- Alkylidyne–metal complexes
  - dimetal compound formation, 157–172
    - anion structure, 168–169
    - four electron donor, 158
    - hyper-closo* cage structure, 167, 169–170
  - IR spectroscopy, 169
  - metallocarbaborane cages, 160, 162, 164, 166–169
  - molecular structure, 159
  - NMR spectra, 165, 169
  - pathways, 166, 170–172
  - reactivity patterns, 162
  - structures, 158, 160–171
  - X-ray diffraction, 158–159, 167
- exo-nido* carbametallaboranes, 172–176
  - molecular structures, 174
  - NMR spectra, 176
  - structures, 173, 175
- Fischer-type, 139
- $\text{HBF}_4 \cdot \text{Et}_2\text{O}$  protonations
  - bidentate phosphines, 149–152
    - product formation, 150–151
    - structures, 150–151
  - monodentate Lewis bases, 142–149
    - icosahedral cage framework, 146–149
    - reactivity pattern, 143–145
    - structures, 143–149
  - X-ray diffraction, 143–144, 146
- history, 137–138
- HX protonations, 152–157
  - anion structure, 153
  - rearrangement process, 154–155
  - structures, 152, 154–156
  - synthetic utility, 156
- lowest unoccupied molecular orbital (LUMO), 139–140
- $\text{M}\equiv\text{C}$  chemistry, 139
- molybdenum complexes
  - $\text{HBF}_4 \cdot \text{Et}_2\text{O}$  protonation, 168–169

- monodentate Lewis bases, 145–146
- HX protonations, 152–154, 156
  - two distinct complex protonation, 160–161, 163, 165
- NMR spectroscopy, 176–181
  - boron-11, 180–181
  - cage-carbon resonances, 179–180
  - carbon-13, 178–180
  - chemical shift ranges, 177–178, 181
  - proton, 177–178
- protonation studies, 139–142
- Schrock-type, 139–140
- structural formulae, 136–138
- synthesis, 137–138
- tungsten complexes
  - exo-nido* carbametallaboranes, 172–173, 175–176
- $\text{HBF}_4 \cdot \text{Et}_2\text{O}$  protonation, 165–172
  - bidentate phosphines, 150–151
  - monodentate Lewis bases, 143–149
- HX protonations, 152–156
  - two distinct complex protonation, 158–165
- X-ray diffraction analysis, 182–183
- Aluminum compounds, *see* Organotin chemistry
- Arsenic clusters, *see* Transition metal clusters

## B

- Bailar twist, 271
- Berry pseudorotation, 275

## C

- Cadmium complexes, *see specific Group metals*
- Cannizzaro reaction, 71–72
- Carbaborane ligands, metal centers, *see* Alkylidyne–metal complexes
- Carbametallaboranes, *see* Alkylidyne–metal complexes
- Catalytic reactions involving CO
  - carbonylation of
    - alcohols, 44–45



- amines, 45–46
- heterocycles, 46
- deoxygenation of
  - aldoximes, 47–48
  - ketoimes, 46–47
  - nitrobenzene, catalytic cycle, 48
  - nitro compounds, 48–49
- Monsanto acetic acid process, 44–45
- Catalytic reactions involving CO and H<sub>2</sub>
  - hydroformylation, 80–89
    - chemoselectivity, 80
    - cyclohexene, mechanism, 88
    - ethylene, catalytic cycle, 86–87
    - formaldehyde, 89
    - mechanistic studies, 87
    - olefins, 80–85
    - regioselectivity, 80, 86–87
  - miscellaneous reactions, 93–95
  - syngas reactions, 74–80
    - catalytic systems, 75
    - Fischer-Tropsch process, 74
    - hydrogenation of carbon monoxide, 76–79
- Catalytic reactions involving CO and H<sub>2</sub>O
  - hydroformylation using water, 99–102
  - hydrohydroxymethylation, 99–101
  - olefins, 100–101
  - Reppe synthesis, 99
  - hydrogenation using water, 102–104
    - nitroaryls, 102
    - nitrobenzene reduction, 103
    - selective reduction, 102
  - miscellaneous reactions, 104–107
  - water–gas shift reaction, 95–99
    - catalytic cycle, 96–97
    - CO exchange kinetics, 97
    - definition, 95
    - equilibrium, 97
    - hydrogen formation, 98
- Catalytic reactions involving H<sub>2</sub>
  - hydrogenation of
    - acetylenes, 60–64
    - aldehydes, 64
    - alkynes, 61–63
    - bis(trifluoromethyl)acetylene, mechanism, 64
    - carbonic acids, 66
    - carbonyls, 64–66
    - ketones, 64
    - nitrogen containing functions, 67–68
    - olefins, 49–60
      - alkenes to alkanes, 50–53
      - asymmetric, 54, 56
      - enantiomer discrimination, 57
      - enantioselective, 55–56
      - ethylene mechanism, 58–59
      - maleic anhydride, catalytic cycle, 59–60
      - photocatalytic, 49, 54
      - selectivity, 54
    - orthoesters, 66
    - hydrosilylation reactions, 72–73
  - hydrogen transfer reactions, 67, 69–72
    - asymmetric reduction, 70–71
    - Cannizzaro reaction, 71–72
  - catalytic, 67, 69
  - Schiff base reductions, 69
  - tetrachloromethane, mechanism, 71
- Chromium complexes, *see* Diboraheterocycle metal complexes; Group 6 metals; Group 8 metals
- Chromium compounds, *see* Organotin chemistry
- C,N-chelating ligands, *see* Organotin chemistry
- Cobalt clusters, *see* Transition metal clusters
- Cobalt complexes, *see* Diboraheterocycle metal complexes; Group 9 metals
- Cobalt compounds, *see* Organotin chemistry
- Copper clusters, *see* Transition metal clusters
- Copper complexes, *see* Diboraheterocycle metal complexes; Group 11 metals
- C,Y-chelating ligands, *see* Organotin chemistry

## D

- 1,4-Diboracyclohexadiene metal complexes, 191–194
- 1,3-Diborafulvene metal complexes, 205–208
- Diboraheterocycle metal complexes
  - acceptor properties, 187–188
  - bifacial coordination, 191
  - chromium complexes, 188–189, 201, 203
  - cobalt complexes, 190–191, 193–194, 198–204, 207–208
  - copper complexes, 203
  - 1,4-diboracyclohexadiene, 191–194

- nido carboranes, 191–192
- synthesis, 192–193
- X-ray structure analysis, 193–194
- 1,3-diborifulvene metal complexes, 205–208
  - molecular structures, 206–207
  - NMR signals, 205
  - X-ray structure analysis, 205–207
- 9,10-dihydro-9,10-diboraanthracene, 197–201
  - bonding, 197, 200
  - molecular structures, 199–200
  - NMR data, 197, 200
  - reactions, 197, 199, 201
  - X-ray structure analysis, 197, 199–200
- 1,4-dihydro-1,4-diboranaphthalene, 194–197
  - molecular structures, 196–197
  - reactions, 194–196
  - X-ray structure analysis, 195–197
- 2,3-dihydro-1,3-diborolyl metal complexes, 202–204
  - EXAFS, 204
  - ligand properties, 202, 204
  - reactions, 203
- donor properties, 187–188
- iron complexes, 189–192, 194–200, 202–208
- manganese complexes, 203
- nickel complexes, 195–198, 200, 202–204
- osmium complexes, 189, 191
- $\pi$ -complex chemistry, 188
- rhodium complexes, 190
- rhodium complexes, 190, 192, 202, 204, 207–208
- ruthenium complexes, 188–189, 191
- syn-facial coordination, 189–190
- tantalum complexes, 189–190
- vanadium complexes, 188–189
- zinc complexes, 195, 203–204
- Diels-Alder cycloaddition, 110
- 9,10-Dihydro-9,10-diboraanthracene metal complexes, 197–201
- 1,4-Dihydro-1,4-diboranaphthalene metal complexes, 194–197
- 2,3-Dihydro-1,3-diborolyl metal complexes, 202–204
- Dimetal compound formation, 157–172
  - protonation of distinct alkylidyne-metal complexes, 157–164
  - protonations with  $\text{HBF}_4 \cdot \text{Et}_2\text{O}$ , 165–172
- Dinuclear metal complexes, *see* Diborahe-terocycle metal complexes
- Diplatinum centers, chemistry
  - dppc bridged complexes, 32–35
    - bond distances, 33–34
    - elimination, 34–35
    - molecular structures, 32–34
    - NMR characterization, 32
    - reactions, 32, 35
  - dppm bridged complexes, 11–32
    - A-frame compounds, 15–19, 21, 24
    - bond distances, 14, 20–23
    - $\text{C}_2\text{H}_4$  elimination, 29
    - coupling constants, 23
    - geometry, 12, 22
    - $\text{H}_2$  elimination mechanism, 26
    - intermediates, 17
    - inversion, 19
    - molecular structures, 11, 13–14, 19–20
    - NMR spectrum, 12, 23–24
    - orbital bonding, 22
    - oxidative addition, 29, 31
    - palladium elimination reactions, 29
    - photochemical decomposition, 31
    - $\text{PPh}_3$  substitution mechanism, 15
    - preparation, 12, 16, 19–20
    - reactions, 11, 13–15, 17–18, 24–25, 28
    - reduction, 25–27
    - structures, 13
    - thermodynamic favorability, 18
    - water-gas shift reaction, 27
    - X-ray diffraction, 14, 17
- dppm related complexes, 13, 16, 18–20, 22, 26, 29–31
  - preparation, 16, 19
  - structures, 13, 19
  - treatment, 20
- halide bridged complexes, 2–3
  - reactions, 2–3
  - Zeise's dimer, 2
- hydride bridged complexes, 3–5
  - characterization, 4
  - dppe syntheses, 4–5
  - molecular structure, 4
  - preparation, 3–4
  - product nuclearity sensitivity, 4
- organic bridging group complexes, 5–7
  - preparation, 6–7

- reactions, 5–7
  - X-ray diffraction characterization, 6
  - Zeise's dimer treatment, 6
  - orthometalated phosphine ligand complexes, 7–10
    - coupling constants, 10
    - dppe ligands, 8
    - molecular structures, 9
    - reactions, 7–10
    - X-ray characterization, 8, 10
  - platinum–platinum bond complexes, 1–2, 35
  - dppc bridged complexes, 32–35
  - dppm bridged complexes, 11–32
  - dppm related complexes, 13, 16, 18–20, 22, 26, 29–31
- F**
- Fischer-Tropsch process, 74
  - Fischer-type alkylidyne–metal complexes, 139
- G**
- Gold clusters, *see* Transition metal clusters
  - Gold complexes, *see* Group 11 metals
  - Group 3–5 metals, trifluoromethyl derivatives, 218
    - cadmium complexes, 218
    - hafnium complexes, 218
    - zirconium complexes, 218
  - Group 6 metals, trifluoromethyl derivatives, 218–221
    - cadmium complexes, 219–220
    - chromium complexes, 220–221
    - CpMo(CO)<sub>2</sub>CF<sub>3</sub>, 218–219
    - CpMo(CO)<sub>2</sub>CF<sub>3</sub> difluorocarbenes, 219–220
    - CpW(CO)<sub>3</sub>CF<sub>3</sub>, 218–219
    - molybdenum complexes, 218–221
    - tungsten complexes, 218–220
  - Group 7 metals, trifluoromethyl derivatives, 221–223
    - cadmium complexes, 221
    - manganese complexes, 221–223
    - Mn(CO)<sub>3</sub>CF<sub>3</sub> carbonylation, 222–223
    - Mn(CO)<sub>3</sub>CF<sub>3</sub> ligand exchange, 221–222
    - Mn(CO)<sub>3</sub>CF<sub>3</sub> synthesis, 221
    - Mn(CO)<sub>3</sub>COCF<sub>3</sub> decarbonylation, 222–223
  - Group 8 metals, trifluoromethyl derivatives
    - cadmium complexes, 224–227
    - chromium complexes, 225
    - cis*-Fe(CO)<sub>4</sub>(CF<sub>3</sub>)<sub>2</sub>, 224–225
    - CpFe(CO)<sub>2</sub>CF<sub>3</sub>, 223–224
    - Fe(diars)(CO)<sub>2</sub>I(COCF<sub>3</sub>), 225
    - iridium complexes, 224
    - iron complexes, 223–225
    - mercury complexes, 226
    - molybdenum complexes, 224
    - osmium complexes, 226–227
    - Os(O) difluorocarbene compounds, 226–227
    - Os(O) trifluoromethyl compounds, 226–227
    - Ru(O) difluorocarbene compounds, 226–227
    - Ru(O) trifluoromethyl compounds, 226–227
    - ruthenium complexes, 226–227
    - ruthenium (II) difluorocarbene compounds, 226
    - ruthenium (II) trifluoromethyl compounds, 226
    - tungsten complexes, 224
  - Group 9 metals, trifluoromethyl derivatives, 227–229
    - cadmium complexes, 227, 229
    - cobalt complexes, 227–228
    - Co(III) — R<sub>f</sub> compounds, kinetics, 228
    - Co(III) — R<sub>f</sub> compounds, reduction, 227–228
    - Co(III) — R<sub>f</sub> compounds, thermodynamics, 228
    - CpCo(CO)(CF<sub>3</sub>)<sub>2</sub> synthesis, 227
    - iridium complexes, 229
    - Ir (III) compounds, 229
    - mercury complexes, 229
    - Rh(CO)(PPh<sub>3</sub>)<sub>2</sub>(CF<sub>3</sub>), 228–229
    - rhodium complexes, 228–229
    - Vaska's complex, 229
  - Group 10 metals, trifluoromethyl derivatives, 230–231
    - nickel complexes, 230
    - palladium complexes, 230
    - platinum (II) compounds, 230–231
    - platinum (IV) compounds, 230–231
    - silver-assisted trifluoromethylations, 230
  - Group 11 metals, trifluoromethyl derivatives, 231–232
    - cadmium complexes, 231–232

gold compounds, 232  
silver compounds, 232  
Group 12 metals, trifluoromethyl derivatives, 233–234  
cadmium complexes, 233–234  
 $\text{Cd}(\text{CF}_3)_2\text{DME}$ , 233–234  
 $\text{Hg}(\text{CF}_3)_2$ , 234  
mercury complexes, 234  
zinc complexes, 233  
 $\text{Zn}(\text{CF}_3)_2\text{L}_2$  synthesis, 233

## H

Hafnium complexes, *see* Group 3–5 metals  
Halide bridged complexes, 2–3  
 $\text{HBF}_4 \cdot \text{Et}_2\text{O}$  protonations  
  bidentate phosphines, 149–152  
  monodentate Lewis bases, 142–149  
Homogeneous catalysis, transition metal clusters, *see* Transition metal clusters  
HX protonations, 152–157  
Hydride bridged complexes, 3–5

## I

Iridium clusters, *see* Transition metal clusters  
Iridium complexes, *see* Group 8 metals;  
  Group 9 metals  
Iron clusters, *see* Transition metal clusters  
Iron complexes, *see* Diboraheterocycle  
  metal complexes; Group 8 metals  
Iron compounds, *see* Organotin chemistry

## K

Karasch addition, 247

## M

Magnesium compounds, *see* Organotin chemistry  
Manganese complexes, *see* Diboraheterocycle metal complexes; Group 7 metals  
Mercury complexes, *see* Group 8 metals;  
  Group 9 metals; Group 12 metals  
Metal complexes of diboraheterocycles, *see*  
  Diboraheterocycle metal complexes  
Molybdenum clusters, *see* Transition metal clusters  
Molybdenum complexes, *see* Alkylidyne–

metal complexes; Group 6 metals;  
Group 8 metals

Monsanto acetic acid process, 44–45

## N

Nickel clusters, *see* Transition metal clusters  
Nickel complexes, *see* Diboraheterocycle  
  metal complexes; Group 10 metals  
Nickel compounds, *see* Organotin chemistry  
Niobium clusters, *see* Transition metal clusters

## O

Organic bridging group complexes, 5–7  
Organotin chemistry  
  aluminum compounds, 282  
  bond angles, 243–244  
  bond lengths, 243  
  characteristics, 243  
  chromium compounds, 247–248  
  cobalt compounds, 247–248, 252  
  coordination geometries, 244–246  
  divalent compounds containing C,  
    Y-chelating ligand, 247–255  
    coalescence temperature, 254–255  
    coordination geometry, 250, 252–253  
    diastereoisomeric structures, 250–251  
    heteroleptic compounds, 252, 254  
    Karasch addition, 247  
    Mössbauer spectroscopy, 253  
    NMR spectra, 250, 252–254  
    reactivity, 255  
    special features, 247  
    stabilization by intramolecular coordination, 249–255  
    structures, 252–255  
    tin as Lewis base, 247–248  
    tin-transition coordination bond, 247–249  
  VSEPR model, 250  
  X-ray crystal structure, 248–250, 253  
iron compounds, 247, 252  
magnesium compounds, 251–252, 282  
nickel compounds, 247, 252  
palladium compounds, 261–262  
platinum compounds, 252  
singlet carbene analog structures, 244  
tetravalent compounds containing C,N-  
  chelating ligand, 260–271

- tetravalent compounds containing C,Y-  
  chelating ligand, 256–288  
  Bailar twist, 271  
  basic fluxional processes, 264  
  Berry pseudorotation, 275  
  chemical shift value, 256–257  
  configuration inversion, mechanism,  
    284  
  coordination geometry, 257–258, 260–  
    261, 263, 268, 281  
  diorganotin dihalides, 279–286  
  diptych derivatives, 259–260, 268  
  EXSY spectroscopy, 260  
  fluxional processes, 264–268  
  geometrical isomers, 285  
  Lewis acidity, 256  
  miscellaneous compounds, 268–271  
  monoanionic compounds, 262–268  
  monoorganotin halides, 286–288  
  Mössbauer spectroscopy, 256–257,  
    279, 287  
  NMR spectroscopy, 256–260, 263–  
    271, 273, 279, 281–286  
  octahedral compound arrangement,  
    279–281  
  schematic projection, 267  
  Sn—C bond reactivity, 261–262  
  Sn-chiral halides, 265  
  stereochemical aspects, 264–268  
  Stille coupling reaction, 261  
  structural features, 277  
  tin centers  
    configuration inversion, 274–275  
    transition states, 275  
  trigonal bipyramidal compound ar-  
    rangement, 281–286  
  triorganotin bromides, pentacoordi-  
    nate, 266–268  
  triorganotin cations, pentacoordinate,  
    269  
  triorganotin chlorides  
    pentacoordinate, 268  
    syabilization, 273  
  triorganotin halides, 262–279  
    hexacoordinate, 270  
    other, 272–274  
    structural correlation, 276–279  
  triptych derivatives, 259–260, 268  
  X-ray structure, 256–259, 261–262,  
    265, 268–269, 276–277, 280–  
    281, 286  
  tin bonds and valency, 242–244  
  tungsten compounds, 248, 250  
  zinc compounds, 248–249  
Orthometalated phosphine ligand com-  
  plexes, 7–10  
Osmium complexes, *see* Diboraheterocycle  
  metal complexes; Group 8 metals
- P**
- Palladium clusters, *see* Transition metal  
  clusters  
Palladium complexes, *see* Group 10 metals  
Palladium compounds, *see* Organotin  
  chemistry  
Platinum complexes, *see* Diplatinum  
  centers, chemistry; Group 10 metals  
Platinum compounds, *see* Organotin chem-  
  istry  
Platinum–platinum bond complexes, 1–2
- R**
- Reppe synthesis, 99  
Rhenium clusters, *see* Transition metal  
  clusters  
Rhenium complexes, *see* Diboraheterocycle  
  metal complexes; Group 9 metals  
Rhodium clusters, *see* Transition metal  
  clusters  
Ruthenium clusters, *see* Transition metal  
  clusters  
Ruthenium complexes, *see* Diboraheterocy-  
  cle metal complexes; Group 8 metals
- S**
- Schrock-type alkylidyne–metal complexes,  
  139–140  
Silver complexes, *see* Group 11 metals  
Stille coupling reaction, 261
- T**
- Tantalum complexes, *see* Diboraheterocycle  
  metal complexes  
Transition metal clusters, *see also* Catalytic  
  reactions  
  alkyne couplings, 117–118  
  allyl alcohol conversion, mechanism, 112

- arene benzylation, 115
- aromatic bond activation, 114–115
- arsenic clusters, catalytic reactions involving CO and  $H_2$ , 81
- carbon–carbon coupling, 112–118
- carbon–nitrogen coupling, 118–121
- catalytic applications, 42–43
- catalytic reactions involving CO, 44–49
  - carbonylation of
    - alcohols, 44–45
    - amines, 45–46
    - heterocycles, 46
  - deoxygenation of
    - nitro compounds, 48–49
    - oximes, 46–48
- catalytic reactions involving CO and  $H_2$ , 74–95
  - homologation reactions, 90–92
  - hydroformylation of olefins, 81–85
  - hydroformylation reactions, 80–89
  - hydrogenation of carbon monoxide, 76–79
  - miscellaneous, 93–95
  - syngas reactions, 74–80
- catalytic reactions involving CO and  $H_2O$ , 95–107
  - hydroformylation using water, 99–102
  - hydrogenation using water, 102–104
  - hydrogen formation, 98
  - hydrohydroxymethylation, 100–101
  - miscellaneous, 104–107
  - nitrobenzene reduction, 103
  - water–gas shift reaction, 95–99
- catalytic reactions involving  $H_2$ , 49–73
  - alkenes to alkanes, 50–53
  - hydrogenation of
    - acetylenes, 60–64
    - alkynes, 61–63
    - carbonyls, 64–66
    - nitrogen containing functions, 67–68
    - olefins, 49–60
  - hydrogen transfer reactions, 67, 69–72
- catalytic reactions involving silanes, 72–73
- catalytic turnover, 43–44
- cobalt clusters
  - catalytic reactions involving
    - CO, 46
    - CO and  $H_2$ , 76, 78–79, 81–85, 88–92, 95
    - CO and  $H_2O$ , 101, 103–104
    - $H_2$ , 51–52, 62, 65, 73
  - isomerization and rearrangement reactions, 108–109, 113–114, 117
- copper clusters, catalytic reactions involving CO and  $H_2$ , 78
- cross aldol-type, 116–117
- definition, 41–42
- Diels-Alder cycloaddition, 110
- diene cyclodimerization, 113–114
- diene isomerization, 108
- enantioselective isomerization, 111
- gold clusters
  - catalytic reactions involving CO and  $H_2$ , 91
  - isomerization and rearrangement reactions, 108
- homogeneous versus heterogeneous catalysis, 42–43
- iridium clusters
  - catalytic reactions involving
    - CO and  $H_2O$ , 101, 103
    - $H_2$ , 51
  - isomerization and rearrangement reactions, 120
- iron clusters
  - catalytic reactions involving
    - CO, 45
    - CO and  $H_2$ , 82–83, 87, 90–91, 93
    - CO and  $H_2O$ , 97–99, 101–102, 105
    - $H_2$ , 49, 61–63, 67–68, 73
  - isomerization and rearrangement reactions, 108–109, 113–114, 121
- isomerization, 107–112
- miscellaneous, 121–122
- molybdenum clusters
  - catalytic reactions involving
    - CO and  $H_2$ , 81
    - $H_2$ , 53, 73
  - isomerization and rearrangement reactions, 121
- nickel clusters
  - catalytic reactions involving  $H_2$ , 51–53, 62–63, 68
  - isomerization and rearrangement reactions, 113
- olefin isomerization, 108, 110
- catalytic cycle, 109
- osmium clusters
  - catalytic reactions involving
    - CO and  $H_2O$ , 97, 100, 103
    - $H_2$ , 50–53, 59–60, 62, 64, 67–68

- isomerization and rearrangement reactions, 109–110, 115, 120–121
  - palladium clusters
    - catalytic reactions involving  $H_2$ , 53
    - isomerization and rearrangement reactions, 108, 121
  - platinum clusters
    - catalytic reactions involving
      - CO and  $H_2$ , 78, 82
      - CO and  $H_2O$ , 103
      - $H_2$ , 53, 63, 70
    - isomerization and rearrangement reactions, 114
  - rearrangement, 112
  - rhenium clusters, catalytic reactions involving CO and  $H_2$ , 78, 92
  - rhodium clusters, catalytic reactions involving
    - CO, 44–45
    - CO and  $H_2$ , 75, 78, 81–89, 92, 94–95
    - CO and  $H_2O$ , 98, 100–107
    - $H_2$ , 51, 55–57, 61, 64–67, 73
  - ruthenium clusters
    - catalytic reactions involving
      - CO, 44–49
      - CO and  $H_2$ , 75–84, 86–93, 95
      - CO and  $H_2O$ , 96–101, 103–107
      - $H_2$ , 49–55, 58–62, 65, 68–73
    - isomerization and rearrangement reactions, 108–113, 116–122
  - tungsten clusters, catalytic reactions involving  $H_2$ , 53
  - Transition metal complexes, trifluoromethyl-containing chemistry, 218–234
    - Group 3–5 metals, derivatives, 218
    - Group 6 metals, derivatives, 218–221
    - Group 7 metals, derivatives, 221–223
    - Group 8 metals, derivatives, 223–227
    - Group 9 metals, derivatives, 227–229
    - Group 10 metals, derivatives, 230–231
    - Group 11 metals, derivatives, 231–232
    - Group 12 metals, derivatives, 233–234
  - early studies, 212–218
    - backbonding, 213
    - $CF_3I$ , 212–215
    - d* block elements, 212–213
    - formation, 213–215
    - preparation, 214–217
    - properties, 213
    - reactions, 214
    - reagents, 216–217
    - $\sigma$ -bonding manifold, 213
    - thermal decarbonylation method, 213–214
    - prospects, 235–236
    - scope, 211–212
    - structural data synopsis, 234–235
  - Trifluoromethyl-containing transition metal complexes, *see* Transition metal complexes, trifluoromethyl-containing
  - Trinuclear metal complexes, *see* Diboraheterocycle metal complexes
  - Tungsten clusters, *see* Transition metal clusters
  - Tungsten complexes, *see* Alkylidyne–metal complexes; Group 6 metals; Group 8 metals
  - Tungsten compounds, *see* Organotin chemistry
- V
- Vanadium complexes, *see* Diboraheterocycle metal complexes
  - Vaska's complex, 229
  - VSEPR model, 250
- W
- Water–gas shift reaction, 95–104
- Z
- Zeise's dimer, 2, 6
  - Zinc complexes, *see* Diboraheterocycle metal complexes; Group 12 metals
  - Zinc compounds, *see* Organotin chemistry
  - Zirconium complexes, *see* Group 3–5 metals

## ***Cumulative List of Contributors***

- Abel, E. W., 5, 1; 8, 117  
 Aguiló A., 5, 321  
 Akkerman, O. S., 32, 147  
 Albano, V. G., 14, 285  
 Alper, H., 19, 183  
 Anderson, G. K., 20, 39; 35, 1  
 Angelici, R. J., 27, 51  
 Aradi, A. A., 30, 189  
 Armitage, D. A., 5, 1  
 Armor, J. N., 19, 1  
 Ash, C. E., 27, 1  
 Ashe III, A. J., 30, 77  
 Atwell, W. H., 4, 1  
 Baines, K. M., 25, 1  
 Barone, R., 26, 165  
 Bassner, S. L., 28, 1  
 Behrens, H., 18, 1  
 Bennett, M. A., 4, 353  
 Bickelhaupt, F., 32, 147  
 Birmingham, J., 2, 365  
 Blinka, T. A., 23, 193  
 Bockman, T. M., 33, 51  
 Bogdanović, B., 17, 105  
 Bottomley, F., 28, 339  
 Bradley, J. S., 22, 1  
 Brew, S. A., 35, 135  
 Brinckman, F. E., 20, 313  
 Book, A. G., 7, 95; 25, 1  
 Brown, H. C., 11, 1  
 Brown, T. L., 3, 365  
 Bruce, M. I., 6, 273, 10, 273; 11, 447, 12, 379; 22, 59  
 Brunner, H., 18, 151  
 Buhro, W. E., 27, 311  
 Byers, P. K., 34, 1  
 Cais, M., 8, 211  
 Calderon, N., 17, 449  
 Callahan, K. P., 14, 145  
 Canty, A. J., 34, 1  
 Cartledge, F. K., 4, 1  
 Chalk, A. J., 6, 119  
 Chanon, M., 26, 165  
 Chatt, J., 12, 1  
 Chini, P., 14, 285  
 Chisholm, M. H., 26, 97; 27, 311  
 Chiusoli, G. P., 17, 195  
 Chojinowski, J., 30, 243  
 Churchill, M. R., 5, 93  
 Coates, G. E., 9, 195  
 Collman, J. P., 7, 53  
 Compton, N. A., 31, 91  
 Connelly, N. G., 23, 1; 24, 87  
 Connolly, J. W., 19, 123  
 Corey, J. Y., 13, 139  
 Corriu, R. J. P., 20, 265  
 Courtney, A., 16, 241  
 Coutts, R. S. P., 9, 135  
 Coyle, T. D., 10, 237  
 Crabtree, R. H., 28, 299  
 Craig, P. J., 11, 331  
 Csuk, R., 28, 85  
 Cullen, W. R., 4, 145  
 Cundy, C. S., 11, 253  
 Curtis, M. D., 19, 213  
 Darensbourg, D. J., 21, 113, 22, 129  
 Darensbourg, M. Y., 27, 1  
 Davies, S. G., 30, 1  
 Deacon, G. B., 25, 237  
 de Boer, E., 2, 115  
 Deeming, A. J., 26, 1  
 Dessy, R. E., 4, 267  
 Dickson, R. S., 12, 323  
 Dixneuf, P. H., 29, 163  
 Eisch, J. J., 16, 67  
 Ellis, J. E., 31, 1  
 Emerson, G. F., 1, 1  
 Epstein, P. S., 19, 213  
 Erker, G., 24, 1



- Ernst, C. R., 10, 79  
 Errington, R. J., 31, 91  
 Evans, J., 16, 319  
 Evans, W. J., 24, 131  
 Faller, J. W., 16, 211  
 Farrugia, L. J., 31, 301  
 Faulks, S. J., 25, 237  
 Fehlner, T. P., 21, 57; 30, 189  
 Fessenden, J. S., 18, 275  
 Fessenden, R. J., 18, 275  
 Fischer, E. O., 14, 1  
 Ford, P. C., 28, 139  
 Forníés, J., 17, 219  
 Forster, D., 17, 255  
 Fraser, P. J., 12, 323  
 Friedrich, H. B., 33, 235  
 Fritz, H. P., 1, 239  
 Fürstner, A., 28, 85  
 Furukawa, J., 12, 83  
 Fuson, R. C., 1, 221  
 Gallop, M. A., 25, 121  
 Garrou, P. E., 23, 95  
 Geiger, W. E., 23, 1; 24, 87  
 Geoffroy, G. L., 18, 207; 24, 249; 28, 1  
 Gilman, H., 1, 89; 4, 1; 7, 1  
 Gladfelter, W. L., 18, 207; 24, 41  
 Gladysz, J. A., 20, 1  
 Glänzer, B. I., 28, 85  
 Green, M. L. H., 2, 325  
 Grev, R. S., 33, 125  
 Griffith, W. P., 7, 211  
 Grovenstein, Jr., E., 16, 167  
 Gubin, S. P., 10, 347  
 Guerin, C., 20, 265  
 Gysling, H., 9, 361  
 Haiduc, I., 15, 113  
 Halasa, A. F., 18, 55  
 Hamilton, D. G., 28, 299  
 Harrod, J. F., 6, 119  
 Hart, W. P., 21, 1  
 Hartley, F. H., 15, 189  
 Hawthorne, M. F., 14, 145  
 Heck, R. F., 4, 243  
 Heimbach, P., 8, 29  
 Helmer, B. J., 23, 193  
 Henry, P. M., 13, 363  
 Heppert, J. A., 26, 97  
 Herberich, G. E., 25, 199  
 Herrmann, W. A., 20, 159  
 Hieber, W., 8, 1  
 Hill, E. A., 16, 131  
 Hoff, C., 19, 123  
 Hoffmeister, H., 32, 227  
 Holzmeier, P., 34, 67  
 Honeyman, R. T., 34, 1  
 Horwitz, C. P., 23, 219  
 Hosmane, N. S., 30, 99  
 Housecroft, C. E., 21, 57; 33, 1  
 Huang, Yaozeng (Huang, Y. Z.), 20, 115  
 Hughes, R. P., 31, 183  
 Ibers, J. A., 14, 33  
 Ishikawa, M., 19, 51  
 Ittel, S. D., 14, 33  
 Jastrzebski, J. T. B. H., 35, 241  
 Jain, L., 27, 113  
 Jain, V. K., 27, 113  
 James, B. R., 17, 319  
 Janiak, C., 33, 291  
 Jenck, J., 32, 121  
 Jolly, P. W., 8, 29; 19, 257  
 Jones, K., 19, 97  
 Jones, M. D., 27, 279  
 Jones, P. R., 15, 273  
 Jordan, R. F., 32, 325  
 Jukes, A. E., 12, 215  
 Jutzi, P., 26, 217  
 Kaesz, H. D., 3, 1  
 Kalck, P., 32, 121; 34, 219  
 Kaminsky, W., 18, 99  
 Katz, T. J., 16, 283  
 Kawabata, N., 12, 83  
 Kemmitt, R. D. W., 27, 279  
 Kettle, S. F. A., 10, 199  
 Kilner, M., 10, 115  
 Kim, H. P., 27, 51  
 King, R. B., 2, 57  
 Kingston, B. M., 11, 253  
 Kisch, H., 34, 67  
 Kitching, W., 4, 267  
 Kochi, J. K., 33, 51  
 Köster, R., 2, 257  
 Krieter, C. G., 26, 297  
 Krüger, G., 24, 1  
 Kudaroski, R. A., 22, 129  
 Kühlein, K., 7, 241  
 Kuivila, H. G., 1, 47  
 Kumada, M., 6, 19; 19, 51  
 Lappert, M. F., 5, 225; 9, 397; 11, 253, 14, 345  
 Lawrence, J. P., 17, 449  
 Le Bozec, H., 29, 163  
 Lednor, P. W., 14, 345

- Linford, L., 32, 1  
 Longoni, G., 14, 285  
 Luijten, J. G. A., 3, 397  
 Lukehart, C. M., 25, 45  
 Lupin, M. S., 8, 211  
 McGlinchey, M. J., 34, 285  
 McKillop, A., 11, 147  
 McNally, J. P., 30, 1  
 Macomber, D. W., 21, 1; 25, 317  
 Maddox, M. L., 3, 1  
 Maguire, J. A., 30, 99  
 Maitlis, P. M., 4, 95  
 Mann, B. E., 12, 135; 28, 397  
 Manuel, T. A., 3, 181  
 Markies, P. R., 32, 147  
 Mason, R., 5, 93  
 Masters, C., 17, 61  
 Matsumura, Y., 14, 187  
 Mayr, A., 32, 227  
 Meister, G., 35, 41  
 Mingos, D. M. P., 15, 1  
 Mochel, V. D., 18, 55  
 Moedritzer, K., 6, 171  
 Molloy, K. C., 33, 171  
 Monteil, F., 34, 219  
 Morgan, G. L., 9, 195  
 Morrison, J. A., 35, 211  
 Moss, J. R., 33, 235  
 Mrowca, J. J., 7, 157  
 Müller, G., 24, 1  
 Mynott, R., 19, 257  
 Nagy, P. L. I., 2, 325  
 Nakamura, A., 14, 245  
 Nesmeyanov, A. N., 10, 1  
 Neumann, W. P., 7, 241  
 Norman, N. C., 31, 91  
 Ofstead, E. A., 17, 449  
 Ohst, H., 25, 199  
 Okawara, R., 5, 137; 14, 187  
 Oliver, J. P., 8, 167; 15, 235; 16, 111  
 Onak, T., 3, 263  
 Oosthuizen, H. E., 22, 209  
 Otsuka, S., 14, 245  
 Pain, G. N., 25, 237  
 Parshall, G. W., 7, 157  
 Paul, I., 10, 199  
 Peres, Y., 32, 121  
 Petrosyan, W. S., 14, 63  
 Pettit, R., 1, 1  
 Pez, G. P., 19, 1  
 Poland, J. S., 9, 397  
 Poliakoff, M., 25, 277  
 Popa, V., 15, 113  
 Pourreau, D. B., 24, 249  
 Powell, P., 26, 125  
 Pratt, J. M., 11, 331  
 Prokai, B., 5, 225  
 Pruett, R. L., 17, 1  
 Rao, G. S., 27, 113  
 Raubenheimer, H. G., 32, 1  
 Rausch, M. D., 21, 1; 25, 317  
 Reetz, M. T., 16, 33  
 Reutov, O. A., 14, 63  
 Rijikens, F., 3, 397  
 Ritter, J. J., 10, 237  
 Rochow, E. G., 9, 1  
 Rokicki, A., 28, 139  
 Roper, W. R., 7, 53; 25, 121  
 Roundhill, D. M., 13, 273  
 Rubezhov, A. Z., 10, 347  
 Salerno, G., 17, 195  
 Slater, I. D., 29, 249  
 Satgé, J., 21, 241  
 Schade, C., 27, 169  
 Schmidbauer, H., 9, 259; 14, 205  
 Schrauzer, G. N., 2, 1  
 Schubert, U., 30, 151  
 Schulz, D. N., 18, 55  
 Schumann, H., 33, 291  
 Schwebke, G. L., 1, 89  
 Seppelt, K., 34, 207  
 Setzer, W. N., 24, 353  
 Seyferth, D., 14, 97  
 Shapakin, S. Yu., 34, 149  
 Shen, Yanchang (Shen, Y. C.), 20, 115  
 Shriver, D. F., 23, 219  
 Siebert, W., 18, 301; 35, 187  
 Sikora, D. J., 25, 317  
 Silverthorn, W. E., 13, 47  
 Singleton, E., 22, 209  
 Sinn, H., 18, 99  
 Skinner, H. A., 2, 49  
 Slocum, D. W., 10, 79  
 Smallridge, A. J., 30, 1  
 Smeets, W. J. J., 32, 147  
 Smith, J. D., 13, 453  
 Speier, J. L., 17, 407  
 Spek, A. L., 32, 147  
 Stafford, S. L., 3, 1  
 Stańczyk, W., 30, 243  
 Stone, F. G. A., 1, 143; 31, 53; 35, 135  
 St, A. C. L., 17, 269

- Suslick, K. M., 25, 73  
Süss-Fink, G., 35, 41  
Sutin, L., 28, 339  
Swincer, A. G., 22, 59  
Tamao, K., 6, 19  
Tate, D. P., 18, 55  
Taylor, E. C., 11, 147  
Templeton, J. L., 29, 1  
Thayer, J. S., 5, 169; 13, 1; 20, 313  
Theodosious, I., 26, 165  
Timms, P. L., 15, 53  
Todd, L. J., 8, 87  
Touchard, D., 29, 163  
Traven, V. F., 34, 149  
Treichel, P. M., 1, 143; 11, 21  
Tsuji, J., 17, 141  
Tsutsui, M., 9, 361; 16, 241  
Turney, T. W., 15, 53  
Tyfield, S. P., 8, 117  
Usón, R., 28, 219  
Vahrenkamp, H., 22, 169  
van der Kerk, G. J. M., 3, 397  
van Koten, G., 21, 151; 35, 241  
Veith, M., 31, 269  
Vezey, P. N., 15, 189  
von Ragué Schleyer, P., 24, 353; 27, 169  
Vreize, K., 21, 151  
Wada, M., 5, 137  
Walton, D. R. M., 13, 453  
Wailles, P. C., 9, 135  
Webster, D. E., 15, 147  
Weitz, E., 25, 277  
West, T., 5, 169; 16, 1; 23, 193  
Wernr, H., 19, 155  
Wiberg, N., 23, 131; 24, 179  
Wiles, D. R., 11, 207  
Wilke, G., 8, 29  
Winter, M. J., 29, 101  
Wojcicki, A., 11, 87; 12, 31  
Yamamoto, A., 34, 111  
Yashina, N. S., 14, 63  
Ziegler, K., 6, 1  
Zuckerman, J. J., 9, 21

This Page Intentionally Left Blank

ISBN 0-12-031135-6



90051



9 780120 311354